FORUM GEOMETRICORUM

A Journal on Classical Euclidean Geometry and Related Areas

published by

Department of Mathematical Sciences
Florida Atlantic University

Volume 16
2016

http://forumgeom.fau.edu

ISSN 1534-1178

Editorial Board

Table of Contents

Forum Geometricorum
Volume 16 (2016) 1–21.

FORUM GEOM
ISSN 1534-1178

On the Coincidences of Pascal Lines

Jaydeep Chipalkatti

Abstract. Let $\mathcal{K}$ denote a smooth conic in the complex projective plane. Pascal's theorem says that, given six points A, B, C, D, E, F on $\mathcal{K}$, the three intersection points $AE \cap BF, AD \cap CF, BD \cap CE$ are collinear. This defines the Pascal line of the array $\begin{bmatrix} A & B & C \\ F & E & D \end{bmatrix}$, and one gets sixty such lines in general by permuting the points. In this paper we consider the variety Ψ of sextuples $\{A, \ldots, F\}$, for which some of the Pascal lines coincide. We show that Ψ has two irreducible components: a five-dimensional component of sextuples in involution, and a four-dimensional component of what will be called 'ricochet configurations'. This gives a complete synthetic characterization of points in Ψ. The proof relies upon Gröbner basis techniques to solve multivariate polynomial equations; the implementation was done in two distinct computer algebra systems.

1. Introduction

1.1. Fix a smooth conic $\mathcal{K}$ in the complex projective plane $\mathbb{P}^2$, and choose six distinct points A, B, C, D, E, F on $\mathcal{K}$. If these are displayed as an array $\begin{bmatrix} A & B & C \\ F & E & D \end{bmatrix}$, then Pascal's theorem says that the three 'cross-hair' intersection points

$$AE \cap BF, \quad AD \cap CF, \quad BD \cap CE,$$

are collinear (see Figure 1).

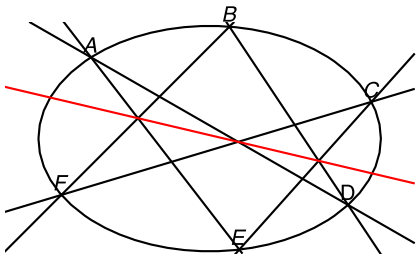

Figure 1. Pascal's theorem

The line containing them (usually called the Pascal line, or just the Pascal) will be denoted as $\left\{ \begin{matrix} A & B & C \\ F & E & D \end{matrix} \right\}$. A different arrangement of the same points, say

Publication Date: March 6, 2016. Communicating Editor: J. Chris Fisher.

$\left\{ \begin{array}{ccc} D & A & C \\ F & B & E \end{array} \right\}$, will *a priori* give a different line. A permutation of rows or columns has no effect on intersection points; for instance,

$$\left\{ \begin{array}{ccc} A & B & C \\ F & E & D \end{array} \right\} = \left\{ \begin{array}{ccc} F & E & D \\ A & B & C \end{array} \right\} = \left\{ \begin{array}{ccc} D & E & F \\ C & B & A \end{array} \right\} \quad \text{etc.,}$$

hence one gets at most $6!/(2 \times 3!) = 60$ possibilities for the Pascal by permuting the points. For a *general* choice of six points, these sixty lines are in fact distinct (see [16]); that is to say, we must be inside a special geometric configuration of some kind if any of the Pascals are to coincide.

1.2. One such configuration is as follows: suppose that the points are in *involution*, i.e., the lines AF, BE, CD are concurrent in the point Q (see Figure 2).

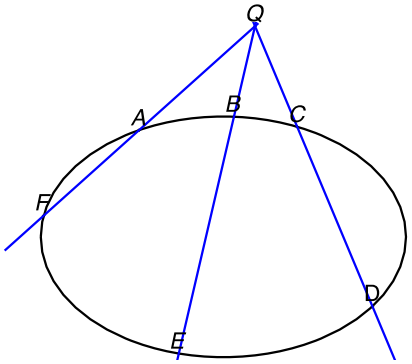

Figure 2. A sextuple in involution

Then it is not difficult to show (see Proposition 1 below), that the following four Pascals become equal:

$$\left\{ \begin{array}{ccc} A & B & C \\ F & E & D \end{array} \right\}, \quad \left\{ \begin{array}{ccc} A & B & D \\ F & E & C \end{array} \right\}, \quad \left\{ \begin{array}{ccc} F & B & C \\ A & E & D \end{array} \right\}, \quad \left\{ \begin{array}{ccc} A & E & C \\ F & B & D \end{array} \right\}. \tag{1}$$

(The pattern is simple; pick any one column from the first array and interchange its entries.) There are no further coincidences, so that a generic involutive configuration has 57 distinct Pascals. It is natural enough to ask whether the converse holds, i.e., whether assuming that some two Pascals coincide forces the initial six points to be in involution. The main result of this paper (Theorem 3 below) says that the answer is 'No, but almost yes.' This requires some explanation.

1.3. Since $\mathcal{K}$ is isomorphic to the projective line $\mathbb{P}^1$, an unordered sextuple of points in $\mathcal{K}$ may be identified with an element in the symmetric product

$$\mathrm{Sym}^6(\mathbb{P}^1) = \frac{(\mathbb{P}^1 \times \mathbb{P}^1 \cdots \times \mathbb{P}^1)}{\text{symmetric group on six objects}} \simeq \mathbb{P}^6.$$

Let $\Delta \subseteq \mathbb{P}^6$ denote the discriminant hypersurface parametrising sextuples where the points are not all distinct. Then we have a morphism

$$\mathbb{P}^6 \setminus \Delta \xrightarrow{\mathfrak{f}} \mathrm{Sym}^{60}(\mathbb{P}^2)^*,$$

which sends a sextuple to all of its Pascals. If $\mathcal{D} \subseteq \mathrm{Sym}^{60}(\mathbb{P}^2)^*$ denotes the 'big diagonal' parametrising repeated lines, then $\Psi = \mathfrak{f}^{-1}(\mathcal{D})$ is the variety of sextuples of distinct points whose Pascals are not all distinct. Our main theorem says that Ψ is a union of two irreducible components $\mathcal{Y}$ and $\mathcal{R}$, where

- $\mathcal{Y}$ is the degree 15 hypersurface of sextuples in involution, and
- $\mathcal{R}$ is the four-dimensional variety of sextuples in what will be called the 'ricochet configuration'.

Since it is $\mathcal{Y}$ which has the larger dimension, a general sextuple in Ψ is in involution.

1.4. The ricochet configuration has not appeared in the literature to the best of my knowledge. I arrived at it after a measure of guesswork, starting from a certain analytic expression in section 3.10 below. It is synthetically constructed as follows:

- Start with arbitrary points A, B, C, D on the conic.
- Let V denote the intersection point of the tangents at A and C, and let F be on the conic such that V, D, F are collinear.
- Let W denote the intersection point of AF and CD.
- Now mark off Z on the conic such that V, B, Z are collinear, and finally E such that W, Z, E are collinear.

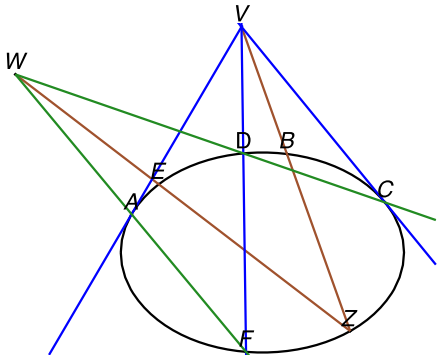

Figure 3. The ricochet configuration

In this situation, the Pascals

$$\left\{ \begin{matrix} A & B & C \\ F & E & D \end{matrix} \right\}, \quad \left\{ \begin{matrix} A & E & C \\ D & B & F \end{matrix} \right\} \tag{2}$$

coincide; this will be proved in section 3.10 below. (The common line is in fact VW, but the diagram would become too baroque for comprehension if any further

lines were added to it.) One can imagine B being struck by V in the direction of Z, bouncing off the conic and getting redirected to E, hence the term 'ricochet'. Another version of this diagram is given on page 11.

The main theorem can be paraphrased as saying that, every sextuple of distinct points whose Pascals are not all distinct must come from[1] either Figure 2 or Figure 3. One can construct Figure 2 starting from an arbitrary choice of Q together with three lines through it, hence $\dim \mathcal{Y} = 5$. Figure 3 is completely determined by the choice of A, B, C, D, hence $\dim \mathcal{R} = 4$.

The proof of the main theorem uses a case-by-case analysis on pairs of Pascals. There are altogether nine cases; each is disposed off by elimination-theoretic computations using Gröbner bases. All such computations were carried out twice, first in MAPLE and then once more in MACAULAY-2 for confirmation.

1.5. The next two sections are devoted to preliminaries. In section 2, we recall the classical labelling schema for Pascals. It is a beautiful combinatorial phenomenon which implicitly involves the unique outer automorphism of the symmetric group on six objects.

The group of automorphisms of $\mathbb{P}^2$ which preserve $\mathcal{K}$ (as a set) is isomorphic to $\mathrm{PSL}(2, \mathbb{C})$. This group acts on all of the varieties mentioned above, and hence it is convenient to use the language of binary forms and SL_2-representations throughout (see section 3). I have included rather more explanation than what would have sufficed for this paper alone, since I should like to refer to it in possible sequels.

The literature on Pascal's theorem is very large. The standard classical reference is by George Salmon (see [19, Notes]). The labelling schema, together with a host of results discovered by Cremona and Richmond are explained by H. F. Baker in his note 'On the *Hexagrammum Mysticum* of Pascal' in [4, Note II, pp. 219–236]. One of the best recent surveys is by Conway and Ryba [6]. We refer the reader to [14, 17] for foundational notions in projective geometry, and to [11] for those in algebraic geometry.

2. The Labelling Schema for Pascals

Start with the following sets

$$\textsc{six} = \{1, 2, 3, 4, 5, 6\}, \quad \text{and} \quad \textsc{ltr} = \{\mathbb{A}, \mathbb{B}, \mathbb{C}, \mathbb{D}, \mathbb{E}, \mathbb{F}\}.$$

(The elements of LTR will eventually stand for points on the conic, but at the moment they are pure letters.) A number duad is a 2-element subset of SIX, e.g., $\{3, 5\}$. A number syntheme is a partition of SIX into three number duads, e.g., $\{\{1, 3\}, \{2, 6\}, \{4, 5\}\}$. We will flatten out the duads and synthemes for readability, i.e., write them as 35 and $13.26.45$ etc. There are similar notions of a letter duad and a letter syntheme answering to the set LTR. For instance, $\mathbb{AE}$ is a letter duad, and $\mathbb{AC}.\mathbb{DE}.\mathbb{BF}$ is a letter syntheme.

[1] These diagrams may specialise further. For instance, the sextuples in section 4.5 admit three distinct centers of involution, leading to several sets of coincident Pascals. Moreover, there are sextuples (see section 4.9) which fit into both diagrams.

Consider the sets ND, NS, LD, LS of number duads, number synthemes, letter duads, and letter synthemes respectively. Each of these four sets has cardinality 15. Now consider the following artfully constructed diagonally symmetric table:

	$\mathbb{A}$	$\mathbb{B}$	$\mathbb{C}$	$\mathbb{D}$	$\mathbb{E}$	$\mathbb{F}$
$\mathbb{A}$		$14.25.36$	$16.24.35$	$13.26.45$	$12.34.56$	$15.23.46$
$\mathbb{B}$	$14.25.36$		$15.26.34$	$12.35.46$	$16.23.45$	$13.24.56$
$\mathbb{C}$	$16.24.35$	$15.26.34$		$14.23.56$	$13.25.46$	$12.36.45$
$\mathbb{D}$	$13.26.45$	$12.35.46$	$14.23.56$		$15.24.36$	$16.25.34$
$\mathbb{E}$	$12.34.56$	$16.23.45$	$13.25.46$	$15.24.36$		$14.26.35$
$\mathbb{F}$	$15.23.46$	$13.24.56$	$12.36.45$	$16.25.34$	$14.26.35$	

A direct verification shows that it defines a bijection $LD \longrightarrow NS$; where for instance, $\mathbb{BC}$ is mapped to $15.26.34$.

2.1. This table can be used to create a label for each Pascal. For instance, consider the array $\begin{bmatrix} A & E & F \\ C & B & D \end{bmatrix}$. Picture it as

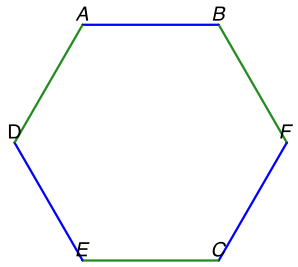

so that each cross-hair intersection is between a blue and a green line forming opposite sides of the hexagon. Use the table above to find the number synthemes corresponding to the blue lines:

$$\mathbb{AB} \rightsquigarrow 14.25.36, \quad \mathbb{FC} \rightsquigarrow 12.36.45, \quad \mathbb{ED} \rightsquigarrow 15.24.36,$$

all of which have the duad 36 in common. Similarly, those corresponding to the green lines

$$\mathbb{AD} \rightsquigarrow 13.26.45, \quad \mathbb{EC} \rightsquigarrow 13.25.46, \quad \mathbb{FB} \rightsquigarrow 13.24.56,$$

have the duad 13 in common. These two duads share the 3, which alternately combines with 1 and 6. Hence the corresponding Pascal $\left\{ \begin{matrix} A & E & F \\ C & B & D \end{matrix} \right\}$ is given the label $k(3, 16)$ or $k(3, 61)$. In summary, starting from an array of points, use the table to extract two duads in the pattern ab, ac; and then the corresponding Pascal is labelled $k(a, bc)$ or $k(a, cb)$. Since $a \in \text{SIX}$, and $\{b, c\} \subseteq \text{SIX} \setminus \{a\}$, there are altogether $6 \times \binom{5}{2} = 60$ labels, as they should be.

The reader may wish to check that the Pascals in (1) are respectively

$$k(1,23), \quad k(4,23), \quad k(5,23), \quad k(6,23).$$

Those in (2) are respectively $k(1,23)$ and $k(1,45)$.

2.2. In the reverse direction, say we are given the label $k(2,35)$. In order to construct the corresponding array, start with the duads $23, 25$. Look for 23 in the table; it appears in positions $\mathbb{AF}, \mathbb{BE}, \mathbb{CD}$. Similarly, 25 appears in $\mathbb{AB}, \mathbb{CE}, \mathbb{DF}$. This determines the hexagon:

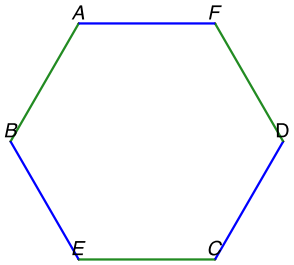

and hence the array[2] as $\begin{bmatrix} A & D & E \\ C & B & F \end{bmatrix}$. In other words, the same table defines a bijection $ND \longrightarrow LS$, which takes 23 to $\mathbb{AF}.\mathbb{BE}.\mathbb{CD}$ etc., and then one can recover the array from the images of the two duads.

2.3. Let $\mathfrak{S}(X)$ denote the symmetric group on the set X. Then the table defines an isomorphism $\mathfrak{S}(\text{LTR}) \longrightarrow \mathfrak{S}(\text{SIX})$. For instance, the image of the transposition $(\mathbb{A}\,\mathbb{B})$ is the product $(1\,4)\,(2\,5)\,(3\,6)$, and the map extends by writing an arbitrary element as a product of transpositions. If we identify LTR and SIX as $\mathbb{A} \rightsquigarrow 1, \mathbb{B} \rightsquigarrow 2, \ldots, \mathbb{F} \rightsquigarrow 6$, then this gives an outer automorphism ω of $\mathfrak{S}(\text{SIX})$, which is completely specified[3] by

$$(1\,2) \xrightarrow{\omega} (1\,4)\,(2\,5)\,(3\,6), \qquad (1\,2\,3\,4\,5\,6) \xrightarrow{\omega} (2\,3\,6)\,(4\,5).$$

(Note that it does not preserve the cycle structure, and hence cannot be inner.) A theorem of Hölder characterises the outer automorphism groups of all finite symmetric groups (see [18, Ch. 7]); it says that

$$\text{Out}(\mathfrak{S}(\{1,2,\ldots,d\})) \simeq \begin{cases} \mathbf{Z}_2 & \text{if } d = 6, \\ \{e\} & \text{otherwise.} \end{cases}$$

Thus, ω represents the unique nontrivial element in $\text{Out}(\mathfrak{S}(\text{SIX}))$. A different identification of LTR with SIX would amount to composing ω with an inner automorphism.

---

[2] It is of course understood that the hexagon is determined only up to rotation and reflection, and the array up to a permutation of rows and columns.

[3] We follow the convention that the cycle $(1\,2\,\ldots\,6)$ takes 1 to 2 etc.

The table above (along with its heavily Greek terminology of duads and synthemes) was in essence constructed by Sylvester (see [21]); however, I did not find his papers easy to follow. What is usually called the *Hexagrammum Mysticum* is a much richer configuration than merely the Pascal lines, and includes the Kirkman points and Cayley-Salmon lines etc. They can all be labelled using the same formalism, and their incidence relations can be read off from the labelling – see the reference to Baker above. Conway and Ryba [6] use an ostensibly different, but fundamentally similar labelling scheme. Other geometric perspectives on the outer automorphism may be found in [13].

3. Binary Forms and Involutions

In this section we will recast the necessary geometric notions in the language of binary forms and SL_2-representations. A similar set-up is used in [5], where rather more detailed explanations are given.

3.1. For a nonnegative integer m, let S_m denote the $(m+1)$-dimensional vector space of homogeneous forms of order m in the variables $\mathbf{x} = \{x_1, x_2\}$. It is an irreducible representation of the group SL_2 of unimodular 2×2 matrices acting linearly on $\mathbf{x}$. Given integers $m, n \geq 0$ and $0 \leq r \leq \min(m, n)$, we have the transvectant morphism

$$S_m \otimes S_n \longrightarrow S_{m+n-2r}, \quad U \otimes V \longrightarrow (U, V)_r;$$

given by the explicit formula

$$(U, V)_r = \frac{(m-r)!\,(n-r)!}{m!\,n!} \sum_{i=0}^{r} (-1)^i \binom{r}{i} \frac{\partial^r U}{\partial x_1^{r-i}\,\partial x_2^i} \frac{\partial^r V}{\partial x_1^i\,\partial x_2^{r-i}}\,. \qquad (3)$$

There is a symbolic calculus for transvectants, which is thoroughly explained in [10, Ch. 1]. The basic theory of SL_2-representations may be found in [9, Ch. 11].

3.2. Throughout, we will work inside the projective plane $\mathbb{P}S_2 \simeq \mathbb{P}^2$; thus a nonzero quadratic form $Q \in S_2$ represents a point $[Q] \in \mathbb{P}^2$. Its polar line is defined to be

$$\ell_Q = \{[R] \in \mathbb{P}S_2 : (R, Q)_2 = 0\}.$$

Every line in $\mathbb{P}^2$ is the polar of a unique point, called its pole. There is a canonical isomorphism of $\mathbb{P}S_2$ with the dual plane $(\mathbb{P}S_2)^*$, which maps $[Q]$ to ℓ_Q.

Given $Q, R \in S_2$, we have $(R, Q)_2 = (Q, R)_2$. Hence $[R] \in \ell_Q$ iff $[Q] \in \ell_R$. The line of intersection of $[Q]$ and $[R]$ is given by the polar of $[(Q, R)_1]$, and the point of intersection of ℓ_Q and ℓ_R is $[(Q, R)_1]$.

3.3. Consider the Veronese imbedding

$$\mathbb{P}S_1 \xrightarrow{\phi} \mathbb{P}S_2, \qquad [u] \longrightarrow [u^2]. \qquad (4)$$

The image of ϕ is a smooth conic $\mathcal{K}$. If $Q = a_0\,x_1^2 + a_1\,x_1\,x_2 + a_2\,x_2^2$, then

$$(Q, Q)_2 = -\frac{1}{2}\,(a_1^2 - 4\,a_0\,a_2).$$

Hence,

$$[Q] \in \mathcal{K} \iff Q \text{ is the square of a linear form } \iff (Q,Q)_2 = 0 \iff [Q] \in \ell_Q.$$

If $Q \in S_2$ factors as $u_1\, u_2$, then the points of intersection of ℓ_Q with $\mathcal{K}$ are $\phi(u_1), \phi(u_2)$. Dually, the tangent to the conic at either $\phi(u_i)$ passes through $[Q]$.

3.4. A sextuple of unordered points $\Gamma = \{\phi(u_1), \ldots, \phi(u_6)\}$ on $\mathcal{K}$ will correspond to the binary sextic form $G_\Gamma = \prod_{i=1}^{6} u_i$, distinguished up to a scalar. Alternately, a nonzero form G in S_6 will give a sextuple Γ_G on $\mathcal{K}$. This gives an isomorphism of $\mathbb{P}S_6$ with $\mathrm{Sym}^6(\mathcal{K})$, where the discriminant hypersurface $\Delta \subset \mathbb{P}S_6$ corresponds to sextuples with repeated points. It will be occasionally convenient to use affine co-ordinates on $\mathcal{K}$, by identifying $\phi(x_1 - \alpha\, x_2)$ with α, and $\phi(x_2)$ with ∞.

Since all incidences and intersections in $\mathbb{P}^2$ can be expressed as transvectants, Pascal's theorem itself can be seen as a transvectant identity (see [15, Theorem 2]). Now define a ***hexad*** to be an injective map $\textsc{ltr} \xrightarrow{h} \mathcal{K}$. We will write $h(\mathbb{A}) = A, \ldots, h(\mathbb{F}) = F$, for the corresponding *distinct* points on $\mathcal{K}$. If HEX denotes the set of all hexads and $\mathcal{L}_k$ the set of all labels, then we have a morphism

$$\mathsf{HEX} \longrightarrow \prod_{\mathcal{L}_k} (\mathbb{P}^2)^*,$$

which maps the hexad to its Pascals. The groups $\mathfrak{S}(\textsc{ltr}), \mathfrak{S}(\textsc{six})$ respectively act on HEX and the direct product compatibly via the isomorphism in section 2.3. Passing to quotients by these actions, we get a morphism

$$\mathbb{P}^6 \setminus \Delta \longrightarrow \mathrm{Sym}^{60}\, (\mathbb{P}^2)^*,$$

which maps a sextuple to the set of its Pascals. For what it is worth, I have calculated all the Pascals for the sextuple $\Gamma = \{0, 1, \infty, 3, -5, 7\}$ using MAPLE, and verified that they are in fact distinct. Hence, they must remain so for a general Γ.

3.5. *The quadratic involution.* Fix a point[4] $Q \in \mathbb{P}S_2$ away from $\mathcal{K}$. It defines an order 2 automorphism (i.e., an involution) σ_Q of $\mathcal{K}$ as follows: if $\mathsf{z} \in \mathcal{K}$, then $\sigma_Q(\mathsf{z})$ is the other point of intersection of $\mathcal{K}$ with the line $Q\mathsf{z}$. Now $\sigma_Q^2(\mathsf{z}) = \mathsf{z}$, and $\sigma_Q(\mathsf{z}) = \mathsf{z}$ exactly when $Q\mathsf{z}$ is tangent to $\mathcal{K}$. If $u \in S_1$ is such that $\phi(u) = \mathsf{z}$, then $\sigma_Q(\mathsf{z})$ corresponds to the linear form $(Q,u)_1$. All of this is pursued further in [1].

Now σ_Q extends to an involution of $\mathbb{P}^2$ by the following recipe: given $R \in \mathbb{P}^2$, let $\mathsf{z}_1, \mathsf{z}_2$ be the (possibly coincident) points where the polar of R intersects $\mathcal{K}$. Then define $\sigma_Q(R)$ to be the pole of the line joining $\sigma_Q(\mathsf{z}_1)$ and $\sigma_Q(\mathsf{z}_2)$. In terms of transvectants,

$$\sigma_Q(R) = (Q,Q)_2\, R - 2\, (Q,R)_2\, Q.$$

Since $\sigma_Q(R)$ is a linear combination of Q and R, the points $Q, R, \sigma_Q(R)$ are collinear. The set of fixed points of σ_Q is Q itself, together with the polar line of Q. Thus, σ_Q is a homology in the sense of [14, Ch. 11].

[4]Henceforth we write Q for $[Q]$ etc. when no confusion is likely.

3.6. Now assume that we have a hexad $\{A, \dots, F\}$ such that

$$\sigma_Q(A) = F, \quad \sigma_Q(B) = E, \quad \sigma_Q(C) = D,$$

as in Diagram 2. Consider the Pascal $\left\{ \begin{array}{ccc} A & B & C \\ F & E & D \end{array} \right\}$. Since σ_Q interchanges the lines AE and BF, it must leave their intersection point invariant. Similarly, σ_Q leaves each of the cross-hair intersections invariant, and hence they must all lie on the polar of Q. It makes no difference to the argument if we select any one column in the array and interchange its entries. We have proved the following proposition.

Proposition 1. *With notation as above, each of the Pascals*

$$\left\{ \begin{array}{ccc} A & B & C \\ F & E & D \end{array} \right\}, \quad \left\{ \begin{array}{ccc} A & B & D \\ F & E & C \end{array} \right\}, \quad \left\{ \begin{array}{ccc} F & B & C \\ A & E & D \end{array} \right\}, \quad \left\{ \begin{array}{ccc} A & E & C \\ F & B & D \end{array} \right\}$$

is equal to the polar line of Q.

As mentioned earlier, these Pascals carry labels $k(r, 23)$ for $r \in \{1, 4, 5, 6\}$. By renaming the points, one would in general obtain four lines in the pattern

$$k(r, ab), \quad r \in \text{SIX} \setminus \{a, b\}.$$

3.7. The proposition becomes easier to visualise if we specialise the diagram as follows. Choose $\mathcal{K}$ to be a circle in the Cartesian plane centered at the origin, and let Q be the point at infinity on the Y-axis. Then σ_Q is simply the reflection in the X-axis, and the three vertical lines AF, BE, CD all pass through Q.

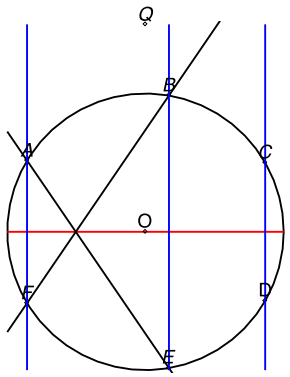

Now each cross-hair intersection such as $AE \cap BF$ will be on the X-axis, which is therefore the common Pascal of the proposition.

3.8. *The involutive hypersurface.* A sextuple of points $\Gamma = \{\mathsf{z}_1, \dots, \mathsf{z}_6\}$ is said to be in involution if it is left invariant by σ_Q for some $Q \in \mathbb{P}^2$, and then Q is said to be its center of involution. (In other words, the sextuple should fit into Diagram 2 for some Q.) Consider the variety

$$\mathcal{Y} = \{[G] \in \mathbb{P}^6 \setminus \Delta : \Gamma_G \text{ is in involution}\}.$$

Change variables so that $Q = x_1\,x_2$. If $\mathsf{z} \in \mathcal{K}$ corresponds to $u = x_1 + \alpha\,x_2$, then $\sigma_Q(\mathsf{z})$ corresponds to[5] $(Q,u)_1 = \square\,(x_1 - \alpha\,x_2)$, and then $u\,(Q,u)_1$ is a quadratic with no $x_1\,x_2$ term. Thus Γ_G is in involution with respect to Q, if and only if G can be written as a form in x_1^2, x_2^2. In other words, $\mathcal{Y}$ is the variety of sextic forms which can be written as

$$c_1\,u_1^6 + c_2\,u_1^4\,u_2^2 + c_3\,u_1^2\,u_2^4 + c_4\,u_2^6, \qquad (c_i \in \mathbb{C}), \tag{5}$$

for some linear forms u_1, u_2 (cf. [20, §260]).

3.9. *The covariants of a binary sextic.* The complete minimal system of covariants of a generic binary sextic is given in [10, p. 156]. We will not reproduce it here; but only note down a few of its members which are relevant to the subject at hand.

Let G denote a generic sextic, and write $\vartheta_{m,q}$ for a covariant of degree-order (m,q). This means that, when written out in full,

$$\vartheta_{m,q} = \sum_{i=0}^{q} \theta_i\,x_1^{q-i}\,x_2^i,$$

where θ_i are homogeneous forms of degree m in the coefficients of G. If $q = 0$, then $\vartheta_{m,0}$ is called an invariant of degree m. Now define

$$\vartheta_{2,4} = (G,G)_4, \quad \vartheta_{3,2} = (G,\vartheta_{2,4})_4, \quad \vartheta_{8,2} = (\vartheta_{2,4},\vartheta_{3,2}^2)_3, \quad \vartheta_{15,0} = ((G,\vartheta_{2,4})_1,\vartheta_{3,2}^4)_8. \tag{6}$$

It is known that $\mathcal{Y}$ is a hypersurface defined by the vanishing of $\vartheta_{15,0}$ (see [1, §4.10]). Moreover, $\vartheta_{8,2}$ evaluated on the form (5) gives $\square\,u_1\,u_2$, which is Q. Thus, if G is in involution, then $\vartheta_{8,2}$ can be used to 'detect' its center if it is unique. (However, if G is arbitrary, then $\vartheta_{8,2}$ has no geometric meaning that I know of.) As we will see in section 4.5, it may happen that a sextuple in a highly special position has more than one center of involution, and then $\vartheta_{8,2}$ vanishes identically.

I have programmed the transvectant formula (3) in MAPLE, so that these covariants can be calculated on a specific G wherever necessary.

3.10. *The ricochet configuration.* Assume that the hexad $\{A,\ldots,F\} \subseteq \mathcal{K}$ is in ricochet configuration as shown in Figure 3.

Proposition 2. *Both the Pascals* $\left\{\begin{array}{ccc} A & B & C \\ F & E & D \end{array}\right\}, \left\{\begin{array}{ccc} A & E & C \\ D & B & F \end{array}\right\}$ *coincide with the line* VW.

Proof. This is a straightforward computation with transvectants. Choose co-ordinates such that

$$A = \phi(x_1), \quad C = \phi(x_2), \quad B = \phi(x_1 - x_2), \quad D = \phi(x_1 - d\,x_2).$$

Then $V = \square\,x_1\,x_2$, and F corresponds to $(V, x_1 - d\,x_2)_1 = \square\,(x_1 + d\,x_2)$. Hence

$$W = (x_1\,(x_1 + d\,x_2), x_2\,(x_1 - d\,x_2))_1 = \square\,(x_1^2 - 2\,d\,x_1\,x_2 - d^2\,x_2^2).$$

[5] Henceforth we will write $\square$ for a multiplicative scalar whose precise value is unimportant. For instance, $\square$ stands for $-\frac{1}{2}$ here.

Now Z is given by $(x_1\,x_2, x_1 - x_2)_1 = \square\,(x_1 + x_2)$, and finally E by

$$(W, x_1 + x_2)_1 = \square\,(x_1 + \frac{d^2 - d}{d+1}\,x_2).$$

One can similarly calculate all the cross-hair intersections and the lines joining them. It turns out that either Pascal is given by the quadratic form $P = x_1^2 + d^2\,x_2^2$; or in other words, it is the polar line of $[P]$. Since $(P, V)_2 = (P, W)_2 = 0$, it must pass through V and W. $\square$

Notice that P factors as $(x_1 + d\,x_2\,\sqrt{-1})\,(x_1 - d\,x_2\,\sqrt{-1})$, i.e., if $VW \cap \mathcal{K} = \{I, J\}$, then I, J have affine co-ordinates $\pm d\,\sqrt{-1}$. This implies that we have cross-ratios

$$\langle\, A, C, I, J \,\rangle = \langle\, D, F, I, J \,\rangle = -1,$$

i.e., I, J is a harmonically conjugate pair with respect to A, C as well as D, F. Moreover, since V, W are determined by A, C, D, the common Pascal is independent of the position of B. These observations suggest that a more conceptual and less computational proof of this proposition should be possible, but I do not see one.

3.11. Once again, the equality of Pascals is easier to see if the line VW is pushed off to infinity. Let $\mathcal{K}$ be the unit circle, with the following arrangement of points.

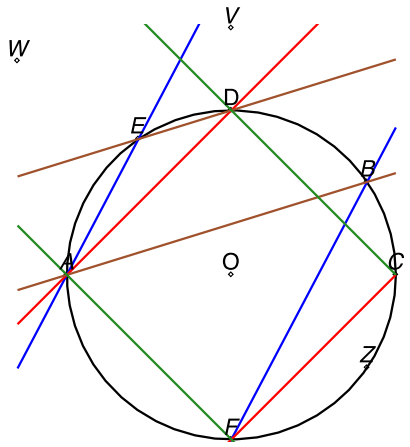

Here $ADCF$ is a square with vertices on the coordinate axes (not shown), and

$$B = (\cos\theta, \sin\theta), \quad Z = (\cos\theta, -\sin\theta), \quad E = (-\sin\theta, \cos\theta), \quad \text{for some } \theta.$$

All vertical lines, such as the tangents at A and C, have V as the common point at infinity. All lines with slope -1, such as AF and CD, have W as the common point at infinity.

Now the lines AE, BF are parallel, and so are AD, CF. Similarly, AB, DE are parallel, and so are AF, CD. It follows that $\left\{ \begin{matrix} A & B & C \\ F & E & D \end{matrix} \right\}$ and $\left\{ \begin{matrix} A & E & C \\ D & B & F \end{matrix} \right\}$ both coincide with the line at infinity. As before, E adjusts itself with the motion of B in such a way that the common Pascal is independent of the position of B.

4. The Main Theorem

In this section we will establish the following theorem.

Theorem 3. *Let Γ be a hexad, and assume that s, t are two labels such that $k(s) = k(t)$ for Γ. Then Γ is either in involution or in ricochet configuration.*

Proof. After applying an automorphism of $\mathcal{K}$, we may assume that the points of Γ are given in affine co-ordinates as

$$A = 0, \quad B = 1, \quad C = \infty, \quad D = p, \quad E = q, \quad F = r, \tag{7}$$

and hence

$$G_\Gamma = x_1\,(x_1 - x_2)\,x_2\,(x_1 - p\,x_2)\,(x_1 - q\,x_2)\,(x_1 - r\,x_2).$$

Now the proof simply goes through all possible s and t, but one can introduce a small technical device to reduce the number of cases.

4.1. Given a label $s = (a, bc)$, write $s' = \{a\}$, and $s'' = \{b, c\}$. For two labels s, t, define their interference matrix

$$I_{st} = \begin{bmatrix} s' \cdot t' & s' \cdot t'' \\ s'' \cdot t' & s'' \cdot t'' \end{bmatrix},$$

where $s' \cdot t''$ means the cardinality of the set $s' \cap t''$ and so on.

For instance, if $s = (1, 23), t = (2, 36)$, then

$$s' = \{1\}, \quad s'' = \{2, 3\}, \quad t' = \{2\}, \quad t'' = \{3, 6\}, \quad \text{and} \quad I_{st} = \begin{bmatrix} 0 & 0 \\ 1 & 1 \end{bmatrix}.$$

After applying a permutation of SIX, we may assume once and for all that $s = (1, 23)$. It corresponds to the array $\begin{bmatrix} A & B & C \\ F & E & D \end{bmatrix}$, and then a direct calculation as in section 3.10 shows that $k(1, 23)$ is given by the quadratic form

$$(q - r)\,x_1^2 + (p\,r - p\,q + p - q)\,x_1\,x_2 + r\,(q - p)\,x_2^2. \tag{8}$$

If t, u are two labels such that $I_{st} = I_{su}$, then one can find a permutation carrying t into u which preserves s, hence it suffices to consider any one example of t for any given interference matrix. The following are all the possibilities for I_{st}.

$$I^{(1)} = \begin{bmatrix} 1 & 0 \\ 0 & 0 \end{bmatrix}, \quad I^{(2)} = \begin{bmatrix} 1 & 0 \\ 0 & 1 \end{bmatrix}, \quad I^{(3)} = \begin{bmatrix} 0 & 0 \\ 1 & 0 \end{bmatrix},$$
$$I^{(4)} = \begin{bmatrix} 0 & 0 \\ 1 & 1 \end{bmatrix}, \quad I^{(5)} = \begin{bmatrix} 0 & 1 \\ 1 & 1 \end{bmatrix}, \quad I^{(6)} = \begin{bmatrix} 0 & 1 \\ 1 & 0 \end{bmatrix},$$
$$I^{(7)} = \begin{bmatrix} 0 & 0 \\ 0 & 0 \end{bmatrix}, \quad I^{(8)} = \begin{bmatrix} 0 & 0 \\ 0 & 1 \end{bmatrix}, \quad I^{(9)} = \begin{bmatrix} 0 & 0 \\ 0 & 2 \end{bmatrix}.$$

Since the whole question is symmetric in s and t, it is unnecessary to consider the transpose of $I^{(3)}$ or $I^{(4)}$.

4.2. Let $I_{st} = I^{(2)} = \begin{bmatrix} 1 & 0 \\ 0 & 1 \end{bmatrix}$. We may assume $t = (1, 24)$, corresponding to the array $\begin{bmatrix} A & D & F \\ C & E & B \end{bmatrix}$. A very similar calculation shows that $k(t)$ is given by

$$(p - r)\, x_1^2 + (r - p\, q)\, x_1\, x_2 + p\, r\, (q - 1)\, x_2^2. \tag{9}$$

If $k(s) = k(t)$, then (8) and (9) must be scalar multiples of each other, and hence the 2×3 matrix of their coefficients must have all of its minors zero. This gives a system of polynomial equations in p, q, r. One solves it by finding a Gröbner basis of the resulting ideal, after imposing an elimination order on the variables (see [2, Ch. 2] or [7, Ch. 3] for the technique). However, in this case, the only solutions are

$p = r = 0$,
$q = 1, r = 0$,
$q = p, r = 0$,
$p = q = 1$,
$q = 1, r = p$,
$p = q = r$.

None of these is legal, since each would force Γ to have a repeated point. We conclude that the two Pascals cannot coincide. Similarly, we get no legal solutions for $I^{(j)}, j = 3, 6, 7, 8$.

4.3. The remaining four cases are geometrically more interesting. They have the common feature that apart from illegal solutions as above (which will not be explicitly mentioned), there is a unique nontrivial solution in every case.

Say $I_{st} = I^{(4)} = \begin{bmatrix} 0 & 0 \\ 1 & 1 \end{bmatrix}$, then we may take $t = (2, 34)$ corresponding to the array $\begin{bmatrix} A & B & D \\ E & C & F \end{bmatrix}$. A similar calculation gives the solution

$$q = \frac{p}{p + 1}, \quad r = \frac{p}{1 - p^2},$$

with p arbitrary. (It is, of course, subject to the constraint that no two points of Γ should coincide, which excludes only finitely many values of p. Henceforth this proviso is tacitly understood whenever we have free parameters.) Substitute the solution into $G = G_\Gamma$ to get a binary sextic whose coefficients are functions of p. Now a rather long calculation using the formulae in (6) shows that $\vartheta_{15,0}(G) = 0$, hence Γ must be in involution. The center of the involution is found to be

$$\vartheta_{8,2}(G) = Q = \Box\, (x_1^2 - 2\, p\, x_1\, x_2 + \frac{p^2}{1 + p}\, x_2^2).$$

The lines AE, CD, BF pass through Q. Hence, by proposition 1, the Pascals

$$\left\{ \begin{matrix} A & B & C \\ E & F & D \end{matrix} \right\}, \quad \left\{ \begin{matrix} A & B & D \\ E & F & C \end{matrix} \right\}, \quad \left\{ \begin{matrix} A & F & C \\ E & B & D \end{matrix} \right\}, \quad \left\{ \begin{matrix} E & B & C \\ A & F & D \end{matrix} \right\} \tag{10}$$

all coincide with each other; or what is the same, $k(4,56) = k(1,56) = k(2,56) = k(3,56)$. Thus we have the curious situation that if $k(1,23), k(2,34)$ coincide, then four other Pascals are also forced to coincide.

Here is a more geometric way to see this configuration: fix Q, A, B, E, F, and allow the line CD to pivot around Q.

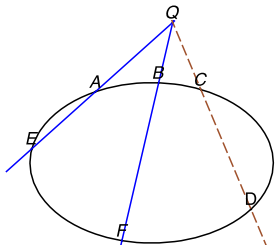

The Pascals in (10) coincide for any position of CD. Furthermore,

$$k(1,23) \rightsquigarrow \underbrace{\left\{ \begin{array}{ccc} A & B & C \\ F & E & D \end{array} \right\}}_{\lambda_1}, \qquad k(2,34) \rightsquigarrow \underbrace{\left\{ \begin{array}{ccc} A & B & D \\ E & C & F \end{array} \right\}}_{\lambda_2}$$

both pass through $Q = AE \cap BF = BF \cap CD$. Let Π_Q denote the pencil of lines through Q; then we have a two-to-one morphism

$$\mathcal{K} \xrightarrow{g_1} \Pi_Q, \qquad C \longrightarrow \lambda_1$$

which maps C to the line joining $BD \cap CE$ with Q. The similar morphism

$$\mathcal{K} \xrightarrow{g_2} \Pi_Q, \qquad C \longrightarrow \lambda_2$$

maps C to the line joining $AC \cap BE$ with Q. Since $\Pi_Q \simeq \mathbb{P}^1$ has a unique rational double cover up to isomorphism[6], there must be an automorphism τ of Π_Q such that $\tau \circ g_1 = g_2$. But then τ must have at least one fixed point (in fact generically two such points), that is to say, a line $\lambda \in \Pi_Q$ such that $\tau(\lambda) = \lambda$. Hence, fixed points of τ correspond to positions of C such that $\lambda_1 = \lambda_2$.

4.4. Assume that $I_{st} = I^{(9)} = \begin{bmatrix} 0 & 0 \\ 0 & 2 \end{bmatrix}$, then we may take $t = (4, 23)$. Using the procedure above, one gets the two parameter solution

$$q = \frac{p\,(r-1)}{p-1},$$

with p, r arbitrary. Then one finds that $\vartheta_{15,0}(G) = 0$, and $\vartheta_{8,2}(G) = Q = x_1^2 - 2\,p\,x_1\,x_2 + p\,r\,x_2^2$. A calculation shows that AF, BE, CD intersect in Q, and we are simply in the generic involutive configuration of section 3.6.

[6]This may be seen as follows: such a cover is completely determined by its two simple branch points, and any two points on $\mathbb{P}^1$ can be taken to any other by the Fundamental Theorem of Projective Geometry.

4.5. Assume that $I_{st} = I^{(5)} = \begin{bmatrix} 0 & 1 \\ 1 & 1 \end{bmatrix}$, then we may take $t = (2, 13)$. The same procedure gives the one-parameter solution

$$q = \frac{p-1}{p}, \quad r = \frac{1}{1-p}.$$

Now $\vartheta_{15,0}(G) = 0$, hence Γ must be in involution. However, $\vartheta_{8,2}(G)$ also vanishes identically, hence one should look for multiple centers. On the other hand, substituting the solution into (8) shows that $k(1, 23)$ is given by

$$T = \frac{p^2 - p + 1}{p\,(p-1)}\,(x_1^2 - x_1\,x_2 + x_2^2) = \Box\,(x_1 + \theta\,x_2)\,(x_1 + \theta^2\,x_2), \qquad \theta = e^{\frac{2\pi\sqrt{-1}}{3}}$$

which is independent of p. The factors of T are suggestive of a connection with 'equi-anharmonicity', i.e., the phenomenon where the cross-ratio of four points on a line admits a threefold symmetry (see [22, Ch. II.8]). Indeed, it turns out that the cyclic group $\mathbf{Z}_3$ acts on the entire structure in such a way that, four distinct groups of Pascals coincide amongst themselves.

Consider the linear transformation ζ of S_1 which acts by

$$x_1 \longrightarrow x_1 - x_2, \quad x_2 \longrightarrow x_1.$$

It induces an action on $\mathbb{P}S_2$ and $\mathcal{K}$, either of which will also be denoted by ζ. Notice that ζ^3 is the scalar multiplication by -1, and hence acts as the identity on $\mathbb{P}S_2$. It is easy to check that the action of ζ on $\mathcal{K}$ stabilizes the set $\Gamma = \{A, \ldots, F\}$, and acts as the permutation $(A\,B\,C)\,(D\,F\,E)$. (That is to say, ζ takes A to B, and D to F etc.) Define points

$$M = \phi(x_1 + \theta\,x_2), \quad N = \phi(x_1 + \theta^2\,x_2),$$

on $\mathcal{K}$, then $\zeta(M) = M, \zeta(N) = N$, and hence the line MN (which is the polar of T) is fixed (as a set) by ζ. Note the cross-ratios

$$\begin{aligned} \langle\, C, A, B, M \,\rangle &= \langle\, \infty, 0, 1, -\theta \,\rangle = -\theta, \\ \langle\, C, A, B, N \,\rangle &= \langle\, \infty, 0, 1, -\theta^2 \rangle = -\theta^2; \end{aligned}$$

which agrees with the fact that $\langle C, A, B, M \,\rangle = \langle\, \zeta(C), \zeta(A), \zeta(B), \zeta(M) \,\rangle = \langle\, A, B, C, M \,\rangle$, and similarly for N. In classical terminology, $\{C, A, B, M\}$ and $\{C, A, B, N\}$ are equi-anharmonic tetrads.

Now let $\alpha = p - 1, \beta = 1, \gamma = -p$, and consider the three quadratic forms:

$$\begin{aligned} Q_6 &= \alpha\,x_1^2 + 2\,\beta\,x_1\,x_2 + \gamma\,x_2^2, \\ Q_4 &= \beta\,x_1^2 + 2\,\gamma\,x_1\,x_2 + \alpha\,x_2^2, \\ Q_5 &= \gamma\,x_1^2 + 2\,\alpha\,x_1\,x_2 + \beta\,x_2^2. \end{aligned}$$

(Notice the cyclic movement of α, β, γ.) Then $(Q_6, T)_2 = (Q_4, T)_2 = (Q_5, T)_2 = 0$, and hence all $[Q_i]$ are on the line MN. The action of ζ on $\mathbb{P}^2$ is such that $[Q_6] \to [Q_4] \to [Q_5] \to [Q_6]$. A simple check shows that the lines AD, BE, CF intersect in Q_6; furthermore AE, CD, BF intersect in Q_4, and AF, CE, BD in

Q_5. Thus Γ is a highly special configuration which is in involution with respect to three different centers – see the diagram below.

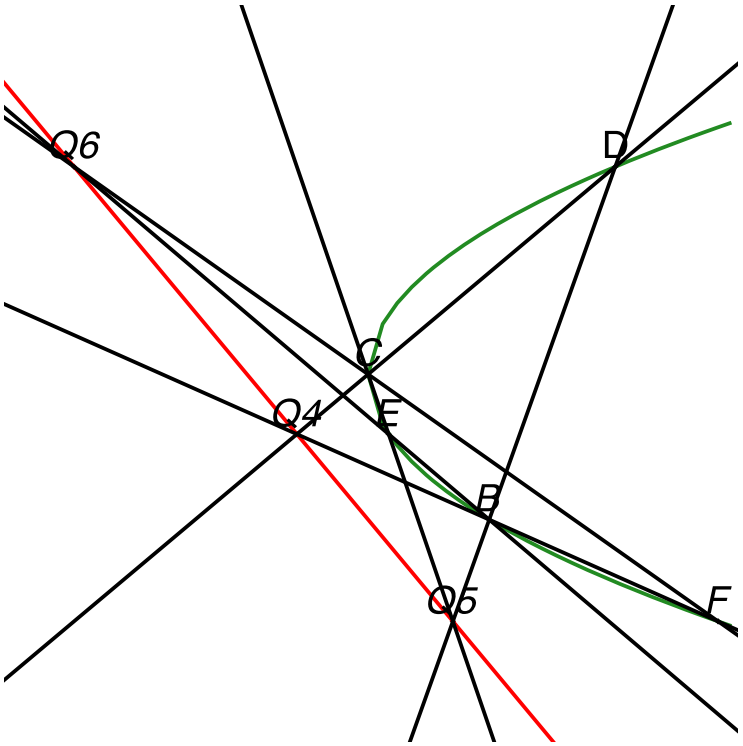

The point A (not shown) is to the far right at infinity. The points M and N, not being real, cannot be shown.

By proposition 1, we have the following sets of coincidences:

$$\begin{aligned} k(1,45) &= k(2,45) = k(3,45) = k(6,45), \\ k(1,56) &= k(2,56) = k(3,56) = k(4,56), \\ k(1,46) &= k(2,46) = k(3,46) = k(5,46). \end{aligned} \tag{11}$$

Or, what comes to the same thing, the map $\mathfrak{S}(\textsc{ltr}) \longrightarrow \mathfrak{S}(\textsc{six})$ sends $(\mathbb{A}\,\mathbb{B}\,\mathbb{C})\,(\mathbb{D}\,\mathbb{F}\,\mathbb{E})$ to $(4\,5\,6)$; the latter induces a cyclic action on the three groups of Pascals in (11), and also explains the subscripts in Q_i.

We are yet to explain the identity $k(1,23) = k(2,13)$. Notice that $k(1,23) \rightsquigarrow \left\{ \begin{array}{ccc} A & B & C \\ F & E & D \end{array} \right\}$ must pass through $AD \cap CF = Q_6$. Applying ζ to the points,

$$\left\{ \begin{array}{ccc} A & B & C \\ F & E & D \end{array} \right\} \xrightarrow{\zeta} \left\{ \begin{array}{ccc} B & C & A \\ E & D & F \end{array} \right\} = \left\{ \begin{array}{ccc} A & B & C \\ F & E & D \end{array} \right\},$$

that is to say, $k(1,23)$ is left invariant by ζ. However, it must pass through $\zeta(Q_6) = Q_4$, and hence must be the line $Q_6Q_4 = MN$. By the same argument, either of

the Pascals

$$k(2,13) \rightsquigarrow \left\{ \begin{array}{ccc} A & B & C \\ D & F & E \end{array} \right\}, \qquad k(3,12) \rightsquigarrow \left\{ \begin{array}{ccc} A & B & C \\ E & D & F \end{array} \right\}$$

is also equal to MN, and thus $k(1,23) = k(2,13) = k(3,12)$.

One suspects that this triply symmetric case is somehow related to the one described by Edge in [8, §3], but the explanation there is phrased in such a way that a clear connection is difficult to see.

4.6. The diagram simplifies considerably if we take $\mathcal{K}$ to be a circle, with $AEBDCF$ a regular hexagon inscribed in $\mathcal{K}$. Then all line-triples of the same color are parallel; that is to say, each Q_i is on the line at infinity.

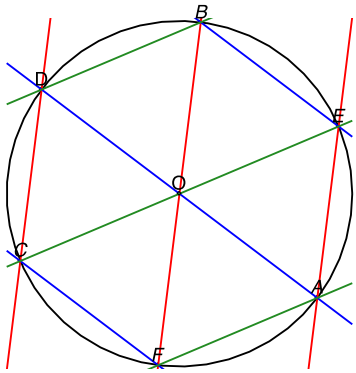

However, this diagram has an extra degree of symmetry (namely O as an additional center of involution) which is absent in the general case. This leads to additional coincidences:

$k(2,13) = k(4,13) = k(5,13) = k(6,13) =$ the polar of $O =$ the line at infinity.

4.7. There remains the case $I_{st} = I^{(1)} = \left[\begin{array}{cc} 1 & 0 \\ 0 & 0 \end{array} \right]$. Assuming $t = (1,45)$, we get the solution

$$q = p\,(1-p)/(1+p), \quad r = -p, \tag{12}$$

with p arbitrary.

It turns out that $\vartheta_{15,0}(G)$ does not vanish as a function of p, hence Γ is not in involution for generic p. (However, see section 4.9 below.) But notice that if we substitute this analytic solution into (7), everything agrees exactly with the proof of Proposition 2, with p in place of d. This shows that Γ is in ricochet configuration, and the proof of Theorem 3 is now complete. □

As mentioned earlier, I used (12) as a starting point, and only afterwards reached the construction in section 1.4. Several false steps were necessary before it was found.

It would be interesting to have an essentially synthetic proof of the main theorem, i.e., one which uses as much classical projective geometry and as little explicit calculation as possible.

4.8. Given an interference pattern I, one may consider the variety

$$\Omega_I = \{[G] \in \mathbb{P}S_6 \setminus \Delta : \text{The sextuple } \Gamma_G \text{ has coincident Pascals in pattern } I\}.$$

These are SL_2-equivariant subvarieties of $\mathbb{P}^6 \setminus \Delta$, and it would be of interest to find their degrees, desingularisations, and defining equations. As we have seen, $\Omega_{I^{(j)}}$ is empty for $j = 2, 3, 6, 7, 8$, and $\Omega_{I^{(9)}} = \mathcal{Y}$. In any of the remaining cases we get a one-parameter solution in p, and since the SL_2-orbit of Γ for a specific p is three-dimensional (see [3]), the variety Ω_I itself must be four-dimensional. It is contained in $\mathcal{Y}$ for $j = 4, 5$, but not for $j = 1$.

I tried to calculate the ideal of the 'ricochet locus' $\mathcal{R} = \Omega_{I^{(1)}}$ inside the coordinate ring of $\mathbb{P}^6$ using elimination of variables (rather as in [1, §4.8]), but could not get the computation to terminate. This is unfortunately a chronic difficulty with practical elimination theory.

4.9. The value of the invariant $\vartheta_{15,0}$ on the 'ricochet' form is:

$$p^{18}\,(p^2{+}3)\,(3\,p^2{+}1)\,(p^2{+}1)\,(p^2{+}p{+}1)\,(p^2{-}p{+}1)\,(p^2{+}2\,p{-}1)^2\,(p^2{-}2\,p{-}1)^2(p{-}1)^3(p{+}1)^3.$$

It vanishes for finitely many p, hence the intersection $\mathcal{R} \cap \mathcal{Y}$ is a finite union of SL_2-orbits. If p is such that this expression vanishes, then the sextuple will be simultaneously in involution and ricochet configuration. In general, this will lead to several sets of coincident Pascals. For instance, if $p = \sqrt{-3}$, then a direct calculation shows that

$$\begin{aligned} &k(1,23) = k(1,45),\\ &k(5,14) = k(5,23),\\ &k(2,15) = k(3,15) = k(4,15) = k(6,15). \end{aligned}$$

It follows that this sextuple is in ricochet configuration in two distinct ways.

It would be of interest to have a complete classification of all sextuples which lead to less than 60 Pascals, together with an explicit enumeration of all coincidences in every case. But such a list is likely to be rather lengthy.

5. Pascals on the Discriminant Locus

Hitherto we have assumed that Γ consists of six distinct points, but all the Pascals are well-defined if any one pair of points is allowed to come together.

5.1. In order to see this, assume that $A = B$, and C, D, E, F are distinct from each other and from A. We will interpret AB as the tangent to $\mathcal{K}$ at A. Given an array of points, one may assume that A occupies the top left corner, and then it is only necessary to consider the following three positions of B.

$$\underbrace{\begin{bmatrix} A & B & D \\ F & E & C \end{bmatrix}}_{I}, \quad \underbrace{\begin{bmatrix} A & C & D \\ B & F & E \end{bmatrix}}_{II}, \quad \underbrace{\begin{bmatrix} A & C & D \\ F & B & E \end{bmatrix}}_{III}. \tag{13}$$

In case I, $AE \cap BF = A$ and the other two cross-hair intersections are on the line AC, hence the Pascal is AC.

In case II, $AF \cap BC$, $AE \cap BD$ both equal A, hence the Pascal is the line joining A to $CE \cap DF$.

In order to see that the Pascal is well-defined in case III, it is enough to show that the points $P = AB \cap CF$, $P' = AE \cap DF$ cannot coincide. If they did, AP would be tangent to the conic at A and would contain E, which is impossible.

5.2. However, if Γ has either a threefold point or two double points, then some of the Pascals become undefined. If $A = B = C$, then $\left\{ \begin{array}{ccc} A & B & C \\ F & E & D \end{array} \right\}$ is no longer defined, since all cross-hair intersections are at A. If $A = B$ and $C = D$, then $\left\{ \begin{array}{ccc} A & B & E \\ C & D & F \end{array} \right\}$ becomes undefined, since the line $AC = AD \cap BC$ will not in general contain the point $AF \cap CE$.

5.3. If $\Gamma \in \Delta$, then it is already clear that many of the Pascals must coincide; for instance, in case I above, the Pascal remains the same for all permutations of D, E, F. In this section we will describe all such coincidences.

The general picture is that the set of labels splits into three types I, II, III as in (13). Type I splits further into 4 classes with 6 elements each, type II into 3 classes with 4 elements each, and type III into 12 classes with 2 elements each. Altogether there are $4 + 3 + 12 = 19$ equivalence classes, such that all Pascals in each class are equal. For a general Γ in Δ, these 19 lines are distinct.

Type I: All Pascals of the form $\left\{ \begin{array}{ccc} A & B & \star \\ \star & \star & C \end{array} \right\}$ are equal, which gives a 6-element equivalence class. To determine their labels, note that we know two of the sides of the corresponding hexagon, namely AC, BC. From the table,

$$\mathbb{AC} \rightsquigarrow 16.24.35, \quad \mathbb{BC} \rightsquigarrow 15.26.34.$$

The label must come from two duads (i.e., one from each number syntheme) which have an element in common. The pair $16, 15$ leads to $k(1, 56)$, and similarly the other possibilities are

$$k(6, 12), \quad k(2, 46), \quad k(4, 23), \quad k(5, 13), \quad k(3, 45).$$

We get three similar equivalence classes by replacing C with D, E, F.

Type II: Consider all arrays of the form $\left[\begin{array}{ccc} A & \star & \star \\ B & \star & \star \end{array} \right]$, where the rightmost 2×2 block is one of

$$\left[\begin{array}{cc} C & D \\ F & E \end{array} \right], \quad \left[\begin{array}{cc} C & F \\ D & E \end{array} \right], \quad \left[\begin{array}{cc} D & E \\ C & F \end{array} \right], \quad \left[\begin{array}{cc} F & E \\ C & D \end{array} \right].$$

The Pascal is the line joining A to $CE \cap DF$ in all cases, hence we have a 4-element equivalence class. The labels are easily determined to be $k(4, 36)$, $k(1, 36)$, $k(3, 14)$, $k(6, 14)$. They are constructed on the following model: start with two number duads ab, cd having no element in common (here $14, 36$), and then combine them as

$$k(a, cd), \quad k(b, cd), \quad k(c, ab), \quad k(d, ab).$$

We get two more such classes from $CD \cap EF$ and $CF \cap DE$. Since $\mathbb{AB} \rightsquigarrow 14.25.36$, picking any two duads out of the three will give one of the three equivalence classes.

Type III: We have

$$\left\{ \begin{array}{ccc} A & C & D \\ F & B & E \end{array} \right\} = \left\{ \begin{array}{ccc} B & C & D \\ F & A & E \end{array} \right\},$$

or what is the same, $k(2,15) = k(5,24)$. The latter Pascal may be written as $\left\{ \begin{array}{ccc} A & F & E \\ C & B & D \end{array} \right\}$, hence in general we have a 2-element equivalence class consisting of

$$\left\{ \begin{array}{ccc} A & P_1 & Q_1 \\ P_2 & B & Q_2 \end{array} \right\} \quad \text{and} \quad \left\{ \begin{array}{ccc} A & P_2 & Q_2 \\ P_1 & B & Q_1 \end{array} \right\},$$

where $\{P_1, P_2, Q_1, Q_2\} = \{C, D, E, F\}$. There are $\frac{4!}{2} = 12$ such classes. Their labels are formed on the following pattern: from the image of $\mathbb{AB} \rightsquigarrow 14.25.36$, pick any of the three duads (say ab), pick another (say cd) and now form the 2-element class of $k(a, bc), k(b, ad)$. (Note that the construction is not symmetric in ab, cd, nor in c, d.)

5.4. In order to assert that there are no further coincidences for a general Γ in Δ, it is sufficient to check this on one example. After choosing,

$$A = B = 0, \quad C = \infty, \quad D = 1, \quad E = -2, \quad F = 3,$$

I have calculated all the Pascals, and verified that there are precisely 19 of them.

In conclusion, if $\mathbb{T}$ denotes the locus of sextic forms which have at least a triple root or two double roots, then we have a morphism $\mathbb{P}^6 \setminus \mathbb{T} \longrightarrow \mathrm{Sym}^{60}(\mathbb{P}^2)^*$ just as in section 1.3. By the main theorem, the preimage of the big diagonal is $\Delta \cup \mathcal{Y} \cup \mathcal{R}$. According to standard procedure, one can blow up $\mathbb{P}^6$ along $\mathbb{T}$ to extend the morphism (see [12, Ch. II.7]); but I will leave this analysis to a sequel.

ACKNOWLEDGEMENT: The author thanks the referee for a thorough reading of the manuscript, and several excellent suggestions.

References

[1] A. Abdesselam and J. Chipalkatti, Quadratic involutions on binary forms, *Mich. Math. J.*, 61 (2012) 279–296.
[2] W. Adams and P. Loustaunau, *An Introduction to Gröbner Bases*, Graduate Studies in Mathematics, vol. 3. American Mathematical Society, 1994.
[3] P. Aluffi and C. Faber, Linear orbits of d-tuples of points in $\mathbb{P}^1$, *J. Reine Angew. Math.*, 445 (1993) 205–220.
[4] H. F. Baker, *Principles of Geometry*, vol. II, Cambridge University Press, 1923.
[5] J. Chipalkatti, On Hermite's invariant for binary quintics, *J. Algebra*, 317 (2007) 324–353.
[6] J. H. Conway and A. Ryba, The Pascal mysticum demystified, *Math. Intelligencer*, 34 (2012) no. 3, 4–8.
[7] D. Cox, J. Little and D. O'Shea, *Ideals, Varieties and Algorithms*, Undergraduate Texts in Mathematics, 3rd edition. Springer, New York, 2007.
[8] W. L. Edge, A footnote on the mystic hexagram, *Math. Proc. Camb. Phil. Soc.*, 77 (1975) 29–42.

[9] W. Fulton and J. Harris, *Representation Theory, A First Course*, Graduate Texts in Mathematics, Springer, New York, 1991.
[10] J. H. Grace and A. Young, *The Algebra of Invariants*, reprinted by Chelsea Publishing Co., New York, 1962.
[11] J. Harris, *Algebraic Geometry, a First Course*, Graduate Texts in Mathematics, Springer, New York, 1992.
[12] R. Hartshorne, *Algebraic Geometry*, Graduate Texts in Mathematics, Springer, New York, 1992.
[13] B. Howard, J. Millson, A. Snowden, and R. Vakil, A description of the outer automorphism of S_6, and the invariants of six points in projective space, *J. Combin. Theory, Ser. A*, 115 (2008) 1296-1303.
[14] L. Kadison and M. T. Kromann, *Projective Geometry and Modern Algebra*, Birkhäuser, Boston, 1996.
[15] F. Leitenberger, Pascal's theorem and quantum deformation, *Letters in Math. Physics*, 51 (2000) 47–53.
[16] D. Pedoe, How many Pascal lines has a sixpoint? *The Mathematical Gazette*, 25 (1941) 110–111.
[17] D. Pedoe, *An Introduction to Projective Geometry*, Pergamon Press, 1963.
[18] J. Rotman, *The Theory of Groups: An Introduction*, Allyn and Bacon, Boston, 1965.
[19] G. Salmon, *A Treatise on Conic Sections*, reprint of the 6th ed. by Chelsea Publishing Co., New York, 2005.
[20] G. Salmon, *Lessons Introductory to Higher Algebra*, reprint of the 5th ed. by Chelsea Publishing Co., New York, 1965.
[21] J. J. Sylvester, Note on the ... six-valued function of six letters, in *Collected Mathematical Papers*, vol. II, pp. 264–271, (also see vol. I, p. 92), Cambridge University Press, 1904–1912.
[22] I. M. Yaglom, *Complex Numbers in Geometry*, (Translation from the Russian by E. J. F. Primrose), Academic Press, New York, 1968.

Jaydeep Chipalkatti: Department of Mathematics, University of Manitoba, Winnipeg, MB R3T 2N2 Canada

E-mail address: Jaydeep.Chipalkatti@umanitoba.ca

Forum Geometricorum
Volume 16 (2016) 23–24.

FORUM GEOM
ISSN 1534-1178

Two Pairs of Archimedean Circles Derived from a Square

Hiroshi Okumura

Abstract. We construct two pairs of Archimedean circles in the square built on the base and on the same side of an arbelos.

Consider an arbelos with two inner semicircles α, β with diameters AO, BO and radii a and b, respectively for a point O on the segment AB. The perpendicular to AB at O is called the axis. It is well known that the two Archimedean circles each tangent to the axis, the outer semicircle (with diameter AB), and to α, β respectively have a common radius $R_{\mathrm{A}} = \frac{ab}{a+b}$ (see [1] and Figure 1).

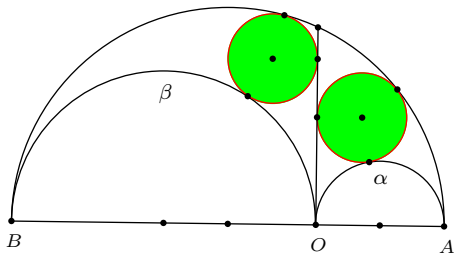

Figure 1

Construct a square $ABDC$ on the same side of AB as the arbelos. Let t_α be the tangent of the semicircle α parallel to AB with point of tangency T_α. Similarly the line t_β and the point T_β are defined. Let E be the intersection of the lines CO and t_β. Since the triangle formed by CO, CD and the axis and the triangle formed by CO, t_β and the axis are similar, the distance from E to the axis equals $\frac{2a}{2a+2b} \cdot b = \frac{ab}{a+b} = R_{\mathrm{A}}$. Hence the circle with center E touching the axis is Archimedean (see Figure 2).

Let F be the the point of intersection of CO and t_α. The distance between F and the axis equals $\frac{2a}{2a+2b} \cdot a = \frac{a^2}{a+b} = a - \frac{ab}{a+b} = a - R_{\mathrm{A}}$. Hence the circle with center F and passing through the point T_α is also Archimedean.

Similarly, there are two Archimedean circles with centers at the intersections of DO and the tangents t_α, t_β. Thus, we have constructed two pairs of Archimedean circles. The centers of these circles, and their orthogonal projections on AB form the vertices of two squares with side lengths a and b respectively.

Publication Date: March 6, 2016. Communicating Editor: Paul Yiu.

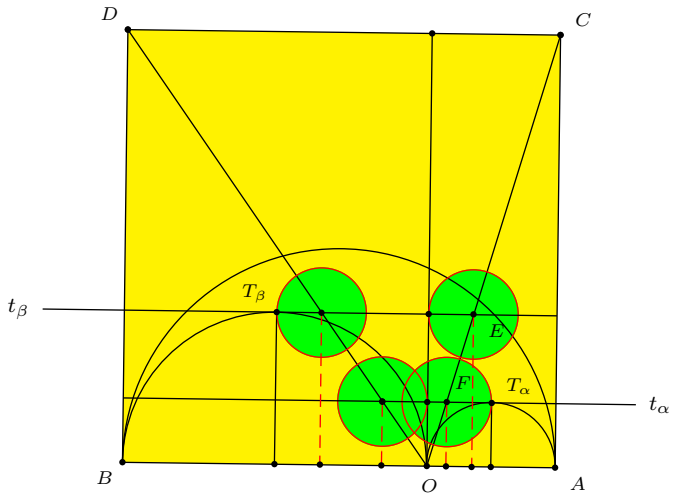

Figure 2

Reference

[1] C. W. Dodge, T. Schoch, P. Y. Woo and P. Yiu, Those ubiquitous Archimedean circles, *Math. Mag.*, 72 (1999) 202–213.

Hiroshi Okumura: Department of Mathematics, Yamato University, 2-5-1 Katayama Suita Osaka 564-0082, Japan

E-mail address: okumura.hiroshi@yamato-u.ac.jp

Forum Geometricorum
Volume 16 (2016) 25–27.

FORUM GEOM
ISSN 1534-1178

Integral Right Triangle and Rhombus Pairs with a Common Area and a Common Perimeter

Shane Chern

Abstract. We prove that there are infinitely many integral right triangle and θ-integral rhombus pairs with a common area and a common perimeter by the theory of elliptic curves.

1. Introduction

We say that a polygon is *integral* (resp. *rational*) if the lengths of its sides are all integers (resp. rational numbers). In a recent paper, Y. Zhang [5] proved that there are infinitely many integral right triangle and parallelogram pairs with a common area and a common perimeter. This type of problem originates from a question of B. Sands, which asked for examples of such right triangle and rectangle pair; see the paper of R. K. Guy [2]. Actually, R. K. Guy gave a negative answer to B. Sands' question, whereas in the same paper showed that there are infinitely many such isosceles triangle and rectangle pairs. Later in 2006, A. Bremner and R. K. Guy [1] replaced isosceles triangle by Heron triangle and proved that such pairs are also infinite.

In this note, we consider such right triangle and rhombus pairs with more restrictions. We say that an integral (resp. rational) rhombus is *θ-integral* (resp. *θ-rational*) if both $\sin\theta$ and $\cos\theta$ are rational numbers. Our result is

Theorem 1. *There are infinitely many integral right triangle and θ-integral rhombus pairs with a common area and a common perimeter.*

2. Proof of the theorem

We start from rational right triangles and θ-rational rhombi. Without loss of generality, we may assume that the rational right triangle has sides $(1-u^2, 2u, 1+u^2)$ with $0<u<1$, and the θ-rational rhombus has side p and intersection angle θ with $0<\theta\leq\pi/2$. Here u and p are both positive rational numbers. Now if the right triangle and rhombus have a common area and a common perimeter, then we have the following Diophantine system

$$\begin{cases} u(1-u^2)=p^2\sin\theta, \\ 1+u=2p. \end{cases} \tag{1}$$

Publication Date: March 6, 2016. Communicating Editor: Paul Yiu.

Since both $\sin\theta$ and $\cos\theta$ are rational numbers, we may set

$$\sin\theta = \frac{2v}{1+v^2},$$

where $0 < v \leq 1$ is a rational number. Note that the case $v = 1$, that is $\theta = \pi/2$, was studied by R. K. Guy in [2]. We thus only need to consider cases $0 < v < 1$. Eliminating p in (1), we have

$$2u^2v^2 - 2uv^2 + 2u^2 + uv - 2u + v = 0. \tag{2}$$

One readily notices that if (2) has infinitely many rational solutions (u, v) with $0 < u, v < 1$, then there exist infinitely many pairs of rational right triangle and θ-rational rhombus with a common area and a common perimeter, and thus infinitely many such (θ-)integral pairs by the homogeneity of these sides.

Now by the transformation

$$(x, y) = \left(-\frac{4uv^2 + 4u + 4v - 4}{v^2}, -\frac{8uv^2 - 4v^2 + 8u + 8v - 8}{v^3}\right),$$

and

$$(u, v) = \left(-\frac{x^3 + 4x^2 + 2xy - y^2 + 4x + 4y}{4x^2 + y^2 + 16x + 16}, \frac{2x + 4}{y}\right),$$

we deduce the following elliptic curve

$$E : y^2 - 3xy - 12y = x^3 + 6x^2 + 8x. \tag{3}$$

Through *Magma*, we compute that $E(\mathbb{Q})$ has rank 1 (generated by point $P = (0, 0)$) and a torsion point of order two $T = (-4, 0)$. Note that

$$[4]P = \left(\frac{5920}{4761}, \frac{5576768}{328509}\right)$$

leads to a solution

$$(u, v) = \left(\frac{552}{1105}, \frac{483}{1264}\right)$$

to (2) satisfying $0 < u, v < 1$. This solution immediately gives a right triangle with side lengths being 1832642, 2439840, and 3051458, and a rhombus with side length being 1830985 and smaller intersection angle being $\arcsin(1221024/1830985)$. They have a common area 2235676628640 and a common perimeter 7323940.

At last, recalling the following result due to H. Poincaré and A. Hurwitz ([4, p. 173]; see also [3, Satz 13]):

Lemma 2 (Poincaré-Hurwitz)**.** *Let E be a nonsingular cubic curve in $\mathbb{P}^2$ which is defined over $\mathbb{Q}$. If the set $E(\mathbb{Q})$ is infinite, then every open subset of $\mathbb{P}^2(\mathbb{R})$ which contains one point of $E(\mathbb{Q})$ must contain infinitely many points of $E(\mathbb{Q})$.*

Now since $[4]P$ gives a suitable solution to (2), from the map $(x, y) \mapsto (u, v)$ and Lemma 2, we conclude that (2) has infinitely many solutions (u, v) satisfying $0 < u, v < 1$. Thus, there are infinitely many pairs of integral right triangle and θ-integral rhombus with a common area and a common perimeter. This ends the proof of Theorem 1.

References

1. A. Bremner and R. K. Guy, Triangle-rectangle pairs with a common area and a common perimeter, *Int. J. Number Theory*, 2 (2006) 217–223.
2. R. K. Guy, My favorite elliptic curve: a tale of two types of triangles, *Amer. Math. Monthly*, 102 (1995) 771–781.
3. A. Hurwitz, Über ternäre diophantische Gleichungen dritten Grades, *Vierteljahrsschr. Naturf. Ges. Zürich*, 62 (1917) 207–229.
4. H. Poincaré, Sur les propriétés arithmétiques des courbes algébriques, *J. Math. Pures Appl. (5)*, 7 (1901) 161–233.
5. Y. Zhang, Right triangle and parallelogram pairs with a common area and a common perimeter, *J. Number Theory*, 164 (2016) 179–190.

Shane Chern: School of Mathematical Sciences, Zhejiang University, Hangzhou, 310027, China
E-mail address: shanechern@zju.edu.cn; chenxiaohang92@gmail.com

Forum Geometricorum
Volume 16 (2016) 29–35.

FORUM GEOM
ISSN 1534-1178

Geogebra Construction of the Roots of Quadratic, Cubic and Quartic Equations

Nikolaos Dergiades

Abstract. We construct geometrically the roots of a quadratic equation, which construction is ruler and compass possible, where the roots are signed segments and the roots of a cubic or quartic equation, that are not ruler and compass constructible, for which we give conic (with intersections of parabolas) dynamic constructions, easily performed via computer applications such as Geogebra etc and apply this construction to the trisection of an acute angle.

1. Introduction

Our attention is for pure geometric constructions of the roots of equations that are the result of real geometric problems, where the coefficients are not simple values [1].

1.1. *Quadratic equation, a ruler and compass construction.* A geometric quadratic equation with unknown a segment x can take the form

$$x^2 + \varepsilon a x + \delta b^2 = 0,$$

where a and b are known segments and $\varepsilon, \delta = \pm 1$. It is easy to see that the above equation has roots the abscissae of the intersections of the circle

$$\left(x + \frac{\varepsilon a}{2}\right)^2 + \left(y + \frac{(\delta+1)b}{2}\right)^2 = \frac{a^2}{4} + \left(\frac{(\delta-1)b}{2}\right)^2 = R^2$$

with the x-axis $y = 0$. It is also easy to see that the above circle passes through the points $A(0, -b)$ and $B(-\varepsilon a, -\delta b)$, and that the distance of these points is $2R$, the diameter of the above circle. Hence the construction of the roots of the quadratic equation consists of constructing the circle with diameter AB and finding its intersections with the x-axis.

1.2. *Not ruler and compass cases.* A geometric construction, that is not possible with ruler and compass, of a segment y sometimes leads to the solution of a cubic or quartic equation. The general form of such a cubic equation is

$$y^3 \pm py^2 \pm q^2 y \pm r^2 s = 0,$$

Publication Date: March 6, 2016. Communicating Editor: Paul Yiu.

where p, q, r, s are lengths of known segments. By the substitution $y = x \mp \frac{p}{3}$ we get the simpler equation

$$x^3 \pm a^2x \pm d^2e = 0 \tag{1}$$

where a, d, e are constructible segments. If $a \neq 0$, then we can construct the segment b such that $d^2e = a^2b$ with the following construction (Figure 1). On a line take the consecutive segments $AB = a$, $BE = e$, Draw $AD \perp AB$, $AD = d$, $AC \perp BD$. If DF is parallel to CE, then $EF = b$.

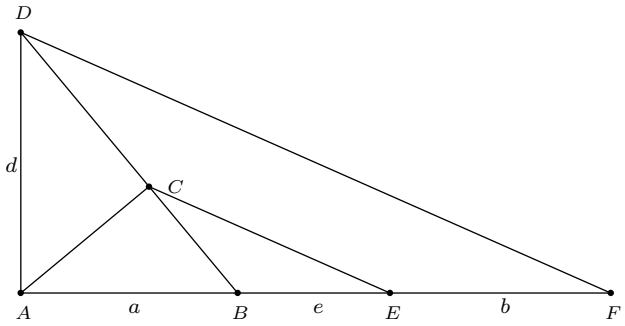

Figure 1

Hence, if $a \neq 0$, we have the equation

$$x^3 + \varepsilon a^2x + \delta a^2b = 0, \qquad \varepsilon, \delta = \pm 1. \tag{2}$$

If $a = 0$, we have the equation

$$x^3 \pm d^2e = 0. \tag{3}$$

Similarly the general form of a quartic equation

$$y^4 \pm py^3 \pm q^2y^2 \pm r^2sy \pm t^2u^2 = 0$$

by the substitution $y = x \mp \frac{p}{4}$ gives the simpler equation

$$x^4 \pm a^2x^2 \pm d^2ex \pm v^2w^2 = 0 \tag{4}$$

where $vw \neq 0$ and a, d, e, v, w are constructible segments.

As previously, if $a \neq 0$, it is easy to construct segments b, c such that (4) has the form

$$x^4 + \varepsilon a^2x^2 + \delta a^2bx + \eta a^2c^2 = 0, \qquad \varepsilon, \delta, \eta = \pm 1. \tag{5}$$

It is easy to see that (4) can have the following other forms

$$x^4 + \varepsilon a^2bx + \eta a^2c^2 = 0, \tag{6}$$

$$x^4 + \varepsilon a^2x^2 + \delta a^2b^2 = 0 \qquad \text{(biquadratic)} \tag{7}$$

and $x^4 - v^2w^2 = 0$ with a trivial construction of the mean proportional of v and w.

2. Cubic equations

2.1. The roots of the cubic equation $x^3+\varepsilon a^2x+\delta a^2b=0$ are the abscissae of the intersections of parabola $x^2=a\left(y-\frac{\varepsilon a}{2}\right)$ with the parabola $y^2=-\delta b\left(x-\frac{a^2}{4\delta b}\right)$ provided that $x\neq 0$, as it is easily seen after elimination of y. Hence we exclude as common point the vertex $A\left(0,\frac{\varepsilon a}{2}\right)$ of the first parabola. These parabolae are easily constructible with Geogebra. The first focus is $F_1\left(0,\ \frac{a}{4}+\frac{\varepsilon a}{2}\right)$ and the directrix is parallel to x-axis at $D_1\left(0,\ -\frac{a}{4}+\frac{\varepsilon a}{2}\right)$. The vertex of the second is $B\left(\frac{a^2}{4\delta b},\ 0\right)$, the focus $F_2\left(-\frac{\delta b}{4}+\frac{a^2}{4\delta b},\ 0\right)$ and the directrix is parallel to y-axis at $D_2\left(\frac{\delta b}{4}+\frac{a^2}{4\delta b},\ 0\right)$. The points A, F_1, D_1 are easily constructible. In order to construct the point B, we construct the point $B'(-\delta b,0)$, the point A' symmetric of A relative to the x-axis. The circumcircle of triangle $AB'A'$ meets again the x-axis at B. The points F_2, D_2 are easily constructible since $F_2B=BD_2=\frac{\delta b}{4}$ (see Figure 2a).

Case 2.1.1. $\varepsilon=\delta=1$ (Figure 2a).

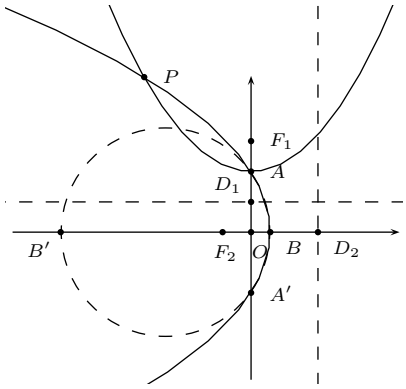

Figure 2a

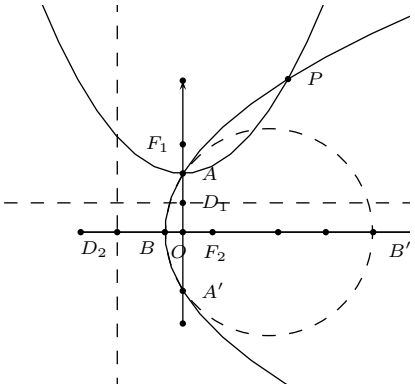

Figure 2b

The parabolae have two common points A, P. Hence we have only one negative root, the abscissa of the point P.

Case 2.1.2. $\varepsilon=1$, $\delta=-1$ (Figure 2b). For $x=-x$ we get case 2.1.1. Hence we have only one positive root.

Case 2.1.3. $\varepsilon=-1$, $\delta=1$ (Figure 2c).

Case 2.1.4. $\varepsilon=\delta=-1$ (Figure 2d). For $x=-x$ we get Case 2.1.3.

Case 2.1.5. $x^3=d^2e$ (Figure 2e). The roots of this equation are the abscissa of the intersections of the parabolas

$$x^2=dy,\qquad y^2=ex,$$

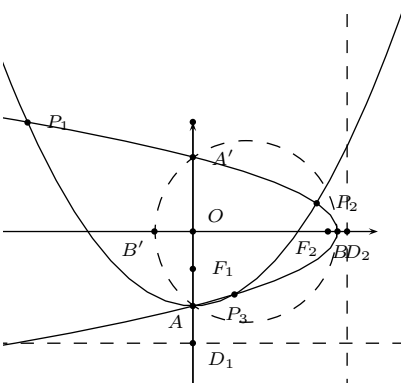

Figure 2c

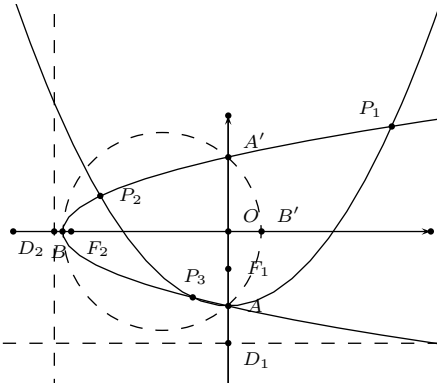

Figure 2d

where $x \neq 0$, $D_1\left(0,\ -\frac{d}{4}\right)$, $D_2\left(-\frac{e}{4},\ 0\right)$. We have only one positive root the abscissa of the point P.

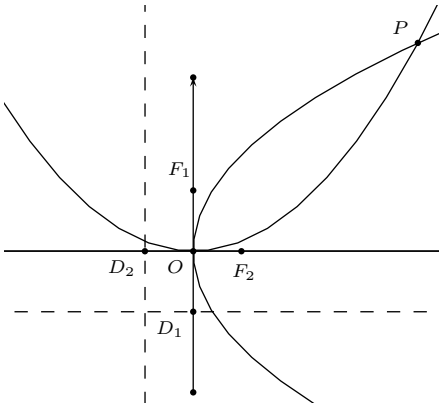

Figure 2e

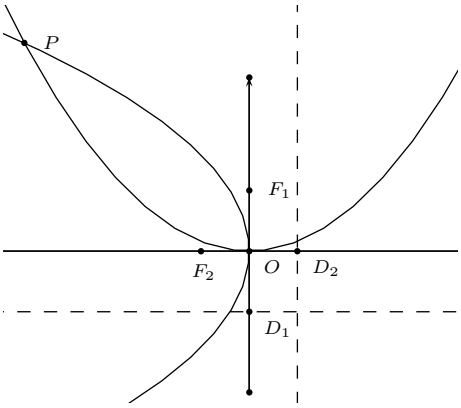

Figure 2f

Case 2.1.6. $x^3 + d^2e = 0$ (Figure 2f). For $x = -x$ we get the previous case Hence we have one negative root.

3. The doubling of a cube

This is a famous problem from antiquity with no ruler and compass solution. If we have a cube with edge a, and we want to construct a second cube with double volume of the first, then the edge x of this cube must be the root of the cubic equation $x^3 = 2a^3$. This equation has the form of Case 2.1.5 where $d = a$, $e = 2a$, and the construction of x is obvious.

4. The trisection of a given acute angle

If triangle ABC has a right angle at A (Figure 3), sidelengths a, b, c, and $\angle B = 3\varphi$, we take a point Z on CA such that $CZ = x$ and BZ trisects the angle B. Hence, $\tan 3\varphi = \frac{b}{c}$, $\tan\varphi = \frac{b-x}{c}$. Since $\tan 3\varphi = \frac{3\tan\varphi - \tan^3\varphi}{1-3\tan^2\varphi}$, we get

$$\frac{b}{c} = \frac{3c^2(b-x) - (b-x)^3}{c(c^2 - 3(b-x)^2)},$$

or

$$x^3 - 3a^2x + 2a^2b = 0.$$

This cubic equation is of the form of Case 2.1.3 where a and b are replaced by $\sqrt{3}a$ and $\frac{2}{3}b$ respectively. Hence we make the following

Construction of the point Z. On the side AB we take the point A_1 such that $AA_1 = \frac{\sqrt{3}}{2}a$, the altitude of the equilateral triangle BCD. Let A_2 be the symmetric of A_1 relative to A. We take the point B_1 on CA such that $B_1A = \frac{2}{3}b$. The circumcircle of triangle $A_1B_1A_2$ meets the line CA at B_2. Let E_1 be the midpoint of AA_2 and D_1 the symmetric of E_1 relative to A_2. We take on B_1B_2 the points E_2, D_2 such that $E_2B_2 = B_2D_2 = \frac{B_1A}{4} = \frac{1}{6}b$. We draw the parabola with focus E_1 and directrix the parallel from D_1 to CA, and the parabola with focus E_2 and directrix the parallel from D_2 to AB.

If P is the common point of the two parabolas with distance d from the line A_1A_2 that is the smallest, then $CZ = d$. Hence the point Z is constructible by this conic construction.

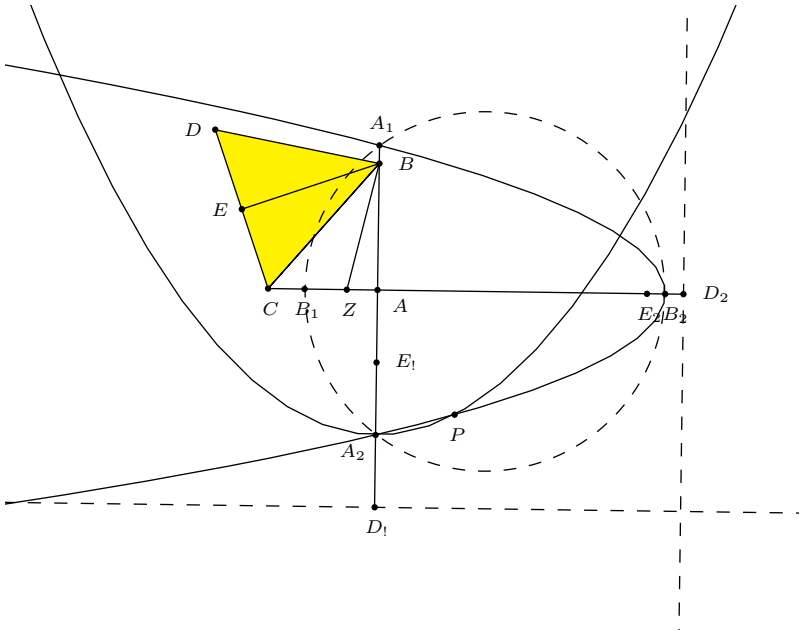

Figure 3

5. Quartic equations

5.1. *The quartic equation* $x^4+\varepsilon a^2x^2+\delta a^2bx+\eta a^2c^2=0$. The roots of the quartic equation are the abscissae of the intersections of parabola $x^2=a\left(y-\frac{\varepsilon a}{2}\right)$ with the parabola $y^2=-\delta b\left(x-\frac{a^2}{4\delta b}+\frac{c^2}{\delta\eta b}\right)$ as it is easily seen after elimination of y. We have almost the same construction as in the case of the cubic equation. The only difference is that if we construct also the points $C(0,c)$, $C'(0,-c)$, then the circumcircle of triangle $B'CC'$, that meets again the x-axis at the point B'', and we translate the second parabola (in the cubic construction) by the vector $-k\overrightarrow{OB''}$. The points F_2, D_2 again are given by $F_2B=BD_2=\frac{\delta b}{4}$.

Example. $\varepsilon=-1$, $\delta=-1$, $\eta=1$ (Figure 4) we refer to case 2.1.3 and (Figure 2d).

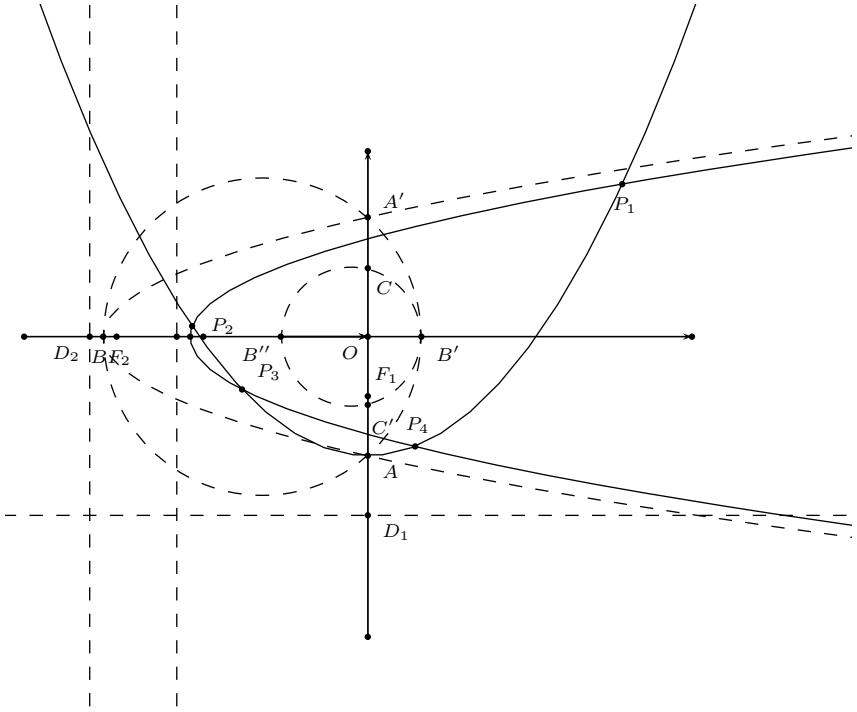

Figure 4

5.2. *The quartic equation* $x^4+\delta a^2bx+\eta a^2c^2=0$. The roots of the quartic equation, as it is easily seen after elimination of y, are the abscissae of the intersections of parabola $x^2=ay$ with the parabola $y^2=-\delta b\left(x+\frac{c^2}{\delta\eta b}\right)$. The first parabola has $A(0,0)$, $D_1\left(0,\ -\frac{a}{4}\right)$ $F_1\left(0,\ \frac{a}{4}\right)$, and the second that has $B\left(-\frac{c^2}{\delta\eta b},\ 0\right)$, $D_2\left(\frac{\delta b}{4},\ 0\right)$, $F_2\left(-\frac{\delta b}{4},\ 0\right)$ is constructed by constructing the points $C(0,c)$, $C'(0,-c)$, $B'(\delta\eta b,0)$, then the circumcircle of triangle $B'CC'$ meets the x-axis at the point B, the vertex of the second parabola.

5.3. *The quartic equation* $y^4 + \varepsilon a^2 y^2 + \delta a^2 b^2 = 0$. This quartic equation is the known biquadratic equation with roots that are ruler and compass constructible. If we put

$$y^2 = ax, \tag{8}$$

then the biquadratic equation becomes the quadratic $x^2 + \varepsilon ax + \delta b^2 = 0$, and since we know the construction of x, then from (8) we know the construction of y.

So we must construct the points $A(0, -b)$, $B(-\varepsilon a, -\delta b)$. The circle with diameter AB meets the x-axis at the points $A_1(x_1, 0)$ and $A_2(x_2, 0)$. If $\eta_1 = \text{sign}(x_1)$ and $\eta_2 = \text{sign}(x_2)$, then we construct the points $B_1(-\eta_1 a, 0)$, $B_2(-\eta_2 a, 0)$. The circles with diameters A_1B_1 and A_2B_2 meet the y-axis at four (if exist both A_1, A_2) points, the ordinates of which are the roots of the biquadratic equation.

Reference

[1] E. W. Weisstein, Carlyle Circle, *MathWorld–A Wolfram Web Resource*, `http://mathworld.wolfram.com/CarlyleCircle.html`.

Nikolaos Dergiades: I. Zanna 27, Thessaloniki 54643, Greece
E-mail address: `ndergiades@yahoo.gr`

Forum Geometricorum
Volume 16 (2016) 37–41.

FORUM GEOM
ISSN 1534-1178

Trisecting an Angle Correctly up to Arcminute

Joseph Tonien

Abstract. We present a simple compass-and-straightedge construction method of approximately trisecting an angle. This method is applicable to both acute and obtuse angles. With an original angle α, the construction gives an angle τ with error $|\epsilon| = |\tau - \alpha/3| < .0155^\circ$.

1. Introduction

Angle trisection is one of a few infamous problems that originated all the way back in ancient times but had required modern mathematics to settle. It was not until in the late 19th centuries that it could be proved rigorously that it is impossible to divide an arbitrary angle into three equal angles using only compass and straightedge.

However, for practical purposes, there are many approximate constructions that can trisect an angle up to a small error [1, 2, 3, 4]. Here we will present a new method of approximate construction. Start with an angle α, the proposed method constructs an angle τ with the error

$$\epsilon = \tau - \frac{\alpha}{3} = \frac{\alpha}{6} - \arctan \frac{\sin \frac{\alpha}{2}}{\sqrt{9 - 4\sin^2 \frac{\alpha}{2}}}.$$

This error is very small (less than an arcminute) which is due to the fact that its Taylor series have zero coefficients in degrees 0, 1, and 2.

$$\epsilon = -\frac{1}{1296}\alpha^3 + \frac{7}{20736}\alpha^5 + \frac{54903553}{3085588961280}\alpha^7 + \dots$$

It is quite simple to calculate this error and it would be a perfect trigonometry problem for students. It is also a nice calculus problem for students to find the Taylor series of the error function and to establish the maximum bound on the error.

Publication Date: March 6, 2016. Communicating Editor: Paul Yiu.

2. The construction

Given an angle $\angle xOy = \alpha$, the construction is as follows (see Figure 1)

- construct the bisector Ot,
- on Oy construct arbitrary points U, A, V such that $OU = UA = AV$,
- construct a circle centre at A with radius equal to OV which meets Ot at B,
- construct a point C on Ot such that $OB = BC$,
- through C, construct a line perpendicular to Ot which meets the line AB at D
- draw OD which makes $\angle xOD = \tau \approx \frac{\alpha}{3}$.

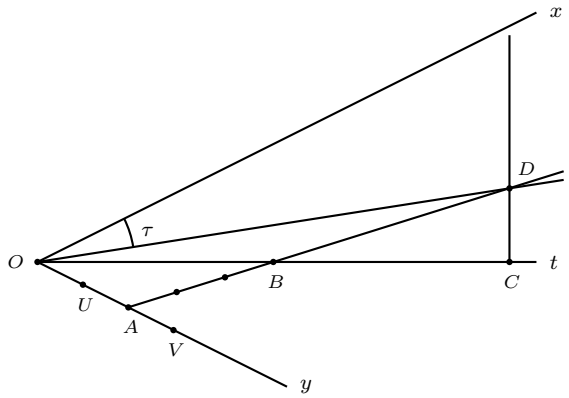

Figure 1. The proposed trisection construction

3. Calculating the error $\epsilon = \tau - \frac{\alpha}{3}$

Using the law of sines on triangle OAB, we have

$$\sin \angle OBA = \frac{2}{3} \sin \angle BOA = \frac{2}{3} \sin \frac{\alpha}{2}.$$

Comparing the two right triangles DOC and DBC we have

$$\tan \angle DOC = \frac{1}{2} \tan \angle DBC = \frac{1}{2} \tan \angle OBA.$$

Thus,

$$\tan \angle DOC = \frac{\sin \angle OBA}{2 \cos \angle OBA} = \frac{\frac{2}{3} \sin \frac{\alpha}{2}}{2\sqrt{1 - \frac{4}{9} \sin^2 \frac{\alpha}{2}}} = \frac{\sin \frac{\alpha}{2}}{\sqrt{9 - 4 \sin^2 \frac{\alpha}{2}}},$$

and

$$\tau = \angle xOD = \frac{\alpha}{2} - \angle DOC = \frac{\alpha}{2} - \arctan \frac{\sin \frac{\alpha}{2}}{\sqrt{9 - 4 \sin^2 \frac{\alpha}{2}}}.$$

We derive the error of the construction:

Theorem 1.

$$\epsilon = \tau - \frac{\alpha}{3} = \frac{\alpha}{6} - \arctan \frac{\sin \frac{\alpha}{2}}{\sqrt{9 - 4\sin^2 \frac{\alpha}{2}}}.$$

Comparing with the errors ϵ_S and ϵ_G of Steinhaus' [3, 4] and Gauld's constructions [2].

$$\epsilon_S = \arctan \frac{2\sin \frac{\alpha}{2}}{1 + 2\cos \frac{\alpha}{2}} - \frac{\alpha}{3},\ \epsilon_G = \arctan \frac{\sin \frac{\alpha}{2} + 2\sin \frac{\alpha}{4}}{\cos \frac{\alpha}{2} + 2\cos \frac{\alpha}{4}} - \frac{\alpha}{3}$$

our method is more accurate than Steinhaus' but a bit weaker than Gauld's. The following table shows the errors in degree.

α	$\lvert\epsilon\rvert$	$\lvert\epsilon_G\rvert$	$\lvert\epsilon_S\rvert$	α	$\lvert\epsilon\rvert$	$\lvert\epsilon_G\rvert$	$\lvert\epsilon_S\rvert$
5	.0000293	.0000073	.0000588	50	.0191908	.0073744	.0597073
10	.0002319	.0000588	.0004704	55	.0225624	.0098235	.0797398
15	.0007694	.0001984	.0015888	60	.0249879	.0127653	.1039094
20	.0017795	.0004704	.0037703	65	.0257239	.0162461	.1326482
25	.0033635	.0009191	.0073744	70	.0238342	.0203129	.1664038
30	.0055737	.0015888	.0127653	75	.0181658	.0250129	.2056412
35	.0083990	.0025243	.0203129	80	.0073259	.0303941	.2508445
40	.0117506	.0037703	.0303941	85	.0103425	.0365048	.3025190
45	.0154458	.0053719	.0433940	90	.0367826	.0433940	.3611934

4. Estimating the error

The error function $\epsilon(\alpha)$ is an odd function, calculting the derivatives,

$$\epsilon'(0) = 0,\ \epsilon^{(3)}(0) = -\frac{1}{216},\ \epsilon^{(5)}(0) = \frac{35}{864},\ \epsilon^{(7)}(0) = \frac{54903553}{612220032},$$

we have the Taylor series

$$\epsilon = -\frac{1}{1296}\alpha^3 + \frac{7}{20736}\alpha^5 + \frac{54903553}{3085588961280}\alpha^7 + \dots$$

We can manipulate the derivative of ϵ as follows

$$\epsilon'(\alpha) = \frac{1}{6} - \frac{3\cos \frac{\alpha}{2}}{2(2 + \cos^2 \frac{\alpha}{2})\sqrt{5 + 4\cos^2 \frac{\alpha}{2}}}$$

$$= \frac{2\sin^2 \frac{\alpha}{2}(\cos^2 \frac{\alpha}{2} + \frac{\sqrt{945}+25}{8})(\frac{\sqrt{945}-25}{8} - \cos^2 \frac{\alpha}{2})}{3(2 + \cos^2 \frac{\alpha}{2})\sqrt{5 + 4\cos^2 \frac{\alpha}{2}}((2 + \cos^2 \frac{\alpha}{2})\sqrt{5 + 4\cos^2 \frac{\alpha}{2}} + 9\cos \frac{\alpha}{2})}$$

It implies that $\epsilon'(\alpha) < 0$ for $\alpha \in [0, \frac{\pi}{4}]$, and so the function $\epsilon(\alpha)$ is decreasing on $[0, \frac{\pi}{4}]$. We have

$$\epsilon(0) = 0 \geq \epsilon(\alpha) \geq \epsilon(\frac{\pi}{4}) = \frac{\pi}{24} - \arctan \frac{1}{\sqrt{32 + 18\sqrt{2}}}.$$

Thus, we derive the following bound:

Theorem 2.

$$\max_{0\le\alpha\le\frac{\pi}{4}} |\epsilon(\alpha)| = \arctan\frac{1}{\sqrt{32+18\sqrt{2}}} - \frac{\pi}{24} < .0155^\circ$$

The above bound is established only for $\alpha \in [0, \frac{\pi}{4}]$. However, we can obtain the same bound for $\alpha \in (\frac{\pi}{4}, 2\pi)$ as follows. If $\alpha \in (\frac{\pi}{4}, 2\pi)$ then we can reduce the trisection of the angle α into the problem of trisection of another angle $\alpha' \in (0, \frac{\pi}{4})$ which is specified in the following table.

$\alpha \in [\frac{\pi}{4}, \frac{2\pi}{4}]$	$\alpha \in [\frac{2\pi}{4}, \frac{3\pi}{4}]$	$\alpha \in [\frac{3\pi}{4}, \frac{4\pi}{4}]$
$\alpha' = \frac{\pi}{2} - \alpha$	$\alpha' = \alpha - \frac{\pi}{2}$	$\alpha' = \pi - \alpha$
$\tau' = \frac{\pi}{6} - \tau$	$\tau' = \tau - \frac{\pi}{6}$	$\tau' = \frac{\pi}{3} - \tau$

$\alpha \in [\frac{4\pi}{4}, \frac{5\pi}{4}]$	$\alpha \in [\frac{5\pi}{4}, \frac{6\pi}{4}]$	$\alpha \in [\frac{6\pi}{4}, \frac{7\pi}{4}]$	$\alpha \in [\frac{7\pi}{4}, 2\pi]$
$\alpha' = \alpha - \pi$	$\alpha' = \frac{3\pi}{2} - \alpha$	$\alpha' = \alpha - \frac{3\pi}{2}$	$\alpha' = 2\pi - \alpha$
$\tau' = \tau - \frac{\pi}{3}$	$\tau' = \frac{\pi}{2} - \tau$	$\tau' = \tau - \frac{\pi}{2}$	$\tau' = \frac{2\pi}{3} - \tau$

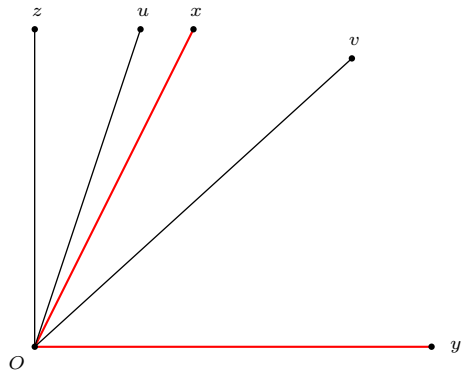

Figure 2. Trisection of α based on the trisection of $\alpha' = \frac{\pi}{2} - \alpha$ when $\alpha \in [\frac{\pi}{4}, \frac{\pi}{2}]$

For example, if $\alpha \in [\frac{\pi}{4}, \frac{\pi}{2}]$ as in Figure 2, then $\alpha' = \frac{\pi}{2} - \alpha$. First, we construct Oz perpendicular to Oy and by our above method, approximately trisect the angle $\alpha' = \angle xOz = \frac{\pi}{2} - \alpha$ by Ou, so we have $\tau' = \angle xOu \approx \frac{\alpha'}{3}$. Construct $\angle uOv = \frac{\pi}{6}$, then $\tau = \angle xOv = \frac{\pi}{6} - \tau'$ is an approximation of $\frac{\alpha}{3}$.

Since

$$|\epsilon'| = |\tau' - \frac{\alpha'}{3}| = |(\frac{\pi}{6} - \tau) - \frac{1}{3}(\frac{\pi}{2} - \alpha)| = |\tau - \frac{\alpha}{3}| = |\epsilon|,$$

the reduction from α to α' gives us the same error. Therefore, for any $\alpha \in (0, 2\pi)$, we can make a construction with an error $|\epsilon| < .0155^\circ$.

References

[1] U. Dudley, *The Trisectors*, Cambridge University Press, 1994.
[2] D. Gauld, Approximate Angle Trisection, *College Mathematics Journal*, 15 (1984) 420–422.
[3] G. Peterson, Approximation to an Angle Trisection, *College Mathematics Journal*, 14 (1983) 166–167.
[4] H. Steinhaus, *Mathematical Snapshots*, Dover Recreational Math, Dover Publications, 3rd edition, 2011.

Joseph Tonien: School of Computing and Information Technology, University of Wollongong, Australia
E-mail address: joseph_tonien@uow.edu.au

Forum Geometricorum
Volume 16 (2016) 43–50.

FORUM GEOM
ISSN 1534-1178

Isogonal Conjugates in a Tetrahedron

Jawad Sadek, Magid Bani-Yaghoub, and Noah H. Rhee

Abstract. The symmedian point of a tetrahedron is defined and the existence of the symmedian point of a tetrahedron is proved through a geometrical argument. It is also shown that the symmedian point and the least squares point of a tetrahedron are concurrent. We also show that the symmedian point of a tetrahedron coincides with the centroid of the corresponding pedal tetrahedron. Furthermore, the notion of isogonal conjugate to tetrahedra is introduced, with a simple formula in barycentric coordinates. In particular, the barycentric coordinates for the symmedian point of a tetrahedron are given.

1. Introduction

The *symmedian point* of a triangle is one of the 6,000 known points associated with the geometry of a triangle [4]. To define the symmedian point, we begin with the concept of isogonal lines. Two lines AR and AS through the vertex A of an angle are said to be isogonal if they are equally inclined from the sides that form $\angle A$. The lines that are isogonal to the medians of a triangle are called symmedian lines [3], pp. 75-76. Figure 1 (a) shows that the symmedian line AP of the triangle ABC is obtained by reflecting the median AM through the corresponding angle bisector AL. The symmedian lines intersect at a single point K known as the symmedian point, also called the Lemoine point. It turns out that the symmedian point of a triangle coincides with the point at which the sum of the squares of the perpendicular distances from the three sides of the triangle is minimum (the *least squares point*, LSP), [1]. Another property of the symmedian point of a triangle is described below. As shown in Figure 1 (b), let $A'B'C'$ the pedal triangle of K (i.e., the triangle obtained by projecting K onto the sides of the original triangle). Then the symmedian point of the triangle ABC and the centroid of the triangle $A'B'C'$ are concurrent.

The existence of symmedian point of a triangle was proved by the the French mathematician Emile Lemoine in 1873 ([3], Chapter 7). Later the symmedian point was defined by Marr for equiharmonic tetrahedrons in 1919 [5]. In the present work we provide the definition and prove the existence of the symmedian point of an arbitrary tetrahedron. Then we show that the symmedian point of a tetrahedron coincides with the LSP of that tetrahedron and the centroid of the corresponding

Publication Date: March 13, 2016. Communicating Editor: Paul Yiu.

The authors would like to thank the anonymous reviewer for the valuable comments and suggestions to improve the quality of the paper and for pointing out reference [6].

petal tetrahedron. Furthermore, we will demonstrate the utility of *least squares solution* for determining the location of the least squares points and hence the symmedian points.

The rest of this paper is organized as follows. In section 2, the existence of the symmedian point of a tetrahedron is proved. In section 3, it is shown that the symmedian point and LSP of a tetrahedron are concurrent. In section 4, the concurrency of the symmedian point and the centroid of the corresponding petal tetrahedron is proved. In section 5, a discussion of the main results is provided.

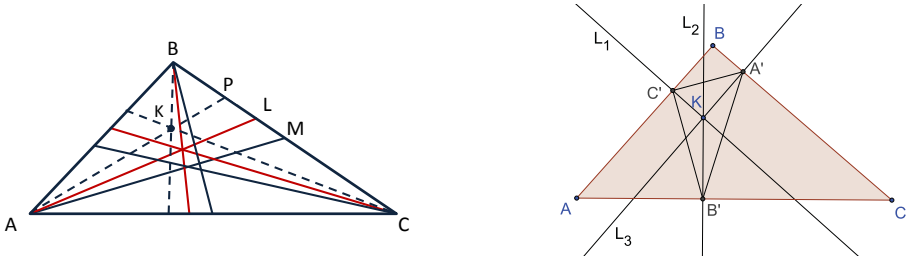

(a) (b)

Figure 1. *(a) The symmedian lines of triangle ABC intersect at the symmedian point K. (b) The symmedian point K of the ABC triangle coincides with the centroid $\widehat{C}$ of its pedal triangle, which is the $A'B'C'$ triangle formed by connecting the intersection points of the perpendicular lines L_1, L_2 and L_3 from K to the sides of the ABC triangle.*

2. Symmedian point of a tetrahedron and barycentric coordinates

Let $ABCD$ be a tetrahedron. Two planes (P) and (Q) through $\overline{AB}$, for instance, are said to be *isogonal* conjugates if they are equally inclined from the sides that form the dièdre angle between the planes of the triangles ABC and ABD. (P) is called the isogonal conjugate of (Q) and vice versa. If a point X of $ABCD$ is joined to vertex A and vertex B, the plane through $\overline{XA}$ and $\overline{XB}$ has an isogonal conjugate at A. Similarly, joining X to vertices B and D, D and C, A and C, B and C, C and D, produce five more conjugate planes. There is no immediately obvious reason why these six conjugates should be concurrent. However, that this is always the case will follow from lemma 2 below. Let M be the midpoint of $\overline{CD}$. The plane containing $\overline{AB}$ and that is isogonal to the plane of triangle ABM is called a *symmedian plane* of tetrahedron $ABCD$. Taking the midpoints of the six sides of the tetrahedron $ABCD$ and forming the associated symmedian planes, we call the intersection point of these symmedian planes the *symmedian point* of the tetrahedron. In this section we show that all six symmedian planes are indeed concurrent at a point. This definition of the symmedian point differs from the one given in [5], which was only defined for equiharmonic tetrahedrons [6]. For the existence of the symmedian point of an arbitrary tetrahedron, we first need the following two lemmas.

Lemma 1. *All six median planes obtained from a side of a tetrahedron and the midpoint of its opposite side are concurrent.*

Proof.
As shown in Figure 2 (a), let M_1 and M_2 be the midpoints of the opposite sides $\overline{CD}$ and $\overline{AB}$, respectively. The two median planes constructed from M_1 and $\overline{AB}$, and from M_2 and $\overline{CD}$ intersect at the line containing the points M_1 and M_2. Similarly, the other median planes constructed from $\overline{AC}$ and M_3, $\overline{BD}$ and M_4 contain $\overline{M_3M_4}$, and the planes formed with $\overline{BC}$ and M_5, and $\overline{AD}$ and M_6, contain $\overline{M_5M_6}$, where M_3, M_4, M_5, and M_6, are the midpoints of $\overline{BD}, \overline{AC}, \overline{AD}$, and $\overline{BC}$, respectively. Thus it is enough to show that the line segments $\overline{M_1M_2}$, $\overline{M_3M_4}$, and $\overline{M_5M_6}$ are concurrent. This can be shown by noticing that $\overline{M_1M_4}$ and $\overline{M_2M_3}$ are parallel to $\overline{AD}$, and $\overline{M_2M_4}$ and $\overline{M_1M_3}$ are both parallel to $\overline{BC}$. Thus the quadrilateral $M_1M_3M_2M_4$ is a parallelogram. It follows that the diagonals $\overline{M_3M_4}$ and $\overline{M_1M_2}$ cross each other at their midpoints. Similar argument shows that the quadrilateral $M_3M_5M_4M_6$ ia a parallelogram with diagonals $\overline{M_5M_6}$ and $\overline{M_3M_4}$ crossing each other at their midpoints. The desired result follows.□

Lemma 2. *Consider the tetrahedron $ABCD$.*

(i): *If L and T are two points on two isogonal planes (P_1) and (P_2), respectively, through $\overline{AB}$, and if $\overline{LR}, \overline{LS}, \overline{TP}, \overline{TQ}$, are the perpendiculars from L and T to the triangles ABC, and ABD, respectively, then*

$$\frac{LR}{LS} = \frac{TQ}{TP} \tag{1}$$

(ii): *If L is on (P_1) and $LR/LS = TQ/TP$, then T is on (P_2), where (P_1) and (P_2) are isogonal planes through $\overline{AB}$.*

Proof.
To show (i) it is enough to show that the two triangles LRS and TQP are similar (see Figure 2 (b)). In fact, $\angle RLS = \angle PTQ = 180^\circ - \angle(\triangle ABC, \triangle ABD)$, where $\angle(\triangle ABC, \triangle ABD)$ is the dièdre angle between the planes of $\triangle ABC$ and $\triangle ABD$. Also, $\angle TPQ = \angle TNQ = \angle(\triangle ABD, (P_2))$, where $\angle(\triangle ABD, (P_2))$ is the dièdre angle between (P_2) and the plane of the triangle ABD, and N is the projection of P onto $\overline{AB}$. To see why notice that $\overline{TP}$ and $\overline{PN}$ are both perpendicular to $\overline{AB}$. Thus $\overline{AB}$ is also perpendicular to $\overline{TN}$. But, $\overline{AB}$ is also perpendicular to $\overline{TQ}$. Hence $\overline{AB}$ is perpendicular to the planes of the triangles QNT and PNT, and so these two triangles are in the same plane. Since the angles at its vertices P and Q are 90°, the quadrilateral $TPNQ$ is a circumscribed quadrilateral (vertices are located on the same circle) and so the equality $\angle TPQ = \angle TNQ$ holds. Similarly, $\angle LSR = \angle LOR = \angle(\triangle ABC, (P_1))$, where O is the projection of R onto $\overline{AB}$. But $\angle(\triangle ABD, (P_2)) = \angle(\triangle ABC, (P_1))$. So $\angle TPQ = \angle LSR$. The similarity of the triangles TQP, and LRS now follows. (ii) follows easily since in the triangles LRS and TQP, $\angle(PTQ) = \angle(RLS)$ and $LR/LS = TQ/TP$.□

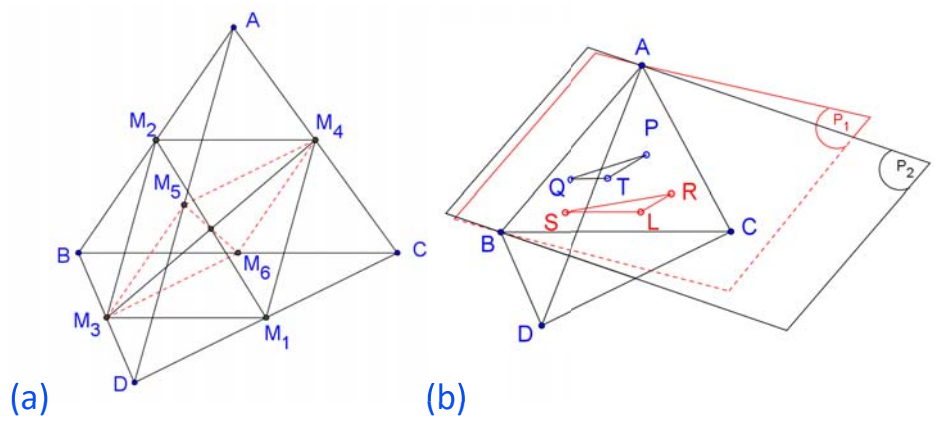

Figure 2. *(a) All six median planes obtained from a side of the $ABCD$ tetrahedron and the midpoint $M_i (1 \leq i \leq 6)$ of its opposite side are concurrent. (b) A representation of the isogonal planes (P_1) and (P_2), and the perpendicular lines from L and T to the triangles ABC and ABD, respectively.*

Now we are ready to show the existence of the symmedian point of a tetrahedron.

Theorem 3. *The symmedian planes are concurrent at a unique point K, the symmedian point of the tetrahedron.*

Proof.
Using Lemma 1, let M be the intersection point of all six median planes. Denote by $S_{\overline{EF}}$ the symmedian plane through a side $\overline{EF}$ and by P^X_{EFG} the orthogonal projection of a point X onto the plane formed by the three points E, F, and G (no three vertices are located on the same line). Let K be the intersection point of the symmedian planes $S_{\overline{AB}}$, $S_{\overline{BC}}$, and $S_{\overline{AC}}$, and let W be the intersection of $S_{\overline{AB}}$ with $S_{\overline{BC}}$ and $S_{\overline{AD}}$. We will show that $W \in S_{\overline{AC}}$. In view of (ii) of Lemma 2, it suffices to show that

$$\frac{WP^W_{ACD}}{WP^W_{ABC}} = \frac{MP^M_{ABC}}{MP^M_{ACD}}.$$

Since W is in $S_{\overline{AD}}$, $S_{\overline{AB}}$, Lemma 2 (i) implies

$$\frac{WP^W_{ACD}}{WP^W_{ABD}} = \frac{MP^M_{ABD}}{MP^M_{ACD}}, \tag{2}$$

and

$$\frac{WP^W_{ABD}}{WP^W_{ABC}} = \frac{MP^M_{ABC}}{MP^M_{ABD}}, \tag{3}$$

Using (2), (3) we have

$$\frac{WP^W_{ACD}}{WP^W_{ABC}} = \frac{WP^W_{ACD}}{WP^W_{ABD}} \times \frac{WP^W_{ABD}}{WP^W_{ABC}} = \frac{MP^M_{ABD}}{MP^M_{ACD}} \times \frac{MP^M_{ABC}}{MP^M_{ABD}} = \frac{MP^M_{ABC}}{MP^M_{ACD}}.$$

Thus W coincides with K. Similar argument shows that the symmedian planes through $\overline{BD}$ and $\overline{CD}$ also pass through K.□

Remark. An identical argument to the proof of Theorem 1 shows that if six planes are concurrent at X, where X is a point in the tetrahedron $ABCD$, then the six conjugate planes are also concurrent at a point X^*, the conjugate of X. In addition, as is in the triangle case, the restriction that X is a point *inside* $ABCD$ is unnecessary.

Now we explore the relationship between the barycentric coordinates of a point X and its isogonal conjugate X^*. Recall that in general, if $x_1, \cdots, x_n$ are the vertices of a simplex in affine space $\mathcal{A}$ and if $(a_1 + \cdots + a_n)X = a_1x_1 + \cdots + a_nx_n$ and at least one of the $a_i's$ does not vanish, then we say that the coefficients $(a_1 : \cdots : a_n)$ are *barycentric coordinates* of X, where $x \in\in \mathcal{A}$ [7]. Also, the barycentric coordinates are homogeneous:

$$(a_1, \cdots, a_n) = (\mu a_1 : \cdots : \mu a_n) \quad \mu \neq 0.$$

Analogous to the triangle case [2], we have the following property for the tetrahedron. Let X be a point in the space. Joining X to each vertex A, B, C, and D, four tetrahedra can be constructed. Let $X = (u : v : w : t)$ and $X^* = (u^* : v^* : w^* : t^*)$ be the barycentric coordinates of X and X^*, respectively, with respect to $ABCD$. Since *the volumes of these tetrahedra are proportional to the barycentric coordinates of* X, using lemma 2, and an argument similar to the proof of Theorem 1, one can establish the following

$$\frac{u^*u}{|\Delta BDC|^2} = \frac{w^*w}{|\Delta ABC|^2} = \frac{v^*v}{|\Delta ADC|^2} = \frac{t^*t}{|\Delta ABD|^2} = \mu,$$

where $|\Delta XYZ|$ denote the area of ΔXYZ. It follows that

$$\begin{aligned} X^* = (u^* : v^* : w^* : t^*) &= (\mu\frac{|\Delta BDC|^2}{u} : \mu\frac{|\Delta ABC|^2}{w} : \mu\frac{|\Delta ADC|^2}{v} : \mu\frac{|\Delta ABD|^2}{t}) \\ &= (\frac{|\Delta BDC|^2}{u} : \frac{|\Delta ABC|^2}{w} : \frac{|\Delta ADC|^2}{v} : \frac{|\Delta ABD|^2}{t}). \quad (4) \end{aligned}$$

(4) gives an extension of isogonal conjugates to tetrahedra with a simple formula in barycentric coordinates. Applying (4) to the centroid $(1 : 1 : 1 : 1)$, we obtain the coordinates of the symmedian point $(|\Delta BDC|^2 : |\Delta ABC|^2 : |\Delta ADC|^2 : |\Delta ABD|^2)$.

3. Concurrency of the Symmedian Point and the Least Squares Point

The LSP of a given tetrahedron $ABCD$ is the point from which the sum of the squares of the perpendicular distances to the four sides of the tetrahedron $ABCD$ is minimized. Now we show that the symmedian point and the LSP of a tetrahedron are concurrent. We start with the following lemma.

Lemma 4. *For a tetrahedron $ABCD$, let M be the midpoint of $\overline{CD}$ and $\overline{MP}$ and $\overline{MQ}$ be the perpendicular line segments from M to ΔABC and ΔABD, respectively. Then we have*

$$\frac{MQ}{MP} = \frac{\textit{area}(\triangle ABC)}{\textit{area}(\triangle ABD)} \tag{5}$$

Similar equalities hold if M is replaced with the midpoints of the other sides of the tetrahedron $ABCD$.

Proof.
Let $\overline{AH}$ be the perpendicular from A to $\triangle BCD$. Now note that

$$\begin{aligned}
\frac{1}{3}MQ \times \text{area}(\triangle ABD) &= \text{volume}(ABMD) \\
&= \frac{1}{3}AH \times \text{area}(\triangle BMD) \\
&= \frac{1}{3}AH \times \text{area}(\triangle BMC) \\
&= \text{volume}(ABCM) \\
&= \frac{1}{3}MP \times \text{area}(\triangle ABC),
\end{aligned}$$

which gives rise to equation (5). □

Now we can prove the concurrency of the symmedian point and the LSP of a tetrahedron.

Theorem 5. *The symmedian point K of tetrahedron $ABCD$ coincides with its LSP.*

Proof.
First, Lemma 2 (i) together with Lemma 4 imply

$$\frac{x}{\text{area}(\triangle ABC)} = \frac{y}{\text{area}(\triangle ABD)} = \frac{z}{\text{area}(\triangle ACD)} = \frac{w}{\text{area}(\triangle BCD)}, \tag{6}$$

where x, y, z, w are the distances from the the symmedian point to the triangles ABC, ABD, ACD, BCD, respectively.
Second, let $\text{area}(\triangle ABC) = a, \text{area}(\triangle ABD) = b, \text{area}(\triangle ACD) = c, \text{area}(\triangle BCD) = d$. By Lagrange's identity,

$$\begin{aligned}
&(x^2+y^2+z^2+w^2)(a^2+b^2+c^2+d^2) - (ax+by+cz+dw)^2 \\
&\qquad = (bx-ay)^2 + (cx-az)^2 + (dx-aw)^2 \\
&\qquad\quad +(cy-bz)^2 + (dy-bw)^2 + (dz-cw)^2.
\end{aligned} \tag{7}$$

Since $a^2+b^2+c^2+d^2$ is constant for all x, y, z, w, and $ax+by+cz+dw = 3\text{vol}(ABCD)$, $(x^2+y^2+z^2+w^2)$ is minimum if and only if the right hand side of (7) is zero. This occurs only when

$$bx = ay,\ cx = az,\ dx = aw,\ cy = bz,\ dy = bw,\ dz = cw.$$

In view of (6), this occurs at the symmedian point K. So the symmedian point coincides with the LSP. □

4. Concurrency of the Symmedian Point and the Centroid of the Corresponding Petal Tetrahedron

In this section we show that the symmedian point of a tetrahedron coincides with the centroid of the corresponding pedal tetrahedron.

Theorem 6. *The symmedian point of a tetrahedron coincides with the centroid of the corresponding pedal tetrahedron.*

Proof.
Let K be the symmedian point of the tetrahedron $ABCD$. Drop the perpendiculars from K to the four sides of the tetrahedron $ABCD$ and let their intersection with $\Delta ABC, \Delta ABD, \Delta ACD, \Delta BCD$ be the points V_1, V_2, V_3, V_4, respectively. Let $\widehat{C}$ be the centroid of the pedal tetrahedron $V_1V_2V_3V_4$ of K. It is well known that $\widehat{C}$ minimizes the sum of the squares of the distances to four vertices V_1, V_2, V_3, V_4. So we have

$$\sum_{i=1}^{4}(\widehat{C}V_i)^2 \leq \sum_{i=1}^{4}(XV_i)^2 \text{ for any } X \in R^3. \tag{8}$$

Suppose $\widehat{C} \neq K$. Drop the perpendiculars from $\widehat{C}$ to the four sides of the tetrahedron $ABCD$ and let their intersection with ΔABC, ΔABD, ΔACD, ΔBCD be the points W_1, W_2, W_3, W_4, respectively. Since K is also the LSP of the tetrahedron $ABCD$

$$\sum_{i=1}^{4}(KV_i)^2 < \sum_{i=1}^{4}(\widehat{C}W_i)^2. \tag{9}$$

Note also that we have $\widehat{C}W_i \leq \widehat{C}V_i$ for each i. So using (8) with $X = K$, we have

$$\sum_{i=1}^{4}(\widehat{C}W_i)^2 \leq \sum_{i=1}^{4}(\widehat{C}V_i)^2 \leq \sum_{i=1}^{4}(KV_i)^2,$$

which contradicts (9). So we must have $\widehat{C} = K$. □

Corollary 7. *The symmedian point and hence the LSP of a tetrahedron belongs to its interior.*

Proof.
Since $K = \widehat{C}$ and $\widehat{C}$ is in the interior of the petal tetrahedron and the pertal tetrahedron is in the interior of the given tetrahedron, the symmedian point K of the given tetrahedron belongs to its interior. □

5. Discussion

In this section we show that our symmedian point of a tetrahedron $ABCD$ is different from the symmedian point defined by Marr [5]. Marr's symmedian point of an equiharmonic tetrahedron (that is, $AD \times BC = AB \times CD = AC \times BD$)

can be defined as the point of intersection of the lines joining the vertices to the symmedian points of the opposite faces. Now we give an example that shows that our symmedian point is different from Marr's symmedian point.

Example 1. Consider the tetrahedron $ABCD$ such that $A(0,0,0)$, $B(1,0,0$, $C(0,1,0)$ and $D(0,0,1)$. Note that the tetrahedron $ABCD$ is equiharmonic and one can compute Marr's symmedian point $\tilde{K} = (1/5, 1/5, 1/5)$. Our symmedian point is $K(1/6, 1/6, 1/6)$. So $\tilde{K} \neq K$.

In summary, the merit of the present work is twofold. First, the definition of the symmedian point of a tetrahedron is a true generalization of the symmedian point of a triangle, because they both coincide with their corresponding least square points. Second, the notion of isogonal conjugate has been extended to tetrahedra, with a simple formula in barycentric coordinates. In particular, a formula for the symmedian point of a tetrahedron has been given in terms of the barycentric coordinates.

References

[1] A. Bogomolny, All About Symmedians, `www.cut-the-knot.org/triangle/symmedians.shtml`.
[2] H. S. M. Coxeter, *Introduction to Geometry*, Wiley, 1963.
[3] R. Honsberger, *Episodes in Nineteenth and Twentieth Century Euclidean Geometry*, MAA, 1995.
[4] C. Kimberling, *Encyclopedia of Triangle Centers*, `http://faculty.evansville.edu/ck6/encyclopedia/ETC.html`.
[5] W. L. Marr, The co-symmedian system of tetrahedra inscribed in a sphere, *Proceedings of the Edinburgh mathematical society*, 37 (1918) 59-64.
[6] J. Neuberg, Memoire sur la tetraedre, *Acad. Royale des Sciences*, 37 (1886) 64.
[7] P. Yiu, The uses of homogeneous barycentric coordinates in plane Euclidean Geometry, *Internat. J. Math. Ed. Sci. Tech.*, 31 (2000) 569–578.

Jawad Sadek: Department of Mathematics, Computer Science and Information Systems, Northwest Missouri State University, Maryville, Missouri 64468-6001, USA
E-mail address: `JAWADS@nwmissouri.edu`

Magid Bani-Yaghoub: Department of Mathematics and Statistics, University of Missouri - Kansas City, Kansas City, Missouri 64110-2499, USA
E-mail address: `baniyaghoubm@umkc.edu`

Noah H. Rhee: Department of Mathematics and Statistics, University of Missouri - Kansas City, Kansas City, Missouri 64110-2499, USA
E-mail address: `RheeN@umkc.edu`

Forum Geometricorum
Volume 16 (2016) 51–56.

FORUM GEOM
ISSN 1534-1178

Archimedes' Arbelos to the n-th Dimension

Antonio M. Oller-Marcén

Abstract. The *arbelos* was introduced in Proposition 4 of Archimedes' Book of Lemmas. It is the plane figure bounded by three pairwise tangent semicircles with diameters lying on the same line. This figure has several interesting properties that have been studied over time. For example, the area of the arbelos equals the area of the circle whose diameter is the portion inside the arbelos of the common tangent to the smaller circles. In this paper we consider n-dimensional analogues of this latter property.

1. Introduction

The *arbelos* ($\acute{\alpha}\rho\beta\eta\lambda o\varsigma$, literally "shoemaker's knife") was introduced in Proposition 4 of Archimedes' Book of Lemmas [2, p. 304]. It is the plane figure bounded by three pairwise tangent semicircles with diameters lying on the same line (see the left-hand side of Figure 1). In addition to the properties proved by Archimedes himself, there is a long list of properties satisfied by this figure. Boas's paper [3] presents some of them and is a good source for references.

It is quite surprising to discover that for 23 centuries no generalizations of this figure were introduced. Sondow [5] extended the original construction considering latus rectum arcs of parabolas instead of semicircles (see the center of Figure 1). In his paper, Sondow proves several interesting properties of his construction (named *parbelos*) that are, in some sense, counterparts of properties of the arbelos. More recently, the author [4] has considered a more general situation where the figure is bounded by the graphs of three functions that are similar, thus extending many of the known properties of the arbelos and parbelos. An example of this general construction (named f-belos) can be seen in the right-hand side of Figure 1.

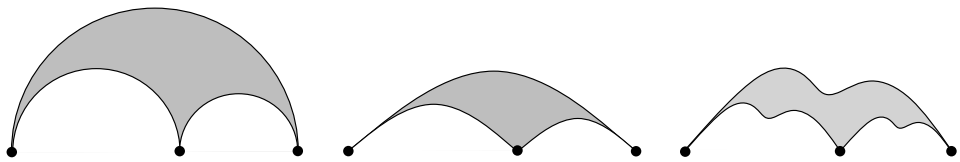

Figure 1. An arbelos (left), a parbelos (center) and an f-belos (right)

The idea of a 3-dimensional arbelos has already been introduced by Abu-Saymed and Hajja [1]. These authors define a 3-dimensional arbelos as the figure bounded by three hemispheres such that two are externally tangent to each other, and internally tangent to the third and whose equatorial circles lie on the same plane (see

Publication Date: March 13, 2016. Communicating Editor: Paul Yiu.

Figure 2). Nevertheless, not much attention has been paid to this possible generalization.

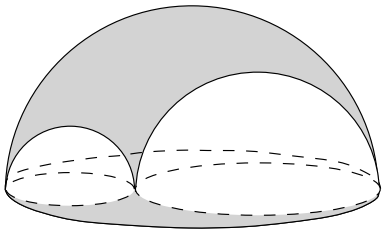

Figure 2. 3-dimensional arbelos

The following result was proved by Archimedes [2, Proposition 4]. We will refer to it as the *fundamental property* of the arbelos.

Proposition 1. *The area of the arbelos* (see Figure 3) *equals the area of the circle whose diameter AB is the portion inside the arbelos of the common tangent to the smaller circles. In other words, the area S of the arbelos is:*

$$S = \pi \left(\frac{\overline{AB}}{2} \right)^2.$$

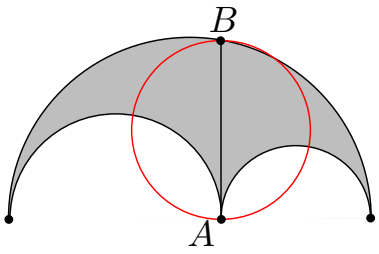

Figure 3. The fundamental property.

Remark. Observe that if R_1 and R_2 are the radii of the inner circles of the arbelos, then $\overline{AB} = 2\sqrt{R_1 R_2}$.

In this paper we will present the analogue of the fundamental property in the 3-dimensional case and we will search for a possible generalization in the n-dimensional case.

2. The fundamental property in 3 dimensions

Let us consider a 3-dimensional arbelos such that the radii of the inner hemispheres are R_1 and R_2. This implies that the outer hemisphere has radius $R_1 + R_2$. Hence, the volume of the arbelos is:

$$V = \frac{1}{2}\left[\frac{4}{3}\pi(R_1+R_2)^3 - \frac{4}{3}\pi R_1^3 - \frac{4}{3}\pi R_2^3\right] = 2\pi R_1 R_2 (R_1+R_2). \qquad (1)$$

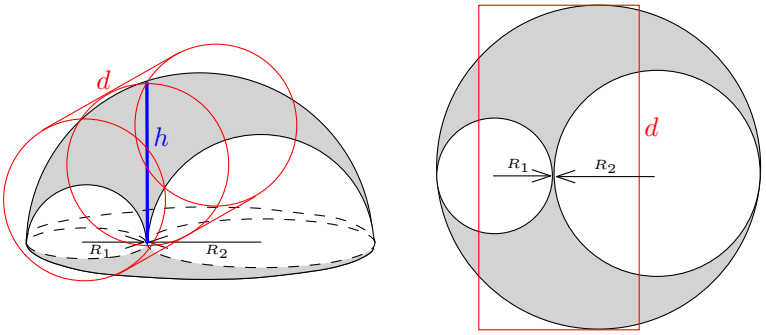

Figure 4. The fundamental property in dimension 3

Let us denote by h the length of the segment which is tangent to both inner hemispheres and perpendicular to the "base plane" (see Figure 4). Clearly we have that $h/2 = \sqrt{R_1 R_2}$. Also observe that $d = 2(R_1 + R_2)$ is precisely the diameter of the outer hemisphere (and also of its equatorial circle). The following result is an analogue of the fundamental property.

Proposition 2. *The volume of the 3-dimensional arbelos equals the volume of a cylinder whose base has diameter h and whose height is the diameter of the outer equatorial circle of the arbelos.*

Proof. The volume of such a cylinder is

$$V_c = \pi \left(\frac{h}{2}\right)^2 2(R_1 + R_2) = 2\pi R_1 R_2 (R_1 + R_2),$$

which coincides with the volume of the arbelos (1). □

3. The fundamental property in n dimensions

In order to extend the fundamental property to an arbitrary dimension we need to consider the volume of an n-dimensional ball. If we denote by $V_n(R)$ the bolumen of an n-dimensional ball of radius R, it is well-known that:

$$V_n(R) = \frac{\pi^{n/2}}{\Gamma\left(\frac{n}{2} + 1\right)} R^n,$$

where Γ denotes Euler Gamma function.

Hence, in order to extend the fundamental property of the arbelos, we are interested in the difference:

$$D_n = \frac{1}{2}\Big[V_n(R_1 + R_2) - V_n(R_1) - V_n(R_2)\Big].$$

In the previous sections we have seen that:

$$D_2 = \pi R_1 R_2 = V_2(h/2),$$
$$D_3 = 2\pi R_1 R_2 (R_1 + R_2) = V_2(h/2) V_1(d/2).$$

where $h/2 = \sqrt{R_1 R_2}$ and $d/2 = R_1 + R_2$.

Clearly we have that

$$D_n = \frac{\pi^{n/2}}{2\Gamma\left(\frac{n}{2}+1\right)}\Big[(R_1+R_2)^n - R_1^n - R_2^n\Big],$$

so we just have to analyze the behavior of $\delta_n(R_1,R_2) = (R_1+R_2)^n - R_1^n - R_2^n$. In particular, we want to express δ_n in terms of R_1R_2 and R_1+R_2.

To do so, for a fixed positive integer n, we recursively introduce a family of numbers $\{A_{p,q}(n) \mid 1 \leq p \leq n/2,\ 1 \leq q \leq n-2p+2\}$ in the following way:

$$A_{1,i}(n) = \binom{n}{i},$$
$$A_{k,i}(n) = A_{k-1,i+1}(n) - A_{k-1,1}(n)\binom{n-2k+2}{i}.$$

Obviously $A_{p,q}(n) \in \mathbb{Z}$ for every p,q for which $A_{p,q}(n)$ makes sense. Moreover, the following lemma gives a closed form for $A_{k,1}(n)$ that will be useful in the sequel. The proof is inductive and we omit.

Lemma 3.

$$A_{k,1}(n) = (-1)^{k+1}\frac{n}{k}\binom{n-k-1}{k-1}.$$

The following result shows how to express $\delta_n(R_1,R_2)$ as a polynomial in (R_1R_2) and (R_1+R_2).

Proposition 4. *For every integer $n \geq 2$, the following holds:*

$$\delta_n(x,y) = (x+y)^n - x^n - y^n = \sum_{k=1}^{\lfloor n/2\rfloor} A_{k,1}(n)(xy)^k(x+y)^{n-2k}.$$

Proof. We will give a sketch of the proof. Due to its recursive nature, details are left to the reader.

$$\begin{aligned}
\delta_n(x,y) &= xy\sum_{k=1}^{n-1}\binom{n}{k}x^{n-k-1}y^{k-1}\\
&= xy\left[\binom{n}{1}(x+y)^{n-2} + \sum_{k=1}^{n-3}\left[\binom{n}{k+1} - \binom{n}{1}\binom{n-2}{k}\right]x^{n-k-2}y^k\right]\\
&= A_{1,1}xy(x+y)^{n-2} + xy\sum_{k=1}^{n-3}A_{2,k}x^{n-k-2}y^k\\
&= A_{1,1}xy(x+y)^{n-2} + (xy)^2\sum_{k=1}^{n-3}A_{2,k}x^{n-k-3}y^{k-1}\\
&= A_{1,1}xy(x+y)^{n-2} + (xy)^2\left[A_{2,1}(x+y)^{n-4} + \sum_{k=1}^{n-5}A_{3,k}x^{n-k-4}y^k\right]
\end{aligned}$$

$$
\begin{aligned}
&= A_{1,1}xy(x+y)^{n-2} + (xy)^2 \sum_{k=1}^{n-3} A_{2,k}x^{n-k-3}y^{k-1} \\
&= A_{1,1}xy(x+y)^{n-2} + (xy)^2 \left[A_{2,1}(x+y)^{n-4} + \sum_{k=1}^{n-5} A_{3,k}x^{n-k-4}y^k \right] \\
&= A_{1,1}xy(x+y)^{n-2} + A_{2,1}(xy)^2(x+y)^{n-4} + (xy)^2 \sum_{k=1}^{n-5} A_{3,k}x^{n-k-4}y^k \\
&\vdots \\
&= \sum_{k=1}^{\lfloor n/2 \rfloor} A_{k,1}(n)(xy)^k(x+y)^{n-2k}.
\end{aligned}
$$

□

With all these ingredients, we can present the main result of the paper. Recall that $h = 2\sqrt{R_1R_2}$ and $d = 2(R_1 + R_2)$.

Theorem 5. *Let $n \geq 2$ be any integer. Then:*

$$D_n = \sum_{k=1}^{\lfloor n/2 \rfloor} \alpha_k(n) \Big[V_2(h/2) \Big]^k V_{n-2k}(d/2),$$

where

$$\alpha_k(n) = \frac{(-2)^{k-1}(n-2k)!!(n-k-1)!}{(n-2)!!k!(n-2k)!}.$$

Proof.

$$
\begin{aligned}
D_n &= \frac{\pi^{n/2}}{2\Gamma\left(\frac{n}{2}+1\right)} \delta_n(R_1,R_2) = \frac{\pi^{n/2}}{2\Gamma\left(\frac{n}{2}+1\right)} \sum_{k=1}^{\lfloor n/2 \rfloor} A_{k,1}(R_1R_2)^k(R_1+R_2)^{n-2k} \\
&= \frac{\pi^{n/2}}{2\Gamma\left(\frac{n}{2}+1\right)} \sum_{k=1}^{\lfloor n/2 \rfloor} (-1)^{k+1} \frac{n}{k} \binom{n-k-1}{k-1} (R_1R_2)^k(R_1+R_2)^{n-2k} \\
&= \sum_{k=1}^{\lfloor n/2 \rfloor} (-1)^{k+1} \frac{\Gamma\left(\frac{n-2k}{2}+1\right)}{k\Gamma\left(\frac{n}{2}\right)} \binom{n-k-1}{k-1} (\pi R_1R_2)^k \frac{\pi^{\frac{n-2k}{2}}}{\Gamma\left(\frac{n-2k}{2}+1\right)} (R_1+R_2)^{n-2k} \\
&= \sum_{k=1}^{\lfloor n/2 \rfloor} \alpha_k(n) \Big[V_2(h/2) \Big]^k V_{n-2k}(d/2).
\end{aligned}
$$

So, to finish the proof we will have a closer look at $\alpha_k(n)$.

$$\begin{aligned}\alpha_k(n) &= (-1)^{k+1}\frac{\Gamma\left(\frac{n-2k}{2}+1\right)}{k\Gamma\left(\frac{n}{2}\right)}\binom{n-k-1}{k-1}\\ &= (-1)^{k-1}\frac{(n-2k)!!\sqrt{\pi}2^{\frac{n-1}{2}}}{2^{\frac{n-2k+1}{2}}k(n-2)!!\sqrt{\pi}}\frac{(n-k-1)!}{(k-1)!(n-2k)!}\\ &= \frac{(-2)^{k-1}(n-2k)!!(n-k-1)!}{(n-2)!!k!(n-2k)!}\end{aligned}$$

□

Remark. Theorem 5 above extends the known results in $n = 2, 3$. In fact:

- In the case $n = 2$ Theorem 5 implies that (recall Proposition 1):

$$D_2 = \alpha_1(2)V_2(h/2)V_0(d/2) = V_2(h/2) = \pi\left(\frac{h}{2}\right)^2 = \pi R_1 R_2.$$

- In the case $n = 3$ we have that (recall Proposition 2):

$$D_3 = \alpha_1(3)V_2(h/2)V_1(d/2) = V_2(h/2)V_1(d/2) = 2\pi R_1 R_2(R_1 + R_2).$$

References

[1] S. Abu-Saymed and M. Hajja, The Archimedean Arbelos in Three-dimensional Space. *Result. Math.*, 52 (2008) 1–16.

[2] Archimedes, *The works of Archimedes*, Dover Publications Inc., Mineola, NY, 2002 (reprint of the 1897 edition and the 1912 supplement, Edited by T. L. Heath).

[3] H. P. Boas, Reflections on the arbelos, *Amer. Math. Monthly*, 113 (2006) 236–249.

[4] A. M. Oller-Marcén, The f-belos, *Forum Geom.*, 13 (2013) 103–111.

[5] J. Sondow, The parbelos, a parabolic analog of the arbelos, *Amer. Math. Monthly*, 120 (2013) 929-935.

Antonio M. Oller-Marcén: Centro Universitario de la Defensa, Academia General Militar, Ctra. de Huesca, s/n, 50090 Zaragoza, Spain

E-mail address: oller@unizar.es

Forum Geometricorum
Volume 16 (2016) 57–61.

FORUM GEOM
ISSN 1534-1178

Another Synthetic Proof of Dao's Generalization of the Simson Line Theorem

Nguyen Van Linh

Abstract. We give a synthetic proof of Dao's generalization of the Simson line theorem.

In [3], Dao Thanh Oai published without proof a remarkable generalization of the Simson line theorem.

Theorem 1 (Dao)**.** *Let ABC be a triangle with its orthocenter H, let P be an arbitrary point on the circumcircle. Let l be a line through the circumcenter and AP, BP, CP meet l at A_1, B_1, C_1, respectively. Denote A_2, B_2, C_2 the orthogonal projections of A_1, B_1, C_1 onto BC, CA, AB, respectively. Then A_2, B_2, C_2 are collinear and the line passing through A_2, B_2, C_2 bisects PH.*

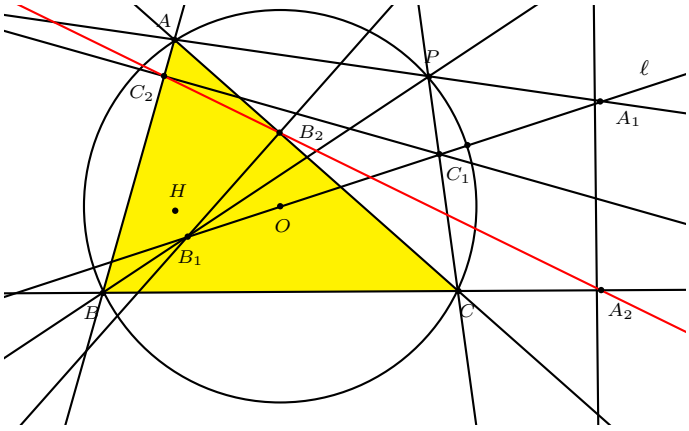

Figure 1. Dao's generalization of Simson line theorem

Note that when l passes through P, the line coincides with the simson line of P with respect to triangle ABC. Two proofs, by Telv Cohl and Luis Gonzalez, can be found in [2]. Nguyen Le Phuoc and Nguyen Chuong Chi have given a synthetic proof in [4]. In this note we give another synthetic proof of Theorem 1 by considering the reformulation.

Theorem 1′ *Let $ABCD$ be a quadrilateral inscribed in circle (O). An arbitrary line l through O intersects the lines AB, BC, CD, DA, AC, BD at X, Y, Z, T,*

Publication Date: March 13, 2016. Communicating Editor: Paul Yiu.

U, V, respectively. Denote by X_1, Y_1, Z_1, T_1, U_1, V_1 the orthogonal projections of X, Y, Z, T, U, V onto CD, AD, AB, BC, BD, AC respectively.
(a) *The six points X_1, Y_1, Z_1, T_1, U_1, V_1 all lie on a line $\mathcal{L}$.*
(b) *If H_a, H_b, H_c, H_d are the orthocenters of triangles BCD, CDA, DAB, ABC respectively, then AH_a, BH_b, CH_c, DH_d share a common midpoint K which lies on the line $\mathcal{L}$.*

We shall make use of two lemmas.

Lemma 2 ([1, Theorem 475])**.** *The locus of a point the ratio of whose powers with respect to two given circles is constant, both in magnitude and in sign, is a circle coaxal with the given circles.*

Lemma 3. *Let M, N, P, Q be the midpoints of AB, BC, CD, DA respectively, and d_M, d_N, d_P, d_Q the perpendiculars from M, N, P, Q to CD, DA, AB, BC respectively. The eight lines AH_a, BH_b, CH_c, DH_d, d_M, d_N, d_P, d_Q are concurrent.*

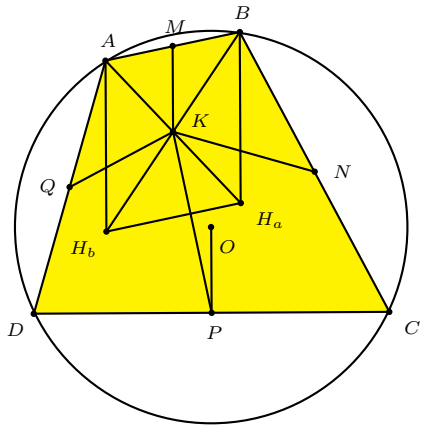

Figure 2. Lemma 3

Proof. Since the distance between one vertex of a triangle and its orthocenter is twice the one between circumcenter and the opposite side, we have $AH_b = 2OP = BH_a$. But $AH_b \parallel BH_a$ then AH_bH_aB is a parallelogram. This means AH_a and BH_b share a common midpoint K. The actually applies to every pair among the four segments AH_a, BH_b, CH_c and DH_d. Therefore, K is the common midpoint of the four segments. Moreover, MK is a midline of triangle ABH_a then $MK \parallel BH_a$, and is perpendicular to CD. It is the line d_M. Similarly, d_N, d_P, d_Q are the lines NK, PK, QK respectively. □

Proof of Theorem 1′

Denote Z_1', X_1' the intersections of Y_1T_1 with AB, CD, respectively.

We will show that the ratios of powers of four points Z_1', X, X_1', Z with respect to (O) and the circle with diameter YT are equal.

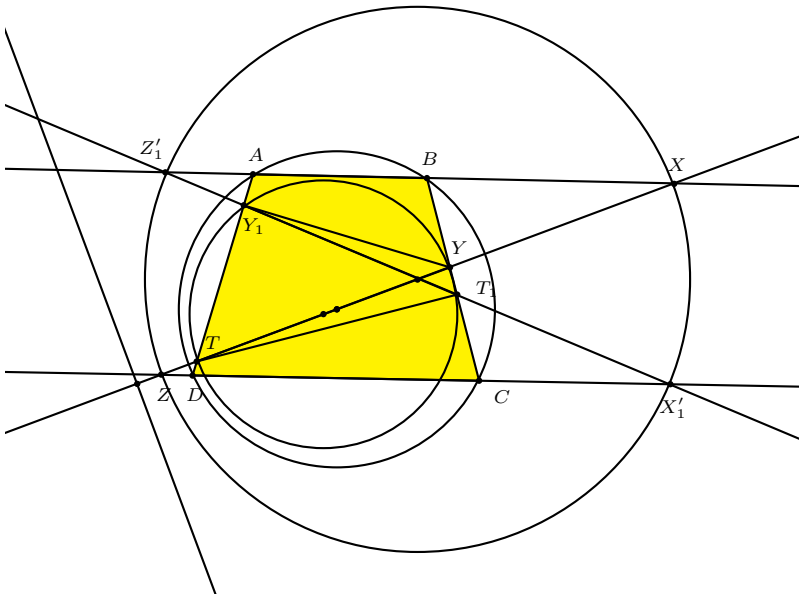

Figure 3. Proof of Theorem 1′(a)

By simple angle chasing, we have
(i) $\angle Z_1'Y_1A = \angle TY_1T_1 = \angle TYT_1 = \angle BYX$,
(ii) $\angle Z_1'AY_1 + \angle XAT = 180°$,
(iii) $\angle Z_1'T_1B = \angle ATX$,
(iv) $\angle Z_1'BT_1 + \angle YBX = 180°$.
From these,

$$\frac{\sin\angle Z_1'Y_1A}{\sin\angle Z_1'AY_1}\cdot\frac{\sin\angle Z_1'T_1B}{\sin\angle Z_1'BT_1} = \frac{\sin\angle XTA}{\sin\angle XAT}\cdot\frac{\sin\angle XYB}{\sin\angle XBY}$$
$$\Longrightarrow \frac{Z_1'A\cdot Z_1'B}{Z_1'Y_1\cdot Z_1'T_1} = \frac{XA\cdot XB}{XY\cdot XT}$$
$$\Longrightarrow \frac{\mathscr{P}_{(O)}(Z_1')}{\mathscr{P}_{(YT)}(Z_1')} = \frac{\mathscr{P}_{(O)}(X)}{\mathscr{P}_{(YT)}(X)}.$$

The same reasoning actually gives

$$\frac{\mathscr{P}_{(O)}(Z_1')}{\mathscr{P}_{(YT)}(Z_1')} = \frac{\mathscr{P}_{(O)}(X)}{\mathscr{P}_{(YT)}(X)} = \frac{\mathscr{P}_{(O)}(X_1')}{\mathscr{P}_{(YT)}(X_1')} = \frac{\mathscr{P}_{(O)}(Z)}{\mathscr{P}_{(YT)}(Z)}.$$

By Lemma 2, the four points X, Z, X_1', Z_1' lie on a circle ω which is coaxal with (O) and the circle with diameter YT. The center of ω obviously lies on l. Therefore, XZ is a diameter of ω. It follows that Z_1' and X_1' are the orthogonal projections of Z, X onto AB and CD respectively. This means X_1' and Z_1' coincide with X_1 and Z_1 respectively. Hence, X_1, Y_1, Z_1, T_1 are collinear on a line $\mathcal{L}$. By a similar reasoning the same line $\mathcal{L}$ also contains U_1 and V_1.

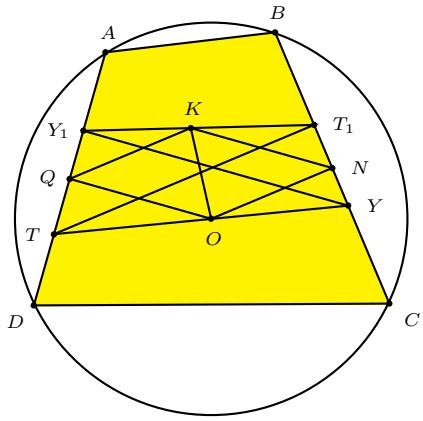

Figure 4. Proof of Theorem 1′(b)

On the other hand, by Lemma 3, QK is parallel to ON, and NK is parallel to OQ. Thus, $ONKQ$ is a parallelogram. From this, $\frac{KN}{Y_1Y} = \frac{OQ}{Y_1Y} = \frac{OT}{TY} = \frac{T_1N}{T_1Y}$. By Thales' theorem, T_1, K, Y_1 are collinear. Therefore, the line $\mathcal{L}$ containing the six points X_1, Y_1, Z_1, T_1, U_1, V_1 also passes through K. This completes the proof of Theorem 1′.

The Simson line theorem has a well-known property which states that *the angle between the Simson lines of two point P and P' is half the angle of the arc PP'*. In Theorem 1, if we choose another point P' on (O) and define A_2', B_2', C_2' analogously to A_2, B_2, C_2 respectively, then the angle between the lines through A_2, B_2, C_2 and A_2', B_2', C_2' is also half the angle of the arc PP'.

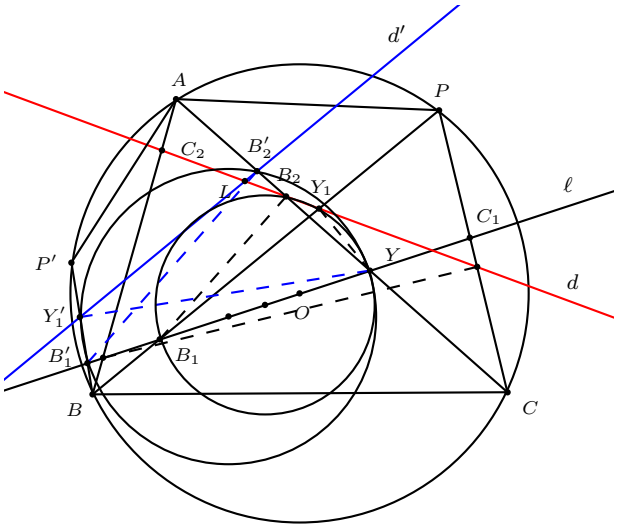

Figure 5. Another property of the generalization of Simson line

Proof. Let Y be the intersection of l and AC, Y_1, Y_1' be the orthogonal projections of Y onto $PB, P'B$, respectively; d and d' the lines through A_2, B_2, C_2 and A_2', B_2', C_2', respectively. Let d meets d' at L.

From the second form of Theorem 1, Y_1 lies on d and Y_1' lies on d'.

We have the directed angle between the lines d and d' given by

$$\begin{aligned}(d, d') &= \angle B_2' L B_2 \\ &= 180^\circ - \angle L B_2 B_2' - \angle L B_2' B_2 \\ &= \angle Y_1' B_1' B_1 - \angle Y_1 B_2 Y \\ &= \angle Y_1' B_1' B_1 - \angle Y_1 B_1 Y \\ &= \angle B_1' B B_1 \\ &= \angle P' B P,\end{aligned}$$

which is half the angle of the arc PP'. □

References

[1] Nathan Altshiller-Court, *College Geometry: An Introduction to the Modern Geometry of the Triangle and the Circle*, Dover Publications, New York, (2007) p.211-213.

[2] A. Bogomolny, *A Generalization of Simson line*, available at `http://www.cut-the-knot.org/m/Geometry/GeneralizationSimson.shtml`

[3] T. O. Dao, Advanced Plane Geometry, message 1781, September 20, 2014.

[4] L. P. Nguyen and C. C. Nguyen, A synthetic proof of Dao's generalization of the Simson line theorem, to appear in *Math. Gazette*.

[5] P. Yiu, Advanced Plane Geometry, message 1783, September 21, 2014.

Nguyen Van Linh: 22 Ba Chua Kho street, Bac Ninh city, Vietnam.
E-mail address: `lovemathforever@gmail.com`

Forum Geometricorum
Volume 16 (2016) 63–67.

FORUM GEOM
ISSN 1534-1178

A Ladder Ellipse Problem

Alan Horwitz

Abstract. We consider a problem similar to the well-known ladder box problem, but where the box is replaced by an ellipse. A ladder of a given length, s, with ends on the positive x- and y- axes, is known to touch an ellipse that lies in the first quadrant and is tangent to the positive x- and y-axes. We then want to find the height of the top of the ladder above the floor. We show that there is a value, $s = s_0$, such that there is only one possible position of the ladder, while if $s > s_0$, then there are two different possible positions of the ladder. Our solution involves solving an equation which is equivalent to a 4-th degree polynomial equation.

The well-known ladder box problem (see [1], [3]) involves a ladder of a given length, say s meters, with ends on the positive x- and y-axes, which touches a given rectangular box (a square in [4]) at its upper right corner (see Figure 1). One then wants to determine how high the top of the ladder is above the floor. Other versions of the problem ([4]) ask how much of the ladder is between the wall (or floor) and the point of contact of the ladder with the box.

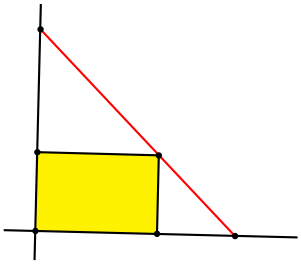

Figure 1

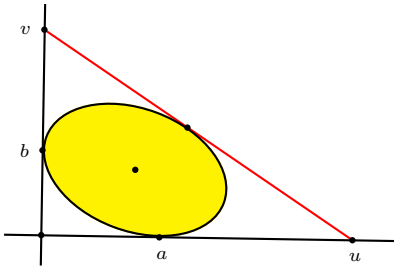

Figure 2

We ask similar questions in this note, but where the box is replaced by an ellipse, E_0, that lies in the first quadrant and is tangent to the positive x- and y-axes at the points $(a, 0)$ and $(0, b)$ (see Figure 2). For example, consider the ellipse with equation $x^2 + 4y^2 + 2xy - 8x - 16y + 16 = 0$, which is tangent to the positive x- and y-axes at the points $(4, 0)$ and $(0, 2)$. If the ladder has length 10 meters, then how high is the top of the ladder above the floor and how many positions of the ladder are possible? One main difference here is that we now allow the ladder to be tangent at any point of E_0 rather than just at the upper right corner of a rectangular

Publication Date: March 19, 2016. Communicating Editor: Paul Yiu.

box. We are also not given the point of tangency of the ladder with the ellipse, just the equation of the ellipse and the length of the ladder. We suppose that the ladder touches the positive x- and y-axes at the points $(u, 0)$ and $(0, v)$, respectively, and we call such a ladder admissible. We then want to find v, which is the height of the top of the ladder above the floor. It is not hard to show that the equation of E_0 must have the form

$$b^2x^2 + a^2y^2 + 2cxy - 2ab^2x - 2a^2by + a^2b^2 = 0, \tag{1}$$

and that if the equation of E_0 is given by (1), then E_0 is tangent to the positive x- and y-axes at the points $(a, 0)$ and $(0, b)$. Note that for (1) to represent an ellipse, we need $a^2b^2 - c^2 > 0$, which is equivalent to

$$ab > |c|. \tag{2}$$

We now assume throughout that T is the triangle with vertices $(0, 0)$, $(u, 0)$, and $(0, v)$ with $u, v > 0$.

Remark. There is another way to look at this problem: Given an ellipse, E_0, inscribed in a right triangle, T, suppose that we know the length of the hypotenuse of T and the points of tangency of E_0 with the other two sides of T. We want to find the lengths of the other sides of T.

The following proposition was proven in [2] for the case when T is the unit triangle. Throughout we let I denote the open interval $(0, 1)$ and I^2 the unit square $= (0, 1) \times (0, 1)$.

We now derive another form for the equation of E_0 which depends on two parameters, which we denote by w and t.

Proposition 1. *Let E_0 be an ellipse inscribed in T, tangent to the x- and y-axes at $T_1 = (ut,\ 0)$ and $T_2 = (0,\ wv)$ for $t, w \in (0,\ 1)$.*

(a) *The ellipse is tangent to the hypotenuse of T at the point*

$$T_3 = \left(\frac{ut(1-w)}{w+t-2wt},\ \frac{vw(1-t)}{w+t-2wt} \right).$$

(b) *The equation of the ellipse E_0 is*

$$\begin{aligned}(vw)^2x^2 + (ut)^2y^2 + 2wt(2w + 2t - 2wt - 1)uvxy \\ - 2ut(vw)^2x - 2wv(ut)^2y + (uvwt)^2 = 0.\end{aligned} \tag{3}$$

Proof. (a) It is well known that the lines joining the vertices of T to the points of tangency of E_0 with the opposite sides are concurrent at a point Q (see Figure 3). By Ceva's theorem,

$$\frac{AT_3}{T_3B} \cdot \frac{BT_2}{T_2O} \cdot \frac{OT_1}{T_1A} = 1 \implies \frac{AT_3}{T_3B} \cdot \frac{v - wv}{wv} \cdot \frac{tu}{u - tu} = 1.$$

Therefore,

$$\frac{AT_3}{T_3B} = \frac{(1-t)w}{(1-w)t},$$

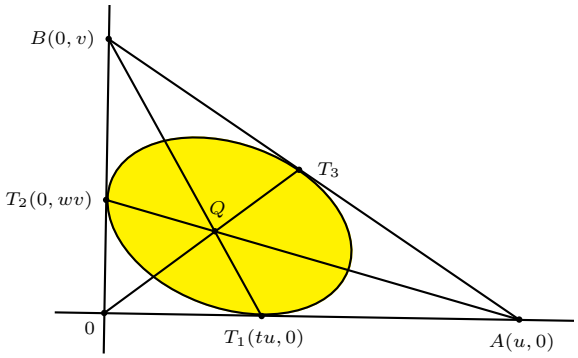

Figure 3

and

$$T_3 = \frac{(1-w)t\cdot A + (1-t)w\cdot B}{(1-t)w+(1-w)t} = \left(\frac{ut(1-w)}{w+t-2wt},\ \frac{vw(1-t)}{w+t-2wt}\right).$$

(b) With $a = tu$ and $b = wv$, the equation of the ellipse E_0 is given by (1) for some c. Since E_0 contains the point T_3, substitution of the coordinates of T_3 gives

$$c = wt(2w+2t-2wt-1)uv.$$

Hence, the equation (3) for the ellipse E_0. □

By Proposition 1(b), with $a = ut$ and $b = vw$, we may rewrite the equation of E_0 as

$$b^2x^2 + a^2y^2 + 2ab(2w+2t-2wt-1)xy - 2ab^2x - 2a^2by + a^2b^2 = 0. \quad (4)$$

Comparing (1) and (4) yields $c = ab(2w+2t-2wt-1)$, which implies that

$$w+t-wt = J, \quad J = \frac{1}{2}\left(1+\frac{c}{ab}\right) \quad (5)$$

for some J. Note that by (2) $ab > c$ and $ab > -c$, which implies that $0 < J < 1$. We want to choose (w,t) so that the ladder has the given length, s. Using $u = \frac{a}{t}$, $v = \frac{b}{w}$, we have $s^2 = u^2+v^2 = \frac{a^2}{t^2} + \frac{b^2}{w^2}$, and since $w = \frac{J-t}{1-t}$ from (5) we have $s^2 = f(t)$, where

$$f(t) = \frac{a^2}{t^2} + \frac{b^2(1-t)^2}{(J-t)^2}. \quad (6)$$

For $t \in I$, $\frac{J-t}{1-t} > 0$ if and only if $t < J$. Also, since $t < 1$, then $1 - \frac{J-t}{1-t} > 0$. Thus we have

$$w = \frac{J-t}{1-t} \Leftrightarrow t < J, \text{ where } t, J \in I. \quad (7)$$

Thus for given s, using (6), we want to solve the equation $f(t) = s^2$ for $t \in (0,J)$. For example, for the ellipse with equation $x^2+4y^2+2xy-8x-16y+16 = 0$, multiplying through by 4 yields the form of the equation given in (1), with $a = 4$, $b = 2$, and $c = 4$. Suppose, say that $s = 10$. That gives $f(t) = \frac{16}{t^2} + \frac{4(1-t)^2}{\left(\frac{3}{4}-t\right)^2}$ and it

is not hard to show that the equation $f(t) = 100$ has two solutions $t_1 = \frac{2}{3}$ and $t_2 \approx 0.43$ in $(0, J)$, $J = \frac{3}{4}$. The corresponding w values are then $w_1 = \frac{J-t_1}{1-t_1} = \frac{1}{4}$ and $w_2 = \frac{J-t_2}{1-t_2} \approx 0.56$, which gives $u_1 = \frac{a}{t_1} = 6$, $v_1 = \frac{b}{w_1} = 8$, $u_2 = \frac{a}{t_2} \approx 9.35$, and $v_2 = \frac{b}{w_2} \approx 3.57$. The corresponding points where the ladder is tangent to E_0 are $T_{3,1} = \left(\frac{36}{7}, \frac{8}{7}\right)$ and $T_{3,2} \approx (3.48, 2.24)$. For this example there are two different positions of the ladder, which is analogous to what happens with the ladder box problem. But are there always two different positions of the ladder ? To help answer this, first we assume that there is an admissible ladder of length s which touches E_0 , so it follows that the equation $f(t) = s^2$ has at least one solution in $(0, J)$. Since $\lim_{t\to 0^+} f(t) = \lim_{t\to J^-} f(t) = \infty$, $f(t) = s^2$ must have at least two solutions in $(0, J)$, counting multiplicities.

Now $f'(t) = -2\left(\frac{a^2}{t^3} - \frac{b^2(1-t)(1-J)}{(J-t)^3}\right)$ and the function of t, $y = \frac{a^2}{t^3}$, is clearly decreasing on $(0, J)$. Since $\frac{d}{dt}\left(\frac{1-t}{(J-t)^3}\right) = \frac{(J-t)^2(3-J-2t)}{(J-t)^6} > 0$ on $(0, J)$, the function of t, $y = \frac{b^2(1-t)(1-J)}{(J-t)^3}$ is increasing on $(0, J)$. Thus the equation $\frac{a^2}{t^3} = \frac{b^2(1-t)(1-J)}{((J-t)^3}$ has at most one solution in $(0, J)$. Since $\lim_{t\to 0^+} f'(t) = -\infty$ and $\lim_{t\to J^-} f'(t) = \infty$, f' has at least one root in $(0, J)$. Hence f' has exactly one root, say t_0, in $(0, J)$, and $\begin{cases} f'(t) < 0 & \text{if } 0 < t < t_0, \\ f'(t) > 0 & \text{if } t_0 < t < J. \end{cases}$. That in turn implies that f is decreasing on $(0, t_0)$ and is increasing on (t_0, J) and so $f(t) = s^2$ has at most two solutions in $(0, J)$. So we can conclude that $f(t) = s^2$ has exactly two solutions in $(0, J)$, *counting multiplicities*. The only way that there would be only one position of the ladder is if $f(t) - s^2$ has a double root in $(0, J)$. Can this actually happen ? To help answer this question, let E_R = rightmost open arc of E_0 between the points, P_H and P_V, on E_0 where the tangents are horizontal or vertical. Clearly there is an admissible ladder tangent to E_0 at any point of E_R. As the point of tangency approaches P_H or P_V, s approaches ∞. Hence there is a unique value $s_0 > 0$ such that there is an admissible ladder of length s tangent to E_0 at any point of E_R if and only if $s \geq s_0$. How does one find s_0? $s_0 = f(t_0)$, where t_0 is the unique root of f' in $(0, J)$ discussed above. For $s = s_0$, there is only one position of the ladder, while if $s > s_0$, then there are two different positions of the ladder. For the example above, $f'(t)$ has one root in $(0, J)$, $t_0 \approx 0.58$. Then $s_0 = f(t_0) \approx 72$.

Remarks. (1) Solving $f(t) = s^2$ is equivalent to solving the 4-th degree polynomial equation

$$p_s(t) = (a^2 - s^2t^2)(J - t)^2 + b^2t^2(1 - t)^2 = 0. \tag{8}$$

Note that one approach for solving the ladder box problem also involves solving a 4th degree polynomial equation.

(2) Another way to solve this problem would be to use an affine map to send E_0 to a circle, C, inscribed in a triangle, T' , which is now not necessarily a right triangle. Then the problem becomes: Suppose that we know the length of one side of a triangle, T', and we know that a circle, C, is inscribed in T' and we know the

points of tangency of the other two sides. Can one find the lengths of these two sides, and if yes, is the answer unique ?

A special Case. Not surprisingly, things simplify somewhat when the ellipse, E_0, is a circle. In that case $b = a$, $c = 0$, and $J = \frac{1}{2}$. The polynomial $p_s(t)$ from (8) factors as a product of two quadratics:

$$p_s(t) = -\frac{1}{4}\left(2(s-a)t^2 - (s-2a)t - a\right)\left(2(s+a)t^2 - (s+2a)t + a\right).$$

It is then easy to show that the critical number s_0 of f is given by $2(\sqrt{2}+1)a$, so that there are two different positions of the ladder when $s > 2(\sqrt{2}+1)a$.

References

[1] P. Baggett and A. Ehrenfeucht, The ladder and box problem: from curves to calculators, Oral presentation, History and Pedagogy of Mathematics, Deajeon, Republic of Korea, July 16-20, 2012.

[2] A. Horwitz, Dynamics of ellipses inscribed in triangles, to appear in *Journal of Science, Technology and Environment*, 5 (2016), Issue 1.

[3] D. Wells, *The Penguin Book of Curious and Interesting Puzzles*, 1992; p. 130.

[4] M. Zerger, The ladder problem, *Math. Mag.*, 60 (1987) 239–242.

Alan Horwitz: Penn State Brandywine, 25 Yearsley Mill Rd., Media, PA 19063, USA
E-mail address: alh4@psu.edu

Forum Geometricorum
Volume 16 (2016) 69–80.

FORUM GEOM
ISSN 1534-1178

Wernick's List: A Final Update

Pascal Schreck, Pascal Mathis, Vesna Marinković, and Predrag Janičić

Abstract. We present a final status of all problems from Wernick's list of triangle construction problems published in 1982 and with a number of unknown status until recently. Our results were obtained by a computer-based system for checking constructibility. We also developed a system for finding elegant constructions for solvable problems and for verifying their correctness. These systems helped in resolving problems open for decades, showing the power of modern computer systems in areas such as symbolic computation, problem solving, and theorem proving.

1. Introduction

In 1982, Wernick presented a list of straightedge and compass construction problems [23] (many of these problems were considered along the centuries, before this list was compiled). Each of them is a *triangle location problem*: the task is to construct a triangle ABC starting from three located points selected from the following set of sixteen characteristic points:

- A, B, C, O: three vertices and circumcenter;
- M_a, M_b, M_c, G: the side midpoints and centroid;
- H_a, H_b, H_c, H: three feet of altitudes and orthocenter;
- T_a, T_b, T_c, I: three feet of the internal angles bisectors and incenter.

There are 560 triples of the above points, but Wernick's list consists only of 139 significantly different non-trivial problems. The triple $\{A, B, C\}$ is trivial and, for instance, the problems $\{A, B, M_a\}$, $\{A, B, M_b\}$, $\{B, C, M_b\}$, $\{B, C, M_c\}$, $\{A, C, M_a\}$, and $\{A, C, M_c\}$ are considered to be symmetric (i.e., analogous). Wernick divided the problems into four categories:

Redundant problems: if there is a point in the given triple such that it is uniquely determined and constructible from the remaining two points, we say that the problem is *redundant* (and we denote it by **R**). For instance, the triple $\{A, B, M_c\}$ is redundant — given points A and B, the point M_c is uniquely determined.

Locus dependent problems: if there exists the required triangle ABC (not a way to construct it, but the triangle itself) only for given points meeting certain constraints, then we say that the problem is *locus dependent* (and we denote it by **L**). All such problems in Wernick's list have infinitely

Publication Date: March 19, 2016. Communicating Editor: Paul Yiu.

many solutions. For instance, for the problem $\{A, B, O\}$, the point O has to belong to the perpendicular bisector of AB, otherwise the corresponding triangle ABC does not exist.

Solvable problems: if there is a construction of the required triangle ABC (whenever it exists, while it does not exist only in some special cases) starting with the given points, we say that the problem is *solvable* or *constructible* (and we denote it by **S**).

Unsolvable problems: if for some given points the required triangle ABC exists, but it is not constructible, then we say that the problem is *unsolvable* or *unconstructible* (and we denote it by **U**).

In the original list, the problem 102 was erroneously marked **S** instead of **L** [18] and the problem 108 was erroneously marked **U** instead of **S** [20]. Wernick's list left 41 problems unresolved/unclassified, but the update from 1996 [18] left only 20 of them. Meanwhile, the problems 90, 109, 110, 111 [21], and 138 [22] were proved to be unsolvable. We are not aware of published solutions for remaining 15 unsolved problems (although there are indications that eight more were resolved [25]). Some of the problems were additionally considered for simpler solutions, like the problem 43 [1, 5], the problem 57 [24], and the problem 58 [4, 21]. Solutions for 59 solvable problems can be found on the Internet [21]. The status for all these problems was determined by ad-hoc attempts, with no systematic solving procedures or computer support involved.

Recently, we developed computer-based systems for checking constructibility for all problems from Wernick's list [20] and for finding constructions for solvable problems [16, 17, 13]. Thanks to the former system, we were able to fill-in all remaining slots in Wernick's list and now the status for all 139 problems is known. They are given in Table 1: there are 74 **S** problems, 39 **U** problems, 3 **R** problems, and 23 **L** problems. The problems are associated with references to the papers resolving their status (for the problems with no references, the status was given in the original Wernick's paper). More on these two systems is given in the following two sections.

2. Computer-Assisted Resolving of Unconstructible Problems

Our first method relies on algebraization of geometric constructions and Galois' results about straightedge and compass constructions of numbers. Let us first recall some classical results.

Let F be a field extension of $\mathbb{Q}$, and G a field extension of F. A number in G is straightedge and compass constructible in F if and only if it is equal to an expression using only numbers in F, arithmetic operations and square radicals. Such a number is algebraic in F, and its degree over F is a power of two. This result is known as Wantzel's result and is often used to prove that a number is not straightedge and compass constructible (for instance, in the demonstration of the impossibility of angle trisection using only straightedge and compass). The conjecture which states the opposite direction is generally false. This is why we also use a stronger result which is a consequence of Galois theory: an algebraic number

1.	A, B, O	L		48.	A, H_a, I	S		94.	M_a, G, T_a	S	
2.	A, B, M_a	S		49.	A, H_b, H_c	S		95.	M_a, G, T_b	U	[18]
3.	A, B, M_c	R		50.	A, H_b, H	L		96.	M_a, G, I	S	[18]
4.	A, B, G	S		51.	A, H_b, T_a	S		97.	M_a, H_a, H_b	S	
5.	A, B, H_a	L		52.	A, H_b, T_b	L		98.	M_a, H_a, H	L	
6.	A, B, H_c	L		53.	A, H_b, T_c	S		99.	M_a, H_a, T_a	L	
7.	A, B, H	S		54.	A, H_b, I	S		100.	M_a, H_a, T_b	U	[18]
8.	A, B, T_a	S		55.	A, H, T_a	S		101.	M_a, H_a, I	S	
9.	A, B, T_c	L		56.	A, H, T_b	U	[18]	102.	M_a, H_b, H_c	L	
10.	A, B, I	S		57.	A, H, I	S	[18]	103.	M_a, H_b, H	S	
11.	A, O, M_a	S		58.	A, T_a, T_b	S	[18]	104.	M_a, H_b, T_a	S	
12.	A, O, M_b	L		59.	A, T_a, I	L		105.	M_a, H_b, T_b	S	
13.	A, O, G	S		60.	A, T_b, T_c	S		106.	M_a, H_b, T_c	U	[18]
14.	A, O, H_a	S		61.	A, T_b, I	S		107.	M_a, H_b, I	U	[18]
15.	A, O, H_b	S		62.	O, M_a, M_b	S		108.	M_a, H, T_a	**S**	[20]
16.	A, O, H	S		63.	O, M_a, G	S		109.	M_a, H, T_b	U	[21]
17.	A, O, T_a	S		64.	O, M_a, H_a	L		110.	M_a, H, I	U	[21]
18.	A, O, T_b	S		65.	O, M_a, H_b	S		111.	M_a, T_a, T_b	U	[21]
19.	A, O, I	S		66.	O, M_a, H	S		112.	M_a, T_a, I	S	
20.	A, M_a, M_b	S		67.	O, M_a, T_a	L		113.	M_a, T_b, T_c	U	[20]
21.	A, M_a, G	R		68.	O, M_a, T_b	U	[18]	114.	M_a, T_b, I	U	[18]
22.	A, M_a, H_a	L		69.	O, M_a, I	S		115.	G, H_a, H_b	U	[18]
23.	A, M_a, H_b	S		70.	O, G, H_a	S		116.	G, H_a, H	S	
24.	A, M_a, H	S		71.	O, G, H	R		117.	G, H_a, T_a	S	
25.	A, M_a, T_a	S		72.	O, G, T_a	U	[18]	118.	G, H_a, T_b	U	[20]
26.	A, M_a, T_b	U	[18]	73.	O, G, I	U	[18]	119.	G, H_a, I	S	[20]
27.	A, M_a, I	S	[18]	74.	O, H_a, H_b	U	[18]	120.	G, H, T_a	U	[18]
28.	A, M_b, M_c	S		75.	O, H_a, H	S		121.	G, H, I	U	[18]
29.	A, M_b, G	S		76.	O, H_a, T_a	S		122.	G, T_a, T_b	U	[20]
30.	A, M_b, H_a	L		77.	O, H_a, T_b	U	[20]	123.	G, T_a, I	U	[20]
31.	A, M_b, H_b	L		78.	O, H_a, I	U	[20]	124.	H_a, H_b, H_c	S	
32.	A, M_b, H_c	L		79.	O, H, T_a	U	[18]	125.	H_a, H_b, H	S	
33.	A, M_b, H	S		80.	O, H, I	U	[18]	126.	H_a, H_b, T_a	S	
34.	A, M_b, T_a	S		81.	O, T_a, T_b	U	[20]	127.	H_a, H_b, T_c	U	[20]
35.	A, M_b, T_b	L		82.	O, T_a, I	S	[18]	128.	H_a, H_b, I	U	[20]
36.	A, M_b, T_c	S		83.	M_a, M_b, M_c	S		129.	H_a, H, T_a	L	
37.	A, M_b, I	S		84.	M_a, M_b, G	S		130.	H_a, H, T_b	U	[18]
38.	A, G, H_a	L		85.	M_a, M_b, H_a	S		131.	H_a, H, I	S	[18]
39.	A, G, H_b	S		86.	M_a, M_b, H_c	S		132.	H_a, T_a, T_b	U	[20]
40.	A, G, H	S		87.	M_a, M_b, H	S	[18]	133.	H_a, T_a, I	S	
41.	A, G, T_a	S		88.	M_a, M_b, T_a	U	[18]	134.	H_a, T_b, T_c	U	[20]
42.	A, G, T_b	U	[18]	89.	M_a, M_b, T_c	U	[18]	135.	H_a, T_b, I	U	[20]
43.	A, G, I	S	[18]	90.	M_a, M_b, I	U	[21]	136.	H, T_a, T_b	U	[20]
44.	A, H_a, H_b	S		91.	M_a, G, H_a	L		137.	H, T_a, I	U	[20]
45.	A, H_a, H	L		92.	M_a, G, H_b	S		138.	T_a, T_b, T_c	U	[22]
46.	A, H_a, T_a	L		93.	M_a, G, H	S		139.	T_a, T_b, I	S	
47.	A, H_a, T_b	S									

Table 1. The definitive status of all Wernick's problems

on F is constructible if and only if the splitting field of its minimal polynomial is an extension of degree 2^m for some m over F. This is equivalent to the fact that the cardinal of the Galois group of the minimal polynomial is also 2^m.

A point is straightedge and compass constructible from a set $\mathcal{B}$ of points if its coordinates are constructible on the extension of $\mathbb{Q}$ containing the coordinates of the points of $\mathcal{B}$. It is obvious that one of the points from $\mathcal{B}$ can have coordinates $(0,0)$, and another one can have coordinates $(k,0)$ where k is a given number. With Wernick's corpus, $\mathcal{B}$ contains three points, two of them can be fixed this way, whereas the third one must have free coordinates (a,b) in order to consider the generic case.

Let us also give a more precise meaning of the labels annotating the problems in Wernick's corpus. A problem has status **S** or **U** if it has solutions in the Euclidean plane, regardless constructibility using straightedge and compass: it has label **S** if it is straightedge and compass constructible, and label **U** (unconstructible) otherwise. The labels **R** and **L** correspond to over-constrained problems and are easy to check by using algebraic tools. We will not discuss this matter further within this text.

The general idea of the method consists of the following steps:

- translate the considered problem into a polynomial system,
- use *regular chains* to obtain a disjunction of irreducible polynomial systems,
- use Wantzel's result or Galois theory to prove constructibility or unconstructibility.

We made this pipeline automatic through an implementation in Maple [11] which offers several powerful tools like the regular chains and the computation of Galois group of a polynomial up to degree 9.

Actually, this idea is used in two different ways:

- First, we try to prove that the problem is not constructible: for this, we consider a *witness*, that is an example of triangle which is a solution of an instance of the problem with rational coordinates for the given points and we apply the method to this example. If this example is not constructible, then the problem is not solvable by straightedge and compass. We implemented a routine for automatically producing witness candidates and checking the whole list for unconstructibility.
- If the first method fails to prove the unconstructibility of the problem (for several witness candidates), we apply the method on the *parametric problem* which represents the general case. The calculi are much harder but complete: if each Galois group has a power of 2 as order, then the problem is constructible. And then, it is theoretically possible to extract a construction [2, 8], but it is very difficult to obtain and even for the simplest problems, the generic construction is geometrically unappealing. See, for instance, the problem 108 below.

Example 1. *We prove the unconstructibility of the problem 122:* $\{G,\ T_a,\ T_b\}$ *by choosing the coordinates* $T_b(0,0)$, $T_a(4,0)$ *and* $G(2,1)$. *Each of these points gives rise to two polynomial equations involving coordinates of points* $A(x_A,y_A)$, $B(x_B,y_B)$, *and* $C(x_C,y_C)$. *The triangularization process for this system of 6 equations gives two systems containing the following disqualifying equations:*
$P(y_C) = y_C^4 - 6y_C^3 - 51y_C^2 - 24y_C + 36$

the splitting field of which is of order 24, meaning that even if the degree of the polynomial is 4, it is not solvable by square radicals, and
$P(y_C) = 2701y_C^3 - 12871y_C^2 + 43008y_C - 28224$
with degree 3. Therefore, this problem is not constructible.

Example 2. *In the problem 108, the given points are T_a, H and M_a, we use the coordinates $(0,0)$ for T_a, $(1,0)$ for M_a, and parametric coordinates (a,b) for H. The triangularization of the corresponding polynomial system gives the following system:*

$$\begin{cases} x_C + x_B - 2 = 0 \\ -a^2 - by_A + x_B^2 + 2a - 2x_B = 0 \\ y_C = 0 \\ y_B = 0 \\ x_A - a = 0 \\ a^3 + aby_A - a^2 + y_A^2 = 0 \end{cases}$$

which is obviously constructible (all the equations have degree at most 2) *and moreover, it is simple enough to solve with square radicals, for instance $y_A = (a/2)(-b \pm \sqrt{b^2 - 4a + 4})$, and to translate the formulas into a straightedge and compass construction that mimics the computation (Figure 1). Recall that it is possible to perform additions, multiplications, divisions and root extract by using ruler and compass constructions.*

This construction might not be elegant, but it is perfectly valid. A new challenge might be to find appealing geometric constructions for problems 108[1] *and 119* (see below).

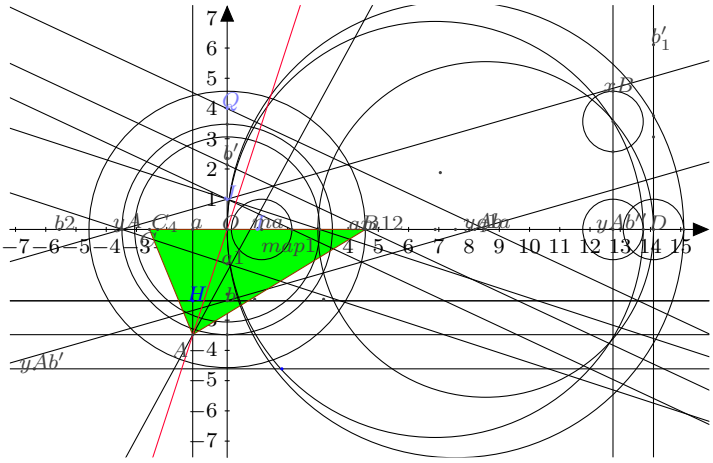

Figure 1. Geometric translation in GeoGebra of the system given in Example 2. Parameters a and b correspond to the *free* point H: this point can be moved and the figure is transformed accordingly.

[1]The GeoGebra figure can be found at url `https://sites.google.com/site/pascalschreck/adg14`

In Appendix, we list relevant polynomials for all the problems with unknown status in [20].

3. Computer-Assisted Solving of Constructible Problems

Our second system, ArgoTriCS, equipped with relevant geometry knowledge, pursues very different aims. It is capable of solving almost all solvable problems from Wernick's list: 66 out of 74 [16, 15, 13]. The system was implemented in PROLOG, has around 6000 lines of code, while the solving times span from a couple of milliseconds to more than an hour. The longest generated construction is the construction for the problem 101: $\{M_a, H_a, I\}$ – it consists of 14 steps (mostly compound construction steps, such as construction of the midpoint of a segment). The system also detects if the problem is redundant or locus dependent. The system produces a construction in a natural language form, and in the format of a dynamic geometry tool GCLC [9], so corresponding illustrations can be also automatically generated. The next example shows an automatically generated solution for the problem $25 : \{A, M_a, T_a\}$ (along with non-degenerate conditions and determination conditions), while the corresponding illustration is given in Figure 2.

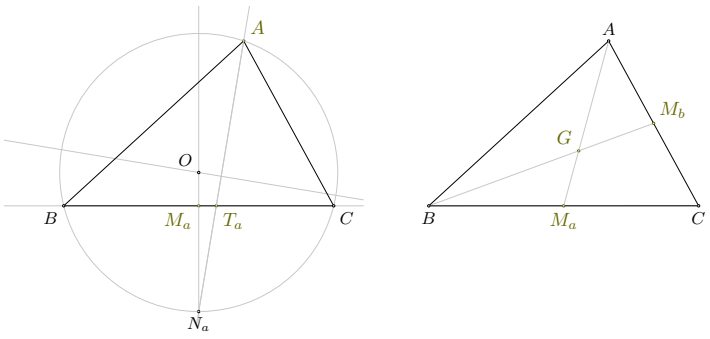

Figure 2. Illustration for the problem 25 (left) and for the problem 84 (right)

Example 3. *Given points A, M_a, and T_a, construct the triangle ABC.*

(1) *Using the point A and the point T_a, construct a line s_a (rule W02);*
(2) *Using the point M_a and the point T_a, construct a line a (rule W02);*
(3) *Using the point M_a and the line a, construct a line m_a (rule W10b);*
(4) *Using the line m_a and the line s_a, construct a point N_a (rule W03);*
(5) *Using the point A and the point N_a, construct a line $m(AN_a)$ (rule W14);*
(6) *Using the line $m(AN_a)$ and the line m_a, construct a point O (rule W03);*
(7) *Using the point A and the point O, construct a circle $k(O, C)$ (rule W06);*
(8) *Using the circle $k(O, C)$ and the line a, construct a point C and a point B (rule W04).*

Non-degenerate conditions: line a and circle $k(O, C)$ intersect; points A and O are not the same; lines $m(AN_a)$ and m_a are not parallel; lines m_a and s_a are not parallel.

Determination conditions: lines $m(AN_a)$ and m_a are not the same; points A and N_a are not the same; lines m_a and s_a are not the same; points M_a and T_a are not the same; points A and T_a are not the same.

Unlike other systems for automatically solving construction problems, the system ArgoTriCS also considers correctness of the constructions generated and invokes automated geometry theorem provers – OpenGeoProver [12] and the provers built in the GCLC tool. Each construction generates three theorems – one for each given point; for instance, if the point G is given, then it should be proved that G is indeed the centroid of the constructed triangle ABC. So, for 92 problems solved by ArgoTriCS (66 **S** problems, and all **L** and **R** problems), there are 276 theorems (some of them trivial – if a triangle vertex is given). Out of 276 theorems, 194 were successfully proved by at least one prover. In addition, for all problems involving only the points $A, B, C, M_a, M_b, M_c, G$, we generated machine verifiable proofs for the correctness of constructions – proofs verified by the proof assistant Isabelle [19]. The next example gives an automatically generated solution for the problem $84 : \{M_a, M_b, G\}$, illustrated in Figure 2.

Example 4. *Given points M_a, M_b, and G, construct the triangle ABC.*

(1) *Using the point M_a and the point G, construct a point A (rule W01);*
(2) *Using the point M_b and the point G, construct a point B (rule W01);*
(3) *Using the point M_a and the point B, construct a point C (rule W01).*

No non-degenerate conditions.
No determination conditions.

For this problem, the central theorem proved formally within the Isabelle proof assistant, with a help of automated theorem provers, is the following:

$$\forall M_a, M_b, G.$$
$$\neg collinear(M_a, M_b, G) \Leftrightarrow \exists A, B, C.(midpoint(M_a, B, C) \wedge$$
$$midpoint(M_b, A, C) \wedge centroid(G, A, B, C) \wedge \neg collinear(A, B, C))$$

The system ArgoTriCS was used for automatically generating a compendium[2] of all problems from the extended Wernick's list (for all 560 triples of characteristic problems) – spanning around 3000 pages, and also an on line encyclopedia with animated solutions for all solved problems [14].

4. Conclusions and Future Work

In this paper we presented the final version of Wernick's list – a list of triangle location problems, presented in 1982 and with a number of construction problems with unknown statuses until recently. These updates were produced by our computer-based systems, while for almost all solvable problems our system can produce elegant constructions with associated illustrations. These results show the

[2]Available online from: `http://www.matf.bg.ac.rs/~vesnap/compendium_wernick.pdf`

power of modern computer systems in areas such as symbolic computation, problem solving and theorem proving.

For future work, we are planning to consider, in analogy, other corpora of triangle construction problems — location problems involving additional points [3] or construction problems based on various geometrical quantities [10, 6, 7].

References

[1] J. Anglesio and V. Schindler, Solution to problem 10719, *Amer. Math. Monthly*, 107 (2000) 952–954.

[2] G. Chen, Les constructions à la règle et au compas par une méthode algébrique (in french), Master's thesis, Université Louis Pasteur, 1992. available at url https://sites.google.com/site/pascalschreck/home/recherche/arti.

[3] H. Connelly, An extension of triangle constructions from located points, *Forum Geom.*, 9 (2009) 109–112.

[4] H. Connelly, N. Dergiades, and J.-P. Ehrmann, Construction of triangle from a vertex and the feet of two angle bisectors, *Forum Geom.*, 7 (2007) 103–106.

[5] E. Danneels, A Simple Construction of a Triangle from its Centroid, Incenter, and a Vertex, *Forum Geom.*, 5 (2005) 53–56.

[6] V. B. Fursenko, Lexicographic account of triangle construction problems (part I) (in Russian), *Mathematics in schools*, 5 (1937) 4–30

[7] V. B. Fursenko, Lexicographic account of triangle construction problems (part II) (in Russian), *Mathematics in schools*, 6 (1937) 21–45.

[8] X. S. Gao and S. C. Chou, Solving geometric constraint systems. II. A symbolic approach and decision of Rc-constructibility, *Computer Aided Design*, 30 (1998) 115–122.

[9] P. Janičić, Geometry constructions language, *Journal of Automated Reasoning*, 44 (2010) 3–24.

[10] L. Lopes, *Manuel de Construction de Triangles*, QED Texte, 1996.

[11] Maplesoft, *Maple 18*, Maplesoft, a division of Waterloo Maple Inc., Waterloo, Ontario.

[12] F. Marić, I. Petrović, D. Petrović, and P. Janičić, Formalization and implementation of algebraic methods in geometry. in Pedro Quaresma and Ralph-Johan Back, editors, Proceedings First Workshop on *CTP Components for Educational Software*, Wrocław, Poland, 31th July 2011, volume 79 of *Electronic Proceedings in Theoretical Computer Science*, pages 63–81. Open Publishing Association, 2012.

[13] V. Marinković, ArgoTriCS – Automated triangle construction solver, to appear in *Journal of Experimental and Theoretical Artificial Intelligence*, 2015.

[14] V. Marinković, On-line compendium of triangle construction problems with automatically generated solutions, *The Teaching of Mathematics*, pages 29–44, 2015.

[15] V. Marinkovic, P. Janicic, and P. Schreck, Computer theorem proving for verifiable solving of geometric construction problems, in Francisco Botana and Pedro Quaresma, editors, *Automated Deduction in Geometry - 10th International Workshop, ADG 2014, Coimbra, Portugal, July 9-11, 2014, Revised Selected Papers*, volume 9201 of *Lecture Notes in Computer Science*, pages 72–93. Springer, 2014.

[16] V. Marinković and P. Janičić, Towards understanding triangle construction problems, in J. Jeuring et al., editor, *Intelligent Computer Mathematics - CICM 2012*, volume 7362 of *Lecture Notes in Computer Science*. Springer, 2012.

[17] V. Marinković, P. Janičić, and P. Schreck, Solving geometric construction problems supported by theorem proving, in *Proceedings of the 10th International Workshop on Automated Deduction in Geometry (ADG 2014)*, pages 121–146. CISUC Technical Report TR 2014/01, University of Coimbra, 2014.

[18] L. F. Meyers, Update on William Wernick's triangle constructions with three located points, *Math. Mag.*, 69 (1996) 46–49.

[19] L. C. Paulson, *Isabelle: a Generic Theorem Prover*, volume 828 of *Lecture Notes in Computer Science*, Springer, 1994.

[20] P. Schreck and P. Mathis. RC-constructibility of problems in Wernick's list, in *Proceedings of the 10th International Workshop on Automated Deduction in Geometry (ADG 2014)*, pages 85–104. CISUC Technical Report TR 2014/01, University of Coimbra, 2014. available at URL `http://www.uc.pt/en/congressos/adg/adg2014/program/proceedings`.
[21] E. Specht, Wernicks Liste (in Deutsch), `http://hydra.nat.uni-magdeburg.de/wernick/`.
[22] A. V. Ustinov, On the construction of a triangle from the feet of its angle bisectors, *Forum Geom.*, 9 (2009) 279–280.
[23] W. Wernick, Triangle constructions vith three located points, *Math. Mag.*, 55 (1982) 227–230.
[24] P. Yiu, Elegant geometric constructions, *Forum Geom.*, 5 (2005) 75–96.
[25] S. Zukowski, Approaching constructability of triangles, *Young Mathematicians Conference*, the Ohio State University, 2010.

Appendix: Summary of our results

We recall here the results used in [20], by giving coordinates of the characteristic points of the problem, and then the last equation of the systems obtained after triangularization using the Maple implementation of regular chains. Fortunately, testing the last equation was enough for the open problems.

Wernick 77 : O, H_a, T_b
Coordinates: $(0,0)$, $(-1,-3)$ and $(-3,0)$.

$$84349y_A^8 + 668100y_A^7 + 908434y_A^6 - 6940782y_A^5 - 32743501y_A^4 - 63643476y_A^3 - 72253168y_A^2 - 56499066y_A - 25568010,$$

the splitting field of which has degree $8! = 40320$ which is not a power of 2: this problem is not RC-constructible.

Wernick 78 : I**,** O**,** H_a
Coordinates: $(0,0)$, $(0,1)$,$(-1,-3)$.

$$P(y_C) = 325y_C^8 + 2050y_C^7 - 75y_C^6 - 11256y_C^5 + 7749y_C^4 + 8964y_C^3 - 107730y_C^2 + 160380y_C - 14580,$$

the splitting field of which has degree $\frac{8!}{105} = 384$ which is not a power of 2. Therefore, this problem is not RC-constructible.

Wernick 81: O**,** T_a**,** T_b
Coordinates: $(0,0)$, $(-1,-3)$ and $(-3,0)$.

$$P(y_C) = 5202928809y_C^8 + 34323168906y_C^7 + 64988457138y_C^6 - 168831818766y_C^5 - 1131189431845y_C^4 - 2336530456944y_C^3 - 2257027274736y_C^2 - 1030105859328y_C - 178376649984,$$

the splitting field of which has degree $8! = 40320$. Therefore, this problem is not RC-constructible.

Wernick 113: T_c**,** T_b**,** M_a
Coordinates: $(0,0)$, $(2,2)$ and $(4,0)$. We get two systems, for the first one we have the polynomial:
$P(y_C) = 25y_C^3 - 94y_C^2 + 160y_C - 128$
and for the second one:
$P(y_C) = 3y_C^3 - 10y_C^2 + 60y_C - 72$.
Therefore, this problem is not RC-constructible.

Wernick 118: T_b**,** H_a**,** G
Coordinates $T_b(0,0)$, $H_a(6,0)$ and $G(4,3)$:

$P(y_C) = y_C^5 + 136y_C^4 - 848y_C^3 + 14112y_C^2 - 52164y_C + 52488.$
Therefore, this problem is not RC-constructible.

Wernick 119 I**,** H_a**,** G
When choosing coordinates $(0,0)$ for I, $(1,-2)$ for H_a and $(1,1)$ for G, we obtain two systems. The second one corresponds to non real solutions, and the first one contains the following polynomial of degree 4:

$P(y_C) = 289y_C^4 - 867y_C^3 - 57528y_C^2 - 99144y_C - 41472,$
the splitting field of which has degree 8 over $\mathbb{Q}$. This result does not mean that the problem is RC-constructible. In order to prove its RC-constructibility, we have to take parameters a and b as coordinates for one of the three points and then compute its Galois group. The triangularization produces a huge system displayed with more than 400 lines and the coefficient of the degree 4 term of the irreducible polynomial we want to test is :

$$\begin{aligned}
&19683a^9 - 59049a^8 + (78732b^2 + 61236)a^7 + (-183708b^2 - 20412)a^6 \\
&+ (118098b^4 + 166212b^2 - 4374)a^5 + (-196830b^4 - 72900b^2 + 2754)a^4 \\
&+ (78732b^6 + 148716b^4 + 10692b^2 + 324)a^3 + (-78732b^6 - 61236b^4 + 3564b^2 - 108)a^2 \\
&+ (19683b^8 + 43740b^6 + 18954b^4 - 756b^2 - 21)a - 6561b^8 - 8748b^6 - 3078b^4 - 108b^2 - 1.
\end{aligned}$$

Maple is powerful enough to compute Galois' group of this huge parameterized polynomial and find:

$$"4T3", \{"D(4)"\}, " - ", 8, \{"(13)", "(1234)"\}$$

From this result, we can conclude that the problem is RC-constructible.

We confirm that result by using Gao and Chou's method [8]. This method leads to heavy computations but allows, in principle, to extract a RC-construction. Unfortunately, it is almost impossible for this concrete problem. The equation of degree 3 considered in that method is huge: this is, for the sake of illustration, just the coefficients for the term of degree 3:

$$\begin{aligned}
&12754584a^{13} + 76527504a^{11}b^2 + 191318760a^9b^4 + 255091680a^7b^6 + 191318760a^5b^8 \\
&+ 76527504a^3b^{10} + 12754584ab^{12} - 55269864a^{12} - 280600848a^{10}b^2 - 573956280a^8b^4 \\
&- 595213920a^6b^6 - 318864600a^4b^8 - 76527504a^2b^{10} - 4251528b^{12} + 93533616a^{11} \\
&+ 416649744a^9b^2 + 731262816a^7b^4 + 629226144a^5b^6 + 263594736a^3b^8 + 42515280ab^{10} \\
&- 72748368a^{10} - 314613072a^8b^2 - 515852064a^6b^4 - 387361440a^4b^6 - 121877136a^2b^8 \\
&- 8503056b^{10} + 18108360a^9 + 115263648a^7b^2 + 214465968a^5b^4 + 155574432a^3b^6 \\
&+ 38263752ab^8 + 8030664a^8 - 4408992a^6b^2 - 48813840a^4b^4 - 42200352a^2b^6 \\
&- 5826168b^8 - 4269024a^7 - 11547360a^5b^2 + 1469664a^3b^4 + 9867744ab^6 - 536544a^6 \\
&+ 2309472a^4b^2 + 2869344a^2b^4 - 1469664b^6 + 355752a^5 + 618192a^3b^2 - 390744ab^4 \\
&+ 55080a^4 - 89424a^2b^2 - 71928b^4 - 9936a^3 - 24624ab^2 - 3024a^2 - 1296b^2 - 264a - 8.
\end{aligned}$$

Wernick 122: T_b**,** T_a**,** G
With coordinates $T_b(0,0)$, $T_a(4,0)$ and $G(2,1)$, we get two systems containing the disqualifying equations:

$P(y_C) = y_C^4 - 6y_C^3 - 51y_C^2 - 24y_C + 36$
the splitting field of which is of order 24 and

$P(y_C) = 2701y_C^3 - 12871y_C^2 + 43008y_C - 28224$
Therefore, this problem is not RC-constructible.

Wernick 123: I**,** T_a**,** G
With the coordinates $(0,0)$, $(4,0)$ and $(2,1)$, we obtain three irreducible triangular systems, but the last one does not have real solutions. The first one contains the polynomial:

$$P(y_C) = 98596y_C^8 - 533172y_C^7 + 1934365y_C^6 - 2612838y_C^5 + 541114y_C^4 + 2325666y_C^3 + 162729y_C^2 - 3815532y_C + 1555848$$

the Galois group of which is:
$"8T44", "[2^4]S(4)", " - ", 384, "(48)", "(18)(45)", "(1238)(4567)"$

And the second one

$P(y_C) = 4y_C^6 - 36y_C^5 + 192y_C^4 - 612y_C^3 + 81y_C^2 + 2025y_C - 3402$

Therefore, this problem is not RC-constructible.

Wernick 127: T_c**,** H_b**,** H_a
Coordinates $(0,0)$, $(0,-6)$ and $(6,-2)$.
$P(y_C) = 8125y_C^4 + 146484y_C^3 + 830844y_C^2 + 1715040y_C + 1049760$

The splitting field of which has degree 24 over $\mathbb{Q}$. Therefore, this problem is not RC-constructible.

Wernick 128: T_c**,** H_b**,** H_a
Coordinates $(0,0)$, $(0,-6)$ and $(6,-2)$.

$P(y_C) = 8125y_C^4 + 146484y_C^3 + 830844y_C^2 + 1715040y_C + 1049760$
which is not RC-resolvable since its splitting field has degree 24. Therefore, this problem is not RC-constructible.

Wernick 132: T_a**,** T_b**,** H_a
Coordinates $(0,0)$, $(4,0)$, and $(-1,3)$.

$$P(y_C) = 9825y_C^6 - 72620y_C^5 + 691848y_C^4 - 403200y_C^3 + 1442880y_C^2 + 10886400y_C - 15552000.$$

Therefore, this problem is not RC-constructible.

Wernick 134: T_c**,** T_b**,** H_a
Coordinates $(0,0)$, $(0,2)$ and $(2,1)$.

$$P(y_C) = 524475y_C^8 - 5345280y_C^7 + 24048076y_C^6 - 62358704y_C^5 + 102412544y_C^4 - 109631360y_C^3 + 75046720y_C^2 - 30134400y_C + 5432000,$$

the Galois group of which is of order 384. Therefore, this problem is not RC-constructible.

Wernick 135: I**,** T_b**,** H_a
With points $I(0,0)$, $T_b(0,2)$ and $H_a(2,-1)$, we get two systems. In the first one, we have the polynomial:

$$\begin{aligned}P(y_C) =& 58968y_C^8 - 194436y_C^7 + 453056y_C^6 - 311496y_C^5 + 319980y_C^4 - 526960y_C^3 \\ &+ 466030y_C^2 - 210025y_C + 28000,\end{aligned}$$

the splitting field of which has degree 40320.
And we have in the second one:
$P(y_C) = 572y_C^5 - 1624y_C^4 + 2088y_C^3 + 2532y_C^2 - 585y_C + 1200$
Therefore, this problem is not RC-constructible.

Wernick 136: T_a**,** T_b**,** H
With points $T_a(0,0)$, $T_b(4,0)$ and $H(2,-1)$, we get two systems. The first one contains the polynomial:

$P(y_C) = 15y_C^4 - 8y_C^3 - 148y_C^2 - 32y_C + 192$
the splitting field of which has degree 24. And we have in the second one:

$P(y_C) = 5705y_C^3 + 25412y_C^2 + 12288y_C - 9216.$
Therefore, this problem is not RC-constructible.

Wernick 137 : I, T_a, H
Coordinates $(0,0)$, (a,b) and $(0,-2)$. We take parameters as coordinates of T_a as we thought that the problem was constructible. We obtain two systems after more than 6 hours of computation. The following polynomial in y_A is the last equation of the first component

$$\begin{aligned}&(9a^4 + (18b^2 + 36b - 12)a^2 + 9b^4 + 36b^3 + 84b^2 + 96b + 64)y_A^4 \\ &+ (18a^4 + (78b^2 + 192b + 48)a^2 + 60b^4 + 192b^3 + 352b^2 + 288b + 128)y_A^3 \\ &+ ((30b + 36)a^4 + (30b^3 + 160b^2 + 256b + 96)a^2 + 148b^4 + 384b^3 + 528b^2 + 320b + 64)y_A^2 \\ &+ ((24b + 24)a^4 + (96b^3 + 224b^2 + 160b + 32)a^2 + 160b^4 + 352b^3 + 320b^2 + 128b)y_A \\ &+ (24b^2 + 24b)a^4 + (80b^3 + 112b^2 + 32b)a^2 + 64b^4 + 128b^3 + 64b^2,\end{aligned}$$

the Galois group of which is:
"$4T5$","$S(4)$","$-$",24,"(14)","(24)","(34)".
The second system provides an equation of degree 3. We can then conclude that this problem is not RC-constructible.

Pascal Schreck: ICube, UMR CNRS 7357, Université de Strasbourg, France
E-mail address: schreck@unistra.fr

Pascal Mathis: ICube, UMR CNRS 7357, Université de Strasbourg, France
E-mail address: mathis@unistra.fr

Vesna Marinković: Faculty of Mathematics, University of Belgrade, Serbia
E-mail address: vesnap@matf.bg.ac.rs

Predrag Janičić: Faculty of Mathematics, University of Belgrade, Serbia
E-mail address: janicic@matf.bg.ac.rs

Forum Geometricorum
Volume 16 (2016) 81–84.

FORUM GEOM
ISSN 1534-1178

An Improvement of Bîrsan's Inequalities for the Sides of a Triangle

Yurii N. Maltsev and Anna S. Kuzmina

Abstract. In terms of the distance d between the circumcenter and the incenter of a triangle, Bîrsan's inequalities can be rewritten as $4((R-d)^2-r^2) \le a^2 \le 4((R+d)^2-r^2)$, where R and r are respectively the circumradius and inradius, and a is the length of a side of the triangle. We improve these inequalities by finding the best lower and upper bounds of a^2.

1. Introduction

Let R and r be the circumradius and the inradius of an arbitrary triangle ABC, O and I be the circumcenter and the incenter of the triangle ABC, $d = OI$ (see Figure 1).

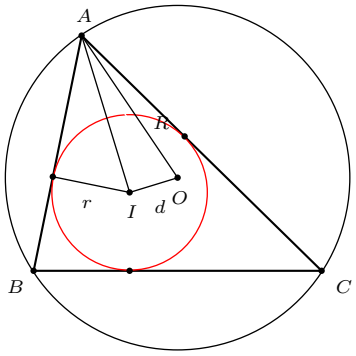

Figure 1

T. Bîrsan [1] has established the following inequalities

$$8R^2-8Rr-4r^2-8R\sqrt{R^2-2Rr} \le a^2 \le 8R^2-8Rr-4r^2+8R\sqrt{R^2-2Rr}, \tag{1}$$

where a is the length of a side of the triangle ABC. By Euler's theorem, $d = \sqrt{R^2-2Rr}$ (see, for example, [2, Theorem 295] or [3]). Hence, Bîrsan inequalities (1)) may been written as

$$4((R-d)^2-r^2) \le a^2 \le 4((R+d)^2-r^2). \tag{2}$$

Publication Date: March 19, 2016. Communicating Editor: Paul Yiu.

This work is supported by a grant from the Ministry of Education and Science of the Russian Federation, project No. 2014/418 for the implementation of State order in the research field (fundamental component).

The authors express gratitude to the referee for valuable remarks.

In this paper, we improve these inequalities by finding the best lower and upper bounds of a^2 for the lengths of the sides. Here is the main result.

Theorem 1. *Let a be the length of a side of a triangle with circumradius R, inradius r, and distance d between the circumcenter and the incenter.*

(a) *If $(\sqrt{2}+1)r \le R$, then*

$$4((R-d)^2-r^2) < 16R^2r^2\frac{(R+d)^2-r^2}{(R+d)^4} \le a^2 \le 4R^2 < 4((R+d)^2-r^2).$$

(b) *If $2r \le R < (\sqrt{2}+1)r$, then*

$$4((R-d)^2-r^2) \le 16R^2r^2\frac{(R+d)^2-r^2}{(R+d)^4} \le a^2 \le 16R^2r^2\frac{(R-d)^2-r^2}{(R-d)^4} \le 4((R+d)^2-r^2).$$

(c) *The improved lower bounds and upper bounds in* (a) *and* (b) *over* (2) *are best possible.*

We shall make use of the following lemma.

Lemma 2. *For any triangle ABC, the circumcenter O is in the interior of the incircle if and only if $2r \le R < (\sqrt{2}+1)r$.*

Proof. The first inequality $2r \le R$ follows from $0 \le d = \sqrt{R(R-2r)}$.

The circumcenter O is in the interior of the incircle of the triangle ABC if and only if $d^2 < r^2$. This condition is equivalent to $R^2 - 2Rr - r^2 < 0$, i.e.,

$$(R-(\sqrt{2}+1)r)(R+(\sqrt{2}+1)r) < 0.$$

Since the second factor is positive, we have $2r \le R < (\sqrt{2}+1)r$. □

Proof of Theorem 1

Let R be the radius of some circle ω, O be the center of ω, r be a number such that $2r \le R$. Denote $d = \sqrt{R^2-2Rr}$. Also, let MN be a diameter of ω. Consider a point I such that I lies in the diameter MN and $|IO| = d$ (see Figure 2).

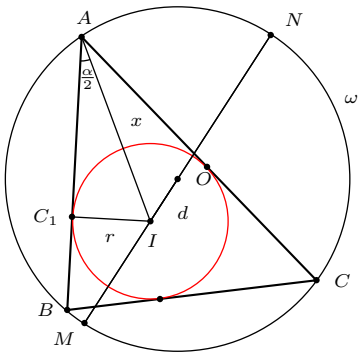

Figure 2

Take an arbitrary point A of the circle ω and draw the tangents AB and AC to the circle with radius r and center I. By Poncelet's closure theorem, the segment BC is also tangent to the circle. Moreover, every triangle with circumradius R and inradius r can be constructed in this way (see also [3]).

For an arbitrary point A on ω, let $x = |AI|$. Assume $|IM| < |IN|$. Since the two circles center I, passing through M and N respectively are tangent to ω, $|MI| \le x \le |IN|$, i.e., $x \in [R-d; R+d]$.

Let $\angle BAC = \alpha$ and C_1 be the orthogonal projection of I on AB. Then $|AC_1| = \sqrt{x^2 - r^2} = x\cos\frac{\alpha}{2}$ and $|IC_1| = r = x\sin\frac{\alpha}{2}$. Hence,

$$a = 2R\sin\alpha = 4R\sin\frac{\alpha}{2}\cos\frac{\alpha}{2} = 4R\cdot\frac{r}{x}\cdot\frac{\sqrt{x^2-r^2}}{x} = 4Rr\frac{\sqrt{x^2-r^2}}{x^2},$$

i.e.,

$$a^2(x) = 16R^2r^2\cdot\frac{x^2-r^2}{x^4}.$$

For the function $a^2(x)$ on the interval $[R-d; R+d]$, we have

$$\frac{d}{dx}(a^2(x)) = 32R^2r^2\cdot\frac{2r^2-x^2}{x^5}.$$

Let $x_0 = \sqrt{2}r$. Clearly, for any $x > 0$, $\frac{d}{dx}(a^2(x))$ is positive, zero, or negative according as $x < x_0$, $= x_0$, or $x > x_0$. Therefore, x_0 is a maximum of $a^2(x)$, provided $x_0 \in [R-d,\ R+d]$, and the function is increasing on $[R-d,\ x_0]$, and decreasing on $[x_0,\ R+d]$.

(a) Let $R - d \le \sqrt{2}r$. Note that in this case $x_0 = \sqrt{2}r < 2r \le R < R+d$. So $x_0 \in [R-d; R+d)$. Furthermore,

$$R - d \le \sqrt{2}r \iff (R-\sqrt{2}r)^2 \le d^2 \iff (\sqrt{2}+1)r \le R.$$

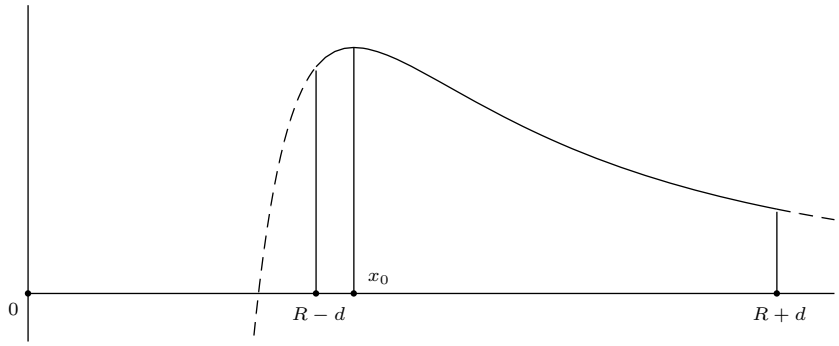

Figure 3

By Lemma 2, the circumcenter O is not in the interior of the incircle of the triangle ABC. Furthermore,

$$\frac{a^2(R-d)-a^2(R+d)}{16R^2r^2} = \frac{(R-d)^2-r^2}{(R-d)^4} - \frac{(R+d)^2-r^2}{(R+d)^4} = \frac{8Rr^2d(R^2-d^2)}{(R-d)^4(R+d)^4} > 0,$$

i.e., $a^2(R-d) > a^2(R+d)$. The maximal value $a^2(x_0) = a^2(\sqrt{2}r) = 4R^2$, and the minimal value $a^2(R+d) = 16R^2r^2\frac{(R+d)^2-r^2}{(R+d)^4}$.

Therefore, for $R \geq (\sqrt{2}+1)r$,

$$16R^2r^2\frac{(R+d)^2-r^2}{(R+d)^4} \leq a^2 \leq 4R^2. \tag{3}$$

(b) Let $R-d > \sqrt{2}r$.

By Lemma 2, the condition $R-d > \sqrt{2}r$ implies that the circumcenter O is in the interior of the incircle. In this case, x_0 is outside the interval $[R-d,\ R+d]$, and the function $a^2(x)$ is decreasing (see Figure 4).

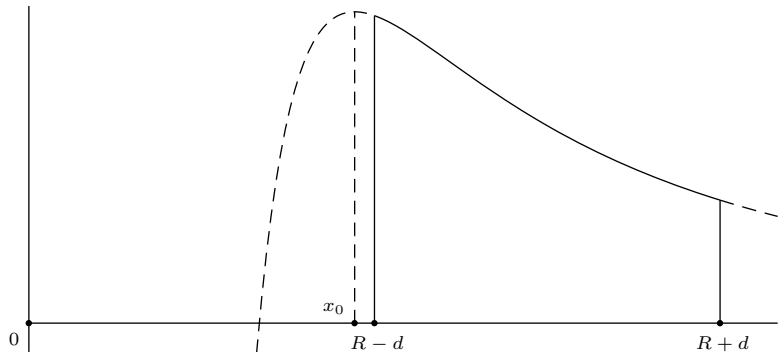

Figure 4

Therefore, $a^2(R-d) \geq a^2 \geq a^2(R+d)$, and we have

$$16R^2r^2\frac{(R+d)^2-r^2}{(R+d)^4} \leq a^2 \leq 16R^2r^2\frac{(R-d)^2-r^2}{(R-d)^4}. \tag{4}$$

(c) Clearly in (3) and (4), the lower and upper bounds cannot be improved.

This completes the proof of Theorem 1.

References

[1] T. Bîrsan, Bounds for elements of a triangle expressed by R, r, and s, *Forum Geom.*, 15 (2015) 99–103.

[2] R. A. Johnson, *Advanced Euclidean Geometry*, Dover reprint, 2007.

[3] V. Soltan and S. Maidman, *Identities and Inequalities in a Triangle* (in Russian), Kishinev, Shtiinca Publishers, 1982.

Yurii N. Maltsev: Altai State Pedagogical University, Barnaul, Russia
E-mail address: maltsevyn@gmail.com

Anna S. Kuzmina: Altai State Pedagogical University, Barnaul, Russia
E-mail address: akuzmina1@yandex.ru

Forum Geometricorum
Volume 16 (2016) 85–94.

FORUM GEOM
ISSN 1534-1178

Solutions of Two Japanese Ellipse Problems

J. Marshall Unger

Abstract. Two premodern Japanese theorems involving an ellipse and tangent circles are stated as problems in [1] (6.4.7 and 6.2.4). Neither can be proven easily by elementary means. But a proof of the second problem follows from another Japanese proposition, for which I give an original proof. It is based on the first part of an elegant proof of a generalization of the first theorem, which I present in edited form.

1. Introduction

Among the many theorems involving ellipses stated as problems in [1], two (6.4.7 and 6.2.4) stand out as particularly challenging. The first theorem (Figure 1) concerns two intersecting tangents to an ellipse and the circles that touch both tangents and the ellipse. If the diameters of the two that touch the ellipse externally are d_1, d_4, and those of the two that touch it internally are d_2, d_3, then $d_1 : d_2 = d_3 : d_4$.

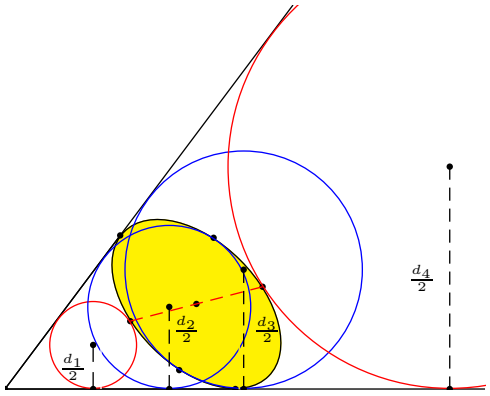

Figure 1

The second theorem states that, in Figure 2,

$$v = \frac{(R-r)\sqrt{Rr+u^2} - u(R+r)}{2\sqrt{Rr}},$$

where u, v are the semi-major and semi-minor axes of the ellipse and R, r are the radii of the two circles touching the ellipse and the sides of the square that are touched by it.

Publication Date: March 29, 2016. Communicating Editor: Paul Yiu.

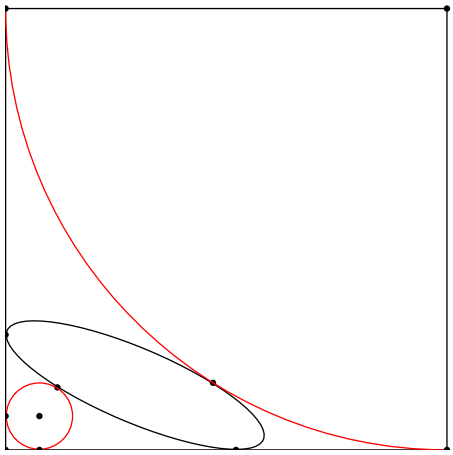

Figure 2

The first theorem is attributed to "S. Iwata" [3], but to "Kosan Iwata (1812 – 1878)" in [1].[1] Iwata does not give the solution, which he found in the spring of 1866, saying it took up 52 pages. Readers are told to drop by the journal office if they want to see the whole thing!

Papers by H. Terao (1885), J. Mizuhara (n.d.), and T. Hayashi (1895) that prove and generalize Iwata's theorem were presented in English by Y. Mikami in [3]. In his paper, Terao Hisashi (1855 – 1923), a founder of modern astronomy in Japan, proves the following theorem, of which Iwata's is a special case:

Theorem (Terao)**.** Given two intersecting tangents to an ellipse or hyperbola, consider the ellipses or hyperbolas, homothetic to one another, that touch the tangents and the first conic. If the major axes of the two that touch the first conic externally are a_1, a_4 and those of the two that touch it internally are a_2, a_3, then $a_1 : a_2 = a_3 : a_4$. So too for the minor axes: $b_1 : b_2 = b_3 : b_4$.

Terao's proof deserves wider recognition, so I have edited Mikami's version and present it in section 2. In section 3, I use the key proposition in Terao's proof to prove a well-known but difficult Japanese theorem not presented in [1]. This proposition makes it easy to prove the second theorem, as shown in section 4.

2. Terao's theorem ([1], 6.4.7)

Take the tangents in Figure 1 to be axes of a (not necessarily orthogonal) coordinate system with origin O. A conic touching both axes at distances $a, b > 0$ from

[1] Iwata's article, signed 岩田專平好算 appeared in 1:1.12.13 (1877) (cited in [1]), followed by a commentary by Fukugawa Riken (paraphrased in [3]). Iwata's personal name was *Senpei* 專平; *Kōsan* 好算 ("loves to calculate") was his pen-name. N.B. the author of [2], Iwata Shikō, is a mid-20th-century mathematician.

O along the x, y axes, respectively, has the equation

$$Q \equiv k^2 \left(\frac{x}{a} + \frac{y}{b} - 1\right)^2 - 4xy = 0$$

for some $k > 0$. Expanding Q,

$$\frac{k^2}{a^2}x^2 + \frac{2(k^2 - 2ab)}{ab}xy + \frac{k^2}{b^2}y^2 - \frac{2k^2}{a}x - \frac{2k^2}{b}y + k^2 = 0,$$

so, as a general conic of the form $Ax^2 + Bxy + Cy^2 + Dx + Ey + F = 0$, its discriminant is

$$B^2 - 4AC = \frac{4(k^2 - 2ab)^2}{a^2b^2} - \frac{4k^4}{a^2b^2} = \frac{16(ab - k^2)}{ab}.$$

We readily see that the discriminant, which is negative for an ellipse and positive for a hyperbola, has the same sign as $ab - k^2$. Let

$$P \equiv k'^2 \left(\frac{x}{a'} + \frac{y}{b'} - 1\right)^2 - 4xy = 0$$

be a second conic touching the same axes. A line through the points where Q and P intersect is

$$Q - P \equiv k^2 \left(\frac{x}{a} + \frac{y}{b} - 1\right)^2 - k'^2 \left(\frac{x}{a'} + \frac{y}{b'} - 1\right)^2 = 0.$$

Since the right side of this equation can be factored into linear terms, it represents a degenerate conic consisting of two intersecting lines, viz. the two common chords (blue in the Figures 3–6) of Q and P. Their equations are

$$k\left(\frac{x}{a} + \frac{y}{b} - 1\right) = \pm k'\left(\frac{x}{a'} + \frac{y}{b'} - 1\right).$$

i.e., one chord is

$$\left(\frac{k}{a} + \frac{k'}{a'}\right)x + \left(\frac{k}{b} + \frac{k'}{b'}\right)y = k + k'$$

and the other is

$$\left(\frac{k}{a} - \frac{k'}{a'}\right)x + \left(\frac{k}{b} - \frac{k'}{b'}\right)y = k - k'.$$

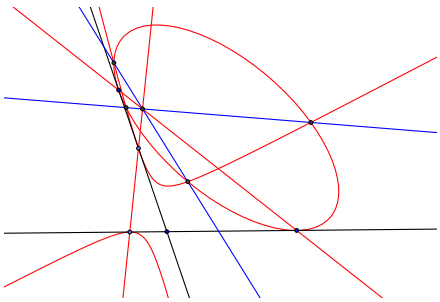

Figure 3

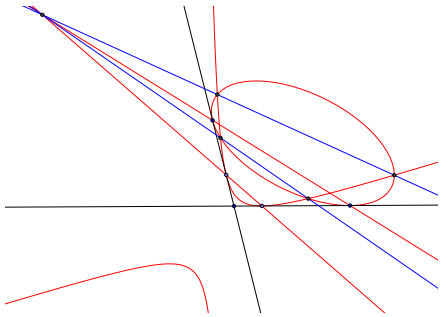

Figure 4

Now suppose we fix a, b, k and vary a', b', k' until the endpoints of one chord or the other coincide and the chord becomes a common tangent of Q and P.

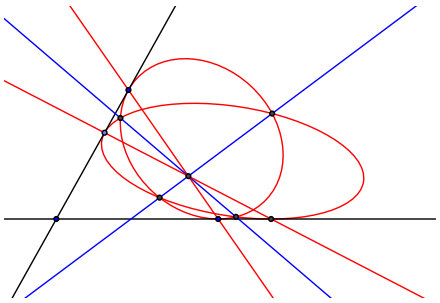

Figure 5

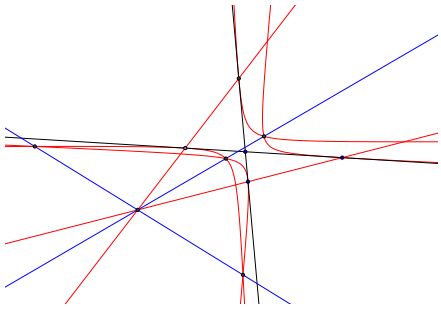

Figure 6

Starting with the first common chord and assuming that $\frac{k}{a}+\frac{k'}{a'}\neq 0$, we use the chord's equation to get y and substitute it into Q, which becomes a quadratic in x. Its two roots are equal if and only if the chord touches Q at a single point, so we set the discriminant to zero and solve. The result is

$$E\equiv k^2k'^2\left(\frac{1}{a}-\frac{1}{a'}\right)\left(\frac{1}{b}-\frac{1}{b'}\right)-(k+k')^2=0.$$

If $\frac{k}{b}+\frac{k'}{b'}=0$ and $\frac{k}{a}+\frac{k'}{a'}\neq 0$, we use one chord's equation to get x and substitute it into Q to get a quadratic in y, but the result is the same. Similarly, starting with the second chord, if $\frac{k}{b}-\frac{k'}{b'}=0$ and $\frac{k}{a}-\frac{k'}{a'}\neq 0$, we get

$$I\equiv k^2k'^2\left(\frac{1}{a}-\frac{1}{a'}\right)\left(\frac{1}{b}-\frac{1}{b'}\right)-(k-k')^2=0.$$

As we are taking Q as fixed, we can say that P belongs to genus E or genus I depending on which chord we start with. If $\frac{k}{b}+\frac{k'}{b'}=0$ and $\frac{k}{a}+\frac{k'}{a'}=0$, then there is no conic in genus E that touches Q, and if $\frac{k}{b}-\frac{k'}{b'}=0$ and $\frac{k}{a}-\frac{k'}{a'}=0$, there is no conic in genus I that touches Q. This occurs when Q and P are homothetic.

Now two ellipses or two hyperbolas (resp. an ellipse and a hyperbola) that touch both axes and each other make contact externally if and only if their centers lie on opposite sides (resp. same side) of the common tangent. Contact that is not external is internal. We now prove that the contact of Q and P is always external for P in genus E.

Suppose that the common tangent of Q and P is the line $t(x,y)=0$. If the centers of Q and P are (g,h) and (g',h'), then $t(g,h)\neq 0$ and $t(g',h')\neq 0$ because the centers certainly do not lie on the tangent. The signs of $t(g,h)$ and $t(g',h')$ are the same if and only if (g,h) and (g',h') lie in the same half-plane. The sign of $\frac{t(g,h)}{t(g',h')}$ is therefore positive when they do.

Because the conic Q is symmetrical, the lines $\frac{\partial Q}{\partial x}=0$ and $\frac{\partial Q}{\partial y}=0$ intersect at its center, so we solve the equations $\frac{k^2}{a}\left(\frac{x}{a}+\frac{y}{b}-1\right)-2y=0$ and $\frac{k^2}{b}\left(\frac{x}{a}+\frac{y}{b}-1\right)-2x=0$ simultaneously to find its coordinates. For Q, this yields

$$g=\frac{k^2a}{2(k^2-ab)},\qquad h=\frac{k^2b}{2(k^2-ab)}.$$

Likewise, for P,

$$g' = \frac{k'^2 a'}{2(k'^2 - a'b')}, \qquad h' = \frac{k'^2 b'}{2(k'^2 - a'b')}.$$

If we start with the first common chord, then Q belongs to genus E and

$$t(x, y) = \left(\frac{k}{a} + \frac{k'}{a'}\right) x + \left(\frac{k}{b} + \frac{k'}{b'}\right) - (k + k').$$

Therefore,

$$\begin{aligned} t(g, h) = & \frac{k^2}{k^2 - ab} + \frac{k^2 k'}{2(k^2 - ab)} \left(\frac{a}{a'} + \frac{b}{b'}\right) - (k + k') \\ = & \frac{(k + k')ab - k^2 k'}{k^2 - ab} + \frac{k^2 k'}{2(k^2 - ab)} \left(\frac{a}{a'} + \frac{b}{b'}\right) \\ = & \frac{(k + k')ab}{k^2 - ab} - \frac{k^2 k'}{k^2 - ab} \left(1 - \frac{1}{2} \left(\frac{a}{a'} + \frac{b}{b'}\right)\right) \\ = & -\frac{ab}{k^2 - ab} \left(\frac{k^2 k'}{ab} \left(1 - \frac{1}{2} \left(\frac{a}{a'} + \frac{b}{b'}\right)\right) - (k + k')\right). \end{aligned}$$

Correspondingly,

$$t(g', h') = -\frac{a'b'}{k'^2 - a'b'} \left(\frac{kk'^2}{a'b'} \left(1 - \frac{1}{2} \left(\frac{a'}{a} + \frac{b'}{b}\right)\right) - (k + k')\right).$$

Thus we have

$$\begin{aligned} \frac{-k'(k^2 - ab)}{ab} t(g, h) = & \frac{k^2 k'^2}{ab} \left(1 - \frac{1}{2} \left(\frac{a}{a'} + \frac{b}{b'}\right)\right) - k'(k + k'), \\ \frac{-k(k'^2 - a'b')}{a'b'} t(g', h') = & \frac{k^2 k'^2}{a'b'} \left(1 - \frac{1}{2} \left(\frac{a'}{a} + \frac{b'}{b}\right)\right) - k(k + k'). \end{aligned}$$

But E may be rewritten

$$\frac{k^2 k'^2}{ab} \left(1 - \frac{1}{2} \left(\frac{a}{a'} + \frac{b}{b'}\right)\right) - k'(k + k') + \frac{k^2 k'^2}{a'b'} \left(1 - \frac{1}{2} \left(\frac{a'}{a} + \frac{b'}{b}\right)\right) - k(k + k') = 0.$$

Therefore, $\frac{-k'(k^2 - ab)}{ab} t(g, h) + \frac{-k(k'^2 - a'b')}{a'b'} t(g', h') = 0$, and

$$\frac{t(g, h)}{t(g', h')} = \frac{-k'(k^2 - ab)}{ab} \cdot \frac{a'b'}{k(k'^2 - a'b')}.$$

Since a, b, k, a', b', k' are all positive, the sign of $\frac{t(g,h)}{t(g',h')}$ depends entirely on the signs of $k^2 - ab$ and $k'^2 - a'b'$. As remarked above, these are positive for an ellipse and negative for a hyperbola. The sign of $\frac{t(g,h)}{t(g',h')}$ is therefore negative when Q and P are both ellipses or both hyperbolas, and positive when one is an ellipse and other a hyperbola. Hence the centers lie on opposite sides in the former case, on the same side in the latter, and the contact is always external for P in genus E. One can prove that the contact is always internal for P in genus I in the same fashion by repeating the steps described above starting with the equation of the second common chord instead of the first.

Now if we select a member of Q with the equation

$$P_0 \equiv k_0^2 \left(\frac{x}{a_0} + \frac{y}{b_0} - 1 \right)^2 - 4xy = 0,$$

then for every conic homothetic to P_0, there exists a constant λ such that $a' = \lambda a_0$, $b' = \lambda b_0$, and $k' = \lambda k_0$. That is,

$$P \equiv k_0^2 \left(\frac{x}{a_0} + \frac{y}{b_0} - \lambda \right)^2 - 4xy = 0,$$

for some $\lambda > 0$. The equations of the major and minor axes of the conics represented by P are linear and homogeneous because their axes are parallel to the corresponding axes of P_0. If, for example, the major axis M_0 is $f(k_0, a_0, b_0, \theta)$, where θ is the angle between the coordinate axes, and major axis M is $f(k', a', b', \theta)$, then

$$f(\lambda k_0, \lambda a_0, \lambda b_0, \theta) = \lambda f(k_0, a_0, b_0, \theta),$$

or $M = \lambda M_0$. Similarly, for the minor axis m, $m = \lambda m_0$.

For the same reason, the tangency conditions E and I can be conflated into

$$k^2 k_0^2 \left(\frac{\lambda}{a} - \frac{1}{a_0} \right) \left(\frac{\lambda}{b} - \frac{1}{b_0} \right) - (\lambda k_0 \pm k)^2 = 0,$$

where it is understood that we select the plus sign to get the equation of E and minus sign to get the equation for I. As a quadratic in λ, this conflated equation is

$$k_0^2 \left(\frac{k^2}{ab} - 1 \right) \lambda^2 - k k_0 \left(\frac{1}{ab_0} + \frac{1}{a_0 b} \pm 2 \right) \lambda + k^2 \left(\frac{k_0^2}{a_0 b_0} - 1 \right)^2 = 0,$$

solving which gives us two values of λ for E and another two for I.

The products of both pairs of roots are equal because the leading coefficients and constant terms in both equations are the same. Writing the products as $\lambda_1 \lambda_4 = \lambda_2 \lambda_3$, we have $\frac{\lambda_1}{\lambda_2} = \frac{\lambda_3}{\lambda_4}$, and, since, for instance, $\frac{m_1}{\lambda_1} = \frac{m_2}{\lambda_2} = \frac{m_3}{\lambda_3} = \frac{m_4}{\lambda_4} = m_0$, the same proportions apply to the respective axes of the conics that touch Q and its two tangents.

This proves Terao's theorem, of which Iwata's is clearly the special case of ellipses in Q and circles in P.

3. The intermediate result

Proposition 98 in the well-known work *Sanpō jojutsu* concerns an ellipse with major and minor axes p, q inscribed in a rectangle of sides m, n, and a circle of diameter d touching the ellipse externally and two adjacent sides of the rectangle internally.

It states that

$$mn + \sqrt{m^2 n^2 - p^2 q^2} - 2 \left(m + n + \sqrt{mn - \sqrt{m^2 n^2 - p^2 q^2}} \right) d + d^2 = 0.$$

A long and difficult algebraic proof of this, ascribed to Ajima Naonobu (1732–1798), is recounted algebraically in [4]. The same proof is interpreted using trigonometry in [6]. According to [4], a simpler proof using matrices appears in [2],

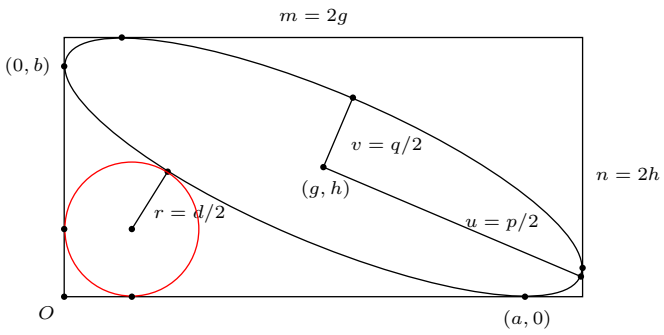

Figure 7

but I have not seen it. The following proof of my own using matrices, inspired by Terao's proof of Iwata's theorem, may be similar to the one in [2].

First, we restate the proposition with modern conventions and a little more care:

Proposition. Given an ellipse with semimajor and semiminor axes u, v inscribed in a rectangle, designate one of its vertices as the origin and take the adjacent sides as the positive x, y axes of a coordinate system. There are two circles that touch the ellipse externally and both these axes. If the center of the ellipse is (g, h), then the radii of these circles are the solutions of

$$gh + \sqrt{g^2h^2 - u^2v^2} - 2\left(g + h + \sqrt{gh - \sqrt{g^2h^2 - u^2v^2}}\right)\rho + \rho^2 = 0.$$

Following Terao, let

$$Q \equiv k^2\left(\frac{x}{a} + \frac{y}{b} - 1\right)^2 - 4xy = 0$$

define the ellipse. In homogeneous coordinates, Q corresponds to the symmetric matrix

$$A = \begin{pmatrix} \frac{1}{a^2} & \frac{1}{ab} - \frac{2}{k^2} & -\frac{1}{a} \\ \frac{1}{ab} - \frac{2}{k^2} & \frac{1}{b^2} & -\frac{1}{b} \\ -\frac{1}{a} & -\frac{1}{b} & 1 \end{pmatrix}.$$

That is, $(x \;\; y \;\; 1) \cdot A \cdot (x \;\; y \;\; 1)^T = 0$. Writing $|M|$ for the determinant of M and A_{33} for the minor of A with its third row and third column omitted, we know that, for a non-degenerate conic, $|A| \neq 0$; for an ellipse, $|A_{33}| > 0$ ($|A_{33}|$ is the discriminant); and for the ellipse to be real, $\mathrm{Tr}(A_{33})|A| < 0$. The first and third conditions always hold for positive a, b, k; the second is equivalent to $k^2 > ab$.

In addition, if λ and μ are the eigenvalues of A_{33}, then the reduced equation of the ellipse is

$$\lambda x^2 + \mu y^2 + \frac{|A_Q|}{|A_{33}|} = 0,$$

or, in canonic form,

$$-\frac{|A_{33}|\lambda}{|A_Q|}x^2 - \frac{|A_{33}|\mu}{|A_Q|}y^2 = 1.$$

This is the equation of the congruent ellipse centered on the origin with major axis on the line $y = 0$. From it, we readily see that $u^2 = -\frac{|A_Q|}{|A_{33}|\lambda}$ and $v^2 = -\frac{|A_Q|}{|A_{33}|\mu}$. Since in general $\lambda\mu = |A_{33}|$, this means that

$$u^2v^2 = \frac{|A_Q|^2}{|A_{33}|^3}.$$

If now $P \equiv k'^2\left(\frac{x}{a'} + \frac{y}{b'} - 1\right)^2 - 4xy = 0$ is a conic that touches the axes at distances a', b' from O, we know (thanks to Terao) that P is externally tangent to Q if and only if

$$k^2k'^2\left(\frac{1}{a} - \frac{1}{a'}\right)\left(\frac{1}{b} - \frac{1}{b'}\right) - (k + k')^2 = 0.$$

If $k'^2 > a'b'$ and $a' = b' = \rho$, P should be the circle of radius ρ centered at (ρ, ρ), and indeed P can be rearranged as $(x - \rho)^2 + (y - \rho)^2 = \rho^2$ provided that $k' = \rho\sqrt{2}$. The external tangency condition thus becomes $2k^2\left(\frac{1}{a} - \frac{1}{\rho}\right)\left(\frac{1}{b} - \frac{1}{\rho}\right) - (k + \rho\sqrt{2})^2$, or, as a quadratic in ρ,

$$k^2 - 2\left(\sqrt{2}k + \frac{k^2}{a} + \frac{k^2}{b}\right)\rho + 2\left(\frac{k^2 - ab}{ab}\right)\rho^2 = 0.$$

To each of it roots, $R > r$, one of a pair of parallel tangents to the ellipse corresponds. The x- and y-intercepts of each tangent, together with O, are the vertices of a right triangle. The incircle of the smaller triangle is the circle with center (r, r) and radius r, and the excircle on the hypotenuse is the one with center (R, R) and radius R. Each circle touches the ellipse at the same point it touches their common tangent. Thus the last equation is a sufficient and necessary condition for constructing the circle in the problem figure exactly for a given ellipse and rectangle.

From its form, we immediately see that $Rr = \frac{k^2ab}{2(k^2-ab)}$. But, as we know, $g = \frac{k^2a}{2(k^2-ab)}$, $h = \frac{k^2b}{2(k^2-ab)}$. Hence, $Rr = bg = ah$. We can therefore substitute $\frac{Rr}{h}$, $\frac{Rr}{g}$ for a, b into either the equation for g or the equation for h. Whichever we choose, the result is

$$k = \frac{Rr\sqrt{2}}{\sqrt{2gh - Rr}}.$$

We can therefore rewrite Q and the external tangency condition exclusively in terms of g, h, R, r. The matrix for this new form of Q is

$$A = \begin{pmatrix} h^2 & Rr - gh & -hRr \\ Rr - gh & g^2 & -gRr \\ -hRr & -gRr & R^2r^2 \end{pmatrix}$$

and the external tangency condition becomes

$$Rr - 2(g + h + \sqrt{2gh - Rr})\rho + \rho^2 = 0.$$

Note that $|A| = -R^2r^2(2gh - Rr)^2$ and $|A_{33}| = Rr(2gh - Rr)$. Hence, from $u^2v^2 = \frac{|A|^2}{|A_{33}|^3}$,

$$\begin{aligned} u^2v^2 &= Rr(2gh - Rr), \\ g^2h^2 - u^2v^2 &= (gh - Rr)^2, \\ \sqrt{g^2h^2 - u^2v^2} &= \pm(gh - Rr). \end{aligned}$$

Selecting the negative sign on the right, we see at once that the external tangency condition is equivalent to

$$gh + \sqrt{g^2h^2 - u^2v^2} - 2\left(g + h + \sqrt{gh - \sqrt{g^2h^2 - u^2v^2}}\right)\rho + \rho^2 = 0.$$

4. Shiraishi's formula ([1, 6.2.4]

We now turn to our the second theorem. The formula

$$v = \frac{(R - r)\sqrt{Rr + u^2} - u(R + r)}{2\sqrt{Rr}}$$

appears in [5] with example data ($R = 36$, $2r = 2$, $2u = 16$, $v = 9$) but no proof.

But let us return to $u^2v^2 = Rr(2gh - Rr)$ in the foregoing proof. This time, we solve for gh, obtaining

$$gh = \frac{R^2r^2 + u^2v^2}{2Rr}.$$

Since $g^2 + h^2 = u^2 + v^2$ (the director circle theorem for ellipses), we have $(g + h)^2 = 2gh + u^2 + v^2$. We can therefore rewrite gh and $g + h$ in the tangency condition

$$Rr - 2(g + h + \sqrt{2gh - Rr})\rho + \rho^2 = 0$$

in terms of u, v, R, r, ρ. Having done so, if we substitute r for ρ, we get

$$r^2 + Rr - 2r\left(\sqrt{\frac{R^2r^2 + u^2v^2}{Rr} - Rr} + \sqrt{\frac{R^2r^2 + u^2v^2}{Rr} + u^2 + v^2}\right) = 0.$$

Substituting instead R for ρ, we get

$$R^2 + Rr - 2R\left(\sqrt{\frac{R^2r^2 + u^2v^2}{Rr} - Rr} + \sqrt{\frac{R^2r^2 + u^2v^2}{Rr} + u^2 + v^2}\right) = 0.$$

Solving either of these for v yields

$$v = \frac{1}{2}\frac{\sqrt{Rr^3 - 2R^2r^2 + rR^3 + 2(R^2 + r^2)u^2 - 2(R^2 - r^2)u\sqrt{Rr + u^2}}}{\sqrt{Rr}}.$$

As the long radicand here factors to $\left((R - r)\sqrt{Rr + u^2} - u(R + r)\right)^2$, we see that one can deduce Shiraishi's formula from the theorem in *Sanpō jojutsu* proven in section 3. Most likely, that was how Shiraishi arrived at it.

5. Concluding remark

Given just R and r in Figure 2, an infinite number of ellipses touch the coordinate axes and both circles. One more condition, such as the length of u, must be given to identify a particular ellipse.

The ellipse always touches the extouch point of the hypotenuse of the larger right triangle defined in section 3, but it need not touch its legs at their extouch points. If it does, it is the Mandart inellipse of the triangle, and one can prove that the distance between the parallel tangents is then exactly $2r$. Shiraishi's example is not a Mandart inellipse, but the theorem is too nice not to mention.

References

[1] H. Fukagawa and D. Pedoe, *Japanese Temple Geometry Problems*, Winnipeg: Charles Babbage Research Centre, 1989.

[2] S. Iwata, *Kikagaku daijiten* (Great encyclopedia of geometry), 6 vols, Tōkyō, 1971–1982.

[3] Y. Mikami (compiled and edited), *Mathematical Papers from the Far East*, Abhandlungen zur Geschichte der mathematischen Wissenschaften mit Einschluss ihrer Anwendungen, 28 (Leipzig: B. G. Teubner, 1910).

[4] N. Nakamura, *Wasan no zukei kōshiki* (Wasan formulae with diagrams), (n.p.: 2008).

[5] N. Shiraishi, *Shamei Sanpu*, 1827.

[6] T. Yoneyama, *Sokuen-jutsu 6: An-shi ikō sokuen-kai ni-jō dai-ni* (Ellipse Methods VI. Two posthumous solutions of Ajima, No. 2), Tōkyō University Bulletin: Natural Sciences (55) 151–161 (Tōkyō: March 2011).

J. Marshall Unger: Emeritus Professor, Department of East Asian Languages & Literatures, The Ohio State University, Columbus, Ohio 43210-1340, USA

E-mail address: unger.26@osu.edu

Forum Geometricorum
Volume 16 (2016) 95–98.

FORUM GEOM
ISSN 1534-1178

The Golden Section in a Planar Quasi Twelve-Point Star

Hartmut Warm

Abstract. A planar quasi twelve-point star is a configuration formed by selected diagonals of a regular dodecagon forming four equilateral triangles and three squares. We show that segments on the sides of the equilateral triangles are divided in the golden ratio by intersections of certain lines and circles.

Historically, the golden section first appears in the division of a diagonal of a regular pentagon by the intersection with another diagonal (see Figure 1): if $ABCDE$ is a regular pentagon, and the diagonals AD and BE intersect at P, then P divides BE and DA in the golden ratio:

$$\frac{BP}{PE} = \frac{DP}{PA} = \varphi = \frac{\sqrt{5}+1}{2}.$$

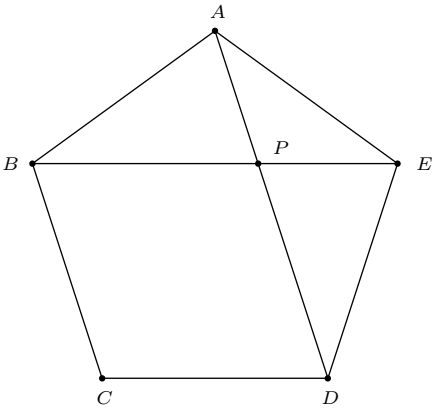

Figure 1

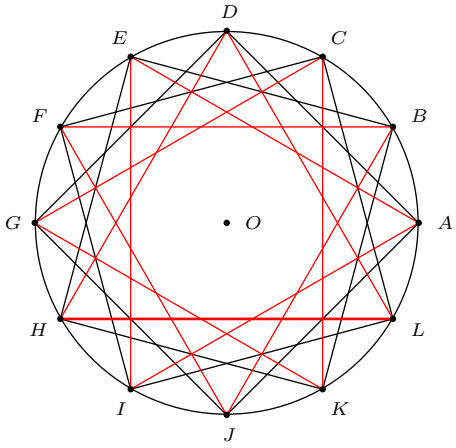

Figure 2

This golden ratio φ also appears in a number of simple geometrical figures. George Odom [2] and Kurt Hofstetter [1] found division of segments in the golden ratio associated with equilateral triangles, Tran [3] used squares. In this note we give a construction associated with a regular dodecagon, leading to division of certain segments in the golden ratio.

Given a circle, center O and radius R, consider twelve points A, B, C, …, J, K, L dividing the circle into 12 equal arcs. There are three inscribed squares $ADGJ$, $BEHK$, $CFIL$ forming a quasi twelve-point star $(12:3)$. Likewise, the

Publication Date: March 29, 2016. Communicating Editor: Paul Yiu.

four inscribed equilateral triangles AEI, BFJ, CGK, DHL form another quasi twelve-point star $(12:4)$. The *planar quasi twelve-point star* in the title refers to the union of $(12:3)$ and $(12:4)$ (see Figure 2).

For convenience, we consider the simpler Figure 3, in which the equilateral triangles AEI and CGK are not shown. The equilateral triangles BFJ and DHL bound a regular hexagon whose sides have length $a = \frac{1}{\sqrt{3}}R$. Figure 3 also shows three circles with center O:
(i) the common inscribed circle of the equilateral triangles, with radius $r = \frac{1}{2}R$,
(ii) the circle $\mathscr{C}$ through the "outer" intersections of the sides of the squares,
(iii) the (dotted) common inscribed circle $\mathscr{C}'$ of the squares, with radius $\frac{1}{\sqrt{2}}R$ (see Figure 4).

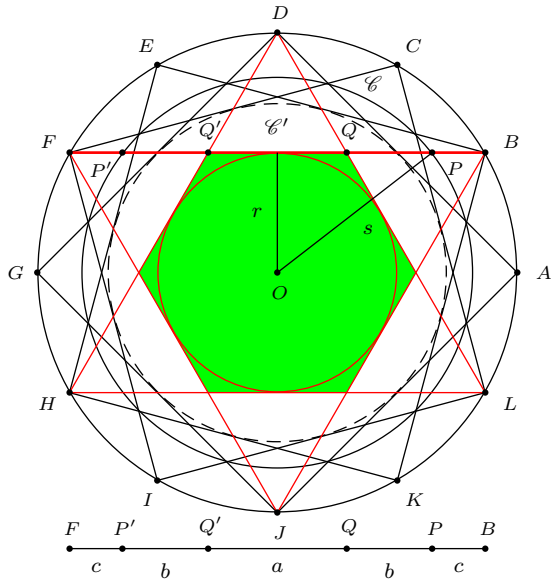

Figure 3

Lemma 1. *The radius of the circle $\mathscr{C}$ is $s = \sqrt{\frac{2}{3}}R$.*

Proof. Let s be the radius of circle $\mathscr{C}$. In Figure 3, the circles $\mathscr{C}$ and $\mathscr{C}'$ are the circumscribed and inscribed circles of a regular hexagon. Therefore,

$$\frac{s}{\frac{1}{\sqrt{2}}R} = \frac{2}{\sqrt{3}} \implies s = \frac{2}{\sqrt{3}} \cdot \frac{1}{\sqrt{2}}R = \sqrt{\frac{2}{3}}R$$

(see Figure 5). □

Remark. This is an adaptation of the proof given in [4, pp.301–302].

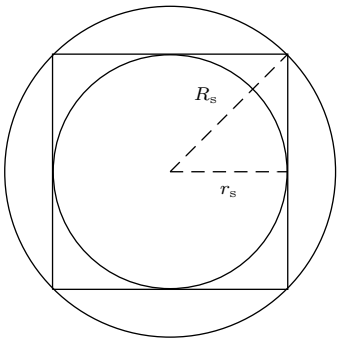

Figure 4: $\frac{R_{\mathrm{s}}}{r_{\mathrm{s}}} = \sqrt{2}$

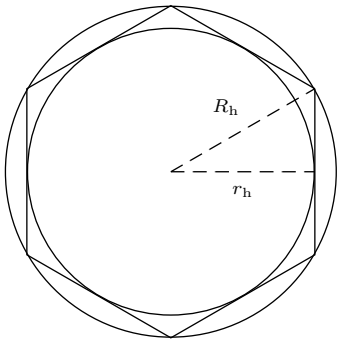

Figure 5. $\frac{R_{\mathrm{h}}}{r_{\mathrm{h}}} = \frac{2}{\sqrt{3}}$

Consider the side BF of the equilateral triangle BFJ and its intersections
(i) P and P' with the circle $\mathscr{C}$,
(ii) Q and Q' with the sides DL and DH of the equilateral triangle DHL.

Proposition 2. (a) *Q divides $Q'P$ and Q' divides QP' in the golden ratio*

$$\frac{Q'Q}{QP} = \frac{QQ'}{Q'P'} = \varphi = \frac{\sqrt{5}+1}{2}.$$

(b) *P divides QB and P' divides $Q'F$ in the golden ratio*

$$\frac{QP}{PB} = \frac{Q'P'}{P'F} = \varphi.$$

Proof. In each case, the equality of the first two ratios follows from symmetry. It is enough to show that the first ratio is equal to φ.

(a) Label the lengths of the segments $Q'Q$, QP, PB as a, b, c as in Figure 3. Since r, $\frac{1}{2}a + b$, and s are the lengths of the sides of a right triangle,

$$\left(\frac{1}{2}a + b\right)^2 = s^2 - r^2 = \left(\frac{2}{3} - \frac{1}{4}\right) R^2 = \frac{5}{12}R^2;$$

$$\frac{1}{2}a + b = \frac{\sqrt{5}}{2\sqrt{3}}R;$$

$$b = \frac{\sqrt{5}}{2\sqrt{3}}R - \frac{1}{2\sqrt{3}}R = \frac{\sqrt{5}-1}{2\sqrt{3}}R = \frac{2}{(\sqrt{5}+1)\sqrt{3}}R = \frac{1}{\varphi\sqrt{3}}R.$$

From this,

$$\frac{a}{b} = \frac{\frac{1}{\sqrt{3}}R}{\frac{1}{\varphi\sqrt{3}}R} = \varphi.$$

(b) Since $b + c = a$, $\frac{c}{b} = \frac{a}{b} - 1 = \varphi - 1 = \frac{1}{\varphi}$. It follows that $\frac{b}{c} = \varphi$. □

References

[1] K. Hofstetter, A simple construction of the golden section, *Forum Geom.*, 2 (2002) 65-66.
[2] G. Odom and J. van de Craats, Elementary Problem 3007, *Amer. Math. Monthly*, 90 (1983) 482; solution, 93 (1986) 572.
[3] Q. H. Tran, The golden section in the inscribed square of an isosceles right triangle, *Forum Geom.*, 15 (2015) 91–92.
[4] H. Warm, *Signature of the Celestial Spheres*, Forest Row, 2010.

Hartmut Warm: Lerchenstr. 41, D-22767 Hamburg, Germany
E-mail address: hw@keplerstern.de

Forum Geometricorum
Volume 16 (2016) 99–114.

FORUM GEOM
ISSN 1534-1178

A Strong Triangle Inequality in Hyperbolic Geometry

Csaba Biró and Robert C. Powers

Abstract. For a triangle in the hyperbolic plane, let α, β, γ denote the angles opposite the sides a, b, c, respectively. Also, let h be the height of the altitude to side c. Under the assumption that α, β, γ can be chosen uniformly in the interval $(0, \pi)$ and it is given that $\alpha + \beta + \gamma < \pi$, we show that the strong triangle inequality $a + b > c + h$ holds approximately 79% of the time. To accomplish this, we prove a number of theoretical results to make sure that the probability can be computed to an arbitrary precision, and the error can be bounded.

1. Introduction

It is well known that the Euclidean and hyperbolic planes satisfy the triangle inequality. What is less known is that in many cases a stronger triangle inequality holds. Specifically,

$$a + b > c + h \tag{1}$$

where a, b, c are the lengths of the three sides of the triangle and h is the height of the altitude to side c. We refer to inequality (1) as the *strong triangle inequality* and note that this inequality depends on which side of the triangle is labeled c.

The strong triangle inequality was first introduced for the Euclidean plane by Bailey and Bannister in [1]. They proved, see also Klamkin [4], that inequality (1) holds for all Euclidean triangles if $\gamma < \arctan\left(\frac{24}{7}\right)$ where γ is the angle opposite side c. Bailey and Bannister also showed that $a + b = c + h$ for any Euclidean isosceles triangle such that $\gamma = \arctan\left(\frac{24}{7}\right)$ and γ is the unique largest angle of the triangle. We let $B = \arctan\left(\frac{24}{7}\right)$ and refer to B as the Bailey-Bannister bound.

In 2007, Baker and Powers [2] showed that the strong triangle inequality holds for any hyperbolic triangle if $\gamma \leq \Gamma$ where Γ is the unique root of the function

$$f(\gamma) = -1 - \cos\gamma + \sin\gamma + \sin\frac{\gamma}{2}\sin\gamma$$

in the interval $[0, \frac{\pi}{2}]$. It turns out that $B \approx 74^\circ$ and $\Gamma \approx 66^\circ$ leading to roughly an 8° difference between the Euclidean and hyperbolic bounds. It appears that the strong triangle inequality holds more often in the Euclidean plane than in the hyperbolic plane.

Let α and β denote the angles opposite the sides a and b, respectively. Under the assumption that the angles α and β can be chosen uniformly in the interval $(0, \pi)$ and $\alpha + \beta < \pi$, Faĭziev et al. [3] showed the strong triangle inequality holds in the

Publication Date: April 1, 2016. Communicating Editor: Paul Yiu.

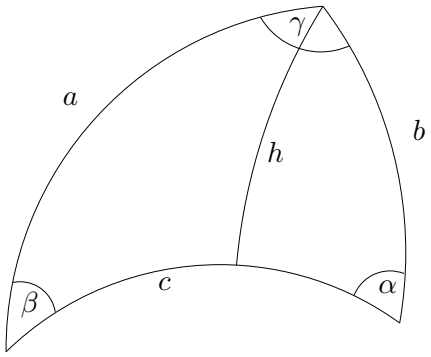

Figure 1. A hyperbolic triangle

Euclidean plane approximately 69% of the time. In addition, they asked how this percentage will change when working with triangles in the hyperbolic plane. In this paper, we answer this question by showing that the strong triangle inequality holds approximately 79% of the time. Moreover, we show that the stated probability can be computed to an arbitrary precision and that the error can be bounded.

Unless otherwise noted, all geometric notions in this paper are on the hyperbolic plane. Since our problem is invariant under scaling, we will assume that the Gaussian curvature of the plane is -1. We will use the notations a, b, c, h, α, β, γ for sides, height, and angles of a given triangle. (See Figure 1.) We will extensively use hyperbolic trigonometric formulas such as the law of sines and the two versions of the law of cosines. We refer the reader to Chapter 8 in [5] for a list of these various formulas.

2. Simple observations

In this section we mention a few simple, but important observations about the main question.

Proposition 1. *If γ is not the unique greatest angle in a triangle, then the strong triangle inequality holds.*

Proof. Suppose that γ is not the greatest angle, say, $\alpha \geq \gamma$. Then $a \geq c$, so $a + b \geq c + b \geq c + h$. Equality could only hold, if $\alpha = \gamma = \pi/2$, which is impossible. □

Proposition 2. *If $\gamma \geq \pi/2$, then the strong triangle inequality does not hold.*

We will start with a lemma that is interesting in its own right.

Lemma 3. *In every triangle the following equation holds.*

$$\sinh c \sinh h = \sinh a \sinh b \sin \gamma$$

Note that in Euclidean geometry the analogous theorem would be the statement that $ch = ab \sin \gamma$, which is true by the fact that both sides of the equation represent twice the area of the triangle. Interestingly, in hyperbolic geometry, the sides of the corresponding equation do not represent the area of the triangle.

Proof. By the law of sines,

$$\frac{\sinh b}{\sin \beta} = \frac{\sinh c}{\sin \gamma},$$

so

$$\sinh c = \frac{\sinh b \sin \gamma}{\sin \beta}.$$

By right triangle trigonometry, $\sinh h = \sinh a \sin \beta$. Multiplying these equations, the result follows. □

Proof of Proposition 2. Note that $a + b > c + h$ if and only if $\cosh(a + b) > \cosh(c + h)$. Using the addition formula for $\cosh$, then the fact that $\cosh h \geq 1$ and $\cosh c \geq 0$, and then the law of cosines, in this order, we get

$$\begin{aligned}
\cos(c + h) &= \cosh c \cosh h + \sinh c \sinh h \geq \cosh c + \sinh c \sinh h \\
&= \cosh a \cosh b - \sinh a \sinh b \cos \gamma + \sinh a \sinh b \sin \gamma \\
&= \cosh a \cosh b + \sinh a \sinh b(\sin \gamma - \cos \gamma)
\end{aligned}$$

Notice that $\sin \gamma - \cos \gamma \geq 1$ if $\pi/2 \leq \gamma \leq \pi$. So

$$\begin{aligned}
&\cosh a \cosh b + \sinh a \sinh b(\sin \gamma - \cos \gamma) \\
\geq\ &\cosh a \cosh b + \sinh a \sinh b \\
=\ &\cosh(a + b).
\end{aligned}$$

□

3. Converting angles to lengths

Since the angles of a hyperbolic triangle uniquely determine the triangle, it is possible to rephrase the condition $a + b > c + h$ with α, β, γ. In what follows, our goal is find a function $f(\alpha, \beta, \gamma)$, as simple as possible, such that $a + b > c + h$ if and only if $f(\alpha, \beta, \gamma) > 0$. Following Proposition 1 and Proposition 2, in the rest of the section we will assume that $\gamma < \pi/2$ is the greatest angle of the triangle.

The following lemma is implicit in [2]. We include the proof for completeness.

Lemma 4. *A triangle satisfies the strong triangle inequality if and only if*

$$\frac{\cos \alpha \cos \beta + \cos \gamma}{\cos \gamma + 1 - \sin \gamma} - 1 < \cosh h.$$

Furthermore, the formula holds with equality if and only if $a + b = c + h$.

Proof. Recall that $a + b > c + h$ if and only if $\cosh(a + b) - \cosh(c + h) > 0$. Using the $\cosh$ addition formula and the law of cosines on $\cosh c$, we have

$$\begin{aligned}
&\cosh(a + b) - \cosh(c + h) \\
=\ &\cosh a \cosh b + \sinh a \sinh b - \cosh c \cosh h - \sinh c \sinh h \\
=\ &\cosh c + \sinh a \sinh b \cos \gamma + \sinh a \sinh b - \cosh c \cosh h - \sinh c \sinh h \\
=\ &\cosh c(1 - \cosh h) + \sinh a \sinh b(\cos \gamma + 1) - \sinh c \sinh h
\end{aligned}$$

By Lemma 3,

$$\begin{aligned}
&\cosh c(1-\cosh h)+\sinh a\sinh b(\cos\gamma+1)-\sinh c\sinh h\\
=\;&\cosh c(1-\cosh h)+\sinh a\sinh b(\cos\gamma+1)-\sinh a\sinh b\sin\gamma\\
=\;&\frac{\sinh a\sinh b}{1+\cosh h}\left[\cosh c\frac{1-\cosh^2 h}{\sinh a\sinh b}+(1+\cosh h)(\cos\gamma+1-\sin\gamma)\right]
\end{aligned}$$

By the fact that $\sinh h=\sinh b\sin\alpha=\sinh a\sin\beta$, we have

$$\frac{1-\cosh^2 h}{\sinh a\sinh b}=\frac{-\sinh^2 h}{\sinh a\sinh b}=\frac{-\sinh b\sin\alpha\cdot\sinh a\sin\beta}{\sinh a\sinh b}=-\sin\alpha\sin\beta,$$

so, using the dual form of the law of cosines,

$$\begin{aligned}
&\cos(a+b)-\cosh(c+h)\\
=\;&\frac{\sinh a\sinh b}{1+\cosh h}\left[-\cosh c\sin\alpha\sin\beta+(1+\cosh h)(\cos\gamma+1-\sin\gamma)\right]\\
=\;&\frac{\sinh a\sinh b}{1+\cosh h}\left[-(\cos\alpha\cos\beta+\cos\gamma)+(1+\cosh h)(\cos\gamma+1-\sin\gamma)\right].
\end{aligned}$$

Since $\frac{\sinh a\sinh b}{1+\cosh h}>0$, we have the strong triangle inequality holds, if and only if

$$\cos\alpha\cos\beta+\cos\gamma<(1+\cosh h)(\cos\gamma+1-\sin\gamma),$$

and the result follows.

A minor variation of the proof shows the case of equality. □

Lemma 5. *For all triangles with* $\gamma>\max\{\alpha,\beta\}$,

$$\frac{\cos\alpha\cos\beta+\cos\gamma}{\cos\gamma+1-\sin\gamma}>1.$$

Proof. Without loss of generality, $0<\alpha\le\beta<\gamma<\pi/2$. Then

$$\begin{aligned}
0>\sin\gamma(\sin\gamma-1)=\sin^2\gamma-\sin\gamma>\sin^2\beta-\sin\gamma\\
\cos^2\beta>\cos^2\beta+\sin^2\beta-\sin\gamma=1-\sin\gamma\\
\cos^2\beta+\cos\gamma>1-\sin\gamma+\cos\gamma,
\end{aligned}$$

so

$$\frac{\cos^2\beta+\cos\gamma}{1-\sin\gamma+\cos\gamma}>1.$$

Since $0<\cos\beta\le\cos\alpha$, we have

$$\frac{\cos^2\beta+\cos\gamma}{1-\sin\gamma+\cos\gamma}\le\frac{\cos\alpha\cos\beta+\cos\gamma}{1-\sin\gamma+\cos\gamma},$$

and the results follows. □

By Lemma 4 and Lemma 5, we can conclude that the strong triangle inequality holds if and only if

$$\left(\frac{\cos\alpha\cos\beta+\cos\gamma}{\cos\gamma+1-\sin\gamma}-1\right)^2<\cosh^2 h. \tag{2}$$

Using the law of cosines,

$$\begin{aligned}\cosh^2 h = &= \sinh^2 h + 1 = \sin^2\beta \sinh^2 a + 1 = \sin^2\beta(\cosh^2 a - 1) + 1 \\ &= \sin^2\beta \left(\frac{\cos\beta\cos\gamma + \cos\alpha}{\sin\beta\sin\gamma}\right)^2 - \sin^2\beta + 1 \\ &= \cos^2\beta + \left(\frac{\cos\beta\cos\gamma + \cos\alpha}{\sin\gamma}\right)^2. \qquad (3)\end{aligned}$$

Equations (2) and (3) together imply the following statement.

Lemma 6. *The strong triangle inequality holds if and only if*

$$f(\alpha,\beta,\gamma) = \cos^2\beta + \left(\frac{\cos\beta\cos\gamma + \cos\alpha}{\sin\gamma}\right)^2 - \left(\frac{\cos\alpha\cos\beta + \cos\gamma}{\cos\gamma + 1 - \sin\gamma} - 1\right)^2 > 0$$

Notes:

(1) $f(\alpha,\beta,\gamma) = 0$ if and only if $a + b = c + h$. The proof of this is a minor variation of that of Lemma 6.
(2) $f(\alpha,\beta,\gamma)$ is symmetric in α and β. This is obvious from the geometry, but it is also not hard to prove directly.
(3) $f(\alpha,\beta,\gamma)$ is quadratic in $\cos\alpha$ and $\cos\beta$.
(4) $f(\alpha,\beta,\gamma)$ is not monotone in either $a + b - c - h$ or in $\cosh(a + b) - \cosh(c + h)$. Therefore it is not directly useful for studying the difference of the two sides in the strong triangle inequality.

Also note that it is fairly trivial to write down the condition $a+b > c+h$ with an inequality involving only α, β, and γ. Indeed, one can just use the law of cosines to compute a, b, and c from the angles, and some right triangle trigonometry to compute h. But just doing this simple approach will result in a formidable formula with inverse trigonometric functions and square roots. Even if one uses the fact that the condition is equivalent to $\cosh(a + b) > \cosh(c + h)$, the resulting naive formula is hopelessly complicated, and certainly not trivial to solve for α and β. Therefore, the importance and depth of Lemma 6 should not be underestimated.

4. Computing probabilities

Motivated by the original goal of computing the probability that the strong triangle inequality holds in hyperbolic geometry, we need to clarify first under what model we compute this probability.

In hyperbolic geometry there exists a triangle for arbitrarily chosen angles, provided that their sum is less than π. So it is natural to choose the three angles independently uniformly at random in $(0,\pi)$, and then aim to compute the probability that the strong triangle inequality holds, given that the sum of the chosen angles is less than π.

Of course, the computation can be reduced to a computation of volumes. Let

$$F = \{(\alpha,\beta,\gamma) \in (0,\pi)^3 : \alpha + \beta + \gamma < \pi,\ \max\{\alpha,\beta\} < \gamma < \pi/2\},$$

and let

$$S = \{(\alpha,\beta,\gamma) \in F : f(\alpha,\beta,\gamma) > 0\}.$$

Since f is continuous when $0 < \gamma < \pi/2$, and S is the level set of f (within F), S is measurable, so its volume is well-defined. The desired probability is then

$$\frac{\mathrm{Vol}(S)}{\pi^3/6},$$

where the denominator is the volume of the tetrahedron for which $\alpha + \beta + \gamma < \pi$.

So it remains to compute the volume of S. Fix $0 < \gamma < \pi/2$, and let

$$P_\gamma = \{(\alpha, \beta) : (\alpha, \beta, \gamma) \in F \text{ and } f(\alpha, \beta, \gamma) > 0\},$$
$$N_\gamma = \{(\alpha, \beta) : (\alpha, \beta, \gamma) \in F \text{ and } f(\alpha, \beta, \gamma) < 0\},$$
$$Z_\gamma = \{(\alpha, \beta) : (\alpha, \beta, \gamma) \in F \text{ and } f(\alpha, \beta, \gamma) = 0\}.$$

(See Figures 2 and 3 for illustration for $\gamma = 1.2$ and $\gamma = 1.3$ respectively.) It is clear that

$$\mathrm{Vol}(S) = \int_0^{\pi/2} \mu(P_\gamma)\, d\gamma,$$

where μ is the 2-dimensional Lebesgue measure.

It is not hard to see why it will be useful for us to solve the equation $f(\alpha, \beta, \gamma) = 0$: it will provide a description of the set Z_γ, which will help us analyze the sets P_γ, and N_γ. This is easy, because f is quadratic in $\cos\beta$. The following extremely useful lemma shows that at most one of the quadratic solutions will lie in F.

Lemma 7. *Let $(\alpha, \beta, \gamma) \in F$ such that $f(\alpha, \beta, \gamma) = 0$. Let*

$$a = \csc^2\gamma - \left(\frac{\cos\alpha}{\cos\gamma + 1 - \sin\gamma}\right)^2,$$
$$b = \frac{\cos\alpha(\cos\gamma + 1)}{\sin^2\gamma},$$
$$c = \left(\frac{\cos\alpha}{\sin\gamma}\right)^2 - \left(\frac{1 - \sin\gamma}{\cos\gamma + 1 - \sin\gamma}\right)^2.$$

Then

$$\cos\beta = \frac{-b - \sqrt{b^2 - 4ac}}{2a}.$$

Proof. By tedious, but simple algebra one can see that $f(\alpha, \beta, \gamma) = 0$ if and only if $a\cos^2\beta + b\cos\beta + c = 0$. To see the result, we will show that if $(\alpha, \beta, \gamma) \in F$, then $(-b + \sqrt{b^2 - 4ac})/(2a) < 0$. We will proceed by showing that for $(\alpha, \beta, \gamma) \in F$, we have $b > 0$, and $c > 0$. The former is trivial. For the latter, here follows the sequence of implied inequalities.

$$1 + \cos\gamma > \sin\gamma(1 + \cos\gamma) = \sin\gamma + \sin\gamma\cos\gamma$$
$$\cos^2\gamma + \sin^2\gamma + \cos\gamma > \sin\gamma + \sin\gamma\cos\gamma$$
$$\cos\gamma(\cos\gamma + 1 - \sin\gamma) > \sin\gamma(1 - \sin\gamma)$$
$$\frac{\cos\alpha}{\sin\gamma} \geq \frac{\cos\gamma}{\sin\gamma} > \frac{1 - \sin\gamma}{\cos\gamma + 1 - \sin\gamma}$$

Squaring both sides will give $c > 0$.

We have shown that $b, c > 0$. If $a = 0$, then $\cos\beta = -c/b < 0$, and that is inadmissible. If $a > 0$, then $b^2 - 4ac < b^2$, so $(-b + \sqrt{b^2 - 4ac})/(2a) < 0$, and similarly, if $a < 0$, then $b^2 - 4ac > b^2$, so $(-b + \sqrt{b^2 - 4ac})/(2a) < 0$ again. □

Recall that a set $R \subseteq \mathbb{R} \times \mathbb{R}$ is called a *function*, if for all $x \in \mathbb{R}$ there is at most one $y \in \mathbb{R}$ such that $(x, y) \in R$. Also $R^{-1} = \{(y, x) : (x, y) \in R\}$. R is *symmetric*, if $R = R^{-1}$. The domain of a function R is the set $\{x : \exists y, (x, y) \in R\}$.

So far we have learned the following about Z_γ.

- Z_γ is a function (by Lemma 7).
- Z_γ is symmetric.
- Z_γ is injective (that is Z_γ^{-1} is function).
- $\mu(Z_\gamma) = 0$.

The last fact follows, because Z_γ is closed, and hence, it is measurable.

Therefore the computation may be reduced to that of $\mu(N_\gamma)$, which will turn out to be more convenient.

Let γ be fixed, and let $0 < \alpha < \gamma$. We will say that α is *all-positive*, if for all β we have $f(\alpha, \beta, \gamma) \geq 0$. Similarly, α is *all-negative*, if for all β, $f(\alpha, \beta, \gamma) \leq 0$. If there is a β' such that $f(\alpha, \beta', \gamma) = 0$, then there are two possibilities: if for all $\beta < \beta'$, we have $f(\alpha, \beta, \gamma) < 0$, and for all $\beta > \beta'$, we have $f(\alpha, \beta, \gamma) > 0$, then we will say α is *negative-positive*. If it's the other way around, we will say α is *positive-negative*.

We will use the function notation $z(\alpha) = \beta$, when $(\alpha, \beta) \in Z_\gamma$; $z(\alpha)$ is undefined if α is not in the domain of Z_γ. When we want to emphasize the dependence on γ, we may write $z_\gamma(\alpha)$ for $z(\alpha)$.

Lemma 8. *If z_γ is defined at α, then*

$$z_\gamma(\alpha) = \cos^{-1}\left(\frac{-b - \sqrt{b^2 - 4ac}}{2a}\right),$$

where a, b, c are as in Lemma 7.

Proof. This is direct consequence of Lemma 7. □

Our next goal is to extend the set F as follows:

$$\overline{F} = \{(\alpha, \beta, \gamma) \in (0, \pi)^3 : \alpha + \beta + \gamma \leq \pi,\ \max\{\alpha, \beta\} \leq \gamma < \pi/2\}.$$

So we are extending F by considering cases where $\alpha + \beta + \gamma = \pi$ and where $\max\{\alpha, \beta\} = \gamma$. For fixed γ such that $0 < \gamma < \pi/2$, the collection $\{P_\gamma, N_\gamma, Z_\gamma\}$ is extended by letting

$$\overline{P}_\gamma = P_\gamma \cup \{(\alpha, \beta) : (\alpha, \beta, \gamma) \in \overline{F} \setminus F \text{ and } a + b > c + h\},$$
$$\overline{N}_\gamma = N_\gamma \cup \{(\alpha, \beta) : (\alpha, \beta, \gamma) \in \overline{F} \setminus F \text{ and } a + b < c + h\},$$
$$\overline{Z}_\gamma = Z_\gamma \cup \{(\alpha, \beta) : (\alpha, \beta, \gamma) \in \overline{F} \setminus F \text{ and } a + b = c + h\}.$$

We will show that with this extension, sequences of points entirely outside of P_γ can not converge to a point in $\overline{P}_\gamma$, and similarly for N_γ. But first, we need a

lemma that, in a way, formalizes the well-known intuition that infinitesimally small hyperbolic triangles are becoming arbitrarily similar to Euclidean triangles.

Lemma 9. *Let $\{(\alpha_i, \beta_i, \gamma_i)\}_{i=1}^{\infty}$ be a sequence in $\mathbb{R}^3$, such that $(\alpha_i, \beta_i, \gamma_i) \to (\alpha, \beta, \gamma)$ with $\alpha_i + \beta_i + \gamma_i < \pi$ for all i, and $\alpha + \beta + \gamma = \pi$. Let a_i, b_i, c_i be the sides of the hyperbolic triangle determined by $\alpha_i, \beta_i, \gamma_i$, and let h_i be the height corresponding to c_i. Furthermore, consider the class of similar Euclidean triangles with angles α, β, γ, and let a, b, c be the sides of an element of this class, and let h be the height corresponding to c. Then*

$$\lim_{i\to\infty} \frac{a_i + b_i - c_i}{h_i} = \frac{a + b - c}{h}.$$

Proof. First we will prove that $a_i/b_i \to a/b$. By the law of sines for both the hyperbolic and Euclidean planes,

$$\frac{\sinh a_i}{\sinh b_i} = \frac{\sin \alpha_i}{\sin \beta_i} \to \frac{\sin \alpha}{\sin \beta} = \frac{a}{b}.$$

Since $a_i, b_i \to 0$, $\lim(\sinh a_i / \sinh b_i) = \lim(a_i/b_i)$, and the claim follows.

Note that applying this to various triangles formed by the height and the sides, this also implies $a_i/h_i \to a/h$, and $b_i/h_i \to b/h$. To see that $c_i/h_i \to c/h$, just observe that $c_i/h_i = (c_i/b_i)(b_i/h_i)$. □

Corollary 10. *Let $\gamma \in (0, \pi/2)$. Let $\{(\alpha_i, \beta_i)\}_{i=1}^{\infty}$ be a sequence in $\mathbb{R}^2$ such that $(\alpha_i, \beta_i) \to (\alpha, \beta)$ with $(\alpha_i, \beta_i, \gamma) \in F$ and $(\alpha, \beta, \gamma) \in \overline{F}$. Then $(\alpha_i, \beta_i) \notin P_\gamma$ implies $(\alpha, \beta) \notin \overline{P}_\gamma$, and $(\alpha_i, \beta_i) \notin N_\gamma$ implies $(\alpha, \beta) \notin \overline{N}_\gamma$.*

Proof. If $(\alpha, \beta, \gamma) \in F$, then this is a direct consequence of the continuity of f. If (α, β, γ) belongs to $\overline{F} \setminus F$, then $\alpha = \gamma$ or $\beta = \gamma$ or $\alpha + \beta + \gamma = \pi$. In the first two cases, all distances in the triangles determined by the angles $\alpha_i, \beta_i, \gamma_i$ converge to the corresponding distances in the limiting isosceles hyperbolic triangle determined by the angles α, β, γ. Finally, if $\alpha + \beta + \gamma = \pi$, then this is a consequence of Lemma 9 with the observation that the strong triangle inequality holds if and only if $\frac{a+b-c}{h} > 1$. □

Recall the notations Γ for the Baker–Powers constant, and B for the Bailey–Bannister constant. We will use the following lemma which was proven by Baker and Powers [2].

Lemma 11. *If $\gamma > \Gamma$, then there exists $\alpha' > 0$ such that for all $0 < \alpha < \alpha'$, the strong triangle inequality fails for the triangle with angles α, α, and γ.*

Lemma 12. *Let $\gamma \in (\Gamma, B)$. Then the set of values of α for which α is negative-positive is an open interval $(0, i_\gamma)$, and z is defined, continuous, and decreasing on this interval. Furthermore, the region N_γ is exactly the region under the function z on the interval $(0, i_\gamma)$.*

See Figure 2 for illustration.

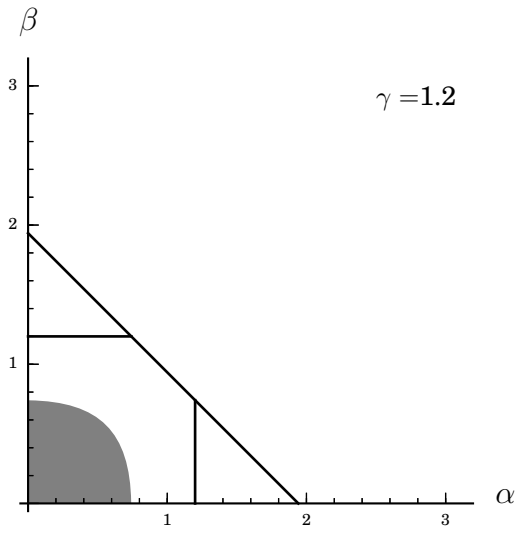

Figure 2. For $\gamma = 1.2$ here, the shaded region is N_γ, and the unshaded is P_γ. The boundary is Z_γ. The horizontal and vertical line segments represent $\beta = \gamma$ and $\alpha = \gamma$, beyond which it is guaranteed that the strong triangle inequality holds. The diagonal $\beta = \pi - \gamma - \alpha$ represents Euclidean triangles.

Proof. First note that the condition on γ implies that every α is either all-positive or negative-positive. Indeed, any other type of α would give rise to a sequence of points in N_γ converging to a point in $\overline{P}_\gamma$. Let C be the set of values of α, for which α is negative-positive. Clearly z is defined on C.

By Lemma 11, there exists $\alpha' > 0$ such that for all $0 < \alpha < \alpha'$, $f(\alpha, \alpha, \gamma) < 0$. This also means that for all $0 < \alpha < \alpha'$, $\alpha \in C$.

Since $\gamma < B$ it follows that the diagonal $\alpha+\beta+\gamma = \pi$ lies in $\overline{P}_\gamma$. Moreover, by Proposition 1, the appropriate vertical line segment $\alpha = \gamma$ belongs to $\overline{P}_\gamma$. Consider the open segment going right from the point $(\alpha'/2, \alpha'/2)$ and ending at the point $(x, \alpha'/2)$ such that $(x, \alpha'/2, \gamma) \in \overline{F} \setminus F$. By Corollary 10, we can not have the open segment entirely in N_γ. So there exists $\alpha'/2 < \alpha_0 < \gamma$ with $(\alpha_0, \alpha'/2) \in Z_\gamma$. We also have that $(0, \alpha_0) \subseteq C$.

By Lemma 8, z is continuous on $(0, \alpha_0)$. Injective continuous functions are monotone, and by symmetry again, z must be monotone decreasing on $(0, \alpha_0)$. The portion of z on $(0, \alpha'/2)$ is "copied" to the portion after α_0, so there exists $\alpha_1 > \alpha_0$ such that $(0, \alpha_1) \subseteq C$, and z is continuous, monotone decreasing on $(0, \alpha_1)$, and $\lim_{\alpha \to \alpha_1^-} z(\alpha) = 0$.

We claim that in fact $(0, \alpha_1) = C$. Suppose not, and there exists $\alpha_2 > \alpha_1$ with $\alpha_2 \in C$. For all $0 < \beta_2 < \min\{z(\alpha_2), \alpha'/2\}$, the horizontal line $\beta = \beta_2$ contains only one point from Z_γ. That implies that in fact the entire open line segment between $(0, \beta_2)$ to $(\min\{\pi - \gamma - \beta_2, \gamma\}, \beta_2)$ lies in $N_\gamma \cup Z_\gamma$. Thereby, we could construct a sequence in $N_\gamma \cup Z_\gamma$ converging to a point in $\overline{P}_\gamma$ contrary to Corollary 10. So the first part of the statement holds with $i_\gamma = \alpha_1$.

The second part of the statement is obvious after the first part, which is necessary to show that there is a well-defined region under the function on the interval $(0, i_\gamma)$. □

For the actual computations, we will need to numerically compute the value of i_γ. Since $i_\gamma = \lim_{\alpha\to 0^+} z(\alpha)$, and since z remains continuous even if we extend the function by its formula for $\alpha = 0$, it is easy to compute its value. In fact it turns out that it has a relatively simple formal expression:

$$i_\gamma = \cos^{-1}\left(\frac{(\sin\gamma - 1)^2 + \cos\gamma}{2\sin\gamma - \cos\gamma - 1}\right).$$

Now we will start to work on the more difficult case when $\gamma \in (B, \pi/2)$. First we need two technical lemmas.

Lemma 13. *$f(\alpha, \beta, \gamma)$ is monotone decreasing in γ.*

Proof. Let

$$f_1(\alpha,\beta,\gamma) = \frac{\cos\beta\cos\gamma + \cos\alpha}{\sin\gamma}, \qquad f_2(\alpha,\beta,\gamma) = \frac{\cos\alpha\cos\beta + \cos\gamma}{\cos\gamma + 1 - \sin\gamma} - 1.$$

Then

$$f(\alpha,\beta,\gamma) = \cos^2\beta + [f_1(\alpha,\beta,\gamma)]^2 - [f_2(\alpha,\beta,\gamma)]^2.$$

Simple computations show

$$\frac{\partial f_1}{\partial\gamma} = \frac{-\cos\beta\sin^2\beta - (\cos\beta\cos\gamma + \cos\alpha)\cos\gamma}{\sin^2\gamma} < 0,$$
$$\frac{\partial f_2}{\partial\gamma} = \frac{1 - \sin\gamma + \cos\alpha\cos\beta(\sin\gamma + \cos\gamma)}{(\cos\gamma + 1 - \sin\gamma)^2} > 0.$$

Since for all $(\alpha, \beta, \gamma) \in F$, clearly $f_1 > 0$, and by Lemma 5, $f_2 > 0$, we get that

$$\frac{\partial f}{\partial\gamma} = 2f_1\frac{\partial f_1}{\partial\gamma} - 2f_2\frac{\partial f_2}{\partial\gamma} < 0.$$

□

Lemma 14. *Let $\gamma \in [B, \pi/2)$. Then all isosceles triangles with angles α, α, and γ fail the strong triangle inequality. Furthermore, these triangles fail with inequality, that is, $(\alpha, \alpha, \gamma) \in N_\gamma$.*

Proof. We will use Lemma 4 with $\alpha = \beta$ and $\gamma = B$. In that case, $\cos\gamma = 7/25$ and $\sin\gamma = 24/25$; also $\cosh h = \cos\alpha/\sin(B/2) = \frac{5}{3}\cos\alpha$. It is elementary to see that to satisfy the inequality of the lemma, even with equality, $\cos\alpha \le 3/5$ is necessary, so $\alpha, \beta \ge \cos^{-1}(3/5)$, and then $\alpha + \beta + \gamma \ge 2\cos^{-1}(3/5) + \tan^{-1}(24/7) = \pi$.

So if $\gamma = B$, then all $(\alpha, \alpha) \in N_\gamma$, and by Lemma 13, this remains true for $\gamma > B$. □

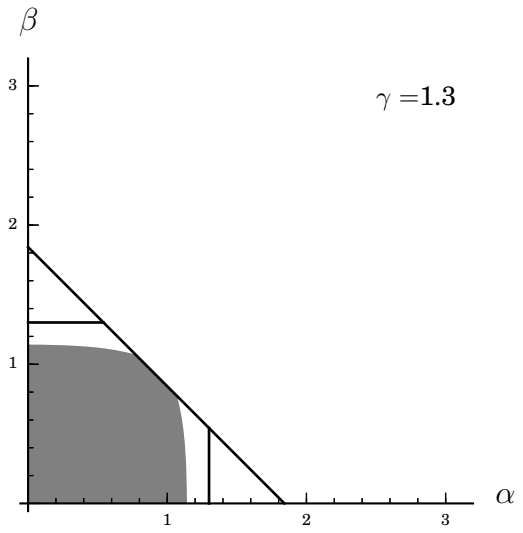

Figure 3. Similar to Figure 2, the shaded region represents N_γ, this time for $\gamma = 1.3$. See caption of Figure 2 for additional explanation of features.

Lemma 15. *Let $\gamma \in [B, \pi/2)$. Then the set of values of α for which α is negative-positive is the union of two open intervals $(0, e_\gamma)$ and $(\pi - \gamma - e_\gamma, i_\gamma)$, and z is continuous and decreasing on these intervals. No value α is positive-negative. Furthermore, the region N_γ is the region under z and under the line $\alpha+\beta+\gamma = \pi$.*

See Figure 3 for illustration.

Proof. Let $\gamma \in [B, \pi/2)$. By [1], there exists $(\alpha, \beta) \notin \overline{P}_\gamma$ on the diagonal $\alpha+\beta+\gamma = \pi$. It is implicit in [3] that the set $\{(\alpha, \beta) \notin \overline{P}_\gamma : \alpha + \beta + \gamma = \pi\}$ is a closed line segment of the line $\alpha + \beta + \gamma = \pi$, and the endpoints of this line segment are the only points of $\overline{Z}_\gamma$ of the line. Also, this line segment is symmetric in α and β. Let the two endpoints of the line segment have coordinates $(e_\gamma, \pi - \gamma - e_\gamma)$, and $(\pi - \gamma - e_\gamma, e_\gamma)$.

By Lemma 14, the open line segment from $(0, 0)$ to $(\frac{\pi-\gamma}{2}, \frac{\pi-\gamma}{2})$ is entirely in N_γ. Let

$$T = \{(\alpha, \beta) : e_\gamma \leq \alpha, \beta \leq \pi - \gamma - e_\gamma \text{ and } \alpha + \beta + \gamma < \pi\}.$$

We will show that $T \subseteq N_\gamma \cup Z_\gamma$. Indeed, suppose a point (α, β) in the interior of T belongs to P_γ. Without loss of generality $\alpha > \beta$. Then there are $\alpha_0 < \alpha < \alpha_1$ with $(\alpha_0, \beta), (\alpha_1, \beta) \in T \cap N_\gamma$, and so by continuity, there are α_0' and α_1' with $(\alpha_0', \beta), (\alpha_1', \beta) \in T \cap Z_\gamma$, contradicting the fact that Z_γ is a function. The statement for the boundary of T follows from Corollary 10.

If $\alpha < e_\gamma$, then α is negative-positive. This is because $(\alpha, \alpha) \in N_\gamma$ and $(\alpha, \min\{\pi - \gamma - \alpha, \gamma\}) \in \overline{P}_\gamma$. So $z_\gamma(\alpha)$ is defined on $(0, e_\gamma)$, and therefore it is continuous on this interval.

Now we will show that $\lim_{\alpha\to e_\gamma^-} z(\alpha) = \pi - \gamma - e_\gamma$. If this is not true, there is $\epsilon > 0$ and a sequence $\alpha_1, \alpha_2, \ldots$ with $\alpha_n \to e_\gamma$ such that $z(\alpha_n) < \pi - \gamma - e_\gamma - \epsilon$. Let $\beta_n = \pi - \gamma - e_\gamma - \epsilon/2$ (a constant sequence). Now the sequence (α_n, β_n) converges to the point $(e_\gamma, \pi - \gamma - e_\gamma - \epsilon/2)$, so a sequence of points in P_γ, converges to a point in $N_\gamma \cup Z_\gamma$. The only way this can happen if $(e_\gamma, \pi - \gamma - e_\gamma - \epsilon/2) \in Z_\gamma$. But the argument can be repeated with $\epsilon/3$ instead of $\epsilon/2$, so $(e_\gamma, \pi - \gamma - e_\gamma - \epsilon/3) \in Z_\gamma$, and this contradicts the fact that Z_γ is a function.

Since $z(\alpha)$ is continuous and bijective on $(0, e_\gamma)$, it is monotone. We will show it must be decreasing. First we note that for $\gamma = B$, z is clearly decreasing, because in that case $e_\gamma = \frac{\pi-\gamma}{2}$, and by symmetry, the function is "copied over" to the interval (e_γ, i_γ), so it can not be increasing and bijective. Then, since f is continuous, $z_\gamma(\alpha)$ is continuous in γ, so if $z_\gamma(\alpha_1) > z_\gamma(\alpha_2)$ for some $\alpha_1 < \alpha_2$ and $z_{\gamma'}(\alpha_1) < z_{\gamma'}(\alpha_2)$ for some $\gamma' > \gamma$, then by the Intermediate Value Theorem, there is a $\gamma < \gamma_0 < \gamma'$ for which $z_{\gamma_0}(\alpha_1) = z_{\gamma_0}(\alpha_2)$, a contradiction. Informally speaking, the function z can not flip its monotonicity without failing injectivity at some point.

We have already seen that α is negative-positive on $(0, e_\gamma)$. By the fact that z is decreasing on this interval, it is implied that α is all-negative on $[e_\gamma, \pi - \gamma - e_\gamma]$, and α is again negative-positive on $(\pi - \gamma - e_\gamma, i_\gamma)$. Finally, α is all-positive on $[i_\gamma, \gamma)$.

The last statement of the lemma is now clear. □

For the actual computations, we will need the value of e_γ. From [3], which describes the equality case for Euclidean geometry, we know that e_γ is the value of α for which

$$\tan\left(\frac{\alpha}{2}\right) + \tan\left(\frac{\beta}{2}\right) = 1,$$

and since the triangle is Euclidean, we have $\alpha/2 + \beta/2 = \pi/2 - \gamma/2$. These equations yield two symmetric solutions for α and β; by our choice in the lemma, we need the smaller of these. We conclude

$$e_\gamma = 2\tan^{-1}\left(\frac{1}{2} - \sqrt{\tan\left(\frac{\gamma}{2}\right) - \frac{3}{4}}\right).$$

For the proof of the next result we let

$$\overline{S} = \{(\alpha, \beta, \gamma) \in F : f(\alpha, \beta, \gamma) \le 0\}$$

and note that $\overline{S}$ is the set of points in F where the strong triangle inequality fails.

Theorem 16. *The probability that the strong triangle inequality holds is*

$$\frac{7}{8} - \frac{6}{\pi^3}\left(\int_\Gamma^B \int_0^{i_\gamma} z_\gamma(\alpha)\, d\alpha d\gamma + \int_B^{\pi/2}\left(\frac{(\pi - \gamma - 2e_\gamma)^2}{2} - e_\gamma^2 + 2\int_0^{e_\gamma} z_\gamma(\alpha)\, d\alpha\right) d\gamma\right).$$

Proof. We break up the integral

$$\int_{\Gamma}^{\pi/2} \mu(N_\gamma)\, d\gamma \tag{4}$$

over two intervals: (Γ, B) and $(B, \pi/2)$. By Lemma 12, in the former interval, N_γ is the region under the function z_γ. So if $\gamma \in (\Gamma, B)$, then $\int_\Gamma^B \mu(N_\gamma)\, d\gamma = \int_\Gamma^B \int_0^{i_\gamma} z_\gamma(\alpha)\, d\alpha\, d\gamma$. If $\gamma \in (B, \pi/2)$, then, by Lemma 15 and symmetry,

$$\int_B^{\pi/2} \mu(N_\gamma)\, d\gamma = \int_B^{\pi/2} \left(2\int_0^{e_\gamma} z_\gamma(\alpha)\, d\alpha - e_\gamma^2 + (\pi - \gamma - 2e_\gamma)^2/2 \right) d\gamma.$$

Thus,

$$\mathrm{Vol}(\overline{S}) = \int_\Gamma^B \int_0^{i_\gamma} z_\gamma(\alpha)\, d\alpha d\gamma + \int_B^{\pi/2} \left(\frac{(\pi - \gamma - 2e_\gamma)^2}{2} - e_\gamma^2 + 2\int_0^{e_\gamma} z_\gamma(\alpha)\, d\alpha \right) d\gamma.$$

By Proposition 2, the strong triangle inequality does not hold if $\gamma \geq \frac{\pi}{2}$. The volume of the tetrahedron for $\gamma \geq \pi/2$ is $\pi^3/48$. Since the volume of the tetrahedron with $\gamma \geq 0$ is $\pi^3/6$ it follows that the required probability is

$$1 - \left(\frac{\mathrm{Vol}(\overline{S})}{\pi^3/6} + \frac{1}{8} \right),$$

and the formula follows. □

5. Theoretical error estimates

We are almost ready to use our favorite computer algebra system to compute the actual number. However, numerical integration will not guarantee accurate results in general. To make sure that we can (theoretically) control the error of computation, we need one more theorem.

Theorem 17. *The volume of $\overline{S}$ may be approximated by arbitrary precision. More precisely, for all $\epsilon > 0$ there is an algorithm to compute a numerical upper bound M and a lower bound m such that $m < \mathrm{Vol}(\overline{S}) < M$ and $M - m < \epsilon$.*

Proof. Lemma 13 implies that in (4) we integrate a monotone increasing function, because $\mu(N_\gamma)$ is the measure of the level set of f at γ. Recall that for a monotone decreasing (respectively, increasing) function, the left Riemann sum overestimates (underestimates) the integral, and the right Riemann sum underestimates (overestimates) it. That is, it is possible to know how precise the the numerical estimate is, and if necessary, it is possible to repeat the computation with higher resolution.

In the actual computation given by Theorem 16, both terms in the parenthesis involve computations of integrals of monotone functions, and the inner integrals in those terms are also computing integrals of monotone functions. So, in essence, the numerical computation involves the integration of a monotone increasing function, whose values may be approximated at arbitrary precision. □

6. Conclusion

We can now use Theorem 16 and the computer algebra system Sage to get the following result.

Corollary 18. *Under the assumption that α, β, γ can be chosen uniformly in the interval $(0, \pi)$ and $\alpha + \beta + \gamma < \pi$, the strong triangle inequality $a + b > c + h$ holds approximately 78.67% of the time.*

Since we know that the strong triangle inequality fails when $\gamma \geq \pi/2$, we could restrict our attention to triangles where $\gamma < \pi/2$. In this case, the inequality $a + b > c + h$ holds approximately 90% of the time. For the Euclidean case, where $\alpha+\beta+\gamma = \pi$ and $\gamma < \pi/2$, it was shown in [3] that the strong triangle inequality holds approximately 92% of the time. Since the calculations in this paper involved volumes and the calculations in [3] involved areas, it is hard to directly compare the hyperbolic and Euclidean probabilities of the strong triangle inequality. We can say, however, that in both planes the strong triangle inequality is likely to hold.

Appendix A. Sage code

The following code will visualize the value $a+b-c-h$ (referred as "strength") of a labelled triangle depending on the angles. It generates 2000 pictures (or "frames"), and each frame will correspond to a fixed value of the angle γ, which grows throughout the frames from 0 to $\pi/2$. The number of frames is defined with the variable `number`. For each frame, the strength is indicated for the angles α, β, as the color of a point in the (α, β) coordinate system. Small positive strength is indicated by blue colors, high positive strength is indicated by red colors. The contours are changing from 0 to 1. Negative strength will be simply the darkest blue. To make the frames more informative, this darkest blue color may be replaced by a distinctive color outside of Sage (e.g. using Imagemagick). A black square on the bottom left corner indicates the points for which γ is the greatest angle. Outside of this square, the strength is proven to be positive. The pictures are saved as numbered `png` files.

```
sage: def strength(al,be,ga): #this is a+b-c-h
...       cha=(cos(be)*cos(ga)+cos(al))/(sin(be)*sin(ga))
...       chb=(cos(al)*cos(ga)+cos(be))/(sin(al)*sin(ga))
...       chc=(cos(al)*cos(be)+cos(ga))/(sin(al)*sin(be))
...       a=arccosh(cha)
...       b=arccosh(chb)
...       c=arccosh(chc)
...       shb=sqrt(chb^2-1)
...       shh=shb*sin(al)
...       h=arcsinh(shh)
...       expression=a+b-c-h
...       return expression
...
sage: def defect(al,be,ga): return pi-al-be-ga
...
sage: var("al be ga")
sage: con=[]
sage: for i in xrange(50): con.append(i/50)
```

```
sage: map=sage.plot.colors.get_cmap('coolwarm')
sage: number=2000
sage: for i in xrange(number):
...       gamma=(i+1)*(pi/2)/(number)
...       p=contour_plot(strength(al,be,ga=gamma),(al,0,pi),(be,0,pi),
...           contours=con,cmap=map,plot_points=1000,
...           figsize=[10,10],region=defect(al,be,ga=gamma))
...       p+=line([(0,pi-gamma),(pi-gamma,0)],color='black')
...       p+=line([(0,gamma),(min(pi-2*gamma,gamma),gamma)],color='black')
...       p+=line([(gamma,0),(gamma,min(pi-2*gamma,gamma))],color='black')
...       p+=text("$\\gamma=$"+str(float(gamma)),(2.5,3),
...           vertical_alignment='top',horizontal_alignment='left')
...       p.save('hyper'+str(i).zfill(4)+'.png')
```

A video generated by this code can be found at

`http://www.math.louisville.edu/~biro/movies/sti.mp4`.

In this video, negative strength is represented by the color green. To generate the video, the following commands were executed in Bash (Linux Mint 17.1, ImageMagick and libav-tools installed). The reason of cropping in the second line is that the default mp4 encoder for avconv (libx264) requires even height and width.

```
for i in hyper*.png; do convert $i -fill green -opaque "#3b4cc0" x$i; done
avconv -i xhyper%04d.png -r 25 -vf "crop=2*trunc(iw/2):2*trunc(ih/2):0:0"
-b:v 500k sti.mp4
```

The following code performs the numerical computation of the integral. We are trying to follow the paper as close as possible, including notations. Note that the numerical integration is performed by Gaussian quadrature, so error bounds are not guaranteed in this code. We use the `mpmath` package and we store 100 decimal digits.

```
sage: from mpmath import *
sage: mp.dps=100
sage: Gamma=findroot(lambda x: -1-cos(x)+sin(x)+sin(x/2)*sin(x),1.15)
sage: Beta=atan(24/7)
...
sage: def i(gamma):
...       return acos(((sin(gamma)-1)^2+cos(gamma))/(2*sin(gamma)-cos(gamma)-1))
...       #return z(gamma,0) #This should give the same result
...
sage: def e(gamma):
...       D=tan(gamma/2)-3/4
...       if D<0:
...           sol=1/2
...       else:
...           sol=1/2-sqrt(D)
...       return 2*atan(sol)
...
sage: def z(gamma,alpha):
...       denominator=cos(gamma)+1-sin(gamma)
...       a=csc(gamma)^2-(cos(alpha)/denominator)^2
...       b=cos(alpha)*(cos(gamma)+1)/sin(gamma)^2
...       c=(cos(alpha)/sin(gamma))^2-((sin(gamma)-1)/denominator)^2
...       d=b^2-4*a*c
...       if d>=0:
...           sol=(-b-sqrt(d))/(2*a)
```

```
...       else:
...           sol=-b/(2*a)
...       if sol>1 or sol<-1:
...           result=0
...       else:
...           result=min(acos(sol),pi-alpha-gamma)
...       return result
...
sage: f = lambda gamma: quad(lambda alpha: z(gamma,alpha),[0,i(gamma)])
sage: g = lambda gamma: (pi-gamma-2*e(gamma))^2/2-e(gamma)^2+
....      2*quad(lambda alpha: z(gamma,alpha),[0,e(gamma)])
sage: int1=quad(f,[Gamma,Beta])
sage: int2=quad(g,[Beta,pi/2])
sage: print "Probability:", 7/8-(6/pi^3)*(int1+int2)
```

Computer code

A version of this paper extended with computer code is available on arXiv.

References

[1] H. R. Bailey and R. Bannister, A stronger triangle inequality, *College Math. J.*, 28 (1997) 182–186.
[2] M. Baker and R. C. Powers, A stronger triangle inequality for neutral geometry, *Forum Geom.*, 7 (2007) 25–29.
[3] V. Faĭziev, R. C. Powers, and P. Sahoo, When can one expect a stronger triangle inequality?, *College Math. J.*, 44 (2013) 24–31.
[4] M. S. Klamkin, A sharp triangle inequality, *College Math. J.*, 29 (1998) 33.
[5] S. Stahl, *The Poincaré Half-Plane*, A gateway to modern geometry, Jones and Bartlett Publishers, Boston, MA, 1993,

Csaba Biró: Department of Mathematics, University of Louisville, Louisville, Kentucky 40292, USA
E-mail address: csaba.biro@louisville.edu

Robert C. Powers: Department of Mathematics, University of Louisville, Louisville, Kentucky 40292, USA
E-mail address: robert.powers@louisville.edu

Forum Geometricorum
Volume 16 (2016) 115–117.

FORUM GEOM
ISSN 1534-1178

The Triangle Construction $\{\alpha, b-c, t_A\}$

Paris Pamfilos

Abstract. We study the problem of constructing a triangle from the data $\{\alpha, b-c, t_A\}$, t_A being the length of the internal angle bisector of angle A of a triangle with side lengths a, b, c, and angles α, β, γ. The key-point is the detection of a parabola intimately related to the construction problem.

1. The problem

Denoting, as usual, by $\{a = |BC|, b = |CA|, c = |AB|\}$ the side-lengths, by $\{\alpha, \beta, \gamma\}$ the angles and by $\{t_A, t_C, t_B\}$ the lengths of the internal bisectors of the triangle ABC, the problem at hand is to construct the triangle, given the data $\{\alpha, b-c, t_A\}$. Figure 1 emphasizes the known parts of the triangle assuming that

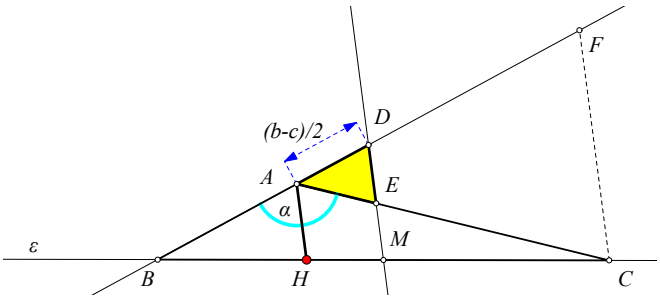

Figure 1. Representing the difference $\frac{b-c}{2}$

$b > c$. The isosceles triangle ADE is created by intersecting the sides $\{AB, AC\}$ with the parallel ME to the bisector AH, from the middle M of the side BC. It is easy to see that, ADE is an isosceles triangle and its lateral sides have the given length $(b-c)/2$. Later, for example, follows by drawing a parallel CF to the bisector AH and noticing that

$$|AD| = |BD| - |AB| = \frac{b+c}{2} - c = \frac{b-c}{2}.$$

In this figure, the known elements are the triangle ADE and the position, relative to ADE, and length of the bisector AH. Thus, the problem reduces to the construction of the appropriate line ε through H, which will define, through its intersections with the lateral sides of ADE, the other two vertices $\{B, C\}$.

Publication Date: April 1, 2016. Communicating Editor: Paul Yiu.

2. The parabola

The three sides of the triangle ABC and the line ME define a parabola ([1, II, p.212]), to which the four lines are tangent, and a key point is, that this parabola is constructible from the given data. Denoting by J the middle of DE and by I the intersection point of the external bisector ζ of the angle $\widehat{A}$ with the medial line of BC, we formulate this property in the following lemma.

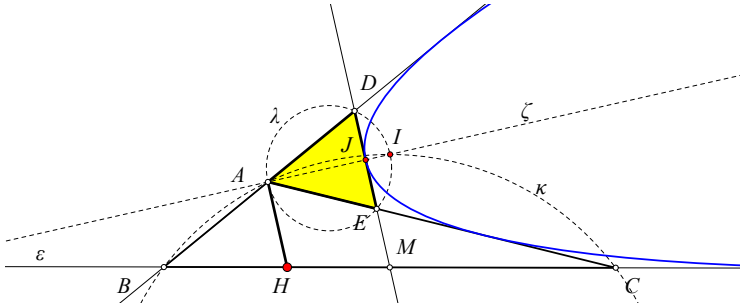

Figure 2. Parabola tangent to $\{AB, BC, CA, DE\}$

Lemma 1. *The parabola, with focus at I and having for tangent at its vertex the line DE, is tangent also to the three sides of the triangle ABC.*

Proof. The lemma results easily from the well known property of parabolas tangent to four lines in general position. It is known that the focus of such a parabola is the intersection point of the circumcircles of the four triangles, formed by three, of the four given lines ([4, p.222]). It suffices here to identify this intersection point with I (See Figure 2), which is trivial. Notice that I is constructible from the given data, since it coincides with the other than A intersection point of the medial line of DE with the circumcircle λ of the triangle ADE. □

3. The solution

Since the parabola is completely defined by the given data, it suffices to construct it and draw from H the tangents to it. This is a ruler and compasses construction, since it only involves the location of intersection points of a parabola and a given line, given the focus and the directrix of the parabola ([5, p. 42]). For the completeness of the exposition, I describe here the construction in a few steps:

(1) Find first the directrix, by drawing the parallel η to DE at the double of its distance from I (See Figure 3).

(2) Find the tangent ξ of the parabola at its intersection point L with the parallel ζ' to its axis ζ from H. This is the intersection point of the line ζ' with the medial line ξ of the segment IN, where N is the intersection point $N = (\zeta', \eta)$.

(3) Draw the parallel ξ' to ξ at double the distance of H from ξ and locate the intersection points $\{P, P'\}$ of the parabola with line ξ'. Lines $\{HP, HP'\}$ are the tangents from H to the parabola, which solve the construction problem.

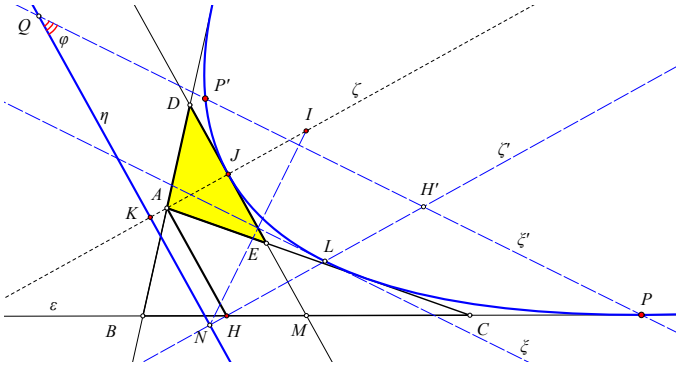

Figure 3. Constructing the tangent to the parabola from H

The intersection points $\{P, P'\}$, of the line ξ' with the parabola, can be constructed, using the angle ϕ of ξ' to η and an Apollonian circle. In fact, consider the intersection point Q of lines $Q = (\xi', \eta)$ and the ratio for arbitrary points X on the line ξ' :

$$\frac{|XI|}{|XQ|} = \frac{|XX_0|}{|XQ|} = \sin(\phi),$$

where X_0 is the projection of X on the directrix η. Hence points $\{P, P'\}$ are the intersections of line ξ' and the Apollonian circle of the segment IQ, for the ratio $k = \sin(\phi)$.

Remarks. (1) The tangent line DE to the parabola was used by Connelly and Randrianantoanina [3] also in some triangle construction problems in another context.

(2) A similar solution can be applied to the construction problem from the elements $\{\alpha, b-c, t'_A\}$, where t'_A denotes the length of the exterior bisector of the angle $\widehat{A}$.

(3) This interpretation of $b-c$ can be used to solve similar construction problems, e.g. from the elements $\{\alpha, b-c, m_A\}$, which is trivial, or $\{\alpha, b-c, h_A\}$, which is more involved ([2, p.144]), m_A and h_A denoting here, respectively, the median and the altitude from A.

References

[1] M. Berger, *Geometry*, vols I, II, Springer Verlag, Heidelberg, 1987.
[2] N. A. Court, *College Geometry*, Dover Publications Inc., New York, 1980.
[3] H. Connelly and B. Randrianantoanina, An angle bisector parallel applied to triangle construction, *Forum Geom.*, 9 (2009) 161–163.
[4] J. L. Hatton, *The Principles of Projective Geometry*, Cambridge University Press, Cambridge, 1913.
[5] I. D'Ignazio and E. Suppa. *Il Problema Geometrico, dal Compasso al Cabri*, interlinea editrice, Teramo, 2001.

Paris Pamfilos: University of Crete, Greece
E-mail address: pamfilos@math.uoc.gr

Forum Geometricorum
Volume 16 (2016) 119–124.

FORUM GEOM
ISSN 1534-1178

Golden Sections of Triangle Centers in the Golden Triangles

Emmanuel Antonio José García and Paul Yiu

Abstract. A golden triangle is one whose vertices are among the vertices of a regular pentagon. There are two kinds of golden triangles, short and tall, which are isosceles triangles with vertical angles 108° and 36° respectively. We consider some basic triangle centers of a short and tall golden triangles sharing one vertex and with the same circumcircle, and exhibit pairs of basic triangle centers divided in the golden ratio by another triangle center.

As is well known, the golden ratio naturally occurs in the regular pentagon, as the ratio of the length of a diagonal d and a side a: $\varphi := \frac{d}{a} = \frac{1}{2}(\sqrt{5}+1)$. The intersection of two diagonals divides each in the golden ratio. If $ABCDE$ is a regular pentagon, and the diagonals AD and BE intersect at P (see Figure 1), then

$$\frac{BE}{BP} = \frac{BP}{PE} = \varphi, \quad \frac{DA}{DP} = \frac{DP}{PA} = \varphi.$$

For later use, we note the following simple trigonometric ratios from Figure 1:

$$\cos 36^\circ = \frac{d/2}{a} = \frac{\varphi}{2}, \qquad \sin 18^\circ = \frac{a/2}{d} = \frac{1}{2\varphi}.$$

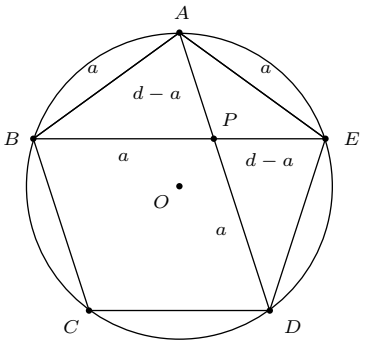

Figure 1. The golden section

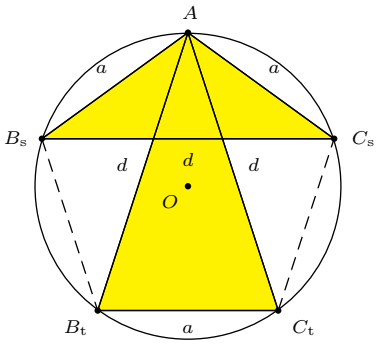

Figure 2. Short and tall golden triangles

Given a regular pentagon, the subtriangles with vertices among those of the pentagon are all isosceles. They fall into two types:
(i) those with three adjacent vertices of the pentagon have angles 108°, 36°, 36°, which we call *short golden triangles*,

Publication Date: April 1, 2016. Communicating Editor: Nikolaos Dergiades.

(ii) those with only two adjacent vertices of the pentagon have angles 36°, 72°, 72°, which we call *tall golden triangles*.

In this note we consider golden sections in the two kinds of golden triangles. For purpose of comparison, we consider a pair of short and tall golden triangles inscribed in the same regular pentagon $AB_{\rm s}B_{\rm t}C_{\rm t}C_{\rm s}$ (see Figure 2). The short golden triangle $\mathbf{T}_{\rm s} := AB_{\rm s}C_{\rm s}$ has sides d, a, a; the tall golden triangle $\mathbf{T}_{\rm t} := AB_{\rm t}C_{\rm t}$ has sides a, d, d. They share the same circumcenter O. Denote by R their common circumradius. Note that the areas Δ_i, $i = {\rm s}, {\rm t}$, of the golden triangles are in the golden ratio:

$$\frac{\Delta_{\rm t}}{\Delta_{\rm s}} = \frac{\frac{1}{2}ad\sin 72^\circ}{\frac{1}{2}a^2\sin 108^\circ} = \frac{d}{a} = \varphi.$$

For $i = {\rm s}, {\rm t}$, since the golden triangle $\mathbf{T}_i$ is isosceles, its triangle centers are all on the (common) perpendicular bisector of the side B_iC_i. We shall call this the *center line* of the golden triangles; It contains the midpoints F_i of B_iC_i (see Figure 3).

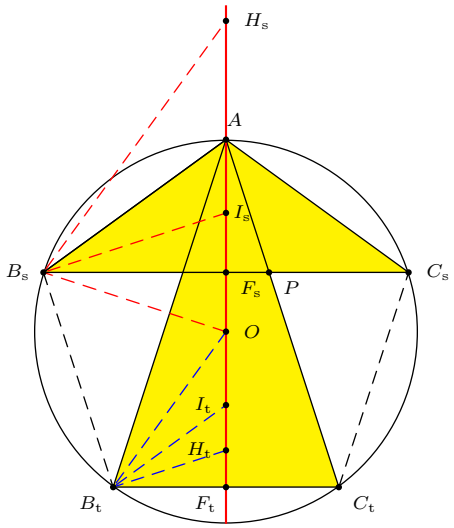

Figure 3

Here are some simple constructions of the basic triangle centers of $\mathbf{T}_{\rm s}$ and $\mathbf{T}_{\rm t}$.

(1) The incenter $I_{\rm s}$ of $\mathbf{T}_{\rm s}$ is the intersection of the center line with the perpendicular of $B_{\rm s}B_{\rm t}$ at $B_{\rm s}$; it is also the reflection of O in the side $B_{\rm s}C_{\rm s}$. From this, the inradius of $\mathbf{T}_{\rm s}$ is

$$r_{\rm s} = F_{\rm s}I_{\rm s} = OF_{\rm s} = R\cos 72^\circ = \frac{R}{2\varphi}.$$

(2) The incenter $I_{\rm t}$ of $\mathbf{T}_{\rm t}$ is the intersection of the diagonals $B_{\rm t}C_{\rm s}$ and $C_{\rm t}B_{\rm s}$. It is also the reflection of A in the side $B_{\rm s}C_{\rm s}$. From this, the inradius of $\mathbf{T}_{\rm t}$ is

$$\begin{aligned} r_{\rm t} &= \frac{a}{2}\tan 36^\circ = R\sin 36^\circ \tan 36^\circ = R\cdot\frac{\sin^2 36^\circ}{\cos 36^\circ} \\ &= R\cdot\frac{1-\left(\frac{\varphi}{2}\right)^2}{\frac{\varphi}{2}} = R\cdot\frac{4-\varphi^2}{2\varphi} = \frac{R}{2}(3\varphi-4). \end{aligned}$$

(3) Let $H_{\rm s}$ be the orthocenter of $\mathbf{T}_{\rm s}$. Clearly $\angle H_{\rm s}OB_{\rm s} = \angle I_{\rm s}OB_{\rm s} = 72^\circ$. Since $H_{\rm s}$ is the isogonal conjugate of O in $\mathbf{T}_{\rm s}$, $\angle H_{\rm s}B_{\rm s}O = 2\angle I_{\rm s}B_{\rm s}O = 2\cdot 36^\circ = 72^\circ$. Therefore, triangle $H_{\rm s}B_{\rm s}O$ is a (tall) golden triangle, and

$$\frac{OH_{\rm s}}{OB_{\rm s}} = \frac{d}{a} = \varphi \implies OH_{\rm s} = \varphi R.$$

Also, by the angle bisector theorem,

$$\frac{H_{\rm s}I_{\rm s}}{I_{\rm s}O_{\rm s}} = \frac{B_{\rm s}H_{\rm s}}{B_{\rm s}O_{\rm s}} = \varphi.$$

This shows that $I_{\rm s}$ *divides* $H_{\rm s}O$ *in the golden ratio.*

Since $B_{\rm s}A$ bisects angle $H_{\rm s}B_{\rm s}I_{\rm s}$, the same reasoning shows that A *divides* $H_{\rm s}I_{\rm s}$ *in the golden ratio*.

(4) In the tall golden triangle $\mathbf{T}_{\rm t}$, the orthocenter $H_{\rm t}$ is the intersection of the center line with the perpendicular to $B_{\rm s}B_{\rm t}$ at $B_{\rm t}$. Note that $B_{\rm t}H_{\rm t} = 2R\cos 72^\circ = 2R\cdot\frac{a/2}{d} = \frac{R}{\varphi}$.

Since $H_{\rm t}$ is the isogonal conjugate of O in $\mathbf{T}_{\rm t}$, by the angle bisector theorem,

$$\frac{OI_{\rm t}}{I_{\rm t}H_{\rm t}} = \frac{B_{\rm t}O}{B_{\rm t}H_{\rm t}} = \varphi.$$

Therefore, $I_{\rm t}$ *divides* $OH_{\rm t}$ *in the golden ratio*

(5) Since O and $I_{\rm t}$ are the reflections of $I_{\rm s}$ and A in $B_{\rm s}C_{\rm t}$, $OI_{\rm t} = AI_{\rm s}$, and

$$\frac{I_{\rm s}O}{OI_{\rm t}} = \frac{I_{\rm s}O}{AI_{\rm s}} = \varphi.$$

Therefore, O *divides* $I_{\rm s}I_{\rm t}$ *in the golden ratio*.

(6) In the tall golden triangle, O *divides* $AH_{\rm t}$ *in the golden ratio.*

$$\frac{AH_{\rm t}}{AO} = \frac{2\cdot R\cos 36^\circ}{R} = 2\cos 36^\circ = \varphi.$$

We summarize these results in the following proposition.

Proposition 1. *Let* $\mathbf{T}_i$, $i = {\rm s}, {\rm t}$ *be golden triangles sharing a common vertex* A *and the same circumcircle with center* O. *Let* H_i *and* I_i *denote the orthocenter and incenter of* $\mathbf{T}_i$.

(a) *The incenter* I_i *divides* H_iO *or* OH_i *in the golden ratio, according as* $i = {\rm s}, {\rm t}$.

(b) *The circumcenter* O *divides each of* $I_{\rm s}I_{\rm t}$ *and* $AH_{\rm t}$ *in the golden ratio.*

(c) A *divides* $H_{\rm s}I_{\rm s}$ *in the golden ratio.*

Some observations by Nikolaos Dergiades:
(i) O is the midpoint of I_sH_t.
(ii) If A' is the antipode of A on the circumcircle, the triangles $I_sH_sB_s$ and OB_sA' are similar to $\mathbf{T}_s$, and since $I_sB_s = OB_s = R$, we have $B_sH_s = B_sA' = R\varphi$.
(iii) The triangle $I_tH_sB_s$ has a right angle at B_s, and since $I_sH_s = I_sB_s$, I_s is the midpoint of H_sI_t.
(iv) The segments $OI_s = \frac{R}{\varphi}$, $I_sB_s = R$, $B_sH_s = R\varphi$ are in geometric progression (with common ratio φ). Since $\varphi = 1 + \frac{1}{\varphi}$, we have $B_sH_s = B_sI_s + OI_s$. This means that the circles $B_s(H_s)$, $I_s(H_s)$ and $O(I_s)$ are concurrent at a point D which lies on the line OB_s (see Figure 4).

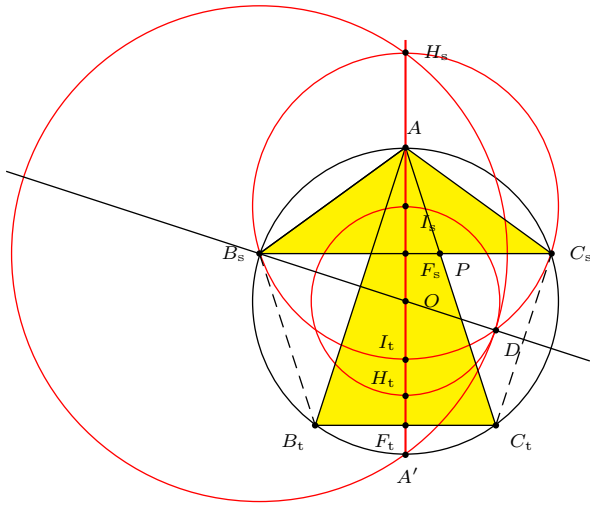

Figure 4

For $i = s, t$, the incircle of $\mathbf{T}_i$ is tangent to the side B_iC_i at its midpoint F_i. Since this midpoint also lies on the nine-point circle of $\mathbf{T}_i$, it is the Feuerbach point of $\mathbf{T}_i$. The nine-point circle of $\mathbf{T}_i$, $i = s, t$, also contains the midpoints $M_{i,b}$. $M_{i,c}$ of the sides AC_i and AB_i.

Proposition 2. (a) *F_s divides F_tA in the golden ratio.*
(b) *The incenter I_t divides F_sF_t in the golden ratio.*

Proof. (a) Let P be the intersection of the diagonals AC_t and B_sC_s (see Figure 3). Since B_sC_s and B_tC_t are parallel,

$$\frac{F_tA}{F_tF_s} = \frac{C_tA}{C_tP} = \varphi.$$

Therefore, F_s divides F_tA in the golden ratio.
(b) Since I_t is the intersection of the diagonals B_sC_t and B_tC_s, $\frac{F_sI_t}{I_tF_t} = \frac{B_sC_s}{B_sC_t} = \varphi$. □

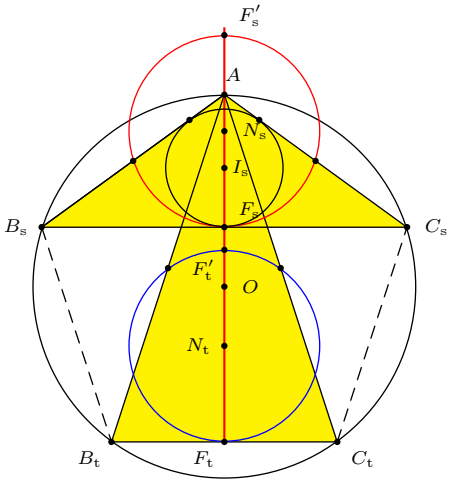

Figure 5

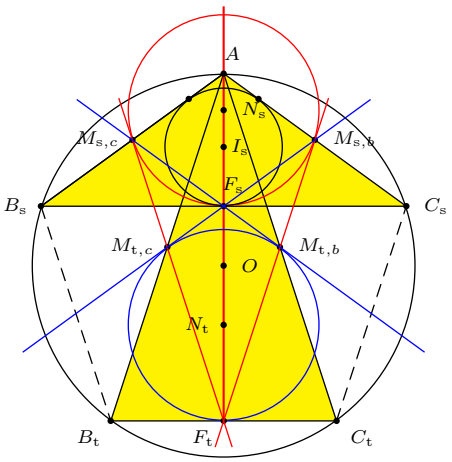

Figure 6

Proposition 3. (a) *For the short golden triangle* $\mathbf{T}_\mathrm{s}$ *with nine-point center* N_s*, the incenter* I_s *divides* $F_\mathrm{s}N_\mathrm{s}$ *in the golden ratio.*

(b) *For the tall golden triangle* $\mathbf{T}_\mathrm{t}$*, the nine-point center* N_t *divides* $F_\mathrm{t}O$ *in the golden ratio* (See Figure 5).

Proof. (a) The inradius of $\mathbf{T}_\mathrm{s}$ is $r_\mathrm{s} = \frac{R}{2\varphi}$. Therefore, $\frac{F_\mathrm{s}N_\mathrm{s}}{F_\mathrm{s}I_\mathrm{s}} = \frac{\frac{R}{2}}{r_\mathrm{s}} = \varphi$, and I_s divides $F_\mathrm{s}N_\mathrm{s}$ in the golden ratio.

(b) $F_\mathrm{t}O = R\cos 36^\circ = \frac{R}{2}\cdot\varphi$. Therefore, $\frac{F_\mathrm{t}O}{F_\mathrm{t}N_\mathrm{t}} = \varphi$, and N_t divides $F_\mathrm{t}O$ in the golden ratio. □

Proposition 4. *For* $\{i,j\} = \{\mathrm{s},\mathrm{t}\}$*, the nine-point center* N_i *of* $\mathbf{T}_i$ *is the reflection of* F_j *in the center* O*.*

Proof. (a) Since I_s is the reflection of O in $B_\mathrm{s}C_\mathrm{s}$,

$$OF_\mathrm{s} = F_\mathrm{s}I_\mathrm{s} = r_\mathrm{s} = \frac{R}{2\varphi},$$

$$ON_\mathrm{s} = OF_\mathrm{s} + F_\mathrm{s}N_\mathrm{s} = \frac{R}{2\varphi} + \frac{R}{2} = \frac{R}{2}\left(\frac{1}{\varphi}+1\right) = R\cdot\frac{\varphi}{2} = R\cos 36^\circ = F_\mathrm{t}O.$$

Therefore, N_s is the reflection of F_t in O.

(b) Since $N_\mathrm{t} - F_\mathrm{t} = N_\mathrm{s} - F_\mathrm{s}$,

$$N_\mathrm{t} = N_\mathrm{s} - F_\mathrm{s} + F_\mathrm{t} = 2\cdot O - F_\mathrm{t} - F_\mathrm{s} + F_\mathrm{t} = 2\cdot O - F_\mathrm{s}$$

is the reflection of F_s in O. □

Therefore, the nine-point center N_s is the antipode of F_t on the circle, center O, passing through F_t, which is the inscribed circle of the regular pentagon. It follows that $\angle N_\mathrm{s}M_{\mathrm{s},b}F_\mathrm{t}$ and $\angle N_\mathrm{s}M_{\mathrm{s},b}F_\mathrm{t}$ are right angles. This means that $F_\mathrm{t}M_{\mathrm{s},b}$ and $F_\mathrm{t}M_{\mathrm{s},c}$ are tangents to the nine-point circle of $\mathbf{T}_\mathrm{s}$ at $M_{\mathrm{s},b}$ and $M_{\mathrm{s},c}$ respectively (see Figure 6). The line $F_\mathrm{t}M_{\mathrm{s},b}$ passes through $M_{\mathrm{t},b}$, which divides $F_\mathrm{t}M_{\mathrm{s},b}$ in the

golden ratio. Similarly, $F_{\rm t}M_{{\rm s},c}$ is the tangent at $M_{{\rm s},c}$ and is divided in the golden ratio by $M_{{\rm t},c}$.

The same reasoning also leads to the following.

(i) The points $M_{{\rm s},b}$, $F_{\rm s}$, $M_{{\rm t},c}$ are collinear, and $F_{\rm s}$ divides $M_{{\rm s},b}M_{{\rm t},c}$ in the golden ratio. Furthermore, the line containing them is tangent to the nine-point circle of $\mathbf{T}_{\rm t}$ at $M_{{\rm t},c}$.

(ii) The points $M_{{\rm s},c}$, $F_{\rm s}$, $M_{{\rm t},b}$ are collinear, and $F_{\rm s}$ divides $M_{{\rm s},c}M_{{\rm t},b}$ in the golden ratio. Furthermore, the line containing them is tangent to the nine-point circle of $\mathbf{T}_{\rm t}$ at $M_{{\rm t},b}$.

We conclude this note with a few more division in the golden ratio with points in Figure 5. The simple proofs are omitted.

For $i = {\rm s}, {\rm t}$, let F_i' be the antipode of F_i on the nine-point circle of $\mathbf{T}_i$. Then
(a) A divides $F_{\rm s}'N_{\rm s}$ in the golden ratio,
(b) $F_{\rm t}'$ divides each of the segments $AN_{\rm t}$ and $F_{\rm t}N_{\rm s}$ in the golden ratio,
(c) O divides $F_{\rm s}'F_{\rm t}$ in the golden ratio,
(d) $I_{\rm s}$ divides $F_{\rm s}'F_{\rm t}'$ in the golden ratio.

Statement (d) follows from Proposition 2(b) and a translation by R along the center line.

Figure 7 summarizes the golden sections in this note, each indicated by a longer solid segment followed by a shorter dotted segment. The endpoints and the division points are indicated on the "center line".

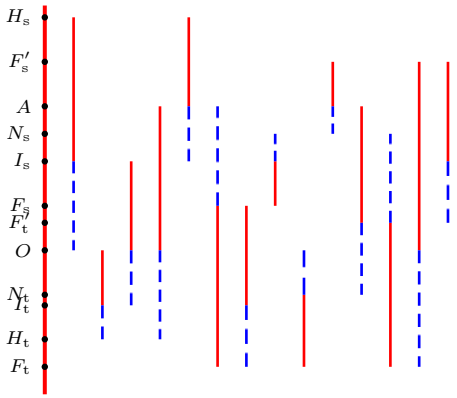

Figure 7

References

[1] M. Bataille, Another simple construction of the golden section, *Forum Geom.*, 11 (2011) 55.
[2] K. Hofstetter, A simple construction of the golden section, *Forum Geom.*, 2 (2002) 65–66.
[3] J. Niemeyer, A simple construction of the golden section, *Forum Geom.*, 11 (2011) 53.

Emmanuel Antonio José García: CEDI Bilingual School, Camila Henríquez Ureña, 20, Santo Domingo, Dominican Republic.
E-mail address: emmanuelgeogarcia@gmail.com

Paul Yiu: Department of Mathematical Sciences, Florida Atlantic University, 777 Glades Road, Boca Raton, Florida 33431-0991, USA
E-mail address: yiu@fau.edu

Forum Geometricorum
Volume 16 (2016) 125–132.

FORUM GEOM
ISSN 1534-1178

Ascending Lines in the Hyperbolic Plane

Dieter Ruoff

Abstract. On the basis of the familiar proportionality theorems a line in the Euclidean plane, which ascends from a horizontal base, can be assigned a constant slope. In a non-Euclidean setting (where the proportionality theorems do not hold) this is not possible: A line segment begins its ascent more slowly than it finishes it, failing to reach at its midpoint half its final height. After reviewing two proofs of this fact we expand on it by comparing the ascent of different line segments. It is hoped that the results presented here, which belong to elementary synthetic non-Euclidean geometry, will contribute to enriching the offerings in the pertinent textbooks.

1. Introduction

Our setting is the elementary non-Euclidean plane, governed by Hilbert's axioms of Bolyai-Lobachevskian Geometry [4, Appendix III]. We consider a triangle ABC with a right angle at C, and the sides a, b, c opposite A, B, C. In this we visualize BC as a horizontal axis with the line segment BA (but for B) lying above it. We are interested in the height of BA above BC at the midpoint M of BC and the midpoint N of BA, represented by the vertical segments MP and QN (Figure 1). That these are different segments will be shown below.

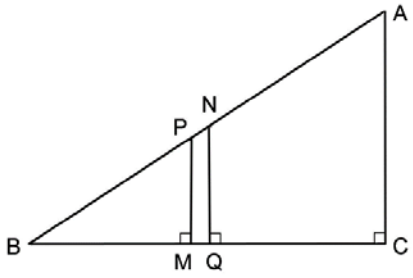

Figure 1

2. Assumptions and notation

We assume a basic knowledge of non-Euclidean geometry (see e.g. [2], [8]). Two non-intersecting lines are either boundary parallels which approach each other towards an end at infinity, or hyperparallels that have exactly one common perpendicular which marks the shortest distance between the lines.

Publication Date: April 12, 2016. Communicating Editor: J. Chris Fisher.

We will also make use of the essential properties of a *Saccheri quadrilateral* $ABCD$, the non-Euclidean counterpart of the Euclidean rectangle. Its base AB and summit CD are joined by sides AD, BC of equal length which form right angles with the base, and acute angles with the summit. Importantly, the summit is longer than the base.

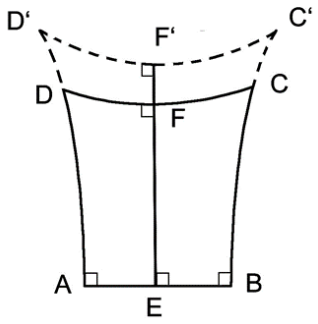

Figure 2

The altitude EF of the Saccheri quadrilateral $ABCD$ joins the midpoint E of the base AB and the midpoint F of the summit CD, and is shorter than the sides BC, AD; it splits the Saccheri quadrilateral into two congruent *Lambert quadrilaterals* which we denote by $FEB\underline{C}$, $FEA\underline{D}$, with the vertices of the three right angles listed first and that of the acute fourth angle underlined. The connection of a Lambert quadrilateral to a Saccheri quadrilateral reveals that the sides through the vertex of its fourth angle are longer than their opposites.

Of two Saccheri quadrilaterals with common base the one with the larger altitude has the larger summit and the smaller summit angles (Figure 2), and of two Saccheri quadrilaterals with common summit the one with the larger altitude has the smaller base and the smaller summit angles (Figure 3).

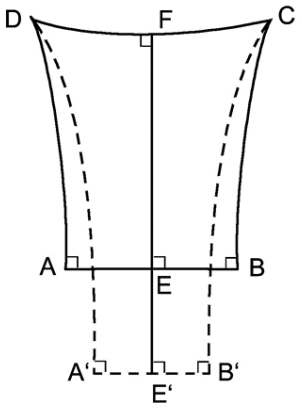

Figure 3

Distinctive for non-Euclidean geometry is the fact that two n-gons do not have to have the same angle sum, and that their area can be measured by their defect, $n \cdot 2\mathbf{R} - 4\mathbf{R} -$ angle sum, where $\mathbf{R}$ denotes the size of a right angle. This means that the larger of two Saccheri quadrilaterals by area has the smaller summit angles, and the larger of two Lambert quadrilaterals has the smaller fourth angle.

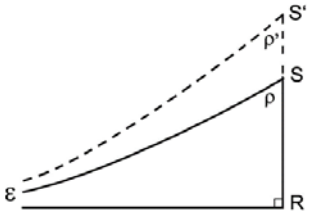

Figure 4

Finally, we point out the role of the acute angle $\rho = \angle RS\epsilon$ of an improper right triangle $RS\epsilon$ which has a right angle at R and in which the sides $R\epsilon$, $S\epsilon$ are boundary parallel (so that the vertex ϵ is actually an end). The angle ρ determines the shape of the triangle completely, and, as angle of parallelism is a function of triangle side RS: $|RS| < |RS'|$ implies $\rho > \rho'$ (Figure 4), [2], [6]. Consider now a triangle ABC with M, N the midpoints of sides BC, BA. It can easily be shown that line MN is hyperparallel to side AC, and that by vertically projecting A, C to the points U, V on line MN we define a Saccheri quadrilateral $UVCA$ with base UV, summit CA; it is called the *associated Saccheri quadrilateral* of triangle ABC on side CA. Its base UV has twice the length of the midpoint connection MN (Figure 5).

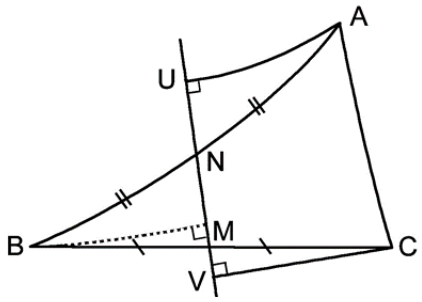

Figure 5

Later we will introduce the notion of an associated Lambert quadrilateral of a right triangle.

3. Results

We refer to the points A, B, C, M, N, P, Q as in connection with Figure 1.

Theorem 1. *For N the midpoint of BA, $|QN| < \frac{1}{2}|CA|$ and $|BQ| > \frac{1}{2}|BC|$* (Figure 6).

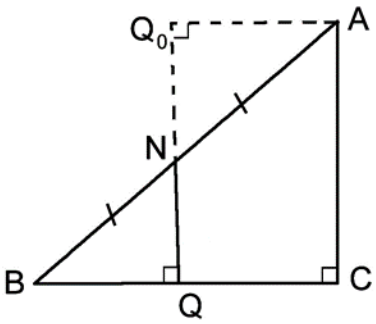

Figure 6

Proof. We rely here on the arguments presented by O. Perron [5]. By point reflection in N move triangle BQN to triangle AQ_0N. The point N then becomes the midpoint of side QQ_0 of the Lambert quadrilateral $Q_0QC\underline{A}$ with fourth angle A. By virtue of the fact that its sides satisfy $|AC| > |Q_0Q|$ and $|AQ_0| > |CQ|$ we obtain the desired inequalities

$$\begin{aligned} 2|QN| = \ |QQ_0| < |CA|, \\ |BQ| = \ |Q_0A| > |QC|. \end{aligned}$$

□

From the second inequality follows that the midpoint M of BC lies between B and Q, and as a result that $|MP| < |QN| < \frac{1}{2}|CA|$ (Figure 1). The result concerning $|MP|$ can also be proved directly.

Theorem 2. *For M the midpoint of BC, $|MP| < \frac{1}{2}|CA|$.*

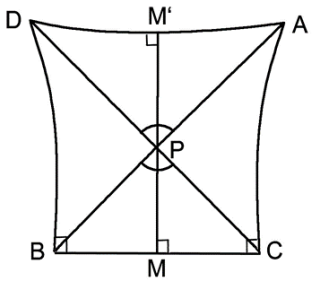

Figure 7

Proof. Complete B, C, A to the Saccheri quadrilateral $BCAD$ with base BC, summit AD, and call M' the intersecting point of lines MP and AD (Figure 7). In the Saccheri quadrilateral $BCAD$ we have $BC < AD$, i.e., in the isosceles triangles PBC and PAD with equal angles at P the base of the former is the shorter. Hence altitude $MP <$ altitude $M'P$. □

We now turn to the main point of this paper, namely to determine how the mentioned heights $|MP|$ and $|NQ|$ compare for line segments BA of different inclination. The answer gives some interesting insight in the structure of a hyperbolic plane.

Theorem 3. *Introduce* (in addition to the points M, N, P, Q, which are related as in Figure 1 to triangle ABC), *the point B' between B and C, and analogously the points M', N', P', Q' related to triangle $AB'C$* (Figure 8). *Then* $|QN| < |Q'N'|$.

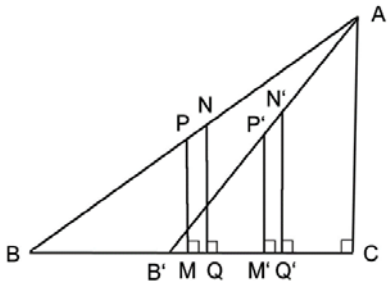

Figure 8

Proof. Proof. We draw the associated Saccheri quadrilaterals $CAUV$ of triangle ABC and $CAU'V'$ of triangle $AB'C$, both on the side CA of these triangles (Figure 9). As we know $|MN| = \frac{1}{2}|VU|$ and $|M'N'| = \frac{1}{2}|V'U'|$, and because the altitude EF of $CAUV$ is larger than the altitude $E'F$ of $CAU'V'$, $|VU| < |V'U'|$. Regarding the summit angles of the two Saccheri quadrilaterals we know especially that $\angle VCA < \angle V'CA$. It follows that

$$|MN| < |M'N'|, \tag{1}$$

and

$$\angle MCV = \mathbf{R} - \angle VCA > \mathbf{R} - \angle V'CA = \angle M'CV'. \tag{2}$$

Based on inequality (2) we conclude that triangle $CM'V'$ lies in the interior of triangle CMV, and, having the smaller area, i.e., the larger angle sum, $\angle CM'V' > \angle CMV$, which is equivalent to

$$\angle QMN < \angle Q'M'N'. \tag{3}$$

Note that if in triangles MQN and $M'Q'N'$ we had $|QN| = |Q'N'|$, inequality (3) would imply $|QM| > |Q'M'|$ and so $|MN| > |M'N'|$, in contradiction to (1). From this it follows easily that also the assumption $|QN| > |Q'N'|$ would lead to a contradiction with (1). Therefore, we must have $|QN| < |Q'N'|$. □

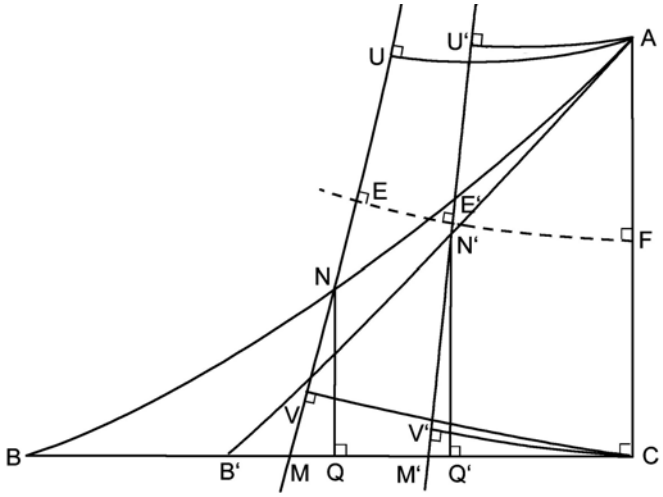

Figure 9

Theorem 4. *Consider the segments MP, $M'P'$ which are perpendicular to BC and pass through the midpoints M, M' of BC, $B'C$ respectively, with B' lying between B and C. For P on BA, and P' on $B'A$, we have $|MP| < |M'P'|$* (Figure 8).

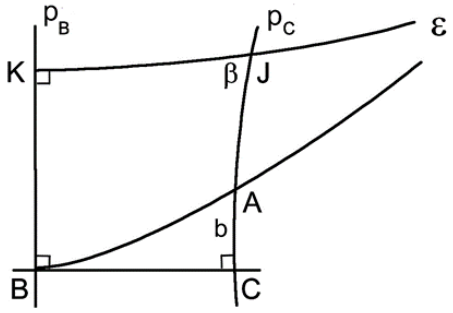

Figure 10

Proof. We make use at this place of the notion of the associated Lambert quadrilateral $KBCJ$ on side BC of a right triangle ABC with hypotenuse AB (see e.g. [1], [2], [3]). Draw the perpendicular lines p_B, p_C to BC through B and C, project the end ϵ of ray BA vertically to the point K of p_B and call J the intersection point of lines $K\epsilon$ and p_C (Figure 10).

A famous theorem by F. Engel establishes that $|BA| = |KJ|$, forming the basis of a ruler and compass construction of a boundary parallel line to a given line through a given point outside it. From among several proofs we point out that of

O. Pund (1907) as presented in [7] which relies entirely on elementary arguments and makes no use of continuity assumptions.

In the context of the proof of Engel's theorem several additional relations between the parts of triangle ABC and $KBC\underline{J}$ are established of which the following is of crucial importance to us: *The angle $\beta = \angle CJK$ is the angle of parallelism of the side $b = CA$ of triangle ABC.* This means that b and β determine each other. Of two Lambert quadrilaterals the one with the smaller fourth angle, and so with the larger area, is associated to a right triangle with the larger related side.

We now add the associated Lambert quadrilateral $K'B'C\underline{J'}$ of triangle $AB'C$ to our figure and note that its fourth angle $\angle CJ'K'$, related again to triangle side $b = CA$, is congruent to $\angle CJK$. This means that $K'B'C\underline{J'}$ and $KBC\underline{J}$ have the same area. Neither polygon contains the other in its interior, and so $|B'C| < |BC|$ implies $|CJ'| > |CJ|$. In addition, translating $K'B'C\underline{J'}$ along p_C so that $\angle CJ'K'$ comes to coincide with $\angle CJK$ we see that the said area equality also requires $|K'J'| < |KJ|$ (Figure 11).

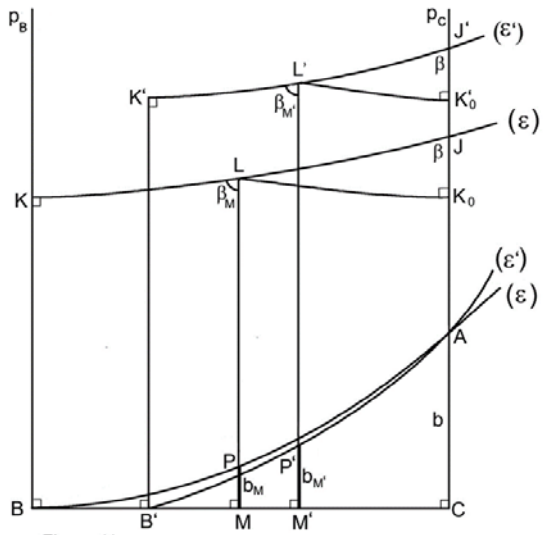

Figure 11

In the following we further need the point L in our figure which completes the Lambert quadrilateral $KBM\underline{L}$, and also the vertical projection K_0 of L in p_C. Analogously we introduce the point L' to complete the Lambert quadrilateral $K'B'M'\underline{L'}$ together with its vertical projection K'_0 in p_C. Lines BP and KL, coinciding with BA and KJ, share the end ϵ which makes $KBM\underline{L}$ the associated Lambert quadrilateral of triangle PBM, and $\beta_M = \angle MLK$, the angle of parallelism of $b_M = |MP|$. Similarly, $\beta_{M'} = \angle M'L'K'$ is the angle of parallelism of $b_{M'} = |M'P'|$. We see at once that ML splits the pentagon BCK_0LK into

the congruent halves $KBM\underline{L}$ and $K_0CM\underline{L}$, especially that $|LK_0| = |LK|$. An analogous statement, applied to pentagon $B'CK_0'L'K'$, yields $|L'K_0'| = |L'K'|$.

As to the triangles JLK_0 and $J'L'K_0'$, they share β and a right angle; so $|L'J'| < |LJ|$ if and only if $|L'K_0'| < |LK_0|$, which, by the above, is equivalent to $|L'J'| < |LJ|$ if and only if $|L'K'| < |LK|$. The parts $L'K'$, $L'J'$ of $K'J'$ are either both smaller than the corresponding parts LK, LJ of KJ, or neither is smaller. Since the sums $K'J' = L'K' + L'J'$ and $KJ = LK + LJ$ satisfy $|K'J'| < |KJ|$, it follows that $|L'K'| < |LK|$, and $|L'J'| < |LJ|$. From the last inequality we easily conclude that the area of triangle $J'L'K_0'$ is smaller than the area of triangle JLK_0.

Note that the Lambert quadrilateral $KBC\underline{J}$ is composed of pentagon BCK_0LK and triangle JLK_0. Likewise $K'B'C\underline{J'}$ is composed of $B'CK_0'L'K'$ and triangle $J'L'K_0'$. The Lambert quadrilaterals have equal areas whereas triangle JLK has a larger area than $J'L'K_0'$. As a result pentagon $KBCK_0L$ has a smaller area than $K'B'CK_0'L'$. This inequality extends to the Lambert quadrilaterals $KBM\underline{L}$ and $K'B'M'\underline{L'}$ which are halves of the respective pentagons: we have area $KBM\underline{L} <$ area $K'B'M'\underline{L'}$ and $\beta_M = \angle MLK > \beta_{M'} = \angle M'L'K'$ for the related fourth angles. As to the right triangles PMB, $P'B'M'$ to which these Lambert quadrilaterals are associated, side MP of the first must be shorter than side $M'P'$ of the second. The claim $b_M = |MP| < b_{M'} = |M'P'|$ is thus established. □

References

[1] R. Bonola, *Non-Euclidean Geometry*, Dover Publications, Inc., New York.

[2] D. Gans, *An Introduction to non-Euclidean Geometry*, Academic Press, Inc., Orlando etc., 1973.

[3] M. J. Greenberg, *Euclidean and Non-Euclidean Geometries*, 4th ed., W.H. Freeman and Co., New York, 2008.

[4] D. Hilbert, *Foundations of Geometry*, Open Court Publishing Co., La Salle, Ill., 1971.

[5] O. Perron, *Nichteuklidische Elementargeometrie der Ebene*, B.G. Teubner, Stuttgart, 1962.

[6] D. Ruoff, On the derivation of the Non-Euclidean angle of parallelism function, *Contributions to Algebra and Geometry*, 36 (1995) 235–241.

[7] M. Simon, *Nichteuklidische Geometrie in elementarer Behandlung* (bearbeitet und herausgegeben von K. Fladt), B.G. Teubner, Leipzig, 1925.

[8] J. R. Smart, *Modern Geometries*, 4th ed., Brooks/Cole Publishing Co., Pacific Grove, CA, 1994.

Dieter Ruoff: CH-8810 Horgen, Switzerland
E-mail address: ruoffd@bluewin.ch

Forum Geometricorum
Volume 16 (2016) 133–139.

FORUM GEOM
ISSN 1534-1178

A Quadrilateral Half-Turn Theorem

Igor Minevich and Patrick Morton

Abstract. If ABC is a given triangle in the plane, P is any point not on the extended sides of ABC or its anticomplementary triangle, Q is the complement of the isotomic conjugate of P with respect to ABC, DEF is the cevian triangle of P, and D_0 and A_0 are the midpoints of segments BC and EF, respectively, a synthetic proof is given for the fact that the complete quadrilateral defined by the lines AP, AQ, D_0Q, D_0A_0 is perspective by a Euclidean half-turn to the similarly defined complete quadrilateral for the isotomic conjugate P' of P. This fact is used to define and prove the existence of a generalized circumcenter and generalized orthocenter for any such point P.

1. Introduction.

The purpose of this note is to give a synthetic proof of the following surprising theorem. We let ABC be an ordinary triangle in the extended Euclidean plane, and we let P be a point which does not lie on the sides of either ABC or its anticomplementary triangle. Furthermore, if K denotes the complement map and P' denotes the isotomic conjugate of P with respect to ABC, then $Q = K(P')$ denotes the *isotomcomplement* of the point P (Grinberg's terminology [3]). Furthermore, let D_0, E_0, F_0 be the midpoints of the sides of ABC opposite A, B, and C, respectively.

We denote by T_P the unique affine map taking ABC to the cevian triangle DEF of P, and we set $A_0B_0C_0 = T_P(D_0E_0F_0)$, the image of the medial triangle of ABC under the map T_P. Then A_0, B_0, C_0 are just the midpoints of segments EF, DF, and DE, respectively. Also, $D_3E_3F_3$ is the cevian triangle of P', so that D_3 is the reflection of the point D across the midpoint D_0 of BC, etc.; $T_{P'}$ is the affine mapping for which $T_{P'}(ABC) = D_3E_3F_3$; and $A_0'B_0'C_0' = T_{P'}(D_0E_0F_0)$. (We are choosing notation to be consistent with the notation in [6], where the cevian triangles of P and Q are $DEF = D_1E_1F_1$ and $D_2E_2F_2$.) The theorem we wish to prove can be stated as follows.

Theorem 1 (Quadrilateral Half-turn Theorem)**.** *If $Q' = K(P)$ is the isotomcomplement of P', the complete quadrilaterals*

$$\Lambda = (AP)(AQ)(D_0Q)(D_0A_0) \ \textit{and} \ \Lambda' = (D_0Q')(D_0A_0')(AP')(AQ')$$

Publication Date: April 15, 2016. Communicating Editor: Paul Yiu.

are perspective by a Euclidean half-turn about the point N_1 = midpoint of AD_0 = midpoint of E_0F_0. In particular, corresponding sides in these quadrilaterals are parallel.

This shows that the symmetry between P and P', initially determined by different reflections across the midpoints of the sides of ABC, is also determined by a Euclidean isometry of the whole plane. However, this isometry permutes the sides of Λ and Λ', so that side AP in Λ does not correspond to AP' in Λ', but to D_0Q', and so forth. There are similar statements corresponding to Theorem 1 for the quadrilaterals $(BP)(BQ)(E_0Q)(E_0B_0)$ and $(CP)(CQ)(F_0Q)(F_0C_0)$.

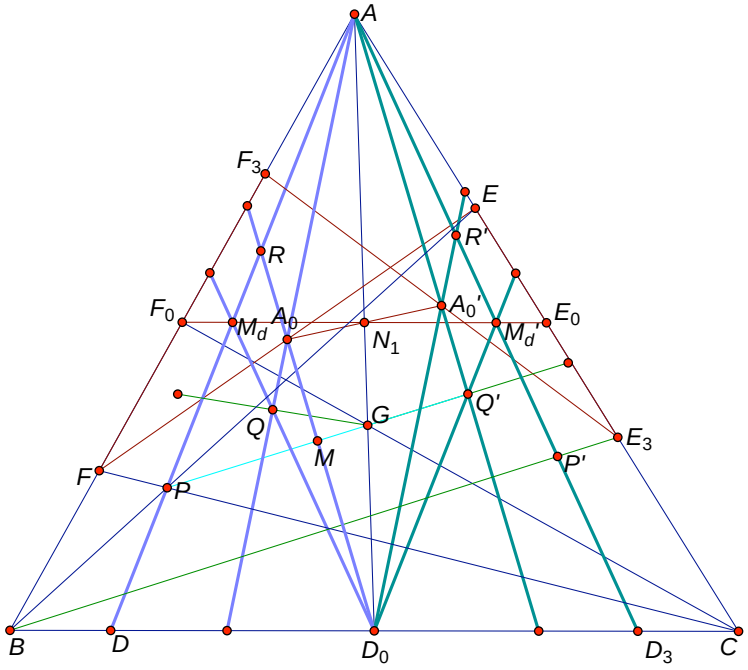

Figure 1. Quadrilateral Half-turn Theorem

2. Preliminaries and proof.

We require two results, for which synthetic proofs can be found in [6].

Theorem 2 ([3, Theorem 3])**.** *Let ABC be a triangle and D, E, F the traces of point P on the sides opposite A, B, and C. Let D_0, E_0, F_0 be the midpoints of the sides opposite A, B, C, and let M_d, M_e, M_f be the midpoints of AD, BE, CF. Then D_0M_d, E_0M_e, F_0M_f meet at the isotomcomplement $Q = K \circ \iota(P)$ of P. (ι is the isotomic map.)*

Corollary 3. *$D_0M_d = D_0Q$ is parallel to AP' and $K(D_3) = M_d$.*

See also Altshiller-Court [1, p.165, Supp. Ex. 10].

Theorem 4 (Grinberg-Yiu [3], [11])**.** *With D, E, F as before, let A_0, B_0, C_0 be the midpoints of EF, DF, and DE, respectively. Then the lines AA_0, BB_0, CC_0 meet at the isotomcomplement Q of P.*

Proof of Theorem 1. (See Figure 1.) Let R and R' denote the midpoints of segments AP and AP', and M_d and M'_d the midpoints of segments AD and AD_3, where $D_3 = AP' \cdot BC$. We first check that the vertices of the complete quadrilateral (see [2])

$$\Lambda = (AP)(AQ)(D_0Q)(D_0A_0)$$

are A, R, M_d, Q, A_0, and D_0. It is clear that A, Q, D_0 are vertices. Further, $M_d = AP \cdot D_0Q$ by Theorem 2 and $A_0 = AQ \cdot D_0A_0$ by Theorem 4.

We now show that D_0, A_0, and R are collinear, from which we obtain $R = AP \cdot D_0A_0$. Since $A_0E_0A'_0F_0$ joins the midpoints of the sides of the quadrilateral FEE_3F_3, it is a parallelogram, so the intersection of its diagonals is the point $A_0A'_0 \cdot E_0F_0 = N_1$. Hence, N_1 bisects $A_0A'_0$ (and with E_0F_0 also AD_0).

Assume that P is an ordinary point. Let M be the midpoint of PQ'; then $K(A) = D_0, K(Q') = M$ (since $K(P) = Q'$), so AQ' is parallel to D_0M. Now R and M are midpoints of sides in triangle $AQ'P$, so RM is a line through $M = K(Q')$ parallel to AQ', hence we have the equality of the lines $RM = D_0M = D_0R$. If $T = A'_0N_1 \cdot D_0R$, then triangles $AN_1A'_0$ and D_0N_1T are congruent ($\angle D_0TN_1 \cong \angle AA'_0N_1$ and AAS), so N_1 bisects A'_0T and $T = A_0$. (Note that N_1, as the midpoint of E_0F_0, lies on AD_0, and A_0 and A'_0 are on opposite sides of this line; hence N_1 lies between A_0 and A'_0.) This shows that D_0, R, and A_0 are collinear. By symmetry, D_0, A'_0, and R' are collinear whenever P' is ordinary.

If $P' = Q$ is infinite, then P is ordinary (it lies on the Steiner circumellipse of ABC), and we may use the congruence $AN_1A_0 \cong D_0N_1A'_0$ to get that $D_0A'_0 || AA_0 = AQ$, which shows that D_0, A'_0, and Q are collinear. Thus, the last vertex of the quadrilateral

$$\Lambda' = (D_0Q')(D_0A'_0)(AP')(AQ')$$

is $R' = AP' \cdot D_0A'_0 = Q$ in this case. By symmetry, we get the same conclusion for Λ when P is infinite (in which case P' is ordinary).

Now consider the hexagon $AM'_dRD_0M_dQ'$ (if P is ordinary). Alternating vertices of this hexagon are on the lines $l = AP$ and $m = D_0Q'$, by Corollary 3, so the theorem of Pappus [2] implies that intersections of opposite sides, namely,

$$AM'_d \cdot D_0M_d, \quad AQ' \cdot RD_0, \quad \text{and } M_dQ' \cdot M'_dR,$$

are collinear. The point $AM'_d \cdot D_0M_d = AP' \cdot D_0Q$ is on the line at infinity because $K(AP') = D_0Q$. By the above argument, $AQ' \cdot RD_0$ is also on the line at infinity. Hence, M_dQ' is parallel to M'_dR. Since $Q'M'_d$ is parallel to $AP = M_dR$ (Theorem 2 and its corollary), $M_dQ'M'_dR$ is a parallelogram and the intersection of the diagonals $Q'R \cdot M_dM'_d$ is the midpoint of $M_dM'_d = K(DD_3)$ (Corollary 3). But this midpoint is $N_1 = K(D_0)$, since D_0 is the midpoint of DD_3. Hence, N_1 also bisects $Q'R$, and by symmetry, QR', when P' is ordinary.

We have shown that N_1 bisects the segments between pairs of corresponding vertices in the sets

$$\{A, R, M_d, Q, A_0, D_0\} \text{ and } \{D_0, Q', M'_d, R', A'_0, A\}.$$

If $P' = Q$ is infinite, we replace R' by Q in the second set of vertices, and we get the same conclusion since Q is then fixed by the half-turn about N_1. This proves the theorem. □

Corollary 5. (a) *If P and P' are ordinary, the Euclidean quadrilaterals RA_0QM_d and $Q'A'_0R'M'_d$ are congruent.*
(b) *If P is ordinary, the points D_0, R, A_0, and $M = K(Q')$ are collinear, where R is the midpoint of segment AP. The point $M = K(Q')$ is the midpoint of segment D_0R.*
(c) *If P' is infinite, then Q, M_d, D_0, A'_0, and $K(A_0)$ are collinear.*

Proof. Part (a) is clear from the proof of the theorem. For part (b), we just have to prove the second assertion. The theorem implies that quadrilateral $AQ'D_0R$ is a parallelogram, since AQ' is parallel to $D_0A_0 = D_0R$, $AR = AP$ is parallel to D_0Q', and $R = AP \cdot D_0A_0$. Thus, segment AQ' is congruent to segment D_0R, and $D_0M = K(AQ')$ is half the length of $AQ' \cong D_0R$. M is clearly on the same side of line D_0Q' as P and R, so M is the midpoint of D_0R. Part (c) follows by applying the complement map to the collinear points $P' = Q, D_3, A$, and A_0, to get that Q, M_d, D_0, and $K(A_0)$ are collinear, and then appealing to the argument in the fourth paragraph of the above proof, which shows that A'_0 is on QD_0. □

3. An affine formula for the generalized orthocenter.

To give an application of Theorem 1, we start with the following definition.

Definition. The point O for which $OD_0 \parallel QD, OE_0 \parallel QE$, and $OF_0 \parallel QF$ is called the *generalized circumcenter* of the point P with respect to ABC. The point H for which $HA \parallel QD, HB \parallel QE$, and $HC \parallel QF$ is called the *generalized orthocenter* of P with respect to ABC.

We have the following affine relationships between Q, O, and H. We let $A'_3B'_3C'_3 = T_{P'}(DEF)$ be the image of the cevian triangle DEF of P under the map $T_{P'}$.

Theorem 6. *The generalized circumcenter O and generalized orthocenter H exist for any point P not on the extended sides of either ABC or its anticomplementary triangle $K^{-1}(ABC)$, and are given by*

$$O = T_{P'}^{-1}K(Q), \quad H = K^{-1}T_{P'}^{-1}K(Q),$$

where $T_{P'}$ is the affine map taking ABC to the cevian triangle $D_3E_3F_3$ of the point P'.

Remark. The formula for the point H can also be written as $H = T_L^{-1}(Q)$, where $L = K^{-1}(P')$ and T_L is the map T_P defined for $P = L$ and the anticomplementary triangle of ABC.

Proof. We will show that the point $\tilde{O} = T_{P'}^{-1}K(Q)$ satisfies the definition of O, namely, that

$$\tilde{O}D_0 \parallel QD, \;\; \tilde{O}E_0 \parallel QE, \;\; \tilde{O}F_0 \parallel QF.$$

It suffices to prove the first relation $\tilde{O}D_0 \parallel QD$. We have that

$$T_{P'}(\tilde{O}D_0) = K(Q)T_{P'}(D_0) = K(Q)A_0'$$

and

$$T_{P'}(QD) = P'A_3',$$

by [6, Theorem 3.7], according to which $T_{P'}(Q) = P'$, and by the definition of the point $A_3' = T_{P'}(D)$. Thus, we just need to prove that $K(Q)A_0' \parallel P'A_3'$. We use the map $\mathcal{S}' = T_{P'}T_P$ from [6, Theorem 3.8], which takes ABC to $A_3'B_3'C_3'$. We have $\mathcal{S}'(Q) = T_{P'}T_P(Q) = T_{P'}(Q) = P'$, since Q is a fixed point of T_P ([6, Theorem 3.2]). Since $\mathcal{S}'$ is a homothety or translation, this gives that $AQ \parallel \mathcal{S}'(AQ) = A_3'P'$. Assuming that P' is ordinary, we have $M' = K(Q)$, as in Corollary 5(b), so by that result

$$K(Q)A_0' = M'A_0' = D_0A_0'.$$

Now Theorem 1 implies that $AQ \parallel D_0A_0'$, and therefore $P'A_3' \parallel K(Q)A_0'$. This proves the formula for O. To get the formula for H, just note that $K^{-1}(OD_0) = K^{-1}(O)A$, $K^{-1}(OE_0) = K^{-1}(O)B$, $K^{-1}(OF_0) = K^{-1}(O)C$ are parallel, respectively, to QD, QE, QF, since K is a dilatation. This shows that $K^{-1}(O)$ satisfies the definition of the point H.

If the point $P' = Q$ is infinite, then it is easy to see from the Definition that $O = H = Q$, and this agrees with the formulas of the theorem, since

$$T_{P'}^{-1}K(Q) = T_{P'}^{-1}(Q) = K \circ [T_{P'}K]^{-1}(Q) = K \circ [T_{P'}K]^{-1}(P') = K(P') = Q,$$

using the fact that $T_{P'}K(P') = P'$ from [6, Theorem 3.7]. □

Corollary 7. *If $P = Ge$ is the Gergonne point of ABC, $P' = Na$ is the Nagel point for ABC, and $Q = I$ is the incenter of ABC, the circumcenter and orthocenter of ABC are given by the affine formulas*

$$O = T_{P'}^{-1}K(Q), \;\; H = K^{-1}T_{P'}^{-1}K(Q).$$

Remark. In the corollary, $K(Q)$ is the Spieker center $X(10)$ of ABC, so the first formula says that $T_{Na}(O) = X(10)$. See [4].

We also prove the following relationship between the traces H_a, H_b, H_c of H on the sides $a = BC, b = CA, c = AB$ and the traces D_2, E_2, F_2 of Q on those sides.

Theorem 8. *If the cevian triangles of P and its isotomic conjugate $P' = \iota(P)$ for ABC are DEF and $D_3E_3F_3$, respectively, then we have the harmonic relations $\mathsf{H}(DD_3, D_2H_a), \mathsf{H}(EE_3, E_2H_b), \mathsf{H}(FF_3, F_2H_c)$. In other words, the point H_a is the harmonic conjugate of D_2 with respect to the points D, D_3 on BC, with similar statements holding for the traces of H and Q on the other sides.*

Proof. Define the points $M = AH_a \cdot QD_3$ and $T = DQ \cdot AD_3$. By Theorem 1, $QD_0||AP' = AD_3$, so since D_0 is the midpoint of DD_3, it follows by considering triangle DTD_3 that Q is the midpoint of DT. By definition of H we also have $DQ||AH_a$, so using similar triangles DTD_3 and H_aAD_3, we see that M is the midpoint of AH_a. Now project the points $H_aDD_2D_3$ on BC from Q to the points $H_aJ_\infty AM$ on AH_a, where $J_\infty = AH_a \cdot QD$ is on the line at infinity. Then the relation $\mathsf{H}(J_\infty M, AH_a)$ yields $\mathsf{H}(DD_3, D_2H_a)$. □

In [8] we will explore the properties of the points O and H in greater depth. In order to give an example of the points O and H, we give their barycentric coordinates in terms of the barycentric coordinates of the point $P = (x, y, z)$. We note that

$$Q = (x', y', z') = (x(y+z), y(x+z), z(x+y)),$$

(see [3], [10]) while

$$K = \begin{pmatrix} 0 & 1 & 1 \\ 1 & 0 & 1 \\ 1 & 1 & 0 \end{pmatrix}, \quad T_{P'}^{-1} = \begin{pmatrix} -xx' & yx' & zx' \\ xy' & -yy' & zy' \\ xz' & yz' & -zz' \end{pmatrix}.$$

From this and Theorem 6 we find that the barycentric coordinates of O and H are

$$\begin{aligned} O &= (x(y+z)^2x'', y(x+z)^2y'', z(x+y)^2z''), \\ H &= (xy''z'', yx''z'', zx''y'') = \left(\frac{x}{x''}, \frac{y}{y''}, \frac{z}{z''}\right), \end{aligned}$$

where

$$x'' = xy + xz + yz - x^2, \;\; y'' = xy + xz + yz - y^2, \;\; z'' = xy + xz + yz - z^2.$$

For example, using the coordinates of O and H it can be shown that if $P = Na$ is the Nagel point, then

$$\begin{aligned} O &= (g(a,b,c), g(b,c,a), g(c,a,b)) = X(6600), \\ &\quad \text{with } \; g(a,b,c) = a^2(b+c-a)(a^2+b^2+c^2-2ab-2ac), \\ H &= (h(a,b,c), h(b,c,a), h(c,a,b)) = X(6601), \\ &\quad \text{with } \; h(a,b,c) = (b+c-a)/(a^2+b^2+c^2-2ab-2ac). \end{aligned}$$

See [4], [5]. Here, $Na = (b+c-a, c+a-b, a+b-c)$, where a, b, c are the side lengths of ABC. (See [5], where these points were given before being listed in [4].) Note that $H = \gamma(X(1617))$, where γ is isogonal conjugation, and $X(1617)$ is the TCC-perspector of $X(57) = \gamma(X(9)) = \gamma(Q)$. We will generalize this fact in [9], by showing (synthetically) in general that $\gamma(H)$ is the TCC-perspector of $\gamma(Q)$.

References

[1] N. Altshiller-Court, *College Geometry, An Introduction to the Modern Geometry of the Triangle and the Circle*, Barnes and Noble, New York, 1952. Reprint published by Dover.

[2] H.S.M. Coxeter, *Projective Geometry*, 2^{nd} edition, Springer, 1987.

[3] D. Grinberg, Hyacinthos Message 6423, January 24, 2003; `http://tech.groups.yahoo.com/group/Hyacinthos`.

[4] C. Kimberling, *Encyclopedia of Triangle Centers*, http://faculty.evansville.edu/ck6/encyclopedia/ETC.html.
[5] I. Minevich and P. Morton, Synthetic cevian geometry, preprint, IUPUI Math. Dept. Preprint Series pr09-01, 2009, http://math.iupui.edu/research/research-preprints.
[6] I. Minevich and P. Morton, Synthetic Foundations of Cevian Geometry, I: Fixed points of affine maps, to appear in *J. of Geometry*, available at http://link.springer.com/article/10.1007/s00022-016-0324-4.
[7] I. Minevich and P. Morton, Synthetic Foundations of Cevian Geometry, II: The center of the cevian conic, http://arXiv.org/abs/1505.05381, 2015.
[8] I. Minevich and P. Morton, Synthetic Foundations of Cevian Geometry, III: The generalized orthocenter, http://arXiv.org/abs/1506.06253, 2015.
[9] I. Minevich and P. Morton, Synthetic Foundations of Cevian Geometry, IV: The TCC-Perspector Theorem, in preparation.
[10] P. Morton, Affine maps and Feuerbach's Theorem, preprint, IUPUI Math. Dept. Preprint Series pr09-05, 2009, http://math.iupui.edu/research/research-preprints.
[11] P. Yiu, Hyacinthos Message 1790, November 10, 2000, http://tech.groups.yahoo.com/group/Hyacinthos.

Igor Minevich: Departmet of Mathematics, Maloney Hall, Boston College, 140 Commonwealth Ave., Chestnut Hill, Massachusetts 02467-3806, USA
E-mail address: igor.minevich@bc.edu

Patrick Morton: Department of Mathematical Sciences, Indiana University - Purdue University at Indianapolis (IUPUI), 402 N. Blackford St., Indianapolis, Indiana 46202, USA
E-mail address: pmorton@math.iupui.edu

Forum Geometricorum
Volume 16 (2016) 141–149.

FORUM GEOM
ISSN 1534-1178

Applying Poncelet's Theorem to the Pentagon and the Pentagonal Star

Arthur Holshouser, Stanislav Molchanov, and Harold Reiter

Abstract. A special case of Poncelet's Theorem states that if all points on circle C_2 lie inside of circle C_1 and if a convex n-polygon, $n \geq 3$, or an n-star, $n \geq 5$, is inscribed in circle C_1 and circumscribed about circle C_2, then there exists a family of such n-polygons and n-stars. Suppose all points on C_2 lie inside of C_1, R, r, are the radii of C_1, C_2 respectively and ρ is the distance between the centers of C_1, C_2. For $n \geq 3$, in a companion paper we give an algorithm that computes the necessary and sufficient conditions on R, r, ρ, where $R > r+\rho, r > 0$, so that if we start at any arbitrary point Q on C_1 and draw successive tangents to C_2 (counterclockwise about the center of C_2) then we will return to Q in exactly n steps and not return to Q in fewer than n steps. This will create the above family of n-polygons and n-stars. However, when $n \geq 5$, this companion paper relies on computers to find these conditions. In some ways, this is a sign of defeat. In this paper, we illustrate for $n = 5$ a technique that can compute these exact same necessary and sufficient conditions on R, r, ρ without using a computer.

1. Introduction

A special case of Poncelet's Theorem states that if all points on circle C_2 lie inside of circle C_1 and if a convex n-polygon, $n \geq 3$, or an n-star, $n \geq 5$, is inscribed in circle C_1 and circumscribed about circle C_2 then there exists a family of such n-polygons and n-stars. Suppose all points on C_2 lie inside of C_1, R, r are the radii of C_1, C_2 respectively and ρ is the distance between the centers of C_1, C_2.

For $n = 5$, we illustrate a technique that can be carried out by hand that computes the necessary and sufficient conditions on R, r, ρ, where $R > r + \rho, r > 0$, so that if we start at any point Q on C_1, and draw successive tangents to C_2 (counterclockwise about the center of C_2) then we will return to Q in exactly 5 steps and not return to Q in fewer than 5 steps.

If we consider $R > \rho \geq 0$ to be arbitrary but fixed and consider $r > 0$ to be a variable, then we end up with two polynomial equations $P(R, \rho, r) = 0, \overline{P}(R, \rho, r) = 0$ that are each of third degree in the variable r. Each of the equations $P(R, \rho, r) = 0, \overline{P}(R, \rho, r) = 0$ has exactly one r-root that satisfies $R > r + \rho, r > 0$. This r-root of $P(R, \rho, r) = 0$ is the value of r so that we get

Publication Date: April 19, 2016. Communicating Editor: Paul Yiu.

a family of pentagonal stars and this r-root of $\overline{P}(R,\rho,r)=0$ is the value of r so that we get a family of pentagons when we start at any arbitrary point Q on C_1.

In this paper, we only deal with the 5-star. The geometric reasoning for the convex pentagon is very similar. Also, we know from the companion paper [4] that the two polynomials $P(R,\rho,r)$, $\overline{P}(R,\rho,r)$ are related by

$$\overline{P}(R,\rho,r)=P(-R,\rho,r)=P(R,\rho,-r).$$

Thus, we can immediately write the polynomial $\overline{P}(R,\rho,r)$ directly from the polynomial $P(R,\rho,r)$ without doing any additional work.

2. A preliminary unfactored form of the polynomial $P(R,\rho,r)$

In this section, for the pentagonal star, we compute a preliminary first version called $P^*(R,\rho,r)$ of the polynomial $P(R,\rho,r)$. Then in Section 3, we refine $P^*(R,\rho,r)$ by factoring it into four irreducible factors

$$P^*(R,\rho,r)=P(R,\rho,r)(2Rr+\theta)(r-R+\rho)^2,$$

where

$$P(R,\rho,r)=\ 8\rho^2Rr^3-4R^2\theta r^2-2R\theta^2r+\theta^3, \tag{1}$$

$$\theta=\ R^2-\rho^2. \tag{2}$$

Of course, for the pentagon we have

$$\overline{P}(R,\rho,r)=P(-R,\rho,r)=P(R,\rho,-r)=-8\rho^2Rr^3-4R^2\theta r^2+2R\theta^2r+\theta^3.$$

The linear factor $r-R+\rho=0$ in $P^*(R,\rho,0)$ is extraneous since we require $R>r+\rho, r>0$. Also, the factor $2Rr+\theta=0$ in $P^*(R,\rho,r)$ is an Euler type of equation which has only an extraneous negative r-root since $\theta>0$.

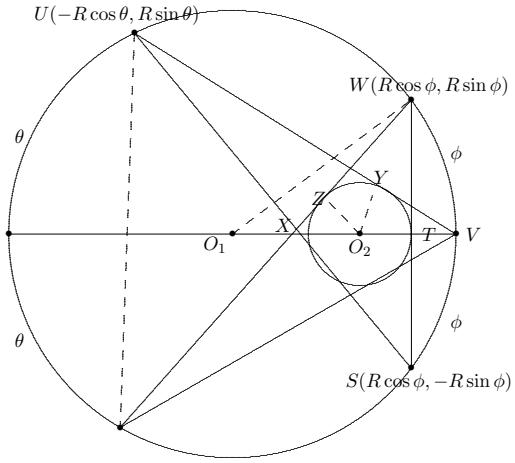

Figure 1. A drawing to compute $P^*(R,\rho,r)=0$

By Poncelet's Theorem, we can use any drawing to compute $P^*(R,\rho,r)=0$ that simplifies the problem. Therefore, by Poncelet's Theorem, the simple drawing of Figure 1 is all that we need to compute $P^*(R,\rho,r)=0$ for the pentagonal star. An analogous drawing is used for the convex pentagon. The θ in Figure 1 is different from the θ in (2)

O_1 is the center of the big circle C_1 and O_2 is the center of the inside circle C_2. R and r are the radii of C_1 and C_2 respectively, and $\rho = O_1O_2$ is the distance between the centers O_1 and O_2. We immediately have
(a) $O_2y = (O_2v)\cdot\sin\frac{\theta}{2} = (R-\rho)\sin\frac{\theta}{2} = r$,
(b) $O_1t = (O_1w)\cdot\cos\phi = R\cos\phi = \rho + r$.

The parametric equation of the line US is

$$\begin{cases} x = R\cos\phi - t\left(R\cos\phi + R\cos\theta\right), \\ y = -R\sin\phi + t\left(R\sin\phi + R\sin\theta\right), \quad t\in R. \end{cases}$$

From these,

$$\begin{aligned} &x\left(\sin\phi+\sin\theta\right)+y\left(\cos\phi+\cos\theta\right) \\ &= R\cos\phi\left(\sin\phi+\sin\theta\right) - R\sin\phi\left(\cos\phi+\cos\theta\right) = R\sin\theta\cos\phi - R\cos\theta\sin\phi \\ &= R\sin\left(\theta-\phi\right) \\ &= 2R\sin\left(\frac{\theta-\phi}{2}\right)\cos\left(\frac{\theta-\phi}{2}\right) \end{aligned}$$

Therefore,

$$\begin{aligned} &2x\sin\left(\frac{\theta+\phi}{2}\right)\cos\left(\frac{\theta-\phi}{2}\right) + 2y\cos\left(\frac{\theta+\phi}{2}\right)\cos\left(\frac{\theta-\phi}{2}\right) \\ &= 2R\sin\left(\frac{\theta-\phi}{2}\right)\cos\left(\frac{\theta-\phi}{2}\right), \end{aligned}$$

and

$$x\sin\frac{\theta+\phi}{2} + y\cos\frac{\theta+\phi}{2} = R\sin\frac{\theta-\phi}{2}$$

is the equation of the line US.

Letting $y=0$ in this equation of the line US, we have

$$O_1x = \frac{R\sin\frac{\theta-\phi}{2}}{\sin\frac{\theta+\phi}{2}}.$$

Therefore,

$$xO_2 = O_1O_2 - O_1x = \rho - O_1x = \rho - \frac{R\sin\frac{\theta-\phi}{2}}{\sin\frac{\theta+\phi}{2}}.$$

Also,

$$O_2z = xO_2\cdot\sin\frac{\theta+\phi}{2} = r = \left[\rho - \frac{R\sin\frac{\theta-\phi}{2}}{\sin\frac{\theta+\phi}{2}}\right]\sin\frac{\theta+\phi}{2}.$$

Therefore,

$$\rho \sin \frac{\theta+\phi}{2} - R \sin \frac{\theta-\phi}{2} = r. \tag{3}$$

Now $\sin^2 \frac{\theta+\phi}{2} = \frac{1-\cos(\theta+\phi)}{2}$ and $\sin^2 \frac{\theta-\phi}{2} = \frac{1-\cos(\theta-\phi)}{2}$. Also, $\sin \frac{\theta+\phi}{2} \sin \frac{\theta-\phi}{2} = \frac{1}{2}\cos\phi - \frac{1}{2}\cos\theta$. Squaring (3) and making these substitutions we have

$$\begin{aligned}
&\rho^2 [1 - \cos(\theta+\phi)] + R^2 [1 - \cos(\theta-\phi)] - 2\rho R [\cos\phi - \cos\theta] = 2r^2, \\
&- R^2 \cos(\theta-\phi) - \rho^2 \cos(\theta+\phi) + 2\rho R [\cos\theta - \cos\phi] = 2r^2 - R^2 - \rho^2, \\
&- R^2 [\cos\theta\cos\phi + \sin\theta\sin\phi] - \rho^2 [\cos\theta\cos\phi - \sin\theta\sin\phi] + 2\rho R [\cos\theta - \cos\phi] \\
&\quad = 2r^2 - R^2 - \rho^2,
\end{aligned}$$

Therefore,

$$\left(-R^2+\rho^2\right)\sin\theta\sin\phi = 2r^2 - R^2 - \rho^2 - 2\rho R(\cos\theta - \cos\phi) + \left(R^2+\rho^2\right)(\cos\theta\cos\phi).$$

Squaring we have

$$\begin{aligned}
&\left(-R^2+\rho^2\right)^2 \left(1-\cos^2\theta\right)\left(1-\cos^2\phi\right) \\
&= \left(-R^2+\rho^2\right)^2 (1-\cos\theta)(1+\cos\theta)(1-\cos\phi)(1+\cos\phi) \\
&= \left[2r^2 - R^2 - \rho^2 - 2\rho R(\cos\theta - \cos\phi) + \left(R^2+\rho^2\right)(\cos\theta\cos\phi)\right]^2.
\end{aligned} \tag{4}$$

Since we have a homogeneous geometric equation in the variables R, r, ρ, it is convenient to let $R = 1$.

From (a), (b) we know that $\sin\frac{\theta}{2} = \frac{r}{R-\rho} = \frac{r}{1-\rho}$ and $\cos\phi = \frac{\rho+r}{R} = \rho + r$.

Therefore, $\cos\theta = 1 - 2\sin^2\frac{\theta}{2} = 1 - 2\left(\frac{r}{1-\rho}\right)^2$ and $\cos\phi = \rho + r$. From these,

$$\begin{aligned}
1 - \cos\theta &= 2\left(\frac{r}{1-\rho}\right)^2, \\
1 + \cos\theta &= 2 - 2\left(\frac{r}{1-\rho}\right)^2 = \frac{2(1-\rho)^2 - 2r^2}{(1-\rho)^2}, \\
1 - \cos\phi &= 1 - \rho - r, 1 + \cos\phi = 1 + \rho + r, \\
\cos\theta - \cos\phi &= 1 - \rho - r - 2\left(\frac{r}{1-\rho}\right)^2, \\
\cos\theta\cos\phi &= (\rho+r)\left(1 - 2\left(\frac{r}{1-\rho}\right)^2\right).
\end{aligned}$$

If we make these substitutions and also put $R = 1$ in (4), multiply the equation by $(1-\rho)^4$, and partially simplify by straightforward calculations, transposing everything to one side of the equation, then we have the following equation which

we call the *preliminary polynomial equation*.

$$\begin{aligned}
&P^*(R,r,\rho)\\
&=\left[\left(2r^2+2\rho r+\rho^2-2\rho-1\right)(1-\rho)^2+4\rho r^2+\left(1+\rho^2\right)\left((1-\rho)^2-2r^2\right)(\rho+r)\right]^2\\
&\quad-4\left(1-\rho^2\right)^2\left[r^2(1-\rho-r)^2(1-\rho+r)(1+\rho+r)\right]\\
&=0.
\end{aligned}$$

3. Factoring the preliminary equation $P^*(R,r,\rho)=0$ into irreducible factors

The above preliminary polynomial equation $P^*(R,r,\rho)=P^*(1,r,\rho)=0$ in the variable r at first glance appears to be intractable. However, if we substitute specific values of ρ, e.g. $\rho=0,\ 1,\ 2$, we quickly conjecture that this polynomial equation can probably be factored into simple factors.

If we substitute $\rho=0$, the preliminary equation becomes

$$P^*(R,\rho,r)=P^*(1,0,r)=\left[2r^2-1+\left(1-2r^2\right)r\right]^2-4r^2\left(1-r^2\right)^2=0,$$

which is equivalent to

$$\begin{aligned}
0=&\ (2r^3-2r^2-r+1)^2-(2r^3-2r)^2\\
=&\ (-2r^2+r+1)(4r^3-2r^2-3r+1)\\
=&\ -(r-1)(2r+1)(r-1)(4r^2+2r-1)\\
=&\ -(r-1)^2(2r+1)(4r^2+2r-1).
\end{aligned}$$

By making other substitutions for ρ, we soon conjecture that

$$P^*(R,r,\rho)=P^*(1,r,\rho)=P(1,r,\rho)\left(2r+1-\rho^2\right)(r-1+\rho)^2=0$$

where $P(1,r,\rho)$ is a 3rd degree polynomial in r.

We now rigorously prove this conjecture. By direct substitution of $r=1-\rho$ into $P^*(1,r,\rho)$ we can easily prove that $r=1-\rho$ is a double r-root of $P^*(1,r,\rho)=0$. To see this, we see that $P^*(1,r,\rho)$ is of the form

$$P^*=[\text{xxx}]^2-[\text{yyy}](1-\rho-r)^2$$

and we only need to show that $[\text{xxx}]=0$ when $r=1-\rho$ to show that $r=1-\rho$ is a double root of $P^*(1,r,\rho)=0$.

Now in $[\text{xxx}]$ when $r=1-\rho$ we see that

$$\begin{aligned}
2r^2+2\rho r+\rho^2-2\rho-1=&\ 2r(\rho+r)+\rho^2-2\rho-1\\
=&\ 2(1-\rho)+\rho^2-2\rho-1\\
=&\ \rho^2-4\rho+1.
\end{aligned}$$

Therefore, in [xxx] when $r = 1 - \rho$ we have

$$\begin{aligned}&(2r^2 + 2\rho r + \rho^2 - 2\rho - 1)(1-\rho)^2 + 4\rho r^2\\ &= (\rho^2 - 4\rho + 1)(1-\rho)^2 + 4\rho(1-\rho)^2\\ &= (\rho^2+1)(1-\rho)^2.\end{aligned}$$

Also, in [xxx] when $r = 1 - \rho$, we have

$$\begin{aligned}(1+\rho^2)((1-\rho)^2 - 2r^2)(\rho + r) =\ & (1+\rho^2)((1-\rho)^2 - 2(1-\rho)^2)\\ =\ & -(1+\rho^2)(1-\rho)^2.\end{aligned}$$

Therefore, when $r = 1 - \rho$,

$$[\text{xxx}] = (\rho^2+1)(1-\rho)^2 - (1+\rho^2)(1-\rho)^2 = 0,$$

and $r = 1 - \rho$ is a double r-root of $P^*(1, r, \rho) = 0$.

The proof that $2r + 1 - \rho^2 = 0$ gives an r-root of $P^*(1, r, \rho) = 0$ takes a little longer but it is completely straightforward.

Therefore, we know that

$$P^*(1, r, \rho) = (ar^3 + br^2 + cr + d)(2r + 1 - \rho^2)(r - 1 + \rho)^2$$

where a, b, c, d need to be determined.

Rewriting $P^*(1, r, \rho) = a_0 r^6 + a_1 r^5 + a_2 r^4 + a_3 r^3 + a_4 r^2 + a_5 r + a_6$, it is fairly easy by straightforward calculations to compute the following coefficients.

$$\begin{aligned}a_0 =\ & 16\rho^2,\\ a_1 =\ & -8(1-\rho)(-\rho^3 + 3\rho^2 + \rho + 1),\\ a_5 =\ & -2(1-\rho)^5(1+\rho)^4,\\ a_6 =\ & (1-\rho)^6(1+\rho)^4.\end{aligned}$$

As an example, we have $a_0 = 4(1+\rho^2)^2 - 4(1-\rho^2)^2 = 16\rho^2$. Also, to compute a_5 we have the following relevant terms,

$$\begin{aligned}&\left(2\rho(1-\rho)^2 r + (\rho^2 - 2\rho - 1)(1-\rho)^2 + (1+\rho^2)(1-\rho)^2 r + (1+\rho^2)(1-\rho)^2\rho\right)^2\\ &= \left(2\rho(1-\rho)^2 r + (1+\rho^2)(1-\rho)^2 r + (\rho^2 - 2\rho - 1)(1-\rho)^2 + (1+\rho^2)(1-\rho)^2\rho\right)^2\\ &= \left((1+\rho)^2(1-\rho)^2 r + (\rho^3 + \rho^2 - \rho - 1)(1-\rho)^2\right)^2\\ &= \left((1+\rho)^2(1-\rho)^2 r - (1+\rho)^2(1-\rho)^3\right)^2.\end{aligned}$$

From this, we see that $a_5 = -2(1-\rho)^5(1+\rho)^4$.

To compute a_6 we let $r = 0$ in $P^*(1, r, \rho)$ and we have

$$\begin{aligned} a_6 &= ((\rho^2 - 2\rho - 1)(1-\rho)^2 + (1+\rho^2)(1-\rho)^2\rho)^2 \\ &= (1-\rho)^4(\rho^3 + \rho^2 - \rho - 1)^2 \\ &= (1-\rho)^4((\rho+1)^2(\rho-1))^2 \\ &= (1-\rho)^6(1+\rho)^4. \end{aligned}$$

The calculation of a_1 is a little longer but it is completely straightforward. However, we must be careful not to overlook anything in computing a_1. Once we know a_0, a_1, a_5, a_6, it is completely straight forward to compute

$$P(1, r, \rho) = ar^3 + br^2 + cr + d = 8\rho^2 r^3 - 4\theta r^2 - 2\theta^2 r + \theta^3,$$

where $\theta = 1 - \rho^2$. So $P^*(1, r, \rho) = P(1, r, \rho) \cdot \left(2r + 1 - \rho^2\right)(r - 1 + \rho)^2$. We now proceed to rigorously prove this. We first note that

$$(8\rho^2 r^3 - 4\theta r^2 - 2\theta^2 r + \theta^3)(2r + \theta) = 16\rho^2 r^4 - 8\theta^2 r^3 - 8\theta^2 r^2 + \theta^4.$$

Therefore, we prove that

$$\begin{aligned} P^*(1, r, \rho) &= (16\rho^2 r^4 - 8\theta^2 r^3 - 8\theta^2 r^2 + \theta^4)(r - 1 + \rho)^2 \\ &= (16\rho^2 r^4 - 8\theta^2 r^3 - 8\theta^2 r^2 + \theta^4)(r^2 - 2(1-\rho)r + (1-\rho)^2). \end{aligned}$$

This equality will be true if and only if the equality correctly computes the above values for a_0, a_1, a_5, a_6, since we have already proved that $2r + \theta$ and $(r - 1 + \rho)^2$ are factors of $P^*(1, r, \rho)$. Now $a_0 = 16\rho^2$ is obviously computed correctly. Also,

$$\begin{aligned} a_1 &= -32\rho^2(1-\rho) - 8(1-\rho^2)^2 \\ &= -8(1-\rho)(4\rho^2 + (1+\rho)^2(1-\rho)) \\ &= -8(1-\rho)(-\rho^3 + 3\rho^2 + \rho + 1), \\ a_5 &= -2(1-\rho)(1-\rho^2)^4 \\ &= -2(1-\rho)^5(1+\rho)^4, \\ a_6 &= (1-\rho^2)^4(1-\rho)^2 \\ &= (1-\rho)^6(1+\rho)^4. \end{aligned}$$

Therefore, we have now rigorously proved that

$$\begin{aligned} P^*(1, r, \rho) &= P(1, r, \rho)(2r + \theta)(r - 1 + \rho)^2 \\ &= (8\rho^2 r^3 - 4\theta r^2 - 2\theta^2 r + \theta^3)(2r + \theta)(r - 1 + \rho)^2 \end{aligned}$$

where $\theta = 1 - \rho^2$.

Of course, this equation can be written for $P^*(R, r, \rho)$ in the three variables R, r, ρ since the equation is a homogeneous geometric equation. This equation $P(R, r, \rho) = P(1, r, \rho)$ is exactly the same equation that we derived in a companion paper by using a computer. This computer derivation was carried out independently by Prof. Benjamin Klein of Davidson College and by Parker Garrison. So we now have three independent verifications of this one equation.

4. Studying $P(R, r, \rho) = P(1, r, \rho)$

If $R = 1 > \rho \geq 0$, we require $R = 1 > r + \rho, r > 0$.

It is easy to show that $P(1, r, \rho) = 8\rho^2 r^3 - 4\theta r^2 - 2\theta^2 r + \theta^3$ is irreducible in the rational field.

Letting $R = 1, 0 < \rho < 1$, we know by Descarte's law of signs that $P(1, r, \rho) = 0$ has two or zero positive r-roots for each fixed $0 < \rho < 1$. For each fixed $0 < \rho < 1$ we show that $P(1, r, \rho) = 0$ has one r-root that satisfies $0 < r < 1 - \rho$. ($\rho = 0$ is easy to deal with.)

Now $P(1, r, \rho) = P(1, +\infty, \rho) > 0$.

Also, $P(1, r, \rho) = P(1, 0, \rho) > 0$. If we show that $P(1, r, \rho) = P(1, 1 - \rho, \rho) < 0$, then it will follow that for each fixed $0 < \rho < 1, P(1, r, \rho) = 0$ will have one r-root that satisfies $0 < r < 1 - \rho$.

Now $P(1, r, \rho) = P(1, 1 - \rho, \rho) < 0$ if and only if

$$(1 - \rho)^3(8\rho^2 - 4(1 + \rho) - 2(1 + \rho)^2 + (1 + \rho)^3) < 0.$$

This is true since

$$\begin{aligned} &(1 - \rho)^3(-4(1 + \rho - 2\rho^2) - (1 + \rho)^2(2 - (1 + \rho))) \\ &= (1 - \rho)^3(-4(1 + 2\rho)(1 - \rho) - (1 + \rho)^2(1 - \rho)) \\ &= -(1 - \rho)^4(4(1 + 2\rho) + (1 + \rho)^2) \\ &< 0. \end{aligned}$$

Therefore, for each $R = 1 > \rho \geq 0$, we see that $P(1, r, \rho) = 0$ has one r-root that satisfies $R = 1 > r + \rho, r > 0$.

If $R = 1 > \rho \geq 0$ are fixed, this r-root is the radius of the inside circle C_2 so that we have a family of 5-stars that are inscribed in C_1 and circumscribed about C_2 when the distance between the centers of C_1, C_2 is ρ, $R = 1$ is the radius of C_1 and r is the radius of C_2.

5. Extending the equation to include convex pentagons

By using analogous reasoning we can show that the companion equation

$$\overline{P}(R, r, \rho) = P(-R, r, \rho) = P(R, -r, \rho) = -8\rho^2 R r^3 - 4R^2\theta r^2 + 2R\theta^2 r + \theta^3 = 0,$$

where $\theta = R^2 - \rho^2$ is the relation between R, r, ρ, $R > r + \rho, r > 0$, so that we have a family of convex pentagons that are inscribed in C_1 and circumscribed about C_2. From the companion paper, we know that the equation $\overline{P}(R, r, \rho) = 0$ for the convex pentagon can be written directly from $\overline{P}(R, r, \rho) = P(-R, r, \rho) = P(R, -r, \rho)$. It is easy to show that for $R = 1 > \rho \geq 0$, there exists exactly one real r-root of $\overline{P}(1, r, \rho) = 0$ that satisfies $R = 1 > r + \rho, r > 0$.

6. Concluding remarks

Everything in this paper was done completely by hand and this adds completeness to a computer only derived solution. The advantage of the computer derived solution is that it is less mentally demanding and requires less thought to carry out.

References

[1] N. A. Court, *College Geometry*, Dover reprint, 2007.
[2] V. Dragović and M. Radnović, *Poncelet Porisms and Beyond, Integrable Billiards, Hyperelliptic Jacobians and Pencials of Quadrics*, Springer, 2011; http://www.springer.com/cda/content/document/cda_downloaddocument/9783034800143-p1.pdf?SGWID=0-0-45-1054140-p174034876.
[3] L. Halbeisen, https://www.math.uzh.ch/fileadmin/math/.../01_14.p..., University of Zurich.
[4] A. Holshouser, S. Molchanov, and H. Reiter, A special case of Poncelet's problem, *Forum Geom.*, 16 (2016) 151–170.
[5] E. Weisstein, Poncelet's Porism, http://mathworld.wolfram.com/PonceletsPorism.html.

Arthur Holshouser: 3600 Bullard St., Charlotte, North Carolina, USA
E-mail address: xxx

Stanislav Molchanov: Department of Mathematics, University of North Carolina Charlotte, Charlotte, North Carolina 28223, USA
E-mail address: smolchan@uncc.edu

Harold Reiter: Department of Mathematics, University of North Carolina Charlotte, Charlotte, North Carolina 28223, USA
E-mail address: hbreiter@email.uncc.edu

Forum Geometricorum
Volume 16 (2016) 151–170.

FORUM GEOM
ISSN 1534-1178

A Special Case of Poncelet's Problem

Arthur Holshouser, Stanislav Molchanov, and Harold Reiter

Abstract. A special case of Poncelet's Theorem states that if circle C_2 lies inside of circle C_1 and if a convex n-polygon, $n \geq 3$, or an n-star, $n \geq 5$, is inscribed in C_1 and circumscribed about C_2, then there exists a family of such n-polygons and n-stars. Suppose C_2 lies inside of C_1 and R, r, are the radii of C_1, C_2 respectively and ρ is the distance between the centers of C_1, C_2. For $n \geq 3$ we give an algorithm that computes the necessary and sufficient conditions on R, r, ρ, where $R > r + |\rho|, r > 0$, so that if we start at any arbitrary point P on C_1 and draw successive tangents to C_2 (counterclockwise about the center of C_2) then we will return to P in exactly n-steps and not return to P in fewer than n-steps. This will create the above family of n-polygons and n-stars. The algorithm uses nothing but rational operations. At the end we illustrate this rational algorithm for $n = 3, 4, 5, 6, 7$ and we will then see an invariant begin to emerge.

1. Introduction

Jean-Victor Poncelet (born July 1, 1788, Metz, France; died December 22, 1867, Paris) was a French mathematician and engineer who was one of the founders of modern projective geometry. As a lieutenant of engineers in 1812, he took part in Napoleon's Russian campaign, in which he was abandoned as dead at Krasnoy and imprisoned at Saratov; he returned to France in 1814. During his imprisonment Poncelet studied projective geometry and wrote *Applications ...*

A special case of Poncelet's Theorem states that if all points on circle C_2 lie inside of circle C_1 and if a convex n-polygon, $n \geq 3$, is inscribed in C_1 and circumscribed about C_2 then there exists a family of such n-polygons. The same thing is true when an n-star, $n \geq 5$, is inscribed in C_1 and circumscribed about C_2 and the n-star goes around the center of C_2 exactly two times or exactly three times or exactly four times, etc. Each member of the family can be constructed by starting at any arbitrary point P on C_1 and drawing successive tangents to C_2 (counterclockwise to the center of C_2) until after exactly n steps and no fewer than n steps were turn to P.

If R, r are the radii of C_1, C_2 respectively and ρ is the distance between the centers, where $R > r + |\rho|, r > 0$, then Poncelet's Theorem and physical reasoning indicates that if $R, \rho, R > |\rho| \geq 0$, are fixed, then r must be the same and unique for all n-polygons, $n \geq 3$, of our family and for all n-stars, $n \geq 5$, of our family that go around the center of C_2 exactly two times, that go around the center of C_2 exactly three times, etc. With $R > |\rho| \geq 0$ being fixed and r being a variable, we develop a rational algorithm for computing this relation between $R, r, \rho, R > r + |\rho|, r > 0$,

Publication Date: April 19, 2016. Communicating Editor: Paul Yiu.

We are grateful to Prof. Ben Klein of Davidson College for his computer generated examples and for his helpful comments.

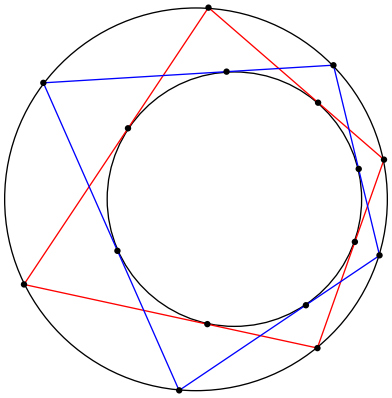

Figure 1. A family of quadrilaterals

for all $n \geq 3$. We do this by studying a very special case for C_1, C_2, P. We assume that C_2 lies inside of C_1 and we define $C_2 : x^2+y^2 = r^2, C_1 : (x-\rho)^2+y^2 = R^2$. We also assume that R, ρ are fixed where $0 \leq |\rho| < R$. Then we compute the necessary and sufficient conditions on R, r, ρ where $R > r + |\rho|, r > 0$, so that if we start at $(x_0, y_0) = (r, -y_1) = \left(r, -\sqrt{R^2 - (r-\rho)^2}\right)$ and draw tangents successively to C_2 (counterclockwise about the origin $(0,0)$) then in exactly $n \geq 3$ steps and not in fewer than n steps we will return to $(x_0, y_0) = (r, -y_1)$.

By Poncelet's Theorem these conditions are also necessary and sufficient so that if we use any arbitrary point P on C_1 in the place of $(x_0, y_0) = (r, -y_1)$ and use the same construction of tangents to C_2 (counterclockwise about $(0,0)$) then we will return to P in exactly n-steps and never return to P in fewer than n-steps. Of course, for each fixed $n \geq 3$, this algorithm is dealing with the n-polygons and the n-stars together to generate one equation $P_n^*(R, r, \rho) = 0$ where P_n^* is a polynomial. However, for each fixed $n \geq 3$, if $R, \rho, R > |\rho| \geq 0$, are fixed and r is a variable and if the positive real r-roots of $P_n^*(R, r, \rho) = 0$ that satisfy $0 < r < R - |\rho|$ are $0 < r_1 < r_2 < \cdots < r_k < R - |\rho|$ then r_k is the radius of C_2 so that we get an n-polygon that goes around $(0,0)$ exactly one time, r_{k-1} is the radius of C_2 so that we get an n-star that goes around $(0,0)$ exactly two times, r_{k-2} is the radius of C_2 so that we get an n-star that goes around $(0,0)$ exactly three times, etc. (Important: see Section 3 for a slight correction to this statement.) We call the n-polygons, $n \geq 3$ and the n-stars, $n \geq 5$, that we generate Poncelet n-polygons and Poncelet n-stars. They can also be called the standard n-gons and the standard n-stars. It may be true that $P_n^*(R, r, \rho) = 0$ has extraneous roots r_i that lie outside of $R > r_i + |\rho|, r_i > 0$. Also, $P_n^*(R, r, \rho) = 0$ might repeat some of the roots r_i. But we can eliminate this multiplicity by agreeing to write $P_n^*(R, r, \rho) = 0$ in the canonical form of Comment 1.

Suppose $n \geq 3$ is fixed. In Section 3 we study exactly how many n-stars can exist and exactly how many times each n-star goes around $(0,0)$. The above list $0 < r_1 < r_2 < \cdots < r_k, R > r_i + |\rho|, r_i > 0$, will include exactly one r_i for

each n-star that can exist. We can see this fact intuitively by letting $R > |\rho| \geq 0$ be fixed and then letting r slowly decrease from $r = R - |\rho|$ to $r = 0$ and studying the action by using physical reasoning.

2. Initial concepts

We first discuss what we mean by an n-star in this note. Suppose we draw a regular n-gon where $n \geq 5$ and number the vertices $1, 2, 3, \cdots, n$ in counterclockwise order. For each $k \in \left\{1, 2, \cdots, \lfloor \frac{n}{2} \rfloor\right\}$ if (n, k) are relatively prime let us start at vertex 1 and draw lines connecting $(1, 1+k)$, $(1+k, 1+2k)$, $(1+2k, 1+3k)$, $(1+3k, 1+4k)$, ..., where the calculations use modulo n arithmetic. Since (n, k) are relatively prime, we will return to vertex 1 in exactly n-steps and in no fewer than n-steps. In doing this we create an n-star that goes around the center of the n-gon exactly k times. Thus, for the 7-gon we can create 7-stars that go around the center $k = 1, k = 2$ or $k = 3$ times where we consider the 7-gon itself as a star.

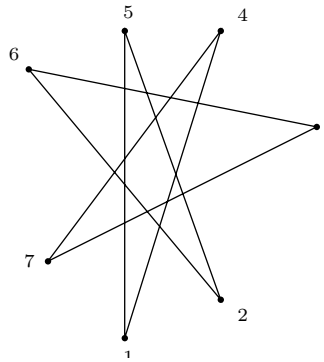

Figure 2a. $n = 7$, $k = 3$

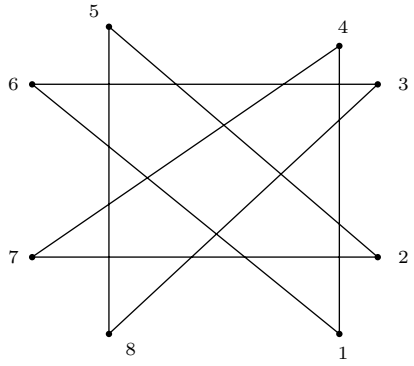

Figure 2b. $n = 8$, $k = 3$

For the 8-gon we can create 8-stars that go around the center $k = 1$ or $k = 3$ times where we consider the 8-gon itself as a star.

Note 1. In this entire note, it is convenient to think of $R, \rho, R > |\rho| \geq 0$, as constants and r, where $R > r + |\rho|, r > 0$, as a variable. By doing this we can use single variable algebra and single variable calculus.

Algorithm 1. Suppose $P(R, r, \rho) = 0,\ Q(R, r, \rho) = 0$ are two polynomial equations (where r is the variable) and we wish to eliminate all r-variable traces of $P(R, r, \rho) = 0$ that are embedded in $Q(R, r, \rho) = 0$ and leave the rest. The following algorithm does this and it also explains exactly what we mean. (In Comment 1 we mention possible overkill.)

(1) First, compute $Q_1 = \gcd(P, Q)$ and write $Q = Q_1 \cdot Q'$ where $\gcd$ denotes greatest common divisor and Q_1 is a polynomial in R, r, ρ. All calculations consider r the variable.

(2) Next, compute $Q_2 = \gcd(P, Q')$ where Q_2 is a polynomial in R, r, ρ and write $Q' = Q_2 \cdot Q''$ so that $Q = Q_1 Q_2 Q''$.

(3) Next, compute $Q_3 = \gcd\left(P, Q''\right)$ where Q_3 is a polynomial and write $Q'' = Q_3 \cdot Q'''$ so that $Q = Q_1 Q_2 Q_3 Q'''$.

$\vdots$

(n) Last, compute $Q_n = \gcd\left(P, Q^{(n-1)}\right)$ where Q_n is a polynomial and write $Q^{(n-1)} = Q_n \cdot Q^{(n)}$ so that $Q = Q_1 \cdot Q_2 \cdots Q_n \cdot Q^{(n)}$. Suppose now that $\gcd\left(P, Q^{(n)}\right) = 1$. That is, $P, Q^{(n)}$ are relatively prime in the variable r. We now define $Q^{(n)}$ to be the part (or divisor) of Q that remains after we eliminate all traces of P in the variable r that are embedded in Q.

Since we will always be writing the equation $Q^{(n)} = 0$, we can also write $Q^{(n)}$ as a polynomial in all of the variables R, r, ρ.

If we wish to eliminate all r-variable traces of several polynomials

$$P_1(R, r, \rho) = 0, \quad P_2(R, r, \rho) = 0, \quad \cdots, P_k(R, r, \rho) = 0$$

that are embedded in polynomial $Q(R, r, \rho) = 0$ and leave the rest we first use the above algorithm with (P_1, Q). Let Q^* be the divisor of Q that remains after all r-traces of P_1 have been eliminated from Q.

We next use the algorithm with (P_2, Q^*), and let Q^{**} be the divisor of Q^* that remains after all r-traces of P_2 have been removed from Q^*. Then we use the algorithm with (P_3, Q^{**}) and let Q^{***} be the divisor of Q^{**} that remains after all r-traces of P_3 have been eliminated from Q^{**} .

We continue the algorithm with each $P_1, P_2 \cdots P_k$ until we end up with $Q^{***\cdots*}$ where $Q^{***\cdots*}$ is the divisor of Q that remains after all r-traces of $P_1, P_2, \cdots, P_k$ have been eliminated from Q.

Comment 1. In applying this algorithm to the problems in this note, from our experience we believe that to eliminate all r-traces of a polynomial $P(R, r, \rho) = 0$ from a polynomial $Q(R, r, \rho) = 0$, then all we have to do is divide $\frac{Q(R,r,\rho)}{P(R,r,\rho)} = Q' = Q^{(n)}$ one time and $Q' = Q^{(n)}$ will automatically be the answer that we are seeking. However, only more practice will tell us whether this is always true or not. As always, we let R, ρ be fixed and r be a variable. Suppose a polynomial $P(R, r, \rho) = 0$ in the rational field is factored $P(R, r, \rho) = P_1^{k_1}(R, r, \rho) \cdot P_2^{k_2}(R, r, \rho) \cdots P_n^{k_n}(R, r, \rho)$ where $P_1, P_2, \cdots P_n$ are distinct polynomials (in the rational field) in the variable r that are each irreducible in the rational field. Then by algebra and calculus we can compute a polynomial $\overline{P}(R, r, a) = \dfrac{P(R, r, \rho)}{\gcd(D_r P, P)} = P_1(R, r, \rho) \cdot P_2(R, r, \rho) \cdots P_n(R, r, \rho)$. D_r is the r-variable derivative. We call $\overline{P}(R, r, \rho)$ the canonical form of $P(R, r, \rho)$. This polynomial $\overline{P}(R, r, \rho) = 0$ will contain the exact same r-root information as $P(R, r, \rho) = 0$ since they have the same r-roots but $\overline{P}(R, r, \rho)$ does not repeat the r-roots. $\overline{P}(R, r, \rho)$ is all that we need. We do not have to compute $P_1, P_2, \ldots, P_k$.

If we agree to write all of our polynomials in this canonical form $\overline{P}(R,r,\rho)$, then in this note it becomes much more likely that Algorithm 1 can be carried out by the above single division $\frac{Q(R,r,\rho)}{P(R,r,\rho)} = Q' = Q^{(n)}$. In any case, if we write all of our polynomials in the above canonical form, Algorithm 1 can always be carried out in just one single step.

3. Analytic machinery

As always, in this note $C_2 : x^2 + y^2 = r^2, C_1 : (x-\rho)^2 + y^2 = R^2$ are the standard definitions of two circles and C_2 lies inside of C_1. That is, $R > r + |\rho|, r > 0$. The origin $(0,0)$ is the center of C_2 and $(\rho,0)$ is the center of C_1.

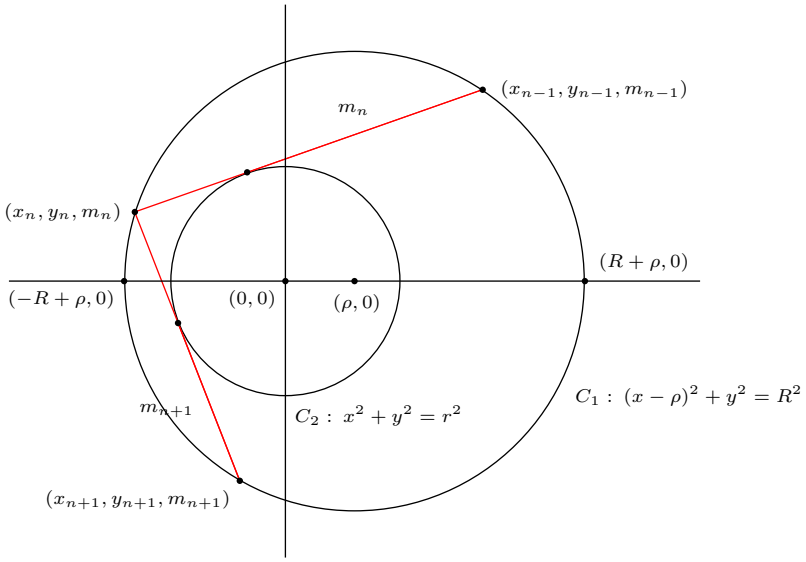

Figure 3. A family of quadrilaterals

In Figure 3 and throughout this paper, the reader may prefer to let $\rho \geq 0$. Suppose $(x_{n-1}, y_{n-1}, m_{n-1}), (x_n, y_n, m_n), (x_{n+1}, y_{n+1}, m_{n+1})$ are drawn in Fig. 3, and suppose that $(x_{n-1}, y_{n-1}), (x_n, y_n), (x_{n+1}, y_{n+1})$ are successive points on circle C_1 and the tangent lines to circle C_2 in Fig. 3 are oriented counterclockwise about the origin $(0,0)$ as indicated by the arrows. Also, $m_n, m_{n+1}, \cdots$ are the reciprocals of the slopes of the tangent lines in Fig. 3. That is, $m_n = \frac{x_n - x_{n-1}}{y_n - y_{n-1}}, m_{n+1} = \frac{x_{n+1} - x_n}{y_{n+1} - y_n}, \cdots$.

For each successive $n, n+1$, the line between (x_n, y_n) and (x_{n+1}, y_{n+1}) can be defined parametrically by the equation $(x,y) = (x_n + m_{n+1}t, y_n + t)$ where $t \in R$ is the parameter.

Using the elementary analytic geometry of the circle, we can easily derive the following recursive equations $(x_n, y_n, m_n) \rightarrow (x_{n+1}, y_{n+1}, m_{n+1})$ for a given starting point (x_0, y_0, m_0).

(1) $m_{n+1} = \dfrac{2x_n y_n}{y_n^2 - r^2} - m_n.$

(2) $x_{n+1} = \dfrac{(-x_n + 2\rho)\, m_{n+1}^2 - 2y_n m_{n+1} + x_n}{m_{n+1}^2 + 1}$.

(3) $y_{n+1} = \dfrac{y_n m_{n+1}^2 - 2\,(x_n - \rho)\, m_{n+1} - y_n}{m_{n+1}^2 + 1}$.

4. A special case of the recursion

As stated previously, this standard special case if the case that we always deal with in this note. Suppose we define $(x_0, y_0, m_0) = \left(r, -\sqrt{R^2 - (r-\rho)^2}, m_0\right)$ and $(x_1, y_1, m_1) = \left(r, \sqrt{R^2 - (r-\rho)^2}, 0\right)$ where the line between (x_0, y_0), (x_1, y_1) is a vertical tangent to circle C_2.

We note that $x_1 = r$ is a rational function of r. Also, we note that y_1 is an irrational function of R, r, ρ but y_1^2 is a rational function of R, r, ρ.

By studying the recursive equations of Section 3, we easily see by using induction that we can write $(x_n, y_n, m_n) = (x_n, Y_n \cdot y_1, M_n \cdot y_1)$ where x_n, Y_n, M_n are rational functions of R, r, ρ and $y_1 = +\sqrt{R^2 - (r-\rho)^2}$. Since $y_1^2 = R^2 - (r-\rho)^2$ is a rational function of R, r, ρ, it follows by induction from $(x_n, y_n, m_n) = (x_n, Y_n \cdot y_1, M_n \cdot y_1)$ and from the recursive equations of Section 3 that

$$(x_{n+1}, y_{n+1}, m_{n+1}) = (x_{n+1}, Y_{n+1} \cdot y_1, M_{n+1} \cdot y_1)$$

where $x_{n+1}, Y_{n+1}, M_{n+1}$ are rational functions of R, r, ρ.

If $(x_0, y_0, m_0) = \left(r, -\sqrt{R^2 - (r-\rho)^2}, m_0\right)$ and $(x_1, y_1, m_1) = \left(r, +\sqrt{R^2 - (r-\rho)^2}, 0\right)$, we see that the recursive equations (1), (2) (3) of Section 3 can now be written for x_n, Y_n, M_n as the following recursion where, of course,

$$\begin{aligned}(x_n, y_n, m_n) &= (x_n, Y_n \cdot y_1, M_n \cdot y_1)\,,\\ (x_{n+1}, y_{n+1}, m_{n+1}) &= (x_{n+1}, Y_{n+1} \cdot y_1, M_{n+1} \cdot y_1)\,,\end{aligned}$$

and where we use $y_1^2 = R^2 - (r-\rho)^2$ and $R > r + |\rho|\,, r > 0$.

(1) $(x_1, Y_1, M_1) = (r, 1, 0)$

(2) $M_{n+1} = \dfrac{2x_n Y_n}{Y_n^2 \cdot y_1^2 - r^2} - M_n$.

(3) $x_{n+1} = \dfrac{(-x_n + 2\rho)\, M_{n+1}^2 \cdot y_1^2 - 2Y_n M_{n+1} \cdot y_1^2 + x_n}{M_{n+1}^2 \cdot y_1^2 + 1}$.

(4) $Y_{n+1} = \dfrac{Y_n M_{n+1}^2 \cdot y_1^2 - 2\,(x_n - \rho)\, M_{n+1} - Y_n}{M_{n+1}^2 \cdot y_1^2 + 1}$.

In these equations, we let R, ρ be constants and let r be the variable. We can even let $R = 1$. There is also no loss of generality if we assume $\rho \geq 0$.

The computer programs run more efficiently if we deal exclusively with polynomials. Therefore, let us write $M_n = \frac{M_n}{\overline{M}_n}, x_n = \frac{x_n}{\overline{x}_n}, Y_n = \frac{Y_n}{\overline{x}_n}$ where we have the five polynomials, $x_n, \overline{x}_n, Y_n, M_n, \overline{M}_n$.

We now have $x_1 = r, \overline{x}_1 = 1, Y_1 = 1, M_1 = 0, \overline{M}_1 = 1, y_1^2 = R^2 - (r-\rho)^2$.

The recursions are as follows.

(1) $M_{n+1} = 2x_n Y_n \overline{M}_n - Y_n^2 M_n y_1^2 + r^2 \overline{x}_n^2 M_n$.

(1′) $\overline{M}_{n+1} = Y_n^2 \overline{M}_n y_1^2 - r^2 \overline{x}_n^2 \overline{M}_n$.

(2) $x_{n+1} = (-x_n + 2\rho\overline{x}_n) M_{n+1}^2 y_1^2 - 2Y_n M_{n+1} \overline{M}_{n+1} y_1^2 + x_n \overline{M}_{n+1}^2$.

(2′) $\overline{x}_{n+1} = \overline{x}_n M_{n+1}^2 y_1^2 + \overline{x}_n \overline{M}_{n+1}^2$.

(3) $Y_{n+1} = Y_n M_{n+1}^2 y_1^2 - 2(x_n - \rho\overline{x}_n) M_{n+1} \overline{M}_{n+1} - Y_n \overline{M}_{n+1}^2$.

We can easily prove by induction that for all $n \geq 1$ and for all real R, r, ρ we have $\overline{x}_n > 0, \overline{x}_{n+1} > 0$.

Therefore, we never have to worry about $\frac{x_n}{\overline{x}_n}, \frac{Y_n}{\overline{x}_n}$ having a common r-root in the range $R > r + |\rho|, r > 0$.

However, to be on the safe side we need to compute the $\gcd\left(M_n, \overline{M}_n\right)$ and throw this $\gcd$ away, in the numerator and denominator of $\frac{M_n}{\overline{M}_n}$.

In this note, we always deal with the fraction form of the recursion and not the polynomial form.

In both the fraction and polynomial forms of the recursion, it appears that the recursive equations will quickly become intractable. However, from our experience, these recursive equations will massively simplify proportional to the expansion. So they remain tractable. This phenomenon is far from random.

Comment 2. It is probably true by induction that for all $n \in \{0, 1, 2, 3, \cdots\}$, $y_1^2 = (R - r + \rho)(R + r - \rho)$ divides $(x_n - r)$.

To see this we see that $x_0 = x_1 = r$ and $y_1^2 | (x_0 - r)$ and $y_1^2 | (x_1 - r)$. From the fraction form of the recursion for x_{n+1} we see that $x_{n+1} - r = \frac{(\quad) y_1^2 + (x_n - r)}{M_{n+1}^2 y_1^2 + 1}$ and from this we see that it is probably true that $y_1^2 | (x_{n+1} - r)$ since $y_1^2 | y_1^2$ and $y_1^2 | (x_n - r)$.

By the same reasoning it is also probably true by induction that $r | x_n$ and $r | M_n$ for all $n \in \{1, 2, 3, \cdots\}$. To see this we see that $r | x_1, r | M_1$ since $x_1 = r, M_1 = 0$.

From the recursion for x_{n+1}, M_{n+1}, we see that it is probably true that $r | x_{n+1}$, $r | M_{n+1}$ for all $n \in \{1, 2, 3, \cdots\}$.

5. Main Problem 1 and Problems $1, 1', 2$

Main Problem 1. Suppose $n \geq 3$ is fixed. Using the standard example that we defined in Section 4, where R, ρ satisfying $R > |\rho| \geq 0$, are fixed, we wish to compute the necessary and sufficient conditions $P_n^*(R, r, \rho) = 0, R > r + |\rho|, r > 0$, where r is considered to be the only variable and where $P_n^*(R, r, \rho)$ is a polynomial in R, r, ρ, so that if we start at the standard point $(x_0, y_0) = (r, -y_1) = \left(r, -\sqrt{R^2 - (r-\rho)^2}\right)$ on C_1 and draw successive tangents to C_2 that are oriented counterclockwise about $(0, 0)$ then we will return to (x_0, y_0) in exactly n

steps and also such that we pass through (x_0, y_0) just one time in n steps. (In this paper, when we say that we arrive at or return to (x_0, y_0) in exactly n steps this always means that we arrive at or return to (x_0, y_0) **at the end** of exactly n steps.)

Note 2. We will call this $P_n^*(R, r, \rho) = 0$, where $R > r + |\rho|, r > 0$ the standard equation or the Poncelet equation. As always, starting at (x_0, y_0), we call the above construction of tangents to C_2 the standard construction and we call $(x_0, y_0) = \left(r, -\sqrt{R^2 - (r-\rho)^2}\right) \to (x_1, y_1) = \left(r, +\sqrt{R^2 - (r-\rho)^2}\right)$ the standard starting points.

Observation 1. We soon define three problems whose solutions are equivalent to Main Problem 1. First, we state the following without proof. By the x-axis symmetry of the standard construction, the proofs are fairly easy and are left to the reader.

Suppose we start at the standard $(x_0, y_0) = (r, -y_1)$ and by using the standard construction we arrive back at (x_0, y_0) in exactly n steps and also we arrive back at (x_0, y_0) just one time in n steps. We call this the standard condition (or the Poncelet condition).

(1) If $n \geq 3$ is odd, then the standard (or Poncelet) condition is met if and only if in exactly $\frac{n+1}{2}$ steps we arrive at one of the two points $(-R + \rho, 0)$, $(R + \rho, 0)$.

Also, we pass through this $(-R + \rho, 0)$ or $(R + \rho, 0)$ point exactly one time in $\frac{n+1}{2}$ steps. Note that we only pass through one of these two points $(-R + \rho, 0), (R + \rho, 0)$.

Exactly which of these two points we arrive at in $\frac{n+1}{2}$ steps depends exactly upon the nature of the n-star that we are dealing with. Of course, a Poncelet n-polygon will arrive at$(-R + \rho, 0)$ in exactly $\frac{n+1}{2}$ steps. The reader can study analogies of Fig. 2 to see this. When $n = 3$, we have no 3-stars and we can only arrive at $(-R + \rho, 0)$ in exactly $\frac{n+1}{2} = 2$ steps. We cannot arrive at $(R + \rho, 0)$ in 2 steps. When $n \geq 5$ is odd, we can have some n-stars (and one n-polygon) that arrive at $(-R + \rho, 0)$ in exactly $\frac{n+1}{2}$ steps, and just one time in $\frac{n+1}{2}$ steps, and we can have some n-stars that arrive at $(R + \rho, 0)$ in exactly $\frac{n+1}{2}$ steps and just one time in $\frac{n+1}{2}$ steps.

(2) If $n \geq 4$ and n is even, then the standard (or Poncelet) condition is met if and only if in exactly $\frac{n}{2}$ steps and just one time in $\frac{n}{2}$ steps, we arrive at $\left(-r, +\sqrt{R^2 - (-r-\rho)^2}\right) = \left(-r, +\sqrt{R^2 - (r+\rho)^2}\right)$.

We note that there are no n-stars when $r = 4$ or $n = 6$. Look at the analogy of Figure 2 for $n = 6$.

From Observation 1, Main Problem 1 is equivalent to the Problems $1, 1', 2$ below.

In Problems $1, 1', 2$ as always we consider R and $\rho, R > |\rho| \geq 0$, to be fixed and r to be a variable where $R > r + |\rho|, r > 0$.

Problem 1. Suppose $n \geq 3$ and n is odd. We wish to find necessary and sufficient conditions $P_n(R,r,\rho)=0$, where $P_n(R,r,\rho)$ is a polynomial in R,r,ρ and $R > r+|\rho|, r>0$, so that if we start at the standard (x_0,y_0) and use the standard construction then we will arrive at $(-R+\rho,0)$ in exactly $\frac{n+1}{2}$ steps and we also pass through $(-R+\rho,0)$ just one time in $\frac{n+1}{2}$ steps.

Problem 1′. Suppose $n \geq 5$ and n is odd. We wish to find necessary and sufficient condition $\overline{P}_n(R,r,\rho)=0$, where $\overline{P}_n(R,r,\rho)$ is a polynomial in R,r,ρ and $R > r+|\rho|, r>0$, so that if we start at the standard (x_0,y_0) and use the standard construction then we will arrive at $(R+\rho,0)$ in exactly $\frac{n+1}{2}$ steps and we also pass through $(R+\rho,0)$ just one time in $\frac{n+1}{2}$ steps.

The solution to Main Problem 1 when $n \geq 3$ and n is odd is $P_n^* = P_n(R,r,\rho) = 0$ or $P_n^* = \overline{P}_n(R,r,\rho)=0$ where $R > r+|\rho|, r>0$.

Problem $1'$ is degenerate with no solution with $R > r+|\rho|, r>0$, when $n=3$.

Problem 2. Suppose $n \geq 4$ and n is even. We wish to find necessary and sufficient conditions $P_n(R,r,\rho)=0$ where $P_n(R,r,\rho)$ is a polynomial in R,r,ρ and $R > r+|\rho|, r>0$, so that if we start at the standard (x_0,y_0) and use the standard construction then we will arrive at $\left(-r,+\sqrt{R^2-(-r-\rho)^2}\right) = \left(-r,+\sqrt{R^2-(r+\rho)^2}\right)$ in exactly $\frac{n}{2}$ steps and we also pass through $\left(-r,\sqrt{R^2-(r+\rho)^2}\right)$ just one time in $\frac{n}{2}$ steps.

The solution to Main Problem 1 when $n \geq 4$ and n is even is $P_n^*(R,r,\rho) = P_n(R,r,\rho)=0, R > r+|\rho|, r>0$.

6. Weaker conditions on R,r,ρ

To solve Problems 1, 1′, 2 we first compute some weaker conditions on R,r,ρ where $R > r+|\rho|, r>0$.

In this section, we start at the standard $(x_0,y_0) \to (x_1,y_1,m_1)$ and we assume that we have computed $(x_n,y_n,m_n) = (x_n, Y_n \cdot y_1, M_n \cdot y_1)$ for each $n \in \{1,2,3,\cdots\}$ by the recursive algorithm of Section 4.

Problem 1*. Suppose $n \geq 3$ and n is odd. We wish to find necessary and sufficient conditions $R_n(R,r,\rho)=0$ where $R_n(R,r,\rho)$ is a polynomial in R,r,ρ and $R > r+|\rho|, r>0$, so that if we start at the standard (x_0,y_0) and use the standard construction of tangents to C_2 then we will arrive at $(-R+\rho,0)$ in exactly $\frac{n+1}{2}$ steps. In Problem 1^* we do not require that we also arrive at $(-R+\rho,0)$ just one time in $\frac{n+1}{2}$ steps.

Problem 1.** Suppose $n \geq 5$ and n is odd. We wish to find necessary and sufficient conditions $\overline{R}_n(R,r,\rho)=0$ where $\overline{R}_n(R,r,\rho)$ is a polynomial in R,r,ρ and $R > r+|\rho|, r>0$, so that if we start at the standard (x_0,y_0) and use the standard construction of tangents to C_2 then we will arrive at $(R+\rho,0)$ in exactly $\frac{n+1}{2}$ steps. In Problem 1^{**} we do not require that we also arrive at $(R+\rho,0)$ just

one time in $\frac{n+1}{2}$ steps. Problem 1^{**} has no solution when $n = 3$ that satisfies $R > r + |\rho|, r > 0$.

Solution to Problems $1^*, 1^{**}$. Problems 1^*, 1^{**} can be solved by settling $x_{\frac{n+1}{2}} = -R + \rho$ and $x_{\frac{n+1}{2}} = R + \rho$ respectively.

This gives the required polynomials $R_n(R, r, \rho) = 0$ and $\overline{R}_n(R, r, \rho) = 0$ where we require $R > r + |\rho|, r > 0$.

These two equations are equivalent to $x_{\frac{n+1}{2}} - r = -R + \rho - r = -(R + r - \rho)$ and $x_{\frac{n+1}{2}} - r = R - r + \rho$ respectively.

Since $y_1^2 = (R + r - \rho)(R - r + \rho)$ probably divides $x_{\frac{n+1}{2}} - r$, we see that we can probably divide out $R + r - \rho$ and $R - r + \rho$ respectively in these two equations. We can now call these new polynomials $R_n(R, r, \rho) = 0, \overline{R}_n(R, r, \rho) = 0$ and as always, we can write $R_n, \overline{R}_n$ in the canonical form. These factors $R + r - \rho = 0, R - r + \rho = 0$ are extraneous since we soon show that they each contradict $R > r + |\rho|, r > 0$. We rarely use the above solutions. The following second solutions are much superior. From Fig. 3, we can solve problem 1^* by using the equality $\frac{x_{\frac{n-1}{2}} - (-R+\rho)}{y_{\frac{n-1}{2}} - 0} = m_{\frac{n+1}{2}}$. That is, $x_{\frac{n-1}{2}} + R - \rho = y_{\frac{n-1}{2}} m_{\frac{n+1}{2}} = Y_{\frac{n-1}{2}} M_{\frac{n+1}{2}} y_1^2$. This is equivalent to

$$\left(x_{\frac{n-1}{2}} - r\right) + (R + r - \rho) = Y_{\frac{n-1}{2}} M_{\frac{n+1}{2}} y_1^2. \qquad (*)$$

Since $y_1^2 \left| \left(x_{\frac{n-1}{2}} - r\right) \right.$ is probably true, we see that $R + r - \rho$ will probably divide out of $(*)$. $R + r - \rho = 0$ is extraneous since $R + r - \rho = 0, r > 0$ implies $\rho = |\rho| = R + r$ and $R \not> r + |\rho| = R + 2r$. After we divide $R + r - \rho$ out of $(*)$, we call the resulting polynomial equation $R'_n(R, r, \rho) = 0$.

Now $R'_n(R, r, \rho) = 0$ is not the solution to Problem 1^*. We now observe that $R_{n-2}(R, r, \rho) = 0$ gives necessary and sufficient conditions so that the standard construction arrives at $(-R + \rho, 0)$ in exactly $\frac{(n-2)+1}{2} = \frac{n-1}{2}$ steps, and this will also solve the above equation $(*)$ since $x_{\frac{n-1}{2}} + R - \rho = 0$ and $Y_{\frac{n-1}{2}} = 0$. Therefore, to compute the true solution to Problem 1^*, we must now eliminate all r-traces of $R_{n-2}(R, r, \rho) = 0$ from the equation $R'_n(R, r, \rho) = 0$ by using Algorithm 1 with emphasis on Comment 1. The divisor of $R'_n(R, r, \rho)$ that is left will be the true necessary and sufficient conditions $R_n(R, r, \rho) = 0, R > r + |\rho|, r > 0$, that solve Problem 1^*.

From Figure 3, we can solve Problem 1^{**} by using the equality $\frac{x_{\frac{n-1}{2}} - (R+\rho)}{y_{\frac{n-1}{2}} - 0} = m_{\frac{n+1}{2}}$. That is, $x_{\frac{n-1}{2}} - R - \rho = y_{\frac{n-1}{2}} m_{\frac{n+1}{2}} = Y_{\frac{n-1}{2}} M_{\frac{n+1}{2}} y_1^2$. This is equivalent to

$$\left(x_{\frac{n-1}{2}} - r\right) - (R - r + \rho) = Y_{\frac{n-1}{2}} M_{\frac{n+1}{2}} y_1^2. \qquad (**)$$

Since $y_1^2 \left| \left(x_{\frac{n-1}{2}} - r\right) \right.$ is probably true, we see that $R - r + \rho$ will probably divide out of $(**)$.

Now $R-r+\rho=0$ is extraneous since $R-r+\rho=0$ implies $\rho=-(R-r)$ which implies $|\rho|=R-r$ and $R \not> r+|\rho|=R$.

After we divide $R-r+\rho$ out of $(**)$, we call the resulting polynomial equation $\overline{R}'_n(R,r,\rho)=0$.

Now $\overline{R}'_n(R,r,\rho)=0$ is not the solution to Problem 1^{**}. We now observe that $\overline{R}_{n-2}(R,r,\rho)=0$ gives necessary and sufficient conditions so that the standard construction arrives at $(R+\rho,0)$ in exactly $\frac{(n-2)+1}{2}=\frac{n-1}{2}$ steps and this will also solve the above equation $(**)$ since $x_{\frac{n-1}{2}}-R-\rho=0$ and $Y_{\frac{n-1}{2}}=0$.

Therefore, to compute the true solution to Problem 1^{**}, we must now eliminate all r-traces of $\overline{R}_{n-2}(R,r,\rho)=0$ from the equation $\overline{R}'_n(R,r,\rho)=0$ by using Algorithm 1 with emphasis on Comment 1. The divisor of $\overline{R}'_n(R,r,\rho)$ that is left will be the true necessary and sufficient conditions $\overline{R}_n(R,r,\rho)=0, R>r+|\rho|, r>0$, that solve Problem 1^{**}.

Problem 2^*. Suppose $n \geq 4$ and n is even. We wish to find necessary and sufficient conditions $R_n(R,r,\rho)=0$ where $R_n(R,r,\rho)$ is a polynomial in R,r,ρ and $R>r+|\rho|, r>0$, so that if we start at the standard (x_0,y_0) and use the standard construction of tangents to C_2 then we will arrive at $\left(-r,+\sqrt{R^2-(-r-\rho)^2}\right)=\left(-r,+\sqrt{R^2-(r+\rho)^2}\right)$ in exactly $\frac{n}{2}$ steps.

In Problem 2^*, we do not require that we also arrive at $\left(-r,+\sqrt{R^2-(-r-\rho)^2}\right)$ just one time in $\frac{n}{2}$ steps.

Solution to Problem 2^*. We first define the equation $x_{\frac{n}{2}}=-r$ where $x_1,x_2,x_3,\cdots$ have been recursively computed. From Comment 2, we know that $r|x_{\frac{n}{2}}$ is probably true.

Therefore, we divide r out of the equation $x_{\frac{n}{2}}=-r$ where $r=0$ is an extraneous factor since it contradicts $r>0$. This defines a polynomial equation $R'_n(R,r,\rho)=0, R>r+|\rho|, r>0$ which gives necessary and sufficient conditions so that if we start at (x_0,y_0) and construct tangents to C_2 in the standard way then we will arrive at one or the other of $\left(-r,-\sqrt{R^2-(-r-\rho)^2}\right)$, $\left(-r,+\sqrt{R^2-(-r-\rho)^2}\right)$ in exactly $\frac{n}{2}$ steps (but not necessarily just one time in $\frac{n}{2}$ steps).

By induction, we know that $R_{n-2}=0, R>r+|\rho|, r>0$, are the necessary and sufficient conditions so that if we start at the standard (x_0,y_0) and use the standard construction of tangents to C_2, then we will arrive at $\left(-r,+\sqrt{R^2-(-r-\rho)^2}\right)$ in exactly $\frac{n-2}{2}=\frac{n}{2}-1$ steps (but not necessarily just one time in $\frac{n}{2}-1$ steps).

Now if the standard and construction starting at (x_0, y_0) arrives at $\left(-r, -\sqrt{R^2 - (-r-\rho)^2}\right)$ in exactly $\frac{n}{2}$ steps, then this construction must also arrive at $\left(-r, +\sqrt{R^2 - (-r-\rho)^2}\right)$ in exactly $\frac{n}{2} - 1$ steps. Therefore, if we eliminate all r-traces of $R_{n-2}(R, r, \rho) = 0, R > r + |\rho|, r > 0$, from $R'_n(R, r, \rho) = 0$ by using Algorithm 1 with emphasis on Comment 1, the divisor of $R'_n(R, r, \rho) = 0$ that is left will be the necessary and sufficient conditions $R_n(R, r, \rho) = 0, R > r + |\rho|, r > 0$, that solves Problem 2*. As always, we can write R_n in the canonical form. If we write R'_n and R_{n-2} in the canonical form, it may be true that we only need to divide $\frac{R'_n(R,r,\rho)}{R_{n-2}(R,r,\rho)} = R_n(R, r, \rho)$.

In any case, if we write R'_n and R_{n-2} in the canonical form, then Algorithm 1 can be carried out in only one step.

7. Solving Problem 1, 1′, 2 and Main Problem 1

Notation 1. We now review the notation. As in Section 6, for each $n \geq 3, n$ odd, $R_n(R, r, \rho) = 0, R > r + |\rho|, r > 0$, are the necessary and sufficient conditions calculated in Section 6 so that the standard construction starting at the standard $(x_0, y_0) = (r, -y_1)$ arrives at $(-R + \rho, 0)$ in exactly $\frac{n+1}{2}$ steps but not necessarily just one time in $\frac{n+1}{2}$ steps.

Also, $\overline{R}_n(R, r, \rho) = 0, R > r + |\rho|, r > 0$, are the necessary and sufficient conditions calculated in Section 6 so that the standard construction starting at the standard $(x_0, y_0) = (r, -y_1)$ arrives at $(R + \rho, 0)$ in exactly $\frac{n+1}{2}$ steps, but not necessarily just one time in $\frac{n+1}{2}$ steps.

Also, $P_n(R, r, \rho) = 0, R > r + |\rho|, r > 0$, and $\overline{P}_n(R, r, \rho) = 0, R > r + |\rho|, r > 0$, are the necessary and sufficient conditions so that the standard construction starting at the standard $(x_0, y_0) = (r, -y_1)$ arrives at $(-R + \rho, 0), (R + \rho, 0)$ respectively in exactly $\frac{n+1}{2}$ steps and passes through $(-R + \rho, 0), (R + \rho, 0)$ just one time in $\frac{n+1}{2}$ steps.

For each $n \geq 4, n$ even, $R_n(R, r, \rho) = 0, R > r + |\rho|, r > 0$, are the necessary and sufficient conditions calculated in Section 6 so that the standard construction starting at the standard $(x_0, y_0) = (-r, -y_1)$ arrives at $\left(-r, +\sqrt{R^2 - (-r-\rho)^2}\right)$ in exactly $\frac{n}{2}$ steps but not necessarily just one time in $\frac{n}{2}$ steps.

Also, for each $n \geq 4, n$ even, $P_n(R, r, \rho) = 0, R > r + |\rho|, r > 0$, are the necessary and sufficient conditions so that the standard construction starting at $(x_0, y_0) = (r, -y_1)$ arrives at $\left(-r, +\sqrt{R^2 - (-r-\rho)^2}\right)$ in exactly $\frac{n}{2}$ steps and passes through $\left(-r, +\sqrt{R^2 - (-r-\rho)^2}\right)$ just one time in $\frac{n}{2}$ steps.

Solution to Problems 1,1′. Suppose $n \geq 3, n$ is odd, is fixed, and the Problems 1,1′ have been solved for all $3 \leq \overline{n} < n$ where $\overline{n}$ is odd. We wish to calculate $P_n(R, r, \rho) = 0, R > r + |\rho|, r > 0$. The calculation of $\overline{P}_n(R, r, \rho) = 0, R >$

$r+|\rho|, r>0$ in Problem $1'$ is exactly the same as the calculation of $P_n(R,r,\rho)=0, R>r+|\rho|, r>0$, in Problem 1.

Suppose $3\le n_1<n_2<\cdots<n_k<n$ is the list of all positive odd integers $\overline{n}$ that lie in $3\le\overline{n}<n$ with the property $(\dagger)$ below.

Of course, as always, for each n_i in the list, $P_{n_i}(R,r,\rho)=0, R>r+|\rho|, r>0$, are the necessary and sufficient conditions so that a (Poncelet) n_i-gon or n_i-star constructed by the standard construction starting at $(x_0,y_0)=(-r,-y_1)$ arrives at $(-R+\rho,0)$ in exactly $\frac{n_i+1}{2}$ steps and passes through $(-R+\rho,0)$ just one time in $\frac{n_i+1}{2}$ steps.

Property $(\dagger)$**.** For each n_i in the list, we require these (Poncelet) n_i-gons or n_i-stars to also arrive at $(-R+\rho,0)$ in exactly $\frac{n+1}{2}$ steps.

In this note, for each odd $3\le n$, we compute the above list $3\le n_1<n_2<\cdots<n_k<n$ of odd $n_i's$ adhoc by simply checking each odd $3\le\overline{n}<n$ to see if $\overline{n}$ has property $(\dagger)$.

For our fixed $n\ge 3, n$ odd, $R_n(R,r,\rho)=0, R>r+|\rho|, r>0$ are the necessary and sufficient conditions computed in Section 7 so that the standard construction starting at the standard $(x_0,y_0)=(r_1-y_1)$ arrives at $(-R+\rho,0)$ in exactly $\frac{n+1}{2}$ steps but not necessarily just one time in $\frac{n+1}{2}$ steps. Now any standard construction that arrives at $(-R+\rho,0)$ in exactly $\frac{n+1}{2}$ steps must either pass through $(-R+\rho,0)$ just one time in exactly $\frac{n+1}{2}$ steps or it has already arrived at $(-R+\rho,0)$ in exactly $\frac{n_i+1}{2}$ steps and passed through $(-R+\rho,0)$ just one time in $\frac{n_i+1}{2}$ steps for some n_i in our list $3\le n_1<n_2<\cdots<n_k<n$.

We now eliminate all r-traces of the polynomials $P_{n_1}=0, P_{n_2}=0,\cdots,P_{n_k}=0$ from the polynomial $R_n=0$ by using Algorithm 1 of Section 3 with emphasis on Comment 1 at the end of Algorithm 1. If we use Comment 1 a simple division may be all that we need to use Algorithm 1.

The polynomial divisor of $R_n(R,r,\rho)=0, R>r+|\rho|, r>0$, that remains after all r-traces of $P_{n_1}=0, P_{n_2}=0,\cdots,P_{n_k}=0$ have been removed from $R_n(R,r,a)=0$ will be the required polynomial $P_n(R,r,\rho)=0, R>r+|\rho|, r>0$, that solves Problem 1. The solution to Problem $1'$ is almost exactly the same.

Solution to Problem 2. Suppose $n\ge 4$, n even, is fixed and suppose Problem 2 has been solved for all $\overline{n}$ where $4\le\overline{n}<n$ and $\overline{n}$ is even.

We wish to calculate $P_n(R,r,\rho)=0, R>r+|\rho|, r>0$. The solution is almost exactly the same as Problems $1, 1'$. Suppose $4\le n_1<n_2<\cdots<n_k<n$ is the list of all positive even integers $\overline{n}$ that lie in $4\le\overline{n}<n$ with the property $(\dagger\dagger)$ below.

Of course, as always for each n_i in the list, $P_{n_i}(R,r,\rho)=0, R>$ r+$|\rho|, r>0$, are the necessary and sufficient conditions so that the standard construction starting at the standard $(x_0,y_0)=(r,-y_1)$ arrives at $\left(-r,+\sqrt{R^2-(-r-\rho)^2}\right)$ in

exactly $\frac{n_i}{2}$ steps and passes through $\left(-r, \sqrt{R^2-(-r-a)^2}\right)$ just one time in $\frac{n_i}{2}$ steps.

Property $(\dagger\dagger)$**.** For each n_i in the list, we require these (Poncelet) n_i-gons or n_i-stars to also arrive at $\left(-r, \sqrt{R^2-(-r-\rho)^2}\right)$ in exactly $\frac{n}{2}$ steps.

In this note, for each even $4 \leq n$, we compute the above list $4 \leq n_1 < n_2 \cdots < n_k < n$ of even n_i's ad hoc by simply checking each even $4 \leq \overline{n} < n$ to see if $\overline{n}$ has property $(\dagger\dagger)$.

Now $R_n(R,r,\rho) = 0, R > r + |\rho|, r > 0$, are the necessary and sufficient conditions computed in Section 7 so that the standard construction starting at the standard $(x_0, y_0) = (r, -y_1)$ arrives at $\left(-r, +\sqrt{R^2-(-r-\rho)^2}\right)$ in exactly $\frac{n}{2}$ steps but not necessarily just one time in $\frac{n}{2}$ steps.

Now any standard construction that arrives at $\left(-r, +\sqrt{R^2-(-r-\rho)^2}\right)$ in exactly $\frac{n}{2}$ steps must arrive at $\left(-r, +\sqrt{R^2-(-r-\rho)^2}\right)$ just one time in $\frac{n}{2}$ steps or it has already arrived at $\left(-r, +\sqrt{R^2-(-r-\rho)^2}\right)$ in exactly $\frac{n_i}{2}$ steps and passed through $\left(-r, +\sqrt{R^2-(-r-\rho)^2}\right)$ just one time in $\frac{n_i}{2}$ steps for some n_i in our list $4 \leq n_1 < \cdots < n_k < n$.

As in Problems $1, 1'$, we now eliminate all r-traces of the polynomial $P_{n_1} = 0, P_{n_2} = 0, \cdots, P_{n_k} = 0$ from $R_n(R,r,\rho) = 0$ using Algorithm 1 of Section 2 with emphasis on Comment 1 at the end of Algorithm 1. If we use Comment 1, a simple division may be all that we need to use Algorithm 1.

The polynomial divisor of $R_n(R,r,\rho) = 0, R > r + |\rho|, r > 0$, that remains after all r-traces of $P_{n_1}, P_{n_2}, \cdots, P_{n_k}$ have been removed from $R_n(R,\rho,P), R > r + |\rho|, r > 0$ will be the required polynomial $P_n(R,r,\rho) = 0, R > r + |\rho|, r > 0$ that solves Problem 2.

Solution to Main Problem 1 As stated in Section 6, the solutions to Problems $1, 1', 2$ give the solution $P_n^* = P_n, P_n^* = \overline{P}_n, P_n^* = P_n$ where $P_n^*(R,r,\rho), R > r + |\rho|, r > 0$, is the polynomial solution to Main Problem 1.

8. Some hand calculated examples

We solve Main Problem 1 for $n = 3, 4$ by hand.

Example 1$(n = 3)$**.** For $n = 3$, it is easy to see that $P_3^*(R,r,\rho) = P_3(R,r,\rho) = R_3(R,r,\rho) = 0$ where $R_3(R,r,\rho) = 0$ is the polynomial computed for Problem 1^* in Section 6 using two different methods. We now give both the long first method and the very short second method.

From Section 6, we see that the Problem 1^* equation $x_{\frac{n+1}{2}} = -R + \rho$ becomes $x_2 = -R + \rho$. The Problem 1^{**}, equation $x_2 = R + \rho$ is degenerate.

From Section 4, $(x_1, Y_1, M_1) = (r, 1, 0)$ and we recall that $y_1^2 = R^2 - (r - \rho)^2$ and $M_2 = \frac{2x_1Y_1}{Y_1^2 \cdot y_1^2 - r^2} - M_1 = \frac{2r}{y_1^2 - r^2} = \frac{2r}{R^2 - 2r^2 + 2\rho r - \rho^2}$.

Using the recursion for x_2 of Section 4 and simplifying we see that $x_2 = -R + \rho$ becomes the following.

$$\frac{4r^2(2\rho - r)y_1^2 - 4ry_1^2\left(R^2 - 2r^2 + 2\rho r - \rho^2\right) + r\left(R^2 - 2r^2 + 2\rho r - \rho^2\right)^2}{4r^2y_1^2 + \left(R^2 - 2r^2 + 2\rho r - \rho^2\right)^2}$$
$$= -R + \rho.$$

This is equivalent to

$$4ry_1^2\left(2\rho r - r^2 - R^2 + 2r^2 - 2\rho r + \rho^2\right) + r\left(R^2 - 2r^2 + 2\rho r - \rho^2\right)^2$$
$$= 4ry_1^2(-Rr + \rho r) + \left(R^2 - 2r^2 + 2\rho r - \rho^2\right)^2(-R + \rho),$$

which is equivalent to

$$4ry_1^2\left(-R^2 + r^2 + Rr - \rho r + \rho^2\right) = -\left(R^2 - 2r^2 + 2\rho r - \rho^2\right)^2(R + r - \rho). \quad (\ddagger)$$

Since $y_1^2 = (R + r - \rho)(R - r + \rho)$ and $R + r - \rho = 0$ is an extraneous equation that contradicts $R > r + |\rho|, r > 0$, we see that $(\ddagger)$ is equivalent to the following

$$4r(-R + r - \rho)\left(-R^2 + r^2 + Rr - \rho r + \rho^2\right) = \left(R^2 - 2r^2 + 2\rho r - \rho^2\right)^2.$$

When we multiply this out and then simplify this becomes $R^4 - 4rR^3 + 4r^2R^2 - 2\rho^2R^2 + 4\rho^2rR + \rho^4 = 0$ which is equivalent to $\left(\left(R^2 - \rho^2\right) - 2rR\right)^2 = 0$. This is equivalent to $P_3^* = R^2 - \rho^2 - 2rR = 0$ which is the standard Euler's equation. The canonical form of Comment 1 would automatically catch this multiplicity. We now solve Example 1 by computing $P_3^* = P_3 = R_3' = R_3$ by using the short second method of Problem 1^* of Section 6.

From $x_1 = r, Y_1 = 1, y_1^2 = (R - r + \rho)(R + r - \rho)$ and $M_2 = \frac{2r}{y_1^2 - r^2} = \frac{2r}{R^2 - 2r^2 + 2\rho r - \rho^2}$ we see that $x_{\frac{n-1}{2}} + R - \rho = Y_{\frac{n-1}{2}} M_{\frac{n+1}{2}} y_1^2$ becomes $x_1 + R - \rho = Y_1 M_2 y_1^2$, which is $r + R - \rho = \frac{2r \cdot (R - r + \rho)(R + r - \rho)}{R^2 - 2r^2 + 2\rho r - \rho^2}$.

Dividing out the extraneous equation $r + R - \rho = 0$ this becomes $R^2 - 2r^2 + 2\rho r - \rho^2 = 2Rr - 2r^2 + 2\rho r$ and we see that $P_3^* = P_3 = R_3' = R_3 = R^2 - \rho^2 - 2rR = 0$.

Note 2. We see that the second method is very superior to the first method. If we try to compute $R_3(R, r, \rho) = 0$ for $n = 3$ by the second method of Section 6, we see that $x_{\frac{n-1}{2}} - R - \rho = Y_{\frac{n-1}{2}} M_{\frac{n+1}{2}} y_1^2$ becomes $x_1 - R - \rho = Y_1 M_2 y_1^2$ which is $r - R - \rho = \frac{2r}{y_1^2 - r^2} y_1^2$. This is equivalent to $-\left(y_1^2 - r^2\right) = 2r(R + r - \rho)$ which simplifies to $\rho^2 = R^2 + 2rR$. This equation is degenerate since we require $R > r + |\rho|, r > 0$. However, we need to keep this equation $\rho^2 - R^2 - 2Rr = 0$ since this factor will divide out of some of the higher level equations that we will encounter. In particular, we use $\rho^2 = R^2 + 2rR$ when we deal with $n = 5$.

Example 2 ($n = 4$). We compute $P_4^*(R, r, \rho) = P_4 = 0$ for $n = 4$. For $n = 4$ it is easy to see that $P_4(R, r, \rho) = R_4'(R, r, \rho) = R_4(R, r, \rho)$ where $R_4'(R, r, \rho)$ is the polynomial computed in Problem 2^* of Section 6. We note that $R_4(R, r, \rho) = R_4'(R, r, \rho)$ since $R_{n-2} = R_2 = 2r$ is degenerate and we are going to divide r out of R_4' anyway. Using the formula for x_2 given in Example 1, we see that $x_2 = -r$ becomes

$$\frac{4r^2y_1^2(2\rho - r) - 4ry_1^2\left(R^2 - 2r^2 + 2\rho r - \rho^2\right) + r\left(R^2 - 2r^2 + 2\rho r - \rho^2\right)^2}{4r^2y_1^2 + \left(R^2 - 2r^2 + 2\rho r - \rho^2\right)^2} = -r,$$

which is equivalent to

$$\begin{aligned} &4r^2y_1^2(2\rho - r) - 4ry_1^2\left(R^2 - 2r^2 + 2\rho r - \rho^2\right) + r\left(R^2 - 2r^2 + 2\rho r - \rho^2\right)^2 \\ &= -r\left(4r^2y_1^2 + \left(R^2 - 2r^2 + 2\rho r - \rho^2\right)^2\right). \end{aligned}$$

Dividing out the extraneous $r = 0$, this becomes

$$4r(2\rho - r)y_1^2 - 4y_1^2\left(R^2 - 2r^2 + 2\rho r - \rho^2\right) + 4r^2y_1^2 = -2\left(R^2 - 2r^2 + 2\rho r - \rho^2\right)^2.$$

Dividing out 2 and simplifying we have

$$2y_1^2\left(R^2 - 2r^2 - \rho^2\right) = \left(R^2 - 2r^2 + 2\rho r - \rho^2\right)^2.$$

Using $y_1^2 = R^2 - r^2 + 2\rho r - \rho^2$ this becomes

$$2\left(R^2 - r^2 + 2\rho r - \rho^2\right)\left(R^2 - 2r^2 - \rho^2\right) = \left(R^2 - 2r^2 + 2\rho r - \rho^2\right)^2.$$

Multiplying out and simplifying we have $R^4 - 2\rho^2R^2 + \rho^4 = 2\rho^2r^2 + 2r^2R^2$, which is $\left(R^2 - \rho^2\right)^2 = 2r^2\left(R^2 + \rho^2\right)$. This is the standard quadrilateral formula.

9. Some computer generated examples

We solve Main Problem 1 for $n = 5, 6, 7$ by using a computer.

Example 3 ($n = 5$). We first compute $R_5'(R, r, \rho) = 0$ of Problem 1^* by using the equality $x_2 + R - \rho - Y_2M_3y_1^2 = 0$ which is equivalent to

$$(x_2 - r) + (R + r - \rho) - Y_2M_3y_1^2 = 0. \qquad (*)$$

Dividing by $R + r - \rho$ and using a computer, we arrive at

$$R_5'(R, r, \rho) = 16\rho^2R^2r^4 + 8R\left(R^2 - \rho^2\right)^2r^3 - 8R^2\left(R^2 - \rho^2\right)^2r^2 + \left(R^2 - \rho^2\right)^4 = 0.$$

From Problem 1^* of Section 6, we know that $R_3(R, r, \rho) = 2Rr + \rho^2 - R^2 = 0$ will also solve $(*)$ where $R_3 = 0$ was computed in Example 1 ($n = 3$). Therefore, we must eliminate all r-traces of $R_3 = 0$ from $R_5' = 0$. We can do this by dividing R_5' by R_3 and letting $R_5(R, r, \rho)$ be the quotient. This gives

$$R_5(R, r, a) = 8\rho^2Rr^3 + 4R^2\left(R^2 - \rho^2\right)r^2 - 2R\left(R^2 - \rho^2\right)^2r - \left(R^2 - \rho^2\right)^3 = 0.$$

It is easy to show that $R_5 = 0$ is irreducible in the rational field. We now let $R = 1$ and by symmetry suppose $0 \le \rho < 1$. We know by Descartes' law of signs that $R_5 = 0$ has one positive r-root for each fixed $0 \le \rho < 1$. For each fixed $0 \le \rho < 1$, we show that $R_5 = 0$ has one r-root that satisfies $0 < r < 1 - \rho$. Now $R_5(R, r, \rho) = R_5(1, 0, \rho) = -(1 - \rho)^3 < 0$. We

now show that $R_5(R,r,\rho) = R_5(1,1-\rho,\rho) > 0$. This is true if and only if $\left[8\rho^2+4(1+\rho)-2(1+\rho)^2-(1+\rho)^3\right](1-\rho)^3 > 0$. This is true if and only if $\left(1-3\rho+3\rho^2-\rho^3\right)(1-\rho)^3 = (1-\rho)6 > 0$, which is true. From this we see that for each $0 \le \rho < 1, R_5 = 0$ has one r-root that satisfies $0 < r < 1-\rho$. Therefore, in general for each $R > |\rho| \ge 0$, we see that $R_5(R,r,\rho) = 0$ has one r-root that satisfies $R > r + |\rho|, r > 0$. We let $P_5^* = R_5$ where $P_5^* = 0$ is one solution to Main Problem 1.

We next compute $\overline{R}_5'(R,r,\rho) = 0$ by using the equality $x_2 - R - \rho - Y_2 M_3 y_1^2 = 0$ which is equivalent to

$$(x_2 - r) - R + r - \rho - Y_2 M_3 y_1^2 = 0. \qquad (©)$$

Dividing by $r - R - \rho$ and using a computer we arrive at

$$\overline{R}_5'(R,r,\rho) = 16\rho^2R^2r^4 - 8R\left(R^2-\rho^2\right)^2r^3 - 8R^2\left(R^2-\rho^2\right)^2r^2 + \left(R^2-\rho^2\right)^4 = 0.$$

Now $\overline{R}_3(R,r,\rho) = -2Rr + \rho^2 - R^2 = 0$ will also solve (©). Therefore, we must eliminate all r-traces of $\overline{R}_3 = 0$ from $\overline{R}_5' = 0$. We can do this by dividing $\overline{R}_5'$ by $\overline{R}_3$ and letting $\overline{R}_5(R,r,\rho)$ be the quotient. This gives

$$\overline{R}_5(R,r,\rho) = -8\rho^2Rr^3 + 4R^2\left(R^2-\rho^2\right)r^2 + 2R\left(R^2-\rho^2\right)^2r - \left(R^2-\rho^2\right)^3 = 0.$$

It is easy to show that $\overline{R}_5 = 0$ is irreducible in the rational field. We now let $R = 1$ and by symmetry suppose $0 < \rho < 1$. We know by Descartes' law of signs that $\overline{R}_5 = 0$ has zero or two positive r-roots for each fixed $0 < \rho < 1$. For each fixed $0 < \rho < 1$ we show that $\overline{R}_5 = 0$ has one r-root that satisfies $0 < r < 1 - \rho$. ($\rho = 0$ is easy to deal with). Now $\overline{R}_5(R,r,\rho) = \overline{R}_5(1,+\infty,\rho) < 0$. Also, $\overline{R}_5(R,r,\rho) = \overline{R}_5(1,0,\rho) < 0$. If we show that $\overline{R}_5(R,r,\rho) = \overline{R}_5(1,1-\rho,\rho) > 0$, then it will follow that for each $0 < \rho < 1, \overline{R}_5 = 0$ has one r-root that satisfies $0 < r < 1 - \rho$. Now $\overline{R}_5(R,r,\rho) = \overline{R}_5(1,1-\rho,\rho) > 0$ if and only if

$$\left(-8\rho^2 + 4(1+\rho) + 2(1+\rho)^2 - (1+\rho)^3\right)(1-\rho)^3 > 0.$$

This is true if and only if

$$\begin{aligned}&\left(4\left(1+\rho-2\rho^2\right) + (1+\rho)^2(2-(1+\rho))\right)(1-\rho)^3\\ =\ &\left(4(1+2\rho)(1-\rho) + (1+\rho)^2(1-\rho)\right)(1-\rho)^3\\ >\ &0.\end{aligned}$$

This is clearly true.

Therefore, in general for each $R > |\rho| \ge 0$, we see that $\overline{R}_5(R,r,\rho) = 0$ has one r-root that satisfies $R > r + |\rho|, r > 0$. We let $P_5^* = \overline{R}_5$ where $P_5^* = 0$ is that second solution to Main Problem 1.

Therefore, $P_5^* = R_5$ and $P_5^* = \overline{R}_5$ are the two solutions to Main Problem 1 for $n = 5$.

Example 4 $(n = 6)$ From Problem 2^*, we define the equation $x_{\frac{n}{2}} = x_3 = -r$. We do this with a computer. From Comment 2 we divide r out of $x_3 = -r$ where $r = 0$ is an extraneous factor since it contradicts $r > 0$. This defines a polynomial equation $R_6'(R, r, \rho) = 0$ which we store in the computer. From Problem 2^*, to compute $R_6 = 0$ we must eliminate all r-traces of $R_4(R.r.\rho) = 2\left(R^2 + \rho^2\right) r^2 - \left(R^2 - \rho^2\right)^2 = 0$ from $R_6'(R, r, \rho) = 0$. This can be done by a single division $\frac{R_6'(R,r,\rho)}{R_4(R,r,\rho)} = R_6(R, r, \rho)$. That is,

$$\begin{aligned} R_6'(R, r, \rho) = &\ R_4(R, r, \rho) \cdot R_6(R, r, \rho) \\ = &\ \left(\left(R^2 - \rho^2\right)^2 - 2\left(\rho^2 + R^2\right) r^2\right) \cdot R_6(R, r, \rho), \end{aligned}$$

where

$$R_6(R, r, \rho) = 16\rho^2 R^2 r^4 + 4\left(\rho^2 + R^2\right)\left(R^2 - \rho^2\right)^2 r^2 - 3\left(R^2 - \rho^2\right)^4 = 0.$$

We now let $R = 1, 0 \leq \rho < 1$. We know from Descartes' Law of signs that $R_6(R, r, \rho) = R_6(1, r, \rho) = 0$ has one positive r-root for each fixed $0 \leq \rho < 1$. We now show that for each fixed $0 \leq \rho < 1, R_6 = 0$ has one r-root that satisfies $0 < r < 1 - \rho$. Now $R_6(R, r, \rho) = R_6(1, 0, \rho) = -3\left(1 - \rho^2\right)^4 < 0$. We now show that $R_6(R, r, \rho) = R_6(1, 1 - \rho, \rho) > 0$ which will finish the proof. Now $R_6(1, 1 - \rho, \rho) > 0$ is true if and only if

$$16\rho^2(1 - \rho)^4 + 4\left(1 + \rho^2\right)(1 + \rho)^2(1 - \rho)^4 - 3(1 + \rho)^4(1 - \rho)^4 > 0.$$

This is equivalent to

$$\begin{aligned} &(16\rho^2 + 4(1 + \rho^2)(1 + \rho)^2 - 3(1 + \rho)^4)(1 - \rho)^4 \\ = &\ (\rho^4 - 4\rho^3 + 6\rho^2 - 4\rho + 1)(1 - \rho)^4 \\ = &\ (1 - \rho)^8 > 0, \end{aligned}$$

which is true. From Problem 2 of Section 7, we know that $P_6^* = P_6 = R_6(R, r, a)$ where $P_6^* = 0$ solves Main Problem 1 for $n = 6$.

Example 5 $(n = 7)$**.** We first compute $R_7'(R, r, \rho) = 0$ of Problem 1^* by using the equality $x_3 + R - \rho - Y_3 M_4 y_1^2 = 0$, which is equivalent to

$$(x_3 - r) + (R + r - \rho) - Y_3 M_4 y_1^2 = 0. \qquad (\P)$$

Dividing by $R + r - \rho$, we arrive at $R_7'(R, r, \rho) = 0$ and we store this in the computer. From Problem 1^* of Section 6, we know that

$$R_5(R, r, \rho) = 8\rho^2 R^2 r^3 + 4R^2\left(R^2 - \rho^2\right)^2 r^2 - 2R\left(R^2 - \rho^2\right)^2 r - \left(R^2 - \rho^2\right)^3 = 0$$

will also solve (¶), where $R_5 = 0$ was computed in Example 3 $(n = 5)$. Therefore, we must eliminate all r-traces of $R_5 = 0$ from $R_7' = 0$. We can do this by dividing

R_7' by R_5 and letting $R_7(R,r,\rho)$ be the quotient. This gives

$$\begin{aligned} R_7(R,r,\rho) = {} & 64\rho^2R^4r^6 - 32\rho^2R\left(R^2-\rho^2\right)\left(R^2+\rho^2\right)r^5 \\ & - 16\rho^2R^2\left(R^2-\rho^2\right)^2r^4 + 8R\left(R^2+3\rho^2\right)\left(R^2-\rho^2\right)^3r^3 \\ & - 4R^2\left(R^2-\rho^2\right)^4r^2 - 4R\left(R^2-\rho^2\right)^5r + \left(R^2-\rho^2\right)^6 \\ = {} & 0. \end{aligned}$$

The equation $\overline{R}_7(R,r,\rho) = 0$ is the same as $R_7(R,r,\rho) = 0$ except that $\overline{R}_7(R,r,\rho) = R_7(-R,r,\rho) = R_7(R,-r,\rho) = 0$. The solution to Main Problem 1 is $P_7^* = R_7$ and $P_7^* = \overline{R}_7$. If we let $R = 1, 0 < \rho < 1$, we can use a computer to show that $R_7(R,r,\rho) = R_7(1,r,\rho) = 0$ has two real r-roots r_1, r_2 that satisfy $0 < r_1 < r_2 < 1-\rho$. These two r-roots give the 7-gon and a 7-star that goes around $(0,0)$ three times when $R = 1$. The equation $\overline{R_7}(R,r,\rho) = \overline{R}_7(1,r,\rho)$ has one r-root r_3 that satisfies $0 < r_3 < 1-\rho$. This r_3 gives a 7-star that goes around $(0,0)$ two times when $R = 1$.

As is consistent with the general pattern, $R_7(R,r,\rho) = R_7(1,1-\rho,\rho) = (1-\rho)^{12}$. We recall that $R_6(1,1-\rho,\rho) = (1-\rho)^8$. Also, $R_5(1,1-\rho,\rho) = (1-\rho)^6$.

Also, $R_4(1,1-\rho,\rho) = 2(1-\rho)^2\left(1+\rho^2\right) - \left(1-\rho^2\right)^2 = (1-\rho)^4$.

Also, $R_3(1,1-\rho,\rho) = 2(1-\rho) - \left(1-\rho^2\right) = (1-\rho)^2$.

In general $R_i(1,1-\rho,\rho) = (1-\rho)^{2n_i}$ where n_i is the r-degree of $R_i(R,r,\rho)$.

10. Discussion

It is fairly obvious that the polynomials R_3, R_4, R_5, R_6, R_7 that we have computed are members of a family. For example they all have powers of 2, i.e. 2, 4, 8, 16, 32, 64,... appearing in them. They also have $\left(R^2-\rho^2\right), \left(R^2-\rho^2\right)^2, \ldots$ appearing in them. In general, they just look alike in some ways. However, the only true invariant that we have discovered for R_3, R_4, R_5, R_6, R_7 is that each R_i satisfies $R_i(R,r,\rho) = R_i(1,1-\rho,\rho) = (1-\rho)^{2n_i}$, where n_i is the $r-$ degree of $R_i(R,r,\rho)$.

References

[1] N. A. Court, *College Geometry*, Dover reprint, 2007.

[2] V. Dragović and M. Radnović, *Poncelet Porisms and Beyond, Integrable Billiards, Hyperelliptic Jacobians and Pencials of Quadrics*, Springer, 2011; http://www.springer.com/cda/content/document/cda_downloaddocument/9783034800143-p1.pdf?SGWID=0-0-45-1054140-p174034876.

[3] L. Halbeisen, https://www.math.uzh.ch/fileadmin/math/.../01_14.p..., University of Zurich.

[4] A. Holshouser, S. Molchanov, and H. Reiter, Applying Poncelet's theorem to the pentagon and the pentagonal star, *Forum Geom.*, 16 (2016) 141–149.

[5] E. Weisstein, Poncelet's Porism, http://mathworld.wolfram.com/PonceletsPorism.html.

Arthur Holshouser: 3600 Bullard St., Charlotte, North Carolina, USA
E-mail address: hbreiter@email.uncc.edu

Stanislav Molchanov: Department of Mathematics, University of North Carolina Charlotte, Charlotte, North Carolina 28223, USA
E-mail address: smolchan@uncc.edu

Harold Reiter: Department of Mathematics, University of North Carolina Charlotte, Charlotte, North Carolina 28223, USA
E-mail address: hbreiter@email.uncc.edu

Forum Geometricorum
Volume 16 (2016) 171–178.

FORUM GEOM
ISSN 1534-1178

Isogonal Conjugacy Through a Fixed Point Theorem

Sándor Nagydobai Kiss and Zoltán Kovács

Abstract. For an arbitrary point X in the plane of a fixed triangle, we study the affine combination of orthogonal projections onto the sidelines of the triangle, with coefficients the absolute barycentric coordinates of X with respect to the triangle. We prove that this map is affine if and only if X lies not on the circumcircle, and the only fixed point of this map is the isogonal conjugate of X.

1. Introduction

In this paper we investigate affine combinations of orthogonal projections onto lines in the plane. In general, this map has the form

$$\phi\colon \mathbf{R}^2 \to \mathbf{R}^2,\ P \mapsto \phi(P) = AP + b,$$

where $A \in \mathbf{R}^{2\times 2}$ is a 2×2 matrix (generally not regular) and b is a vector. This map is a collineation, not necessarily injective. Nevertheless, the image set of ϕ is an affine subspace. The image space is $\mathbf{R}^2$ if and only if A is regular, and we call ϕ an affine map in this case, as usual. (In this case ϕ is a bijective collineation.)

Specifically, we fix a triangle ABC, and for $X \in \mathbf{R}^2$, consider the affine combination of orthogonal projections with respect to the sides of ABC, with coefficients the absolute barycentric coordinates of X with respect to ABC. We call this map the *weighted pedal map* ϕ_X (see Section 2). We prove that the weighted pedal map ϕ_X is affine if and only if X does not lie on the circumcircle. If X is on the circumcircle, then the image space is the Simson line of the antipodal point of X.

In the affine case we prove that the only fixed point of ϕ_X is the isogonal conjugate of the point X. Note, the isogonal conjugate X^* of a point X in the plane of the triangle ABC is constructed geometrically by reflecting the lines AX, BX, and CX about the angle bisectors at A, B, and C. The three reflected lines then concur at the isogonal conjugate X^* ([4]).

Finally, we investigate the image of the circumcircle in special cases.

Throughout this paper we work with barycentric coordinates. We follow conventions in [3]. Let ABC be the fundamental triangle with angles A, B, C and side lengths $BC = a$, $CA = b$, $AB = c$. Every finite point P in the plane has a unique absolute barycentric coordinates (u, v, w) for which $P = uA + vB + wC$ and $u + v + w = 1$. For any $\lambda \in \mathbf{R} \setminus \{0\}$, $(u', v', w') = \lambda(u, v, w)$ are the homogeneous (or relative) barycentric coordinates of P and we write $P = (u' : v' : w')$.

Publication Date: April 26, 2016. Communicating Editor: Paul Yiu.

Let $S_A = \frac{b^2+c^2-a^2}{2} = bc\cos A$, $S_B = \frac{a^2+c^2-b^2}{2} = ac\cos B$, $S_C = \frac{a^2+b^2-c^2}{2} = ab\cos C$. S denotes twice the area of triangle ABC. We shall freely use the following identities:

$$\begin{aligned} S^2 &= b^2c^2 - S_A^2 = c^2a^2 - S_B^2 = a^2b^2 - S_C^2, \\ S^2 &= a^2S_A + S_BS_C = b^2S_B + S_CS_A = c^2S_C + S_AS_B, \\ S^2 &= S_BS_C + S_CS_A + S_AS_B, \\ 2S^2 &= a^2S_A + b^2S_B + c^2S_C, \\ 2S_AS_B &= a^2S_A + b^2S_B - c^2S_C. \end{aligned}$$

2. The weighted pedal map

Definition. Let X be a point in the plane of the triangle ABC. Denote by (α, β, γ) the absolute barycentric coordinates of X with respect to the triangle ABC, i.e.

$$X = \alpha A + \beta B + \gamma C,\ \alpha + \beta + \gamma = 1.$$

Define the *weighted pedal map* $\phi_X : \mathbf{R}^2 \to \mathbf{R}^2$ by

$$\phi_X(P) = \alpha\pi_a(P) + \beta\pi_b(P) + \gamma\pi_c(P), \tag{1}$$

where π_a, π_b, π_c denote the orthogonal projections onto the sidelines a, b, c respectively.

From the point of view of linear algebra, ϕ_X is an affine combination of orthogonal projections onto the sidelines of the triangle ABC. In particular, if X is the centroid of the triangle, then ϕ_X is the average of orthogonal projections onto the sidelines.

From a geometrical point of view $\phi_X(P)$ has the same barycentric coordinates with respect to the pedal triangle $P_aP_bP_c$ of P as X has with respect to ABC, provided P is not on the circumcircle. In the latter case the pedal triangle degenerates, but affine combinations of points P_a, P_b and P_c are still meaningful.

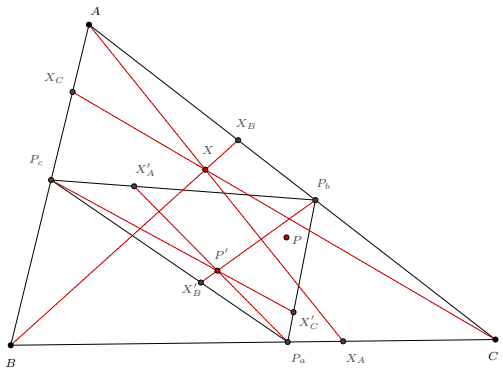

Figure 1. Construction of $\phi_X(P)$ (part I)

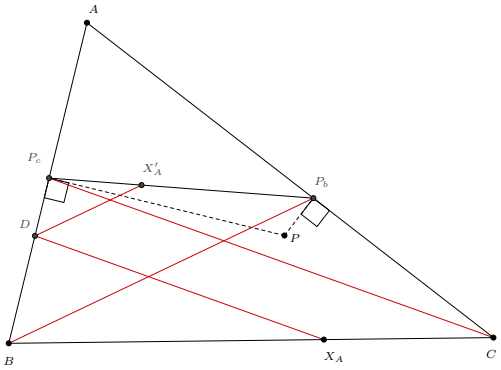

Figure 2. Construction of $\phi_X(P)$ (part II)

Figures 1–2 show the construction of $\phi_X(P)$. Let $X_AX_BX_C$ the Ceva triangle of the point X (Figure 1.) The only problem is to construct points X'_A, X'_B, X'_C such that

$$\frac{BX_A}{X_AC} = \frac{P_aX'_A}{X'_AP_c}, \qquad \frac{CX_B}{X_BA} = \frac{P_cX'_B}{X'_BP_a}, \qquad \frac{AX_C}{X_CB} = \frac{P_aX'_C}{X'_CP_b}.$$

because the Ceva point of the triangle $X'_AX'_BX'_C$ is $P' = \phi_X(P)$. Figure 2 shows the obvious construction of the point X'_A, where $X_AD \| CP_c$ and $DX'_A \| BP_b$.

Let the point P in the plane of the triangle ABC have absolute barycentric coordinates (u, v, w), i.e.

$$P = u \cdot A + v \cdot B + w \cdot C,$$

where $u + v + w = 1$.

It is well-known (see e.g. [5, p. 52]) that

$$\pi_a(P) = \frac{(a^2v + uS_C) \cdot B + (a^2w + uS_B) \cdot C}{a^2}, \tag{2}$$

$$\pi_b(P) = \frac{(b^2w + vS_A) \cdot C + (b^2u + vS_C) \cdot A}{b^2}, \tag{3}$$

$$\pi_c(P) = \frac{(c^2u + wS_B) \cdot A + (c^2v + wS_A) \cdot B}{c^2}. \tag{4}$$

Substituting from (2)-(4) we get

$$\phi_X(P) = \left((\beta+\gamma)u + \beta\frac{S_C}{b^2}v + \gamma\frac{S_B}{c^2}w\right)A + \left(\alpha\frac{S_C}{a^2}u + (\gamma+\alpha)v + \gamma\frac{S_A}{c^2}w\right)B + \left(\alpha\frac{S_B}{a^2}u + \beta\frac{S_A}{b^2}v + (\alpha+\beta)w\right)C. \tag{5}$$

The sum of coefficients of A, B, C in (5) is 1. Thus, (5) gives the absolute barycentric coordinates of $\phi_X(P)$.

Theorem 1. *ϕ_X is an affine map if and only if X is not on the circumcircle.*

Proof. ϕ_X is an affine map if and only if the image of a triangle is a triangle. We give a necessary and sufficient condition that $\{\phi_X(A), \phi_X(B), \phi_X(C)\}$ to be an affine independent point set. From (5) we get

$$\phi_X(A) = (1-\alpha)A + \frac{\alpha S_C}{a^2}B + \frac{\alpha S_B}{a^2}C = (a^2(\beta+\gamma) : \alpha S_C : \alpha S_B)$$
$$\phi_X(B) = \frac{\beta S_C}{b^2}A + (1-\beta)B + \frac{\beta S_A}{b^2}C = (\beta S_C : (\gamma+\alpha)b^2 : \beta S_A)$$
$$\phi_X(C) = \frac{\gamma S_B}{c^2}A + \frac{\gamma S_A}{c^2}B + (1-\gamma)C = (\gamma S_B : \gamma S_A : (\alpha+\beta)c^2).$$

It follows that ϕ_X is affine if and only if

$$\Delta = \begin{vmatrix} (\beta+\gamma)a^2 & \alpha S_C & \alpha S_B \\ \beta S_C & (\gamma+\alpha)b^2 & \beta S_A \\ \gamma S_B & \gamma S_A & (\alpha+\beta)c^2 \end{vmatrix} \neq 0. \tag{6}$$

A direct expansion of the determinant gives

$$\begin{aligned}\Delta &= S^2(\alpha+\beta+\gamma)(\beta\gamma a^2 + \gamma\alpha b^2 + \alpha\beta c^2) \\ &= S^2(\beta\gamma a^2 + \gamma\alpha b^2 + \alpha\beta c^2).\end{aligned}$$

We know that

$$\beta\gamma a^2 + \gamma\alpha b^2 + \alpha\beta c^2 = 0$$

is the equation of the circumcircle [5, p. 63]. (6) is equivalent to X not lying on the circumcircle. □

Theorem 2. *Suppose that X is on the circumcircle. The image space of the map ϕ_X is the Simson line of the antipodal point of X.*

Proof. First we prove that if X is on the circumcircle then the matrix defined in (6) is of rank 2, i.e. the image space is a line. For an indirect proof, suppose that all the 2×2 minors of the matrix in (6) have zero determinant. For example,

$$\begin{aligned}\begin{vmatrix} (1-\alpha)a^2 & \alpha S_C \\ \beta S_C & (1-\beta)b^2 \end{vmatrix} &= (1-\alpha)(1-\beta)a^2b^2 - \alpha\beta a^2b^2\cos^2 C \\ &= a^2b^2(\gamma + \alpha\beta\sin^2 C) = 0.\end{aligned}$$

Analogously, $\alpha + \beta\gamma\sin^2 A = 0$ and $\beta + \gamma\alpha\sin^2 B = 0$. By addition we get

$$\underbrace{(\alpha+\beta+\gamma)}_{1} + \underbrace{(\alpha\beta\sin^2 C + \beta\gamma\sin^2 A + \alpha\gamma\sin^2 B)}_{0} = 0,$$

which is a contradiction.

The center of the circumcircle is

$$O = \left(\frac{a^2S_A}{2S^2}, \frac{b^2S_B}{2S^2}, \frac{c^2S_C}{2S^2}\right). \tag{7}$$

The antipodal point of X is

$$X' = 2O - X = \left(\frac{a^2S_A}{S^2} - \alpha, \frac{b^2S_B}{S^2} - \beta, \frac{c^2S_C}{S^2} - \gamma\right).$$

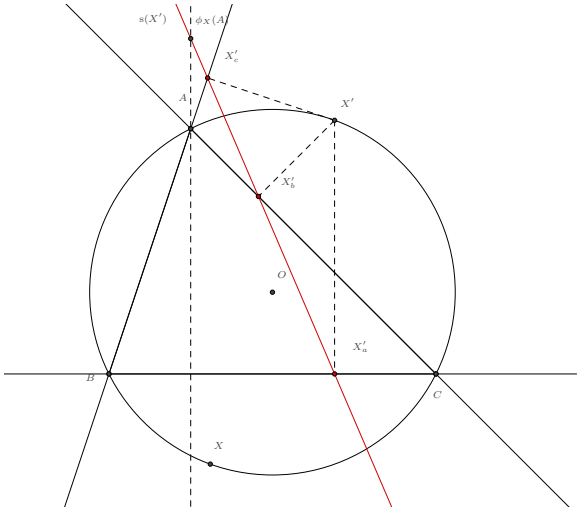

Figure 3. Image space of ϕ_X in the degenerate case

The orthogonal projection of X' onto the lines BC, AC, AB are

$$X'_A = (0 : S_B\alpha + a^2\gamma : S_C\alpha + a^2\beta),$$
$$X'_B = (S_A\beta + b^2\gamma : 0 : S_C\beta + b^2\alpha),$$
$$X'_C = (S_A\gamma + c^2\beta : S_B\gamma + c^2\alpha : 0),$$

respectively (see Figure 3). If $X' \neq C$, then the Simson line of X' passes through X'_A and X'_B. (If $X' = C$, then $X'_A = X'_B = C$ and we use points X'_A and X'_C, but everything goes through analogously.) We check that $\phi_X(A) = (a^2(\beta+\gamma) : \alpha S_C : \alpha S_C)$ lies on the line $X'_AX'_B$. Indeed,

$$\begin{vmatrix} a^2(\beta+\gamma) & \alpha S_C & \alpha S_B \\ 0 & a^2\gamma + \alpha S_B & a^2\beta + \alpha S_C \\ b^2\gamma + \beta S_A & 0 & b^2\alpha + \beta S_C \end{vmatrix}$$

$$= a^2 S_C(\alpha+\beta+\gamma)\underbrace{(\beta\gamma a^2 + \gamma\alpha b^2 + \alpha\beta c^2)}_{0}$$

$$= 0.$$

□

It is easy to give the inverse transformation of ϕ_X, where X is not on the circumcircle. Let $\phi_X(P) = u'A + v'B + w'C$, where $u' + v' + w' = 1$. From (5) we get

$$u = \frac{1}{\Delta}\begin{vmatrix} u' & \beta\frac{S_C}{b^2} & \gamma\frac{S_B}{c^2} \\ v' & \gamma+\alpha & \gamma\frac{S_A}{c^2} \\ w' & \beta\frac{S_A}{b^2} & \alpha+\beta \end{vmatrix},$$

where $\Delta = S^2(\beta\gamma a^2 + \gamma\alpha b^2 + \alpha\beta c^2)$. After expansion:

$$u = \frac{1}{\Delta b^2 c^2}\left((\alpha b^2 c^2 + \beta\gamma S^2)u' + (\underbrace{S^2\gamma - c^2 S_C}_{\lambda_c})\beta v' + (\underbrace{S^2\beta - b^2 S_B}_{\lambda_b})\gamma w'\right)$$

$$= \frac{1}{\Delta b^2 c^2}\left((\alpha b^2 c^2 + \gamma\beta S^2)u' + \lambda_c\beta v' + \lambda_b\gamma w'\right), \tag{8}$$

Analogously, with $\lambda_a = S^2\alpha - a^2 S_A$ we get

$$v = \frac{1}{\Delta c^2 a^2}\left(\lambda_c\alpha u' + (c^2 a^2\beta + S^2\gamma\alpha)v' + \lambda_a\gamma w'\right) \tag{9}$$

$$w = \frac{1}{\Delta a^2 b^2}\left(\lambda_b\alpha u' + \lambda_a\beta v' + (a^2 b^2\gamma + S^2\alpha\beta)\gamma w'\right). \tag{10}$$

In the case where X is the circumcenter, ϕ_X is central similarity with scale factor $1/2$. This fact follows from the next theorem.

Theorem 3. *Let O denote the circumcenter of the triangle ABC. The image of the circumcircle under the map ϕ_O is the nine-point circle of ABC.*

It is possible to determine the equation of the image of the circumcircle using the 'inverse transformation principle', by substituting (8), (9), (10) into the equation of the circumcircle. After a long calculation we get the equation of the nine-point circle. Here we outline a geometric proof.

Proof. Let k be the circumcircle. Since ϕ_O is an affine map, $\phi_O(k)$ is an ellipse. We display below 6 points of the nine-point circle on $\phi_O(k)$. From these it follows that $\phi_O(k)$ is the nine-point circle. First of all, with $(u, v, w) = (1, 0, 0)$ for A, and (α, β, γ) given by (7) for O, we have, by (5),

$$\begin{aligned}
\phi_O(A) &= \left(\frac{b^2 S_B + c^2 S_C}{2S^2}\right)A + \frac{S_A S_C}{2S^2}B + \frac{S_A S_B}{2S^2}C \\
&= \left(\frac{S^2 + S_B S_C}{2S^2}\right)A + \frac{S_A S_C}{2S^2}B + \frac{S_A S_B}{2S^2}C \\
&= \frac{1}{2}A + \frac{1}{2}\left(\frac{S_B S_C}{S^2}A + \frac{S_A S_C}{S^2}B + \frac{S_A S_B}{S^2}C\right) \\
&= \frac{A + H}{2},
\end{aligned}$$

where H is the orthocenter of ABC. Similarly, $\phi_O(B) = \frac{B+H}{2}$ and $\phi_O(C) = \frac{C+H}{2}$. Note that the points $\frac{A+H}{2}$, $\frac{B+H}{2}$, $\frac{C+A}{2}$ are on the nine-point circle.

Let $A' = 2O - A$, $B' = 2O - B$ and $C' = 2O - C$ the antipodal points of A, B and C on the circumcircle. After substitution into (5), making use of (7), we get

$$\phi_O(A') = \frac{B + C}{2}, \qquad \phi_O(B') = \frac{C + A}{2}, \qquad \phi_O(C') = \frac{A + B}{2}.$$

These images are the midpoints of the sides of triangle ABC; they lie on the nine-point circle. □

3. A fixed point theorem for the weighted pedal map

Theorem 4. *Suppose X is not on the circumcircle. The only fixed point of the weighted pedal map ϕ_X is the isogonal conjugate of X: $\phi_X(X^*) = X^*$.*

Proof. We prove that the fixed point has barycentric coordinates

$$(a^2\beta\gamma : b^2\gamma\alpha : c^2\alpha\beta)$$

with respect to the triangle ABC.

P is a fixed point of the map (1) if and only if

$$\begin{aligned}(\gamma+\beta)u + \beta\frac{S_C}{b^2}v + \gamma\frac{S_B}{c^2}w &= u\\ \alpha\frac{S_C}{a^2}u + (\alpha+\gamma)v + \gamma\frac{S_A}{c^2}w &= v\\ \alpha\frac{S_B}{a^2}u + \beta\frac{S_A}{b^2}v + (\alpha+\beta)w &= w\end{aligned}$$

i.e.

$$\begin{aligned}-\alpha u + \beta\frac{S_C}{b^2}v + \gamma\frac{S_B}{c^2}w &= 0\\ \alpha\frac{S_C}{a^2}u - \beta v + \gamma\frac{S_A}{c^2}w &= 0\\ \gamma\frac{S_B}{a^2}u + \beta\frac{S_A}{b^2}v - \gamma w &= 0.\end{aligned} \tag{11}$$

The matrix of this homogeneous system of linear equations has rank 2, because it has zero determinant, but

$$\begin{vmatrix} -\alpha & \beta\frac{S_C}{b^2} \\ \alpha\frac{S_C}{a^2} & -\beta \end{vmatrix} = \frac{\alpha\beta S^2}{a^2b^2} \neq 0.$$

It means that solutions are generated with one nonzero vector. With direct substitution it is easy to see that $(a^2\beta\gamma, b^2\alpha\gamma, c^2\alpha\beta)$ solves (11). □

Remark. A list of isogonal conjugate pairs is given in [4]; see also [1]. If X is the centroid of the triangle, than ϕ_X is the average of the orthogonal projections π_a, π_b and π_c. In this case X^* is the symmedian point, and geometric analysis of Theorem 4 gives a well-known property of the symmedian point, namely, *the symmedian point is the centroid of its pedal triangle, and it is the only point with this property* (see, for example, [2]).

We conclude this note with an application of Theorem 4.

Theorem 5. *If the orthocenter H does not lie on the circumcircle, then the image of the circumcircle k by the weighted pedal map ϕ_H is an inscribed ellipse.*

Proof. Note, the isogonal conjugate of the orthocenter is the circumcenter O, which is the only fixed point of ϕ_H. Thus $\phi_X(H)$ is an ellipse with center O.

Let F denote the intersection point of tangent lines to the circumcircle at A and B (see Figure 4.) F has the absolute barycentric coordinates $\left(\frac{a^2}{2S_C}, \frac{b^2}{2S_C}, -\frac{c^2}{2S_C}\right)$.

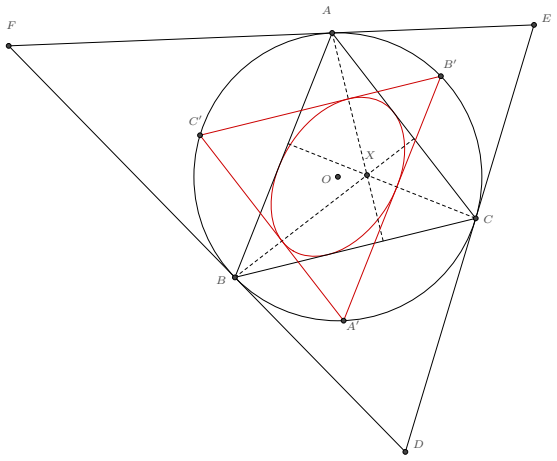

Figure 4. An inscribed ellipse

After calculation we get

$$\phi_X(F) = C' = \left(\frac{a^2 S_A}{S^2}, \frac{b^2 S_B}{S^2}, -\frac{S_A S_B}{S^2} \right).$$

This is the antipode of C on the circumcircle. Repeating this construction for A and B, we get points A', B'. Since k is the inscribed circle of the tangential triangle DEF with center O, $\phi_X(k)$ is an inscribed ellipse of the triangle $A'B'C'$ with center $\phi_X(O) = O$. After point reflection in point O, $\phi_X(k)$ remains fixed and this fact gives the statement.

□

References

[1] C. Kimberling, *Encyclopedia of Triangle Centers*, `http://faculty.evansville.edu/ck6/encyclopedia/ETC.html`.
[2] C. Pohoata, A short proof of Lemoine's theorem, *Forum Geom.*, 8 (2008) 97–98.
[3] A. A. Ungar, *Barycentric Calculus in Euclidean and Hyperbolic Geometry, A comparative introduction*, World Scientific Publishing Co. Pte. Ltd., Hackensack, NJ, 2010.
[4] E. W. Weisstein, Isogonal conjugate, `http://mathworld.wolfram.com/IsogonalConjugate.html`.
[5] P. Yiu, *Introduction to the geometry of the triangle*, 2002; `http://math.fau.edu/Yiu/GeometryNotes020402.pdf`.

S. Nagydobai Kiss: 'Constatin Brâncuşi' Technology Lyceum, Satu Mare, Romania
E-mail address: `d.sandor.kiss@gmail.com`

Zoltán Kovács: Institute of Mathematics and Computer Science, University of Nyíregyháza, Nyíregyháza, Sóstói ú. 31/b, Hungary
E-mail address: `kovacs.zoltan@nye.hu`

Forum Geometricorum
Volume 16 (2016) 179–184.

FORUM GEOM
ISSN 1534-1178

A Recursive Formula for the Circumradius of the n-Simplex

Kenta Kobayashi

Abstract. We present a recursive formula which gives the circumradius of the n-simplex in terms of the circumradius of its facets. Our formula shows that the circumradius of the n-simplex is closely related to the distances from each vertex to the circumcenter of the opposite facet. In particular, our formula shows that the circumradius of the tetrahedron can be expressed by the areas of the pedal triangles of each facet. We could only prove the formula for $n \leq 5$, but numerical results strongly suggest that our formula holds true for any n.

1. Recursive Formula

Consider a general n-simplex K in the n-dimensional Euclidean space $\mathbb{E}^n$. Let $P_1, P_2, \cdots, P_{n+1}$ be the vertices of K, and let K_i be the facet which opposes the vertex P_i. Moreover, let V be the volume and R the circumradius of K; and let V_i be the volume, R_i the circumradius and C_i the circumcenter of K_i. Then we proved the following theorem:

Theorem 1. *For $2 \leq n \leq 5$, the following recursive formula holds true:*

$$R^2 = \frac{\dfrac{1}{4n^2V^2}\displaystyle\sum_{i=1}^{n+1}(R_i^2 - L_i^2)^2V_i^4 + \frac{1}{2}\sum_{i=1}^{n+1}(3R_i^2 - L_i^2)V_i^2 + n^2V^2}{\displaystyle\sum_{i=1}^{n+1}V_i^2} \tag{1}$$

where L_i denotes the length of P_iC_i (Figure 1 shows the situation when $n = 3$).

This formula shows that the circumradius of K is closely related to the lengths R_i and L_i. For $n = 2$, this formula is easily shown by parallelogram law, Heron's formula and the law of sines. We proved this formula for $2 \leq n \leq 5$ using the computer algebra system Mathematica, the details of which are explained in Section 3. Although the general proof has not been obtained yet, we checked this formula for 100 random simplices for each n up to 50 on the Mathematica. We carried out verification using rational number arithmetic for random simplices whose vertices are random lattice points and the formula was satisfied each time.

Publication Date: April 29, 2016. Communicating Editor: Paul Yiu.

The author would like to thank Prof. Takuya Tsuchiya for the useful discussions during my visit to Ehime University without which this work would not have been conceived.

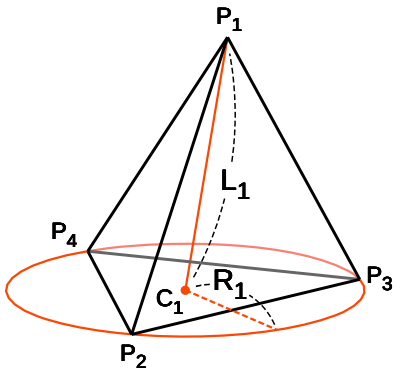

Figure 1. Distance from a vertex to the circumcenter of the opposite facet

2. Three-dimensional Case

In this section we consider the three-dimensional case, that is, when K is a tetrahedron. We can derive the following result from Theorem 1:

Theorem 2. *The circumradius of the tetrahedron K is expressed as*

$$R^2 = \frac{\displaystyle\sum_{i=1}^{4} \left(1 + \frac{4W_i^2 R_i^2}{9V^2}\right) R_i^2 S_i^2}{S_1^2 + S_2^2 + S_3^2 + S_4^2}$$

where S_i denotes the area of K_i and W_i denotes the area of the pedal triangle defined by the foot of the perpendicular from P_i to the three sides of K_i (Figure 2). *That is, R^2 can be considered as the weighted mean of*

$$\left(1 + \frac{4W_i^2 R_i^2}{9V^2}\right) R_i^2$$

with respect to S_i^2.

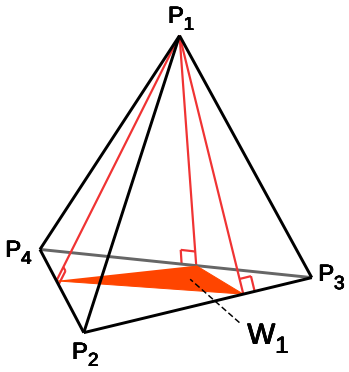

Figure 2. Pedal triangle defined by the foot of the perpendicular from a vertex

Proof. From Theorem 1, the circumradius of the tetrahedron K is expressed as

$$R^2 = \frac{\dfrac{1}{36V^2}\displaystyle\sum_{i=1}^{4}(R_i^2 - L_i^2)^2 S_i^4 + \frac{1}{2}\sum_{i=1}^{4}(3R_i^2 - L_i^2)S_i^2 + 9V^2}{S_1^2 + S_2^2 + S_3^2 + S_4^2}.$$

Now let F_i be the foot of the perpendicular from P_i to K_i, and let H_i and D_i be the lengths of P_iF_i and F_iC_i, respectively. Then, using the relations

$$V = \frac{S_i H_i}{3}, \qquad L_i^2 = H_i^2 + D_i^2,$$

our formula can be rewritten in the following form:

$$R^2 = \frac{\displaystyle\sum_{i=1}^{4}\left(R_i^2 + \frac{(R_i^2 - D_i^2)^2}{4H_i^2}\right)S_i^2}{S_1^2 + S_2^2 + S_3^2 + S_4^2}.$$

Then, using the relation $4W_iR_i^2 = S_i|R_i^2 - D_i^2|$ ([1, pp.139-141]), we have the expression to be proved. □

It is unclear whether there is a higher-dimensional analogue of this reformulation.

3. Proof Using Computer Algebra System

In this section, we outline how to prove Theorem 1 by using a computer algebra system. For this purpose we have to calculate the volume, the circumradius and the circumcenter of the given simplex.

Let K be the given n-simplex whose vertices are represent by position vectors $\boldsymbol{p}_1, \boldsymbol{p}_2, \cdots, \boldsymbol{p}_{n+1}$. Then the volume V and the circumradius R of K are obtained by the Cayley-Menger Determinant as follows [2][3, pp. 124]:

$$V^2 = \frac{(-1)^{n+1}}{2^n(n!)^2}\det(\widehat{\boldsymbol{A}}), \qquad R^2 = -\frac{\det(\boldsymbol{A})}{2\det(\widehat{\boldsymbol{A}})}, \tag{2}$$

$$\boldsymbol{A} = \begin{pmatrix} 0 & \alpha_{12} & \alpha_{13} & \cdots & \alpha_{1\,n+1} \\ \alpha_{21} & 0 & \alpha_{23} & \cdots & \alpha_{2\,n+1} \\ \alpha_{31} & \alpha_{32} & 0 & \cdots & \alpha_{3\,n+1} \\ \vdots & \vdots & \vdots & \ddots & \vdots \\ \alpha_{n+1\,1} & \alpha_{n+1\,2} & \alpha_{n+1\,3} & \cdots & 0 \end{pmatrix}, \quad \widehat{\boldsymbol{A}} = \begin{pmatrix} 0 & 1 & \cdots & 1 \\ 1 & & & \\ \vdots & & \boldsymbol{A} & \\ 1 & & & \end{pmatrix},$$

$$\alpha_{ij} = \|\boldsymbol{p}_i - \boldsymbol{p}_j\|^2,$$

where $\|\cdot\|$ denotes the Euclidean norm. Furthermore, the position vector of the circumcenter of K is obtained as

$$\boldsymbol{c} = s_1\boldsymbol{p}_1 + s_2\boldsymbol{p}_2 + \cdots + s_{n+1}\boldsymbol{p}_{n+1} \tag{3}$$

where $s_1, s_2, \cdots, s_{n+1}$ are the solutions of the following system of linear equations:

$$\begin{pmatrix} \beta_{11} & \beta_{12} & \cdots & \beta_{1n} & 0 \\ \beta_{21} & \beta_{22} & \cdots & \beta_{2n} & 0 \\ \vdots & \vdots & \ddots & \vdots & \vdots \\ \beta_{n1} & \beta_{n2} & \cdots & \beta_{nn} & 0 \\ 1 & 1 & \cdots & 1 & 1 \end{pmatrix} \begin{pmatrix} s_1 \\ s_2 \\ \vdots \\ s_n \\ s_{n+1} \end{pmatrix} = \begin{pmatrix} \beta_{11}/2 \\ \beta_{22}/2 \\ \vdots \\ \beta_{nn}/2 \\ 1 \end{pmatrix},$$

$$\beta_{ij} = (\boldsymbol{p}_i - \boldsymbol{p}_{n+1}) \cdot (\boldsymbol{p}_j - \boldsymbol{p}_{n+1}),$$

where $\cdot$ denotes the Euclidean dot product.

To prove Theorem 1, we first let

$$\boldsymbol{p}_1 = \begin{pmatrix} 0 \\ 0 \\ 0 \\ \vdots \\ 0 \end{pmatrix}, \boldsymbol{p}_2 = \begin{pmatrix} x_{12} \\ 0 \\ 0 \\ \vdots \\ 0 \end{pmatrix}, \boldsymbol{p}_3 = \begin{pmatrix} x_{13} \\ x_{23} \\ 0 \\ \vdots \\ 0 \end{pmatrix}, \cdots, \boldsymbol{p}_{n+1} = \begin{pmatrix} x_{1\,n+1} \\ x_{2\,n+1} \\ x_{3\,n+1} \\ \vdots \\ x_{n\,n+1} \end{pmatrix},$$

and represent R^2, V^2, R_i^2, V_i^2 and L_i^2 in terms of x_{12} to $x_{n\,n+1}$ by (2) and (3). We then confirm that both sides of (1) are equal. The Mathematica script for proving our formula is given in Section 4. The script was tested using Wolfram Mathematica 9.0 on a PC with Microsoft Windows 8.1 operating system, Intel Core i5 processor and 8GB memory. We could confirm that our formula holds for $2 \leq n \leq 5$. However, the computational cost of using a computer algebra system grows very rapidly as n increases; we therefore could not succeed in proving the theorem for $n \geq 6$.

4. Mathematica script

For the reproducibility of the proof, we provides Mathematica script for proving our formula by the procedures explained in Section 3.

```
NN[x_] = x.x;

n = 5;  (* Dimension of the space *)

(* Set the coordinates of the vertices *)
P = Table[If[i<j,x[i,j],0],{i,n},{j,n+1}];

(* Obtain the volume and the circumradius of K *)
(* by the Cayley-Menger Determinant            *)
A = Factor[Table[NN[P[[All,i]]-P[[All,j]]],{i,n+1},{j,n+1}]];
B = PadLeft[A,{n+2,n+2},1];
B[[1,1]] = 0;
V = Factor[(-1)^(n+1)*Det[B]/2^n/(n!)^2];
R = Factor[-Det[A]/Det[B]/2];

(* Obtain the volume and the circumradius of        *)
```

```
(* the facets of K by the Cayley-Menger Determinant *)
v = ConstantArray[0,n+1];
r = ConstantArray[0,n+1];
For[k=1,k<=n+1,k++,
    a = Drop[A,{k},{k}];
    b = Drop[B,{k+1},{k+1}];
    v[[k]] = Factor[(-1)^n*Det[b]/2^(n-1)/((n-1)!)^2];
    r[[k]] = Factor[-Det[a]/Det[b]/2];
]

(* Obtain the circumcenter of the facets of K *)
e = ConstantArray[0,n+1];
For[k=1,k<=n+1,k++,
    p = Drop[P,{},{k}];
    a = Factor[Table[(p[[All,i]]-p[[All,n]])
        .(p[[All,j]]-p[[All,n]]),{i,n-1},{j,n-1}]];
    a = PadRight[a,{n-1,n},0];
    a = PadRight[a,{n,n},1];
    b = Table[a[[i,i]]/2,{i,n}];
    b[[n]] = 1;
    s = LinearSolve[a,b];
    e[[k]] = Factor[NN[p.s-P[[All,k]]]];
]

(* Obtain the circumradius of K by our formula *)
(* and compare it with R                       *)
F = n^2*V;
vs = 0;
For[k=1,k<=n+1,k++,
    F = F+((r[[k]]-e[[k]])^2*v[[k]]/V/4/n^2
        +(3*r[[k]]-e[[k]])/2)*v[[k]];
    vs = vs+v[[k]];
]
F = F/vs;

If[Factor[F-R]==0,
    Print["Proved!"], Print["Failed"]
];
```

5. Conclusion

We found a recursive formula which gives the circumradius of the n-simplex in terms of the circumradius of its facets. We could only prove the formula for $n \leq 5$ by the aid of computer algebra system Mathematica, but numerical results strongly suggest that our formula holds true for any n. We therefore invite anyone interested in this problem to try to prove general cases.

References

[1] R. A. Johnson, *Modern Geometry: An Elementary Treatise on the Geometry of the Triangle and the Circle*, Houghton Mifflin, Boston, MA, 1929.

[2] H. S. M. Coxeter, The Circumradius of the General Simplex, *Math. Gazette*, 15 (1930) 229–231.
[3] D. M. Y. Sommerville, *An Introduction to the Geometry of n Dimensions*, Dover Publications, New York, 1958.

Kenta Kobayashi: Graduate School of Commerce and Management, Hitotsubashi University, Naka 2-1, Kunitachi-City, Tokyo, 186-8601, Japan
E-mail address: kenta.k@r.hit-u.ac.jp

Forum Geometricorum
Volume 16 (2016) 185–186.

FORUM GEOM
ISSN 1534-1178

A Proof of the Butterfly Theorem Using Ceva's Theorem

Cesare Donolato

Abstract. A proof is given of the butterfly theorem by using a simple auxiliary construction and Ceva's theorem.

The two well-known theorems considered here are illustrated, for instance, in [2], each with a selected proof; see [2, p.45, Theorem 2.81] for the butterfly theorem and [2, p.5, Theorem 1.22] for Ceva's theorem. In [1] about twenty different proofs of the butterfly theorem are described, with comments on their features, related references and historical information.

In this note the butterfly theorem is proved by preliminarily adding some auxiliary lines to its usual illustrative diagram. Then Ceva's theorem is used as a lemma within this extended graph, and the butterfly theorem itself follows from elementary geometry.

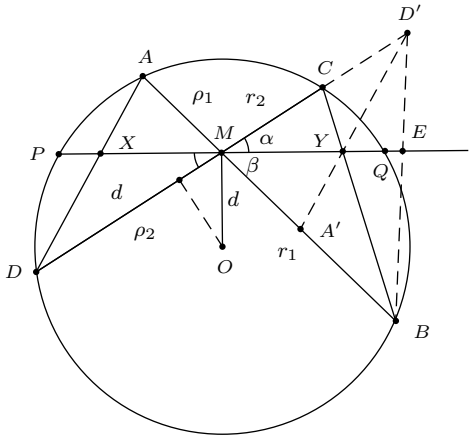

Figure 1

Theorem 1 (The Butterfly Theorem)**.** *Through the midpoint M of a chord PQ of a circle, two other chords AB and CD are drawn. Chords AD and BC intersect PQ at points X and Y, respectively. Then M is also the midpoint of XY.*

We introduce the points A' and D' that are the symmetric of A and D about M, respectively. Hence, $MA' = MA$ and $MD' = MD$. Next we connect the point

Publication Date: May 3, 2016. Communicating Editor: Paul Yiu.

D' to A' and B, and call E the intersection of $D'B$ with the line through P and Q (Figure 1). Thus we have constructed triangle MBD' with cevians $D'A'$, ME, and BC. We show that the segment $D'A'$ cuts the chord PQ at the same point Y as BC, i.e., that the three cevians are concurrent at Y. This property will be proved by applying Ceva's theorem to triangle MBD'.

Lemma 2. *In triangle MBD', the cevians $D'A'$, ME, and BC are concurrent at Y.*

Proof. We set $MA' = MA = \rho_1$, $MB = r_1$, $MC = r_2$, and $MD' = MD = \rho_2$. We observe that $\frac{BE}{ED'}$ is equal to the ratio $\frac{r_1 \sin\beta}{\rho_2 \sin\alpha}$ of the respective distances of B and D' from the line PQ. Moreover, $A'B = r_1 - \rho_1$, and $D'C = \rho_2 - r_2$ (see Figure 1). Now,

$$\frac{BE}{ED'} \cdot \frac{D'C}{CM} \cdot \frac{MA'}{A'B} = \frac{r_1 \sin\beta}{\rho_2 \sin\alpha} \cdot \frac{\rho_2 - r_2}{r_2} \cdot \frac{\rho_1}{r_1 - \rho_1} = \frac{(\rho_2 - r_2)\sin\beta}{(r_1 - \rho_1)\sin\alpha} \qquad (1)$$

since $\rho_1 r_1 = \rho_2 r_2$ by the intersecting chords theorem (see, e.g., [2, p.28, Theorem 2.11]).

The differences appearing in (1) can be written in terms of the distance $d = OM$ of the circle center O to the chord PQ, and the angles α and β. Figure 1 shows that the projection of OM onto the chord CD has length $d\sin\alpha$, so that we get $\rho_2 = \frac{CD}{2} + d\sin\alpha$, and $r_2 = \frac{CD}{2} - d\sin\alpha$. Hence, $\rho_2 - r_2 = 2d\sin\alpha$. Similarly, we find $r_1 - \rho_1 = 2d\sin\beta$. Substituting these expressions into (1) we obtain

$$\frac{BE}{ED'} \cdot \frac{D'C}{CM} \cdot \frac{MA'}{A'B} = 1.$$

By Ceva's theorem, the cevians $D'A'$, ME, and BC are concurrent. The common point is clearly Y. □

Proof of the Butterfly Theorem. We observe that triangle $MA'D'$ is congruent by construction to triangle MAD, because two sides of the first (MA', MD') are equal to two sides of the second (MA, MD), and the included angles are equal. It follows that $\angle MD'Y = \angle MDX$. Consequently, triangles $MD'Y$ and MDX are also congruent, since they have equal two pairs of angles ($\angle MD'Y = \angle MDX$, and $\angle YMD' = \angle XMD$, vertical angles), as well as the included sides ($MD' = MD$). This congruence implies that the corresponding sides MY and MX are equal. Therefore, M is the midpoint of XY and the butterfly theorem is proved. □

References

[1] A. Bogomolny, The Butterfly Theorem, `http://www.cut-the-knot.org/pythagoras/Butterfly.shtml`.

[2] H. S. M. Coxeter and S. L. Greitzer, *Geometry Revisited*, Mathematical Association of America, Washington, D.C., 1967.

Cesare Donolato: Via dello Stadio 1A, 36100 Vicenza, Italy
E-mail address: `cesare.donolato@alice.it`

Forum Geometricorum
Volume 16 (2016) 187–191.

FORUM GEOM
ISSN 1534-1178

Some Loci in the Animation of a Sangaku Diagram

Junghyun Lee, Minyoung Hwang, and Cheolwon Bae

Abstract. In a symmetric partition of a regular n-gon into n congruent subtriangles and a regular n-gon in the center, we determine the loci of the incenter and points of tangency of the incircle a subtriangle.

A famous Sangaku problem ([1, Problem 2.1.7], [2]) asks to partition an equilateral triangle into four subtriangles with congruent incircle (see Figure 1). Ito and Wimmer [3] considered the same problem for general regular polygons (see Figure 2 for the case of a regular pentagon). In this note, we consider a dynamic situation by letting the congruent subtriangles by the sides of the regular polygon vary, and examine the loci of various points in the configuration.

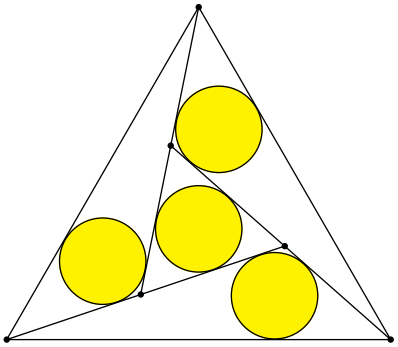

Figure 1

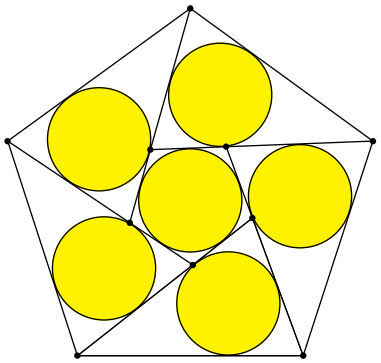

Figure 2

Given a regular n-gon $\mathcal{P} := A_1A_2\cdots A_n$, $k = 1, 2, \ldots, n$, with center O, pass a line $\ell_k(\theta)$ through the vertex A_k such that the directed angle $(A_kA_{k+1}, \ell_k(\theta)) = \theta \in \left(0, \pi - \frac{2\pi}{n}\right)$. Here indices are taken modulo n so that $A_{n+1} = A_1$ etc. Let $A'_k(\theta)$ be the intersection of $\ell_k(\theta)$ and $\ell_{k+1}(\theta)$ (see Figure 3). When there is no danger of confusion, we shall simply write A'_k for $A'_k(\theta)$. Then the regular n-gon $\mathcal{P}$ is partitioned into
(i) n congruent triangles $A'_kA_kA_{k+1}$ for $k = 1, 2, \ldots, n$, and
(ii) a regular n-gon $\mathcal{P}' = A'_1A'_2\cdots A'_n$ at the center.

Publication Date: May 18, 2016. Communicating Editor: Paul Yiu.
The authors thank their teacher Mr. Cha Seungkyun for his guidance and help.

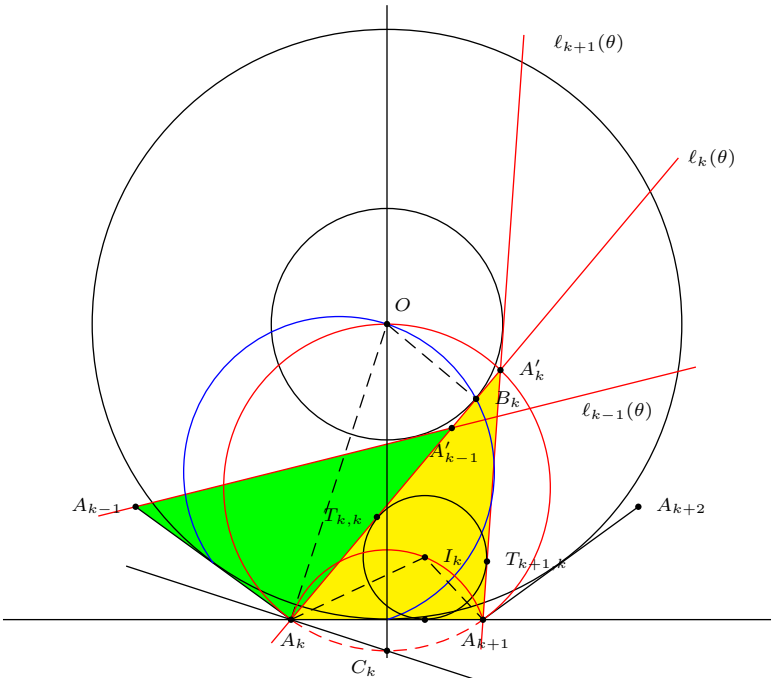

Figure 3

It is clear that the center of the regular n-gon $A'_1A'_2\cdots A'_n$ is the fixed point O. On the other hand, the locus of $A'_k(\theta)$ is the part of the circle OA_kA_{k+1} in the interior of $\mathcal{P}$. This is because

$$\angle A_kA'_kA_{k+1} = \left(\frac{2\pi}{n}+\theta\right) - \theta = \frac{2\pi}{n} = \angle A_kOA_{k+1},$$

from which A_k, A'_k, O, and A_{k+1} are concyclic.

Suppose the incircle of $\mathcal{P}'$ touches the sides $A'_{k-1}A'_k$ at B_k, the midpoint of A'_{k-1} and A'_k on ℓ_k. Since OB_k is perpendicular to $A'_{k-1}A'_k$, it is perpendicular the line $\ell_k(\theta)$ through A_k. Therefore, OB_kA_k is a right angle, and B_k lies on the part of the circle with diameter OA_k inside the regular polygon $\mathcal{P}$. If M_{k-1} and M_k are the midpoints of $A_{k-1}A_k$ and A_kA_{k+1}, then this is the arc of the circle $M_{k-1}OM_k$ in the interior of $\mathcal{P}$.

Now we consider the incircle of triangle $\mathbf{T}_k = A'_kA_kA_{k+1}$, with incenter I_k, and tangent to ℓ_k, ℓ_{k+1} at the points $T_{k,k}$, $T_{k+1,k}$ respectively.

Note that

$$\angle A_kI_kA_{k+1} = \frac{\theta}{2} + \frac{2\pi}{n} + \frac{1}{2}\left(\pi - \frac{2\pi}{n} - \theta\right) = \frac{\pi}{2} - \frac{\pi}{n}$$

is independent of θ. This means that the locus of I_k is the part of a circle through A_k and A_{k+1} in the interior of $\mathcal{P}$. Its center C_k is the intersection of the perpendicular bisector of A_kA_{k+1} and the *external* bisector of angle $A_{k-1}A_kA_{k+1}$.

We summarize these simple results in the following proposition.

Proposition 1. *Let $\mathcal{P} := A_1A_2\cdots A_n$ be a regular n-gon with center O. For $k = 1, 2, \ldots, n$, let $\ell_k(\theta)$ be the line through the vertex A_k such that the directed angle $(A_kA_{k+1}, \ell_k(\theta)) = \theta$ (with indices taken modulo n). As θ varies in $\left(0, \pi - \frac{2\pi}{n}\right)$, the loci of*
(a) *the intersection $A'_k(\theta)$ of $\ell_k(\theta)$ and $\ell_{k+1}(\theta)$ is the part of the circle OA_kA_{k+1} in the interior of $\mathcal{P}$,*
(b) *the point of tangency B_k of the incircle of the regular n-gon $A'_1A'_2\cdots A'_n$ with the line $\ell_k(\theta)$ is the part of the circle $OM_{k-1}M_k$ in the interior of $\mathcal{P}$, M_k being the midpoint A_kA_{k+1},*
(c) *the incenter I_k of triangle $A'_kA_kA_{k+1}$ is the arc of the circle, center C_k, passing through A_{k-1}, C_k being the intersection of the perpendicular bisector of A_kA_{k+1} and the external bisector of angle $A_{k-1}A_kA_{k+1}$.*

We compute some of the lengths in this configuration. In Figure 3, let a be the length of a side of the regular n-gon $\mathcal{P}$. Suppose in triangle $A'_kA_kA_{k+1}$, $A'_kA_{k+1} = b$ and $A_kA'_k = c$. By the law of sines,

$$\begin{aligned} b &= \frac{a}{\sin\frac{2\pi}{n}}\sin\theta, \\ c &= \frac{a}{\sin\frac{2\pi}{n}}\sin\left(\frac{2\pi}{n}+\theta\right). \end{aligned}$$

Theorem 2. *For $k = 1, 2, \ldots, n$, let $T_{k,k}$ and $T_{k+1,k}$ be the points of tangency of the incircle of triangle $A'_kA_kA_{k+1}$ with the lines $\ell_k(\theta)$ and $\ell_{k+1}(\theta)$ respectively. θ varies in $\left(0, \pi - \frac{2\pi}{n}\right)$, the loci of $T_{k,k}$ and $T_{k+1,k}$ are the parts of limaçon inside the regular n-gon $\mathcal{P}$, symmetric with respect to the perpendicular bisector of A_kA_{k+1}.*

Proof. The point of tangency $T_{k,k}$ is the point on $\ell_k(\theta)$ uniquely determined by the length of $A_kT_{k,k}$. Now, in triangle $A'_kA_kA_{k+1}$,

$$\begin{aligned} A_kT_{k,k} &= \frac{1}{2}(a+c-b) \\ &= \frac{a}{2} + \frac{a}{2\sin\frac{2\pi}{n}}\left(\sin\left(\frac{2\pi}{n}+\theta\right) - \sin\theta\right) \\ &= \frac{a}{2} + \frac{a}{2\sin\frac{2\pi}{n}}\cdot 2\cos\left(\frac{\pi}{n}+\theta\right)\sin\frac{\pi}{n} \\ &= \frac{a}{2} + \frac{a}{2\cos\frac{\pi}{n}}\cdot\cos\left(\frac{\pi}{n}+\theta\right). \end{aligned}$$

Let C_k be the intersection of the perpendicular bisector of A_kA_{k+1} and the external angle of $A_{k-1}A_kA_{k+1}$. Note that $A_kC_k = \frac{a}{2\cos\frac{\pi}{n}}$. In a polar coordinate system with pole at A_k and polar axis the half line A_kA_{k+1}, the equation

$$\rho = \frac{a}{2\cos\frac{\pi}{n}}\cos\left(\frac{\pi}{n}+\theta\right)$$

represents the circle with A_kC_k as diameter. Therefore,

$$\rho = \frac{a}{2} + \frac{a}{2\cos\frac{\pi}{n}}\cos\left(\frac{\pi}{n}+\theta\right)$$

is a limaçon: If the circle with diameter A_kC_k intersects $\ell_k(\theta)$ at D_k, then $T_{k,k}$ is the point obtained by translating D_k by $\frac{a}{2}$ (along A_kD_k); see Figure 4 for the case of a regular pentagon $A_1A_2A_3A_4A_5$ with $k = 1$.

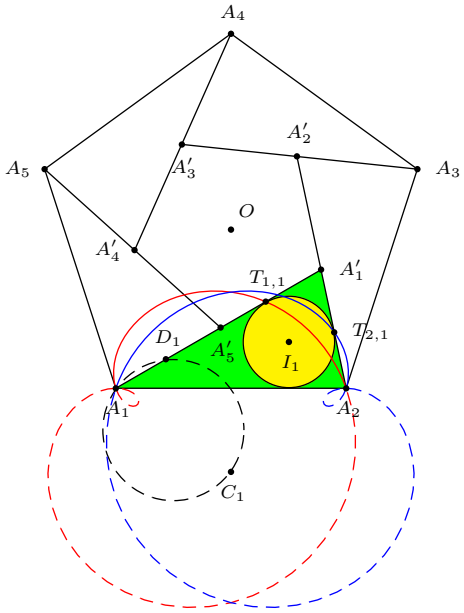

Figure 4

The locus of $T_{k+1,k}$ is clearly the reflection of the locus of $T_{k,k}$ in the perpendicular bisector of A_kA_{k+1}. It is determined by

$$A_{k+1}T_{k+1,k} = \frac{1}{2}(a - c + b) = \frac{a}{2} - \frac{a}{2\cos\frac{\pi}{n}} \cdot \cos\left(\frac{\pi}{n} + \theta\right).$$

This is the limaçon with respect to the circle diameter $A_{k+1}C_k$ and length $\frac{a}{2}$. □

References

[1] H. Fukagawa and D. Pedoe, *Japanese Temple Geometry Problems*, Charles Babbage Research Centre, Winnipeg, 1989.
[2] H. Fukagawa and T. Rothman, *Sacred Mathematics*, Princeton University Press, 2008.
[3] N. Ito and H. Wimmer, H, A Sangaku-type problem with regular polygons, triangles, and congruent incircles, *Forum Geom.*, 13 (2013) 185–190.

Junghyun Lee: Changwon Science High School, 159 beon-gil 30, Pyeongsan-ro, Uichang-gu, Changwon-si, Gyeongsangnam-do, Korea
E-mail address: science0229@gmail.com

Minyoung Hwang: Changwon Science High School, 159 beon-gil 30, Pyeongsan-ro, Uichang-gu, Changwon-si, Gyeongsangnam-do, Korea
E-mail address: myhwang99@naver.com

Cheolwon Bae: Changwon Science High School, 159 beon-gil 30, Pyeongsan-ro, Uichang-gu, Changwon-si, Gyeongsangnam-do, Korea
E-mail address: cw2184@naver.com

Forum Geometricorum
Volume 16 (2016) 193–205.

FORUM GEOM
ISSN 1534-1178

Septic Equations are Solvable by 2-fold Origami

Joachim König and Dmitri Nedrenco

Abstract. In this paper we prove that a generic polynomial equation of degree 7 over the rationals is solvable by 2-fold origami. In particular we show how to septisect an arbitrary angle and to take arbitrary seventh roots. This extends the work of Alperin, Lang (2006) and Nishimura (2015) on 2-fold origami and significantly improves previously known results on the solvability of septic equations by multi-fold origami. Furthermore we give exact crease patterns for folding polynomials with Galois groups A_7 resp. $PSL_3\mathbb{F}_2$.

1. Motivation

Almost every paper about geometry can start with "Ancient Greeks already knew how to…". Ancient Greeks knew how to trisect an angle, for example by neusis [11, Theorem 9.3] or with a conchoid of Nicomedes [3]. But they could not trisect an angle with a ruler and compasses. After Wantzel we know that it is indeed impossible [13]. In the 1930s Margherita Beloch found out that one can trisect an angle by paper folding [2], [6]. Her ideas were almost forgotten and a new wave of origamists was needed to describe the power of paper folding. By the end of the second millennium it was proven that paper folding can solve arbitrary (rational) quartic polynomials, so every 2-3-tower over $\mathbb{Q}$ is constructible by means of paper folding.

By *paper folding* we mean the so called 1-fold origami; only one foldline is allowed in each folding step, cf. [1]. Generalizing this, one defines n-fold origami by allowing n fold lines (simultaneously) arising in each folding step. In 2006 Alperin and Lang developed axioms for 2-fold origami and calculated ideals describing each of the axioms: two simultaneous fold lines can be produced in every folding step (think, for instance, of folding a letter). They proved (cf. [1, Theorem 1]), using the method of Lill [6], [10], that

Theorem 1. *Every polynomial of degree n can be solved by $(n-2)$-fold origami.*

So in particular you need at most 3-fold origami to solve quintics. Alperin and Lang asked whether you can do better. Nishimura showed that every quintic is solvable by means of one 2-fold axiom (AL4a6ab in the Alperin and Lang notation). He did it by interpreting this axiom geometrically (and some quite involved calculations). It is a remarkable improvement of Theorem 1. We try to take this

Publication Date: May 18, 2016. Communicating Editor: Paul Yiu.

game a little bit further and investigate whether one can solve every septic equation with one or more 2-fold axioms. We see this work as a continuation of the papers [1] and [12].

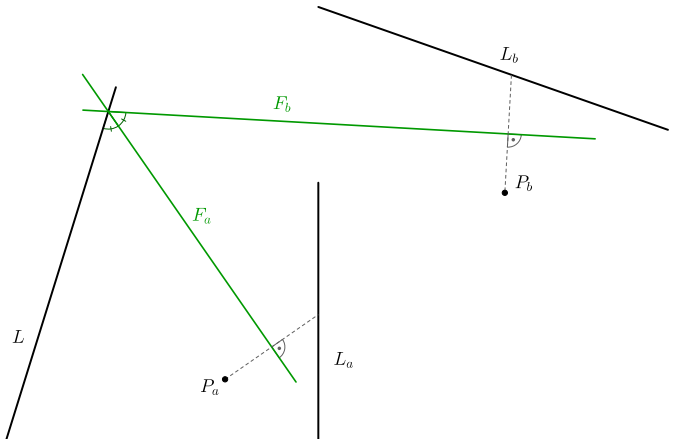

Figure 1. Axiom AL4a6ab used by Nishimura. $L^{F_a} = F_b,\ P_a^{F_a} \in L_a,\ P_b^{F_b} \in L_b$. Notation of the points and lines as in [12].

2. Setting

We use the notation of a *point*, *line*, *folded point* and *folded line* as Alperin and Lang do, cf. [1, pp. 4–5] for exact definitions and formulas.

The list of 2-fold axioms given by Alperin and Lang is impressive and too long in order to try every axiom. So we did some calculations in order to filter out the axioms which yield irreducible polynomials of degree 7 for the slope of one of the fold lines: These are[1]: AL3a5b6b7a, AL3a5b6b7b, AL3a5b7ab and AL6ab8. From the geometrical point of view and after consulting [1, §7.1.1] we decided that AL6ab8 is suitable. Let us describe it.

Assume that we have already constructed four points and two lines. We seek to fold one point onto the first line and the second point onto the second line such that the third point folded by the first foldline meets the fourth point folded by the second foldline, cf. Figure 2.

From the basic origami theory we know that folding one point not on a given line onto this line yields as a fold line a tangent to the parabola defined by the point and line [11, Theorem 10.3]. We fix the line m and the points $P \notin m$ and $Q \neq P$ and we let the tangent l to the parabola with focus P and directrix m vary over the set of all tangents to this parabola. Then the reflexion image Q^l of Q across l moves along a cubic curve, cf. Figure 3. This curve was discussed for instance in [11, p. 150], [7, pp. 76], [5].

[1]One might think of “AL” as Alignment or Alperin-Lang.

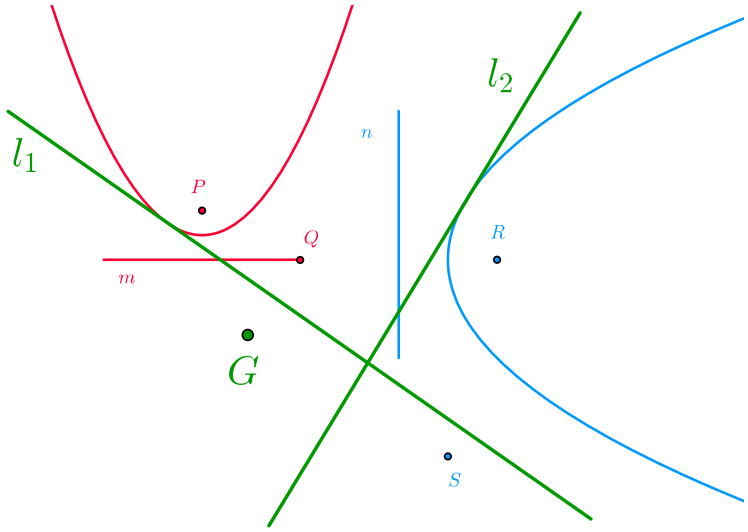

Figure 2. A representation of the axiom AL6ab8. $Q^{l_1} = G = S^{l_2}$, $P^{l_1} \in m$, $R^{l_2} \in n$.

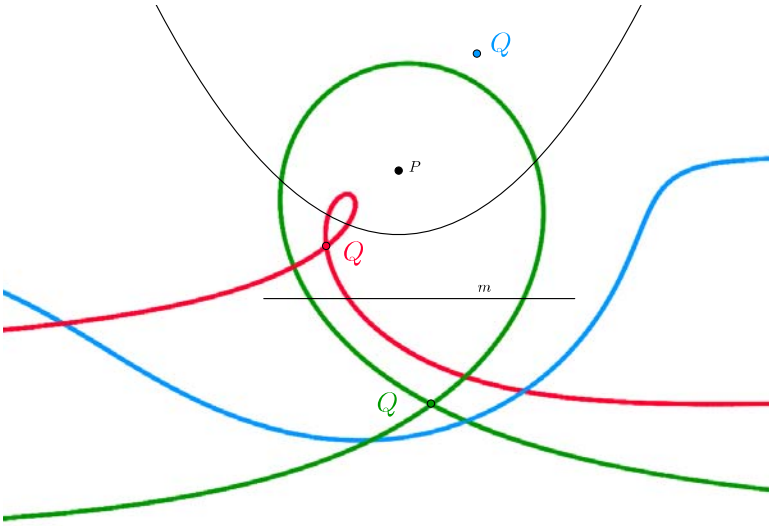

Figure 3. Three different origami cubic curves for three different positions of Q. A point Q is folded across each tangent to the parabola with directrix m and focus P. Note that the blue curve has an isolated *real* point Q, but obviously there are no such isolated points if you look at this curve in $\mathbb{P}_2\mathbb{C}$ where it naturally lives.

Let us be more specific here. Let $m = \{(x, y) \in \mathbb{R}^2 \mid ax + by + 1 = 0\}$ be a given line with origami-constructible[2] a, b. Let $P = (c, d) \in \mathbb{R}^2, P \notin m$ and $Q = (e, f) \in \mathbb{R}^2$, $Q \neq P$ be two given points with origami-constructible

[2]We will use *origami-constructible* for 1-*fold origami-constructible*.

coefficients c, d, e, f. It is well-known how to find the image of a point by reflexion across a line, cf. [1, Definition 3]. The equation of an arbitrary tangent l to a parabola with focus P and directrix m is easily calculated, too. So if we put this together, we can calculate the equation of the moving point Q^l. It is:

$$\begin{aligned}
&ax^3 + bx^2y + axy^2 + by^3 \\
&+ (-ac - ae + bd - bf + 1)x^2 + (-2ad - 2bc)xy + (ac - ae - bd - bf + 1)y^2 \\
&+ (2ace + 2adf - ae^2 - af^2 + 2bcf - 2bde - 2e)x \\
&+ (-2acf + 2ade + 2bce + 2bdf - be^2 - bf^2 - 2f)y \\
&- ace^2 + acf^2 - 2adef + ae^3 + aef^2 - 2bcef + bde^2 - bdf^2 + be^2f + bf^3 + e^2 + f^2 \\
&= 0.
\end{aligned}$$

Obviously, this curve passes through Q, so if we change the coordinate system to $X := x - e$ and $Y := y - f$ and simplify a little bit the curve will have the equation:

$$(X^2 + Y^2)(aX + bY) + t_1X^2 + t_2XY + t_3Y^2 = 0 \tag{1}$$

with $t_1 = -ac+2ae+bd+1, t_2 = -2ad+2af-2bc+2be, t_3 = ac-bd+2bf+1 \in \mathbb{Q}(a, b, c, d, e, f)$. We call this curve a (*circular nodal*) origami cubic curve and denote it by $\mathcal{C} := \mathcal{C}(a, b, c, d, e, f)$.

The letters a, b, c, d, e, f will be used throughout the paper in the sense just explained. We pause for a second to show a converse to the necessary condition for an origami cubic curve.

In the definition of the line $m = \{(x, y) \mid ax + by + 1 = 0\}$ there is no loss of generality assuming $a \neq 0$. Then we divide the equation (1) by a and set $t_0 := \frac{b}{a}$ getting

$$\begin{aligned}
&(X^2 + Y^2)(X + t_0Y) + (-c + 2e + t_0d + \frac{1}{a})X^2 \\
&+ (-2d + 2f - 2t_0c + 2t_0e)XY + (c - t_0d + 2t_0f + \frac{1}{a})Y^2 = 0.
\end{aligned}$$

We show that the coefficients at X^2, XY, and Y^2 can take arbitrary values t_1, t_2, t_3 (for given t_0, e, f and suitable choices of a, c, d). To achieve this, we have to solve the system of equations

$$\begin{aligned}
t_0 &= \frac{b}{a}, \\
t_1 &= -ac + 2ae + t_0ad + 1, \\
t_2 &= -2d + 2f - 2t_0c + 2t_0e, \\
t_3 &= ac - t_0ad + 2t_0af + 1
\end{aligned}$$

for given t_0, t_1, t_2, t_3, e, f and unknown variables a, b, c, d. This system is solved by

$$\begin{aligned} a &:= \frac{2}{2t_0 f - t_1 - t_3 + 2e}, \\ b &:= t_0 a, \\ c &:= \frac{2t_0^2 e - t_0 t_2 - t_1 + t_3 + 2e}{2t_0^2 + 2}, \\ d &:= \frac{2t_0^2 f + t_0 t_1 - t_0 t_3 - t_2 + 2f}{2t_0^2 + 2}. \end{aligned}$$

We have therefore shown the following

Lemma 2. *Let t_0, t_1, t_2, t_3, e, f be real numbers, and let $X := x - e$ and $Y := y - f$. Then the cubic curve given by*

$$(X^2 + Y^2)(X + t_0 Y) + t_1 X^2 + t_2 XY + t_3 Y^2 = 0$$

is an origami cubic curve $\mathcal{C}(a, b, c, d, e, f)$ with a, b, c, d in the field generated by t_0, t_1, t_2, t_3, e, f over $\mathbb{Q}$. That is, there exists a parabola (given by directrix $\{(x, y) \mid ax + by + 1 = 0\}$ and focus (c, d)) such that the image of the given point (e, f) under reflection across the tangents of the parabola is exactly the given cubic.

Remark. For certain values of t_0, t_1, t_2, t_3, e, f the denominator of a (and b) in the above solution may vanish. This, however, does not mean that there is no solution, but rather that the directrix of the parabola passes through the origin and therefore cannot be represented in the form $g_{a,b} := \{(x, y) \in \mathbb{R}^2, ax + by + 1 = 0\}$ as above. Furthermore one can see that if the cubic curve is irreducible then the point (c, d) in the above solution will not lie on the line $g_{a,b}$, i.e. they really define a parabola.

In the following, interpreting AL6ab8 geometrically, we construct two parabolas and two tangents to them such that two given points are superposed by folding across these tangents. Finding these tangents resp. folds l_1 and l_2 as in Figure 2 is equivalent to finding the intersection points of two (origami) cubics.

By the Bézout Theorem there are nine (projective) complex intersection points of two cubics. The equation (1) reveals that, in our situation, the two origami cubic curves will have two intersection points at infinity, so we get generically seven affine intersection points. This yields an equation of degree 7, cf. the following section.

The Galois group of this equation is S_7 in the generic case, but we noticed that, for suitable values for the points and lines, smaller group such as A_7 and $PSL_3\mathbb{F}_2$ occur as well (see Figures 4 and 5 for concrete crease patterns for these groups). This observation led to the natural question *Which subgroups of S_7 are realizable by 2-fold axioms?* Even stronger: *Is every septic equation solvable by 2-fold axioms?*

3. Generic Septic Equations

We want to find suitable values for the given points and lines, such that the arising origami cubic curves intersect in a point with the "right" minimal polynomial, i.e. minimal polynomial with the wanted Galois group, for instance. We have seen that it suffices in many cases to fix one of the two parabolas. In the axiom AL6ab8 we drop the generality and specify one half of the data. Let n be the line with the equation $y = -1$. Let $R = (0, 1)$ and $S = (0, 0)$, cf. Figure 2. So we fold the origin across the tangents of the parabola with the equation $y = \frac{1}{4}x^2$. If (X, Y) is an intersection point of the two arising origami cubic curves and $W := \frac{X}{Y}$ (this is, up to sign, just the slope of the fold line across which $(0, 0)$ is reflected to (X, Y)), the following equation of degree 7 is satisfied by W:

$$
\begin{aligned}
&W^7 + \left(\frac{3}{2}e + \frac{1}{2}ft_0 + t_0 - \frac{1}{2}t_1\right) W^6 \\
&+ \left(\frac{3}{4}e^2 + \frac{1}{2}eft_0 + et_0 - \frac{1}{2}et_1 + \frac{1}{4}f^2 - \frac{1}{4}ft_2 + f - \frac{1}{2}t_2\right) W^5 \\
&+ \left(\frac{1}{8}e^3 + \frac{1}{8}e^2ft_0 + \frac{1}{4}e^2t_0 - \frac{1}{8}e^2t_1 + \frac{1}{8}ef^2 - \frac{1}{8}eft_2 + \frac{1}{2}ef - \frac{1}{4}et_2 + \frac{1}{2}e + \frac{1}{8}f^3t_0\right. \\
&\quad \left. + \frac{3}{4}f^2t_0 - \frac{1}{8}f^2t_3 + \frac{3}{2}ft_0 - \frac{1}{2}ft_3 - \frac{1}{2}t_3\right) W^4 \\
&+ \left(\frac{3}{4}e^2 + \frac{1}{2}eft_0 - \frac{1}{2}et_1 + \frac{1}{4}f^2 - \frac{1}{4}ft_2\right) W^3 \\
&+ \left(\frac{1}{4}e^3 + \frac{1}{4}e^2ft_0 + \frac{1}{4}e^2t_0 - \frac{1}{4}e^2t_1 + \frac{1}{4}ef^2 - \frac{1}{4}eft_2 + \frac{1}{2}ef - \frac{1}{4}et_2 + \frac{1}{4}f^3t_0\right. \\
&\quad \left. + \frac{3}{4}f^2t_0 - \frac{1}{4}f^2t_3 - \frac{1}{2}ft_3\right) W^2 + \\
&+ \frac{1}{8}e^3 + \frac{1}{8}e^2ft_0 - \frac{1}{8}e^2t_1 + \frac{1}{8}ef^2 - \frac{1}{8}eft_2 + \frac{1}{8}f^3t_0 - \frac{1}{8}f^2t_3 \\
&= 0.
\end{aligned}
\tag{2}
$$

We see that the coefficient at W^1 is zero (which can of course always be achieved for a general equation of degree 7 by substituting W^{-1} for W and applying a linear transformation). The question is therefore whether the remaining six coefficients can take arbitrary values $s_1, \ldots, s_6$ for suitable choices of t_0, t_1, t_2, t_3, e, f. As the resulting system of equations is linear in $t_0, \ldots, t_3$, we can assign arbitrary values to four of the coefficients (say, the coefficients at $W^6, \ldots, W^3$).

More precisely, this is achieved by setting

$$
\begin{aligned}
t_0 &:= \frac{2s_1e + s_2f - \frac{3}{2}e^2 - \frac{1}{2}f^2 - s_4(f + 2)}{ef + 2e}, \\
t_1 &:= 3e + ft_0 + 2t_0 - 2s_1, \\
t_2 &:= \frac{4s_1e - 3e^2 + f^2 + 4f - 4s_2}{2 + f}, \\
t_3 &:= \frac{-2s_1e^2 + 4s_2e + e^3 + 4e + f^3t_0 + 6f^2t_0 + 12ft_0 - 8s_3}{4f + 4 + f^2}.
\end{aligned}
$$

The polynomial we obtain in this way from Formula (2) is

$$W^7 + s_1W^6 + s_2W^5 + s_3W^4 + s_4W^3 + C_1W^2 + C_2 = 0, \tag{3}$$

where

$$\begin{aligned} C_1 := \frac{1}{4(ef^2+4ef+4e)}\Big(& -2s_1e^3f - 4s_1e^3 - 2s_1ef^3 - 12s_1ef^2 - s_2e^2f^2 + 2s_2e^2f \\ & + 8s_2e^2 - s_2f^4 - 6s_2f^3 + 8s_3ef^2 + 16s_3ef + s_4e^2f^2 + 4s_4e^2f + 4s_4e^2 + s_4f^4 \\ & + 8s_4f^3 + 12s_4f^2 + \frac{1}{2}e^4f + e^4 + e^2f^3 + 4e^2f^2 - 8e^2f + \frac{1}{2}f^5 + 3f^4\Big), \\ C_2 := \frac{1}{4(ef^3+6ef^2+12ef+8e)}\Big(& -2s_1e^3f^2 - 4s_1e^3f - 2s_1ef^4 - 8s_1ef^3 - s_2e^2f^3 \\ & + 4s_2e^2f - s_2f^5 - 4s_2f^4 + 4s_3ef^3 + 8s_3ef^2 + s_4e^2f^3 + 6s_4e^2f^2 + 12s_4e^2f \\ & + 8s_4e^2 + s_4f^5 + 6s_4f^4 + 8s_4f^3 + \frac{1}{2}e^4f^2 - 2e^4 + e^2f^4 + 2e^2f^3 - 6e^2f^2 \\ & + \frac{1}{2}f^6 + 2f^5\Big). \end{aligned}$$

Now we are ready to show the main result.

Theorem 3. *A generic equation of degree* 7 *can be solved by* 2*-fold origami.*

Proof. If we set $f = 0$ in equation (3), then we obtain

$$W^7+s_1W^6+s_2W^5+s_3W^4+s_4W^3+\frac{1}{16}(e^3-4e^2s_1+8es_2+8es_4)W^2-\frac{1}{16}e^3+\frac{1}{4}es_4 = 0. \tag{4}$$

Replacing W by W^{-1}, we obtain a septic equation with vanishing coefficient at W^6. After multiplying W with an appropriate factor and dividing by the leading coefficient, we even get a monic septic polynomial of the form $W^7 + a_1W^5 + a_2W^4+a_3W^3+a_4W^2+a_5W+a_5$, where the a_i are rational functions in $s_1, \ldots, s_4$ and e.

We investigate whether for suitable choices of $s_1, \ldots, s_4$ and e *any* equation of the form

$$W^7 + a_1W^5 + a_2W^4 + a_3W^3 + a_4W^2 + a_5W + a_5 \ = 0 \tag{5}$$

with real-valued coefficients $a_1, \ldots, a_5$, can be obtained. This leads to a system of polynomial equations in the variables $s_1, \ldots, s_4$ and e over the function field $\mathbb{Q}(a_1, \ldots, a_5)$. Gröbner basis methods show that the system can be solved by e satisfying the equation

$$
\begin{aligned}
&p_e(a_1,\dots,a_5)\\
&:= e^8 + \frac{e^6}{a_5^3}\big(48a_1^2a_2a_5^2 + 40a_1a_2^4a_5 - 176a_1a_2^2a_5^2 - 56a_1a_4a_5^2 + 112a_1a_5^3 + 4a_2^7\\
&\qquad - 40a_2^5a_5 - 40a_2^3a_4a_5 + 128a_2^3a_5^2 + 136a_2a_4a_5^2 - 128a_2a_5^3\big)\\
&\quad + \frac{e^4}{a_5^4}\big(368a_1^4a_2^2a_5^2 + 448a_1^4a_5^3 - 64a_1^3a_2^5a_5 - 192a_1^3a_2^3a_5^2 - 1248a_1^3a_2a_4a_5^2\\
&\qquad - 1280a_1^3a_2a_5^3 + 448a_1^2a_2^4a_4a_5 - 96a_1^2a_2^4a_5^2 + 1888a_1^2a_2^2a_4a_5^2 + 128a_1^2a_2^2a_5^3\\
&\qquad + 896a_1^2a_4^2a_5^2 - 896a_1^2a_4a_5^3 + 1792a_1^2a_5^4 + 128a_1a_2^5a_4a_5 - 64a_1a_2^5a_5^2\\
&\qquad - 1184a_1a_2^3a_4^2a_5 - 544a_1a_2^3a_4a_5^2 + 512a_1a_2^3a_5^3 - 320a_1a_2a_4^2a_5^2 - 640a_1a_2a_4a_5^3\\
&\qquad - 1024a_1a_2a_5^4 - 32a_2^6a_4^2 + 64a_2^6a_4a_5 - 16a_2^6a_5^2 + 352a_2^4a_4^2a_5 - 736a_2^4a_4a_5^2\\
&\qquad + 192a_2^4a_5^3 + 800a_2^2a_4^3a_5 - 1600a_2^2a_4^2a_5^2 + 2816a_2^2a_4a_5^3 - 768a_2^2a_5^4 - 896a_4^3a_5^2\\
&\qquad + 3584a_4^2a_5^3 - 3584a_4a_5^4 + 1024a_5^5\big)\\
&\quad + \frac{e^2}{a_5^5}\big(256a_1^7a_5^3 + 1024a_1^6a_2a_5^3 - 1024a_1^5a_2^2a_4a_5^2 + 1536a_1^5a_2^2a_5^3 - 3584a_1^5a_4a_5^3\\
&\qquad - 2048a_1^4a_2^3a_4a_5^2 + 1024a_1^4a_2^3a_5^3 + 4608a_1^4a_2a_4^2a_5^2 - 8704a_1^4a_2a_4a_5^3\\
&\qquad + 512a_1^3a_2^4a_4^2a_5 - 1024a_1^3a_2^4a_4a_5^2 + 256a_1^3a_2^4a_5^3 + 12800a_1^3a_2^2a_4^2a_5^2\\
&\qquad - 6656a_1^3a_2^2a_4a_5^3 - 3584a_1^3a_4^3a_5^2 + 14336a_1^3a_4^2a_5^3 - 3072a_1^2a_2^3a_4^3a_5\\
&\qquad + 6144a_1^2a_2^3a_4^2a_5^2 - 1536a_1^2a_2^3a_4a_5^3 - 27648a_1^2a_2a_4^3a_5^2 + 15360a_1^2a_2a_4^2a_5^3\\
&\qquad + 7168a_1a_2^2a_4^4a_5 - 12288a_1a_2^2a_4^3a_5^2 + 3072a_1a_2^2a_4^2a_5^3 + 14336a_1a_4^4a_5^2\\
&\qquad - 14336a_1a_4^3a_5^3 + 64a_2^5a_4^4 - 768a_2^3a_4^4a_5 - 4608a_2a_4^5a_5 + 11264a_2a_4^4a_5^2\\
&\qquad - 2048a_2a_4^3a_5^3\big)\\
&\quad + \frac{1}{a_5^5}\big(-1024a_1^3a_2^3a_4^4 + 6144a_1^2a_2^2a_4^5 - 12288a_1a_2a_4^6 + 8192a_4^7\big)\\
&= 0
\end{aligned}
$$

and $s_1,\dots,s_4$ lying in the field extension of $\mathbb{Q}(a_1,\dots,a_5)$ generated by e.

But obviously e^2 is a root of a quartic polynomial. As quadratic and quartic polynomials can be solved by 1-fold origami, e is an origami-constructible number – and so are $s_1,\dots,s_4$. Therefore, by substituting $t_0,\dots,t_3$ and then a,b,c,d as described above, all the values for our 2-fold step are constructible numbers. If we can, in addition, choose them as real numbers – for which it is sufficient that e is real – then we can solve the generic septic equation (5) by 2-fold origami.

While the above polynomial $p_e(a_1,\dots,a_5)$ of degree 8 may of course have no real roots for certain choices of $a_1,\dots,a_5$, we will show that there is always a polynomial

$$W^7 + b_1W^5 + b_2W^4 + b_3W^3 + b_4W^2 + b_5W + b_5$$

generating the same field extension as the analogous polynomial in $a_1,\dots,a_5$, such that $p_e(b_1,\dots,b_5)$ has a real root.

Firstly, observe that $p_0(a_1,\dots,a_5) = -1024\cdot a_4^4a_5^{-5}\cdot(a_1a_2-2a_4)^3$ and $\lim_{e\to+\infty} p_e = +\infty$. If we can enforce $a_5(a_1a_2-2a_4) > 0$, then p will change

its sign somewhere between 0 and $+\infty$ and therefore have a real root. Now for $w \in \mathbb{R}$ a root of $W^7 + a_1W^5 + a_2W^4 + a_3W^3 + a_4W^2 + a_5W + a_5$ and $\lambda \in \mathbb{Q}$, we can bring the minimal polynomial of $w + \frac{\lambda}{w}$ into the form $W^7 + b_1W^5 + b_2W^4 + b_3W^3 + b_4W^2 + b_5W + b_5$ via linear transformations. The term $b_5(b_1b_2 - 2b_4)$ is a rational function in the a_i and λ; as we are only interested in the sign of this expression, we can multiply it by arbitrary squares and thus obtain a square-free polynomial F in $a_1, \ldots, a_5$ and λ.

Viewing F as a polynomial in λ over $\mathbb{Q}(a_1, \ldots, a_5)$, we observe that F splits as $F(\lambda) = F_1(\lambda) \cdot F_2(\lambda)$ with F_1, F_2 polynomials in λ of degree 5 and 7 respectively. But F_1 and F_2 will both have a real root, and generically these roots will not coincide; this means that the expression $b_5(b_1b_2 - 2b_4)$ will change its sign at some point, so if we choose $\lambda \in \mathbb{Q}$ in a suitable interval, $b_5(b_1b_2 - 2b_4)$ will be positive, and $p_e(b_1, \ldots, b_5)$ will have a real root. But this means that we can construct $w + \frac{\lambda}{w}$, and therefore w as well, with 2-fold origami, so every real root of a generic septic equation is constructible by 2-fold origami. □

Remark. Note that our "generic" form can be obtained without loss of generality, if we view the coefficients as transcendentals; however, for certain specializations, like polynomials of the form $W^7 - A$ this is not possible by linear transformations. We will deal with equations $W^7 - A = 0$ in 4.2.

Also, throughout the proof, we deal with rational functions in certain coefficients; of course, for a bad choice of the coefficients, these might not be well-defined due to vanishing denominators. The term "generic" polynomial should always be understood in the sense that the denominators have to behave well.

4. Solvable groups

We showed above that a generic equation of degree 7 is solvable by 2-fold origami, but there are some important cases which seem not to be included in the generic result, like 2-folding of seventh roots. We deal with this separately and show more generally that every solvable $\{2, 3, 5, 7\}$-extension of $\mathbb{Q}$ is solvable by 2-fold origami.

4.1. *Angle septisection.* If you are an origami artist you have quite often to create some difficult marks to proceed. Usually these are some divisions of a segment, like third parts. It can occur that you need a third part of an angle[3]. Robert Lang found an exact angle quintisection with 2-fold origami, which is impossible by 1-fold origami, and [1] and [12] put this result on a more general basis. As far as we know an exact angle septisection for a general angle has not been given by means of k-fold origami for $k < 5$. Robert Lang did find an approximate solution [9], though, and used it for the construction of his famous scorpion.

Let $\varphi \in (0, 2\pi)$ be an angle, $A = 2\cos(\varphi)$ and $x = 2\cos(\varphi/7)$. Then one easily verifies with de Moivre's formula that $x^7 - 7x^5 + 14x^3 - 7x - A = 0$. If we

[3]By the way, the possibility of angle trisection is one of the advantages of 1-fold origami over euclidean constructions.

can solve this equation for arbitrary $A \in (-2, 2)$, then we can septisect an arbitrary angle. The following theorem states that we can do this with 2-fold origami.

Theorem 4. *Septisection of arbitrary angles $\varphi \in (0, 2\pi)$ is possible with 2-fold origami.*

Proof. We take the polynomial from equation (4), replace W with W^{-1} (so the polynomial has vanishing coefficient at W^6 instead of W^1), and multiply W with a constant factor in order to let the constant and the linear coefficient take the same value. Denote the resulting polynomial by $h_1(W)$. Then we treat $W^7 - 7W^5 + 14W^3 - 7W - A$ in the same way (that is, multiply W with factor $\frac{A}{7}$) and denote the result by $h_2(W)$. Now compare the coefficients of h_1 and h_2. The arising system of equations over $\mathbb{Q}(A)$ is solved by $s_2 = 0 = s_4$ and

$$s_1 := \frac{\begin{array}{c}4302592(-28+A^2)(-196+14A^2+3A^4)e\\ +196A^4(5488+560A^2+A^4)e^3 - A^6(28+3A^2)e^5\end{array}}{153664A^2(21952-784A^2-252A^4+A^6)},$$
$$s_3 := \frac{-3764768(-112+A^4)e - 98A^2(784+280A^2+A^4)e^3 + A^6e^5}{5488(21952-784A^2-252A^4+A^6)},$$

where e fulfills

$$e^6 - \frac{38416}{A^2}e^4 + \frac{-7529536A^4+210827008A^2-843308032}{A^6}e^2 - \frac{210827008}{A^2} = 0.$$

As all the other unknown coefficients a, b, c, d of our initial point and line setting can be expressed as rational functions in these, we are done if we can construct e as a real number; but the above sextic polynomial in e can be solved by solving cubic and quadratic equations, i. e. by 1-fold origami. It remains to be seen whether e can be chosen as a real number. As

$$p(x) = x^6 - \frac{38416}{A^2}x^4 + \frac{-7529536A^4+210827008A^2-843308032}{A^6}x^2 - \frac{210827008}{A^2}$$

is negative at 0 and $\lim_{x\to+\infty} p(x) = +\infty$, such a real number e exists, indeed. □

4.2. *Folding seventh roots.* We try to specialize all intermediate coefficients of the polynomial in equation (3) to zero. This corresponds to constructing seventh roots. So we compare coefficients of the polynomial in (3) with those of the polynomial $W^7 + s$, where s is any positive real number. This leads to two equations in e and f over the field $\mathbb{Q}(s)$. This system of equations has a solution in the function field defined by

$$\begin{aligned}&f^{10}t^2 + 2f^{10}t + f^{10} + 24f^9t^2 + 24f^9t + 252f^8t^2 - 84f^8t + 1536f^7t^2\\ &- 1264f^7t + 6048f^6t^2 - 1008f^6t + 16128f^5t^2 + 5376f^5t + 29568f^4t^2\\ &+ 3584f^4t + 36864f^3t^2 - 6144f^3t + 29952f^2t^2 + 14336ft^2 + 3072t^2 = 0,\end{aligned}$$

where $t := s^2$. This defines a rational function field $\mathbb{Q}(f, t)$ over $\mathbb{Q}(t)$, and therefore we can find a parameter w such that $\mathbb{Q}(w) = \mathbb{Q}(f, t)$ and express t as a rational

function in it; computer calculation yields $t = 2^{10}\frac{w^7}{(w+7)^7(w+1)^2(w+3)}$ for a suitable parameter w.

Remember that we want to solve $X^7 + \sqrt{t} = 0$. Multiply X with a factor $\sqrt{\frac{2w}{w+7}}$, we can transform this to $X^7 + \sqrt{T} = 0$, where $T = \frac{8}{(w+1)^2(w+3)}$. Note that the square root that is introduced in this transformation does not lead to any problems, as square roots are of course constructible by 1-fold origami.

But now we can specialize T to an arbitrary positive value; w will then be the (w.l.o.g. real) root of a cubic equation, and we can solve this equation with 1-fold origami. Now e and f lie in the field generated by w and $\sqrt{t}$, which is at most a quadratic extension of $\mathbb{Q}(w)$. As we can w.l.o.g. multiply T with positive rational 7th powers, the field $\mathbb{Q}(w, \sqrt{T})$ can even be enforced to be real because for $T > 0$ small enough, for the equation $8 = T(w+1)^2(w+3)$ will always have a *positive* solution w, and therefore t will be positive with T as well. So the construction is completed.

Together with angle septisection shown above, this result leads to the following

Theorem 5. *Let $K \mid \mathbb{Q}$ be a finite solvable Galois extension of degree $2^a \cdot 3^b \cdot 5^c \cdot 7^d$ with $a, b, c, d \in \mathbb{N}_0$. Then K is solvable by 2-fold origami.*

Proof. Galois theory says that the extension $K \mid \mathbb{Q}$ can be solved by repeatedly taking (square, cubic, fifth and seventh) roots. Now taking the n-th root of any complex number can be achieved by taking the real n-th root of its absolute value, combined with angle n-section.

Square roots and cubic roots can be taken by 1-fold origami. Nishimura [12] and Lang [8] showed that in particular fifth roots and quintisection can be taken with 2-fold origami. This leaves $n = 7$, and we showed above how to septisect arbitrary angles and take seventh roots of reals. □

5. Crease patterns for nonsolvable transitive groups in S_7

In the previous section we showed that every polynomial whose Galois group is a solvable subgroup of S_7 can be solved by 2-fold origami. Now we turn to nonsolvable transitive groups in S_7. These are S_7, A_7 and $PSL_3\mathbb{F}_2 \cong PSL_2\mathbb{F}_7$, cf. [4, p. 60, Table 2.1]. With the methods of Section 3, one could give many explicit constructions for each of these groups; however these constructions would in general be quite lengthy and involved as they require for instance the folding of solutions of quartic equations.

We give explicit examples of folds with very nice initial coordinates that lead to Galois groups A_7 and $PSL_3\mathbb{F}_2$ (the generic case S_7 is left out as almost all folds with axiom AL6ab8 lead to this Galois group).

First, we want to give a realization of A_7 by specializing the axiom AL6ab8. We put

$$m : x = -2,\ P = (-4, -1),\ Q = (1, 2)$$

for the first parabola set, cf. Figure 4. Furthermore we set

$$n : y = -1,\ R = (0, 1),\ S = (1, 0)$$

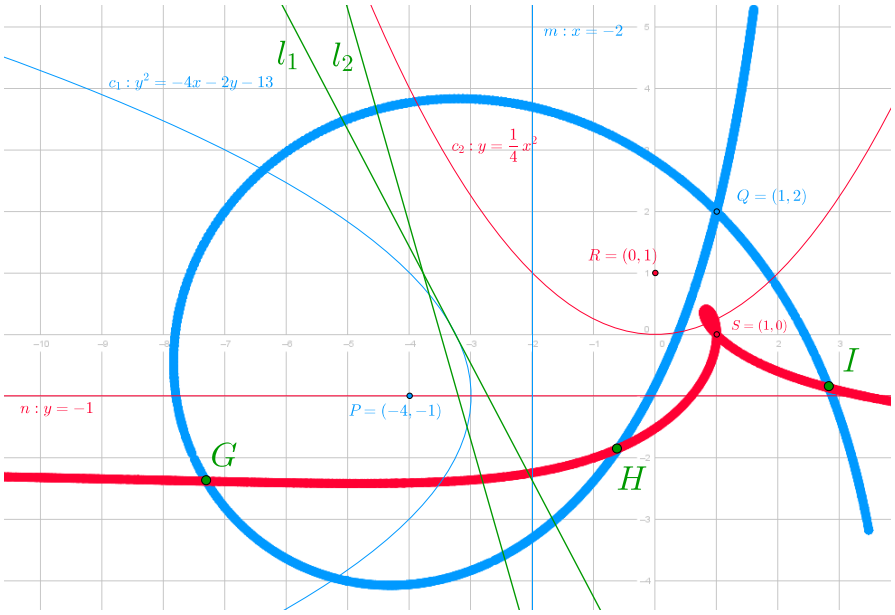

Figure 4. Crease pattern for A_7 by AL6ab8. G, H, I are the intersection points of the two bold cubics in red and blue. The green foldlines l_1 and l_2 arise by folding Q resp. S on G.

for the second parabola set. Putting these numbers into the equations we dealt with above, we get a polynomial h of degree 7, describing the intersection points of the two cubics, such that $\mathrm{Gal}(h \mid \mathbb{Q}) \cong A_7$. More precisely, the slope of the foldline l_2 is a root of the polynomial $y^7 + y^6 - 8y^5 + 3y^4 + y^3 - 3y^2 + 2y - 1$. The discriminant of this polynomial is equal to $2^8 \cdot 31^2 \cdot 157^2$, so it is a square and the Galois group must be contained in A_7. In fact, equality holds, as one verifies with a computer algebra program such as Magma.
Note that this polynomial has exactly three real roots, corresponding to the three intersection points of our cubics in the affine plane. The slope of the line l_2 in Figure 4 is the real root of approximate value -3.49.

Now, let us describe how to construct $PSL_3\mathbb{F}_2$ by AL6ab8. As depicted in Figure 5, set

$$m : y = \frac{1}{2}x - 1,\ P = (-\frac{16}{5}, -\frac{12}{5}),\ Q = (-3, -3);$$
$$n : y = -2,\ R = (0, 0),\ S = (1, -1).$$

Again the two cubics intersect in three real points; the slope of fold line l_2 fulfills the equation

$$y^7 + 3y^6 - 3y^4 + 5y^3 + y^2 - 10y - 1 = 0,$$

whose Galois group surprisingly turns out to be $PSL_3\mathbb{F}_2$. It is notable that this polynomial is very simple and the number field generated by one of its roots has very small discriminant, namely $2^6 \cdot 383^2$.

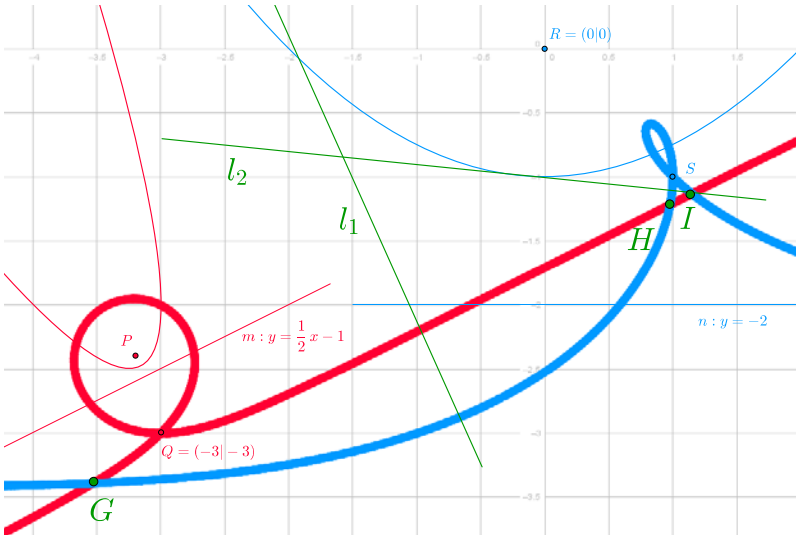

Figure 5. Crease pattern for $PSL_3\mathbb{F}_2$ by AL6ab8. The green foldlines l_1 and l_2 arise by folding Q resp. S on H.

References

[1] R. Alperin and R. Lang, One-, two, and multi-fold origami axioms, *Origami 4* (2006) 371–393.

[2] M. Beloch, Sulla risoluzione dei problemi di terzo e quarto grado col metodo del ripiegamento della carta, *Scritti Matematici Offerti a Luigi Berzolari*, Pavia (1936) 93–96.

[3] E. Brieskorn and H. Knörrer, *Plane Algebraic Curves*, Springer, 2012.

[4] J. Dixon and B. Mortimer, *Permutation groups*, Springer, 1996.

[5] E. Frigerio and H. Huzita, A possible example of system expansion in origami geometry, in *Proceedings of the First International Meeting of Origami Science and Technology*, edited by H. Huzita, Ferrara, (1989) 53–79.

[6] T. Hull, Solving cubics with creases: the work of Beloch and Lill, *Amer. Math. Monthly*, 118 (2011) 307–315.

[7] T. Hull, *Project Origami, Activities for exploring origami*, CRC Press, 2012.

[8] R. Lang, Angle Quintisection, `http://www.langorigami.com/science/math/quintisection/quintisection.pdf`

[9] R. Lang, Origami Constructions, `http://www.langorigami.com/science/math/hja/origami_constructions.pdf`

[10] E. Lill, Resolution graphique des equations numériques dún degré quelconque à une inconnue, *Nouv. Annales Math.*, Ser. 2, 6 (1867) 359–362.

[11] G. Martin, *Geometric constructions*, Springer, 1998.

[12] Y. Nishimura, Solving quintic equations by two-fold origami, *Forum Mathematicum*, 27 (2015) 1379–1387.

[13] P. Wantzel, Recherches sur les moyens de reconnaître si un problème de géométrie peut se résoudre avec la règle et le compas, *Journal de Mathématiques pures et appliquées*, 2.1 (1837) 366–372.

Joachim König: Department of Mathematics, Würzburg University, 97074 Würzburg, Germany
E-mail address: `joachim.koenig@mathematik.uni-wuerzburg.de`

Dmitri Nedrenco: Department of Mathematics, Würzburg University, 97074 Würzburg, Germany
E-mail address: `dmitri.nedrenco@mathematik.uni-wuerzburg.de`

Forum Geometricorum
Volume 16 (2016) 207–225.

FORUM GEOM
ISSN 1534-1178

On the Diagonal and Inscribed Pentagons of a Pentagon

Paris Pamfilos

Abstract. In this article we study two projective maps f and g, naturally associated with a pentagon. We show that, in the generic case, these maps have three distinct fixed points and discuss their reduction to some kind of canonical form, relative to the triangle of these three fixed points. In addition we give descriptions and geometric characterizations of the non-generic pentagons, called axial symmetric and their exceptional case of polygons projectively equivalent to the canonical pentagon.

1. Introduction

Given a pentagon p, Kasner [6] seems to be the first one, who studied two other pentagons naturally related to p. The first one, denoted by $p^1 = \mathcal{D}(p)$ is the *diagonal pentagon* $p^1 = A^1B^1C^1D^1E^1$, having for vertices the intersection points of the diagonals of the pentagon of reference p. The second one, denoted by $p_1 = \mathcal{I}(p)$ is the *inscribed pentagon* $p_1 = A_1B_1C_1D_1E_1$, having for vertices the points of contact of the sides of p with the conic inscribed in p. The labeling convention adopted corresponds to vertex V of p the vertex V^1 of p^1 and V_1 of p_1. Vertex V^1 is the intersection point of the diagonals of p, which do not contain V. Vertex V_1 is the contact point of the opposite to V side with the inscribed conic.

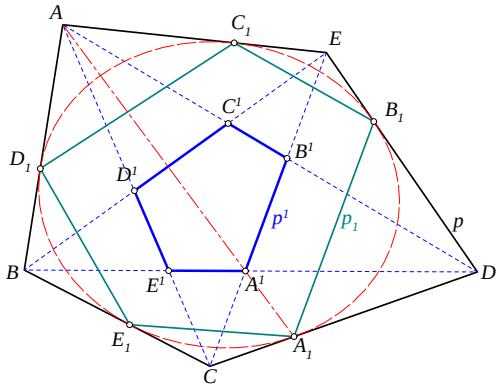

Figure 1. The *diagonal* $p^1 = \mathcal{D}(p)$ and the *inscribed* $p_1 = \mathcal{I}(p)$ of the pentagon p

Remark. By Brianchon's theorem, in its version for pentagons, points V, V^1 and V_1 are collinear for every vertex V of p.

Publication Date: May 23, 2016. Communicating Editor: Paul Yiu.

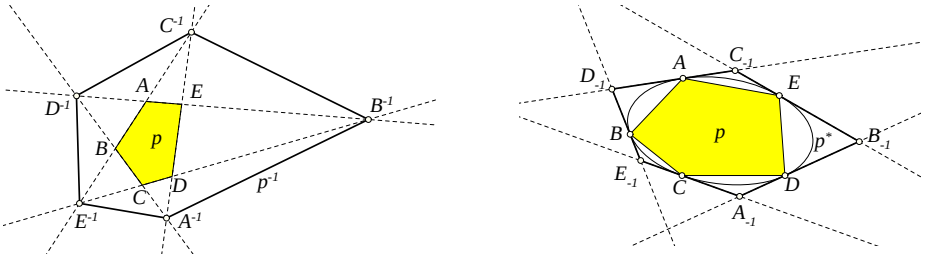

Figure 2. $p^{-1} = \mathcal{D}^{-1}(p)$ and $p_{-1} = \mathcal{I}^{-1}(p)$

The construction of the diagonal and inscribed polygons can be repeated and so it makes sense to write compositions of the two operators introduced, like $\mathcal{D}^k(p) = \mathcal{D}(\mathcal{D}(...\mathcal{D}(p)...))$ (k times), and analogously $\mathcal{I}^k(p) = \mathcal{I}(\mathcal{I}(...\mathcal{I}(p)...))$. It makes even sense to use negative exponents, since $p^{-1} = \mathcal{D}^{-1}(p)$ can be defined as the pentagon, which results by extending the sides of p and taking their intersections. Analogously is defined $p_{-1} = \mathcal{I}^{-1}(p)$ as the pentagon whose sides are tangent to the circumconic of p at its vertices. I call the set of polygons $\mathcal{D}_p = \{p^n = \mathcal{D}^n(p) : n \in \mathbb{Z}\}$ the *diagonal series* of p and the set $\mathcal{I}_p = \{p_n = \mathcal{I}^n(p) : n \in \mathbb{Z}\}$ the *inscribed series* of p.

2. The circumconics

Theorem 1. *For every pentagon p the polars π_Q of points Q of the circumconic of $p^{-1} = \mathcal{D}^{-1}(p)$, with respect to the circumconic c_p of p, are tangent to the circumconic c^1 of its diagonal pentagon $p^1 = \mathcal{D}(p)$.*

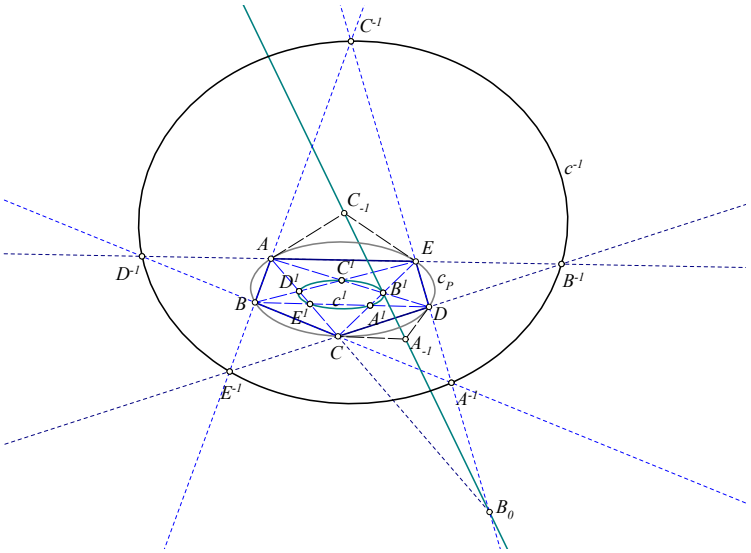

Figure 3. The circumconic of the pentagon

For the proof consider the pentagon $p^{-1} = A^{-1}B^{-1}C^{-1}D^{-1}E^{-1}$ and its diagonals $\mathcal{D}(p^{-1}) = p = ABCDE$ and $\mathcal{D}(p) = p^1 = A^1B^1C^1D^1E^1$. The polars of points of the circumconic c^{-1} of p^{-1} with respect to the circumconic c_p of p are tangent to the circumconic c_1 of p_1. In fact, from the complete quadrilateral $q = ACDE$ follows that the polar of B^{-1} with respcect to the circumconic c_p of pentagon p passes through B^1. From Pascal's theorem, in its variant for pentagons, we know that the tangent to c^1 at B^1 intersects the opposite side D^1E^1 at a point B_0 on line DE. But the polar of B^{-1} w.r.t. c_p passes also through B_0. Hence this tangent coincides with the polar of B^{-1} w.r.t. c_p. The same reasoning applies to all five vertices of p^{-1} and shows that the envelope of polars of points of c_{-1} passes through the vertices of p^1, hence it coincides with the circumconic c^1 of p^1.

Corollary 2. *The polar B^1B_0 of the vertex B^{-1} of $p^{-1} = \mathcal{D}^{-1}(p)$ with respect to the circumconic c_p of p passes through the vertices A_{-1}, C_{-1} of $p_{-1} = \mathcal{I}^{-1}(p)$.*

Corollary 3. *The two operators commute $\mathcal{D}(\mathcal{I}(p)) = \mathcal{I}(\mathcal{D}(p))$.*

The proof of the first corollary follows from the reciprocity of the pole-polar relation. Since the polars of A_{-1}, C_{-1}, which are respectively the lines CD, AE, pass through B^{-1}, the polar of B^{-1} will pass in turn through A_{-1}, C_{-1}.

The second corollary, which is Kasner's theorem ([6], [5]), follows from the previous corollary and the proper definitions of the operators $\mathcal{D}$ and $\mathcal{I}$. In fact, by the

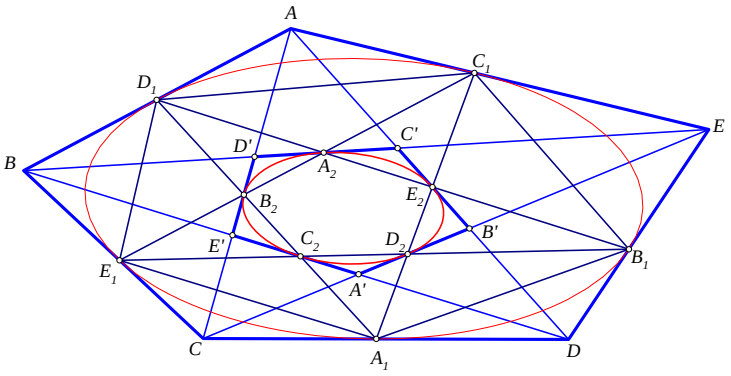

Figure 4. $\mathcal{D}(\mathcal{I}(p)) = \mathcal{I}(\mathcal{D}(p))$.

previous theorem, the intersection point E_2 of lines B_1D_1 and C_1A_1 is the contact point of the tangent AD of the conic inscribed in $p' = \mathcal{D}(p)$. This means that E_2 is a vertex of $\mathcal{I}(\mathcal{D}(p))$. But simultaneously it is a vertex of $\mathcal{D}(A_1B_1C_1D_1E_1) = \mathcal{D}(\mathcal{I}(p))$. This shows that the two constructions lead to polygons with identical vertices and proves the claimed property.

3. The basic homographies

Theorem 4. *For every pentagon there is a homography f which maps the vertices of every pentagon q of the series $\{\mathcal{D}^n(p) : n \in \mathbb{Z}\}$ to the corresponding vertices of its diagonal pentagon $\mathcal{D}(q)$.*

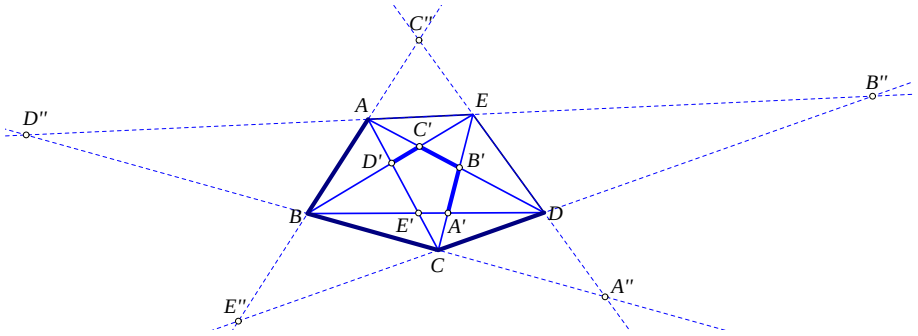

Figure 5. The homography f preserving the diagonal series

For the proof, consider the homography f which maps the four vertices A, B, C, D of the pentagon $p = ABCDE$ to the corresponding vertices A', B', C', D' of its diagonal pentagon. We show first, that also for the fifth vertex $f(E) = E'$ ([3, p. 64]). For this, consider the pentagon $p'' = \mathcal{D}^{-1}(p)$. Since, by its definition, $f(CD) = C'D', f(AB) = A'B'$ we have $f(E'') = f(AB \cap CD) = A'B' \cap C'D' = E$. From this it follows that $f(B'') = B$. This, because f maps the line CD to line $C'D'$ and f, being a homography respects the cross-ratio. Hence the cross ratio (E'', C, D, B'') maps to the same cross ratio $(E, C', D', f(B''))$. But from the pencil of lines at A : $A(B, D', C', E)$ we have that $(E, C', D', B) = (B'', D, C, E'') = (E'', C, D, B'')$. It follows that $(E, C', D', f(B'')) = (E, C', D', B)$, hence $f(B'') = B$. Analogously we show that $f(C'') = C$. Then $E = AB'' \cap DC''$ maps via f to $A'B \cap D'C = E$, as claimed. The argument shows also that the same homography f, which maps the vertices of p to those of $\mathcal{D}(p)$, maps also the vertices of $p'' = \mathcal{D}^{-1}(p)$ to those of p. Hence, inductively, we can prove that this is true also for any polygon of the series $\{\mathcal{D}^n(p) : n \in \mathbb{Z}\}$, as claimed.

Lemma 5. *For every pentagon p the cross ratios $(A_1C_2B_2D_1)$ and $(AC'B'D)$ are equal. Here $p = ABCDE$, $A'B'C'D'E' = \mathcal{D}(p)$, $A_1B_1C_1D_1E_1 = \mathcal{I}(p)$ and $A_2B_2C_2D_2E_2$ is the composite $\mathcal{I}(\mathcal{D}(p))$.*

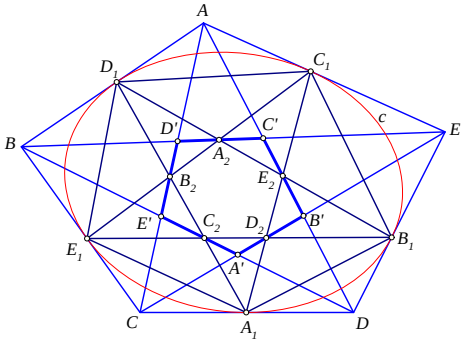

Figure 6. The basic equality $(A_1C_2B_2D_1) = (AC'B'D)$

The proof follows by noticing that the cross ratio $(A_1C_2B_2D_1)$ equals to the one of the four points A_1, B_1, C_1, D_1 on the conic c inscribed in p. This in turn is equal to the cross ratio defined on the tangent of c at E_1 by the four tangents to the same conic at these points. The pencil joining point E to these points on the tangent at E_1 coincides with the pencil $E(C, D, A, B)$. This pencil defines on line AD the cross ratio $(B'DAC') = (AC'B'D)$, as claimed.

Theorem 6. *For every pentagon there is a homography g which maps the vertices of every pentagon q of the series $\{\mathcal{I}^n(p) : n \in \mathbb{Z}\}$ to the corresponding vertices of its inscribed pentagon $\mathcal{I}(q)$.*

For the proof, consider the homography g which maps the four vertices A, B, C, D of the pentagon $p = ABCDE$ to the corresponding vertices A_1, B_1, C_1, D_1 of its inscribed pentagon $p_1 = \mathcal{I}(p) = A_1B_1C_1D_1E_1$. It follows that $g(E' = AC \cap BD) = g(AC) \cap g(BD) = E_2$. It follows also that D' maps via g to D_2. In fact, since g preserves the cross ratio, $(CE'D'A) = (C_1E_2g(D')A_1)$. But, by the previous lemma, $(CE'D'A) = (C_1E_2D_2A_1)$, hence $g(D') = D_2$. Analogously $g(A') = A_2$. Thus, line $g(CA') = C_1A_2$ and $g(BD') = B_1D_2$, thereby proving that $g(E = CA' \cap BD') = C_1A_2 \cap B_1D_2 = E_1$, as claimed. It follows that g maps the incircle of p to the incircle of $p_1 = A_1B_1C_1D_1E_1$ and sends simultaneously the vertices of p_1 to those of $\mathcal{I}(p_1)$. The proof of the theorem follows from an obvious induction.

Corollary 7. *The two homographies f, g, defined by the previous theorems and preserving correspondingly the diagonal and inscribed series, commute.*

This follows immediately from the fact that the two maps have compositions $f \circ g$ and $g \circ f$ coinciding on the five vertices of p. Since they are also projective maps, they coincide everywhere.

Obviously the homographies f, g defined previously, realize the operators $\mathcal{D}$ and $\mathcal{I}$ by means of projective maps. I denote them respectively by f_p and g_p.

Corollary 8. *The homography $f_{\mathcal{I}(p)}$ coincides with f_p. Analogously $g_{\mathcal{D}(p)}$ coincides with g_p.*

This is a consequence of the commutativity of f, g. In fact, referring to Figure 4, if $A_1B_1C_1D_1E_1 = p_1 = \mathcal{I}(p)$ and $A_2B_2C_2D_2E_2 = \mathcal{D}(\mathcal{I}(p))$, we have $A_2 = f(A_1)$ and the analogous equalities for the other vertices of p_1 and p_2. This is because f maps the inconic of p to the inconic of $\mathcal{D}(p)$ and the points of tangency to corresponding points of tangency. Analogous is the proof for the homography g_p.

Theorem 9. *For every point X of the plane points $X, f(X), g(X)$ are collinear.*

For the proof we show first that this property is valid for every point X of the line AE of pentagon p. Besides A, E line AE contains also the vertices $C_1 \in \mathcal{I}(p)$ and B', D', which are vertices of $\mathcal{D}^{-1}(p)$. These five points map via f to corresponding points on line $e = BD$ and via g on line $d = E_1A_1$ of $\mathcal{I}(p)$. By the properties proven above we see that in each case of these five the corresponding

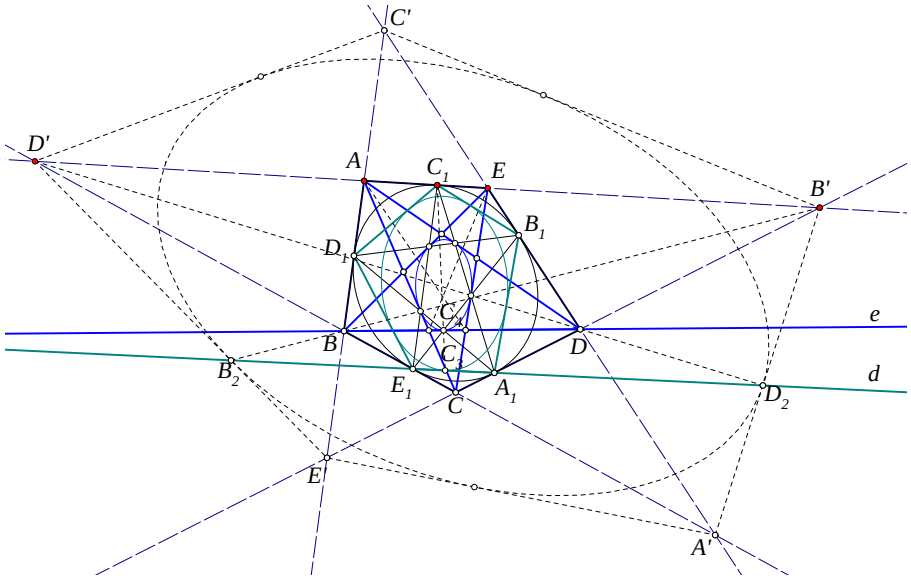

Figure 7. Collinearity of $X, f(X), g(X)$

points $X, f(X), g(X)$ are always collinear. The restrictions f', g' of f and g on line AE produce homographies mapping this line to e and d respectively. By well known theorem the line defined by points $X, f'(X)$ for X in AE envelope a conic c. Analogously, also the lines $X, g'(X)$ envelope a conic c'. Since these conics have five common tangents, they coincide. It follows that $X, f(X), g(X)$ are collinear for every point on line AE. An analogous argument shows that this triad of points is collinear also for every X on the lines which support the sides of p. Taking a system of coordinates, by means of which the homographies f, g are described by matrices respectively U and V, the condition of collinearity is equivalent with the vanishing of the determinant

$$|X, UX, VX| = 0.$$

This defines a cubic, which by the proof sofar, is satisfied by the five line-sides of the polygon p. Hence it is satisfied identically on the plane, as claimed.

4. The canonical representation

Let $p = ABCDE$ be an arbitrary convex pentagon and consider the unique homography h_p, which maps the first four vertices A, B, C, D of p correspondingly to the four points $A_0 = (0, 1)$, $B_0 = (0, 0)$, $C_0 = (1, 0)$, $D_0 = (1, 1)$, defined in an ordinary cartesian system of coordinates. The homography h_P maps the fifth point E of p to a point $E_0 = (a, b)$ and it is readily seen that the convexity assumption implies that (a, b) belongs to the domain $\mathcal{M}$ defined by

$$\mathcal{M} = \{(a, b) : 0 < a < 1 \text{ and } 1 < b\}.$$

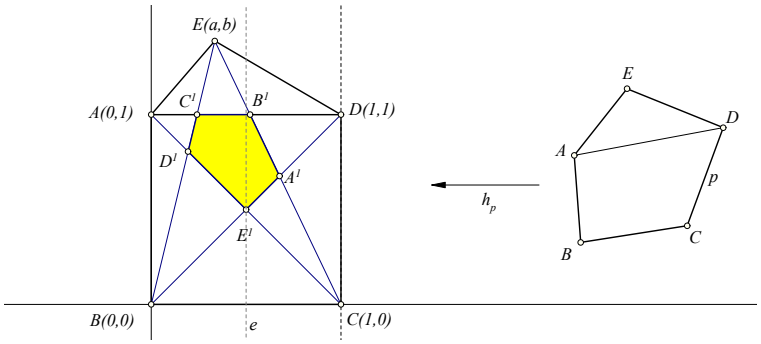

Figure 8. The canonical representation of p

In the rest of this section we identify p with its image $h_p(p)$. By this identification, all labeled convex polygons $p = ABCDE$ are parameterized by points $E(a, b)$ of the plane, whose coordinates satisfy the above restrictions. The representation is not really one-to-one, since the axial symmetry with respect to the middle-parallel e between lines AB and CD corresponds congruent pentagons. Thus, by restricting a to the interval $(0, \frac{1}{2}]$ or $[\frac{1}{2}, 1)$ the representation becomes a bijective one.

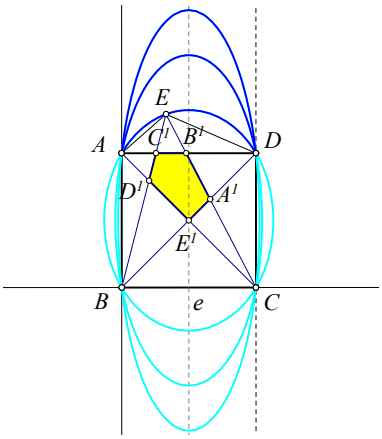

Figure 9. Arcs of constancy of cross ratio $E(ABCD)$

Note that in this representation the circumconic of the pentagon maps to an ellipse passing through A, B, C, D and having its center at E^1. Also the arcs of these ellipses falling inside the domain $\mathcal{M}$ are characterizing the classes of pentagons for which the cross ratio $E(ABCD)$ is constant ([2, p.3]). Given the arc of the ellipse on which lies point E, its precise location on it can be determined by another cross ratio from the remaining four defined by the pentagon, e.g. from $A(BCDE)$. It is also readily seen, for example by applying Brouwer's theorem ([4, p. 341]), that the homography $f : p \longrightarrow p^1$ has a fixed point lying inside p. We

need though a more detailed information on the fixed points of f and g and for this purpose we compute their matrices with respect to the homogeneous coordinates associated with a standard cartesian system of coordinates.

Lemma 10. *The matrices F and G of the projectivities correspondingly f and g, with respect to the projective basis $\{A=(0,1,1), B=(0,0,1), C=(1,0,1), D=(1,1,1)\}$, are*

$$F = \begin{pmatrix} a(b-1)(b+a-1) & (1-a)a^2 & a(a-b)(b+a-1) \\ (2a-1)(b-1)b & (1-a)ab & ab(a-b) \\ (2a-1)(b-1)b & (1-a)a & ab(a-b) \end{pmatrix},$$

$$G = \begin{pmatrix} -ab(b-1) & (a-1)a^2 & a(b-a)(b+a-1) \\ (1-2a)(b-1)b & (a-1)a(2b-1) & ab(b-a) \\ (1-2a)(b-1)b & (a-1)a & a(b^2-b-a+1) \end{pmatrix}.$$

The two matrices satisfy

$$F + G = (a-1)a(b-1)I,$$

where I is the identity matrix.

The proof is a standard computation in homogeneous coordinates, which I omit. The linear relation between F and G gives another proof of Theorem 9, which, among other things, implies that the two projectivities f and g have common fixed points.

Lemma 11. *The function*

$$k(a,b) = \frac{b(b-a)(b+a-1)}{a(a-1)(b-1)},$$

restricted in the domain $\mathcal{M}$, is C^∞ differentiable and possesses an absolute maximum

$$k_{max} = -\frac{11+5\sqrt{5}}{2},$$

attained at the point $(a_0,b_0) = \left(\frac{1}{2}, \frac{3+\sqrt{5}}{4}\right)$.

In fact, the differentiability is clear. To see the statement on the maximum consider for the moment b fixed and the partial function

$$k_b(x) = \frac{b(b-x)(b+x-1)}{x(x-1)(b-1)}.$$

Its derivatives are

$$k_b'(x) = -b^2\frac{2x-1}{(x(x-1))^2}, \qquad k_b''(x) = (2b^2)\frac{3x^2-3x+1}{(x(x-1))^3}.$$

Its unique extremum is at $x=\frac{1}{2}$ and the value of $k_b''\left(\frac{1}{2}\right) = -32b^2 < 0$. Thus the function has a local maximum in the interval $(0,1)$, whose value is

$$h(b) = k_b\left(\frac{1}{2}\right) = -\frac{b(2b-1)^2}{b-1},$$

and from the form of the derivative follows that this is also an absolute maximum of k_b. Repeating the previous procedure for the function

$$h(x) = -\frac{x(2x-1)^2}{x-1},$$

we find that its derivatives are

$$h'(x) = -\frac{(2x-1)(4x^2-6x+1)}{(x-1)^2} \qquad h''(x) = -2\frac{4x^3-12x^2+12x-3}{(x-1)^3}.$$

The roots of the first derivative, besides $x_0 = \frac{1}{2}$, which does not fall into the interval $(1,\infty)$ we are considering the function, are

$$x_1 = \frac{3-\sqrt{5}}{4} \text{ and } x_2 = \frac{3+\sqrt{5}}{4}.$$

From these only the second x_2 is compatible with our condition $b = x_2 > 1$, for which the corresponding value of the second derivative is

$$h''(x_2) = -16\frac{(\sqrt{5}+3)(3\sqrt{5}-5)}{(\sqrt{5}-1)^3} < 0.$$

Thus, $h(x)$ has at x_2 a local maximum, which, as seen from the form of the derivative, it is a global maximum in the interval $(1,\infty)$. From the analysis we made follows that the maximum of $h(x)$ which is

$$h(x_2) = -\frac{11+5\sqrt{5}}{2} = -11.09016994374948...$$

This coincides with the maximum of the function $k(a,b)$ restricted in the domain $(0,1)\times(1,\infty)$, as was claimed.

Lemma 12. *With the exception of the point $E_0(a_0,b_0)$, where the function $k(a,b)$ obtains its maximum in the domain $\mathcal{M}$, for all other points $E(a,b) \in \mathcal{M}$ the matrix F has three distinct real eigenvalues.*

In fact, the characteristic polynomial of F is found to be the negative of the polynomial

$$x^3 - m\cdot x^2 + m\cdot nx + m^2\cdot n,$$

where $m = (a-1)a(b-1)$ and $n = b(b-a)(b+a-1)$.

Setting for $x = y\cdot m$ and dividing the resulting equation by m^3 we find the equivalent of the equation in y :

$$y^3 - y^2 + ky + k = 0,$$

where $k = \frac{n}{m} < 0$. Obviously the roots of the characteristic polynomial of f can be determined by solving this equation and the inequality involved follows from the assumptions on a, b made at the beginning of the section. By the well known criterion of the nature of the roots of a cubic equation ([1, p.84]), this has three distinct real roots if and only if its discriminant

$$G^2 + 4H^3 < 0,$$

with $G = \frac{2}{27}(18k-1)$, $H = \frac{1}{9}(3k-1)$. It follows that

$$G^2 + 4H^3 = \frac{4}{27}k \cdot (k^2 + 11k - 1).$$

Since, by our assumptions, $k < 0$, this expression is negative if and only if k is outside the interval defined by the roots of the quadratic polynomial in k, which are

$$k_1 = \frac{-11 - 5\sqrt{5}}{2}, \qquad k_2 = \frac{-11 + 5\sqrt{5}}{2}.$$

Since we are interested in negative values for k and $k_2 = 0.09016994374947\ldots$, it follows that there are three real distinct roots for all k which satisfy

$$k < k_1 = -\frac{11 + 5\sqrt{5}}{2},$$

which, as claimed, is the maximum of the function $k(a,b) = \frac{n}{m}$.

Theorem 13. *With the exception of one class of projective equivalent pentagons, for all other pentagons the corresponding homography f has always three real fixed points.*

The proof of the theorem follows immediately from the previous lemmata.

5. The exceptional class

From the analysis in the preceding paragraph follows that the only class of projectively equivalent pentagons, whose corresponding homography f may have another configuration than the one of three distinct real fixed points is the class of

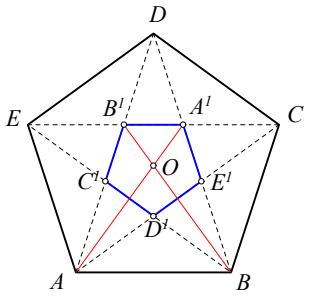

Figure 10. The exceptional class of regular pentagons

regular pentagons. Indeed, for the regular pentagon $p = ABCDE$ the associated homography f, mapping p to its diagonal $p' = A'B'C'D'E'$ coincides with an homothety. The fixed points of the homothety, from the projective viewpoint, are the center of the polygon and the line at infinity. Thus, in view of the previous results, and since in this case f has infinite many fixed points, the corresponding canonical representation, should map the regular polygon to the exceptional point

$$E_0(a_0, b_0) = \left(\frac{1}{2}, \frac{3+\sqrt{5}}{4}\right).$$

Figure 11 confirms this behavior. It illustrates how this special case corresponds to the exceptional point E_0.

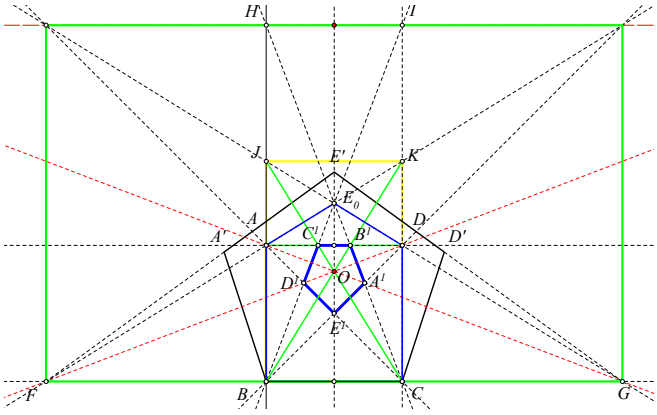

Figure 11. The exceptional class of regular pentagons

The figure shows the regular pentagon $p' = A'BCD'E'$ and its image $p = ABCDE_0$ under the homography fixing points B and C and mapping A' and D', correspondingly to A, D. It is easily seen that this homography maps also point E' to E_0, thus identifying the class of regular pentagons with the exceptional class in the sense explained above. The diagonal polygon $p^1 = A^1B^1C^1D^1E^1 = f(p)$ is constructed as usual and it is easily seen that f has an isolated fixed point O, which is the common point of all lines through $X, f(X)$. Indeed, in this case f coincides with a *homology* and as such has an isolated fixed point and a whole line of fixed points, represented in the figure by point O and line HI respectively. The figure reveals some simple relations concerning the locations of the fixed point and the fixed line of f with respect to the pentagon p. Rectangle $BCKJ$ is a *golden* one and point O is its center. The cross ratio $(FBBG) = (AC^1B^1D) = (BD^1C^1E_0)$ has the value of the golden section. Rectangle $ADIH$ results from $BCKJ$ and a parallel translation by BA. This and some other relations, suggested by the figure, are easily seen and are left as exercises. The discussion so far shows that the following theorem is true.

Theorem 14. *The class of pentagons which are projectively equivalent to the regular pentagon, is characterized by the fact that f is a homology, the ratio being necessarily equal to $-\frac{\sqrt{5}-1}{\sqrt{5}+1}$. It is also characterized as the only class of pentagons for which the lines which join X to $Y = f(X)$ pass all through a fixed point.*

6. Axial symmetric pentagons

There are some special classes of pentagons, for which their canonical representatives have point E lying on line e. I call them *axial symmetric*. They are characterized by the fact that line $e = E^1E^{-1}$, where $E^1 = AC \cap BD$ and $E^{-1} = AB \cap CD$, passes through E. Equivalently, the *harmonic homology* ([3,

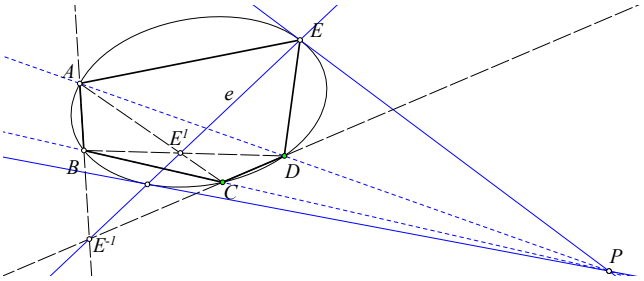

Figure 12. Axial symmetric pentagons

p.56]) whose fixed line is e and whose isolated fixed point P is the pole of e with respect to the circumconic of the pentagon, fixes E and interchanges the points of the pairs (A, D) and (B, C) (See Figure 12). By the canonical representation of §4 these pentagons correspond to points $E(a, b)$ with $a = \frac{1}{2}$. Thus their canonical forms are reflection-symmetric with respect to the axis $e(x = \frac{1}{2})$. The next theorem is an immediate consequence of the discussion so far.

Theorem 15. *Every class of projective equivalent axial symmetric pentagons corresponds to a unique point on the axis $e(x = \frac{1}{2})$. The class is uniquely determined by the value of the cross-ratio $E(ABCD)$.*

For all such pentagons, which are different from the exceptional one of §5, their corresponding homogrpahy f has the point at infinity W of line BC coinciding

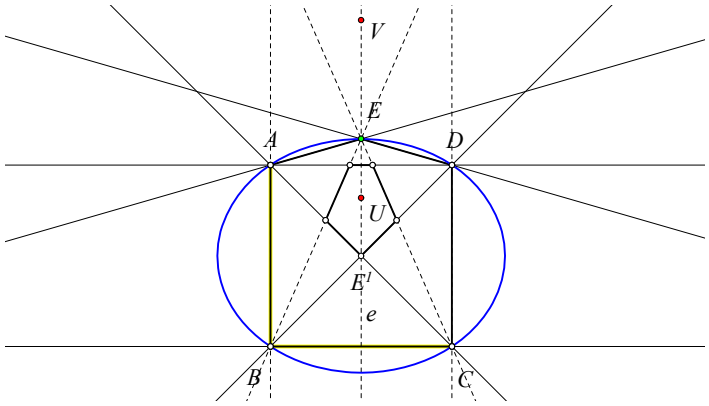

Figure 13. Canonical form of axial symmetric pentagons

with one of its fixed points, the other two fixed points U, V of f lying on line e (See Figure 13). From the representation of the homography given in §4, the coordinates of the fixed points are easily calculated and seen to be given by

$$U = \left(\frac{1}{2}, b^2 - c\right), \qquad V = \left(\frac{1}{2}, b^2 + c\right),$$

where $c = \sqrt{(b-1)((b+1)(b^2+1)+1))}$. Thus, in this case, the autopolar triangle UVW with respect to the circumconic of $ABCDE$, has one side coinciding with e and the other two coinciding respectively with the parallels to BC from U and V. Points U and V on line e are characterized by the fact that they are simultaneously harmonic conjugate with respect to the circumconic c of the pentagon and also with respect to the inconic $c_1 = g(c)$ of the pentagon.

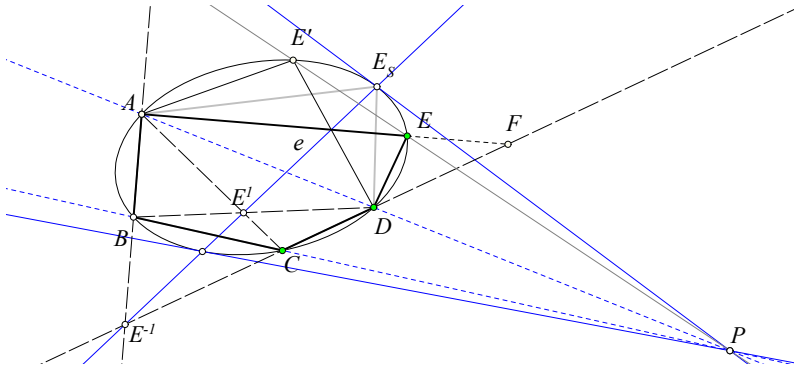

Figure 14. Generic pentagon $ABCDE$ and corresponding axial symmetric $ABCDE_S$

In the generic case of non axial symmetric pentagons $p = ABCDE$, the harmonic homology with respect to the line $e = E^1E^{-1}$ defines a projectively equivalent to p pentagon $p' = ABCDE'$ and an intersection point E_S of the line e with the circumconic c of p defines a corresponding axial symmetric pentagon $p_S = ABCDE_S$, such that the cross ratios are equal $E_S(ABCD) = E(ABCD)$. The location of E on the arc, say, DE_S of c is uniquely determined by the cross ratio $A(BCDE) = A(E^{-1}CDF)$, where $F = AE \cap CD$. Thus, as noticed in §4, the class of projectively equivalent pentagons to p is uniquely determined by the values of the two cross ratios $E(ABCD)$ and $A(BCDE)$.

Among the axial symmetric pentagons, the exceptional class of regular pentagons is also distinguished by the following simple feature.

Theorem 16. *The axial symmetric pentagon $ABCDE$, with axis passing through E, belongs to the class of the regular pentagons if and only if the cross-ratios $A(BCDE)$ and $E(ABCD)$ of two adjacent vertices are equal.*

The proof follows from a calculation of the equation resulting by equating the two ratios. It is seen that the locus of points defining such pentagons is a reducible cubic. One component of it consists of the ellipse c^*, which is tangent to lines CB, CD, respectively at B and D and passes through A. The other component of the cubic is the line AC. The ellipse c^* passes also through the exceptional point E_0 and defines the arc with endpoints E_0 and D lying in the domain of interest $\mathcal{M}$. The points of this arc are the only points of the domain $\mathcal{M}$ for which the equality of the cross ratio occurs. The theorem results from the fact that point E_0 is the only intersection point of this arc with the axis $e(x = \frac{1}{2})$.

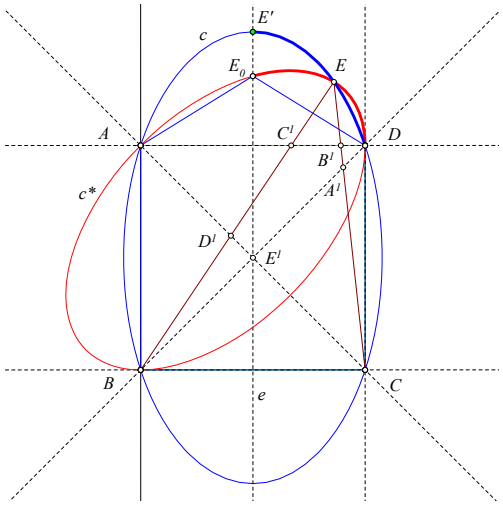

Figure 15. Geometric locus of equal ratios for adjacent vertices

Note that each one of the ellipses c, passing through points A, B, C, D, E' and representing, with their arcs falling into the domain $\mathcal{D}$, classes of pentagons with constant cross ratio $E'(ABCD)$, either do not intersect the arc E_0D of c^* or intersect it at one point E. The values v of the cross ratio for which there is an intersection point are easily seen to be all $v \leq g$, where g is the value of the golden ratio $g = \frac{\sqrt{5}+1}{2}$. They correspond to ellipses c, which intersect the axis e at a point lying higher than E_0. For all other values $v > g$ there are no polygons with two equal cross ratios for adjacent vertices. These values correspond to ellipses c that intersect the axis e at a point E' lying lower than E_0.

7. Autopolar conics

From the discussion in the previous paragraphs follows that for all pentagons, whose canonical representation $p = ABCDE$ has $E \neq E_0$, the corresponding homography f has three distinct real fixed points, which in the sequel are denoted by U, V, W.

Theorem 17. *For every pentagon, which is not projectively equivalent to a regular one, the three fixed points of the homography f build an autopolar triangle with respect to its circumconic and also with respect to its inscribed conic.*

The pentagon $p = ABCDE$ is considered in its canonical form, as this is described in §4. With the notation introduced in that section, and a standard computation in homogeneous coordinates, it is readily seen that the circumconic c and the inconic c' of the pentagon are represented correspondingly by the matrices

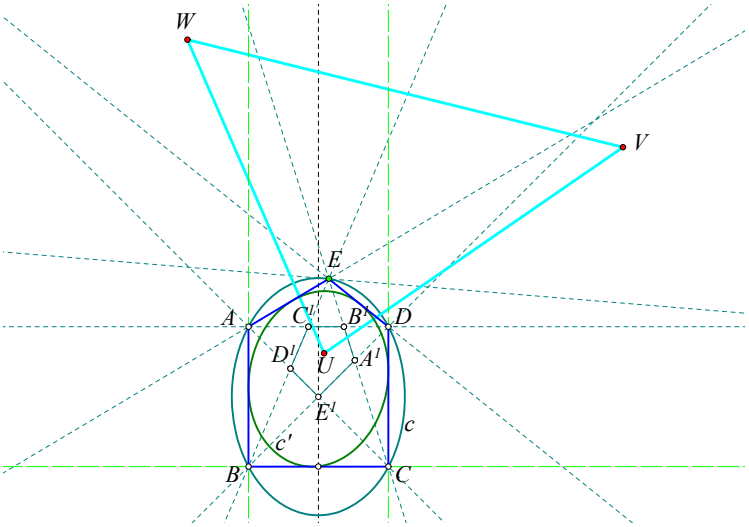

Figure 16. Autopolar triangle UVW of the fixed points of f

$$C = \begin{pmatrix} 2b(b-1) & 0 & b(1-b) \\ 0 & 2a(1-a) & a(a-1) \\ b(1-b) & a(a-1) & 0 \end{pmatrix},$$

$$C' = \begin{pmatrix} (2b-1)^2 & (1-2a)b & (a-b)(2b-1) \\ (1-2a)b & b^2 & b(a-b) \\ (a-b)(2b-1) & b(a-b) & (b-a)^2 \end{pmatrix}.$$

The proof for the inscribed conic is similar to that for the circumscribed conic of the pentagon, which reduces to a commutativity relation of matrices. The matrix C and the matrix F of §4, describing the homography f in the selected projective basis, are related by the following equation

$$C \cdot F = F^t \cdot C,$$

where F^t denotes the transposed of the matrix F. This is easily seen to imply that the polar line with respect to the circumconic c of every fixed point of f is an invariant line, which is equivalent to the statement of the theorem.

8. Reference to fixed points

In this section we assume that the pentagon $ABCDE$ is not an exceptional one i.e. it is not projectively equivalent to a regular pentagon. Under this assumption it seems appropriate to change to a coordinate system with basis points $U(1,0,0), V(0,1,0), W(0,0,1)$ and $E(1,1,1)$ coinciding respectively with the fixed points of the homography f and the centroid of triangle UVW. Using also an additional homography we may reduce the configuration to that of an equilateral triangle UVW and its centroid E. Next figure ilustrates some coincidences of points and lines, which lead to important conditions on the projectivities f and g.

The homography f is uniquely determined by the fact that it fixes points U, V, W

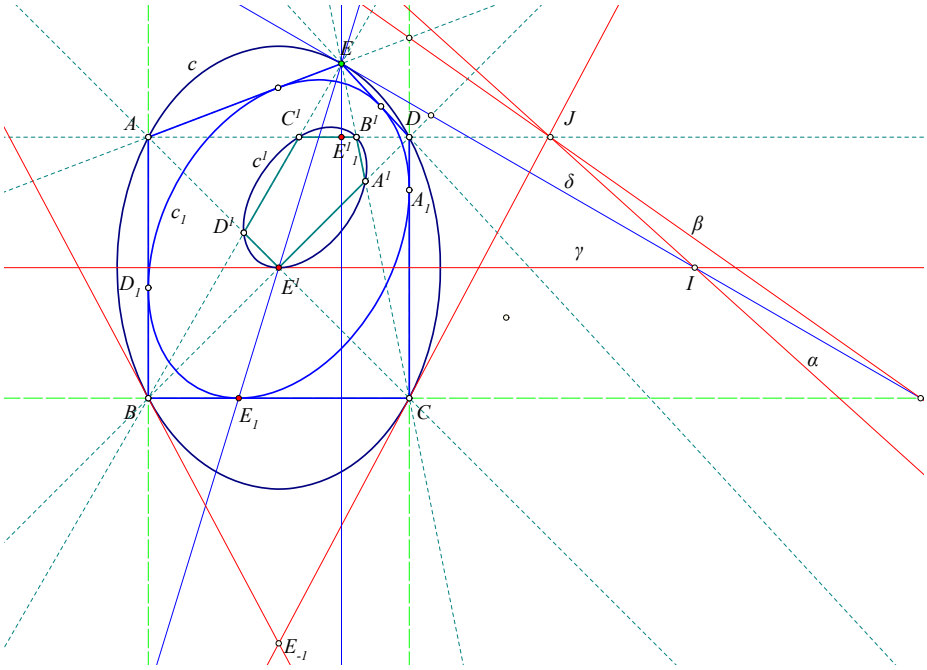

Figure 17. Coincidence relations

and maps point E to a certain point $E^1(k, l, m)$. In order to have a map with three isolated fixed points the numbers k, l and m must be non-zero and pairwise different. Homography g is determined in a similar way, by its property to fix the same points with f and mapping E to another point $E_1(k', l', m')$. By the previous discussion, points E^1, E_1 and E are collinear. Thus, we may assume that they are related by a linear relation of the form

$$E_1 = sE^1 + tE \quad \Longleftrightarrow \quad (k', l', m') = (\, s \cdot k + t,\ s \cdot l + t,\ s \cdot m + t).$$

Thus, the corresponding matrices, representing f and g, may then be assumed to be :

$$F = \begin{pmatrix} k & 0 & 0 \\ 0 & l & 0 \\ 0 & 0 & m \end{pmatrix} \quad \text{and} \quad G = \begin{pmatrix} s \cdot k + t & 0 & 0 \\ 0 & s \cdot l + t & 0 \\ 0 & 0 & s \cdot m + t \end{pmatrix}.$$

The circumconic c and the inscribed conic c_1 of the pentagon are autopolar with respect to the triangle UVW, hence they may be represented respectively in the form

$$(c)\ ax^2 + by^2 + cz^2 = 0 \quad \text{and} \quad (c_1)\ a'x^2 + b'y^2 + c'z^2 = 0.$$

By the previous discussion $c_1 = g(c)$. From this condition follows immediately that the coefficients (a', b', c') can be taken to be

$$(a', b', c') = \left(\frac{a}{(sk+t)^2}, \frac{b}{(sl+t)^2}, \frac{c}{(sm+t)^2} \right).$$

Since point $E(1,1,1)$ lies on c the coefficients of the conic must also satisfy

$$a + b + c = 0.$$

The following table contains the coordinate expressions of points, lines and conics which are relevant in subsequent verifications of coincidences (See Figure 17). These coincidences follow from the theory discussed so far or/and by performing appropriate calculations in coordinates. The symbol $p(X, c)$ denotes the polar of point X with respect to the conic c. When X is on c this coincides with its tangent at X.

kind	notation	coordinates
point	E	$(1,1,1)$
point	$E^1 = f(E)$	(k,l,m)
point	$E_1 = g(E)$	$(sk+t, sl+t, sm+t)$
point	$E_1^1 = g(f(E))$	$(k(sk+t), l(sl+t), m(sm+t))$
point	$E_{-1} = g^{-1}(E)$	$(1/(sk+t), ...)$
conic	c	(a,b,c)
conic	$c^1 = f(c)$	$(a/k^2, ...)$
conic	$c_1 = g(c)$	$(a/(sk+t)^2, ...)$
line	$\delta = p(E, c)$	(a,b,c)
line	$\alpha = p(E_1^1, c)$	$(ak(sk+t), ...)$
line	$\beta = p(E_1^1, c_1)$	$((ak)/(sk+t), ...)$
line	$\gamma = p(E^1, c^1)$	$(a/k, ...)$
line	$\zeta = p(E_1, c_1)$	$(a/(sk+t), ...)$
line	$\eta = E^1 E_1^1$	$((l-m)/k, ...)$
point	$I = \alpha \cap \gamma$	$(k(l-m))/a, ...)$
point	$J = \alpha \cap \beta$	$((m^2-l^2)(m+l+2k)/(ak), ...)$
point	$K = \gamma \cap \zeta$	$(k(l^2-m^2)/a, ...)$

The coincidence of lines $\alpha = p(E_1^1, c)$, $\delta = p(E, c)$ and $\gamma = p(E^1, c^1)$ at point I leads to a vanishing determinant whose value is

$$\frac{abc(l-k)(m-l)(k-m)(t+(m+l+k)s)}{klm}.$$

Since the constants k, l, m are pairwise different, and the conic assumed non-degenerate, this implies

$$t + (k+l+m) \cdot s = 0.$$

The three last equations of the table took into account this fact. Also in the process of reduction it is obvious that also the conditions

$$kl + lm + mk \neq 0 \quad \text{and} \quad k + l + m \neq 0$$

are valid.

The concurrence of lines E_1^1J, $\gamma = p(E^1, c^1)$ and $\zeta = p(E_1, c_1)$ at a point leads also to a vanishing determinant, which amounts to an equation of the form

$$a \cdot A + b \cdot B + c \cdot C = 0.$$

Here the coefficients are $A = k^2((m+l)^2+kl+lm+mk)$ and B, C result from the same formula by cyclically permuting k, l and m. Thus, the vector (a, b, c) satisfies the previous equation, as well as the condition $a + b + c = 0$. The two vectors $(1, 1, 1)$ and (A, B, C) are though dependent. This is proved by contradiction. In fact, if they were independent, the coefficients (a, b, c) would be a multiple of their vector product. But this is found to be a non-zero multiple of

$$((k + l + m)(kl + lm + mk) + klm) \begin{pmatrix} m - l \\ k - m \\ l - k \end{pmatrix}.$$

Thus if $((k+l+m)(kl+lm+mk)+klm)$ were non-zero, then the tangent line of the conic c at $E(1, 1, 1)$, which is given by $ax+by+cz = 0$ would be identical with the line EE^1, which is described by the equation $(m-l)x+(k-m)y+(l-k)z = 0$. But this is impossible. Hence the dependence of the two vectors and the vanishing of the factor. This proves the following theorem.

Theorem 18. *The coefficients (k, l, m) determining the homography f of a generic pentagon, referred to its basis of fixed points, with one of its vertices at $E(1, 1, 1)$, satisfy the cubic equation*

$$(x + y + z)(xy + yz + zx) + xyz = 0.$$

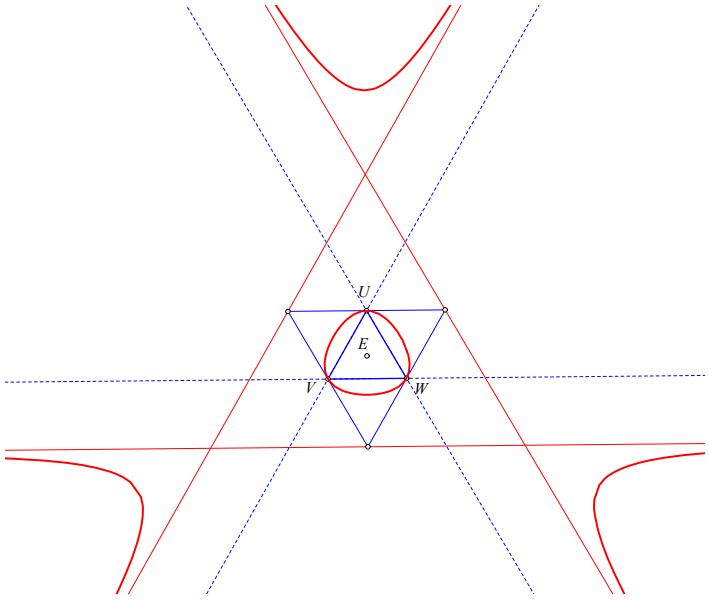

Figure 18. The cubic $(x + y + z)(xy + yz + zx) + xyz = 0$

References

[1] W. Burnside, *Theory of Equations*, Hodges, Figgis and Co., Dublin, 1886.
[2] M. Chasles, *Traite de Sections Coniques*, Gauthier-Villars, Paris, 1865.
[3] H. S. M. Coxeter, *The Real Projective Plane*, McGraw-Hill Book Company, Inc., New York, 1949.
[4] J. Dugundji, *Topology*, Allyn and Bacon Inc., Boston, 1966.
[5] L. Hofmann, Synthetic proof of professor Kassner's pentagon theorem, *Amer. Math. Monthly*, 35 (1928) 356–358.
[6] E. Kasner, A projective theorem on the plane pentagon, *Amer. Math. Monthly*, 35 (1928) 352–356.

Paris Pamfilos: University of Crete, Greece
E-mail address: pamfilos@math.uoc.gr

Forum Geometricorum
Volume 16 (2016) 227–232.

FORUM GEOM
ISSN 1534-1178

Regular Polytopic Distances

Poo-Sung Park

Abstract. Let M be an n-dimensional regular polytope of simplices, hypercubes, or orthoplexes and r be the circumscribed radius of M. If q^4 is the average of fourth powers of distances between a point and vertices of M and s^2 is the average of squares of those distances, then

$$q^4 + \frac{4(n+1)}{n^2} r^4 = \left(s^2 + \frac{2}{n} r^2 \right)^2 .$$

1. Introduction

In his book *Mathematical Circus*, Martin Gardner posed a beautifully symmetric formula satisfied by distances between an arbitrary point and vertices of an equilateral triangle. That is, if a, b, and c are the distances between a point P and three vertices of an equilateral triangle of side d, the relation

$$3(a^4 + b^4 + c^4 + d^4) = (a^2 + b^2 + c^2 + d^2)^2$$

holds (Figure 1).

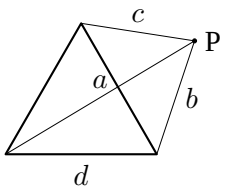

$3(a^4 + b^4 + c^4 + d^4)$
$= (a^2 + b^2 + c^2 + d^2)^2$

Figure 1. Equilateral triangle

This result was generalized in two ways by J. Bentin [1, 2]. One is about $(n-1)$-dimensional simplices of side d_0. In this case, if the n distances are denoted by $d_1, d_2, \ldots, d_n$, then

$$n(d_0^4 + d_1^4 + \cdots + d_n^4) = (d_0^2 + d_1^2 + \cdots + d_n^2)^2$$

holds (Figure 2).

Another way of Bentin's generalizations is about regular polygons. If we denote the average of fourth powers of distances by q^4 and the average of squares of distances by s^2, then

$$q^4 + 3r^4 = (s^2 + r^2)^2$$

Publication Date: May 23, 2016. Communicating Editor: Paul Yiu.

This research was supported by Basic Science Research Program through the National Research Foundation of Korea (NRF) funded by the Ministry of Education (NRF-2013R1A1A2010614).

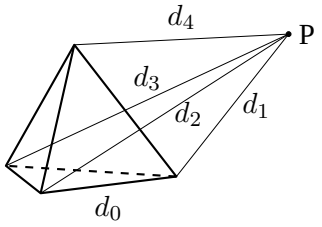

$$4(d_0^4 + d_1^4 + d_2^4 + d_3^4 + d_4^4) = (d_0^2 + d_1^2 + d_2^2 + d_3^2 + d_4^2)^2$$

Figure 2. Regular tetraheron

for arbitrary regular polygon of circumscribed radius r (Figure 3). This formula for equilateral triangles coincides with the above one introduced by Gardner.

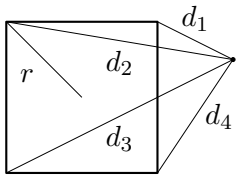

$$q^4 + 3r^4 = (s^2 + r^2)^2$$

Figure 3. Square

It is natural to ask whether similar formulas might be obtained for other regular polytopes. We can find ones for cubes and octahedrons. Besides, the results are extended to the higher dimension, that is, hypercubes and orthoplexes.

2. Main results

It is well known that there are only five regular polyhedrons. In dimension 4 there are 6 kinds of regular polytopes. But, dimension 5 or higher allows only three kinds of regular polytopes: n-simplex, n-cube, n-orthoplex. These regular polytopes are denoted by using Schläfli symbols (see [3]).

$$\begin{aligned}
n = 2: &\quad \{k\}, \text{where } k \geq 3 \text{ is an arbitrary integer} \\
n = 3: &\quad \{3,3\}, \{3,4\}, \{4,3\}, \{3,5\}, \{5,3\} \\
n = 4: &\quad \{3,3,3\}, \{3,3,4\}, \{4,3,3\}, \{3,4,3\}, \{3,3,5\}, \{5,3,3\} \\
n \geq 5: &\quad \{3^{d-1}\}, \{3^{d-2}, 4\}, \{4, 3^{d-2}\}
\end{aligned}$$

We find distance relations for n-simplex, n-cube, n-orthoplex with $n \geq 2$. Note that 2-simplex is an eqilateral triagle, 2-cube is a square, and 2-orthogonal is also a square.

Theorem 1. *For n-dimensional regular simplices, let q^4 be the average of fourth power of distances between $n+1$ vertices and a point and s^2 be the average of squares of those distances. If r is the circumscribed radius, then*

$$q^4 + \frac{4(n+1)}{n^2} r^4 = \left(s^2 + \frac{2}{n} r^2 \right)^2 .$$

Proof. Just restatement of Bentin's. □

Theorem 2. *For n-dimensional cubes, let q^4 be the average of fourth power of distances between 2^n vertices and a point and s^2 be the average of squares of those distances. If r is the circumscribed radius, then*

$$q^4 + \frac{4(n+1)}{n^2} r^4 = \left(s^2 + \frac{2}{n} r^2 \right)^2 .$$

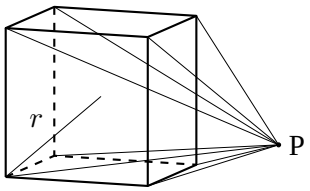

$$q^4 + \frac{16}{9} r^4 = \left(s^2 + \frac{2}{3} r^2 \right)^2$$

Figure 4. Cube

Proof. The number of vertices of an n-dimensional cube is 2^n. We may assume that the vertices are represented by $\pm a\mathbf{e}_1 \pm a\mathbf{e}_2 \pm \cdots \pm a\mathbf{e}_n$ in $\mathbb{R}^n$, where $\mathbf{e}_i$ is the elementary unit vector. Then the circumscribed radius is $r = \sqrt{n}a$.

Each vertex is determined by the sequence of 1 or -1. Using functions $\sigma_i : \{1, 2, \ldots, n\} \to \{1, -1\}$ for $i = 1, \ldots, 2^n$, we may write each vertex V_i as

$$(\sigma_i(1)a, \sigma_i(2)a, \ldots, \sigma_i(n)a) .$$

Let $P = (x_1, \ldots, x_n)$ and $\ell^2 = x_1^2 + \cdots + x_n^2$. Then,

$$\begin{aligned} d_i^2 = \|P - V_i\|^2 &= \sum_{k=1}^{n} (x_k - \sigma_i(k)a)^2 \\ &= \sum_{k=1}^{n} \left(x_k^2 - 2x_k\sigma_i(k)a + a^2 \right) \\ &= \ell^2 + na^2 - 2a \sum_{k=1}^{n} \sigma_i(k)x_k \end{aligned}$$

Summing up all d_i^2, we obtain

$$\begin{aligned} 2^n s^2 = d_1^2 + \cdots + d_{2^n}^2 &= \sum_{i=1}^{2^n} \left(\ell^2 + na^2 - 2a \sum_{k=1}^{n} \sigma_i(k)x_k \right) \\ &= 2^n(\ell^2 + na^2) - 2a \sum_{k=1}^{n} \sum_{i=1}^{2^n} \sigma_i(k)x_k. \end{aligned}$$

Since $\sum_{i=1}^{2^n} \sigma_i(k) = 0$,

$$ns^2 + 2r^2 = n(\ell^2 + na^2) + 2na^2 = n(\ell^2 + (n+2)a^2).$$

Now, consider d_i^4. Note that

$$\begin{aligned} d_i^4 &= \left(\ell^2 + na^2 - 2a\sum_{k=1}^{n}\sigma_i(k)x_k\right)^2 \\ &= \ell^4 + n^2a^4 + 4a^2\left(\sum_{k=1}^{n}\sigma_i(k)x_k\right)^2 \\ &\quad + 2\ell^2na^2 - 4na^3\sum_{k=1}^{n}\sigma_i(k)x_k - 4\ell^2a\sum_{k=1}^{n}\sigma_i(k)x_k. \end{aligned}$$

Then,

$$\begin{aligned} 2^nq^4 &= d_1^4 + \cdots + d_{2^n}^4 \\ &= 2^n\left(\ell^4 + n^2a^4 + 2\ell^2na^2\right) \\ &\quad + 4a^2\sum_{i=1}^{2^n}\left(\sum_{k=1}^{n}\sigma_i(k)x_k\right)^2 - (4na^3 + 4\ell^2a)\sum_{i=1}^{2^n}\sum_{k=1}^{n}\sigma_i(k)x_k. \end{aligned}$$

Since

$$\left(\sum_{k=1}^{n}\sigma_i(k)x_k\right)^2 = \sum_{k=1}^{n}x_k^2 + \sum_{k\neq j}\sigma_i(k)\sigma_i(j)x_kx_j$$

and

$$\sum_{i=1}^{2^n}\sigma_i(k)\sigma_i(j) = 0 \text{ with } j \neq k,$$

we obtain

$$2^nq^4 = 2^n(\ell^4 + n^2a^4 + 2\ell^2na^2 + 4a^2\ell^2)$$

and thus

$$\begin{aligned} n^2q^4 + 4(n+1)r^4 &= n^2(\ell^4 + n^2a^4 + 2\ell^2na^2 + 4a^2\ell^2) + 4(n+1)n^2a^4 \\ &= n^2(\ell^4 + n^2a^4 + 2\ell^2na^2 + 4a^2\ell^2 + 4(n+1)a^4) \\ &= n^2(\ell^4 + 2(n+2)\ell^2a^2 + (n+2)^2a^4) \\ &= (ns^2 + 2r^2)^2, \end{aligned}$$

which is the required result. □

Theorem 3. *For n-dimensional orthoplexes, let q^4 be the average of fourth power of distances between $2n$ vertices and a point and s^2 be the average of squares of those distances. If r is the circumscribed radius, then*

$$q^4 + \frac{4(n+1)}{n^2}r^4 = \left(s^2 + \frac{2}{n}r^2\right)^2.$$

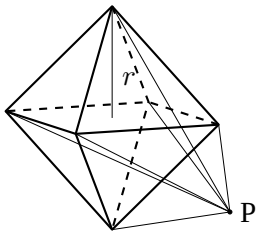

$$q^4 + \frac{16}{9}r^4 = \left(s^2 + \frac{2}{3}r^2\right)^2$$

Figure 5. Octahedron

Proof. An n-dimensional orthoplex has $2n$ vertices. We may assume that the vertices are represented by $V_{i,+} = a\mathbf{e}_i$ and $V_{i,-} = -a\mathbf{e}_i$ for $i = 1, 2, \ldots, n$. Then the circumscribed radius is $r = a$.

Let $P = (x_1, \ldots, x_n)$ and $\ell^2 = x_1^2 + \cdots + x_n^2$. Then,

$$\begin{aligned} d_{i,+}^2 &= \|P - V_{i,+}\|^2 \\ &= x_1^2 + \cdots + x_{i-1}^2 + (x_i - a)^2 + x_{i+1}^2 + \cdots + x_n^2 \\ &= x_1^2 + \cdots + x_{i-1}^2 + x_i^2 + x_{i+1}^2 + \cdots + x_n^2 - 2x_i a + a^2 \\ &= \ell^2 - 2x_i a + a^2 \end{aligned}$$

and

$$\begin{aligned} d_{i,-}^2 &= \|P - V_{i,-}\|^2 \\ &= x_1^2 + \cdots + x_{i-1}^2 + (x_i + a)^2 + x_{i+1}^2 + \cdots + x_n^2 \\ &= \ell^2 + 2x_i a + a^2 \end{aligned}$$

Thus,

$$2ns^2 = \sum_{i=1}^{n} (d_{i,+}^2 + d_{i,-}^2) = 2n\ell^2 + 2na^2$$

and

$$ns^2 + 2r^2 = n\ell^2 + na^2 + 2a^2 = n\ell^2 + (n+2)a^2.$$

Since

$$\begin{aligned} d_{i,+}^4 &= \left(\ell^2 - 2x_i a + a^2\right)^2 \\ &= \ell^4 + 4x_i^2 a^2 + a^4 - 4\ell^2 x_i a - 4x_i a^3 + 2\ell^2 a^2 \end{aligned}$$

and

$$\begin{aligned} d_{i,-}^4 &= \left(\ell^2 + 2x_i a + a^2\right)^2 \\ &= \ell^4 + 4x_i^2 a^2 + a^4 + 4\ell^2 x_i a + 4x_i a^3 + 2\ell^2 a^2, \end{aligned}$$

we obtain

$$\begin{aligned} 2nq^4 &= \sum_{i=1}^{n}(d_{i,+}^4 + d_{i,-}^4) \\ &= 2n\ell^4 + 8(x_1^2 + \cdots + x_n^2)a^2 + 2na^4 + 4n\ell^2a^2 \\ &= 2n\ell^4 + 8\ell^2a^2 + 2na^4 + 4n\ell^2a^2. \end{aligned}$$

Thus,

$$\begin{aligned} n^2q^4 + 4(n+1)r^4 &= n^2\ell^4 + 4n\ell^2a^2 + n^2a^4 + 2n^2\ell^2a^2 + 4(n+1)a^4 \\ &= n^2\ell^4 + 2n\ell^2(n+2)a^2 + (n+2)^2a^4 \\ &= (ns^2 + 2r^2)^2. \end{aligned}$$

We are done. □

References

[1] J. Bentin, Regular simplicial distances, *Math. Gaz.* **79**(March 1995), p. 106.
[2] J. Bentin, Regular polygonal distances, *Math. Gaz.* **81**(July 1997), pp. 277–279.
[3] H.S.M.Coxeter, *Regular Polytopes*, Dover Publications Inc., New York 1973.

Poo-Sung Park: Department of Mathematics Education, Kyungnam University, Changwon-si, 631-701, Republic of Korea
E-mail address: pspark@kyungnam.ac.kr

Forum Geometricorum
Volume 16 (2016) 233–239.

FORUM GEOM
ISSN 1534-1178

Area of the Orthic Quadrilaterals of a Convex Cyclic Orthodiagonal Quadrilateral

Grégoire Nicollier

Abstract. Among all orthic quadrilaterals inscribed in a given convex cyclic orthodiagonal quadrilateral, the orthic quadrilateral of the side midpoint rectangle has the largest area. We give here a short and simple proof of this recently established fact by describing the orthic quadrilaterals, inscribed or not, as a symmetric difference of orthic triangles and computing their area.

1. Introduction

We consider a convex cyclic orthodiagonal quadrilateral $\mathcal{Q} = ABCD$ (Figure 1). Its perpendicular diagonals AC and BD intersect at O. We set $OA = a$, $OB = b$, $OC = c$, and $OD = d$. Let $\mathcal{R} = KLMN$ be a rectangle with sides parallel to the diagonals of $\mathcal{Q}$ and vertices K, L, M, and N on the sidelines AB, BC, CD, and DA of $\mathcal{Q}$, respectively. The orthogonal projections of the vertices of $\mathcal{R}$ on the opposite sidelines of $\mathcal{Q}$ generate the *orthic quadrilateral* $\mathcal{R}^* = K^*L^*M^*N^*$ of $\mathcal{R}$. $\mathcal{R}$ and $\mathcal{R}^*$ are concyclic [1]. The *principal* orthic quadrilateral $\mathcal{R}_p^*$ is the orthic quadrilateral of the side midpoint rectangle. It was conjectured in [1] and proven recently in [2] that the principal orthic quadrilateral has the largest area among the orthic quadrilaterals $\mathcal{R}^*$ *inscribed* in $\mathcal{Q}$ (this restriction is missing in [2] although it is necessary since the area of $\mathcal{R}^*$ tends to infinity as K moves away from $\mathcal{Q}$ on the sideline AB). We give here another (simpler, shorter, and more enlightening) proof of this result by describing the orthic quadrilaterals, inscribed or not, as a symmetric difference of orthic triangles and computing their area.

We consider the diagonals as the axes of a Cartesian coordinate system with origin O and $A = (a, 0)$, $B = (0, b)$. We set $K = (x, y)$ on the line AB, which implies $y = b(1 - x/a)$, and write $\mathcal{R} = \mathcal{R}(x)$, $\mathcal{R}^* = \mathcal{R}^*(x)$. The solution for $a = b = c = d$ is immediate: $\mathcal{Q}$ is a square, $\mathcal{R}^*(x)$ is $\mathcal{R}(x)$ rotated by $\pi/2$ of area $4|x(x - a)|$. From now on we suppose $a < c$ and $b \le d$ without loss of generality.

2. The orthic quadrilateral of a diagonal

Let $\mathcal{R}_v^* = K_v^*L_v^*M_v^*N_v^*$ be the orthic quadrilateral of the *vertical* diagonal $\mathcal{R}_v = \mathcal{R}(0) = BBDD$ (Figure 2). Triangle BCD is acute as $a < c$. The orthic triangle of BCD is $K_v^*ON_v^*$. By a well-known property of the orthocenter, A

Publication Date: June 2, 2016. Communicating Editor: Paul Yiu.

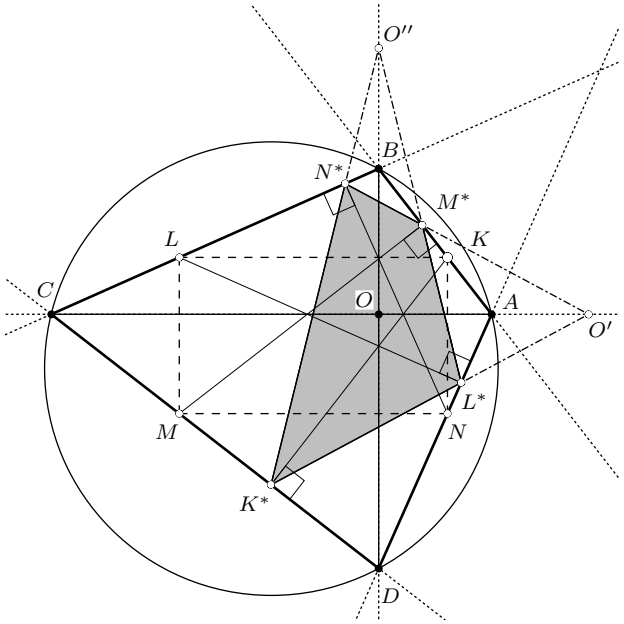

Figure 1. Inscribed orthic quadrilateral $\mathcal{R}^* = K^*L^*M^*N^*$ generated by rectangle $\mathcal{R} = KLMN$

is the reflection of the orthocenter H in the line BD. The reflection in the line BD maps thus the lines of the altitudes BK_v^* and DN_v^* of triangle BCD to the sidelines BA and DA of triangle BAD, respectively, and the sidelines BC and DC of BCD to the altitudes BL_v^* and DM_v^* of BAD. The reflections of K_v^* and N_v^* in the line BD are hence M_v^* and L_v^*, respectively. As the altitudes of a triangle are the angle bisectors of its orthic triangle, the points K_v^*, O, and L_v^* are collinear, as are the points M_v^*, O, and N_v^*. The following theorem is proven (Figures 2 and 3).

Theorem 1. *The orthic quadrilateral $\mathcal{R}_v^* = K_v^*L_v^*M_v^*N_v^*$ of the diagonal $\mathcal{R}_v = BBDD$ is symmetric in the diagonal BD. The sides $K_v^*L_v^*$ and $M_v^*N_v^*$ intersect at O. Triangles $K_v^*ON_v^*$ and $L_v^*OM_v^*$ are the orthic triangles of BCD and BAD, respectively. The orthic quadrilateral of the other diagonal has similar properties.*

By well-known formulæ, $\mathcal{Q}$ and triangle BCD have the circumdiameter

$$2\rho = \sqrt{AB^2 + CD^2} = \sqrt{BC^2 + DA^2} = \sqrt{a^2 + b^2 + c^2 + d^2} \tag{1}$$

and the area of the orthic triangle of (any triangle) BCD is

$$\frac{1}{2\rho} BC \cdot CD \cdot DB \cdot \left| \cos \widehat{CDB} \cos \widehat{DBC} \cos \widehat{BCD} \right| . \tag{2}$$

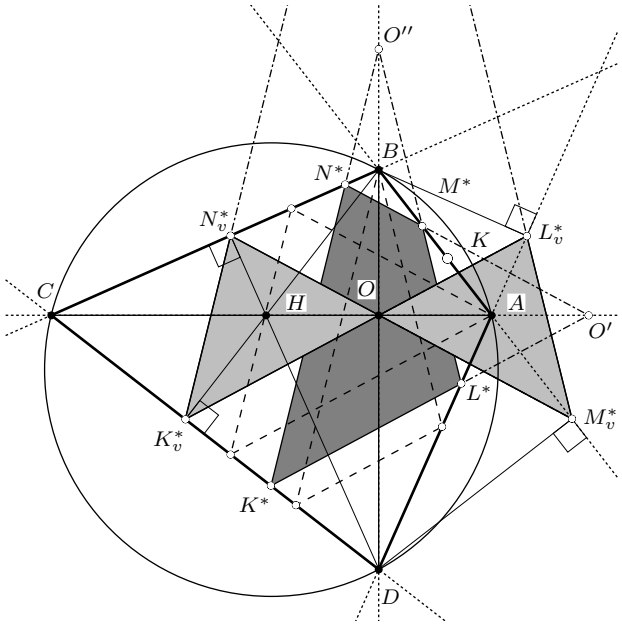

Figure 2. Orthic quadrilateral $\mathcal{R}_v^* = K_v^* L_v^* M_v^* N_v^*$ generated by the diagonal $BBDD$; first and last inscribed orthic quadrilaterals (dashed)

Remember that $ac = bd$ by the inscribed angle theorem. By expressing the sides of triangle BCD with b, c, d and using the cosine rule, one obtains

$$\cos \widehat{BCD} = \frac{c^2 - bd}{BC \cdot CD} = \frac{c(c-a)}{BC \cdot CD}. \tag{3}$$

Using (1)–(3), one finds easily for $a < c$

$$\operatorname{area}(\mathcal{R}_v^*) = \frac{2ac^2(c-a)(b+d)}{\sqrt{a^2+b^2+c^2+d^2}\sqrt{b^2+c^2}\sqrt{c^2+d^2}}. \tag{4}$$

3. Construction of $\mathcal{R}^*$ from homothetic copies of the halves of $\mathcal{R}_v^*$

We denote the homothety of ratio λ about P by $\mathsf{h}(P, \lambda)$ and refer to Figures 1 and 2.

Theorem 2. *Suppose $a < c$.*

(1) *The vertices of $\mathcal{R}(x)$ are the images of the vertices B and D of $\mathcal{R}_v = \mathcal{R}(0)$ under the homotheties $\mathsf{h}(A, 1 - x/a)$ for K and N and $\mathsf{h}(C, 1 - x/a)$ for L and M.*

(2) *The vertices K^* and N^* of $\mathcal{R}^*(x)$ are the images of the vertices K_v^* and N_v^* of $\mathcal{R}_v^*$ under the homothety $\mathsf{h}\big(C, 1 + 2x/(c-a)\big)$. The vertices L^* and M^* are the images of L_v^* and M_v^* under $\mathsf{h}\big(A, 1 - 2cx/(a(c-a))\big)$. The self-intersection point O of $\mathcal{R}_v^*$ has the same image O' under both homotheties: the sidelines K^*L^* and M^*N^* intersect thus at O'.*

(3) *The orthic quadrilateral $\mathcal{R}^*$ is the closure of the symmetric difference of triangles $K^*O'N^*$ and $L^*O'M^*$, which are the orthic triangles of the images of BCD and BAD under the respective homotheties.*

Proof. We only prove the assertion about K^* (the other assertions have similar proofs or are almost immediate). Using (3), one obtains

$$CK_v^* = BC\cos\widehat{BCD} = \frac{c(c-a)}{CD}. \tag{5}$$

The cosine angle difference identity gives

$$\begin{aligned}&\cos\left(\widehat{BAO} - \widehat{OCD}\right)\\ &= \cos\left(\arctan\frac{b}{a} - \arctan\frac{d}{c}\right) = \frac{ac+bd}{AB\cdot CD} = \frac{2ac}{AB\cdot CD}.\end{aligned} \tag{6}$$

As $BK = BA\cdot x/a$, one has by (6)

$$K_v^*K^* = BK\cos\left(\widehat{BAO} - \widehat{OCD}\right) = \frac{2cx}{CD} \tag{7}$$

and by (5) and (7)

$$\frac{CK^*}{CK_v^*} = 1 + \frac{K_v^*K^*}{CK_v^*} = 1 + \frac{2x}{c-a}. \qquad \square$$

Theorem 3. *Suppose $a < c$ and $b \le d$. The orthic quadrilateral $\mathcal{R}^*(x)$ is then inscribed in the convex cyclic orthodiagonal quadrilateral $\mathcal{Q}$ if and only if*

$$\left(1 - \frac{a}{c}\right)\frac{a}{2} \le x \le \left(1 + \frac{b}{d}\right)\frac{a}{2}.$$

On this interval, the area of $\mathcal{R}^*(x)$ is

$$\operatorname{area}(\mathcal{R}_v^*)\,\frac{2(c+a)}{a^2(c-a)}x(a-x) \tag{8}$$

– see (4) *– and attains its maximal value for the principal orthic quadrilateral $\mathcal{R}_p^* = \mathcal{R}^*(a/2)$:*

$$\operatorname{area}\left(\mathcal{R}_p^*\right) = \frac{c+a}{2(c-a)}\operatorname{area}(\mathcal{R}_v^*) = \frac{ac^2(a+c)(b+d)}{\sqrt{a^2+b^2+c^2+d^2}\sqrt{b^2+c^2}\sqrt{c^2+d^2}}. \tag{9}$$

Proof. We set $\operatorname{area}(\mathcal{R}_v^*) = \mu_v$ and refer to Figure 2. As long as $\mathcal{R}^*$ is inscribed in $\mathcal{Q}$, its area equals

$$\operatorname{area}\left(K^*O'N^*\right) - \operatorname{area}\left(L^*O'M^*\right) = \frac{\mu_v}{2}\left(1 + \frac{2x}{c-a}\right)^2 - \frac{\mu_v}{2}\left(1 - \frac{2cx}{a(c-a)}\right)^2$$

by Theorems 1 and 2. $\mathcal{R}^*$ is inscribed for the first time in $\mathcal{Q}$ when $L^*O'M^*$ collapses to A, that is, for $x = (1 - a/c)\cdot a/2$. And $\mathcal{R}^*$ is inscribed for the last time in $\mathcal{Q}$ when M^* and N^* coincide with B: this is the case for $y = (1 - b/d)\cdot b/2$, which is the vertical version of $x = (1 - a/c)\cdot a/2$, where $y = b(1 - x/a)$ is the ordinate of K, that is, when $x = (1 + b/d)\cdot a/2$. $\square$

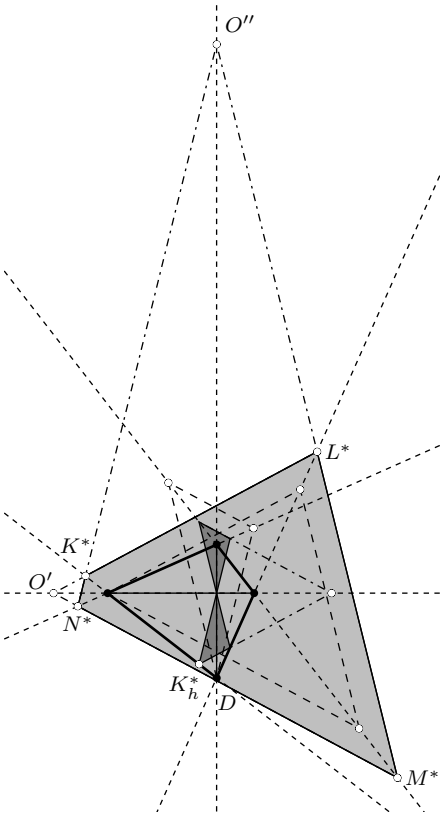

Figure 3. $\mathcal{R}_h^* = K_h^* L_h^* M_h^* N_h^*$ generated by the diagonal $ACCA$ and three other orthic quadrilaterals

Remark. $\mathcal{R}_v^*$ has a larger area than the principal orthic quadrilateral if and only if $c > 3a$.

4. Area of the orthic quadrilaterals

We show that the area of $\mathcal{R}^*(x)$ is a piecewise quadratic polynomial in x. We suppose $a < c$, $b < d$ and set $\mathcal{R}_h^* = \mathcal{R}^*(a)$, the orthic quadrilateral of the *horizontal* diagonal $\mathcal{R}_h = \mathcal{R}(a) = ACCA$ (Figure 3): $\mu_h = \operatorname{area}(\mathcal{R}_h^*)$ is obtained from (4) by interchanging a and b as well as c and d. As $ac = bd$, Theorem 3 and a direct calculation starting from the two versions of (4) show that

$$2\operatorname{area}\left(\mathcal{R}_p^*\right) = \frac{c+a}{c-a}\operatorname{area}(\mathcal{R}_v^*) = \frac{d+b}{d-b}\operatorname{area}(\mathcal{R}_h^*)\,. \tag{10}$$

Theorem 2 can be reformulated for $\mathcal{R}^*(x)$, $\mathcal{R}_h$, $\mathcal{R}_h^*$, and $y = b(1 - x/a)$ with homotheties

$$\mathsf{h}\big(D,\, 1 + 2y/(d-b)\big) \quad \text{and} \quad \mathsf{h}\big(B,\, 1 - 2dy/(b(d-b))\big)$$

and a common image O'' of O on the line BD (Figures 2 and 3). $\mathcal{R}^*$ is the closure of the symmetric difference of triangles $K^*O''L^*$ and $M^*O''N^*$ as well as of $K^*O'N^*$ and $L^*O'M^*$.

As long as O' is on the left of C, for $x \leq (a-c)/2$, triangle $K^*O'N^*$ is the tip of triangle $L^*O'M^*$ (Figure 3): the area of their symmetric difference is thus given by (8) with opposite sign.

For x from $(a-c)/2 = (1-c/a)\cdot a/2$ to $(1-a/c)\cdot a/2$, where $O' = A$ (Figure 2), the two triangles share only O' and their areas have to be added. Then, until $O'' = B$ (Figure 2), the orthic quadrilateral is inscribed in $\mathcal{Q}$ and its area is given by (8).

For O'' below B (Figure 3), the area of the symmetric difference of $K^*O'N^*$ and $L^*O'M^*$ is

$$\operatorname{area}\left(K^*O''L^*\right)+\operatorname{area}\left(M^*O''N^*\right) = \frac{\mu_h}{2}\left(1+\frac{2y}{d-b}\right)^2+\frac{\mu_h}{2}\left(1-\frac{2dy}{b(d-b)}\right)^2$$

from $x = (1+b/d)\cdot a/2$, $y = (1-b/d)\cdot b/2$ to $y = (b-d)/2 = (1-d/b)\cdot b/2$, $x = (1+d/b)\cdot a/2$ when O'' reaches D (Figure 3).

For $y < (b-d)/2$, when O'' is below D, triangle $K^*O''L^*$ is the tip of $M^*O''N^*$ and $\operatorname{area}(\mathcal{R}^*) = -\operatorname{area}(K^*O''L^*) + \operatorname{area}(M^*O''N^*)$.

If $b = d$, the area of $\mathcal{R}^*(x)$ for $x \geq a$, after the inscribed cases, is again given by (8) with opposite sign. Using (8) and (10), the results can now be simplified and summarized. With the change of variable $x = \xi a/2$ one obtains a further simplification by considering the *normalized area* of $\mathcal{R}^*(\xi a/2)$ given by

$$\frac{\operatorname{area}\left(\mathcal{R}^*(\xi a/2)\right)}{\operatorname{area}\left(\mathcal{R}_p^*\right)}.$$

(We leave the details to the reader!)

Theorem 4. *For $a \leq c$ and $b \leq d$, the normalized area of $\mathcal{R}^*(\xi a/2)$ is* (Figure 4)

$$\frac{\operatorname{area}\left(\mathcal{R}^*(\xi a/2)\right)}{\operatorname{area}\left(\mathcal{R}^*(a/2)\right)} = \begin{cases} \dfrac{c-a}{c+a}\left(\dfrac{c^2+a^2}{(c-a)^2}\xi^2-2\xi+2\right), & 1-\dfrac{c}{a} < \xi < 1-\dfrac{a}{c} \\ \dfrac{d+b}{d-b}\left(\dfrac{d^2+b^2}{(d+b)^2}\xi^2-2\xi+2\right), & 1+\dfrac{b}{d} < \xi < 1+\dfrac{d}{b} \\ \left|\xi^2-2\xi\right|, & \textit{otherwise.} \end{cases}$$

(*The first interval, whose endpoints correspond to $O' = C$ and $O' = A$, is empty for $a = c$. The second interval, whose endpoints correspond to $O'' = B$ and $O'' = D$, is empty for $b = d$. The area of $\mathcal{R}^*(a/2) = \mathcal{R}_p^*$ is given by* (9).)

The area of $\mathcal{R}^*(\xi a/2)$ is thus a piecewise quadratic polynomial in ξ that is differentiable everywhere except at $\xi = 0$ when $a = c$ ($\mathcal{R}_v^*$ degenerates) and at $\xi = 2$ when $b = d$ ($\mathcal{R}_h^*$ degenerates). The normalized area is $2\xi - \xi^2$ exactly when the orthic quadrilateral is inscribed in $\mathcal{Q}$. The normalized area is further strictly greater than $\left|\xi^2-2\xi\right|$ on the intervals $1-c/a < \xi < 1-a/c$ and $1+b/d < \xi < 1+d/b$,

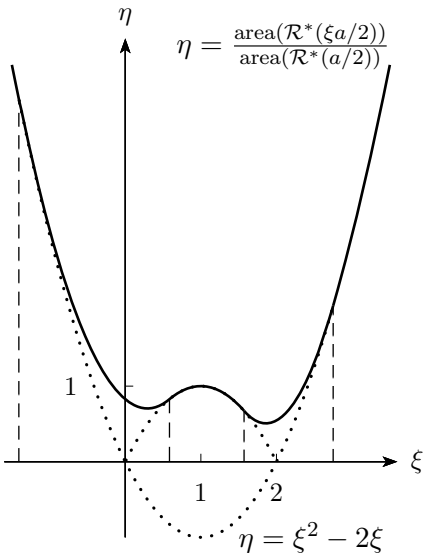

Figure 4. Normalized area of the orthic quadrilaterals for the convex orthodiagonal quadrilateral whose unit circumcircle is centered at $\left(-\frac{2}{5}, -\frac{1}{4}\right)$: c, $a = \frac{\sqrt{15}}{4} \pm \frac{2}{5}$ and d, $b = \frac{\sqrt{21}}{5} \pm \frac{1}{4}$

its two local minima are

$$\frac{c^2 - a^2}{c^2 + a^2} \quad \text{at} \quad \xi = \frac{(c-a)^2}{c^2 + a^2} \quad \text{and} \quad \frac{d^2 - b^2}{d^2 + b^2} \quad \text{at} \quad \xi = \frac{(d+b)^2}{d^2 + b^2},$$

and its unique local maximum corresponds to the principal orthic quadrilateral.

References

[1] M. F. Mammana, B. Micale, and M. Pennisi, Orthic quadrilaterals of a convex quadrilateral, *Forum Geom.*, 10 (2010) 79–91.

[2] F. Pierro and G. Vincenzi, On a conjecture referring to orthic quadrilaterals, *Beitr. Algebra Geom.*, 57 (2016) 441–451.

Grégoire Nicollier: University of Applied Sciences of Western Switzerland, Route du Rawyl 47, CH–1950 Sion, Switzerland

E-mail address: gregoire.nicollier@hevs.ch

Forum Geometricorum
Volume 16 (2016) 241–248.

FORUM GEOM
ISSN 1534-1178

Cevian Projections of Inscribed Triangles and Generalized Wallace Lines

Gotthard Weise

Abstract. Let $\Delta = ABC$ be a reference triangle and $\Delta' = A'B'C'$ an inscribed triangle of Δ. We define the cevian projection of Δ' as the cevian triangle Δ_P of a certain point P. Given a point P not on a sideline, all inscribed triangles with common cevian projection Δ_P form a family $\mathcal{D}_P = \{\Delta(t) = A_tB_tC_t,\ t \in \mathbb{R}\}$. The parallels of the lines AA_t, BB_t, CC_t through any point of a certain circumconic $\mathcal{C}_P$ intersect the sidelines a, b, c in collinear points X, Y, Z, respectively. This is a generalization of the well-known theorem of Wallace.

1. Notations

Let $\Delta = ABC$ be a positive oriented reference triangle with the sidelines a, b, c. A point P in the plane of Δ is described by its homogeneous barycentric coordinates u, v, w in reference to Δ: $P = (u : v : w)$, a line $\ell : ux+vy+wz = 0$ by $\ell = [u : v : w]$.

For a point $P = (u : v : w)$ not on a sideline, denote by $\Delta_P = P_aP_bP_c$ its cevian triangle with the vertices

$$P_a = (0 : v : w), \quad P_b = (u : 0 : w), \quad P_c = (u : v : 0), \tag{1}$$

and the sidelines

$$p_a = [-vw : wu : uv], \quad p_b = [vw : -wu : uv], \quad p_c = [vw : wu : -uv]. \tag{2}$$

The directions of these sidelines (as points of intersection with the infinite line) are

$$\begin{aligned} L_a &= (u(v-w) : -v(w+u) : w(u+v)) \\ L_b &= (u(v+w) : v(w-u) : -w(u+v)) \\ L_c &= (-u(v+w) : v(w+u) : w(u-v)) \,. \end{aligned} \tag{3}$$

The medial operator m on points maps P to the point

$$mP = (v+w : w+u : u+v) =: \ M \tag{4}$$

so that the centroid G divides the segment PM in the ratio $2 : 1$ (see, for example, [4]).

Publication Date: June 2, 2016. Communicating Editor: Paul Yiu.

Thanks are due to Paul Yiu for his lively interest in the paper, for valuable suggestions and especially for the examples in section 3.

The circumconic $pyz+qzx+rxy=0$ with perspector $(p:q:r)$ has the center

$$(p(q+r-p):q(r+p-q):r(p+q-r)) \tag{5}$$

(see, for example, [5]).

2. Cevian projection of an inscribed triangle

Let $\mathcal{T}$ be the set of all inscribed triangles $\Delta' = A'B'C'$ and $\mathcal{T}_{\text{cev}}$ the set of all cevian triangles of Δ. We define a map $\text{cevpro} : \mathcal{T} \to \mathcal{T}_{\text{cev}}$ with $\text{cevpro}(\Delta') = \Delta_P$ by the following geometrical construction.

Construction 1. *Given an inscribed triangle $\Delta' = A'B'C'$, which is not perspective to Δ, suppose the lines AA', BB', CC' bound a nondegenerate triangle $\Delta^* := A^*B^*C^*$ (with $A^* = BB' \cap CC'$ etc). The parallels of the sidelines a^*, b^*, c^* of Δ^* through A^*, B^*, C^* intersect a, b, c at the points A'', B'', C'', respectively. Let P_a, P_b, P_c be the midpoints of the segments $A'A''$, $B'B''$, $C'C''$. We define* $\text{cevpro}(\Delta') := P_aP_bP_c$*, and call it the* cevian projection *of* Δ' (see Figure 1).

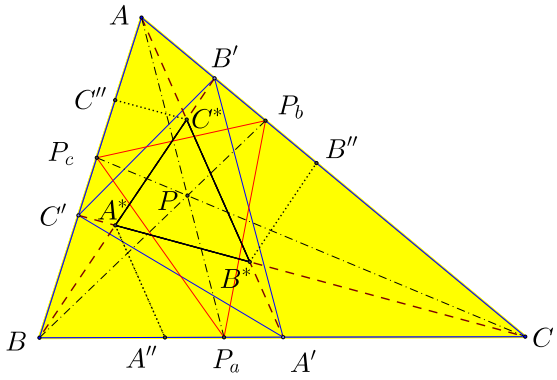

Figure 1

Proposition 2. *If $A'B'C'$ is not a cevian triangle, $P_aP_bP_c$ is a cevian triangle, i.e., the lines AP_a, BP_b, CP_c are concurrent.*

Proof. Let us describe the vertices of Δ' by homogeneous barycentric coordinates:

$$A' = (0:d:1-d), \quad B' = (1-e:0:e), \quad C' = (f:1-f:0), \tag{6}$$

for real numbers d, e, f. From this it follows

$$AA' = a^* = [0:d-1:d], \quad BB' = b^* = [e:0:e-1], \quad CC' = c^* = [f-1:f:0], \tag{7}$$

and

$$\begin{aligned} A^* &= BB' \cap CC' = (f(1-e):(1-e)(1-f):ef) \\ B^* &= CC' \cap AA' = (fd:d(1-f):(1-f)(1-d)) \\ C^* &= AA' \cap BB' = ((1-d)(1-e):de:e(1-d)) \,. \end{aligned} \tag{8}$$

The directions of a^*, b^*, c^* are the infinite points

$$L_{a^*} = (1 : -d : d-1), \quad L_{b^*} = (e-1 : 1 : -e), \quad L_{c^*} = (-f : f-1 : 1). \tag{9}$$

With the abbreviations

$$p = 1 - e + ef, \quad q = 1 - f + fd, \quad r = 1 - d + de, \tag{10}$$

the parallels of a^*, b^*, c^* through A^*, B^*, C^* respectively, have the representation[1]

$$\begin{aligned} l_{A^*} &= A^*L_{a^*} = [\odot : -fr : (1-e)q] \\ l_{B^*} &= B^*L_{b^*} = [(1-f)r : \odot : -dp] \\ l_{C^*} &= C^*L_{c^*} = [-eq : (1-d)p : \odot]. \end{aligned} \tag{11}$$

They intersect a, b, c at the points

$$\begin{aligned} A'' &= (0 : (1-e)q : fr)\,, \\ B'' &= (dp : 0 : (1-f)r)\,, \\ C'' &= ((1-d)p : eq : 0)\,. \end{aligned} \tag{12}$$

As midpoints of the segments $A'A''$, $B'B''$, $C'C''$ we obtain

$$\begin{aligned} P_a &= (0 : p + (q-r) : p - (q-r))\,, \\ P_b &= (q - (r-p) : 0 : q + (r-p))\,, \\ P_c &= (r + (p-q) : r - (p-q) : 0)\,, \end{aligned} \tag{13}$$

and the lines AP_a, BP_b, CP_c are

$$\begin{aligned} AP_a &= [0 : -p + (q-r) : p + (q-r)]\,, \\ BP_b &= [q + (r-p) : 0 : -q + (r-p)] \\ CP_c &= [-r + (p-q) : r + (p-q) : 0]\,. \end{aligned} \tag{14}$$

It is obvious that the column sums of $\det(AP_a, BP_b, CP_c)$ vanish. Thus, the lines are concurrent at the point

$$\begin{aligned} P &= \left(\frac{1}{q+r-p} : \frac{1}{r+p-q} : \frac{1}{p+q-r}\right) \\ &= \left(p^2 - (q-r)^2 : q^2 - (r-p)^2 : r^2 - (p-q)^2\right). \end{aligned} \tag{15}$$

Triangle $P_aP_bP_c$ is the cevian triangle of P. □

3. Examples

Construction 1 does not apply when the inscribed triangle $A'B'C'$ is a cevian triangle. Now, $A'B'C'$ is a cevian triangle if and only if $(1-d)(1-e)(1-f) = def$. If $A'B'C'$ is the cevian triangle of Q, then formulas (15) and (10) give $P = Q$.

[1] $\odot$ means: There is no necessity to calculate this coordinate.

3.1. *Cevian projection of a pedal triangle.* Let $Q = (x : y : z)$ be a point not on the Darboux cubic ($K004$ in [1])

$$\sum_{\text{cyclic}} (S_{AB} + S_{CA} - S_{BC})x(c^2y^2 - b^2z^2) = 0$$

so that its pedal triangle $A'B'C'$ is not a cevian triangle. The cevian projection of $A'B'C'$ is the cevian triangle of the point

$$P = \left(\frac{1}{f(x,y,z)} : \frac{1}{f(y,z,x)} : \frac{1}{f(z,x,y)}\right),$$

where

$$f(x,y,z) = S^2(a^2yz + b^2zx + c^2xy) + 2a^2(S_Ay + b^2z)(S_Az + c^2y).$$

If Q lies on the Darboux cubic and $A'B'C'$ is the cevian triangle of P', then formulas (15) and (10) gives $P = P'$.

3.2. *Cevian projection of a degenerate inscribed triangle.* Since we do not assume $A'B'C'$ to be a cevian triangle, $A^*B^*C^*$ is perspective with ABC if and only if $(1-d)(1-e)(1-f) = -def$, i.e., the triangle $A'B'C'$ is degenerate. If the line containing A', B', C' is the trilinear polar of a point $Q = (x : y : z)$, then
(i) $A^*B^*C^*$ is the anticevian triangle of Q,
(ii) A'', B'', C'' are collinear, and the line containing them is the trilinear polar of the cevian quotient $G/Q = (x(y+z-x) : y(z+x-y) : z(x+y-z))$,
(iii) $P_aP_bP_c$ is the cevian triangle of the point P with homogeneous barycentric coordinates $\left(\frac{x}{y-z} : \frac{y}{z-x} : \frac{z}{x-y}\right)$, which is the fourth intersection of the circumconics with centers Q and G/Q (see Figure 2).

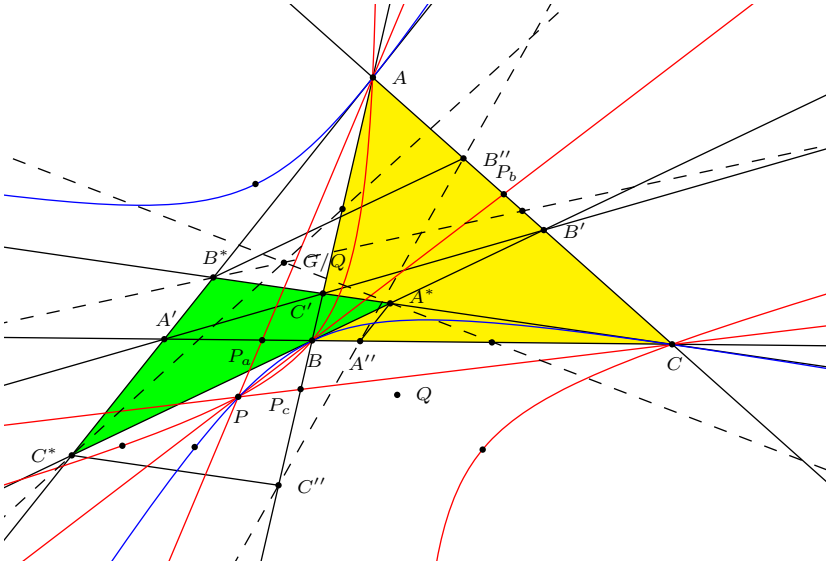

Figure 2

For example, if A', B', C' are the intersections of the sidelines with the Lemoine axis $\frac{x}{a^2}+\frac{y}{b^2}+\frac{z}{c^2}=0$, then
(i) $A^*B^*C^*$ is the tangential triangle,
(ii) A'', B'', C'' are the intersections of the sidelines with the trilinear polar of the circumcenter O,
(iii) $P_aP_bP_c$ is the cevian triangle of the Euler reflection point on the circumcircle, which is the common point of the reflections of the Euler line in the three sidelines of Δ.

3.3. *Wallace lines.* Suppose A', B', C' are the pedals of a point

$$Q=\left(\frac{a^2}{(S_B-S_C)(S_A+t)}:\frac{b^2}{(S_C-S_A)(S_B+t)}:\frac{c^2}{(S_A-S_B)(S_C+t)}\right)$$

on the circumcircle, the cevian projection of the (degenerate) pedal triangle of Q is the cevian triangle of

$$P=\left(\frac{S_A(S_{BB}+S_{CC})-S_{BC}(S_B+S_C)+(S_{AB}+S_{AC}-2S_{BC})t}{(S_B-S_C)^2(S_A+t)^2}:\cdots:\cdots\right)$$

As Q varies on the circumcircle, the locus of P is the quintic

$$\sum_{\text{cyclic}}x^3(S_By-S_Cz)^2+3xyz\sum_{\text{cyclic}}a^2(b^2+c^2)yz=0.$$

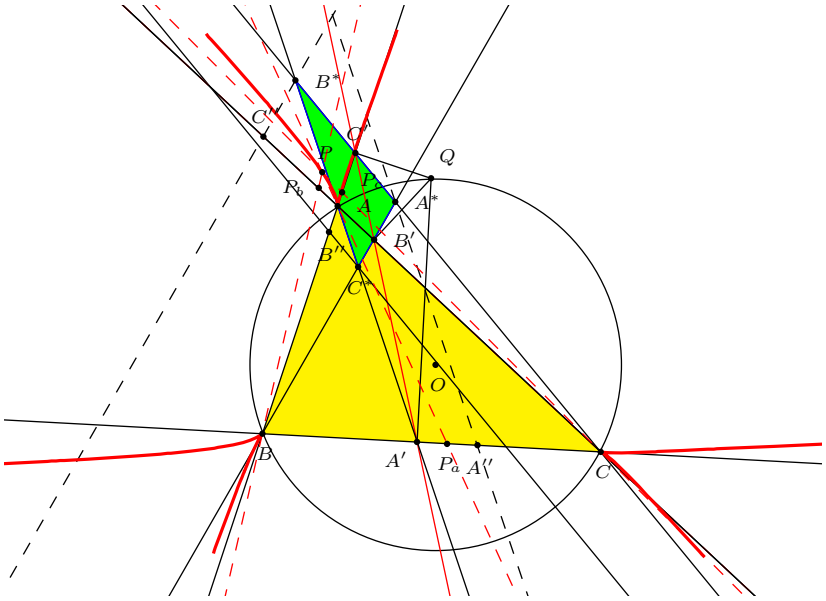

Figure 3

4. Inscribed triangles with a given cevian projection

Now we want to "invert" the map cevpro. A cevian triangle Δ_P with $P = (u : v : w)$ is given, and we search for all inscribed triangles Δ' with $\mathrm{cevpro}(\Delta') = \Delta_P$. Note that in Figure 1, $A'B''$, $A''B'$ and $P_aP_b(= p_c)$ are parallel; they all have infinite point $(p, -q, -p+q)$ with p, q given in (10). Beginning with an arbitrary point A' on the sideline a, and A'' the reflection of A' in P_a, we construct B' as the intersection of the parallel of p_c through A'' with the sideline b, and similarly C' on c so that $\mathrm{cevpro}(A'B'C') = P_aP_bP_c$.

Proposition 3. *The family $\mathcal{D}_P = \{\Delta(t) : t \in \mathbb{R}\}$ with $\Delta(t) = A_tB_tC_t$ given by*

$$\begin{aligned} A_t &= (0 : uv - t : wu + t), \\ B_t &= (uv + t : 0 : vw - t), \\ C_t &= (wu - t : vw + t : 0), \end{aligned} \tag{16}$$

is the set of all inscribed triangles with the common cevian projection Δ_P.

Proof. With $A_t = (0 : uv - t : uw + t)$, $t \in \mathbb{R}$, one can represent every point on the sideline a. Then $A_{-t} = (0 : uv + t : uw - t)$ is the reflection of A_t in P_a. An easy computation shows that the parallel of P_aP_b through A_{-t}, that is the line $A_{-t}L_c$, intersects the sideline b at $B_t = (uv + t : 0 : vw - t)$. Similarly $C_t = (wu - t : wv + t : 0)$. □

Remarks. (1) The cevian triangle itself is in the family $\mathcal{D}_P$: $\Delta(0) = \Delta_P$.

(2) The reflections of B_t in P_b and C_t in P_c are respectively

$$B_{-t} = (uv - t : 0 : vw + t) \quad \text{and } C_{-t} = (wu + t : vw - t : 0).$$

Here are some further details: the infinite points of AA_t, BB_t, CC_t are

$$\begin{aligned} L_{a^*} &= (-u(v+w) : uv - t : wu + t), \\ L_{b^*} &= (uv + t : -v(w+u) : vw - t), \\ L_{c^*} &= (wu - t : vw + t : -w(u+v)). \end{aligned} \tag{17}$$

Proposition 4. *For every triangle $\Delta(t) = A_tB_tC_t$ of the family $\mathcal{D}_P$, the medial triangle of $\Delta(t)$ is inscribed in Δ_P.*

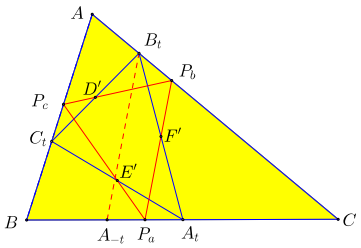

Figure 4

Proof. The segments A_tA_{-t} and A_tB_t are divided by the parallel P_aP_b of $A_{-t}B_t$ through P_a in the ratio $\frac{A_tP_a}{P_aA_{-t}} = 1 = \frac{A_tF'}{F'B_t}$ (see Figure 4). □

5. Generalized Wallace lines

Let $P = (u : v : w)$ be a point not on the sidelines, $\mathcal{D}_P = \{\Delta(t) : t \in \mathbb{R}\}$ the family of inscribed triangles with common cevian projection Δ_P, and $\mathcal{C}_P$ the circumconic (of ABC) with center mP.

Proposition 5. *For all $\Delta(t) \in \mathcal{D}_P$ and all points $Q \in \mathcal{C}_P$ holds true: The intersections X, Y, Z of the parallels of AA_t, BB_t, CC_t through Q with a, b, c, respectively, are collinear.*

The line containing X, Y, Z we call a *generalized Wallace line* (see Figure 5).

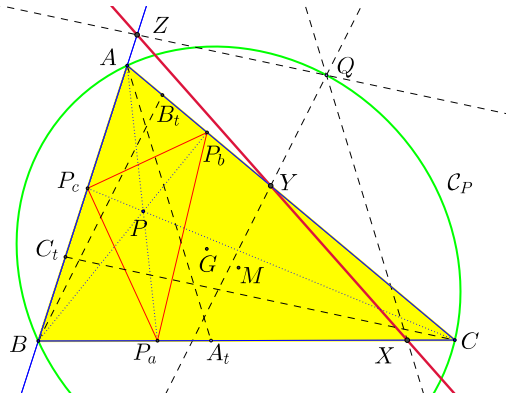

Figure 5

Proof. Let $Q = (x : y : z)$. Then the parallels of AA_t, BB_t, CC_t through Q are respectively the lines $l_a = QL_{a^*}$, $l_b = QL_{b^*}$, $l_c = QL_{c^*}$ (with L_{a^*}, L_{b^*}, L_{c^*} given in (17)):

$$\begin{aligned} l_a &= [(wu+t)y - (uv-t)z : -u(v+w)z - (wu+t)x : (uv-t)x + u(v+w)y], \\ l_b &= [(vw-t)y + v(w+u)z : (uv+t)z - (vw-t)x : -v(w+u)x - (uv+t)y)], \\ l_c &= [-w(u+v)y - (vw+t)z : (wu-t)z + w(u+v)x : (vw+t)x - (wu-t)y]. \end{aligned} \tag{18}$$

These lines intersect a, b, c respectively at the points X, Y, Z:

$$\begin{aligned} X &= (0 : (uv-t)x + u(v+w)y : u(v+w)z + (wu+t)x)\,, \\ Y &= (v(w+u)x + (uv+t)y : 0 : (vw-t)y + v(w+u)z)\,, \\ Z &= ((wu-t)z + w(u+v)x : w(u+v)y + (vw+t)z : 0)\,. \end{aligned} \tag{19}$$

The points X, Y, Z are collinear if and only if the determinant of (X, Y, Z) vanishes. After a longer calculation we find from (19):

$$\begin{aligned} &\det(X, Y, Z) \\ &= (x+y+z)(t^2 + uvw(u+v+w))\,(u(v+w)yz + v(w+u)zx + w(u+v)xy)\,. \end{aligned}$$

Now, the last factor defines the circumconic $\mathcal{C}_P$ with center $mP = (v+w : w+u : u+v)$, with equation

$$u(v+w)yz + v(w+u)zx + w(u+v)xy = 0. \tag{20}$$

Therefore, for Q in $\mathcal{C}_P$, the points X, Y, Z are collinear. □

Remark. It is easy to verify that the reflections of P in P_a, P_b, P_c are points of $\mathcal{C}_P$.

Let H be the orthocenter of Δ. In the case $\{P = H,\ t = 0\}$ we have the well-known theorem of Wallace. The special cases $\{P$ arbitrary, $t = 0\}$ and $\{P = G, t \in \mathbb{R}\}$ are dealt with by O. Giering in the papers [2] and [3].

References

[1] B. Gibert, *Catalogue of Triangle Cubics*, http://bernard.gibert.pagesperso-orange.fr/ctc.html

[2] O. Giering, Affine and Projective Generalization of Wallace Lines, *Journal for Geometry and Graphics*, 1, no. 2 (1997) 119–133.

[3] O. Giering, Sätze vom Wallace-Typ, *Informationsblätter der Geometrie* (*IBDG*), 32, no. 1 (2013) 43–45.

[4] S. Sigur, *Affine Theory of Triangle Conics*, http://www.paideiaschool.org/, Teacherpages/Steve_Sigur/resources/conic-types-web/conic.htm.

[5] P. Yiu, *Introduction to the Geometry of the Triangle*, 2001, new version of 2013, http://math.fau.edu/yiu/YIUIntroductionToTriangleGeometry130411.pdf

Gotthard Weise: Buchloer Str. 23, D-81475 München, Germany
E-mail address: gotthard.weise@tele2.de

Forum Geometricorum
Volume 16 (2016) 249–256.

FORUM GEOM
ISSN 1534-1178

Some Collinearities in the Heptagonal Triangle

Abdilkadir Altintaş

Abstract. With the methods of barycentric coordinates, we establish several collinearities in the heptagonal triangle, formed by a side and two diagonals of different lengths of a regular heptagon.

1. The regular heptagon

Consider a regular heptagon $AA'C'A''BCB'$ inscribed in a circle, each side of length a. The diagonals are of two kinds. Those with 3 vertices on the defining minor arc have the same length b, and those with 4 vertices on the defining minor arc have the same length c. There are seven of each kind. The lengths a, b, c satisfy some simple relations.

Lemma 1. (a) $a^2 = c(c-b)$,
(b) $b^2 = a(c+a)$,
(c) $c^2 = b(a+b)$,
(d) $\frac{1}{a} = \frac{1}{b} + \frac{1}{c}$.

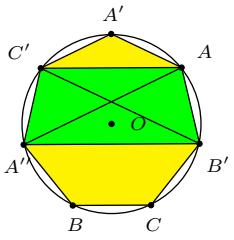

Figure 1(a)

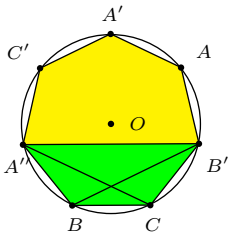

Figure 1(b)

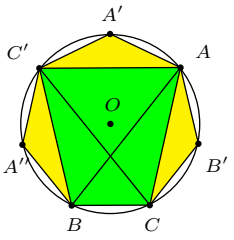

Figure 1(c)

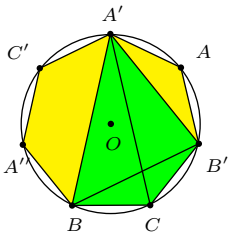

Figure 1(d)

Proof. Applying Ptolemy's theorem to the quadrilaterals
(a) $A''B'AC'$, we obtain $c^2 = a^2 + bc \implies a^2 = c(c-b)$;
(b) $BCB'A''$, we obtain $b^2 = a(c+a)$;
(c) $BCAC'$, we obtain $c^2 = b(a+b)$;
(d) $BCB'A'$, we obtain $bc = ca + ab \implies \frac{1}{a} = \frac{1}{b} + \frac{1}{c}$. □

Corollary 2. *The roots of the cubic polynomial* $t^3 - 2t^2 - t + 1$ *are* $-\frac{b}{c}$, $\frac{c}{a}$, *and* $\frac{a}{b}$.
(a) $b^3 + 2b^2c - bc^2 - c^3 = 0$,
(b) $c^3 - 2c^2a - ca^2 + a^3 = 0$,
(c) $a^3 - 2a^2b - ab^2 + b^3 = 0$.

Publication Date: June 8, 2016. Communicating Editor: Paul Yiu.

2. The heptagonal triangle

Consider the triangle ABC imbedded in the regular heptagon $AA'C'A''BCB'$. We call this the heptagonal triangle. It has angles $A = \frac{\pi}{7}$, $B = \frac{2\pi}{7}$, $C = \frac{4\pi}{7}$, and sidelengths $BC = a$, $CA = b$, $AB = c$ satisfying the relations given in Lemma 1. Basic properties of the heptagonal triangle can be found in [1]. We establish several collinearity relations in the triangle ABC by the method of barycentric coordinates. A basic reference is [2]. The paper [3] contains results on the heptagonal triangle obtained by complex number coordinates.

In the heptagonal triangle ABC, let
(i) AX, BY, CZ be the angle bisectors, concurrent at the incenter I,
(ii) AD, BE, CF be the medians, concurrent at the centroid G, and
(iii) AD', BE', CF' be symmedians, concurrent at the symmedian point K.

In homogeneous barycentric coordinates with reference to the heptagonal triangle ABC,

$$\begin{array}{llll} X = (0 : b : c), & Y = (a : 0 : c), & Z = (a : b : 0), & I = (a : b : c); \\ D = (0 : 1 : 1) & E = (1 : 0 : 1), & F = (1 : 1 : 0), & G = (1 : 1 : 1); \\ D' = (0 : b^2 : c^2), & E' = (a^2 : 0 : c^2), & F' = (a^2 : b^2 : 0), & K = (a^2 : b^2 : c^2). \end{array}$$

Proposition 3. (a) *Y, Z, G are collinear.*
(b) *E', F', I are collinear.*
(c) *G, I, D' are collinear.*
(d) *E, X, K are collinear.*

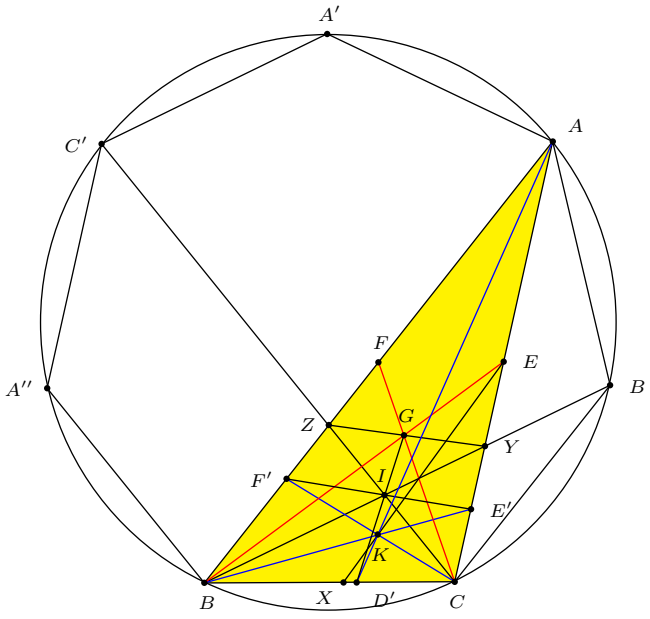

Figure 2

Proof. (a) The equation of the line YZ is

$$0 = \begin{vmatrix} x & y & z \\ a & 0 & c \\ a & b & 0 \end{vmatrix} = -bcx + cay + abz = abc\left(-\frac{x}{a} + \frac{y}{b} + \frac{z}{c}\right).$$

This is clearly satisfied if $(x : y : z) = (1 : 1 : 1)$ by Lemma 1(d). Therefore, the line YZ contains the centroid G of triangle ABC.

(b) The equation of the line $E'F'$ is

$$0 = \begin{vmatrix} x & y & z \\ a^2 & 0 & c^2 \\ a^2 & b^2 & 0 \end{vmatrix} = -b^2c^2x + c^2a^2y + a^2b^2z = a^2b^2c^2\left(-\frac{x}{a^2} + \frac{y}{b^2} + \frac{z}{c^2}\right).$$

By Lemma 1 (d) again, this is clearly satisfied if $(x : y : z) = (a : b : c)$. Therefore, the line $E'F'$ contains the incenter I of triangle ABC.

(c) The equation of the line GI is

$$0 = \begin{vmatrix} x & y & z \\ 1 & 1 & 1 \\ a & b & c \end{vmatrix} = (b-c)x + (c-a)y + (a-b)z.$$

With $(x, y, z) = (0, b^2, c^2)$, we have $(c-a)b^2+(a-b)c^2 = (b-c)(bc-ca-ab) = 0$ by Lemma 1 (d). Therefore, G, I, D' are collinear.

(d) The equation of the line EX is

$$0 = \begin{vmatrix} x & y & z \\ 0 & b & c \\ 1 & 0 & 1 \end{vmatrix} = bx + cy - bz.$$

With $(x, y, z) = (a^2, b^2, c^2)$, we have

$$bx + cy - bz = a^2b + b^2c - bc^2 = b(a^2 - c(c-b)) = 0$$

by Lemma 1(a). Therefore, E, X, K are collinear. □

Proposition 4. (a) *O, Z, D are collinear.*
(b) *O, F, Y are collinear.*
(c) *Let the median BE intersect the bisector CZ at T.*
(i) *The points F', T, Y are collinear*
(ii) *The points O, T, K are collinear.*

Proof. (a) Since $\angle ZCB = \angle ZBC = \frac{2\pi}{7}$, $ZB = ZC$. Clearly, $OB = OC$. Therefore, the line OZ is the perpendicular bisector of BC, and passes through its midpoint D (see Figure 3).

(b) The equation of the line FY is

$$0 = \begin{vmatrix} x & y & z \\ 1 & 1 & 0 \\ a & 0 & c \end{vmatrix} = -cx + cy + az.$$

With $(x, y, z) = (a^2(b^2 + c^2 - a^2), b^2(C^2 + a^2 - b^2), c^2(a^2 + b^2 - c^2))$, we have

$$-cx + cy + az = c(a^2 + b^2 - c^2)(a(c+a) - b^2) = 0$$

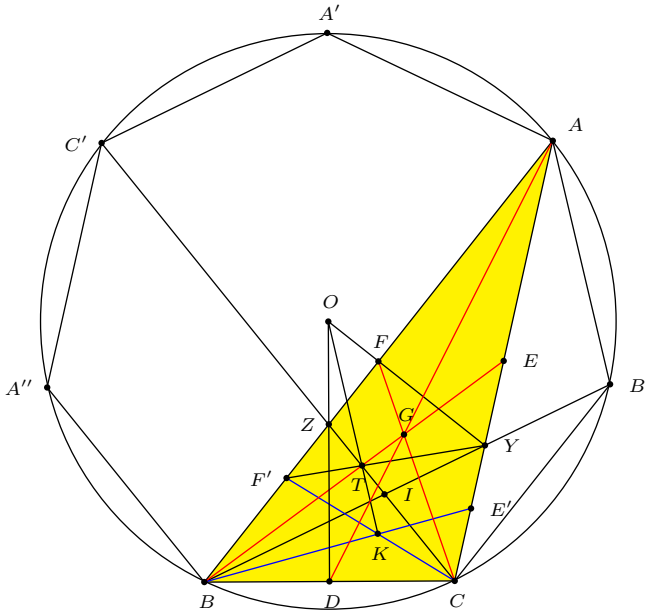

Figure 3

by Lemma 1 (b). Therefore, the points O, F, Y are collinear.

(c) The intersection of the median BE and the bisector CZ is $T = (a : b : a)$.

(i) The equation of YF' is

$$0 = \begin{vmatrix} x & y & z \\ a & 0 & c \\ a^2 & b^2 & 0 \end{vmatrix} = -b^2cx + a^2cy + ab^2z.$$

With the coordinates of T, we have

$$-b^2ca + a^2cb + ab^2a = ab(-bc + ca + ab) = 0$$

by Lemma 1 (a). Therefore, Y, T, F' are collinear.

(ii) The equation of the Brocard axis OK is

$$\frac{b^2 - c^2}{a^2}x + \frac{c^2 - a^2}{b^2}y + \frac{a^2 - b^2}{c^2}z = 0,$$

(see [2, p. 111]). With $(x, y, z) = (a, b, a)$, the left hand side becomes

$$\frac{b^2 - c^2}{a} + \frac{c^2 - a^2}{b} + \frac{a(a^2 - b^2)}{c^2} = \frac{-ab}{a} + \frac{bc}{b} + \frac{a \cdot (-ca)}{c^2} = \frac{c(c - b) - a^2}{c} = 0$$

by Lemma 1. Therefore, the points O, T, K are collinear. □

Let the line AI intersect the circumcircle at J. This is the point $J = \left(-\frac{a^2}{b+c} : b : c\right) = (-a^2 : b(b+c) : c(b+c))$.

Proposition 5. *Let H and N be the orthocenter and nine-point center of the heptagonal triangle ABC.*

(a) *B, J, H are collinear.*

(b) *E', Z, N are collinear.*

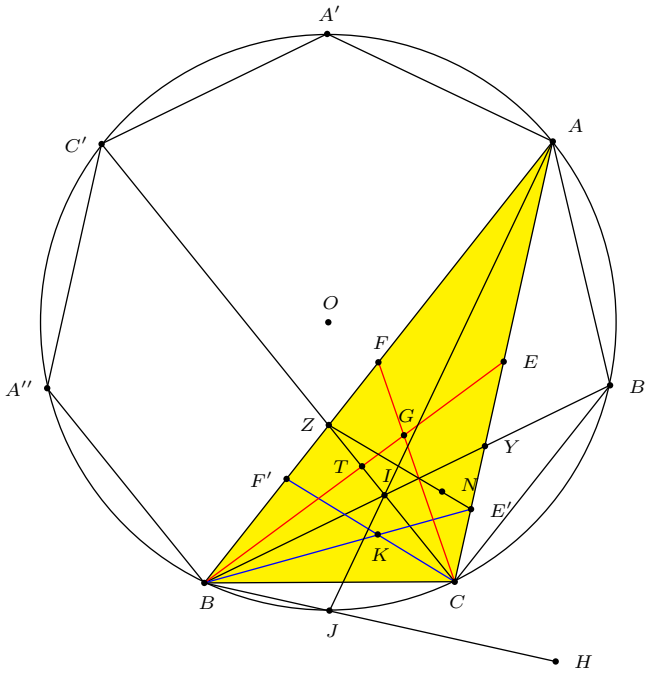

Figure 4

Proof. (a) The line BJ has equation

$$0 = \begin{vmatrix} x & y & z \\ 0 & 1 & 0 \\ -a^2 & b(b+c) & c(b+c) \end{vmatrix} = c(b+c)x + a^2 z.$$

If $(x : y : z)$ are the homogeneous barycentric coordinates of H, then $x : z = a^2 + b^2 - c^2 : b^2 + c^2 - a^2$. Since

$$\begin{aligned} & c(b+c)(a^2+b^2-c^2) + a^2(b^2+c^2-a^2) \\ = & -a^4 + a^2(b^2+bc+2c^2) - c(b+c)(c^2-b^2) \\ = & -(a^4 - a^2((b+c)^2 + c(c-b)) + c(c-b)(b+c)^2) \\ = & -(a^2-(b+c)^2)(a^2-c(c-b)) \\ = & 0 \end{aligned}$$

by Lemma 1 (a). Therefore, B, J, H are collinear.

(b) The line $E'Z$ has equation

$$0 = \begin{vmatrix} x & y & z \\ a^2 & 0 & c^2 \\ a & b & 0 \end{vmatrix} = -bc^2x + ac^2y + a^2bz.$$

The nine-point center N has coordinates

$$(a^2(b^2+c^2) - (b^2-c^2)^2 : b^2(c^2+a^2) - (c^2-a^2)^2 : c^2(a^2+b^2) - (a^2-b^2)^2).$$

Substituting these into $-bc^2x + ac^2y + a^2bz$, we obtain

$$\begin{aligned}
&(c^2-a^2)b^5 - 2(c^2-a^2)(c^2+a^2)b^3 + c^2a(c^2+a^2)b^2 + (c^2-a^2)(c^4+a^4)b \\
&\qquad - c^2a(c^2-a^2)^2 \\
&= (c^2-a^2)\left(b^5 - 2(c^2+a^2)b^3 + (c^4+a^4)b - c^2a(c^2-a^2)\right) + ab^2c^2(c^2+a^2) \\
&= bc\left(b^5 - 2(c^2+a^2)b^3 + (c^4+a^4)b - c^2a(bc) + abc(c^2+a^2)\right) \\
&= bc\left(b^5 - 2(c^2+a^2)b^3 + (c^2+a^2)^2b - 2a^2bc^2 + abc\cdot a^2)\right) \\
&= b^3c\left((c^2+a^2-b^2)^2 - a^2c(2c-a)\right) \\
&= b^2c\left((c^2+a^2-a(c+a))^2 - a^2c(2c-a)\right) \\
&= b^2c\left(c^2(c-a)^2 - a^2c(2c-a)\right) \\
&= b^2c^2\left(c(c-a)^2 - a^2(2c-a)\right) \\
&= b^2c^2\left(c^3 - 2c^2a - ca^2 + a^3\right) \\
&= 0
\end{aligned}$$

by Corollary 2 (b). Therefore, E', Z and N are collinear. □

The Jerabek hyperbola

$$a^2(b^2-c^2)(b^2+c^2-a^2)yz + b^2(c^2-a^2)(c^2+a^2-b^2)zx + c^2(a^2-b^2)(a^2+b^2-c^2)xy = 0$$

of a triangle ABC is the circum-rectangular hyperbola through the circumcenter O and the orthocenter H (see [2, p.110]). It also contains the symmedian point K. Consider the intersections P and Q of the hyperbola with the median CF and the bisector CZ respectively. These are the points

$$P = (2a^2b^2 - c^2(a^2+b^2-c^2) : 2a^2b^2 - c^2(a^2+b^2-c^2) : c^2(a^2+b^2-c^2)), \quad (1)$$

$$\begin{aligned}
Q = {} & (a(a^3b + a^2(2b^2-c^2) + ab(b^2-c^2) - c^2(b^2-c^2)) \\
& : b(a^3b + a^2(2b^2-c^2) + ab(b^2-c^2) - c^2(b^2-c^2)) \\
& : (a+b)c^2(a^2+b^2-c^2)).
\end{aligned} \quad (2)$$

Figure 5 shows the Jerabek hyperbola of the heptagonal triangle.

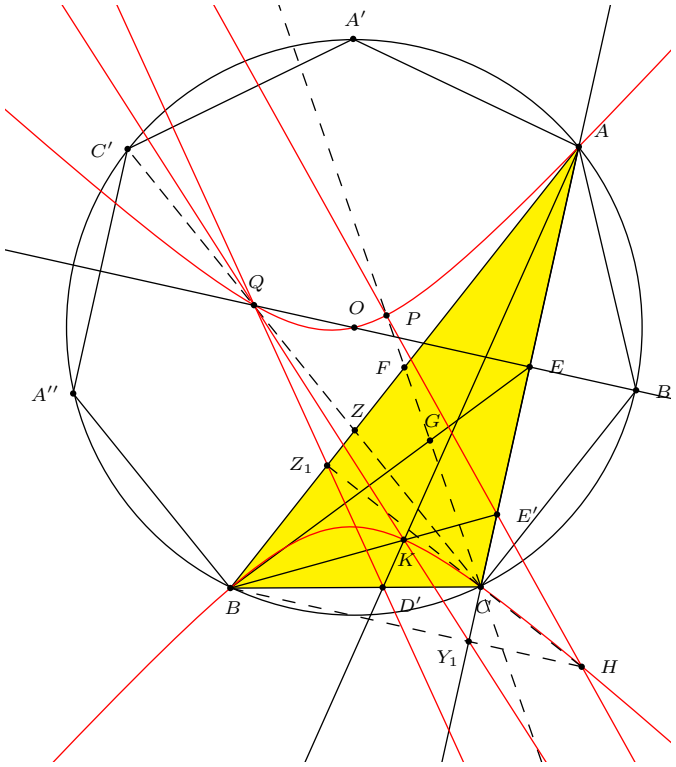

Figure 5

Proposition 6. *Let BY_1 and CZ_1 be altitudes of the heptagonal triangle ABC.*
(a) *H, E', P are collinear.*
(b) *O, E, Q are collinear.*
(c) *K, Y_1, Q are collinear.*
(d) *D', Z_1, Q are collinear.*

Proof. (a) The equation of the line $E'H$ is

$$c^2(a^2+b^2-c^2)(b^2+c^2-a^2)x + (c^2-a^2)(c^2+a^2-b^2)^2y \\ - a^2(a^2+b^2-c^2)(b^2+c^2-a^2)z = 0.$$

With the coordinates of P given in (1), we have

$$\begin{aligned} &-2(c^2-a^2)(c^2+a^2-b^2)(a^2b^2(b^2-a^2)+(a^4-a^2b^2-b^4)c^2+(b^2-a^2)c^4) \\ &= -2(c^2-a^2)(c^2+a^2-b^2)\cdot ab(a+b)(a^3-2a^2b-ab^2+b^3) \\ &= 0 \end{aligned}$$

by Lemma 1 (c) and Corollary 2(c). Therefore, the points H, E', P are collinear.

(b) The equation of the line OE is

$$-b^2x + (c^2-a^2)y + b^2z = 0.$$

With the coordinates of Q given in (2), we have

$$b(c^2-a^2)(a+b+c)(a+b-c)(b(a+b)-c^2)=0$$

by Lemma 1 (c). Therefore, O, E, Q are collinear.

In homogeneous barycentric coordinates,

$$Y_1 = (a^2+b^2-c^2 : 0 : b^2+c^2-a^2),$$
$$Z_1 = (c^2+a^2-b^2 : b^2+c^2-a^2 : 0).$$

(c) The equation of the line KY_1 is

$$b^2(b^2+c^2-a^2)x+(c^2-a^2)(c^2+a^2-b^2)y-b^2(a^2+b^2-c^2)z=0.$$

With the coordinates of Q given in (2), we have

$$b(c^2-a^2)(b^2+c^2-a^2)(c^2+a^2-b^2)(b(a+b)-c^2)=0$$

by Lemma 1 (c). Therefore, K, Y_1, Q are collinear.

(d) The equation of the line $D'Z_1$ is

$$c^2(b^2+c^2-a^2)x-c^2(c^2+a^2-b^2)y+b^2(c^2+a^2-b^2)z=0.$$

With the coordinates of Q given in (2), we have

$$c^2(b(a+b)-c^2)(b^2+c^2-a^2)((b-a)c^2+a^3+a^2b+ab^2-b^3)=0$$

by Lemma 1 (c) again. Therefore, D', Z_1, Q are collinear.

□

References

[1] L. Bankoff and J. Garfunkel, The heptagonal triangle, *Math. Mag.*, 46 (1973) 7–19.
[2] P. Yiu, *Introduction to the Geometry of the Triangle*, Florida Atlantic University Lecture Notes, 2001; with corrections, 2013, `http://math.fau.edu/Yiu/Geometry.html`
[3] P. Yiu, Heptagonal triangles and their companions, *Forum Geom.*, 9 (2009) 125–148.

Abdilkadir Altintaş: Emirdag Anadolu Lisesi, 03600 Emirdag Afyon - Turkey
E-mail address: `archimedes26@yandex.com`

Forum Geometricorum
Volume 16 (2016) 257–267.

FORUM GEOM
ISSN 1534-1178

Locus of Centroids of Similar Inscribed Triangles

Francisco Javier García Capitán

Abstract. We study the locus of the centroids of families of similar triangles inscribed in a given triangle.

1. Miquel circles

Given a triangle ABC and three points X, Y, Z on the sidelines BC, CA, AB respectively, the three Miquel circles are the circumcircles of the triangles AYZ, BZX, and CXY. According to Miquel's theorem, the three Miquel circles concur at a point, the Miquel point of X, Y, Z.

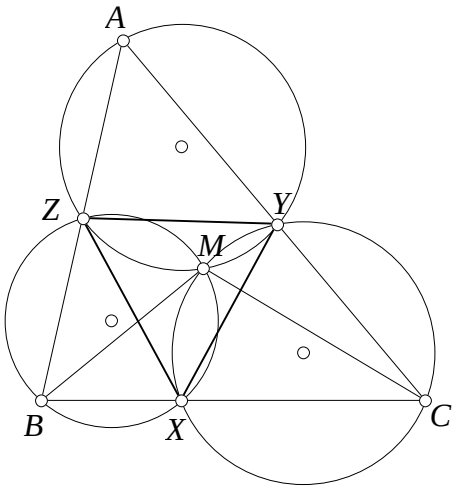

Figure 1

It is well known that if XYZ remains similar to a given triangle, the point M is fixed. The converse is also true: given a point M with homogeneous barycentric coordinates (u, v, w) with reference to ABC, if for X, Y, Z on the lines BC, CA, AB respectively, the circumcircles of AYZ, BZX, and CXY pass through M, then all such triangles XYZ are mutually similar. If $X_0Y_0Z_0$ is the pedal triangle of M, then every such triangle XYZ satisfies

$$\angle X_0MX = \angle Y_0MY = \angle Z_0MZ\ (=\ \theta).$$

Publication Date: June 20, 2016. Communicating Editor: Paul Yiu.

If $t = \tan\theta$, the vertices of the triangle are

$$\begin{aligned} X_t =\ & (0,\ (a^2+b^2-c^2)u + 2a^2v - 2Stu,\ (c^2+a^2-b^2)u + 2a^2w + 2Stu), \\ Y_t =\ & (2b^2u + (a^2+b^2-c^2)v + 2Stv,\ 0,\ (b^2v + c^2 - a^2)v + 2b^2w - 2Stv), \\ Z_t =\ & (2c^2u + (c^2+a^2-b^2)w - 2Stw,\ 2c^2v + (b^2+c^2-a^2)w + 2Stw,\ 0) \end{aligned} \tag{1}$$

in homogeneous barycentric coordinates. For basic formulas in barycentric coordinates, see [2].

2. The locus of the centroid of triangles XYZ

Note that in (1) above, the coordinate sums of X_t, Y_t, Z_t are respectively $2a^2(u+v+w)$, $2b^2(u+v+w)$, $2c^2(u+v+w)$. The centroid of $X_tY_tZ_t$ is the point

$$G_t = G_0 + 2t\cdot a^2b^2c^2S\left(\frac{v}{b^2}-\frac{w}{c^2},\ \frac{w}{c^2}-\frac{u}{a^2},\ \frac{u}{a^2}-\frac{v}{b^2}\right),$$

where

$$\begin{aligned} G_0 \ =\ & (a^2(4b^2c^2u + c^2(a^2+b^2-c^2)v + b^2(c^2+a^2-b^2)w), \\ & b^2(c^2(a^2+b^2-c^2)u + 4a^2c^2v + a^2(b^2+c^2-a^2)w), \\ & c^2(b^2(c^2+a^2-b^2)u + a^2(b^2+c^2-a^2)v + 4a^2b^2w)) \end{aligned}$$

is the centroid of the pedal triangle of M. Note that for $M = K = (a^2, b^2, c^2)$, the symmedian point of triangle ABC, $G_t = G_0 = K$.

For $M \neq K$, the coordinates of G_t are linear functions of t, the locus of G_t is a straight line $\ell(M)$. The line $\ell(M)$ clearly contains G_0 and the infinite point

$$J(M) := \left(\frac{v}{b^2}-\frac{w}{c^2},\ \frac{w}{c^2}-\frac{u}{a^2},\ \frac{u}{a^2}-\frac{v}{b^2}\right). \tag{2}$$

This is the infinite point of the line

$$\frac{u}{a^2}x + \frac{v}{b^2}y + \frac{w}{c^2}z = 0,$$

the trilinear polar of $M^* := \left(\frac{a^2}{u},\ \frac{b^2}{v},\ \frac{c^2}{w}\right)$, the isogonal conjugate of M. We summarize this in the following theorem.

Theorem 1. *Let $M \neq K$ be a point with homogeneous barycentric coordinates (u, v, w) with reference to ABC. The locus of the centroids of triangles XYZ with Miquel point M is the line $\ell(M)$ through the centroid G_0 of the pedal triangle of M parallel to the trilinear polar of the isogonal conjugate of M.*

The line $\ell(M)$ has barycentric equation

$$\sum_{\text{cyclic}} \left(\begin{array}{c} b^2c^2u^2 - 2c^2a^2v^2 - 2a^2b^2w^2 - a^2(b^2+c^2-a^2)vw \\ +b^2(-a^2+b^2+2c^2)wu + c^2(-a^2+2b^2+c^2)uv \end{array} \right) x = 0. \tag{3}$$

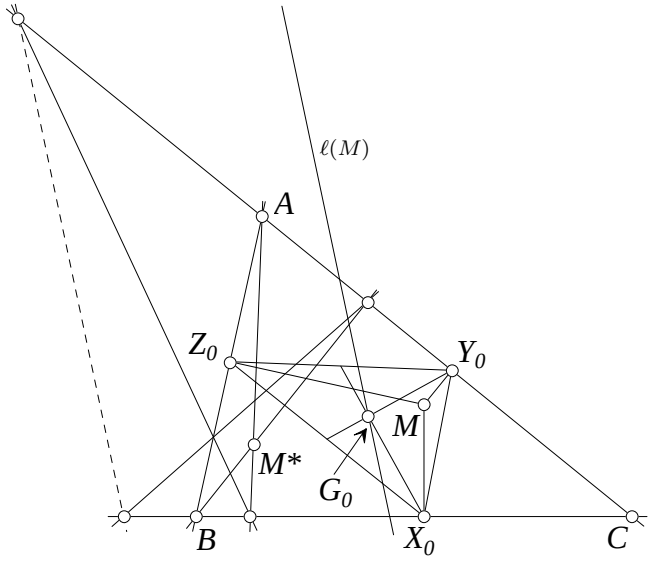

Figure 2

Example 1.

	M	$\ell(M)$	$J(M)$
(i)	G	$\sum_{\text{cyclic}}(a^4-4a^2(b^2+c^2)+b^4+5b^2c^2+c^4)x=0$	$X(512)$
(ii)	O	$\sum_{\text{cyclic}}(b^2+c^2-2a^2)x=0$	$X(523)$
(iii)	H	line joining O and	$X(520)$
(iv)	I	$\sum_{\text{cyclic}}(a^2-2a(b+c)+b^2+bc+c^2)x=0$	$X(513)$
(v)	$X(55)$	line joining $X(7)$ and	$X(514)$
(vi)	$X(56)$	line joining $X(8)$ and	$X(522)$
(vii)	$X(99)$	$\sum_{\text{cyclic}}\frac{x}{a^2(b^2+c^2)-2b^2c^2}=0$	$X(888)$
(viii)	$X(110)$	$\sum_{\text{cyclic}}\frac{x}{b^2+c^2-2a^2}=0$	$X(690)$

3. Parallelism and orthogonality

Proposition 2. *The lines $\ell(M)$ and $\ell(M')$ are parallel if and only if the line MM' passes through the symmedian point of triangle ABC.*

Proof. Let $M=(u,v,w)$ and $M'=(u',v',w')$ in homogeneous barycentric coordinates. The lines $\ell(M)$ and $\ell(M')$ are parallel if and only if the trilinear polars of M and M' are parallel. Equivalently, $J(M)$ lies on the line $\frac{u'}{a^2}x+\frac{v'}{b^2}y+\frac{w'}{c^2}z=0$:

$$\begin{aligned}0 &= \frac{u'}{a^2}\left(\frac{v}{b^2}-\frac{w}{c^2}\right)+\frac{v'}{b^2}\left(\frac{w}{c^2}-\frac{u}{a^2}\right)+\frac{w'}{c^2}\left(\frac{u}{a^2}-\frac{v}{b^2}\right)\\ &= \frac{1}{a^2b^2c^2}\left(a^2(v'w-vw')+b^2(w'u-wu')+c^2(u'v-uv')\right).\end{aligned}$$

Since $(v'w - vw')x + (w'u - wu')y + (u'v - uv')z = 0$ represents the line MM', the condition is equivalent to the line MM' containing (a^2, b^2, c^2), the symmedian point of triangle ABC. □

Corollary 3. *If M lies on the Brocard axis, the line $\ell(M)$ is perpendicular to Euler line.*

Proof. If M lies on the Brocard axis, by Theorem 1,

$$\begin{aligned} J(M) = \ & J(O) = \left(\frac{b^2 S_B}{b^2} - \frac{c^2 S_C}{c^2}, \frac{c^2 S_C}{c^2} - \frac{a^2 S_A}{a^2}, \frac{a^2 S_A}{a^2} - \frac{b^2 S_B}{b^2} \right) \\ = \ & (S_B - S_C, S_C - S_A, S_A - S_B), \end{aligned}$$

which is the triangle center $X(523)$ in [1], the infinite point of the perpendicular to the Euler line. Therefore, $\ell(M)$ is perpendicular to the Euler line. □

Corollary 4. *The locus of the centroids of equilateral inscribed triangles is formed by two lines perpendicular to Euler line.*

Proof. This follows from the fact that equilateral inscribed triangles have Miquel points the isodyanamic points $X(15)$ or $X(16)$ on the Brocard axis. The locus is formed by the lines

$$\sum_{\text{cyclic}} (\sqrt{3}(a^2(b^2 + c^2) - (b^4 + c^4)) \pm 2(b^2 + c^2 - 2a^2)S)x = 0,$$

S being twice the area of triangle ABC. □

Proposition 5. *Let $M = (u, v, w)$. The locus of M' for which $\ell(M') \perp \ell(M)$ is the line*

$$\sum_{\text{cyclic}} (-2b^2c^2u + c^2(a^2 + b^2 - c^2)v + b^2(c^2 + a^2 - b^2)w)x = 0. \tag{4}$$

Proof. For $M' = (x, y, z)$, $\ell(M) \perp \ell(M')$ if and only if

$$S_A \left(\frac{v}{b^2} - \frac{w}{c^2} \right) \left(\frac{y}{b^2} - \frac{z}{c^2} \right) + S_B \left(\frac{w}{c^2} - \frac{u}{a^2} \right) \left(\frac{z}{c^2} - \frac{x}{a^2} \right) + S_C \left(\frac{u}{a^2} - \frac{v}{b^2} \right) \left(\frac{x}{a^2} - \frac{y}{b^2} \right) = 0.$$

Rearrangement with the substitutions $S_A = \frac{b^2 + c^2 - a^2}{2}$ etc leads to (4) above. □

Example 2.

	M	locus of M' for which $\ell(M') \perp \ell(M)$	inf. point
(i)	G	$\sum_{\text{cyclic}} (a^2(b^2 + c^2) - (b^4 + c^4))x = 0$	$X(523)$
(ii)	O	$\sum_{\text{cyclic}} \frac{2a^4 - a^2(b^2+c^2) - (b^2-c^2)^2}{a^2} x = 0$	$X(8675)$
(iii)	I	$\sum_{\text{cyclic}} \frac{a^2(b+c) - 2abc - (b+c)(b-c)^2}{a} x = 0$	$X(9001)$
(iv)	$X(55)$	$\sum_{\text{cyclic}} \frac{2a^3 - a^2(b+c) - (b+c)(b-c)^2}{a^2} x = 0$	$X(9000)$
(v)	$X(56)$	$\sum_{\text{cyclic}} \frac{2a^4 - a^3(b+c) - a^2(b-c)^2 + a(b+c)(b-c)^2 - (b^2-c^2)^2}{a^2} x = 0$	$X(8999)$
(vi)	$X(110)$	$\sum_{\text{cyclic}} \frac{2a^6 - 2a^4(b^2+c^2) + a^2(b^4+c^4) - (b^2+c^2)(b^2-c^2)^2}{a^2} x = 0$	$X(526)$

Proposition 6. *Let $\mathscr{L}_i:\ p_ix+q_iy+r_iz=0$, $i=1,2$, be two lines through the symmedian point K, and J_1, J_2 the infinite points of $\ell(M_1)$, $\ell(M_2)$ for M_i on $\mathscr{L}_i$ respectively. Then points J_1 and J_2 correspond to perpendicular lines if and only if*

$$(q_1+r_1)p_2+(r_1+p_1)q_2+(p_1+q_1)r_2=0.$$

Remark. In other words, the point $Q=(q_1+r_1:r_1+p_1:p_1+q_1)$ lies on the line $\mathscr{L}_2$.

Construction 7. *Given a line $\mathscr{L}_1$ containing the symmedian point K, construct*
(i) *$Q=$ the complement of the isotomic conjugate of the trilinear pole of $\mathscr{L}_1$,*
(ii) *the line $\mathscr{L}_2=KQ$.*

For arbitrary points M on $\mathscr{L}_1$ and M' on $\mathscr{L}_2$, $\ell(M)\perp\ell(M')$.

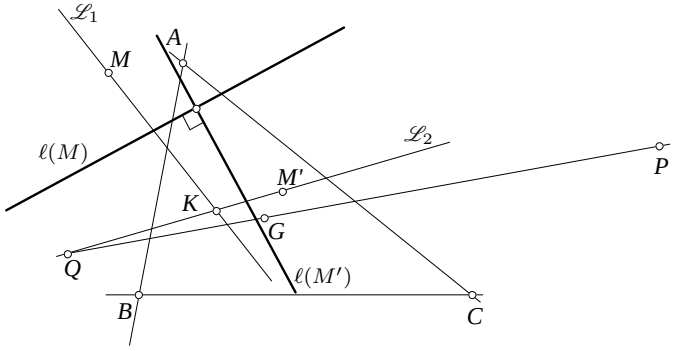

Figure 3

Proposition 8. *The locus of M for which $\ell(M)$ contains a given point $P(u,v,w)$ is the circle $\Gamma(P)$*

$$\begin{aligned}&(a^2+b^2+c^2)(u+v+w)(a^2yz+b^2zx+c^2xy)\\&-(x+y+z)\left(\sum_{\text{cyclic}}b^2c^2(2v+2w-u)x\right)=0.\end{aligned}$$

with center

$$\begin{aligned}O(P)=\ &(a^2((a^4-2a^2(b^2+c^2)+b^4-8b^2c^2+c^4)u\\&+(a^4-a^2(2b^2-c^2)+(b^2-c^2)(b^2+2c^2))v\\&+(a^4+a^2(b^2-2c^2)-(b^2-c^2)(2b^2+c^2)w),\\&\cdots,\cdots).\end{aligned}$$

and passing through the symmedian point K.

For $M=G$, the centroid, this is the circle

$$(a^2+b^2+c^2)(a^2yz+b^2zx+c^2xy)-(x+y+z)(b^2c^2x+c^2a^2+a^2b^2z)=0$$

with center $X(182)$, the midpoint of OK.

Proposition 9. *The tangent of* $\Gamma(P)$ *at* K *is parallel to* $\ell(P)$.

Proof. The tangent of $\Gamma(P)$ at K is the line[1]

$$\frac{(b^2+c^2)u-a^2v-a^2w}{a^2}x+\frac{-b^2u+(c^2+a^2)v-b^2w}{b^2}y+\frac{-c^2u-c^2v+(a^2+b^2)w}{c^2}z=0.$$

This has infinite point

$$\begin{aligned}
&\Bigg(\frac{-b^2u+(c^2+a^2)v-b^2w}{b^2}-\frac{-c^2u-c^2v+(a^2+b^2)w}{c^2},\\
&\quad\frac{-c^2u-c^2v+(a^2+b^2)w}{c^2}-\frac{(b^2+c^2)u-a^2v-a^2w}{a^2},\\
&\quad\frac{(b^2+c^2)u-a^2v-a^2w}{a^2}-\frac{-b^2u+(c^2+a^2)v-b^2w}{b^2}\Bigg)\\
&=\Bigg(\frac{(c^2+a^2+b^2)v}{b^2}-\frac{(a^2+b^2+c^2)w}{c^2},\frac{(a^2+b^2+c^2)w}{c^2}-\frac{(b^2+c^2+a^2)u}{a^2},\\
&\quad\frac{(b^2+c^2+a^2)u}{a^2}-\frac{(c^2+a^2+b^2)v}{b^2}\Bigg)\\
&=(a^2+b^2+c^2)\left(\frac{v}{b^2}-\frac{w}{c^2},\frac{w}{c^2}-\frac{u}{a^2},\frac{u}{a^2}-\frac{v}{b^2}\right)
\end{aligned}$$

equal to $J(P)$. Therefore the tangent is parallel to $\ell(P)$. □

Here is a construction of the center $O(P)$ of the circle $\Gamma(P)$.

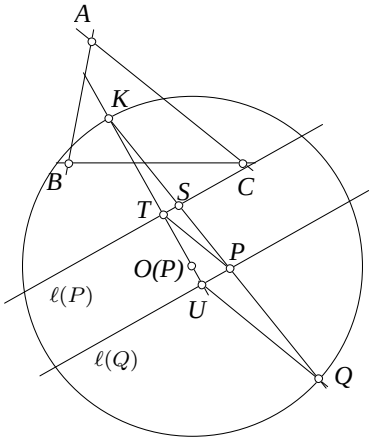

Figure 4

[1]Given the homogeneous (quadratic) equation of a conic, the tangent at a point (u,v,w) can be obtained by replacing x^2, y^2, z^2 by ux, vy, wz, and yz, zx, xy by $\frac{1}{2}(wy+vz)$, $\frac{1}{2}(uz+wx)$, $\frac{1}{2}(vx+uy)$ respectively.

Construction 10. *Given a point $P \neq K$, construct*
(1) *the line $\ell(P)$ to intersect KP at S;*
(2) *the orthogonal projections*
T of K on $\ell(P)$, and
U of P on KT;
(3) *the parallel of PT through U to intersect the line KP at Q, (the line $\ell(Q)$ passes through P);*
(4) *the perpendicular bisector of KQ to intersect KT at $O(P)$.*
$O(P)$ is the center of $\Gamma(P)$.

4. Envelopes

Proposition 11. *If M traverses a line $\mathscr{L}$, the lines $\ell(M)$ envelope a parabola whose axis is parallel to the trilinear polar of the isogonal conjugate of the infinite point of $\mathscr{L}$.*

Focus

$$\begin{aligned} F = \ & \big(a^4p^2 + b^2(c^2+a^2-b^2)q^2 + c^2(a^2+b^2-c^2)r^2 \\ & - (c^2+a^2-b^2(a^2+b^2-c^2)qr - c^2a^2rp - a^2b^2pq, \\ & \cdots, \cdots\big). \end{aligned}$$

Directrix

$$\begin{aligned} \sum_{\text{cyclic}} \ & (a^2((b^2+c^2-a^2)^2 + 8b^2c^2)p \\ & + b^2(a^4 + a^2(-2b^2+c^2) + (b^2-c^2)(b^2+2c^2))q \\ & + c^2(a^4 + a^2(b^2-2c^2) - (b^2-c^2)(2b^2+c^2))r)x \\ = \ & 0. \end{aligned}$$

For example, if $\mathscr{L}$ is the Lemoine axis $\frac{x}{a^2} + \frac{y}{b^2} + \frac{z}{c^2} = 0$, the parabola has barycentric equation

$$\sum_{\text{cyclic}} (b^2+c^2-2a^2)^2yz - (x+y+z)\left(\sum_{\text{cyclic}} (a^4 - 4b^2c^2)x\right) = 0.$$

It has focus the Parry point[2]

$$X(111) = \left(\frac{a^2}{b^2+c^2-2a^2}, \ \frac{b^2}{c^2+a^2-2b^2}, \ \frac{c^2}{a^2+b^2-2c^2}\right),$$

and directrix the line

$$\sum_{\text{cyclic}} (a^4 - a^2(b^2+c^2) + 4b^2c^2)x = 0$$

[2]The Parry point is the isogonal conjugate of the infinite point of the line GK.

which is the perpendicular to the line GK from the intersection of the Euler line and the Simson line of the Steiner point. [3]

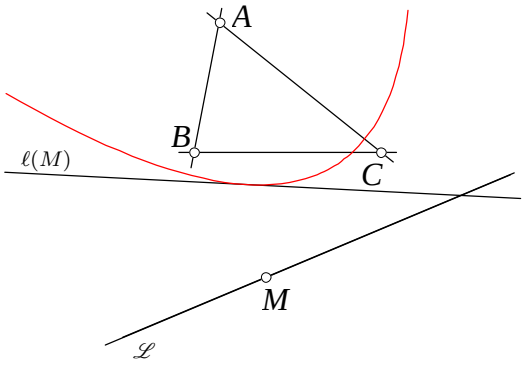

Figure 5

Proposition 12. *If M is a point on the circumcircle, the line $\ell(M)$ is tangent to the Steiner inellipse.*

Proof. If $M = \left(\frac{a^2}{(b^2-c^2)(a^2+\tau)}, \frac{b^2}{(c^2-a^2)(b^2+\tau)}, \frac{c^2}{(a^2-b^2)(c^2+\tau)}\right)$ on the circumcircle, the centroid of the (degenerate) pedal triangle of M is the point

$$\begin{aligned} G_0 = \ & (c^2a^2 + a^2b^2 - 2b^2c^2 - (b^2 + c^2 - 2a^2)\tau) \\ & \cdot (a^2(a^2(b^2 + c^2) - (b^4 + c^4)) + (2a^4 - a^2(b^2 + c^2) - (b^2 - c^2)^2)\tau), \\ & \cdots, \cdots). \end{aligned}$$

The trilinear polar of M^* is the line

$$\frac{x}{(b^2 - c^2)(a^2 + \tau)} + \frac{y}{(c^2 - a^2)(b^2 + \tau)} + \frac{z}{(a^2 - b^2)(c^2 + \tau)} = 0$$

with infinite point

$$\begin{aligned} J(\tau) = \ & ((b^2 - c^2)(a^2 + \tau)(a^2(b^2 + c^2) - 2b^2c^2 - (b^2 + c^2 - 2a^2)\tau), \\ & (c^2 - a^2)(b^2 + \tau)(b^2(c^2 + a^2) - 2c^2a^2 - (c^2 + a^2 - 2b^2)\tau), \\ & (a^2 - b^2)(c^2 + \tau)(c^2(a^2 + b^2) - 2a^2b^2 - (a^2 + b^2 - 2c^2)\tau)). \end{aligned}$$

The line $\ell(M)$ contains G_0 and $J(\tau)$. It has barycentric equation

$$\sum_{\text{cyclic}} \frac{x}{a^2(b^2 + c^2) - 2b^2c^2 - (b^2 + c^2 - 2a^2)\tau} = 0.$$

This is the tangent to the Steiner inellipse

$$x^2 + y^2 + z^2 - 2yz - 2zx - 2xy = 0$$

[3] This intersection is the triangle center $X(1513) = ((a^2(b^2 + c^2) - (b^4 + c^4))(3a^4 + (b^2 - c^2)^2), \cdots, \cdots)$.

at the point[4]

$$T(\tau) = ((a^2(b^2+c^2) - 2b^2c^2 - (b^2+c^2-2a^2)\tau)^2, \cdots, \cdots).$$

□

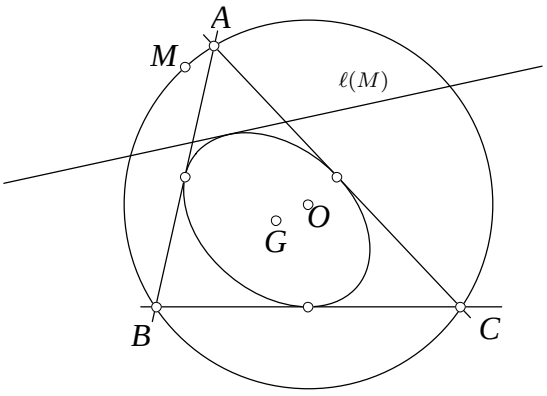

Figure 6

Corollary 13. *The Steiner inellipse is the envelope of $\ell(M)$ for M on the circumcircle of triangle ABC.*

Remark. If S_t is the Steiner point, the fourth intersection of the cirucumcircle and the Steiner circum-ellipse, and the line $M(\tau)S_t$ intersects the Steiner circum-ellipse at $T'(\tau)$, then $T(\tau)$ is the midpoint of G and $T'(\tau)$.

5. The inverse problem

We solve the inverse problem of finding the point $M(u,v,w)$ so that $\ell(M)$ is a given line $\mathscr{L}: \ px+qy+rz=0$ not containing the symmedian point K. This has to satisfy two conditions:
(i) $J(M)$ is the infinite point of $\mathscr{L}$, and
(ii) the centroid of the pedal triangle of M lies on $\mathscr{L}$.

$$\begin{aligned}
&\frac{q-r}{a^2}u + \frac{r-p}{b^2}v + \frac{p-q}{c^2}w = 0,\\
&\frac{4a^2p + (a^2+b^2-c^2)q + (c^2+a^2-b^2)r}{a^2}u\\
&\quad + \frac{(a^2+b^2-c^2)p + 4b^2q + (b^2+c^2-a^2)r}{b^2}v\\
&\quad + \frac{(c^2+a^2-b^2)p + (b^2+c^2-a^2)q + 4c^2r}{c^2}w = 0.
\end{aligned}$$

[4]If (u,v,w) is an infinite point, then (u^2,v^2,w^2) is a point on the Steiner inellipse, and the tangent at that point is $\frac{x}{u}+\frac{y}{v}+\frac{z}{w}=0$.

Solving these equations, we obtain

$$\begin{aligned}&u : v : w\\ &= a^2(-a^2p^2 + 2b^2q^2 + 2c^2r^2 + (b^2 + c^2 - a^2)qr - (b^2 + 2c^2 - a^2)rp - (2b^2 + c^2 - a^2)pq)\\ &: b^2(2a^2p^2 - b^2q^2 + 2c^2r^2 - (2c^2 + a^2 - b^2)qr + (c^2 + a^2 - b^2)rp - (c^2 + 2a^2 - b^2)pq)\\ &: c^2(2a^2p^2 + 2b^2q^2 - c^2r^2 - (a^2 + 2b^2 - c^2)qr - (2a^2 + b^2 - c^2)rp + (a^2 + b^2 - c^2)pq).\end{aligned}$$

Example 3.

	$\mathscr{L}$	M
(i)	orthic axis	$X(187)$
(ii)	Lemoine axis	$X(352)$

Remarks. (1) $X(187)$ is the midpoint of the isodynamic points .

(2) $X(352)$ is a point on the circle through the centroid and the isodynamic points.

We conclude with a construction of M from $\ell(M)$.

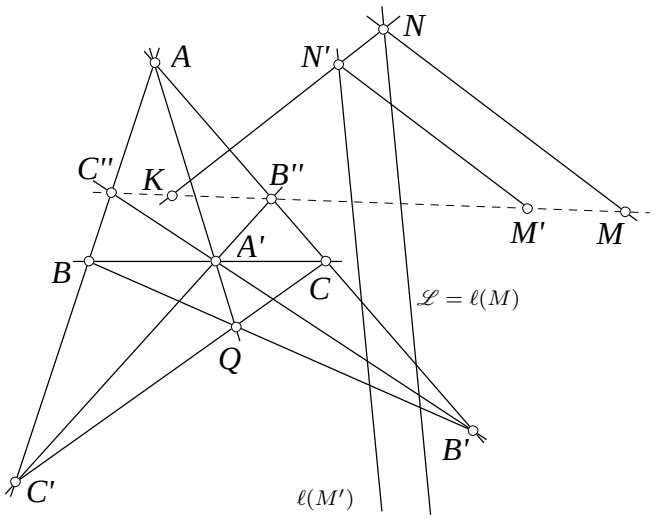

Figure 7

Construction 14. *Given a line $\mathscr{L}$, construct*
(i) *the isogonal conjugate Q of the infinite point of $\mathscr{L}$,*
(ii) *the cevian triangle $A'B'C'$ of Q and the points $B'' = C'A' \cap CA$ and $C'' = A'B' \cap AB$, (the line $B''C''$ passes through the symmedian point K),*
(iii) *the line $\ell(M')$ for any point M' on the line $B''C''$, (this line is parallel to $\mathscr{L}$),*
(iv) *any line through K intersecting $\mathscr{L}$ and $\ell(M')$ at N and N' respectively,*
(v) *the parallel through N to $M'N'$ to intersect $B''C''$ at M.*

The point M has $\ell(M)$ equal to the given line $\mathscr{L}$.

References

[1] C. Kimberling, *Encyclopedia of Triangle Centers*, available at http://faculty.evansville.edu/ck6/encyclopedia/ETC.html.

[2] P. Yiu, *Introduction to the Geometry of the Triangle*, Florida Atlantic University Lecture Notes, 2001; with corrections, 2013, available at http://math.fau.edu/Yiu/Geometry.html

Francisco Javier García Capitán: Departamento de Matemáticas, I.E.S. Alvarez Cubero, Avda. Presidente Alcalá-Zamora, s/n, 14800 Priego de Córdoba, Córdoba, Spain

E-mail address: garciacapitan@gmail.com

Forum Geometricorum
Volume 16 (2016) 269–272.

FORUM GEOM
ISSN 1534-1178

Some Golden Sections in the Equilateral and Right Isosceles Triangles

Dao Thanh Oai

Abstract. Associated with the equilateral triangle and the right isosceles triangles and their circumcircles, we exhibit some segments that are divided in the golden ratio.

1. Equilateral triangles

A segment AB is said to be divided in the golden ratio by a point P if $\frac{AB}{AP} = \frac{AP}{PB}$. In this case, the division ratio is the golden ratio $\varphi := \frac{\sqrt{5}+1}{2}$, which satisfies

$$\varphi^2 = \varphi + 1. \tag{1}$$

Proposition 1. *Consider an equilateral triangle ABC with its sides AC and AB divided into five equal parts by points E_k, F_k, $k = 1, 2, 3, 4$, so that $AE_k = AF_k = \frac{k}{5} \cdot BC$. If the circle (AE_4F_4) intersects BC at G and H* (see Figure 1)*, then G divides HB in the golden ratio.*

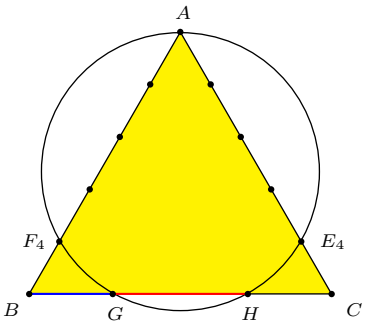

Figure 1

Proof. Suppose each side of the equilateral triangle has length 5. If $BG = x$, then $BH = 5 - x$. By Ptolemy's theorem,

$$BG \cdot BH = BF_4 \cdot BA \implies x(5-x) = 1 \cdot 5 \implies x^2 - 5x + 5 = 0,$$

and $x = \frac{5-\sqrt{5}}{2}$. It follows that $GH = 5 - 2x = \sqrt{5}$, and

$$\frac{HG}{GB} = \frac{5-2x}{x} = \frac{2\sqrt{5}}{5-\sqrt{5}} = \frac{2}{\sqrt{5}-1} = \frac{\sqrt{5}+1}{2} = \varphi.$$

□

Publication Date: June 20, 2016. Communicating Editor: Paul Yiu.

Proposition 2. *Let E be the point on the side AC of an equilateral triangle ABC such that $AE = \frac{1}{4} \cdot AC$. The perpendicular from E to AB intersects*
(i) *the perpendicular to BC at C at F, and*
(ii) *the circle with center B and radius BC at G and H* (see Figure 2).
(a) *G divides EF in the golden ratio.*
(b) *E divides HF in the golden ratio.*

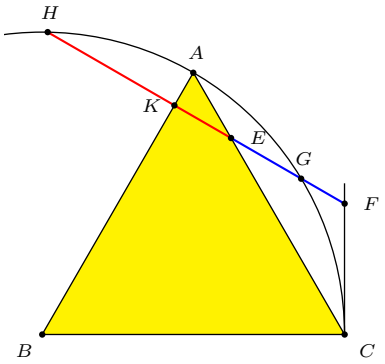

Figure 2

Proof. Suppose each side of the equilateral triangle ABC has length 4. Triangle FCE is isosceles with base angle $30°$, $CE = 3$, and $FC = \frac{CE}{2\cos 30°} = \sqrt{3}$. If the line HF intersects AB at K, then $EK = AE \sin 60° = \frac{\sqrt{3}}{2}$.

If $FG = y$, then $GE = \sqrt{3} - y$ and $GK = GE + EK = \frac{3\sqrt{3}}{2} - y$. Since K is the midpoint of the chord GH, $FH = FG+GH = FG+2GK = y+3\sqrt{3}-2y = 3\sqrt{3} - y$. By Ptolemy's theorem,

$$FG \cdot FH = FC^2 \implies y(3\sqrt{3} - y) = 3 \implies y^2 - 3\sqrt{3}y + 3 = 0,$$

and

$$y = \frac{3\sqrt{3} - \sqrt{15}}{2} = \frac{\sqrt{3}(3 - \sqrt{5})}{2} = \frac{\sqrt{3}(6 - 2\sqrt{5})}{4} = \frac{\sqrt{3}(\sqrt{5} - 1)^2}{4} = \frac{\sqrt{3}}{\varphi^2}.$$

(a) $EG = EF - FG = \sqrt{3} - y = \sqrt{3}\left(1 - \frac{1}{\varphi^2}\right) = \sqrt{3} \cdot \frac{\varphi^2 - 1}{\varphi^2} = \sqrt{3} \cdot \frac{\varphi}{\varphi^2} = \frac{\sqrt{3}}{\varphi}$. Therefore, $\frac{EF}{EG} = \varphi$, and G divides EF in the golden ratio.

(b) $HF = 3\sqrt{3} - y = \sqrt{3}\left(3 - \frac{1}{\varphi^2}\right)$ and $HE = HF - \sqrt{3} = 2\sqrt{3} - y = \sqrt{3}\left(2 - \frac{1}{\varphi^2}\right)$. Therefore,

$$\frac{HF}{HE} = \frac{3\varphi^2 - 1}{2\varphi^2 - 1} = \frac{2\varphi^2 + (\varphi + 1) - 1}{2(\varphi + 1) - 1} = \frac{\varphi(2\varphi + 1)}{2\varphi + 1} = \varphi,$$

and E divides HF in the golden ratio. □

2. Isosceles right triangles

Figure 3 shows a right isosceles triangle ABC with the equal sides AC and AB divided into five equal parts, at E_k, F_k, $k = 1, 2, 3, 4$, so that $AE_k = AF_k = \frac{k}{5} \cdot AB$. The circle (AE_3F_3) intersect BC at F and G.

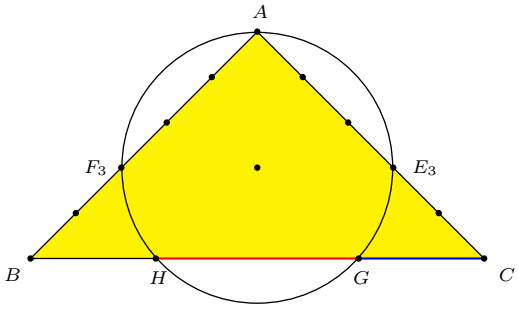

Figure 3

Proposition 3. *G divides HC in the golden ratio.*

Proof. In a Cartesian coordinate system with $A = (0, 5)$, $B = (-5, 0)$, and $C = (5, 0)$, the division points are $E_k = (k, 5 - k)$ and $F_k = (-k, 5 - k)$ for $k = 1, 2, 3, 4$. The circle AE_3F_3 has center $(0, 2)$ and radius 3; it has equation $x^2 + (y - 2)^2 = 9$ and intersects the line BC at $G = (\sqrt{5}, 0)$ and $H = (-\sqrt{5}, 0)$. Therefore, $HG = 2\sqrt{5}$ and $GC = 5 - \sqrt{5} = \sqrt{5}(\sqrt{5} - 1)$. The point G divides HC in the golden ratio since

$$\frac{HG}{GC} = \frac{2\sqrt{5}}{\sqrt{5}(\sqrt{5} - 1)} = \frac{2}{\sqrt{5} - 1} = \frac{\sqrt{5} + 1}{2} = \varphi.$$

□

Extend E_1F_1 to intersect the circumcircles of AE_3F_3 and ABC at G' and H' respectively (see Figure 4). Tran [2] has found that F_1 divides E_1G' in the golden ratio. It is also true that G' divides F_1H' in the golden ratio.

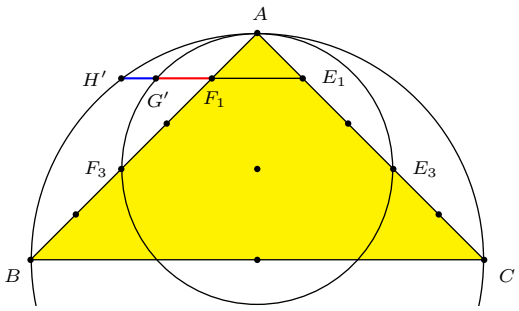

Figure 4

Figure 5 shows a right isosceles triangle ABC with $\angle ACB = 90^\circ$, and the sides AC, AB trisected at E, F respectively. The segment EF is extended to intersect the quadrant of the circumcircle at G and the perpendicular from B at H.

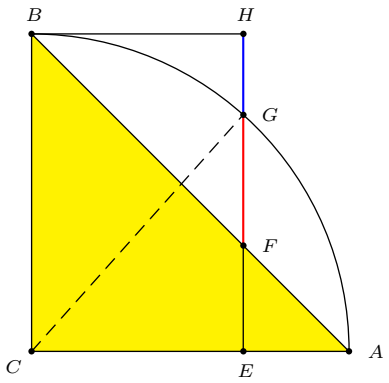

Figure 5

Proposition 4. *G divides FH in the golden ratio.*

Proof. Suppose $AC = BC = 3$. Then $FH = EH - EF = 3 - 1 = 2$, and $FG = EG - EF = \sqrt{CG^2 - CF^2} - EF = \sqrt{3^2 - 2^2} - 1 = \sqrt{5} - 1$. Therefore, $\frac{FH}{FG} = \frac{2}{\sqrt{5}-1} = \varphi$, and G divides FH in the golden ratio. □

References

[1] G. Odom and J. van de Craats, Elementary Problem 3007, *Amer. Math. Monthly*, 90 (1983) 482; solution, 93 (1986) 572.

[2] Q. H. Tran, The golden section in the inscribed square of an isosceles right triangle, *Forum Geom.*, 15 (2015) 91–92.

Dao Thanh Oai: Cao Mai Doai, Quang Trung, Kien Xuong, Thai Binh, Viet Nam
E-mail address: daothanhoai@hotmail.com

Forum Geometricorum
Volume 16 (2016) 273–281.

FORUM GEOM
ISSN 1534-1178

Regular Polygons and the Golden Section

Djura Paunić and Paul Yiu

Abstract. Given an isosceles triangle and its circumcircle, we construct a chord parallel to the base so that the endpoints and the intersections with the other two sides of the triangle are divided in the golden ratio. This generalizes results of Hagge and Odom for equilateral triangles, and Tran for a "half-square". We apply this construction to an isosceles triangle formed by two consecutive sides of a regular n-gon.

1. The golden section line of an isosceles triangle

This note is on an extension to regular polygons of elegant results on the golden section of segments associated with an equilateral triangle (Hagge [2] and Odom [4]) and a square (Tran [5]) with its circumcircle (see Figures 1 and 2). In each case, Y divides ZP and Z divides YQ in the golden ratio.

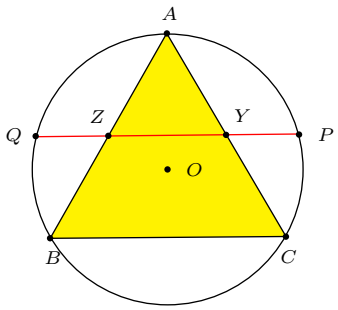

Figure 1

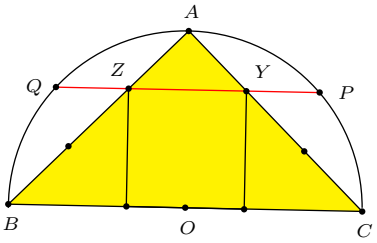

Figure 2

Let AB and AC be two consecutive sides of a regular n-gon inscribed in a circle, so that triangle ABC is isosceles with base angle $\theta = \frac{\pi}{n}$. Consider the problem of constructing a line parallel to BC, intersecting AB at Z, AC at Y, and the circle at P and Q (with P on the same side of OA as Y), such that Y divides ZP and Z divides YQ in the golden ratio $\varphi := \frac{\sqrt{5}+1}{2}$ (see Figure 3). The point Y divides ZP in the golden ratio if and only if $PY \cdot PZ = YZ^2$. Now, $PY \cdot PZ = PY \cdot YQ = CY \cdot YA$ by the intersecting chords theorem. Therefore, Y divides ZP in the golden ratio if and only if

$$\frac{CY}{YA} = \frac{CY \cdot YA}{YA^2} = \frac{YZ^2}{YA^2} = \frac{BC^2}{CA^2} = \frac{BC^2}{AB^2}.$$

Publication Date: July 13, 2016. Communicating Editor: Li Zhou.

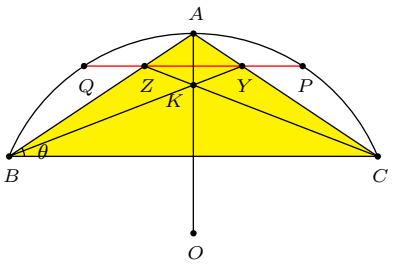

Figure 3

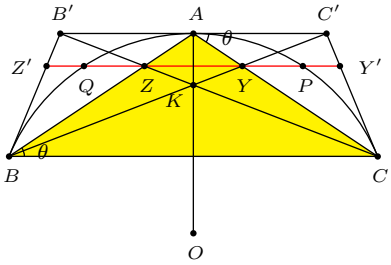

Figure 4

By symmetry, also $\frac{BZ}{ZA} = \frac{BC^2}{CA^2}$. Denote by K the intersection of the lines BY and CZ. With reference to triangle ABC, the point K has homogeneous barycentric coordinates $(BC^2 : CA^2 : AB^2)$. This is the symmedian point (see [7, §4.5.1]), and the problem is solved easily by constructing the tangents to the circle at the vertices A, B, C. Let the tangents at B and C intersect the tangent at A at B' and C' respectively. Then Y is the intersection of AC with BC' and Z that of AB and CB'. These points Y and Z determine the chord PQ of the circle such that Y divides ZP in the golden ratio (see Figure 4). Furthermore, if the chord PQ is extended to intersect BB' at Z' and CC' at Y', then P divides YY' and Q divides ZZ' in the golden ratio. We prove this by establishing a more general result on a symmetric trapezoid (see Figure 4).

Proposition 1. *Given an isosceles triangle ABC with $AB = AC$, let $BB'C'C$ be the symmetric trapezoid such that BB', $B'C'$ and $C'C$ are tangent to the circumcircle of ABC at B, A, C respectively. Let Y be the intersection of AC with BC' and Z that of AB and CB'. Extend the line YZ to intersect BB' at Z', CC' at Y', and the circle at P and Q so that P is between Y, Y', and Q is between Z and Z'. Then*
(a) *Y and Z are trisection points of the segment $Y'Z'$,*
(b) *Y divides ZP and Z divides YQ in the golden ratio,*
(c) *P divides YY' and Q divides ZZ' in the golden ratio.*

Proof. (a) By the similarity of triangles BYZ and $BC'A$ and that of triangles $CY'Y$ and $CC'A$, we have

$$\frac{YZ}{C'A} = \frac{BZ}{BA} = \frac{CY}{CA} = \frac{Y'Y}{C'A}.$$

Therefore, $YZ = Y'Y$. The same reasoning shows that $YZ = ZZ'$. Therefore, Y and Z trisect the segment $Y'Z'$.

(b) Let K be the intersection of BC' and CB'. Since B' is the intersection of the tangents at A and B to the circumcircle of triangle ABC, and C' that of the tangents at A and C, K is the symmedian point of triangle ABC. With reference to this triangle, K has homogeneous barycentric coordinates $(BC^2 : CA^2 : AB^2)$. The point Y is the trace of K on the side CA. It has coordinates $(BC^2 : 0 : AB^2)$.

Therefore,

$$CY : YA = BC^2 : AB^2 = 4\cos^2\theta : 1,$$

where θ is the base angle of the isosceles triangle ABC.[1] From the similarity of triangles CYZ and CAB',

$$\begin{aligned}
\frac{YZ}{AB'} = \frac{CY}{CA} = \frac{CY}{CY + YA} &= \frac{\frac{CY}{YA}}{1 + \frac{CY}{YA}} = \frac{4\cos^2\theta}{1 + 4\cos^2\theta} \\
\implies YZ = \frac{4\cos^2\theta \cdot AB'}{1 + 4\cos^2\theta} &= \frac{2AB'\cos\theta \cdot 2\cos\theta}{1 + 4\cos^2\theta} = \frac{AC \cdot 2\cos\theta}{1 + 4\cos^2\theta} \\
\implies YZ^2 = \frac{AC \cdot 4\cos^2\theta}{1 + 4\cos^2\theta} &\cdot \frac{AC}{1 + 4\cos^2\theta} = CY \cdot YA.
\end{aligned}$$

By the intersecting chords theorem, $CY \cdot YA = PY \cdot YQ = PY \cdot PZ$. Therefore, $PY \cdot PZ = YZ^2$, and $\frac{PZ}{YZ} = \frac{YZ}{PY}$. This shows that Y divides PZ in the golden ratio.

(c) Let M be the midpoint of YZ. It also bisects PQ and $Y'Z'$. By (a), $YY' = 2MY$. By (b), $YP = \frac{2MY}{\varphi}$. Therefore, $\frac{YY'}{YP} = \varphi$, and P divides YY' in the golden ratio. □

We call the line containing Y, Z, P, Q, Y', Z' the *golden section line* of the isosceles triangle ABC. With reference to a Cartesian coordinate system with origin O, so that A is the point $(0, R)$, the points B and C are respectively $B(-R\sin 2\theta,\ R\cos 2\theta)$ and $C(R\sin 2\theta,\ R\cos 2\theta)$. Since $CY : YA = 4\cos^2\theta : 1 = 2(1 + \cos 2\theta) : 1$, Y is the point

$$\begin{aligned}
(x, y) &= \frac{(R\sin 2\theta,\ R\cos 2\theta) + 2(1 + \cos 2\theta)(0, R)}{3 + 2\cos 2\theta} \\
&= \frac{(R\sin 2\theta,\ R(2 + 3\cos 2\theta))}{3 + 2\cos 2\theta}.
\end{aligned} \tag{1}$$

Proposition 2. *Let AB_1C_1 and AB_2C_2 be isosceles triangles inscribed in the same circle, center O, with points Y_i, Z_i, P_i, Q_i, Y_i', Z_i', $i = 1, 2$, on their golden section lines. The lines Y_1Y_2, Z_1Z_2, P_1P_2, Q_1Q_2, $Y_1'Y_2'$, $Z_1'Z_2'$ are concurrent at a point on the line OA.*

Proof. Let the line Y_1Y_2 intersect OA at T. By symmetry, the line Z_1Z_2 also intersects OA at the same point. Triangles TY_1Z_1 and TY_2Z_2 are similar. Since Y_i divides P_iZ_i in the golden ratio, $Z_iP_i = \varphi Z_iY_i$. It follows that

$$\frac{Z_1P_1}{Z_2P_2} = \frac{Z_1Y_1}{Z_2Y_2} = \frac{TZ_1}{TZ_2}.$$

Therefore, triangles TZ_1P_1 and TZ_2P_2 are similar, $\angle P_1TZ_1 = \angle P_2TZ_2$. This shows that P_1, P_2, and T are collinear. Since $Z_iY_i' = 2Z_iY_i$, the same reasoning shows that Y_1', Y_2', and T are collinear. By symmetry in OA, each of the lines

[1] We do not assume $\theta = \frac{\pi}{n}$ for some positive integer $n \geqslant 3$.

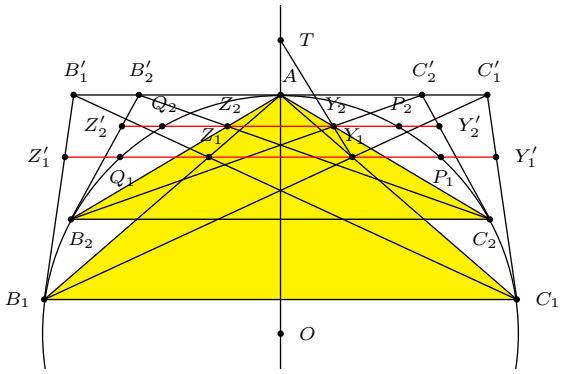

Figure 5

Q_1Q_2, and $Z_1'Z_2'$ also contains the point T. Therefore, the six lines are concurrent at T on OA. □

Remark. In a Cartesian coordinate system with origin O in which A is the point $(0, R)$, the coordinates of Y_i, $i = 1, 2$, are

$$Y_i = \left(\frac{R \sin 2\theta_i}{3 + 2\cos 2\theta_i}, \frac{R(2 + 3\cos 2\theta_i)}{3 + 2\cos\theta_i} \right),$$

where θ_i is the base angle of the isosceles triangle AB_iC_i. The line Y_1Y_2 intersects OA at

$$T = \left(0, \frac{2\cos(\theta_1 + \theta_2) + 3\cos(\theta_1 - \theta_2)}{3\cos(\theta_1 + \theta_2) + 2\cos(\theta_1 - \theta_2)} R\right) = \left(0, \frac{5 + \tan\theta_1 \tan\theta_2}{5 - \tan\theta_1 \tan\theta_2} R\right). \tag{2}$$

2. Regular polygons

By taking $\theta = \frac{\pi}{n}$ for a positive integer $n \geqslant 3$, we apply Proposition 1 to regular n-gons.

Proposition 3. *Let $A_1A_2 \cdots A_n$ and $A_1'A_2' \cdots A_n'$ be regular n-gons such that A_k is the midpoint of $A_k'A_{k+1}'$ (for $k = 1, 2, \ldots, n$ and indices taken modulo n). Let Y_k be the intersection of A_kA_{k-1} and $A_{k+1}A_k'$, and Z_k that of A_kA_{k+1} and $A_{k-1}A_{k+1}'$. Construct the line Y_kZ_k to intersect*
(i) *$A_{k-1}A_k'$ at Y_k', $A_{k+1}A_{k+1}'$ at Z_k',*
(ii) *the circumcircle of the regular n-gon $A_1A_2 \cdots A_n$ at P_k and Q_k so that P_k is between Y_k and Y_k', and Q_k is between Z_k and Z_k'.*
Then
(a) *Y_k and Z_k are trisection points of the segment $Y_k'Z_k'$,*
(b) *Y_k divides Z_kP_k and Z_k divides Y_kQ_k in the golden ratio,*
(c) *P_k divides Y_kY_k' and Q_k divides Z_kZ_k' in the golden ratio.*

It follows from Proposition 3 that the golden section line of an isosceles triangle formed by two adjacent sides of a regular n-gon is constructible with ruler and compass if and only if the regular n-gon is constructible. By Gauss' theorem, this

is the case precisely when n is the product of a power of 2 and distinct Fermat primes of the form $2^{2^k}+1$.

For $n=5$, we consider a regular pentagon $AB_sB_tC_tC_s$. The isosceles triangles AB_sC_s and AB_tC_t are called the *short* and *tall golden triangles* respectively, with base angles $\theta_s = 36°$, $\theta_t = 72°$ (see [1]). The lines Y_sY_t, Z_sZ_t, P_sP_t, Q_sQ_t, $B_sB'_s$, and $C_sC'_s$ are concurrent (Proposition 2) at the point

$$T = \left(0,\ \frac{2\cos 108° + 3\cos(-36°)}{3\cos 108° + 2\cos(-36°)}\right) = \left(0,\ \frac{2\left(-\frac{1}{2\varphi}\right) + 3\cdot\frac{\varphi}{2}}{3\left(-\frac{1}{2\varphi}\right) + 2\cdot\frac{\varphi}{2}}\right) = (0, (\varphi{+}1)R)$$

according to formula (2). The point A divides TO in the golden ratio: $TA : AO = \varphi : 1$ (see Figure 6).

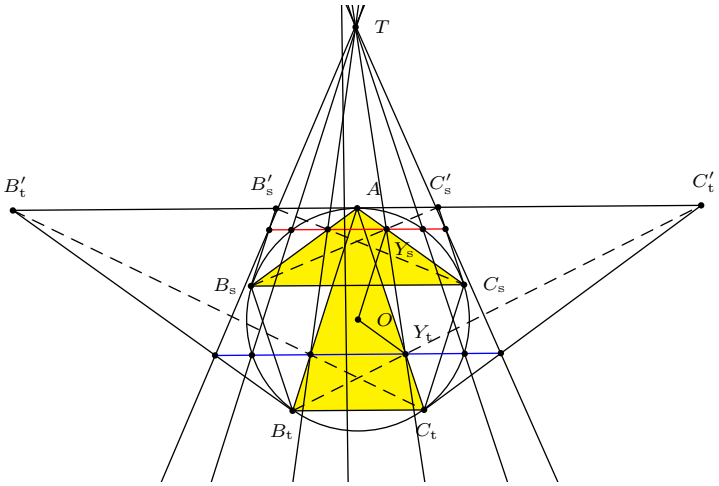

Figure 6

Figure 6 also shows a simple alternative to the construction of the golden section lines for the golden triangles. For the short golden triangle AB_sC_s, the point Y_s can be constructed as the intersection of AC_s and the parallel through O to C_sC_t. The reflection of Y_s in OA is the point Z_s, and Y_sZ_s is the golden section line for the isosceles triangle AB_sC_s. For the tall golden triangle AB_tC_t, Y_t is the intersection of AC_t with the parallel through O to AC_s. The reflection of Y_t in OA is the point Z_t, and Y_tZ_t is the golden section line for the isosceles triangle AB_tC_t.

Since AY_s is parallel to OY_t, it follows that Y_s divides TY_t in the golden ratio; similarly for the other pairs of corresponding points on the golden section lines.

3. A diagonal of a regular n-gon as a golden section line

Consider for an isosceles triangle $A_1A_{k+1}A_{n-k+1}$, $k+1 \le \lfloor \frac{n}{2} \rfloor$, from a regular n-gon $A_1A_2\cdots A_n$ with circumradius R, the possibility of its golden section line

being a diagonal of the regular n-gon. The golden section line is at a distance

$$\frac{2R\sin\frac{k\pi}{n}\cdot\sin\frac{k\pi}{n}}{1+4\cos^2\frac{k\pi}{n}} = R\cdot\frac{1-\cos\frac{2k\pi}{n}}{3+2\cos\frac{2k\pi}{n}}$$

from the vertex A_1. This line is the diagonal $A_{h+1}A_{n-h+1}$ if and only if this distance is $2R\sin\frac{h\pi}{n}\cdot\sin\frac{h\pi}{n} = 2R\sin^2\frac{h\pi}{n} = R\left(1-\cos\frac{2h\pi}{n}\right)$. Cancelling the common factor R, and simplifying, this condition becomes

$$\frac{2+3\cos\frac{2k\pi}{n}}{3+2\cos\frac{2k\pi}{n}} = \cos\frac{2h\pi}{n}. \tag{3}$$

For $n = 10$, $k = 2$, we have

$$\frac{2+3\cos\frac{2\pi}{5}}{3+2\cos\frac{2\pi}{5}} = \frac{2+\frac{3}{2\varphi}}{3+\frac{1}{\varphi}} = \frac{4\varphi+3}{2(3\varphi+1)} = \frac{\varphi}{2} = \cos\frac{2\pi}{10}.$$

The condition (3) is satisfied with $h = 1$.

Also, for $n = 10$ and $k = 4$,

$$\frac{2+3\cos\frac{4\pi}{5}}{3+2\cos\frac{4\pi}{5}} = \frac{2-\frac{3\varphi}{2}}{3-\varphi} = \frac{4-3\varphi}{2(3-\varphi)} = -\frac{1}{2\varphi} = \cos\frac{2\cdot 3\pi}{10}.$$

The condition (3) is satisfied with $h = 3$.

We summarize these in the following proposition.

Proposition 4. *In a regular decagon $A_1A_2\cdots A_{10}$, the golden section line of the isosceles triangles $A_1A_3A_9$ and $A_1A_5A_7$ are respectively the diagonals A_2A_{10} and A_4A_8* (see Figure 7).

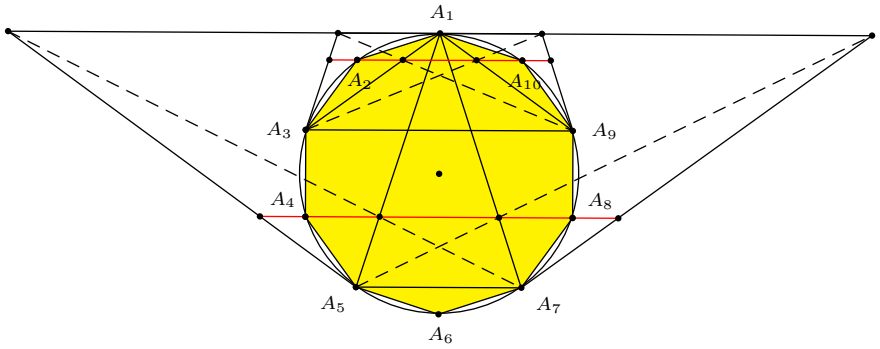

Figure 7

4. Golden section line as a side or diagonal of an inscribed regular n-gon

Proposition 3 generalizes results of Hagge [2] and Odom [4] for equilateral triangles and Tran [5] for squares to regular polygons. In Figures 8 and 9, the segment YZ is a side of a regular n-gon, $n = 3, 4$, inscribed in the isosceles triangle $A_nA_1A_2$. Figure 10, communicated by Gerhard Wanner [6], is the case of a regular hexagon, where YZ is a diagonal of a regular hexagon inscribed in the isosceles triangle. We say that a regular n-gon is inscribed in ABC if each side of ABC contains at a vertex or a side of the n-gon. We show that this is possible only for $n = 3, 4, 6$.

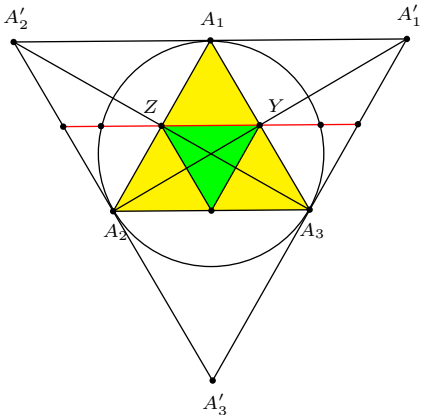

Figure 8

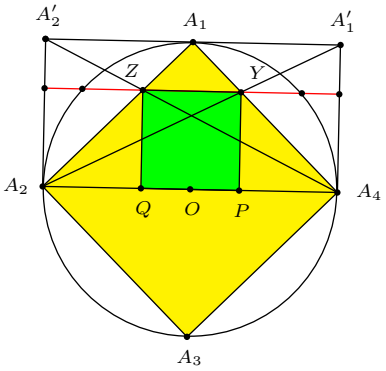

Figure 9

Proposition 5. *For an isosceles triangle formed by two consecutive sides of a regular n-gon, the golden section line is a side or a diagonal of an inscribed regular n-gon if and only if $n = 3, 4, 6$.*

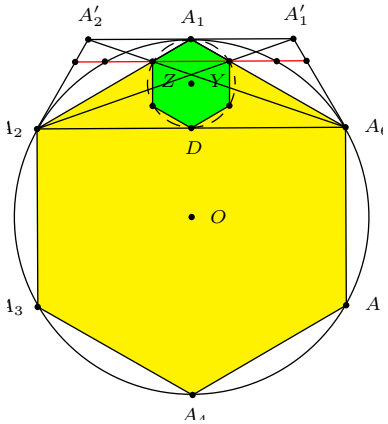

Figure 10

Proof. It is enough to prove the necessity part. The sufficiency part is indicated in Figures 8, 9, 10.

Let ℓ be the length of a side of a regular n-gon inscribed in the isosceles triangle $A_1A_2A_n$ with $A_1A_2 = A_1A_n = a$ and $\angle A_1A_2A_n = \angle A_1A_nA_2 = \frac{\pi}{n}$.

Suppose YZ is a side of the inscribed regular n-gon. Then its length is $\ell = 2a\frac{\cos\frac{\pi}{n}}{1+4\cos^2\frac{\pi}{n}}$, and its distance from A_2A_n is $A_nY\sin\frac{\pi}{n} = 4a\frac{\sin\frac{\pi}{n}\cos^2\frac{\pi}{n}}{1+4\cos^2\frac{\pi}{n}}$.

(i) If n is odd, A_2A_n contains a vertex of the n-gon. In this case

$$\begin{aligned}
&\frac{\ell}{2}\cot\frac{\pi}{2n} = 4a\frac{\sin\frac{\pi}{n}\cos^2\frac{\pi}{n}}{1+4\cos^2\frac{\pi}{n}} \implies a\frac{\cos\frac{\pi}{n}\cot\frac{\pi}{2n}}{1+4\cos^2\frac{\pi}{n}} = 4a\frac{\sin\frac{\pi}{n}\cos^2\frac{\pi}{n}}{1+4\cos^2\frac{\pi}{n}}\\
\implies\ &\cot\frac{\pi}{2n} = 4\sin\frac{\pi}{n}\cos\frac{\pi}{n} \implies \cos\frac{\pi}{2n} = 8\sin^2\frac{\pi}{2n}\cos\frac{\pi}{2n}\cos\frac{\pi}{n}\\
\implies\ &1 = 4\left(1-\cos\frac{\pi}{n}\right)\cos\frac{\pi}{n} \implies \left(2\cos\frac{\pi}{n}-1\right)^2 = 0 \implies \cos\frac{\pi}{n} = \frac{1}{2}.
\end{aligned}$$

This shows that the only possibility is $n = 3$ (see Figure 7).

(ii) If n is even, A_2A_n contains a side of the n-gon. In this case,

$$\frac{2a\cos\frac{\pi}{n}}{1+4\cos^2\frac{\pi}{n}}\cot\frac{\pi}{n} = \frac{4a\sin\frac{\pi}{n}\cos^2\frac{\pi}{n}}{1+4\cos^2\frac{\pi}{n}} \implies \sin^2\frac{\pi}{n} = \frac{1}{2}.$$

Therefore, $n = 4$ (see Figure 8).

Now suppose each of A_1A_2 and A_1A_n contains a side of the n-gon. In this case, $\ell = A_1Y = \frac{a}{1+4\cos^2\frac{\pi}{n}}$.

(iii) If n is even, then A_2A_n contains a vertex of the n-gon, and $\frac{\ell}{\sin\frac{\pi}{n}} = a\sin\frac{\pi}{n}$.

$$\frac{a}{\sin\frac{\pi}{n}\left(1+4\cos^2\frac{\pi}{n}\right)} = a\sin\frac{\pi}{n} \implies \cos^2\frac{\pi}{n} = \frac{3}{4}.$$

This is possible only when $n = 6$ (see Figure 10). In this case, $CY : YA = 3 : 1$. There is an easier construction of YZ: If D is the intersection of BC and OA, then the circle with diameter AD intersects A_1A_n and A_1A_2 at Y and Z.

(iv) If n is odd, then A_2A_n contains a side of the n-gon, and $\frac{\ell}{2}\cot\frac{\pi}{2n} = a\sin\frac{\pi}{n}$.

$$\begin{aligned}
&\frac{a\cot\frac{\pi}{2n}}{2\left(1+4\cos^2\frac{\pi}{n}\right)} = a\sin\frac{\pi}{n} \implies \cos\frac{\pi}{2n} = 2\sin\frac{\pi}{n}\sin\frac{\pi}{2n}\left(1+4\cos^2\frac{\pi}{n}\right)\\
\implies\ &1 = 4\sin^2\frac{\pi}{2n}\left(1+4\cos^2\frac{\pi}{n}\right) = 2\left(1-\cos\frac{\pi}{n}\right)\left(1+4\cos^2\frac{\pi}{n}\right)\\
\implies\ &8\cos^3\frac{\pi}{n} - 8\cos^2\frac{\pi}{n} + 2\cos\frac{\pi}{n} - 1 = 0. \qquad (4)
\end{aligned}$$

Therefore, $2\cos\frac{\pi}{n}$ is a root of the irreducible polynomial $f(x) = x^3-2x^2+x-1 \in \mathbb{Z}[x]$. But there is no integer n satisfying this condition. By Lehmer's theorem [3, Theorem 3.9], $2\cos\frac{\pi}{n}$ is an algebraic integer of degree $m := \frac{\phi(2n)}{2}$, where ϕ is the Euler totient function. If $f(x)$ is the minimal polynomial of $2\cos\frac{\pi}{n}$, then $x^m f(x+x^{-1})$ is the cyclotomic polynomial Φ_{2n}. Now there are only two integers

n for which $\frac{\phi(2n)}{2} = 3$. These are $n = 7, 9$. Since

$$x^3 f(x + x^{-1}) = x^6 - 2x^5 + 4x^4 - 5x^3 + 4x^2 - 2x + 1$$

is not the same as $\Phi_{14}(x) = x^6 - x^5 + x^4 - x^3 + x^2 - x + 1$ or $\Phi_{18}(x) = x^6 - x^3 + 1$, this shows that there is no integer n satisfying (4) □

References

[1] E. A. J. García and P. Yiu, Golden section of triangle centers in the golden triangles, *Forum Geom.*, 16 (2016) 119–124.

[2] K. Hagge, Der goldene Schnitt, *Z. f. math. und naturw. Unterr.*, 42 (1911) 28–31.

[3] I. Niven, *Irrational Numbers*, Carus Monograph, Number 11, MAA, 1956.

[4] G. Odom, and J. van de Craats, Elementary Problem 3007, *Amer. Math. Monthly*, 90 (1983) 482; solution, 93 (1986) 572.

[5] Q. H. Tran, The golden section in the inscribed square of an isosceles right triangle, *Forum Geom.*, 15 (2015) 91–92.

[6] G. Wanner, Private communication, March 27, 2016.

[7] P. Yiu, *Introduction to the Geometry of the Triangle*, Florida Atlantic University Lecture Notes, 2001; with corrections, 2013, available at
`http://math.fau.edu/Yiu/Geometry.html`

Djura Paunić: Department of Mathematics and Informatics, University of Novi Sad, 4 Trg Dositeja Obradovića, 21000 Novi Sad, Serbia

E-mail address: `djura@dmi.uns.ac.rs`

Paul Yiu: Department of Mathematical Sciences, Florida Atlantic University, 777 Glades Road, Boca Raton, Florida 33431-0991, USA

E-mail address: `yiu@fau.edu`

Forum Geometricorum
Volume 16 (2016) 283–290.

FORUM GEOM
ISSN 1534-1178

A Distance Property of the Feuerbach Point and Its Extension

Sándor Nagydobai Kiss

Abstract. We prove that among the distances from the inner Feuerbach point of a triangle to the midpoints of the three sides, one is equal to the sum of the remaining two. The same is true if the inner Feuerbach point is replaced by any one of the outer Feuerbach points.

1. Introduction

The famous Feuerbach theorem asserts that the nine-point circle of a triangle is tangent to the incircle and each of the excircles. The point of tangency with the incircle is the Feuerbach point ; it is in the interior of the triangle. We call it the *inner* Feuerbach point. The points of tangency with the excircles are exterior to the triangle, and are called the *exterior* Feuerbach points. In this note we give an interesting distance property of F_e (Theorem 1 and Figure 1 below), and its analogues for the exterior Feuerbach points.

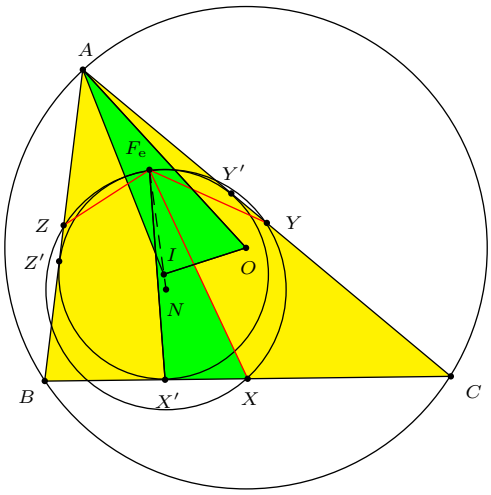

Figure 1

Theorem 1. *If F_e is the inner Feuerbach point of triangle ABC, and X, Y, Z are the midpoints of the sides BC, CA, AB, respectively, then one of the distances F_eX, F_eY, F_eZ is equal of the sum of the two others.*

Publication Date: July 15, 2016. Communicating Editor: Paul Yiu.

We make use of standard notations in triangle geometry (see [3]). Given triangle ABC, denote by a, b, c the lengths of the sides BC, CA, AB respectively, s the semiperimeter, Δ the area, and R, r the circumradius and inradius respectively. In homogeneous barycentric coordinates, the inner Feuerbach point is

$$F_{\rm e} = ((s-a)(b-c)^2 :\ (s-b)(c-a)^2 :\ (s-c)(a-b)^2). \tag{1}$$

We shall simplify calculations in this paper by employing the notations

$$u := s-a = \frac{b+c-a}{2}, \quad v := s-b = \frac{c+a-b}{2}, \quad w := s-c = \frac{a+b-c}{2}.$$

In terms of u, v, w,

$$F_{\rm e} = (u(v-w)^2 :\ v(w-u)^2 :\ w(u-v)^2), \tag{2}$$

with coordinate sum

$$\begin{aligned}\sigma_{\rm e} :=&\ u(v-w)^2 + v(w-u)^2 + w(u-v)^2\\ =&\ (v+w)(w+u)(u+v) - 8uvw \qquad (3)\\ =&\ abc - 8r^2 s =\ 4Rrs - 8r^2 s\\ =&\ 4rs(R-2r) =\ \frac{4\Delta}{R}\cdot R(R-2r) =\ \frac{4\Delta}{R}\cdot OI^2 \qquad (4)\end{aligned}$$

by Euler's formula ([1, Theorem 297]), where O and I are the circumcenter and incenter of the triangle.

Working with the distance formula, we also make use of

$$S_A := \frac{b^2+c^2-a^2}{2}, \quad S_B := \frac{c^2+a^2-b^2}{2}, \quad S_C := \frac{a^2+b^2-c^2}{2}.$$

Lemma 2. (1) $v+w=a$, $w+u=b$, $u+v=c$, *and* $u+v+w=s$.
(2) *The inradius and the exradii are*

$$r = \frac{\Delta}{s}, \quad r_a = \frac{\Delta}{u}, \quad r_b = \frac{\Delta}{v}, \quad r_c = \frac{\Delta}{w}.$$

(3) $uvw = r^2 s = r\Delta$.
(4) $vw+wu+uv = r(4R+r)$.
(5) $S_A = us - vw$, $S_B = vs - wu$, $S_C = ws - uv$.

Proof. (4)

$$\begin{aligned}vw+wu+uv =&\ \frac{uvw}{u} + \frac{uvw}{v} + \frac{uvw}{w} =\ \frac{r\Delta}{u} + \frac{r\Delta}{v} + \frac{r\Delta}{w}\\ =&\ r(r_a+r_b+r_c) =\ r(4R+r),\end{aligned}$$

since $r_a+r_b+r_c = 4R+r$ (see [1, §298 (c)]).
(5) $S_A = \frac{b^2+c^2-a^2}{2} = \frac{(w+u)^2+(u+v)^2-(v+w)^2}{2} = u(u+v+w)-vw = us-vw$. □

Proposition 3. $F_{\rm e}X = \frac{R}{2\cdot OI}\cdot|b-c|$.

Proof. We make use of the distance formula (see [3, §7.1]) for two points $P = (u,v,w)$ and $Q = (u',v',w')$ in *absolute* barycentric coordinates:

$$PQ^2 = S_A(u-u')^2 + S_B(v-v')^2 + S_C(w-w')^2.$$

The absolute barycentric coordinates of $F_{\rm e}$ are

$$(x_{\rm e}, y_{\rm e}, z_{\rm e}) = \frac{1}{\sigma_{\rm e}}(u(v-w)^2, v(w-u)^2, w(u-v)^2).$$

Since the midpoint X of BC has absolute barycentric coordinates $\left(0, \frac{1}{2}, \frac{1}{2}\right)$, and

$$\begin{aligned} y_{\rm e} - \frac{1}{2} &= \frac{1}{2\sigma_{\rm e}}\left(2v(w-u)^2 - \sigma_{\rm e}\right) \\ &= \frac{-1}{2\sigma_{\rm e}}\left(u(v-w)^2 - v(w-u)^2 + w(u-v)^2\right) \\ &= \frac{1}{2\sigma_{\rm e}}(v-w)(w+u)(u-v); \\ z_{\rm e} - \frac{1}{2} &= \frac{1}{2\sigma_{\rm e}}(v-w)(w-u)(u+v), \end{aligned}$$

the distance of $F_{\rm e}X$ is given by

$$\begin{aligned} F_{\rm e}X^2 &= S_A\cdot x_{\rm e}^2 + S_B\left(y_{\rm e}-\frac{1}{2}\right)^2 + S_C\left(z_{\rm e}-\frac{1}{2}\right)^2 \\ &= \frac{(v-w)^2}{4\sigma_{\rm e}^2}\left(4(us-vw)u^2(v-w)^2 + (vs-wu)(w+u)^2(u-v)^2\right. \\ &\qquad \left. +(ws-uv)(w-u)^2(u+v)^2\right) \\ &= \frac{(v-w)^2}{4\sigma_{\rm e}^2}\left(s(4u^3(v-w)^2 + v(w+u)^2(u-v)^2 + w(w-u)^2(u+v)^2)\right. \\ &\qquad \left. -u(4uvw(v-w)^2 + w(w+u)^2(u-v)^2 + v(w-u)^2(u+v)^2)\right). \end{aligned}$$

It turns out that both $4u^3(v-w)^2 + v(w+u)^2(u-v)^2 + w(w-u)^2(u+v)^2$ and $4uvw(v-w)^2 + w(w+u)^2(u-v)^2 + v(w-u)^2(u+v)^2$ are equal to

$$(w+u)(u+v)((v+w)(w+u)(u+v) - 8uvw) = (w+u)(u+v)\sigma_{\rm e}.$$

Therefore,

$$\begin{aligned} F_{\rm e}X^2 &= \frac{(v-w)^2}{4\sigma_{\rm e}^2}\cdot(s-u)(w+u)(u+v)\sigma_{\rm e} \\ &= \frac{(v+w)(w+u)(u+v)}{4\sigma_{\rm e}}\cdot(v-w)^2 \\ &= \frac{abc}{4\sigma_{\rm e}}\cdot(b-c)^2 = \frac{R^2}{4\cdot OI^2}\cdot(b-c)^2, \end{aligned}$$

with σ_e given by (4) and $abc = 4R\Delta$. This gives $F_{\rm e}X = \frac{R}{2\cdot OI}\cdot|b-c|$. □

Proof of Theorem 1. If Y and Z are the midpoints of CA and AB respectively, then analogous to the result of Proposition 3,

$$F_eY = \frac{R}{2\cdot OI}\cdot|c-a| \quad \text{and} \quad F_eZ = \frac{R}{2\cdot OI}\cdot|a-b|.$$

Thus, F_eX, F_eY, F_eZ are in the proportions of $|b-c|$, $|c-a|$, $|a-b|$. It is clear that in the latter triad, one of the terms (the greatest) is the sum of the remaining two. The same holds for the former triad F_eX, F_eY, F_eZ. This completes the proof of Theorem 1.

Proposition 4. *Let the incircle of triangle ABC touch the sides BC, CA, AB at X', Y', Z' respectively. The triangles F_eXX', F_eYY', F_eZZ' are similar to the triangles AOI, BOI, COI respectively.*

Proof. It is enough to prove the similarity of triangles F_eXX' and AOI (see Figure 1). Since $BX' = s-b = \frac{c+a-b}{2}$, $XX' = \left|\frac{a}{2} - \frac{c+a-b}{2}\right| = \frac{1}{2}|b-c|$. By Proposition 3, $\frac{F_eX}{AO} = \frac{XX'}{OI} = \frac{|b-c|}{2\cdot OI}$. It remains to show that $\frac{F_eX'}{AI} = \frac{|b-c|}{2\cdot OI}$ also. For this, we compute the length of F_eX'.

The absolute barycentric coordinates of X' are $\frac{1}{a}(0, s-c, s-b) = \frac{1}{v+w}(0,w,v)$. Now,

$$y_e - \frac{w}{v+w} = \frac{v(w-u)^2}{\sigma_e} - \frac{w}{v+w} = \frac{v(v+w)(w-u)^2 - w\sigma_e}{(v+w)\sigma_e}$$
$$= \frac{u(v-w)((v+w)(w+u)-4vw)}{(v+w)\sigma_e},$$

see Lemma 5(a) below. Similarly,

$$z_e - \frac{v}{v+w} = \frac{-u(v-w)((u+v)(v+w)-4vw)}{(v+w)\sigma_e}.$$

Therefore,

$$F_eX'^2 = S_Ax_e^2 + S_B\left(y_e - \frac{w}{v+w}\right)^2 + S_C\left(z_e - \frac{v}{v+w}\right)^2 = \frac{u^2(v-w)^2}{(v+w)^2\sigma_e^2}\cdot\mathscr{F},$$

where

$$\mathscr{F} = S_A(v+w)^2(v-w)^2 + S_B((v+w)(w+u)-4vw)^2 + S_C((u+v)(v+w)-4vw)^2. \tag{5}$$

We shall establish in Lemma 5(b) below that $\mathscr{F} = 4vw(v+w)\sigma_e$. From this,

$$F_eX'^2 = \frac{u^2(v-w)^2}{(v+w)^2\sigma_e^2}\cdot 4vw(v+w)\sigma_e = \frac{4u^2vw(v-w)^2}{(v+w)\sigma_e}$$
$$= \frac{4u\cdot r^2s(b-c)^2}{(v+w)\cdot\frac{4rs}{R}\cdot OI^2} = \frac{u\cdot Rr(b-c)^2}{(v+w)OI^2}$$

Now,

$$AI^2 = \frac{r^2}{\sin^2\frac{A}{2}} = \frac{uvw}{s}\cdot\frac{(w+u)(u+v)}{vw} = \frac{u(w+u)(u+v)}{s}.$$

Therefore,

$$\frac{F_{\mathrm{e}}X'^2}{AI^2} = \frac{u\cdot Rr(b-c)^2}{(v+w)OI^2}\cdot\frac{s}{u(w+u)(u+v)} = \frac{Rrs(b-c)^2}{4abc\cdot OI^2} = \frac{(b-c)^2}{4\cdot OI^2},$$

and $\frac{F_{\mathrm{e}}X'}{AI} = \frac{|b-c|}{2\cdot OI}$. The completes the proof of the similarity of triangles $F_{\mathrm{e}}XX'$ and AOI. □

Lemma 5. (a) $v(v+w)(w-u)^2 - w\sigma_{\mathrm{e}} = u(v-w)((v+w)(w+u)-4vw)$.
(b) *The polynomial* $\mathscr{F}$ *defined in* (5) *is* $4vw(v+w)\sigma_{\mathrm{e}}$.

Proof. (a) Using (3) for σ_{e}, we have

$$\begin{aligned}
& v(v+w)(w-u)^2 - w\sigma_{\mathrm{e}}\\
=\ & v(v+w)(w-u)^2 - w((v+w)(w+u)(u+v)-8uvw)\\
=\ & (v+w)(v(w-u)^2 - w(w+u)(u+v)) + 8uvw^2\\
=\ & (v+w)(u^2v - uw^2 - u^2w - 3uvw) + 8uvw^2\\
=\ & u((v+w)(uv-uw-w^2-3vw) + 8vw^2)\\
=\ & u(u(v^2-w^2) - (v+w)w(3v+w) + 8vw^2)\\
=\ & u(u(v^2-w^2) - w((v+w)(3v+w) - 8vw))\\
=\ & u(u(v^2-w^2) - w(v-w)(3v-w))\\
=\ & u(v-w)(u(v+w) + w(w-3v))\\
=\ & u(v-w)((v+w)(w+u)-4vw).
\end{aligned}$$

(b) The polynomial $\mathscr{F}$ defined in (5) is

$$\begin{aligned}
\mathscr{F} =\ & (us-vw)(v+w)^2(v-w)^2 + (vs-wu)((v+w)(w+u)-4vw)^2\\
& + (ws-uv)((u+v)(v+w)-4vw)^2.
\end{aligned}$$

Note that the coefficient of s is

$$\begin{aligned}
& u(v+w)^2(v-w)^2 + v((v+w)(w+u)-4vw)^2 + w((u+v)(v+w)-4vw)^2\\
=\ & u(v+w)^2(v-w)^2 + v(v+w)^2(w+u)^2 - 8v^2w(v+w)(w+u) + 16v^3w^2\\
& + w(u+v)^2(v+w)^2 - 8vw^2(u+v)(v+w) + 16v^2w^3\\
=\ & (v+w)\big(u(v+w)(v-w)^2 + v(v+w)(w+u)^2 + w(u+v)^2(v+w)\\
& - 8v^2w(w+u) - 8vw^2(u+v) + 16v^2w^2\big)\\
=\ & (v+w)\big(u(v+w)(v-w)^2 + v(v+w)(w+u)^2 + w(u+v)^2(v+w)\\
& - 8uvw(v+w)\big)\\
=\ & (v+w)^2\big(u(v-w)^2 + v(w+u)^2 + w(u+v)^2 - 8uvw\big)\\
=\ & (v+w)^2\left((v+w)(w+u)(u+v) - 8uvw\right)\\
=\ & (v+w)^2\sigma_{\mathrm{e}}.
\end{aligned}$$

The sum of the terms in $\mathscr{F}$ without s is

$$\begin{aligned}
&-vw(v+w)^2(v-w)^2 - wu((v+w)(w+u)-4vw)^2 \\
&\qquad\qquad - uv((u+v)(v+w)-4vw)^2 \\
=\ &-vw(v+w)^2(v-w)^2 - wu(v+w)^2(w+u)^2 + 8uvw^2(v+w)(w+u) - 16uv^2w^3 \\
&\qquad\qquad - uv(u+v)^2(v+w)^2 + 8uv^2w(u+v)(v+w) - 16uv^3w^2 \\
=\ &-(v+w)\left(vw(v+w)(v-w)^2 + wu(v+w)(w+u)^2 + uv(u+v)^2(v+w)\right. \\
&\qquad\qquad \left. -8uvw^2(w+u) - 8uv^2w(u+v) + 16uv^2w^2\right) \\
=\ &-(v+w)\left((v+w)\left(vw(v-w)^2 + wu(w+u)^2 + uv(u+v)^2\right)\right. \\
&\qquad\qquad \left. -8uvw(u(v+w)+(v-w)^2)\right) \\
=\ &-(v+w)\left((v+w)(w+u)(u+v)(u(v+w)+(v-w)^2)\right. \\
&\qquad\qquad \left. -8uvw(u(v+w)+(v-w)^2)\right) \\
=\ &-(v+w)(u(v+w)+(v-w)^2)\left((v+w)(w+u)(u+v)-8uvw\right) \\
=\ &-(v+w)(u(v+w)+(v-w)^2)\sigma_{\mathrm{e}}.
\end{aligned}$$

Therefore,

$$\begin{aligned}
\mathscr{F} &= (v+w)^2\sigma_{\mathrm{e}}s - (v+w)(u(v+w)+(v-w)^2)\sigma_{\mathrm{e}} \\
&= (v+w)\sigma_{\mathrm{e}}\left((v+w)(u+v+w) - (u(v+w)+(v-w)^2)\right) \\
&= 4vw(v+w)\sigma_{\mathrm{e}}.
\end{aligned}$$

□

2. Outer Feuerbach points

The nine-point circle is also tangent to each of the excircles. If the excircle (I_a) touches BC at X_a, and the extensions of AC and AB at Y_a, Z_a respectively, then the outer Feuerbach point F_a is the intersection of the nine-point circle with the segment joining I_a to the nine-point center N (see Figure 2). In homogeneous barycentric coordinates,

$$F_a = (-s(b-c)^2 :\ (s-c)(c+a)^2 :\ (s-b)(a+b)^2).$$

Note that these can be obtained from the coordinates of $-F_{\mathrm{e}}$ by changing (a,b,c) into $(-a,b,c)$. Under this transformation, (u,v,w,s) becomes $(s,-w,-v,u)$. In terms of u, v, w,

$$F_a = (-s(v-w)^2 : w(s+v)^2 : v(s+w)^2)$$

with coordinate sum σ_a which can be obtained from

$$-\sigma_{\mathrm{e}} = -(v+w)(w+u)(u+v) + 8uvw$$

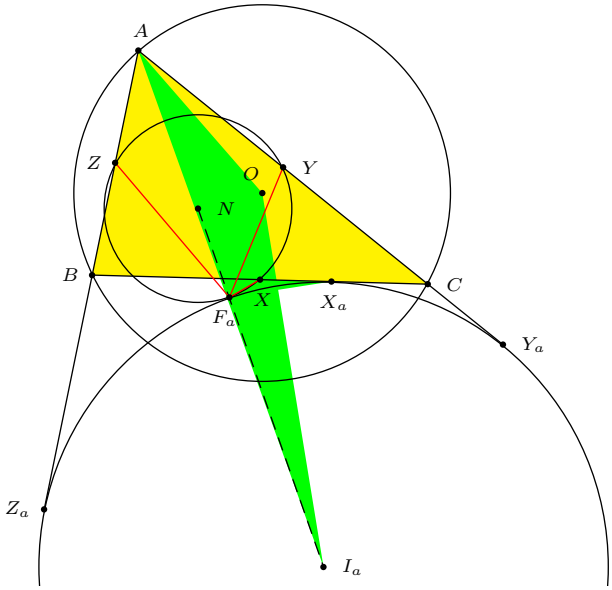

Figure 2

by the transformation (u, v, w, s) becomes $(s, -w, -v, u)$. Thus,

$$\begin{aligned}\sigma_a &= (v+w)(w+u)(u+v) + 8vws \\ &= 4\Delta(R + 2r_a) \\ &= \frac{4\Delta}{R} \cdot R(R + 2r_a) = \frac{4\Delta}{R} \cdot OI_a^2,\end{aligned}$$

where I_a is the A-excenter of the triangle (see [1, §295]).

The transformations $(a, b, c) \to (-a, b, c)$ and $(u, v, w, s) \to (s, -w, -v, u)$ also wrap X' and X_a, Y' and Y_a, Z' and Z_a. Therefore, we can easily translate the results in the previous section about the incircle into results on the excircles.

First of all, the translation of the distance formulas:

$$\begin{array}{lcl} F_eX = \frac{R}{2\cdot OI}|b-c| & \to & F_aX = \frac{R}{2\cdot OI_a}|b-c|; \\ F_eY = \frac{R}{2\cdot OI}|c-a| & \to & F_aY = \frac{R}{2\cdot OI_a}(c+a); \\ F_eZ = \frac{R}{2\cdot OI}|a-b| & \to & F_aZ = \frac{R}{2\cdot OI_a}(a+b). \end{array}$$

Since $a + \max(b, c) = (a + \min(b, c)) + |b - c|$, we easily obtain the following analogue of Theorem 1.

Proposition 6. *If the nine-point circle touches the A-excircle at F_a, then one of F_aX, F_aY, F_aZ is the sum of the remaining two.*

The analogues of Proposition 4 also hold. From the relation

$$\frac{F_eX'}{AI} = \frac{|b-c|}{2\cdot OI},$$

we obtain

$$\frac{F_aX_a}{AI_a} = \frac{|b-c|}{2 \cdot OI_a} = \frac{XX_a}{OI_a} = \frac{F_aX}{AO}.$$

The similarity of triangles F_aXX_a and AOI_a follows (see Figure 2). Similar results hold for the other two excircles.

References

[1] R. A. Johnson, *Advanced Euclidean Geometry*, 1929, Dover reprint 2007.

[2] M. J. G.Scheer, A simple vector proof of Feuerbach's theorem, *Forum Geom.*, 11 (2011) 205–210.

[3] P. Yiu, *Introduction to the Geometry of the Triangle*, Florida Atlantic University Lecture Notes, 2001; with corrections, 2013, available at
`http://math.fau.edu/Yiu/Geometry.html`

S. Nagydobai Kiss: 'Constatin Brâncuşi' Technology Lyceum, Satu Mare, Romania
E-mail address: `d.sandor.kiss@gmail.com`

Forum Geometricorum
Volume 16 (2016) 291–298.

FORUM GEOM
ISSN 1534-1178

Euclidean Figures and Solids without Incircles or Inspheres

Dimitris M. Christodoulou

Abstract. All classical convex planar Euclidean figures that possess incircles have areas $A = pr/2$, where p is the perimeter, r is the radius of the incircle, and the factor of 2 represents the dimension of the space. Similarly, all classical convex Euclidean solids that possess inspheres have volumes $V = Sr/3$, where S is the total surface area, r is the radius of the insphere, and the factor of 3 represents the dimension of the space. Elementary figures such as parallelograms and trapezoids without an incircle still obey the same area relation, but then r is the harmonic mean of the radii of the two internally tangent circles to opposite sides. Similarly, common solids without an insphere (notably cylinders and prisms) still obey the same volume relation, but then r is the harmonic mean of the three internally tangent spheres to their faces.

1. Introduction

Coxeter and Greitzer [2] show early in their book that the area of a triangle can be expressed as $A = sr$, where s is the semiperimeter and r is the inradius. This result can also be written as [1]

$$A = \frac{1}{2}pr \ , \tag{1}$$

where $p = 2s$ is the perimeter of the triangle. The use of s by [2] implies that the authors did not intend to compare their result to other classical results obtained for regular polygons (e.g., $A = pa/2$, where a is the apothem), probably because the equation $A = sr$ is valid for any triangle, regular or not. On the other hand, some comparisons have been made in print between objects and figures that are regular, such as regular polygons and regular polyhedra (e.g., Rowland 2015), where it was noticed that the equations $A = pa/2$ and

$$V = \frac{1}{3}Sr \ , \tag{2}$$

where V is the volume and S is the total surface area, are precisely similar except for the factors of 2 and 3 that appear because of the dimension of the space in each case.

This investigation started with the following question: Which global property does the ratio A/p or V/S represent in any Euclidean figure or solid, respectively?

Publication Date: July 22, 2016. Communicating Editor: Paul Yiu.

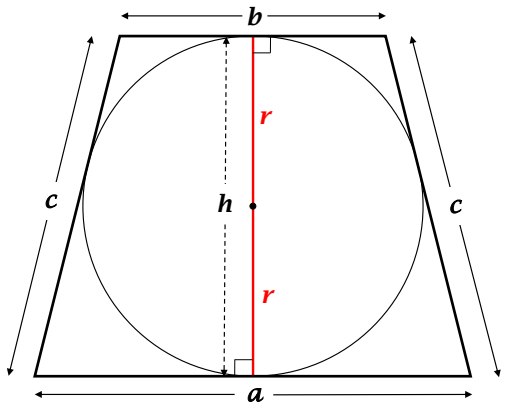

Figure 1. Isosceles trapezoid with bases a, b, legs c, inradius r, and altitude $h = 2r$.

These ratios represent a property with dimensions of length that should be characteristic of the entire object and not of any particular side and altitude. The above classical results indicate that for figures with an inscribed circle, the ratio A/p is related to the inradius; similarly, for three-dimensional solids with an insphere, the ratio V/S is related to the inradius of the insphere. This includes any rhombus, square, regular polygon, and one special isosceles trapezoid in two dimensions; and any cube, cone, and regular pyramid in three dimensions, respectively.

Notably absent from the above lists are parallelograms, rectangles, and arbitrary trapezoids; as well as rectangular prisms and right cylinders in three dimensions. So we set out to investigate such common cases in Euclidean geometry in which an incircle or an insphere cannot be drawn. For these cases, the above equations (1) and (2) are still valid, except that the inradius r has to be replaced by the harmonic mean of the radii of internally tangent circles or spheres.

In § 2, we analyze the ratio A/p in two-dimensional Euclidean figures and in § 3, we analyze the ratio V/S in three-dimensional Euclidean solids. Finally, in § 4, we discuss briefly and interpret our results in terms of the mean curvature [3, 5] defined by such tangent circles and spheres for these objects.

2. Two-Dimensional Figures

Eq. (1) can be derived quite easily for two-dimensional figures such as squares, rhombuses, and circles. But it is not obvious how it applies to trapezoids. Symmetry tells us that there exists a special isosceles trapezoid with bases a, b, congruent sides c, and altitude h between the bases that possesses an incircle (Fig. 1). Then:

Theorem 1. *If eq. (1) holds for an isosceles trapezoid, then* $c = (a + b)/2$.

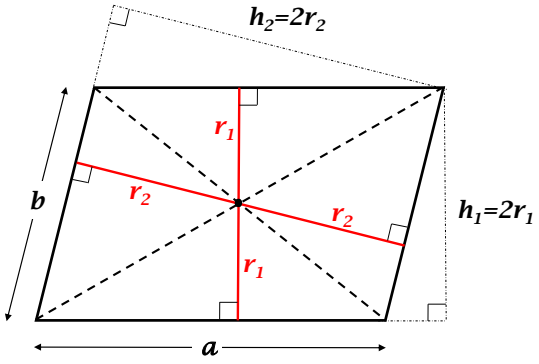

Figure 2. Parallelogram with sides a, b, altitudes $h_1 = 2r_1$, $h_2 = 2r_2$, and without an incircle.

Proof. An inscribed circle with radius r must be tangent to the bases, so $r = h/2$ (Fig. 1). Substituting this equation and the perimeter $p = a + b + 2c$ into eq. (1):

$$A = \frac{1}{2}pr = \frac{1}{2}(a + b + 2c)\frac{h}{2} = \frac{1}{2}\left(\frac{a+b}{2} + c\right)h \, . \tag{3}$$

Comparing this result to the well-known formula $A = (a + b)h/2$, we find that $\frac{a+b}{2} + c = a + b$ which implies that $c = (a + b)/2$. □

It is also interesting to note that for this special isosceles trapezoid, the altitude is the geometric mean of the bases, i.e., $h = \sqrt{ab}$.

Next we prove the converse of Theorem 1:

Theorem 2. *If $c = (a + b)/2$, then eq. (1) holds for this isosceles trapezoid.*

Proof. We begin with the well-known formula $A = (a + b)h/2$. An inscribed circle with radius r must be tangent to the bases, so $h = 2r$ (Fig. 1). Then

$$A = \frac{1}{2}(a + b)h = \frac{1}{2}(a + b)2r \, . \tag{4}$$

Then, we rewrite $(a + b)2 = (a + b) + (a + b) = (a + b) + 2c = p$, using the hypothesis. Therefore, $(a + b)2 = p$ and by substitution to eq. (4), we find eq. (1). □

Rectangles and parallelograms do not possess an incircle. Nevertheless, we can draw two different circles that will be internally tangent between opposite parallel sides. Let r_1 and r_2 be the radii of these circles (Fig. 2). Then:

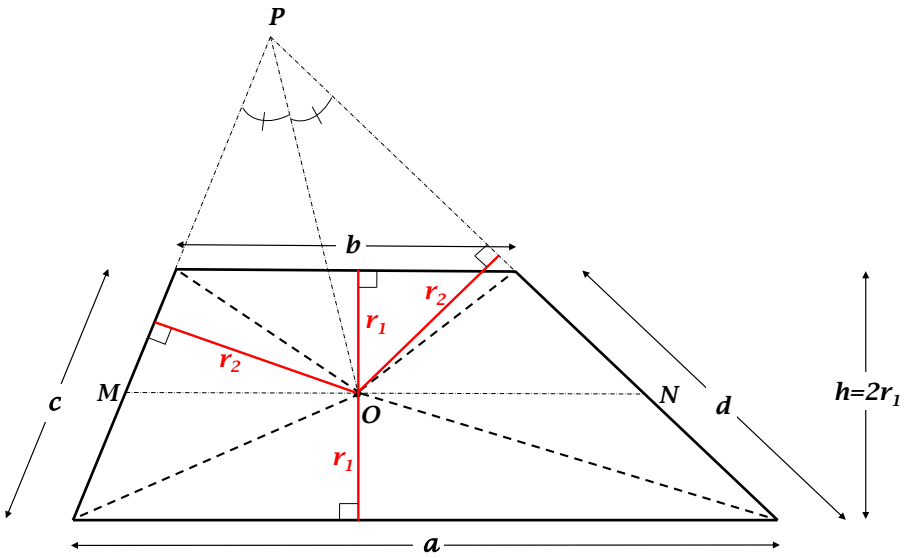

Figure 3. Trapezoid with bases a, b, legs c, d, altitude $h = 2r_1$, and without an incircle.

Theorem 3. *In rectangles and parallelograms with two internally tangent circles to opposite sides, eq. (1) holds, where r is the harmonic mean of r_1 and r_2.*

Proof. For rectangles of dimensions L and W, the proof is trivial given that $r_1 = L/2$, $r_2 = W/2$, and $p = 4(r_1 + r_2)$:

$$\frac{A}{p} = \frac{LW}{2(L+W)} = \frac{r_1 r_2}{r_1 + r_2} = \frac{1}{2}\left(\frac{2r_1 r_2}{r_1 + r_2}\right) . \tag{5}$$

For parallelograms of dimensions a and b and altitudes h_1 and h_2, we find that $h_1 = 2r_1$ and $h_2 = 2r_2$ (Fig. 2). We draw the diagonals to partition the figure into four triangles of equal area, and we sum up their areas to obtain the total area:

$$A = 2 \cdot \frac{1}{2} a r_1 + 2 \cdot \frac{1}{2} b r_2 = a r_1 + b r_2 . \tag{6}$$

Since $p = 2(a + b)$, we can write

$$\frac{A}{p} = \frac{a r_1 + b r_2}{2(a+b)} . \tag{7}$$

But $a r_1 = b r_2$ $(= A/2)$, in which case $b/a = r_1/r_2$. Substituting into eq. (7), we find after some algebra that

$$\frac{A}{p} = \frac{1}{2}\left(\frac{2r_1 r_2}{r_1 + r_2}\right) . \tag{8}$$

□

The same result (eq. [8]) can be proven for the arbitrary trapezoid without an incircle. First, we need to find the common center of the two circles that are internally tangent to the bases and to the legs, respectively. Let P be the point at which the legs meet when they are extended (Fig. 3). This center O is located at the intersection of the midsegment $\overline{MN}$ (so that it is equidistant from the bases) and the bisector of $\angle$P (so that it is equidistant from the legs). By construction, O is interior to the trapezoid. Let r_1 be the distance of O from the bases and r_2 be the distance of O from the legs. Then:

Theorem 4. *In trapezoids with two internally tangent circles to opposite sides, eq. (1) holds, where r is the harmonic mean of r_1 and r_2.*

Proof. For a trapezoid with bases a and b, legs c and d, and altitude h, we find that $h = 2r_1$ (Fig. 3). We draw segments from O to the vertices of the trapezoid to partition the figure into four triangles, and we sum up their areas to obtain the total area:

$$A = \frac{1}{2}(a+b)r_1 + \frac{1}{2}(c+d)r_2 \; . \tag{9}$$

The area of the trapezoid can also be expressed as

$$A = \frac{1}{2}(a+b)h = \frac{1}{2}(a+b)2r_1 = (a+b)r_1 \; . \tag{10}$$

Equating the two expressions for A, we find that $c + d = (a + b)r_1/r_2$. Using this equation to eliminate $c + d$ from the perimeter, we find that $p = a + b + c + d = (a + b)(r_1 + r_2)/r_2$. Then using this equation for p and eq. (10), we find that

$$\frac{A}{p} = \frac{(a+b)r_1}{(a+b)(r_1+r_2)/r_2} = \frac{r_1 r_2}{r_1+r_2} \; , \tag{11}$$

which is equivalent to eq. (1) with $r = 2r_1r_2/(r_1 + r_2)$. □

3. Three-Dimensional Solids

Eq. (2) can be derived quite easily for three-dimensional solids such as cubes and other regular polyhedra [4], and spheres. But it is not obvious how it applies to cones, cylinders, regular polygonal pyramids, and rectangular prisms. We give below only the proofs for cones and cylinders; the other proofs are similar.

Consider a cone of base radius R, height H, and slant height L (Fig. 4). A sphere of radius r can always be inscribed into this cone. Then:

Theorem 5. *Eq. (2) holds for any cone.*

Proof. Certain radii of the sphere are normal to the base of the cone and to its lateral surface (Fig. 4). A vertical cross-section through the vertex V and the center of the base C contains two similar triangles (VDO and VCB) from which we derive the proportion

$$\frac{R}{r} = \frac{L}{x} \; , \tag{12}$$

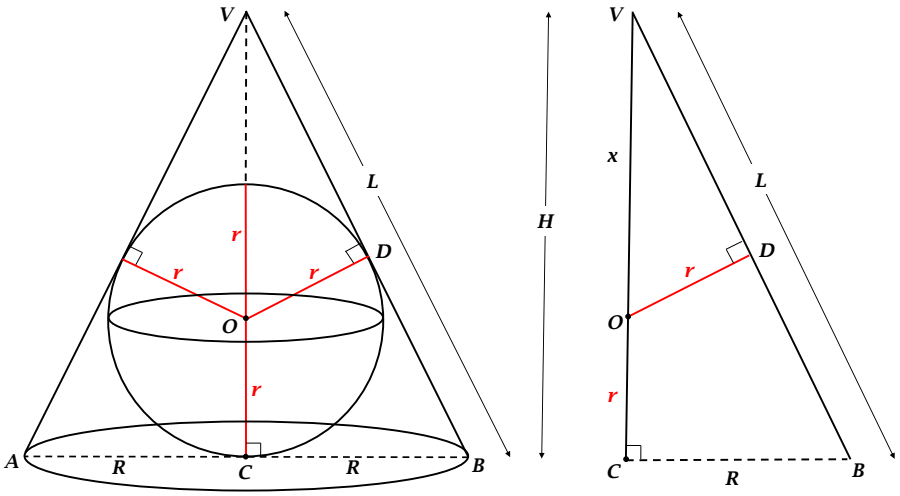

Figure 4. Cone of radius R, height H, and slant height L with an insphere of radius r. Triangles VDO and VCB on the cross-section VAB are similar (AA Similarity Postulate).

where x is the hypotenuse of the smaller triangle (see Fig. 4). This is used in the total surface area S of the cone to eliminate L:

$$S = \pi R^2 + \pi RL = \pi R^2 \left(1 + \frac{x}{r}\right) = \frac{\pi R^2 H}{r} \,, \tag{13}$$

since $r + x = H$. This equation implies that $\pi R^2 H = Sr$. Using this equation into the volume formula of the cone $V = \pi R^2 H/3$, then eq. (2) is obtained. □

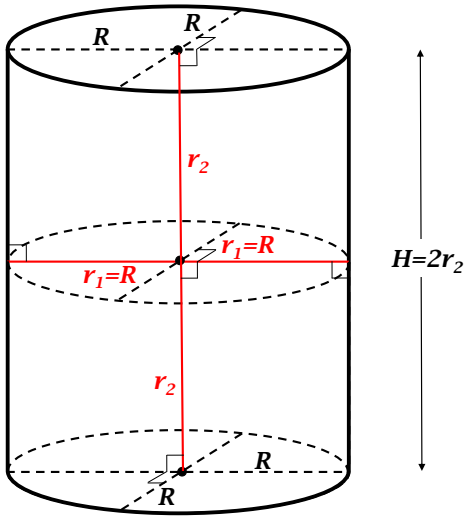

Figure 5. Cylinder of radius $R = r_1$, height $H = 2r_2$, and without an insphere.

There also exists one special cylinder in which a sphere of radius r can be inscribed. Its height then is $H = 2r$. Eq. (2) holds for that cylinder too, but the proof is trivial and is omitted. In general, a sphere cannot be inscribed in an arbitrary cylinder. In that case, we consider a cylinder with base radius R and height H in which we can draw two spheres: one internally tangent to the lateral surface with radius $r_1 = R$; and another internally tangent to the bases with radius $r_2 = H/2$ (Fig. 5). Then:

Theorem 6. *In cylinders with two such internally tangent spheres, eq. (2) holds, where r is the harmonic mean of r_1, r_1, and r_2.*

Proof. We use $r_2 = H/2$ to eliminate the height from the well-known formulae for V and S for a cylinder. Then we obtain $V = 2\pi r_1^2 r_2$, $S = 2\pi r_1(r_1 + 2r_2)$, and their ratio is

$$\frac{V}{S} = \frac{r_1 r_2}{r_1 + 2r_2} = \frac{1}{3}\left(\frac{3}{\frac{2}{r_1} + \frac{1}{r_2}}\right) . \tag{14}$$

□

Radius r_1 enters twice in the harmonic mean because the sphere that is internally tangent to the lateral surface covers two of the three principal directions in three-dimensional space. This is understood when eq. (14) is compared to the corresponding result for an arbitrary rectangular prism that has three different internally tangent spheres with radii r_1, r_2, and r_3:

$$\frac{V}{S} = \frac{1}{3}\left(\frac{3}{\frac{1}{r_1} + \frac{1}{r_2} + \frac{1}{r_3}}\right) . \tag{15}$$

4. Discussion

We have shown that eqs. (1) and (2) hold for a variety of classical Euclidean figures and solids, respectively. In cases where an incircle or an insphere cannot be drawn, the radius r in these equations reverts to a harmonic mean of the radii of the circles or spheres that are internally tangent to the sides or faces of the figures or solids, respectively. We note that no such general results can be obtained by using the radii of the circumscribed circles and spheres. Therefore, it appears that the inradius r is the most important global property of these objects in any dimension; and that the ratio of "content to boundary" (A/p or V/S) is equal to r/N, where $N \geq 2$ is the dimension of space.

The concept of mean curvature

$$K_m \equiv \frac{1}{N}\sum_{i=1}^{N} K_i \, , \tag{16}$$

from differential geometry [3, 5] allows us to rewrite the equations in all cases as

$$A = \frac{p}{\frac{1}{r_1} + \frac{1}{r_2}} = \frac{p}{2K_m} \, , \tag{17}$$

and as

$$V = \frac{S}{\frac{1}{r_1} + \frac{1}{r_2} + \frac{1}{r_3}} = \frac{S}{3K_m} \,, \tag{18}$$

where the reciprocals of the radii represent the principal curvatures K_i in the N dimensional space. We see now that the ratios A/p and V/S (of content to boundary) are equal to

$$\frac{\text{Content}}{\text{Boundary}} = \frac{\rho_m}{N} \,, \tag{19}$$

where

$$\rho_m \equiv \frac{1}{K_m} \,, \tag{20}$$

is the radius of the mean curvature K_m in each object. This answers the question posed in the Introduction.

Eq. (17) is only approximately valid for an ellipse with semi-axes $a = r_1$ and $b = r_2$. Similarly, in the case of a circular sector with an incircle, eq. (1) is approximate and becomes more accurate in the limit of small opening angles θ (i.e., for $\theta \to 0$). But the errors are remarkably small in both of these cases. We believe that the problem with the ellipse is that the circle about the two vertices is nowhere interior to the figure. And the problem with the circular sector is that its perimeter combines two linear segments with an arc. However, as $\theta \to 0$, the arc length approaches that of a straight line segment and this is why the error term then becomes minimal.

References

[1] R. G. Brown, *Advanced Mathematics*, 2003, McDougal-Littell, Evanston IL.

[2] H. S. M. Coxeter and S. L. Greitzer, *Geometry Revisited*, 1967, Math. Assoc. America, Washington, DC.

[3] A. Gray, Normal Curvature, in *Modern Differential Geometry of Curves and Surfaces with Mathematica*, 2nd ed., 1967, CRC Press, Boca Raton, FL.

[4] E. Rowland, `http://thales.math.uqam.ca/~rowland/investigations/polyhedra-project.html`, 2015.

[5] R. Schneider, *Convex Bodies: The Brunn-Minkowski Theory*, 2nd ed., 2014, Cambridge Univ. Press, Cambridge, UK.

Dimitris M. Christodoulou: Department of Mathematical Sciences, University of Massachusetts Lowell, Lowell, Massachusetts 01854, USA

E-mail address: `dimitris_christodoulou@uml.edu`

Forum Geometricorum
Volume 16 (2016) 299–311.

FORUM GEOM
ISSN 1534-1178

The Feuerbach Point and the Fuhrmann Triangle

Nguyen Thanh Dung

Abstract. We establish a few results on circles through the Feuerbach point of a triangle, and their relations to the Fuhrmann triangle. The Fuhrmann triangle is perspective with the circumcevian triangle of the incenter. We prove that the perspectrix is the tangent to the nine-point circle at the Feuerbach point.

1. Feuerbach point and nine-point circles

Given a triangle ABC, we consider its intouch triangle $X_0Y_0Z_0$, medial triangle $X_1Y_1Z_1$, and orthic triangle $X_2Y_2Z_2$. The famous Feuerbach theorem states that the incircle $(X_0Y_0Z_0)$ and the nine-point circle (N), which is the common circumcircle of $X_1Y_1Z_1$ and $X_2Y_2Z_2$, are tangent internally. The point of tangency is the Feuerbach point $F_{\rm e}$. In this paper we adopt the following standard notation for triangle centers: G the centroid, O the circumcenter, H the orthocenter, I the incenter, $N_{\rm a}$ the Nagel point. The nine-point center N is the midpoint of OH.

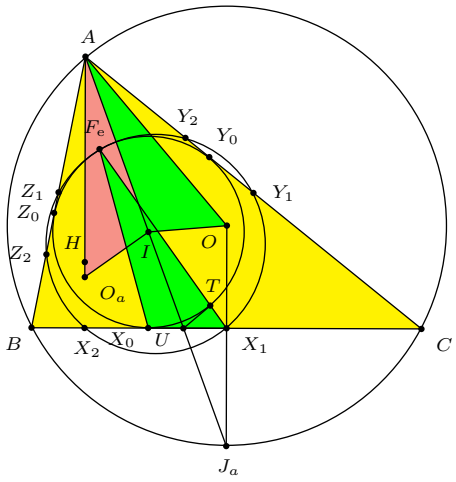

Figure 1

Proposition 1. *Let ABC be a non-isosceles triangle.*

(a) *The triangles $F_{\rm e}X_0X_1$, $F_{\rm e}Y_0Y_1$, $F_{\rm e}Z_0Z_1$ are directly similar to triangles AIO, BIO, CIO respectively.*

(b) *Let O_a, O_b, O_c be the reflections of O in IA, IB, IC respectively. The lines IO_a, IO_b, IO_c are perpendicular to $F_{\rm e}X_1$, $F_{\rm e}Y_1$, $F_{\rm e}Z_1$ respectively.*

Publication Date: July 25, 2016. Communicating Editor: Paul Yiu.

Proof. (a) It is enough to prove the direct similarity of triangles $F_eX_0X_1$ and AOI. We work with the notion of directed angles (see [2, §§16–19]). Assume that $AB < AC$. Let U and J_a be the intersections of the line AI with BC and the circumcircle (O) respectively. Draw a tangent UT to the incircle (I) (see Figure 1). The points F_e, T, X_1 are collinear (see [1, Theorem 215]). Hence, modulo π,

$$\begin{aligned}(X_0X_1,\ X_0T) &\equiv \frac{\pi}{2} - (X_0T,\ X_0I) \equiv\ (IX_0,\ IJ_a)\\ &\equiv\ (J_aO,\ J_aA) \equiv\ (AJ_a,\ AO) \equiv (AI,\ AO) \equiv -(AO,\ AI).\end{aligned}$$

On the other hand,

$$\frac{X_0T}{X_0X_1} = \frac{2r\sin X_0IJ_a}{\frac{b-c}{2}} = \frac{2r}{R}\cdot\frac{\sin\frac{B-C}{2}}{\sin B-\sin C} = \frac{r}{R\sin\frac{A}{2}} = \frac{AI}{AO}.$$

Therefore, triangles X_0TX_1 and AIO are inversely similar.

Since $(F_eX_0,\ F_eX_1) \equiv\ -(X_0T,\ X_0X_1) \pmod\pi$, and $(X_1F_e,\ X_1X_0) \equiv -(X_1X_0, X_1T) \pmod\pi$, triangles $F_eX_0X_1$ and X_0TX_1 are oppositely similar. It follows that $F_eX_0X_1$ and AIO are *directly* similar.

(b) Triangle AIO_a is oppositely similar to triangle $F_eX_0X_1$. Since $AO_a \perp X_0X_1$, it follows that $IO_a \perp F_eX_1$. Similarly, $IO_b \perp F_eY_1$ and $IO_c \perp F_eZ_1$. □

The Feuerbach point F_e is also the Poncelet point of the quadrilateral $ABCI$. This means that F_e is the common point of the nine-point circles of the four triangles IBC, ICA, IAB, and ABC. The circles $(F_eX_0X_1)$, $(F_eY_0Y_1)$, $(F_eZ_0Z_1)$ are therefore the nine-point circles of triangles IBC, ICA, IAB respectively. Each of them passes through the midpoints of two of the segments AI, BI, CI. Denote by N_a, N_b, N_c the nine-point centers of the triangles IBC, ICA, IAB respectively. We shall prove in Theorem 5 below that N_a, N_b, N_c are equidistant from N, the nine-point center of ABC.

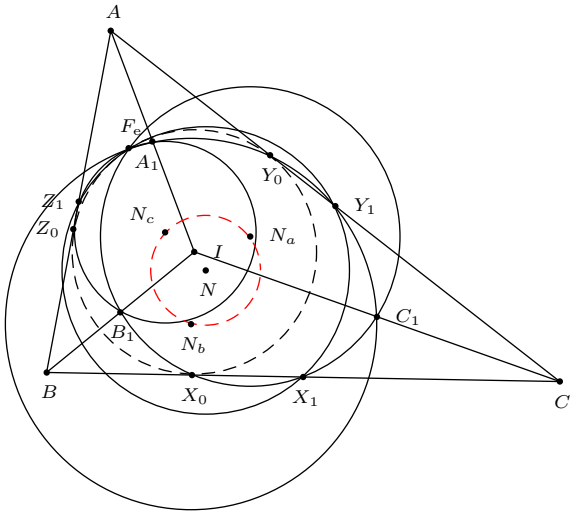

Figure 2

2. Fuhrmann triangle and Fuhrmann circle

The triangle $N_aN_bN_c$ is closely related to the Fuhrmann triangle. Let $J_aJ_bJ_c$ be the circumcevian triangle of the incenter I, and J'_a, J'_b, J'_c the reflections of J_a in BC, J_b in CA, J_c in AB respectively. These reflections form the Fuhrmann triangle $J'_aJ'_bJ'_c$. Now, J_a is the center of the circumcircle of IBC, which also passes through the excenter I_a. The nine-point center of IBC is the midpoint between I and the reflection of its circumcenter in the side BC. [1] Therefore, N_a is the midpoint of IJ'_a. Similarly, N_b and N_c are the midpoints of IJ'_b and IJ'_c. In other words, $N_aN_bN_c$ is the image of the Fuhrmann triangle under the homothety h with center I and ratio $\frac{1}{2}$. [2]

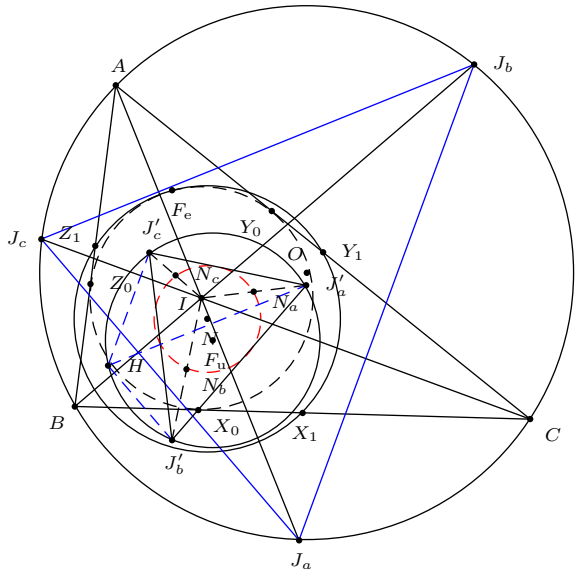

Figure 3

Basic results about the Feuerbach point and the Fuhrmann triangle can be found in [1, §§215–216] and [2, §§320–324, 367–372]. A proof of the Feuerbach theorem is given in [4].

The Fuhrmann circle is the circumcircle of the Fuhrmann triangle. It contains HN_a as a diameter ([2, Theorem 369]). The center of the Fuhrmann circle is the midpoint F_u of HN_a. Here is an alternative description.

Proposition 2. *The center of the Fuhrmann circle is the reflection of I in N.*

---

[1] If ABC is a triangle with centroid G and circumcenter O, its nine-point center is $N = \frac{3G-O}{2} = \frac{A+((B+C)-O)}{2} = \frac{A+O'}{2}$, where $O' = B + C - O = 2 \cdot \frac{B+C}{2} - O$ is the reflection of O in (the midpoint of) BC.

[2] Throughout this paper, h denotes this specific homothety. For every point P, $\mathsf{h}(P) = \frac{1}{2}(I+P)$, the midpoint of IP.

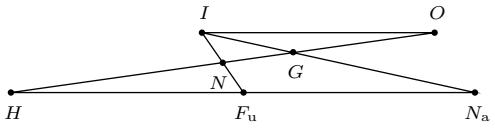

Figure 4

Proof.

$$F_{\rm u} = \frac{H + N_{\rm a}}{2} = \frac{H + (3G - 2I)}{2} = \frac{H + (H + 2 \cdot O) - 2I}{2} = H + O - I = 2N - I.$$

□

Proposition 3. *The Fuhrmann triangle $J'_aJ'_bJ'_c$ and the circumcevian triangle of I are oppositely similar.*

Proof. Since the circumcircle of $J'_aJ'_bJ'_c$ contains H, and $HJ'_a \parallel J_cJ_b$ etc. (see Figure 3),

$$(J'_aJ'_b,\ J'_aJ'_c) \equiv (HJ'_b,\ HJ'_c) \equiv (J_cJ_a,\ J_bJ_a) \equiv -(J_aJ_b,\ J_aJ_c) \pmod{\pi}.$$

Similarly, $(J'_bJ'_c,\ J'_bJ'_a) \equiv -(J_bJ_c,\ J_bJ_a) \pmod{\pi}$. The two triangles $J'_aJ'_bJ'_c$ and $J_aJ_bJ_c$ are oppositely similar. □

Since the vertices of $J_aJ_bJ_c$ are on the angle bisectors of ABC and the sides are perpendicular to these bisectors, the triangle $J_aJ_bJ_c$ has orthocenter I. This is also true for the Fuhrmann triangle.

Proposition 4. *The Fuhrmann triangle has orthocenter I.*

Proof. We begin with the excentral triangle $I_aI_bI_c$, where I_a, I_b, I_c are the excenters of triangle AC. It is well known that it has orthocenter I and circumcenter $I' = 2 \cdot O - I$, the reflection of I in O. Therefore, the centroid of the excentral triangle is

$$\frac{I_a + I_b + I_c}{3} = \frac{2I' + I}{3} = \frac{4 \cdot O - I}{3}.$$

From this we have

$$I_a + I_b + I_c = 4 \cdot O - I.$$

Since J_a is the center of the circle (IBC), which also passes through I_a, $J_a = \frac{I+I_a}{2}$. Now, for the Fuhrmann triangle, we have

$$J'_a = 2 \cdot \frac{B + C}{2} - J_a = \frac{2(B + C) - (I + I_a)}{2}.$$

and analogous expressions for J_b' and J_c'. The centroid of the Fuhrmann triangle is therefore

$$\begin{aligned} G' &= \frac{J_a' + J_b' + J_c'}{3} = \frac{4(A+B+C) - 3I - (I_a + I_b + I_c)}{6} \\ &= \frac{12G - 3I - (4 \cdot O - I)}{6} = \frac{6G - 2 \cdot O - I}{3} \\ &= \frac{3G + (3G - 2 \cdot O) - I}{3} = \frac{3G + H - I}{3}. \end{aligned}$$

Its orthocenter is

$$H' = 3G' - 2F_{\mathrm{u}} = (3G + H - I) - (H + N_{\mathrm{a}}) = 3G - N_{\mathrm{a}} - I = 2I - I = I.$$

□

Theorem 5. *The triangle $N_aN_bN_c$ has circumcenter N, circumradius $\frac{OI}{2}$, and orthocenter I.*

Proof. The triangle $N_aN_bN_c$ is the image of the Fuhrmann triangle under h. It has circumcenter $\mathsf{h}(2N - I) = \frac{I+(2N-I)}{2} = N$ and orthocenter $\mathsf{h}(I) = \frac{I+I}{2} = I$.

Since the Fuhrmann circle has diameter HN_{a}, which is parallel to and equal to twice OI (see Figure 4), its circumradius is OI. It follows that the circumradius of $N_aN_bN_c$ is $\frac{OI}{2}$. □

Corollary 6. *The circumcircle of $N_aN_bN_c$ is the nine-point circle of the Fuhrmann triangle.*

Proof. Since the Fuhrmann triangle has orthocenter I, the point N_a, being the midpoint of IJ_a', lies on its nine-point circle. Similarly, N_b and N_c are on the same nine-point circle. Therefore, the circumcircle of $N_aN_bN_c$ is the nine-point circle of the Fuhrmann triangle. □

Consider the midpoints A_1, B_1, C_1 of AI, BI, CI respectively.

Proposition 7. *The orthocenter of triangle $A_1B_1C_1$ lies on the circumcircle of $N_aN_bN_c$.*

Proof. Triangle $A_1B_1C_1$ is the image of ABC under the homothety h. Its orthocenter H' is the midpoint of IH. Since I is the orthocenter of the Fuhrmann triangle, and H lies on the Fuhrmann circle, it follows that H' lies on the nine-point circle of the Fuhrmann triangle, which is the circle $(N_aN_bN_c)$. □

Theorem 8. *The N_aX_1, N_bY_1, N_cZ_1 are concurrent at the Spieker center of triangle ABC.*

Proof. In triangle $J_a'IJ_a$, N_a and X_1 are the midpoints of the sides $J_a'I$ and $J_a'J_a$. Therefore, N_aX_1 is parallel to J_aI, the bisector of angle A. In the medial triangle $X_1Y_1Z_1$, the line N_aX_1 is the bisector of angle X_1. Similarly, N_bY_1 and N_cZ_1 are the bisectors of angles Y_1 and Z_1. The three lines N_aX_1, N_bY_1, N_cZ_1 are concurrent at the Spieker center, the incenter of the medial triangle $X_1Y_1Z_1$. □

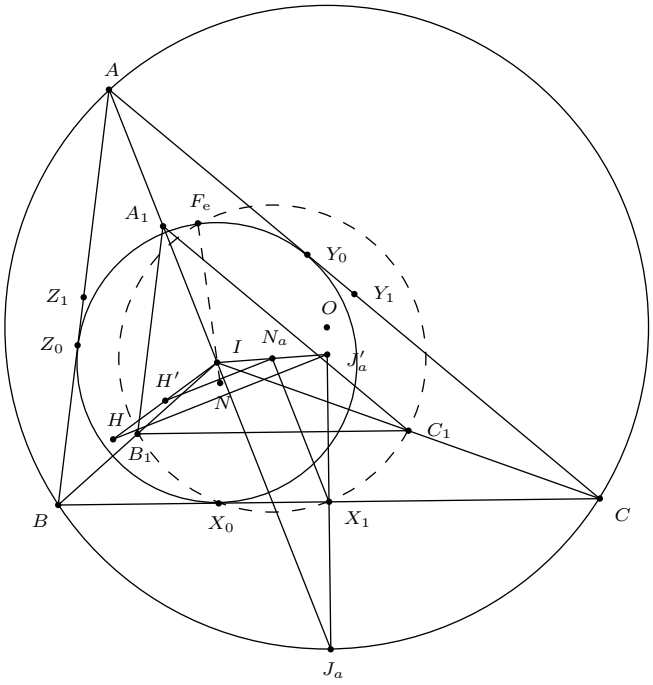

Figure 5

Remark. This point of concurrency is also the antipode of the orthocenter H' of $A_1B_1C_1$ on the circle $N_aN_bN_c$. Since this circle has center N and contains $H' = \frac{I+H}{2}$, the antipode of H' is

$$2N - H' = O + H - \frac{I+H}{2} = \frac{2\cdot O + H - I}{2} = \frac{3G - I}{2},$$

which divides IG in the ratio $3 : -1$. This is the Spieker center.

3. The residual triangles of the orthic triangle

Consider the orthic triangle $X_2Y_2Z_2$. Let X_3, Y_3, Z_3 be the midpoints of its sides Y_2Z_2, Z_2X_2, X_2Y_2 respectively, and let
O_1, I_1, F_1 be the circumcenter, incenter and Feuerbach point of triangle AY_2Z_2,
O_2, I_2, F_2 those of BZ_2X_2, and
O_3, I_3, F_3 those of CX_2Y_2.

Note that the circumcenter O_1 is the midpoint of AH, and is a point on the nine-point circle of ABC.

Theorem 9. *The lines F_1X_3, F_2Y_3, F_3Z_3 are perpendicular to OI.*

Proof. Let the line AI intersect BC at A'. Draw a line passing through A' parallel to Y_2Z_2, intersecting AC and AB at B' and C' respectively. Triangle $AB'C'$ is

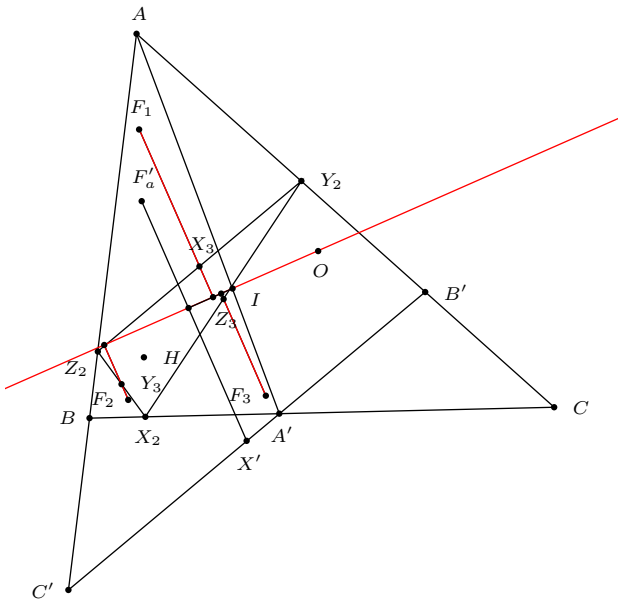

Figure 6

the reflection of ABC in AI, and is homothetic to triangle AY_2Z_2. Under this homothety, F_1 corresponds to the reflection F_a' of F_e in AI. Also, X_3 corresponds to the midpoint X' of $B'C'$. It follows that $F_1X_3 \parallel F_a'X'$. By Lemma 1(ii), $F_a'X' \perp OI$. Therefore, $F_1X_3 \perp OI$. Similarly, F_2Y_3 and F_3Z_3 are also perpendicular to OI. □

Theorem 10. *The lines O_1I_1, O_2I_2, O_3I_3 are concurrent at the Feuerbach point F_e.*

Proof. Since A, Y_2, H, Z_2 are concyclic, the circumcenter N_1 is the midpoint of AH. Let O' be the reflection of O in AI. By Proposition 1(b), $O'I \perp F_eX_1$. Now, N_1X_1 is a diameter of nine-point circle of ABC. This means that $N_1F_e \perp F_eX_1$. Therefore, $O'I$ and O_1F_e are parallel.

Since the reflection of triangle AY_2Z_2 in AI is homothetic to ABC, the incenter I_1 of AY_2Z_2 is the intersection of AI with the parallel to $O'I$ through O_1. This is the line N_1F_e. From this we conclude that I_1 is the intersection of N_1F_e with AI. The line O_1I_1 passes through F_e; similarly for the lines O_2I_2 and O_3I_3. □

4. Perspectivity and orthology of $J_aJ_bJ_c$ and $J_a'J_b'J_c'$

The triangles $J_aJ_bJ_c$ and $J_a'J_b'J_c'$ are clearly perspective at O. They are also axis-perspective. This means that the three points

$$X = J_bJ_c \cap J_b'J_c', \quad Y = J_cJ_a \cap J_c'J_a', \quad Z = J_aJ_b \cap J_a'J_b',$$

are collinear.

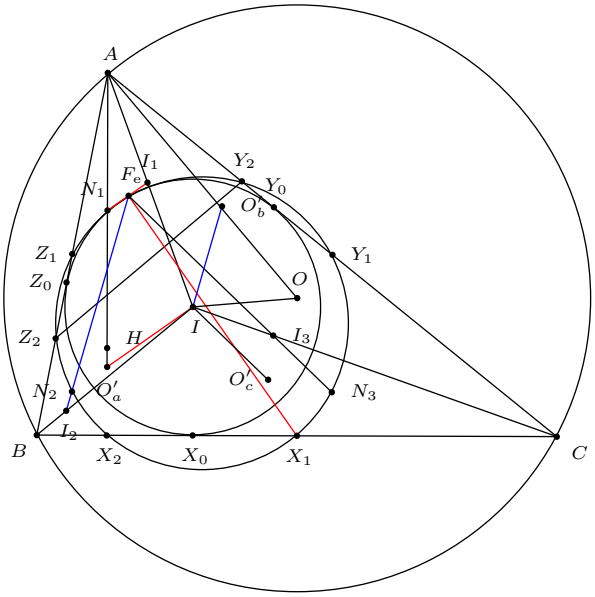

Figure 7

Theorem 11. *The line containing X, Y, Z is the tangent to the nine-point circle at the Feuerbach point.*

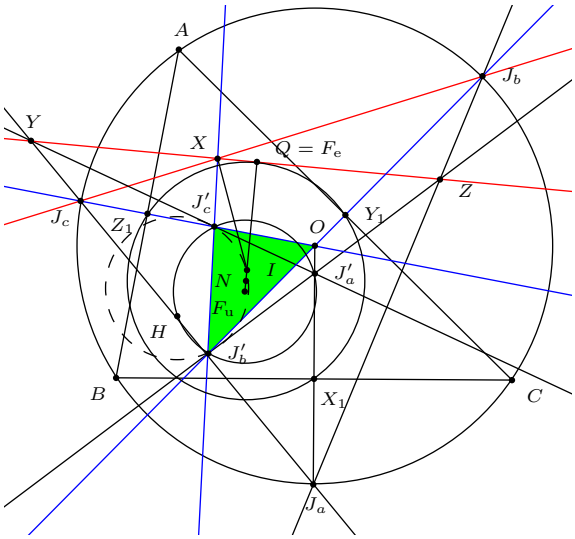

Figure 8

Proof. Applying Menelaus' theorem to triangle $OJ'_bJ'_c$ with transversal XJ_bJ_c, we have

$$\frac{J'_bX}{XJ'_c}\cdot\frac{J'_cJ_c}{J_cO}\cdot\frac{OJ_b}{J_bJ'_b}=-1 \implies \frac{J'_bX}{XJ'_c}=-\frac{J_cO}{J'_cJ_c}\cdot\frac{J_bJ'_b}{OJ_b}=-\frac{J_bJ'_b}{J_cJ'_c}.$$

Therefore,

$$\frac{XJ'_b}{XJ'_c}=\frac{J_bJ'_b}{J_cJ'_c}=\frac{\sin^2\frac{B}{2}}{\sin^2\frac{C}{2}}=\left(\frac{\sin\frac{B}{2}}{\sin\frac{C}{2}}\right)^2$$

On the other hand,

$$\frac{IJ'_b}{IJ'_c}=\frac{\sin\frac{B}{2}}{\sin\frac{C}{2}}.$$

Therefore, $\frac{XJ'_b}{XJ'_c}=\left(\frac{IJ'_b}{IJ'_c}\right)^2$. This means that IX is tangent to the circle $(IJ'_bJ'_c)$, and $IX^2=XJ'_b\cdot XJ'_c$. Thus, X lies on the radical axis of the Fuhrmann circle and the point-circle I. The same is true for Y and Z. This shows that the perspectrix XYZ is perpendicular to the line joining $F_{\rm u}$ and I, which is the same as the line NI. If XYZ intersects NI at Q,

$$QF_{\rm u}^2-QI^2=(QF_{\rm u}-QI)(QF_{\rm u}+QI)=IF_{\rm u}\cdot 2QN=4NI\cdot QN=2(R-2r)QN.$$

It follows that $2(R-2r)QN=\rho^2=OI^2=R(R-2r)$, and $QN=\frac{R}{2}$. This means that Q lies on the nine-point circle of triangle ABC, and is the Feuerbach point $F_{\rm e}$. The line XYZ is the tangent to the nine-point circle at $F_{\rm e}$. □

Theorem 12. *The triangles $J_aJ_bJ_c$ and $J'_aJ'_bJ'_c$ are orthologic.*

(a) *The perpendiculars from J'_a to J_bJ_c etc are concurrent at the Nagel point $N_{\rm a}$.*

(b) *The perpendiculars from J_a to $J'_bJ'_c$ etc are concurrent at the superior of the Feuerbach point.*

Proof. (a) The perpendiculars from J'_a to J_bJ_c, J'_b to J_cJ_a, and J'_c to J_aJ_b are the lines

$$\begin{aligned}(b-c)x+\quad by-\quad cz&=0,\\ -ax+(c-a)y+\quad cz&=0,\\ ax-\quad by+(a-b)z&=0.\end{aligned}$$

These three lines are concurrent at the point $(x:y:z)$, where

$$\begin{aligned}x:y:z&=\begin{vmatrix}c-a & c\\ -b & a-b\end{vmatrix}:-\begin{vmatrix}-a & c\\ a & a-b\end{vmatrix}:\begin{vmatrix}-a & c-a\\ a & -b\end{vmatrix}\\ &=a(b+c-a):a(c+a-b):a(a+b-c)\\ &=b+c-a:c+a-b:a+b-c.\end{aligned}$$

This is the Nagel point.

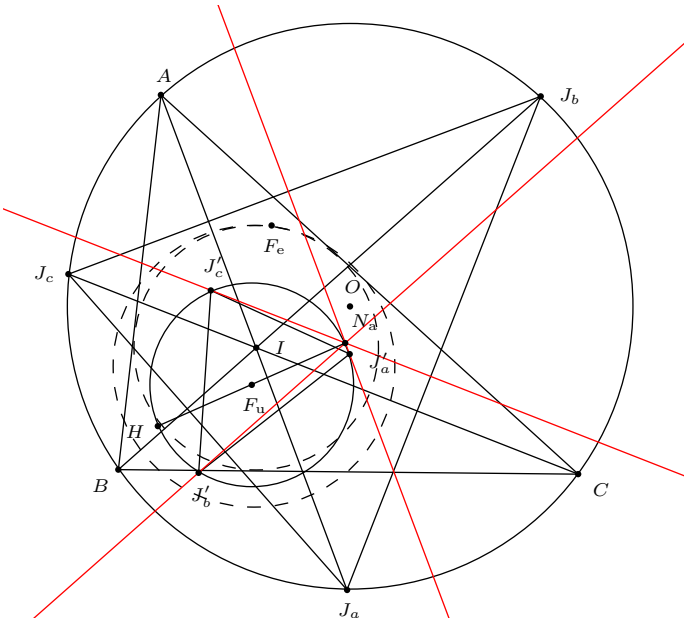

Figure 9

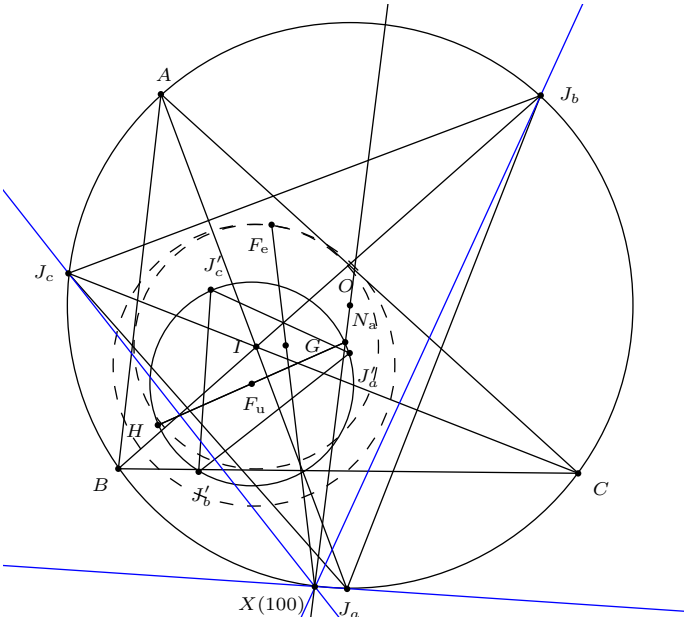

Figure 10

(b) The perpendiculars from J_a to $J'_bJ'_c$, J_b to $J'_cJ'_a$, and J_c to $J'_aJ'_b$ are the lines

$$\begin{aligned} -(b+c)(b-c)x+ \quad & a(c-a)y+ \quad a(a-b)z=0,\\ b(b-c)x-(c+a)(c-a)y+ \quad & b(a-b)z=0,\\ c(b-c)x+ \quad & c(c-a)y-(a+b)(a-b)z=0. \end{aligned}$$

These three lines are concurrent at the point $(x : y : z)$, where

$$\begin{aligned}&(b-c)x : (c-a)y : (a-b)z\\ &= \begin{vmatrix}-(c+a) & b\\ c & -(a+b)\end{vmatrix} : -\begin{vmatrix}b & b\\ c & -(a+b)\end{vmatrix} : \begin{vmatrix}b & -(c+a)\\ c & c\end{vmatrix}\\ &= a(a+b+c) : b(a+b+c) : c(a+b+c).\end{aligned}$$

Therefore, $(x : y : z) = \left(\frac{a}{b-c} : \frac{b}{c-a} : \frac{c}{a-b}\right)$. This is the triangle center $X(100)$ in [3]. It is the superior of the Feuerbach point. □

Remarks. (1) The Nagel point N_a is the triangle center $X(74)$ of the Fuhrmann triangle.

(2) The superior of the Feuerbach point is the triangle center $X(100)$. It is $X(74)$ of $J_aJ_bJ_c$.

Theorem 13. *The seven circles $IJ_aJ'_a$, $IJ_bJ'_b$, $IJ_cJ'_c$, $AJ'_bJ'_c$, $BJ'_cJ'_a$, $CJ'_aJ'_b$ and the circumcircle (O) have a common point K. Moreover, let J be the intersection point of the ray HF_e and the circumcircle (O) and I be the incenter of ABC. Then, K, I, J are collinear.*

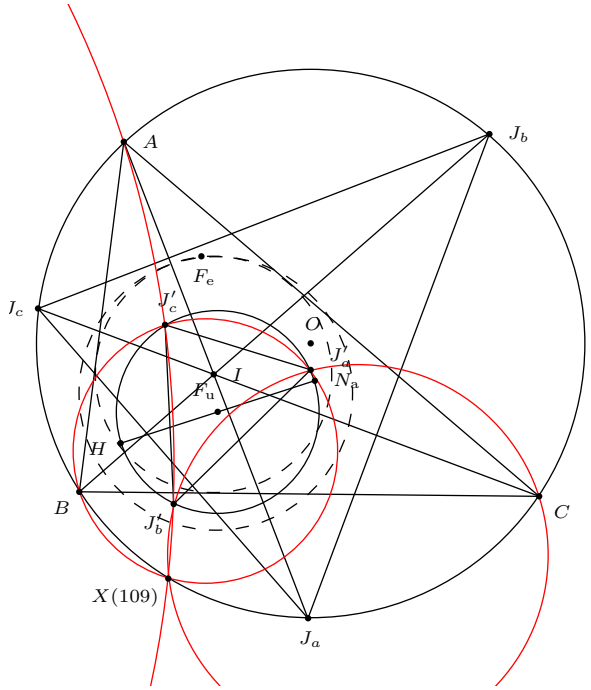

Figure 11

Proof. The equation of the circle $AJ'_bJ'_c$ is

$$(b^2-bc+c^2-a^2)(a^2yz+b^2zx+c^2xy)-(x+y+z)f(x,y,z)=0,$$

where

$$f(x,y,z) = c^2(c-a)(c+a-b)y - b^2(a-b)(a+b-c)z.$$

This contains the point

$$X(109) = \left(\frac{a^2}{(b-c)(b+c-a)} : \frac{a^2}{(b-c)(b+c-a)} : \frac{a^2}{(b-c)(b+c-a)}\right)$$

on the circumcircle since

$$f\left(\frac{a^2}{(b-c)(b+c-a)}, \frac{a^2}{(b-c)(b+c-a)}, \frac{a^2}{(b-c)(b+c-a)}\right)$$
$$= c^2b^2 - b^2c^2 = 0.$$

Therefore, the circle $AJ_b'J_c'$ contains $X(109)$. Similarly, the circles $BJ_c'J_a'$ and $CJ_a'J_b'$ also contain the same point.

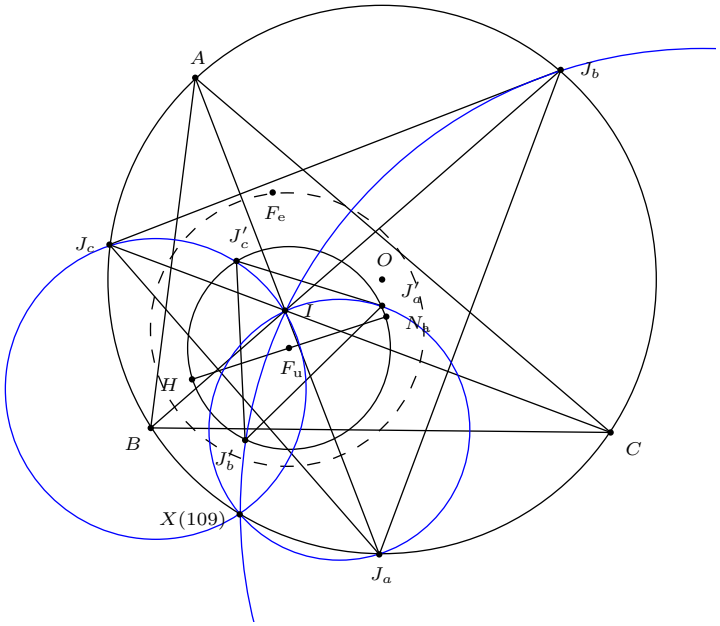

Figure 12

The equation of the circle IJ_aJ_b' is

$$(b-c)(a+b+c)(b+c-a)(a^2yz + b^2zx + c^2xy) - (x+y+z)g(x,y,z) = 0,$$

where

$$g(x,y,z) = bc(b-c)(b+c)(b+c-a)x - a^2c(c-a)(c+a-b)y - a^2b(a-b)(a+b-c)z.$$

This contains the point $X(109)$ with coordinates given above since

$$g\left(\frac{a^2}{(b-c)(b+c-a)}, \frac{a^2}{(b-c)(b+c-a)}, \frac{a^2}{(b-c)(b+c-a)}\right)$$
$$= a^2bc(b+c) - a^2b^2c - a^2bc^2 = 0.$$

Similarly, the circles $IJ_bJ'_b$ and $IJ_cJ'_c$ contain the same point.

□

References

[1] N. A. Court, *College Geometry*, Dover reprint, 2007.
[2] R. A. Johnson, *Advanced Euclidean Geometry*, Dover reprint, 2007.
[3] C. Kimberling, *Encyclopedia of Triangle Centers*, available at `http://faculty.evansville.edu/ck6/encyclopedia/ETC.html`.
[4] M. J. G. Scheer, A simple vector proof of Feuerbach's theorem, *Forum Geom.*, 11 (2011) 205–210.
[5] J. Vonk, The Feuerbach point and reflections of the Euler line, *Forum Geom.*, 9 (2009) 47–55.

Nguyen Thanh Dung: Chu Van An high school for Gifted students, 55 To Son street, Chi Lang ward, Lang son province, Viet Nam

E-mail address: `nguyenthanhdungcva@gmail.com`

Forum Geometricorum
Volume 16 (2016) 313–316.

FORUM GEOM
ISSN 1534-1178

Similarities on a Sphere

Pascal Honvault

Abstract. We define dilations and similarities on a sphere with the use of quaternions. As an application, we produce a simple algorithm for the calculation of the angles of a polyhedron.

1. Introduction

The orientation preserving similarities of the usual plane are well known: They are composition of translations, rotations and dilations. We can define as well rotations and dilations on a sphere in a simple manner by the use of quaternions. The big advantage of quaternions is to facilitate the calculation of the composition $R_2 \circ R_1$ of two rotations in the usual 3D-space ([2]), and to avoid singularities like the poles.

We begin by looking for the local similarities on the unit sphere S^2 of the usual 3D-real euclidean space $\mathbb{R}^3$. We say that f is a local similarity of S^2 if there exist neighbourhoods V_Ω, $V_{\Omega'}$ of points Ω, Ω' such that $f : V_\Omega \to V_{\Omega'}$ preserves the distance ratios. Recall that the exponential map $exp_\Omega : m \in T_\Omega \mapsto M \in V_\Omega$ sends points m in a neighbourhood of Ω in the tangent plane T_Ω to points M in the unit sphere. Geometrically, it corresponds to laying off a length equal to Ωm along the geodesic that passes through m in the direction of $\overrightarrow{\Omega m}$. So we can define the local induced map $\tilde{f} : T_\Omega \to T_{\Omega'}$ by $\tilde{f} = exp_{\Omega'}^{-1} \circ f \circ exp_\Omega$. Indeed, it is a local plane similarity because distance ratios and angles from Ω are preserved. If we specialize to positive similarities with a fixed point Ω, we then obtain that $f = exp_\Omega \circ \tilde{f} \circ exp_\Omega^{-1}$ is a local rotation or dilation of center Ω (or their composition), which we want now to describe in terms of quaternions.

2. Local similarities in terms of quaternions

We first recall some basic facts and notations about the space $\mathbb{H}$ of quaternions. We will denote by $\mathbf{q} = a + q$ or $\mathbf{q} = (a, q)$ a quaternion of scalar part (or real part) a and vector part (or imaginary part) q, with $q = bi + cj + dk$, $(b, c, d) \in \mathbb{R}^3$. $\mathbb{H}$ is then an associative, anticommutative real algebra of dimension 4 with respect to the usual addition and the multiplication rule:

$$ii = jj = kk = -1,\ ij = k,\ jk = i,\ ki = j.$$

Publication Date: September 27, 2016. Communicating Editor: Paul Yiu.

We also identify the number q with the vector (b, c, d) of $\mathbb{R}^3$. The conjugate $\mathbf{q}^*$ of $\mathbf{q}$ is defined by $\mathbf{q}^* = a - q$, in such a way that $\mathbf{q}\mathbf{q}^* = \mathbf{q}^*\mathbf{q} = a^2 + b^2 + c^2 + d^2$ is the usual euclidean norm of $\mathbb{R}^4$. This leads us to define the set of unit quaternions $\mathbb{H}(\|1\|)$. In fact, we can introduce a scalar product on $\mathbb{H}$ by $\mathbf{q} \cdot \mathbf{q}' = aa' + bb' + cc' + dd'$ and $\mathbf{q}\mathbf{q}^*$ is nothing but $\mathbf{q} \cdot \mathbf{q} = \|\mathbf{q}\|^2$. On the second hand, each unit quaternion $\mathbf{q}$ can be rewritten as $\cos(\varphi) + \sin(\varphi)u$ where u is a pure imaginary and unit quaternion. Finally, we can represent rotations $R_{\vec{u},\theta}$ with axis $\mathbb{R}\vec{u}$ ($\vec{u}$ unitary) and angle θ by the quaternion $\mathbf{q} = \cos(\theta/2) + \sin(\theta/2)u$ in the following manner: $R_{\vec{u},\theta}(\vec{v}) = \mathbf{q}v\mathbf{q}^*$. Moreover, the mapping $\mathbf{q} \in \mathbb{H}(\|1\|) \mapsto R \in SO(3)$ is a group homomorphism for multiplication and composition, that is the composition of two rotations is represented by the product of two unit quaternions.

Next, let us look at spherical dilation. We fix a point $\Omega \in S^2$ and a real positive number λ. The dilation $H_{\Omega,\lambda}$ of center Ω and ratio λ is a map from the spherical cap $V_{\Omega,\pi/\lambda} = \left\{M \in S^2 : \angle O\Omega M < \pi/\lambda\right\}$ to S^2. By noting M' the image of M and $\mathscr{C}_{\Omega,M}$ the meridian of origin Ω passing through M, it is defined by: $M' \in \mathscr{C}_{\Omega,M}$ and $\widetilde{\Omega M'} = \lambda \cdot \widetilde{\Omega M}$. This motion may be described by quaternion interpolation ([3]) in the following way. Let $\mathbf{q_0} = q_0$ and $\mathbf{q} = q$ be the unit quaternions (and purely imaginary) representing the vectors $\overrightarrow{O\Omega}$ and $\overrightarrow{OM}$. Then the quaternion (where θ is the angle between q_0 and q)

$$\mathbf{q}'(\lambda) = q'(\lambda) = \frac{q_0 \cdot \sin(1-\lambda)\theta + q \cdot \sin(\lambda\theta)}{\sin(\theta)}$$

is exactly the quaternion representing M'. It is also denoted by $Slerp(\lambda; q_0, q)$ and it is known as "Spherical Linear Interpolation". Let us summarize the previous results.

Theorem 1. *The local positive similarities of the unit sphere S^2 with a fixed point Ω are the rotations $R_{\overrightarrow{O\Omega},\delta}$, the dilations $H_{\Omega,\lambda}$ of center Ω, and their compositions. They can be algebraically represented by quaternions as:*

- $R_{\overrightarrow{O\Omega},\delta} : v \mapsto qvq^*$ *where* $q = \cos\dfrac{\delta}{2} + \sin\dfrac{\delta}{2} \cdot \omega$,
- $H_{\Omega,\lambda} : v \mapsto Slerp(\lambda; \omega, v) = \dfrac{\omega \cdot \sin(1-\lambda)\theta + v \cdot \sin(\lambda\theta)}{\sin(\theta)}$,

where ω is the quaternion representing Ω and $\theta = \angle(\widehat{\omega, v})$.

3. Application to polyhedra

We apply here the above results to compute some angles of a given polyhedral angle. As in our technical report ([4]), we are interested in the calculation of the last three angles of such a polyhedra. That is, let $\mathscr{P}$ be a polyhedral angle of vertex p and degree n, and $F_1, ..., F_n$ its faces. It intersects the unit sphere of center p in a spherical polygon $(q_0, q_1, ..., q_{n-1}, q_n = q_0)$. If we fix the internal angles $\alpha_1 = \angle q_0 p q_1, \ldots, \alpha_{n-1} = \angle q_{n-2} p q_{n-1}$ of the faces $F_1, ..., F_{n-1}$ and the external (dihedral) angles $\delta_1 = \angle(F_1, F_2), \ldots, \delta_{n-2} = \angle(F_{n-2}, F_{n-1})$, then the polyhedron is entirely known up to a motion (see [1] for rigidity-type results). Thus we may compute the last three angles $\alpha_n = \angle q_{n-1} p q_n$, $\delta_{n-1} = \angle(F_{n-1}, F_n)$ and

$\delta_n = \angle(F_n, F_1)$. The angles α_i are measured in $]0, \pi[$ and are equal to the lengths of the geodesic arcs $\widetilde{q_{i-1}q_i}$, whereas the angles δ_i are measured in $]0, 2\pi[$ and are equal to the angles $(\widetilde{q_iq_{i-1}}, \widetilde{q_iq_{i+1}})$.

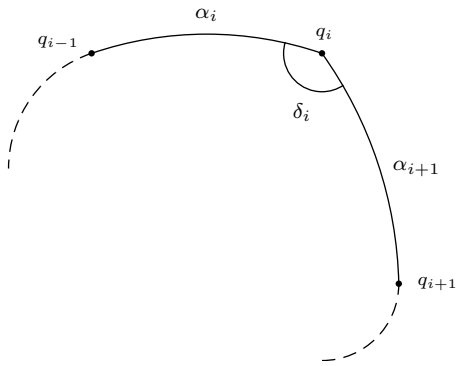

Figure 1. Polygonal view of $\mathscr{P}$ on S^2

If we associate with each point $q_i = (b, c, d)$ the quaternion $\mathbf{q_i} = q_i = bi + cj + dk$, then we have the simple following relationship between q_{i-1}, q_i and q_{i+1}:

$$\begin{aligned} q_{i+1} &= Slerp(\frac{\alpha_{i+1}}{\alpha_i}; q_i, Q_iq_{i-1}Q_i^*) \\ &= \frac{\sin(\alpha_i - \alpha_{i+1})q_i + \sin(\alpha_{i+1})Q_iq_{i-1}Q_i^*}{\sin(\alpha_i)} \end{aligned} \tag{1}$$

with $Q_i = \cos(\frac{\delta_i}{2}) + \sin(\frac{\delta_i}{2})q_i$. For this calculation, we also need the value of θ which is here $\arccos q_i \cdot (Q_iq_{i-1}Q_i^*)$ (because $Slerp$ is independent of the sign of θ). For the algorithm, we fix the values $q_0 = i, q_1 = \cos(\alpha_1)i + \sin(\alpha_1)j$, and we compute q_{n-1} step by step by using the equation (1) for $i = 1$ to $n - 2$.

Now we can compute $\alpha_n = \arccos(\mathbf{q_{n-1}}.\mathbf{q_n}) = \arccos\dfrac{q_{n-1}q_0^* + q_0q_{n-1}^*}{2}$.

For the last two dihedral angles, we will use the following lemma.

Lemma 2. *Let u, v be two unit vectorial quaternions, $q = \cos(\delta/2) + \sin(\delta/2)u$ and $Q = \cos(\delta) + \sin(\delta)u$. Then $Q = \dfrac{(u \cdot v)u \wedge v + (qvq^*)((u \cdot v)u - v)}{1 - (u \cdot v)^2}$.*

Proof. Recall that if $q = \cos(\delta/2)+\sin(\delta/2)u$ is a unit quaternion and v a vectorial quaternion, then

$$qvq^* = \cos(\delta)v + (1 - \cos(\delta))(u.v)u + \sin(\delta).u \wedge v \tag{2}$$

and that the product of two vectorial quaternions q_1 and q_2 is

$$q_1q_2 = -(q_1.q_2) + q_1 \wedge q_2.$$

So, if v is unitary, then

$$(qvq^*)v = -\cos(\delta) + (1 - \cos(\delta))(u \cdot v)(-(u \cdot v) + u \wedge v) + \sin(\delta)(u \wedge v) \wedge v.$$

By the vector triple product formula $(u \wedge v) \wedge w = (u.w)v - (v.w)u$, this leads to

$$\begin{aligned}(qvq^*)v = & -(\cos(\delta) + \sin(\delta)u) - (u \cdot v)^2(1 - \cos(\delta)) + \sin(\delta)(u \cdot v)v \\ & + (1 - \cos(\delta))(u \cdot v)u \wedge v.\end{aligned}$$

We have similarly

$$(qvq^*)u = -(u \cdot v)(\cos(\delta) + \sin(\delta)u) - (u \cdot v)(1 - \cos(\delta)) + \sin(\delta)v - \cos(\delta)u \wedge v.$$

Thus, $(qvq^*)(v - (u \cdot v)u) = Q((u \cdot v)^2 - 1) + (u.v)u \wedge v$ and this proves the lemma. □

Now, formula (1) tells us that

$$Q_i q_{i-1} Q_i^* = \frac{\sin(\alpha_i)q_{i+1} - \sin(\alpha_i - \alpha_{i+1})q_i}{\sin(\alpha_{i+1})}. \tag{3}$$

Thus, we have by Lemma 2

$$\cos(\delta_i) + \sin(\delta_i)q_i = \frac{\cos(\alpha_{i+1})(\cos(\alpha_i) + q_i q_{i-1}) + q_{i+1}(\cos(\alpha_i)q_i - q_{i-1})}{\sin(\alpha_{i+1})\sin(\alpha_i)}$$

giving us the values of δ_{n-1} and δ_n by identifying the real and imaginary parts.

Theorem 3. *The dihedral angles δ_{n-1} and δ_n are given by*

$$\begin{aligned}&\cos(\delta_{n-1}) + \sin(\delta_{n-1})q_{n-1} \\ &= \frac{\cos(\alpha_n)(\cos(\alpha_{n-1}) + q_{n-1}q_{n-2}) + q_0(\cos(\alpha_{n-1})q_{n-1} - q_{n-2})}{\sin(\alpha_n)\sin(\alpha_{n-1})}, \\ &\cos(\delta_n) + \sin(\delta_n)q_0 \\ &= \frac{\cos(\alpha_1)(\cos(\alpha_n) + q_0 q_{n-1}) + q_1(\cos(\alpha_n)q_0 - q_{n-1})}{\sin(\alpha_1)\sin(\alpha_n)}.\end{aligned}$$

References

[1] A. D. Alexandrov, *Convex polyhedra*, Springer, 2010.
[2] J. Hladik and P. E. Hladik, *Quaternions réels, duaux, complexes*, Ellipses, Paris, 2016.
[3] Q. J. Ge and B. Ravani, Computer aided geometric design of motion interpolants, *Journal of Mechanical Design*, 116 (1994) no.13, 756–762.
[4] P. Honvault, Angles of polyhedral angles, Technical report, Cahiers du LMPA, 2016.

Pascal Honvault: Univ. Littoral Côte d'Opale, EA 2597, LMPA - Laboratoire de Mathématiques Pures et Appliquées Joseph Liouville, F-62228 Calais (France), CNRS, FR 2956, France
E-mail address: pascal.honvault@lmpa.univ-littoral.fr

Forum Geometricorum
Volume 16 (2016) 317–321.

FORUM GEOM
ISSN 1534-1178

A Strengthened Version of the Erdős-Mordell Inequality

Dao Thanh Oai, Nguyen Tien Dung and Pham Ngoc Mai

Abstract. We present a strengthened version of the Erdős-Mordell inequality and its proofs.

1. The main result

In 1935, Paul Erdős proposed the following inequality as Problem 3740 in the AMERICAN MATHEMATICAL MONTHLY.

Theorem 1 ([1])**.** *If from a point O inside a given triangle ABC, the perpendiculars OD, OE, OF are drawn to its sides, then $OA+OB+OC \geq 2(OD+OE+OF)$. Equality hold if and only if triangle ABC be an equilateral triangle.*

There is an extensive literature on the Erdős-Mordell inequality; some proofs can be found in [1, 2, 3]. In this article, we give a strengthened version of Theorem 1 and its proofs.

Theorem 2 ([4])**.** *Let ABC be a triangle inscribed into a circle (O), and P be a point inside the triangle. Let D, E, F be the orthogonal projections of P onto BC, CA, AB respectively, and H, K, L be the orthogonal projections of P onto the tangents to (O) at A, B, C respectively. Then $PH + PK + PL \geq 2(PD + PE + PF)$.*

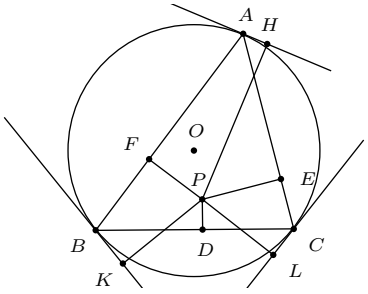

Figure 1

We give two proofs of Theorem 2.

Publication Date: October 13, 2016. Communicating Editor: Paul Yiu.

2. The first proof

Lemma 3. *The cyclic quadrilateral $PEHF$ is a convex quadrilateral.*

Proof. Case 1. If $\angle BAC < 90^\circ$, $\angle PAB$ and $\angle PAC$ are acute angles. Then the points E, F are on the the rays AC, AB respectively. Hence, the ray AP is between the rays AE and AF (see Figures 2a and 2b).

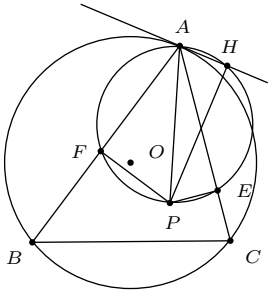

Figure 2a

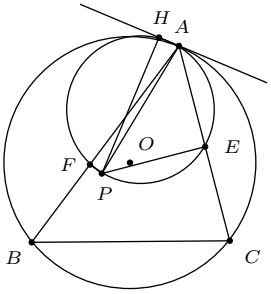

Figure 2b

Notice that four points P, E, H, F lie on a circle with diameter AP. The cyclic quadrilateral $PEHF$ is a convex quadrilateral.
Case 2. If $\angle BAC \geq 90^\circ$, the ray AO is between the rays AB and AC. Let G be the intersection of AO and BC. Without loss of the generality, we may assume that the point P is inside triangle AGC or on the segment AG ($P \neq A, G$). We have $\angle GAC = 90^\circ - \angle ABC$, and is acute. Therefore E lies on the ray AC (see Figures 3a and 3b).

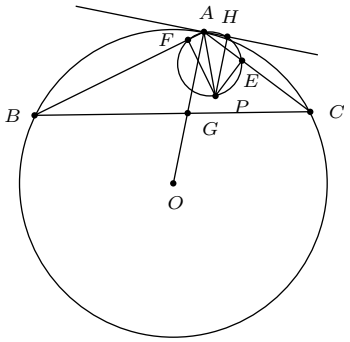

Figure 3a

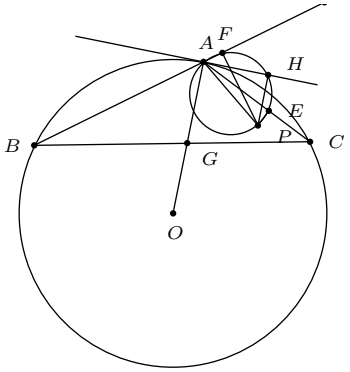

Figure 3b

Since $OA \parallel PH$, H and P lie on the same side of the line AO. Then the ray AE is between the rays AH and AP. Notice that four points P, E, H, F lie on a circle with diameter AP. The cyclic quadrilateral $PEHF$ is a convex quadrilateral. $\square$

First proof of Theorem 2. According to Lemma 3, the cyclic quadrilaterals $PEHF$, $PFKD$, and $PDLE$ are convex. Applying Ptolemy's theorem to quadrilateral $PEHF$, we have $PH \cdot EF = PE \cdot HF + PF \cdot HE$. Thus,

$$\begin{aligned} PH &= \frac{HF}{EF} \cdot PE + \frac{HE}{EF} \cdot PF \\ &= \frac{\sin HEF}{\sin EHF} \cdot PE + \frac{\sin HFE}{\sin EHF} \cdot PF \\ &= \frac{\sin C}{\sin A} \cdot PE + \frac{\sin B}{\sin A} \cdot PF \\ &= \frac{c}{a} \cdot PE + \frac{b}{a} \cdot PF, \end{aligned}$$

where a, b, c are the lengths of the sides BC, CA, AB of triangle ABC.

Similarly,

$$\begin{aligned} PK &= \frac{a}{b} \cdot PF + \frac{c}{b} \cdot PD, \\ PL &= \frac{b}{c} \cdot PD + \frac{a}{c} \cdot PE. \end{aligned}$$

Combining these equations we obtain

$$\begin{aligned} PH + PK + PL &= \left(\frac{b}{c} + \frac{c}{b}\right) PD + \left(\frac{c}{a} + \frac{a}{c}\right) PE + \left(\frac{a}{b} + \frac{b}{a}\right) PF \\ &\geq 2(PD + PE + PF). \end{aligned}$$

Equality holds if and only if $a = b = c$, i.e., ABC is an equilateral triangle.

3. The second proof

Consider the function with two variables

$$f(P) = PH + PK + PL - 2(PD + PE + PF)$$

for an arbitrary point P inside triangle ABC. (By using the formula for the distance from a point to a line, we can extend $f(P)$ to a linear function on $\mathbb{R}^2$). Because triangle ABC is convex, $f(P)$ attains its minimum at one of the three vertices of triangle ABC.

We have

$$\begin{aligned} f(A) &= AK + AL - 2 \cdot AD \\ &= c \sin C + b \sin B - 2c \sin B \\ &= 2R(\sin B - \sin C)^2 \\ &\geq 0. \qquad (*) \end{aligned}$$

See Figures 4a and 4b. Similarly, $f(B), f(C) \geq 0$. Therefore, $f(P) \geq 0$ for every point P inside and on the perimeter of triangle ABC.

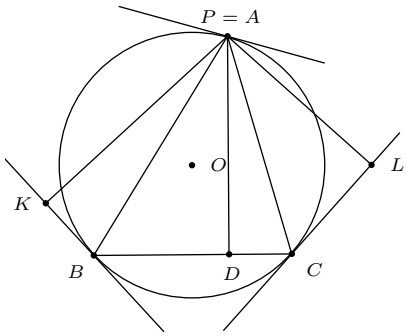

Figure 4a

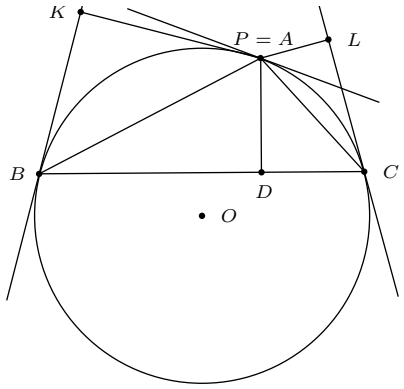

Figure 4b

4. A weighted version

Theorem 4. *Let ABC be a triangle inscribed into a circle (O), and P be a point inside the triangle. Let D, E, F be the orthogonal projections of P onto BC, CA, AB respectively, and H, K, L be the orthogonal projections of P onto the tangents to (O) at A, B, C respectively. Then*

$$x^2 \cdot PH + y^2 \cdot PK + z^2 \cdot PL \geq 2yz \cdot PD + 2zx \cdot PE + 2xy \cdot PF$$

for $x, y, z \in \mathbb{R}$.

Proof. Similar to the second proof of Theorem 2, we set

$$f(P) = x^2 \cdot PH + y^2 \cdot PK + z^2 \cdot PL - 2yz \cdot PD - 2zx \cdot PE - 2xy \cdot PF.$$

Then (*) becomes

$$\begin{aligned} f(A) &= y^2 \cdot AK + z^2 \cdot AL - 2yz \cdot AD \\ &= y^2 c \sin C + z^2 b \sin B - 2yzc \sin B \\ &= 2R(y \sin C - z \sin B)^2 \\ &\geq 0. \end{aligned}$$

Similarly, $f(B), f(C) \geq 0$. From the convexity of triangle ABC, we conclude that $\min f(P) \geq 0$ for P inside or on the perimeter of triangle ABC. □

References

[1] P. Erdős, L. J. Mordell, and D. F. Barrow, Problem 3740, *Amer. Math. Monthly*, 42 (1935) 396; solutions, ibid., 44 (1937) 252–254.

[2] C. Alsina and R. B. Nelsen, A visual proof of the Erdős-Mordell inequality, *Forum Geom.*, 7 (2007) 99–102.

[3] H. Lee, Another proof of the Erdős-Mordell theorem, *Forum Geom.*, 1 (2001) 7–8.

[4] T. O. Dao, Advanced Plane Geometry, message 3374, July 24, 2016.

Dao Thanh Oai: Cao Mai Doai, Quang Trung, Kien Xuong, Thai Binh, Vietnam.
E-mail address: daothanhoai@hotmail.com

Nguyen Tien Dung: Long Bien, Hanoi, Vietnam.
E-mail address: tiendung12121993@gmail.com

Pham Ngoc Mai: 91 Chua Lang, Dong Da, Hanoi, Vietnam.
E-mail address: phamngocmai@ftu.edu.vn

Forum Geometricorum
Volume 16 (2016) 323–329.

FORUM GEOM
ISSN 1534-1178

Apollonian Circumcircles of IFS Fractals

József Vass

Abstract. Euclidean triangles and IFS fractals seem to be disparate geometrical concepts, unless we consider the Sierpiński gasket, which is a self-similar collection of triangles. The "circumcircle" hints at a direct link, as it can be derived for three-map IFS fractals in general, defined in an Apollonian manner. Following this path, one may discover a broader relationship between polygons and IFS fractals.

1. Introduction

The Sierpiński gasket evolves as a limit set by iteratively shrinking an equilateral triangle towards its three vertices, as illustrated below. This iteration can be

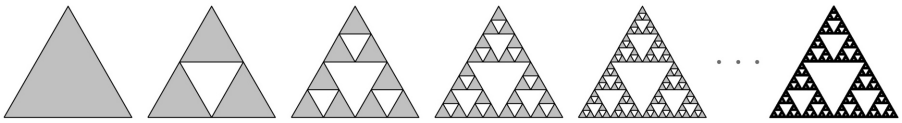

Figure 1. This converges to an attractor with Hausdorff dimension $\log_2 3$ (hence "fractal").

viewed as the collective action of three contractive affine transformations T_k with contraction factors $\lambda_k \in (0,1)$ and fixed points $p_k \in \mathbb{C}$ at the vertices. Adding rotations $\vartheta_k \in (-\pi, \pi]$ to the actions of T_k for a little more generality, their trajectories will be logarithmic spirals, and will take the form

$$T_k(z) = p_k + \varphi_k(z - p_k) \ \ (z \in \mathbb{C},\ k = 1,2,3)$$

where $\varphi_k = \lambda_k \mathrm{e}^{\vartheta_k \mathrm{i}}$ and their collective action can be represented by the map

$$\mathrm{H}(S) := T_1(S) \cup T_2(S) \cup T_3(S)$$

which has a unique attractor $F = \mathrm{H}(F)$ over compact sets as shown by Hutchinson [6], commonly called an "IFS fractal" where IFS stands for "iterated function system". In this sense, three-map IFS fractals are generalized triangular fractals, or "trifractals". Their definition can of course be generalized to any dimension $d \geq 1$ with one-or-more contractions, not far removed from Nature considering that the Romanesco broccoli is a 3D IFS fractal, due to botanical L-systems being close relatives of such fractals [10].

Publication Date: October 20, 2016. Communicating Editor: Paul Yiu.

2. Apollonian Circumcircles

2.1. *Trifractals.* Let us consider the vague problem of generalizing the Euclidean circumcircle to trifractals. Observing that due to the scaling action of T_k the circumcircle of the Sierpiński gasket F is tangential to the circumcircles of each subfractal $T_k(F)$, we might attempt an analogous Apollonian definition in general. The conditions for inner tangentiality of a circle $C = (c, r) \in \mathbb{C} \times \mathbb{R}_+$ with its iterates $T_k(C)$ are

$$|T_k(c) - c| + \lambda_k r = r \ \ (k = 1, 2, 3).$$

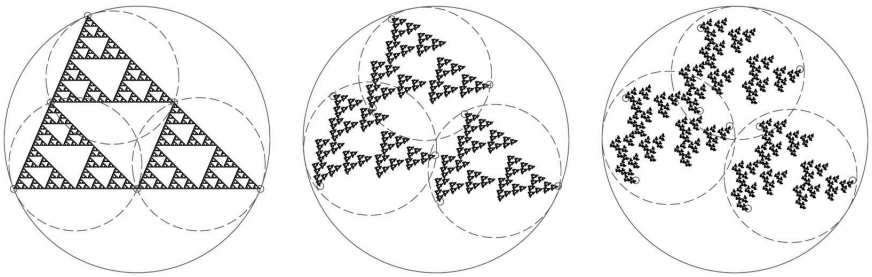

Figure 2. The circumcircle varying under perturbation of the IFS rotations.

These three equations in three real unknowns $r, \mathrm{Re}(c), \mathrm{Im}(c)$ can be reduced to

$$|p_k - c|^2 - \alpha_k^2 r^2 = 0 \ \text{ with } \ \alpha_k := \frac{1 - |\varphi_k|}{|1 - \varphi_k|} \ \ (k = 1, 2, 3).$$

Denoting $p_{k1} := \mathrm{Re}(p_k),\ p_{k2} := \mathrm{Im}(p_k),\ x := \mathrm{Re}(c),\ y := \mathrm{Im}(c)$ and expanding these conditions, then multiplying each by the factors $p_{31}-p_{21},\ p_{11}-p_{31},\ p_{21}-p_{11}$ respectively, and lastly summing the three equations, several terms drop out in the resulting equation, which we denote as $E_1 = 0$. We may do similarly with the factors $p_{32}-p_{22},\ p_{12}-p_{32},\ p_{22}-p_{12}$, resulting in an analogous equation $E_2 = 0$. Taking $E_1 + E_2\mathrm{i} = 0$ and collecting terms, we get an equation of the following form

$$Ar^2 + B - (C\mathrm{i})c = 0$$

with these constants

$$\begin{aligned} A &:= (\alpha_3^2 - \alpha_2^2)p_1 + (\alpha_1^2 - \alpha_3^2)p_2 + (\alpha_2^2 - \alpha_1^2)p_3, \\ B &:= (|p_2|^2 - |p_3|^2)p_1 + (|p_3|^2 - |p_1|^2)p_2 + (|p_1|^2 - |p_2|^2)p_3 \\ C &:= 2(p_2 - p_1) \times (p_2 - p_3) \end{aligned}$$

with the complex cross product $z_1 \times z_2 := \mathrm{Re}(z_1)\mathrm{Im}(z_2) - \mathrm{Im}(z_1)\mathrm{Re}(z_2)$ for $z_{1,2} \in \mathbb{C}$.

The above equation is solvable for the center c in terms of the radius r iff $C \neq 0$, meaning iff the fixed points $p_{1,2,3}$ are non-collinear. In that case, the center takes the form $c = c_0 + ar^2$ with $c_0 = B/C\mathrm{i},\ a = A/C\mathrm{i}$. If the fractal were Sierpiński, then $\vartheta_k = 0$ and thus $\alpha_k = 1$ held for each k, implying $A = 0$. So c_0 is the center of the circumcircle of $p_{1,2,3}$ and let its radius be $r_0 := |p_1 - c_0|$.

To find the fractal circumcircle radius r, let us expand one of the tangentiality conditions, say the first one $|p_1 - c|^2 - \alpha_1^2 r^2 = 0$, resulting after some algebraic manipulation in the equation

$$|a|^2 r^4 + 2Dr^2 + r_0^2 = 0$$

$$D := a \bullet c_0 + \frac{1}{C}(\alpha_1^2\, p_2 \times p_3 + \alpha_2^2\, p_3 \times p_1 + \alpha_3^2\, p_1 \times p_2) = a \bullet c_0 - \left(a \bullet p_1 + \frac{\alpha_1^2}{2}\right)$$

where $\bullet$ is the dot product for complex vectors.

If $a = 0$ ($\Leftrightarrow A = 0$), then $\alpha_{1,2,3}$ are equal since $p_{1,2,3}$ are non-collinear, so $r = r_0/\alpha_1$ and $c = c_0$. On the other hand, if $a \neq 0$ then we can solve the above equation as a quadratic for r^2. Taking the square root we get

$$r = \frac{1}{|a|}\sqrt{-D \pm \sqrt{D^2 - (|a| r_0)^2}}$$

implying two solution circles if $p_{1,2,3}$ are non-collinear and $D \leq -|a| r_0$, with $c = c_0 + a r^2$. The smaller one may be preferable to be defined as "the circumcircle" of a trifractal.

Note that if $\vartheta_k = 0$ for some $k \in \{1, 2, 3\}$, then $\alpha_k = 1$, so by the corresponding circumcircle condition, we get that $|p_k - c| = r$. This implies that the corresponding fixed point p_k lies on the circumcircle. In fact for Sierpiński trifractals with $\vartheta_k = 0\ \forall k$, all three fixed points lie on the circumcircle, as expected.

2.2. *Bifractals.* In the case of two IFS contractions, if the rotations are both zero then the attractor is a Cantor set along the segment connecting the two fixed points. The one-dimensional "bounding ball" is the segment itself, while the two-dimensional one is a circular disk centered at the midpoint. We might wonder if the latter can be generalized, possibly again in an Apollonian manner.

In our attempt, we take a completely different approach than for trifractals, based on the following intuitive figure depicting the sought circumcircle $C = (c, r)$ and its iterates $A = (a, r_A)$ and $B = (b, r_B)$ according to the contractions T_1 and T_2.

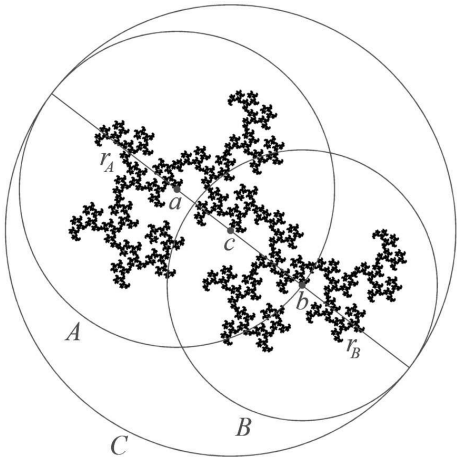

Figure 3. The circumcircle of a bifractal.

Based on the figure, we see that the following equations must hold:

$$c = \frac{1}{2}((a - r_A u) + (b + r_B u)),$$
$$r = \frac{1}{2}(r_A + r_B + |b - a|) \text{ with } u := \frac{b-a}{|b-a|}.$$

Since T_1 maps C to A and T_2 maps C to B, we have that $A = (a, r_A) = (T_1(c), \lambda_1 r)$ and $B = (b, r_B) = (T_2(c), \lambda_2 r)$. So defining $\mathrm{M} = (m_1, m_2) : \mathbb{C} \times \mathbb{R}_+ \to \mathbb{C} \times \mathbb{R}_+$ as

$$m_1(c, r) := \frac{T_1(c) + T_2(c)}{2} + r\frac{\lambda_2 - \lambda_1}{2}\frac{T_2(c) - T_1(c)}{|T_2(c) - T_1(c)|},$$
$$m_2(c, r) := \frac{\lambda_1 + \lambda_2}{2} r + \frac{|T_2(c) - T_1(c)|}{2}$$

for $T_1(c) \neq T_2(c)$ the sought circumcircle will be its fixed point $(c, r) = \mathrm{M}(c, r)$.

For the second component $m_2(c, r) = r$ we get that $r = |T_2(c) - T_1(c)|/2(1 - \lambda)$ denoting $\lambda := (\lambda_1 + \lambda_2)/2$. Plugging this into the first fixed point equation $m_1(c, r) = c$ we get with $\nu := (\lambda_2 - \lambda_1)/2(1 - \lambda)$ the formula for the center

$$c = \frac{(1 - \nu)(1 - \varphi_1)p_1 + (1 + \nu)(1 - \varphi_2)p_2}{(1 - \nu)(1 - \varphi_1) + (1 + \nu)(1 - \varphi_2)}$$

and remarkably it is a "complex combination" of the fixed points $p_{1,2}$. Plugging this formula for c into the expression $r = |T_2(c) - T_1(c)|/2(1 - \lambda)$ we get that

$$r = \frac{1}{1 - \lambda} \frac{|1 - \varphi_1|\,|1 - \varphi_2|}{|(1 - \nu)(1 - \varphi_1) + (1 + \nu)(1 - \varphi_2)|} |p_2 - p_1|.$$

This formula implies that $r \neq 0$ (since $p_1 = p_2$ would degenerate the fractal to a point) so by its earlier relationship to $|T_2(c) - T_1(c)|$ we see that $T_1(c) \neq T_2(c)$. Therefore this derivation shows that the fixed point of M exists and it is unique. Note that by further investigation, we find that M is not a contractive map in general.

2.3. *Polyfractals.* In the case of more than two IFS contractions – "polyfractals" – it may be tempting to consider when the convex hull of the IFS fixed points is a cyclic polygon. Perhaps its circumcircle could be "blown up" as for trifractals.

For now assume instead that the IFS rotations are all equal – "equiangular" – and of the form $\vartheta := \vartheta_k = 2\pi N/M,\ M \in \mathbb{N},\ N \in [0, M) \cap \mathbb{Z}$. Such a fractal F generated by the contractions $T_1, \ldots, T_n$ can also be generated as a Sierpiński fractal. Meaning with a new IFS, we can generate the same fractal but with zero rotations.

To see this, first of all let us observe that the identity $F = \mathrm{H}(F)$ inductively implies that

$$F = \mathrm{H}(F) = \ldots = \mathrm{H}^L(F) \ \ (L \in \mathbb{N}).$$

Notice that due to the definition of H "addresses" a of length L (denoted $|a| = L$) are generated as $a = a(1) \ldots a(L)$ where $a(\cdot) \in \{1, \ldots, n\}$ with corresponding

affine contractions

$$T_a(z) = p_a + \varphi_a(z - p_a)$$

where it can be shown via induction [14] that $\varphi_a := \varphi_{a(1)} \cdot \ldots \cdot \varphi_{a(L)}$ with complex argument $\arg(\varphi_a) \equiv \vartheta L \pmod{2\pi}$ and $p_a := T_a(0)/(1-\varphi_a)$ where $T_a = T_{a(1)} \circ \ldots \circ T_{a(L)}$.

So at the iteration level $L_* := M/\gcd(N, M)$ we have $\vartheta L_* \equiv 0 \pmod{2\pi}$ giving any map T_a a zero rotation angle. Therefore F is generated as a Sierpiński fractal by the n^{L_*} IFS contractions T_a of level $|a| = L_*$ implying that the convex hull is $\mathrm{Conv}(F) = \mathrm{Conv}(p_a : |a| = L_*)$. Thus if the extremal points $\mathrm{Ext}(p_a : |a| = L_*)$ lie on a circle, then the boundary $\partial\mathrm{Conv}(F)$ is a cyclic polygon, implying a circumcircle for the polyfractal F generated by the IFS $\{T_a : |a| = L_*\}$.

Finding a circumcircle in the non-equiangular case, perhaps when $\mathrm{Ext}(p_1, \ldots, p_n)$ lie on a circle, is left open to the reader.

3. Bounding Spheres

3.1. *A General Bounding Sphere.* If we consider the circumcircle problem in a broader sense as the problem of bounding the attractor of any IFS in $\mathbb{R}^d$ $(d \in \mathbb{N})$, it hinges on the containment property

$$\mathrm{H}(B(c,r)) \subset B(c,r) \text{ where } B(c,r) := \{z \in \mathbb{C} : \|z - c\|_2 \le r\}$$

which implies inductively for any level that $B(c,r) \supset \mathrm{H}^L(B(c,r)) \to F$ $(L \to \infty)$.

Let us now take more general IFS contractions $T_k(z) = p_k + M_k(z - p_k)$ where $z, p_k \in \mathbb{R}^d$ and $M_k \in \mathbb{R}^{d\times d}$, $\lambda_k := \|M_k\|_2 < 1$ in the matrix norm induced by the Euclidean norm. The map H will still have an attractor F [6]. The above containment property becomes

$$\|T_k(c) - c\|_2 + \lambda_k r \le r \quad (k = 1, \ldots, n)$$

a weaker form of the tangential conditions for trifractals. Rewriting the left side and estimating it using these new notations, we get

$$\varrho(z) := \max_{1\le k\le n} \|p_k - z\|_2 \quad (z \in \mathbb{R}^d) \text{ and}$$

$$\lambda_* := \max_{1\le k\le n} \|M_k\|_2, \quad \mu_* := \max_{1\le k\le n} \|I - M_k\|_2,$$

$$\|(I - M_k)(p_k - c)\|_2 + \lambda_k r \le \|I - M_k\|_2 \, \|p_k - c\|_2 + \lambda_* r \le \mu_* \varrho(c) + \lambda_* r.$$

So to satisfy the containment property optimally, we require $\mu_*\varrho(c) + \lambda_* r = r$ implying that $r = r(c) := \mu_*\varrho(c)/(1 - \lambda_*)$. So taking any $c \in \mathbb{R}^d$, such as the centroid of $p_1, \ldots, p_n$, the closed ball $B(c, r(c))$ will be a bounding sphere of the fractal F.

Clearly a minimizer of $\varrho(\cdot)$ also minimizes the corresponding radius $r(\cdot)$. This minimizer is known to be unique, so denote it as $c_* := \mathrm{argmin}_{c\in\mathbb{R}^d} \ \varrho(c)$. The corresponding sphere $B(c_*, \varrho(c_*))$ is called the "minimal bounding sphere" of $p_1, \ldots, p_n \in \mathbb{R}^d$, and its determination is called the "Smallest Bounding-Sphere Problem", first investigated in modern times by Sylvester [13] in 1857. Several algorithms exist for finding the exact parameters of the optimal sphere, and the

fastest run in linear time, such as the algorithms of Fischer et al. [4], Larsson [7], Megiddo [9], and Welzl [16].

If we wish to improve the tightness of a bounding sphere, it can be done easily by exploiting the self-similarity of $F = \mathrm{H}(F)$. Having such a sphere $C = B(c, r)$ and taking its L-level iterate $\mathrm{H}^L(C)$, we can compute the minimal bounding sphere $B(c', r')$ of the n^L centers $\mathrm{H}^L(\{c\})$, and then $B(c', r' + \lambda_*^L r)$ will be a tighter bounding sphere of F. For large enough L, we can get within any $\varepsilon > 0$ accuracy of the fractal.

Nevertheless, one might wonder how the circumcircle compares in the plane to the one derived above. According to our numerical experiments for bifractals, in about $2/3$ of randomized cases the circumcircle has a smaller radius, but this general bounding circle still remains competent, and in a few cases it is even tighter than the circumcircle.

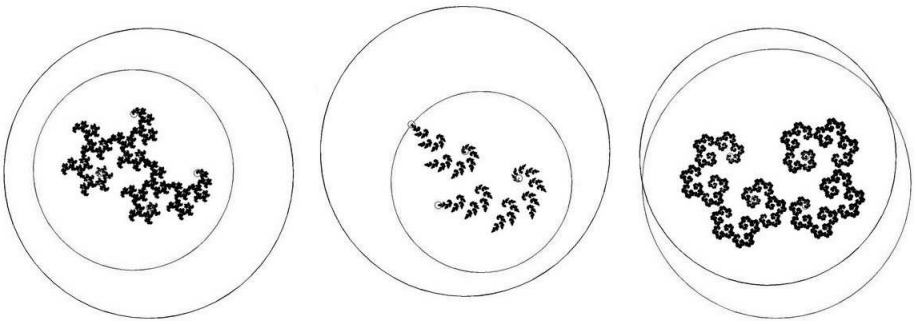

Figure 4. The circumcircle vs. the general bounding circle (top) for two contractions.

Philosophically speaking, the above "general bounding sphere" reduces the problem of bounding an IFS fractal with an infinite number of points, to that of a finite number of points, the fixed points of the IFS.

3.2. *Other Bounds.* Dubuc and Hamzaoui [2] find a bounding circle similar to our last one, but it remains unclear how the optimal center may be found. Rice [11] introduces a method for n-map IFS, similar to the circumcircle definition of this paper, but also relying on an optimization algorithm. Canright [1] gives an algorithmic method as well. Sharp et al. [3, 12] determine bounding circles with a given fixed center for the purpose of fitting the attractor on the screen. Martyn [8] gives an algorithm that seeks the tightest bounding sphere of an IFS fractal, via some potentially expensive subroutines.

As noted earlier, tightness can be improved to an arbitrary accuracy by further iteration, making this aspect of bounding less relevant. The circles and spheres introduced in this paper are special in that they are given by explicit formulas, unlike those in the literature.

4. Concluding Remarks

The reader may have found the formulation of equiangular polyfractals as a Sierpiński fractal somewhat peculiar, as it also implies the finiteness of extrema. The question arises if this can be shown in general; meaning is it true that any IFS fractal has a finite number of extremal points? This is answered by the author in the paper [15] focused on the determination of the convex hull of IFS fractals, which seems like a natural inquiry regarding bounding.

Indeed bounding F by some invariant compact set $S \supset \mathrm{H}(S)$ is a key prerequisite of various algorithms for IFS fractals – such as the ray tracing of 3D IFS fractals [5] – and the convex hull is often ideal in terms of efficiency [14].

References

[1] D. Canright, Estimating the spatial extent of the attractors of iterated function systems, *Computers and Graphics*, 18 (1994) 231–238.

[2] S. Dubuc and R. Hamzaoui, On the diameter of the attractor of an IFS, Technical report, *C. R. Math. Rep. Sci. Canada*, 1994.

[3] A. Edalat, D. W. Sharp, and R. L. While, Bounding the attractor of an IFS, Technical report, Imperial College, 1996.

[4] K. Fischer, B. Gärtner, and M. Kutz, Fast smallest-enclosing-ball computation in high dimensions, in *Algorithms - ESA*, 630–641, Springer, 2003.

[5] J. C. Hart and T. A. DeFanti, Efficient antialiased rendering of 3-D linear fractals, *Computer Graphics*, 25 (1991) 91–100.

[6] J. E. Hutchinson, Fractals and self similarity, *Indiana University Mathematics Journal*, 30 (1981) 713–747.

[7] T. Larsson, Fast and tight fitting bounding spheres, *Proceedings of The Annual SIGRAD Conference*, 27–30, November 2008.

[8] T. Martyn, Tight bounding ball for affine IFS attractor, *Computers & Graphics*, 27 (2003) 535–552.

[9] N. Megiddo, Linear-time algorithms for linear programming in R^3 and related problems, *SIAM Journal on Computing*, 12 (1983) 759–776.

[10] P. Prusinkiewicz and A. Lindenmayer, *The Algorithmic Beauty of Plants*, Springer- Verlag, second edition, 1996.

[11] J. Rice, Spatial bounding of self-affine iterated function system attractor sets, in *Graphics Interface*, 1996, 107–115.

[12] D. W. Sharp and R. L. While, A tighter bound on the area occupied by a fractal image, Technical report, Imperial College, 1999.

[13] J. J. Sylvester, A question in the geometry of situation, *Quarterly Journal of Mathematics*, 1 (1857) 79.

[14] J. Vass, On the Geometry of IFS Fractals and its Applications, PhD thesis, University of Waterloo, 2013.

[15] J. Vass. On the exact convex hull of IFS fractals, Submitted, arXiv/1502.03788, 2015.

[16] E. Welzl, Smallest enclosing disks (balls and ellipsoids), *New Results and New Trends in Computer Science*, Lecture Notes in Computer Science, 555 (1991) 359–337.

József Vass: Faculty of Mathematics, University of Waterloo, Canada
E-mail address: jvass@uwaterloo.ca, jozsef.vass@outlook.com

Forum Geometricorum
Volume 16 (2016) 331–336.

FORUM GEOM
ISSN 1534-1178

A Characterization of the Rhombus

Paris Pamfilos

Abstract. In this article we discuss a simple characterization of the rhombus by considering the triangles formed by a point and each of the sides of the rhombus.

1. The characteristic property

A rhombus $AB\Gamma\Delta$ has a symmetry center coinciding with the intersection point O of its diagonals, defining four triangles $\{OAB, OB\Gamma, O\Gamma\Delta, O\Delta A\}$, which are congruent. (see Figure 1). One can inversely ask, if there is another kind of quadri-

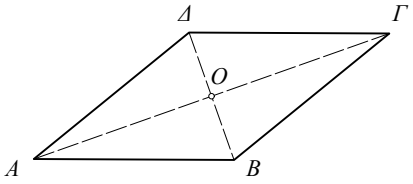

Figure 1. Four congruent triangles

lateral with the same property. The answer is no, and this is the subject of the following theorem.

Theorem 1. *A quadrilateral $AB\Gamma\Delta$ is a rhombus, if and only if, there is a point O in its plane, such that the four triangles*

$$OAB,\ OB\Gamma,\ O\Gamma\Delta,\ O\Delta A \quad \textit{are congruent}. \tag{*}$$

The formulation of the theorem is quite general and refers to arbitrary quadrilaterals, convex, non-convex, self-intersecting, but, nevertheless, non-degenerate, i.e. having no three vertices collinear. The proof is amusing, since it scarcely needs something more in background than pure logic. It is however not totally trivial, its tricky part being the arrangement of the angles around the point O.

The key-idea arises then naturally and consists in the study of the possible configurations of two "adjacent" triangles, which share a common side, like for example $\{OAB, OB\Gamma\}$.

The necessity part of the condition $(*)$ being trivial, the following sections supply the details of the proof for the sufficiency part. Below we often refer to this condition as the "fundamental assumption".

The figures that follow seem, some times, to deviate from a correct graphical representation of this assumption. This is though necessary and reflects the incompatibility of the assumption with some other additional assumptions made in each case.

Publication Date: October 20, 2016. Communicating Editor: Paul Yiu.

2. Congruent triangles with a common side

The following lemma is trivial, and its proof can be read from Figure 2. In this

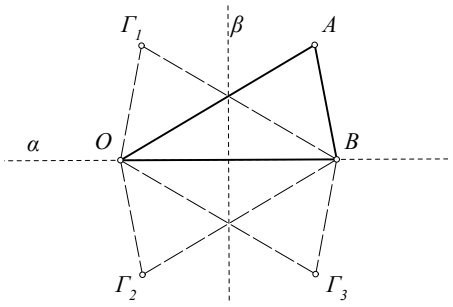

Figure 2. Congruent triangles with a common side

are seen also the symmetry axes of the configuration, which are α : the line OB, and β : the medial line of OB.

Lemma 2. *Given the triangle OAB, there are three other, congruent to it, triangles sharing with it the side OB.*

Returning to the initial problem, we can imagine, that if a point O, satisfying the fundamental assumption $(^*)$ exists, and we fix the triangle OAB, then the vertex Γ of the quadrilateral in question must have one of the positions $\{\Gamma_1, \Gamma_2, \Gamma_3\}$. The proof then, results naturally by repeating this simple construction for each one of the possibilities

$$O\Gamma_1,\ O\Gamma_2,\ O\Gamma_3, \qquad (**)$$

and considering analogously the three possible places for the vertex Δ. It turns out, that only $O\Gamma_3$ and one, out of the three, possibilities for it, is compatible with $(^*)$ and leads to the rhombus.

In this section we adopt for Γ the position Γ_1 of the previous figure and examine the three resulting possibilities for the Δ's as shown in the figure 3-I. The first case,

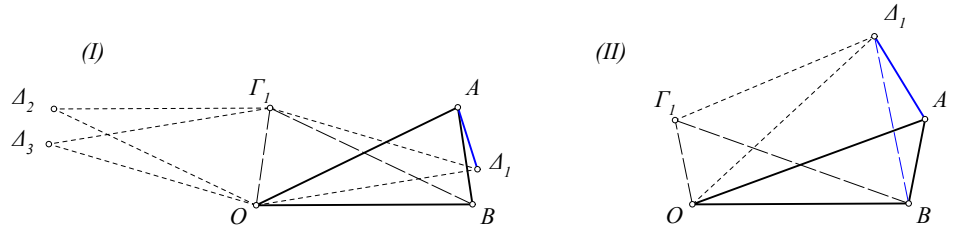

Figure 3. $\{\Delta_1, \Delta_2, \Delta_3\}$ for Γ_1 ... and incompatible $\{\Gamma_1, \Delta_1\}$

seen in this figure, resulting by selecting $\{\Gamma_1, \Delta_1\}$, leads to an incompatibility with $(^*)$.

In fact, from the assumed congruence of triangles $\{OAB, O\Delta_1 A\}$, follows the equality of the angles $\widehat{OA\Delta_1} = \widehat{OAB}$ and $\widehat{AOB} = \widehat{AO\Delta_1}$. Hence, either the two triangles coincide, which is not acceptable, or they are symmetric with respect to AO. In the later case line $B\Delta_1$, which is parallel to $O\Gamma_1$, is orthogonal to OA. In addition, from the fundamental assumption, follows the equality of the angles $\widehat{\Delta_1 OA} = \widehat{O\Delta_1\Gamma_1}$. This implies, that the quadrilateral $OA\Delta_1\Gamma_1$ must be an isosceles trapezium with a right angle at O (see Figure 3-II), hence a rectangle. This implies, in turn, that $\{B, A, \Delta_1\}$ are collinear, which is not acceptable.

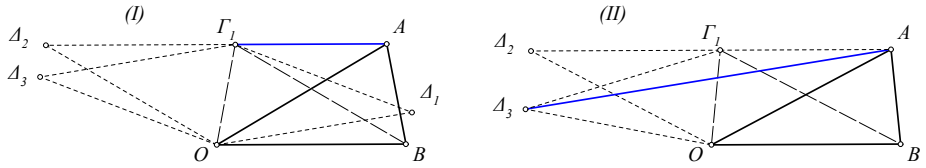

Figure 4. Incompatible $\{\Gamma_1, \Delta_2\}$ ... and incompatible $\{\Gamma_1, \Delta_3\}$

The position Δ_2 for Δ leads directly to impossibility, since in that case, as is easily seen, the points $\{A, \Gamma_1, \Delta_2\}$ are collinear (see Figure 4-I), which is not acceptable.

Finally, the position Δ_3 leads also to incompatibility (see Figure 4-II). In fact, in this case the triangles $\{OAB, O\Delta_3 A, O\Delta_3\Gamma_1\}$, supposed to be congruent, must have also equal the angles opposite to equal sides, and this implies the equality of the angles $\{\widehat{OA\Delta_3}, \widehat{O\Gamma_1\Delta_3}\}$. However, since $\{A, \Gamma_1, \Delta_2\}$ are collinear and $O\Gamma_1\Delta_2\Delta_3$ is a cyclic quadrilateral, this implies that A must coincide with either Γ_1 or Δ_2. The coincidence of A with Γ_1 is not acceptable, and the coincidence of A

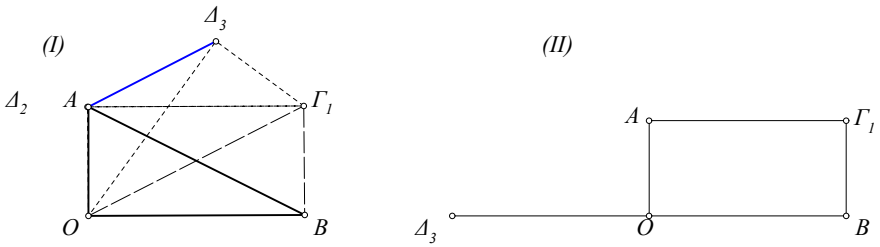

Figure 5. Case with coincident $\{A, \Delta_2\}$

with Δ_2 leads to a parallelogram $OB\Gamma_1 A$ with equal diagonals, hence a rectangle (see Figure 5-I). This implies that $AO\Delta_3$ is a right angle, hence either Δ_3 coincides with B, which is not acceptable, or it is symmetric to B with respect to AO, which is incompatible with $(^*)$ (see Figure 5-II).

The discussion made in this section shows that the position $\Gamma = \Gamma_1$ leads, in all cases, to incompatibilities with the fundamental assumption. The next sections handle analogously the cases for Γ_2 and Γ_3.

3. Γ_2 : **three incompatibilities**

Taking Γ to be at the position Γ_2 of the initial Figure 2, the possible positions for Δ under the assumption $(^*)$ are seen in Figure 6. The cases of $\{\Delta_1, \Delta_2\}$ are

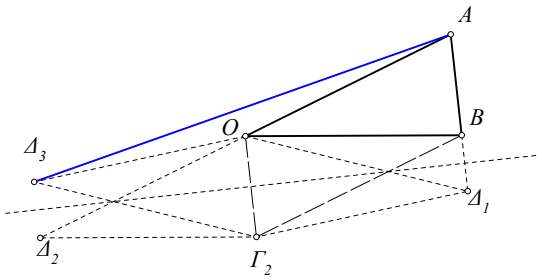

Figure 6. All $AB\Gamma_2\Delta_i$ incompatible

excluded immediately, since in the first $\{A, B, \Delta_1\}$ are collinear and in the second $\{A, O, \Delta_2\}$ are collinear and the triangle $AO\Delta_2$ is degenerate. The third case $\Delta = \Delta_3$ is also excluded, since then, under the fundamental assumption, the angles $\widehat{\Delta_3 AO} = \widehat{OAB}$, and the congruency of triangles $\{\Delta_3 AO, BAO\}$ imply that A lies on the medial line of the segment $B\Delta_3$, which is line $O\Gamma_2$. Hence $\{O, \Gamma_2, A\}$ must be collinear, which is not possible, since $\{AB, O\Gamma_2\}$ are parallel in this case.

4. Γ_3 : **one compatibility**

The last possibility is to choose for Γ the place Γ_3 in Figure-2. Then the possible places for the vertex Δ are shown in Figure 7-I. The first case with $\Delta = \Delta_1$

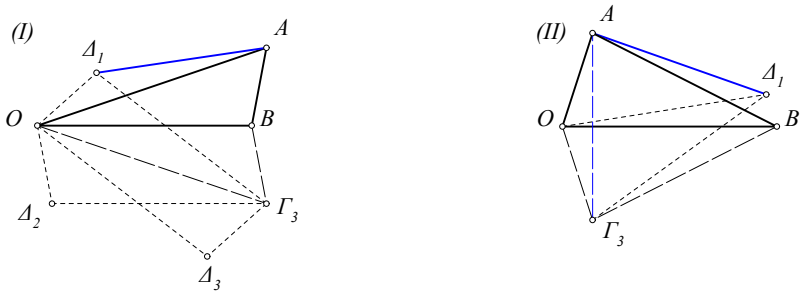

Figure 7. Case $AB\Gamma_3\Delta_1$ incompatible

leads to incompatibility. In fact, in this case the assumed congruent triangles $\{OA\Delta_1, O\Delta_1\Gamma_3\}$ imply the equality of angles $\widehat{O\Delta_1 A} = \widehat{O\Delta_1\Gamma_3}$. This implies that A is either coincident with Γ_3, which is incompatible, or it is the symmetric of Γ_3 with respect to $O\Delta_1$. In the later case Δ_1 must lie on the medial line of $A\Gamma_3$ which is OB. Since it lies, in this case, also on the parallel $B\Delta_1$ to $O\Gamma_1$, this is impossible.

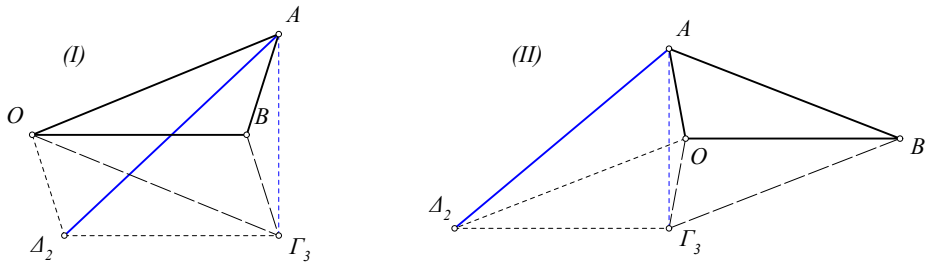

Figure 8. Case $AB\Gamma_3\Delta_2$ incompatible

In the case of $\Delta = \Delta_2$ of Figure 8-I, the triangles $\{OA\Delta_2, O\Delta_2\Gamma_3\}$ assumed congruent, would imply the equality of angles $\widehat{O\Delta_2\Gamma_3} = \widehat{O\Delta_2 A}$. This would imply, either coincidence of $\{A, \Gamma_3\}$, which is not acceptable, or coincidence of A with the symmetric of Γ_3 with respect to $O\Delta_2$. In this case it is readily seen, that, under the fundamental assumption, Δ_2 lies on the medial line of $A\Gamma_3$ and points $\{\Delta_2, O, B\}$ must be collinear (see Figure 8-II), which is not possible, since $\{\Delta_2\Gamma_3, OB\}$ are parallel in this case.

The only acceptable configuration results for $\Delta = \Delta_3$, which is seen in Figure 9-I. The requirement of congruency of triangles $\{OAB, OA\Delta_3\}$ implies that point

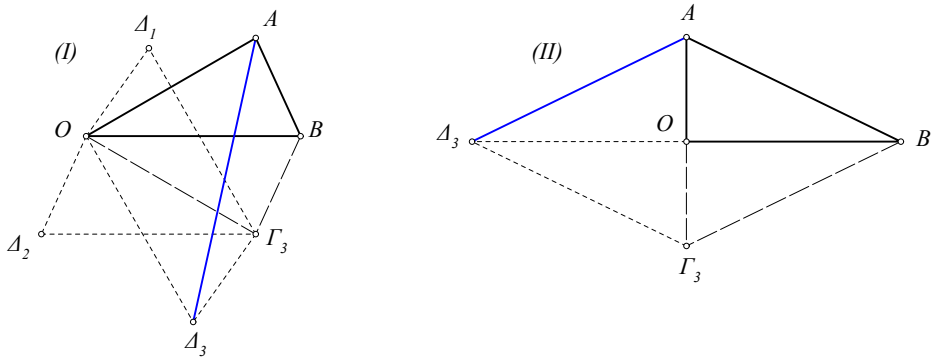

Figure 9. The only compatible case $AB\Gamma_3\Delta_3$

Δ_3, either coincides with B, which is not acceptable, or it is the symmetric of B with respect to AO. Since Δ_3 is also the symmetric of B with respect to $O\Gamma_3$, the two symmetrics coincide when $\{A, O, \Gamma_3\}$ are collinear and OB is orthogonal to AO (see Figure 9-II). This last case produces the rhombus $AB\Gamma_3\Delta_3$ and completes the proof of the sufficiency part of the theorem.

Remark. It is trivial to see that, for triangles, the only one species with an analogous to the previous property, i.e. triangles $AB\Gamma$, for which there is a point O in their plane, such that the triangles $\{OAB, OB\Gamma, O\Gamma A\}$ are congruent, are the equilaterals. For general polygons, however, I don't know alternative characterizations for the analogously defined category. Certainly, one can construct examples

by gluing together copies of the same triangle, or rotating a triangle about a ver-

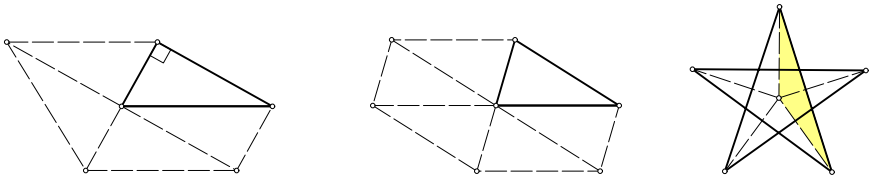

Figure 10. Polygons with the analogous property

tex, as seen in Figure 10. The knowledge, though, of a simple geometric property, giving another aspect of this class of polygons, seems to be missing.

Paris Pamfilos: University of Crete, Greece
E-mail address: pamfilos@math.uoc.gr

Forum Geometricorum
Volume 16 (2016) 337–338.

FORUM GEOM
ISSN 1534-1178

A Proof of the Butterfly Theorem Using the Similarity Factor of the Two Wings

Martin Celli

Abstract. We give a new proof of the butterfly theorem, based on the use of several expressions involving the similarity factor of the two wings.

The aim of this article is to give a new proof of the butterfly theorem.

Butterfly Theorem. *Let M be the midpoint of a chord PQ of a circle, through which two other chords AB and CD are drawn. If A and D are on opposite sides of PQ, and AD, BC intersect PQ at X and Y respectively, then M is also the midpoint of XY.*

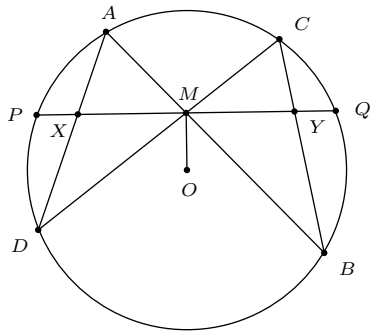

Figure 1

Let O be the center of the circle. The points A and C belong to the same half-plane defined by PQ; the points B and D to the other half-plane, which we may assume containing O (see Figure 1). Several classic and recent proofs of this theorem are known ([1], [2]). The two wings AMD and CMB are clearly similar. Let α be the similarity factor:

$$\alpha = \frac{AM}{CM} = \frac{DM}{BM} = \frac{AD}{CB}.$$

We show that

$$\frac{\sin AXM}{\sin CYM} = \alpha, \tag{1}$$

and deduce the butterfly theorem from this.

Publication Date: November 1, 2016. Communicating Editor: Paul Yiu.

In triangle ADM,

$$\begin{aligned} DM^2 - AM^2 &= ||\overrightarrow{DO} + \overrightarrow{OM}||^2 - ||\overrightarrow{AO} + \overrightarrow{OM}||^2 \\ &= (OD^2 + OM^2 + 2\overrightarrow{DO} \cdot \overrightarrow{OM}) - (OA^2 + OM^2 + 2\overrightarrow{AO} \cdot \overrightarrow{OM}) \\ &= 2(\overrightarrow{DO} - \overrightarrow{AO}) \cdot \overrightarrow{OM} \\ &= 2\overrightarrow{DA} \cdot \overrightarrow{OM} \\ &= 2AD \times OM \sin AXM, \end{aligned}$$

since the angle between $\overrightarrow{DA}$ and $\overrightarrow{OM} = \frac{\pi}{2} - \angle AXM$. Therefore,

$$\sin AXM = \frac{DM^2 - AM^2}{2AD \times OM}.$$

Similarly, in triangle CBM,

$$\sin CYM = \frac{BM^2 - CM^2}{2CB \times OM}.$$

It follows that

$$\begin{aligned} \frac{\sin AXM}{\sin CYM} &= \frac{DM^2 - AM^2}{2AD \times OM} \times \frac{2CB \times OM}{BM^2 - CM^2} \\ &= \frac{CB}{AD} \times \frac{DM^2 - AM^2}{BM^2 - CM^2} \\ &= \frac{1}{\alpha} \times \alpha^2 \\ &= \alpha. \end{aligned}$$

This establishes (1). From this, the butterfly theorem follows:

$$XM = AM \times \frac{\sin MAX}{\sin AXM} = \alpha CM \times \frac{\sin MCY}{\alpha \sin CYM} = CM \times \frac{\sin MCY}{\sin CYM} = YM.$$

References

[1] A. Bogomolny, Butterfly theorem. Interactive Mathematics Miscellany and Puzzles, `http://www.cut-the-knot.org/pythagoras/Butterfly.shtml`.

[2] C. Donolato, A proof of the butterfly theorem using Ceva's theorem, *Forum Geom.*, 16 (2016) 185–186.

Martin Celli: Departamento de Matemáticas, Universidad Autónoma Metropolitana-Iztapalapa, Av. San Rafael Atlixco, 186. Col. Vicentina. Del. Iztapalapa. CP 09340, México, D.F.

E-mail address: `cell@xanum.uam.mx`

Forum Geometricorum
Volume 16 (2016) 339–344.

FORUM GEOM
ISSN 1534-1178

The 19 Congruent Jacobi Triangles

Glenn T. Vickers

Abstract. With a given triangle and three angles, Jacobi's theorem involves the construction of a new triangle. An investigation into the case when these two triangles are congruent is presented. It is claimed that there are always nineteen possibilities and that they fall into four distinct classes.

Jacobi Triangles.

With ABC being any triangle, construct the points P, Q, R so that

$$\angle RAB = \angle QAC = \alpha,\ \angle PBC = \angle RBA = \beta \text{ and } \angle QCA = \angle PCB = \gamma.$$

These points form a *Jacobi triangle* for ABC and Jacobi's theorem states that the lines $AP,\ BQ$ and CR are concurrent (at the Jacobi point K), see Figure 1. Proofs of this result are readily available e.g. [1, pp.55-56] and [2]. Let Δ be the area and a, b, c be the lengths of the sides of ABC. With

$$X = 2\Delta(\cot\alpha + \cot A),\ Y = 2\Delta(\cot\beta + \cot B),\ Z = 2\Delta(\cot\gamma + \cot C),$$

the coordinates of the key points are (using areal coordinates based upon ABC)

$$P(-a^2, Z, Y),\ Q(Z, -b^2, X),\ R(Y, X, -c^2),\ K(1/X, 1/Y, 1/Z).$$

This note gives details for the cases when the triangles ABC and PQR are congruent. It is straightforward to write down the necessary conditions for this to occur and numerical experiments suggest that there are always nineteen real solutions (excluding degenerate cases with at least one of α, β, γ being zero). Even for an equilateral triangle, they are distinct. They fall into four distinct groups as listed below. In the figures, the triangle ABC is the one with dashed lines and its circumcircle and circumcenter are shown. The position of K is indicated by a cross.

The properties of Classes 2 and 3 were first noticed from the figures and then verified algebraically with the aid of Maple. Thus informative proofs are not available.

Class 1. This has a unique member given by

$$\alpha = \pi/2 - A,\ \beta = \pi/2 - B,\ \gamma = \pi/2 - C.$$

The points P, Q, R are diametrically opposite A, B, C on the circumcircle of ABC so that PQR corresponds to a rotation of ABC by π. Also K is the center of the circumcircle.

Publication Date: November 1, 2016. Communicating Editor: Paul Yiu.

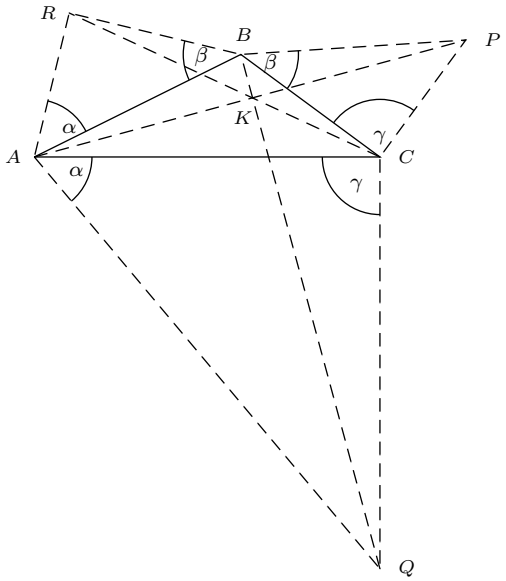

Figure 1. The points P, Q, R are constructed on a base triangle ABC with pairs of angles equal as shown. Jacobi's theorem states that AP, BQ, CR are concurrent and K will be used for the common point.

Class 2. The six members of this group satisfy

$$a^2X + b^2Y + c^2Z = 0$$

which implies that K lies on the circumcircle of ABC. This is illustrated in Figure 2. It will be seen that the six triangles form two groups of three, the orientations within a group being the same. Furthermore they correspond to rotations of $\pm 2\pi/3$

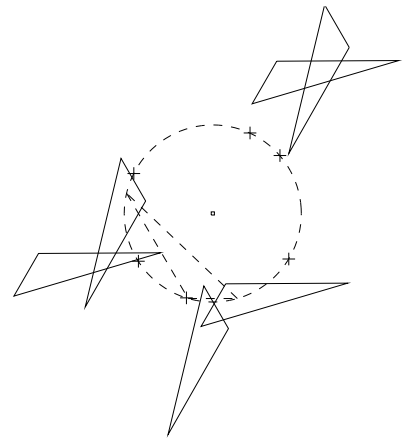

Figure 2. Class 2: The Jacobi points lie on the circumcircle of ABC.

of ABC. No simple formula for the values of X, Y, Z has been found. However, for an isosceles triangle ($b = a$) solutions are

$$X, Y = c^2u \pm [(a^2 + 2a^2u - c^2u)(3a^2 - 2a^2u - c^2u)]^{1/2},\ Z = -2a^2u$$

where

$$(-16a^4 - 16a^2c^2 + 8c^4)u^3 + (8a^4 - 4a^2c^2 - 4c^4)u^2 + (20a^4 - 4a^2c^2 + 2c^4)u + (6a^4 - 3a^2c^2) = 0.$$

Class 3. The six members of this group satisfy

$$X + Y + Z = (a^2 + b^2 + c^2)/2 \Rightarrow \cot\alpha + \cot\beta + \cot\gamma = 0. \qquad (1)$$

However, they form two disparate groups, each with three members.

Class 3A. Here the circumcircles of PQR and ABC touch, see Figure 3. The orientation of the Jacobi triangles involves a reflection as well as a rotation. The analytic solution for this case also appears to be unwieldy but when $b = a$ it may be written as

$$X, Y = \frac{-c^2 \pm 3c\sqrt{c^2 + 8a^2}}{4},\ Z = a^2 + c^2$$

and, as the third root,

$$X = Y = 2a^2,\ Z = c^2/2 - 3a^2.$$

The coordinates of the three points of contact are

$$(c \pm \sqrt{c^2 + 8a^2},\ c \mp \sqrt{c^2 + 8a^2},\ 4c) \text{ and } (2a^2, 2a^2, -c^2).$$

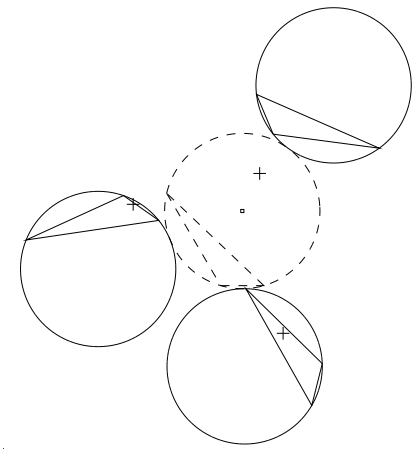

Figure 3. Class 3A: The circumcircle of PQR touches that of ABC.

Class 3B. The members of this sub-class satisfy the additional condition

$$X \cot \alpha = Y \cot \beta = Z \cot \gamma.$$

This condition together with (1) implies that

$$1/X + 1/Y + 1/Z = 0$$

and so K is at infinity. Indeed PQR has the same orientation as ABC, (see Figure 4).

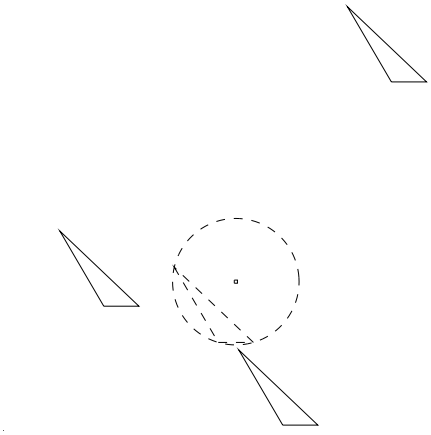

Figure 4. Class 3B: The orientations of the Jacobi triangles are the same as that of ABC. The Jacobi points are at infinity.

These conditions also imply that the circumcircles of AQR, PBR and PQC all touch that of ABC and this is shown in Figure 5. For this case the analytic solution for the general case is reasonably concise; the three values of X satisfy the equation

$$6X^3 + (a^2 - 5b^2 - 5c^2)X^2 + (b^4 + c^4 - a^2b^2 - a^2c^2)X + b^2c^2(a^2 + b^2 + c^2) = 0.$$

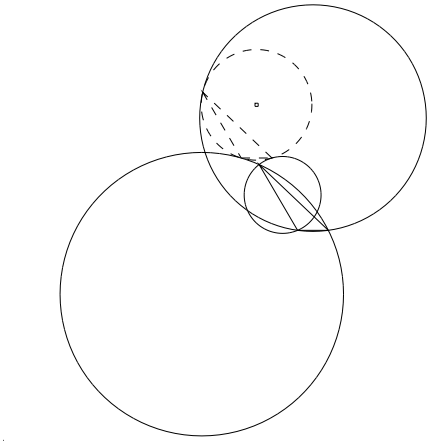

Figure 5. Class 3B: This shows that the circumcircles of AQR, PBR, PQC touch that of ABC.

Class 4. The six members of this group satisfy both

$$\sin 2\alpha + \sin 2\beta + \sin 2\gamma = 0$$

and

$$\frac{\sin(A+2\alpha)}{\sin A} = \frac{\sin(B+2\beta)}{\sin B} = \frac{\sin(C+2\gamma)}{\sin C}.$$

These conditions were encountered in [2] and provided the instigation of this note. They correspond to the reciprocal triangles that occur when K is at infinity so that

$$1/X + 1/Y + 1/Z = 0.$$

There are three pairs of solutions one of which is as follows:

$$\begin{aligned}
\cot 2\alpha &= \frac{1}{2\sin A \cos\frac{1}{3}(B-C)} - \cot A, \\
\cot 2\beta &= \frac{-1}{2\sin B \cos\frac{1}{3}(B+2C)} - \cot B, \\
\cot 2\gamma &= \frac{-1}{2\sin C \cos\frac{1}{3}(2B+C)} - \cot C
\end{aligned}$$

and as subsidiary relations,

$$A = -2\alpha + \beta + \gamma + \pi,\ B = \alpha - 2\beta + \gamma,\ C = \alpha + \beta - 2\gamma.$$

These determine two sets of values for α, β, γ and the two triangles have the same orientation, see Figure 6.

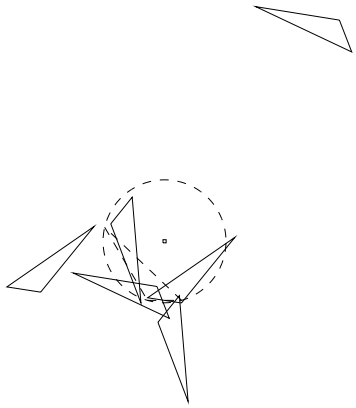

Figure 6. Class 4: There are now three similarly oriented pairs, rotated by $2\pi/3$ from one another. The Jacobi points are at infinity.

Furthermore, the three orientations (i.e. one for each pair) are rotated by $2\pi/3$ with respect to each other. The circumcircles of AQR, PBR, PQC, PBC, AQC, ABR all have the same radius, (see Figure 7), the value being the same for each pair.

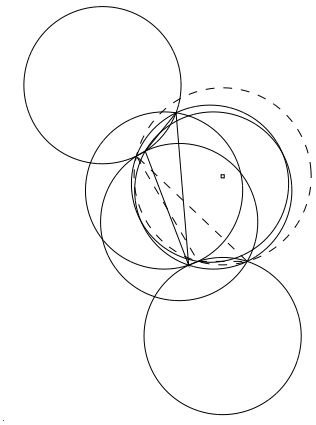

Figure 7. Class 4: To show that the circumradii of AQR, PBR, PQC, PBC, AQC, ABR are equal.

It may be shown that these solutions satisfy not only

$$\frac{1}{\cot A + \cot \alpha} + \frac{1}{\cot B + \cot \beta} + \frac{1}{\cot C + \cot \gamma} = 0$$

(which is equivalent to $1/X + 1/Y + 1/Z = 0$) but also

$$\frac{1}{\cot A + \cot 2\alpha} + \frac{1}{\cot B + \cot 2\beta} + \frac{1}{\cot C + \cot 2\gamma} = 0.$$

References

[1] P. Baptist, *Die Entwicklung der Neueren Dreiecksgeometrie*, Wissenschaftsverlag, Mannheim/ Leipzig/Wein/Zurich, 1992.

[2] G. T. Vickers, Reciprocal Jacobi triangles and the McCay cubic, *Forum Geom.*, 15 (2015) 179–183.

Glenn T. Vickers: 5 The Fairway, Sheffield S10 4LX, United Kingdoms
E-mail address: glennmarilynvickers@gmail.com

Forum Geometricorum
Volume 16 (2016) 345–346.

FORUM GEOM
ISSN 1534-1178

Another synthetic proof of the butterfly theorem using the midline in triangle

Tran Quang Hung

Abstract. We give a new synthetic proof of the butterfly theorem, based on the use of midline in triangle, and cyclic quadrilateral.

This article is to give a new proof of the butterfly theorem.

Butterfly Theorem. *Let M be the midpoint of a chord AB of a circle. Through M two other chords CD and EF are drawn. If C and F are on opposite sides of AB, and CF, DE intersect AB at G and H respectively, then M is also the midpoint of GH.*

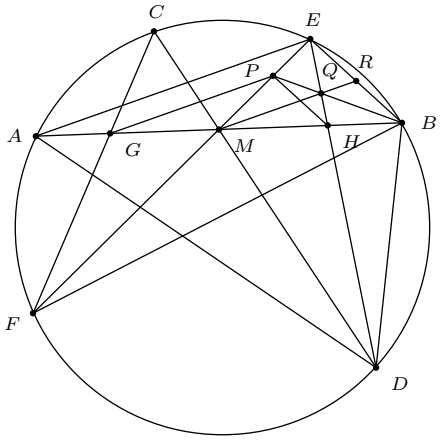

Figure 1

Let P be the point on segment ME such that $GP \parallel AE$. PB intersects EH at Q. We have $\angle PGB = \angle EAB = \angle EFB = \angle PFB$. This shows that quadrilateral $FGPB$ is cyclic. We get $\angle QBM = \angle PBG = \angle PFG = \angle EFC = \angle EDC = \angle QDM$. Therefore, quadrilateral $DMQB$ is also cyclic. From this, $\angle QMB = \angle QDB = \angle EDB = \angle EAB$, and $MQ \parallel AE$. Since M is the midpoint of AB, by the midline theorem, MQ passes through the midpoint R of EB. By Ceva's theorem for triangle MEB and Thales's theorem for triangle MEA, we get $\frac{MH}{MB} = \frac{MP}{ME} = \frac{MG}{MA}$. Since $MA = MB$, we have $MG = MH$.

Publication Date: November 3, 2016. Communicating Editor: Paul Yiu.

References

[1] A. Bogomolny, Butterfly theorem, *Interactive Mathematics Miscellany and Puzzles*, http://www.cut-the-knot.org/pythagoras/Butterfly.shtml.
[2] M. Celli, A proof of the butterfly theorem using the similarity factor of the two wings, *Forum Geom.*, 16 (2016) 337–338.
[3] C. Donolato, A proof of the butterfly theorem using Ceva's theorem, *Forum Geom.*, 16 (2016) 185–186.

Tran Quang Hung: High school for Gifted students, Hanoi University of Science, Vietnam National University, Hanoi, Vietnam

E-mail address: analgeomatica@gmail.com

Forum Geometricorum
Volume 16 (2016) 347–354.

FORUM GEOM
ISSN 1534-1178

Two Six-Circle Theorems for Cyclic Pentagons

Grégoire Nicollier

Abstract. Miquel's pentagram theorem is true for any pentagon. We consider the pentagram obtained by producing the sides of a pentagon and prove two further six-circle theorems, the first for a cyclic pentagram and the second for a cyclic pentagon. If the pentagram is cyclic, consecutive circumcircles of the ear edges issued from the same pentagon vertex have concyclic alternate intersections. If the pentagon is cyclic, alternate intersections of the circumcircles of the rooted ears issued from the same pentagon vertex are concyclic (a rooted ear is an ear extended by the neighboring sides of the pentagon). Among related results, we also show that the circumcircle of an ear producing opposite sides of a cyclic quadrilateral and the circumcircle of the corresponding rooted ear are both tangent to the same two circles centered at the circumcenter of the quadrilateral.

1. Introduction

Take any planar pentagon, not necessarily simple and convex, and consider the pentagram obtained by producing the sides of the pentagon. By Miquel's theorem, the circumcircles of consecutive ears meet at five concyclic points besides the pentagon vertices (Figure 1). We prove two further six-circle theorems, the first for a *cyclic* pentagram and the second for a *cyclic* pentagon (Section 2). Larry Hoehn [5] found that, for any pentagon, the circumcircles of the ear edges issued from the same pentagon vertex have a common radical center: we show that alternate intersections of such consecutive circumcircles are concyclic when the pentagram is cyclic (Figure 2). Dao Thanh Oai [3] discovered experimentally with dynamic geometry software that alternate intersections of the circumcircles of the *rooted* ears issued from the same vertex of a cyclic pentagon are concyclic (a rooted ear is an ear extended by the neighboring sides of the pentagon): we prove this conjecture by explicit computations and show that this immediately follows from the fact that these circumcircles have a common radical center (Figure 3). Using similar computations, we obtain related results in Section 3. Here are two examples: the circumcircles of Miquel's theorem have a common radical center when the pentagon is cyclic; the circumcircle of an ear producing opposite sides of a cyclic quadrilateral and the circumcircle of the corresponding rooted ear are both tangent to the same two circles centered at the circumcenter of the quadrilateral. We also give a short computational proof of Dao's theorem on six circumcenters associated with a cyclic hexagon [2, 4, 1].

2. The six-circle theorems

Theorem 1. *Consider a pentagon $A_1A_2A_3A_4A_5$ (possibly nonconvex or self-intersecting) and the pentagram with ear apices $E_{k+0.5} = A_{k-1}A_k \cap A_{k+1}A_{k+2}$*

Publication Date: November 3, 2016. Communicating Editor: Paul Yiu.

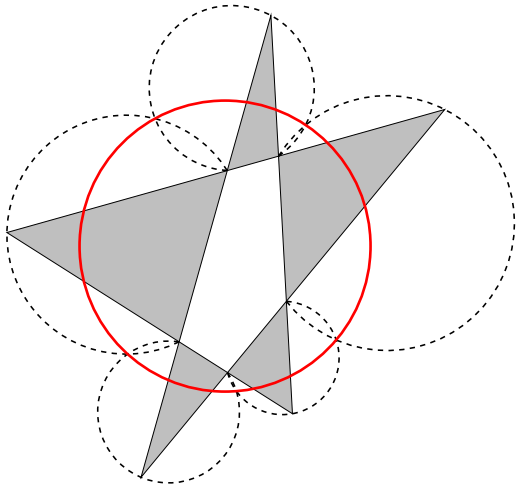

Figure 1

obtained by producing the pentagon sides (*index k is taken modulo* 5). *Let $\mathcal{C}_k$ be the circumcircle of the ear edges issued from the pentagon vertex A_k: the consecutive circumcircles $\mathcal{C}_k$ and $\mathcal{C}_{k+1}$ intersect at the ear apex $E_{k+0.5}$ and at a second point denoted by $I_{k+0.5}$.*

(1) *Taken in pairs, the circumcircles $\mathcal{C}_k$ have concurrent radical axes.*
(2) *If the ear apices are concyclic, so are the points $I_{k+0.5}$* (Figure 2). *Further the circumcenter of the ear apices, the circumcenter of the points $I_{k+0.5}$, and the radical center of the circumcircles $\mathcal{C}_k$ are then collinear.*

Proof. The first part was proven in [5] for consecutive circumcircles and generalized in [6]; the radical center theorem immediately establishes the assertion for all pairs of circumcircles. For the second part, the radical center lies outside the five circumcircles when the ear apices are concylic and is thus the center of a circle $\mathcal{C}$ orthogonal to all $\mathcal{C}_k$, which are thus invariant under the reflection about $\mathcal{C}$. This reflection permutes $E_{k+0.5}$ and $I_{k+0.5}$ for all k and maps the circumcircle of the $E_{k+0.5}$ to a circle, that of the $I_{k+0.5}$: the two circle centers and the inversion center are collinear. □

Theorem 2. *Consider a cyclic pentagon $A_1A_2A_3A_4A_5$ (convex or not) and the pentagram with ear apices $E_{k+0.5} = A_{k-1}A_k \cap A_{k+1}A_{k+2}$ obtained by producing the pentagon sides* (*index k is taken modulo* 5). *Let I_k be the second point besides A_k where the circumcircles of the rooted ears $A_kE_{k+1.5}A_{k+3}$ and $A_kE_{k-1.5}A_{k-3}$ issued from A_k intersect* (Figure 3).

(1) *The points I_k are concyclic.*
(2) *Taken in pairs, the circumcircles of the rooted ears have concurrent radical axes.*
(3) *The circumcenters O of $A_1A_2A_3A_4A_5$ and I of $I_1I_2I_3I_4I_5$ and the concurrency point J of the radical axes are collinear.*

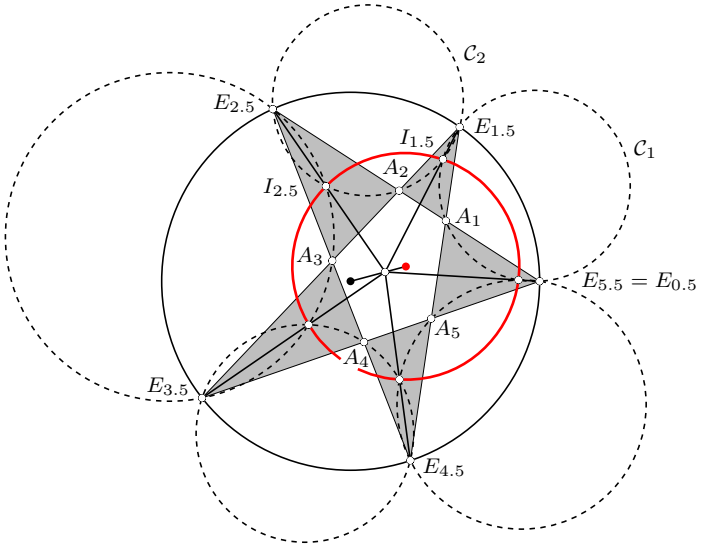

Figure 2

Proof. Note that the existence of a radical center for the circumcircles of the rooted ears implies the two other assertions as in Theorem 1: lying inside these five circumcircles, the radical center is the center of a circle $\mathcal{C}$ that has diameters as common chords with the circumcircles. The circumcircles of the rooted ears are thus invariant under a reflection about $\mathcal{C}$ followed by a half-turn about the radical center. This transformation permutes A_k and I_k for all k and maps the circumcircle of the A_k to a circle, that of the I_k: the two circle centers and the inversion center are collinear.

We prove here the whole theorem by explicit computations. We suppose without loss of generality that the affixes of the pentagon vertices A_k are the unit complex numbers $a_k = e^{i\alpha_k}$. (We sometimes identify points with their affixes for simplicity!) Simple angle chasing shows [4] that the apex angle of the ear $A_kE_{k+0.5}A_{k+1}$ and the rooted ear $A_{k-1}E_{k+0.5}A_{k+2}$ is

$$\pi + \frac{\alpha_{k-1} + \alpha_k - \alpha_{k+1} - \alpha_{k+2}}{2}. \tag{1}$$

Let the circumcenter $C_{k+0.5}$ of the rooted ear $A_{k-1}E_{k+0.5}A_{k+2}$ have the affix $c_{k+0.5}$: by the central angle theorem and (1), one has

$$c_{k+0.5} - a_{k-1} = (c_{k+0.5} - a_{k+2})a_{k-1}a_k\,\overline{a_{k+1}a_{k+2}}$$

and therefore

$$\begin{aligned} c_{k+0.5} &= \frac{a_{k-1}a_ka_{k+2} - a_{k-1}a_{k+1}a_{k+2}}{a_{k-1}a_k - a_{k+1}a_{k+2}} \\ &= e^{i(\alpha_{k-1}+\alpha_{k+2})/2} \sin\frac{\alpha_k - \alpha_{k+1}}{2} \csc\frac{\alpha_{k-1} + \alpha_k - \alpha_{k+1} - \alpha_{k+2}}{2} \end{aligned} \tag{2}$$

by using

$$e^{i\varphi} - e^{i\psi} = 2ie^{i(\varphi+\psi)/2} \sin \frac{\varphi - \psi}{2}. \tag{3}$$

The midpoint M of $A_{k-1}A_{k+2}$ has the affix

$$e^{i(\alpha_{k-1}+\alpha_{k+2})/2} \cos \frac{\alpha_{k-1} - \alpha_{k+2}}{2}$$

and

$$MA_{k-1} = \left| \sin \frac{\alpha_{k-1} - \alpha_{k+2}}{2} \right|.$$

Being the hypotenuse of $C_{k+0.5}MA_{k-1}$, the circumradius $r_{k+0.5}$ of the rooted ear $A_{k-1}E_{k+0.5}A_{k+2}$ is thus

$$r_{k+0.5} = \left| \sin \frac{\alpha_{k-1} - \alpha_{k+2}}{2} \csc \frac{\alpha_{k-1} + \alpha_k - \alpha_{k+1} - \alpha_{k+2}}{2} \right| \tag{4}$$

by the Pythagorean theorem (after simplification).

The circumcircles centered at $C_{k+1.5}$ and $C_{k-1.5}$ intersect at A_k and

$$I_k = \frac{(a_k a_{k+1} - a_k a_{k+2} - a_{k+1} a_{k+2}) a_{k+3}^2 - (a_k a_{k-1} - a_k a_{k-2} - a_{k-1} a_{k-2}) a_{k-3}^2}{\left(a_k a_{k+1} + a_{k+2}^2 - a_{k+1} a_{k+2}\right) a_{k+3} - \left(a_k a_{k-1} + a_{k-2}^2 - a_{k-1} a_{k-2}\right) a_{k-3}}. \tag{5}$$

We found (5) with Mathematica (after simplification) as the second solution of the system formed by the Cartesian equations of one circumcircle – given by (2) and (4) – and of the radical axis of the two circumcircles, knowing the first solution a_k.

The five intersection points I_k lie on a circle centered at

$$I = \frac{\sum_{k=1}^{5} e^{i\alpha_k} \sin(\alpha_{k+3} - \alpha_{k+2})}{\sum_{k=1}^{5} \sin(\alpha_k - \alpha_{k+2})} \tag{6}$$

and the lines $A_k I_k$ concur at

$$J = \frac{\sum_{k=1}^{5} e^{i\alpha_k} \sin(\alpha_{k+3} - \alpha_{k+2})}{\sum_{k=1}^{5} \left[\sin(\alpha_k - \alpha_{k+2}) - \sin(\alpha_k - \alpha_{k+1})\right]}. \tag{7}$$

The line IJ contains thus the circumcenter $O = 0$ of the cyclic pentagon.

We found the results (6) and (7) again with Mathematica: I by computing the intersection of the perpendicular bisectors of I_1I_2 and I_2I_3 given by their Cartesian equations and noticing that the formula for I is shift-invariant; J by solving the system of the Cartesian equations of the lines A_1I_1 and OI and noticing that the formula for J is shift-invariant.

It remains to show that the radical axis of two circumcircles of consecutive rooted ears contains J. This follows from the radical center theorem: for example the radical center of the first, second, and fourth circumcircles is J as two of the radical axes are A_3I_3 and A_1I_1. □

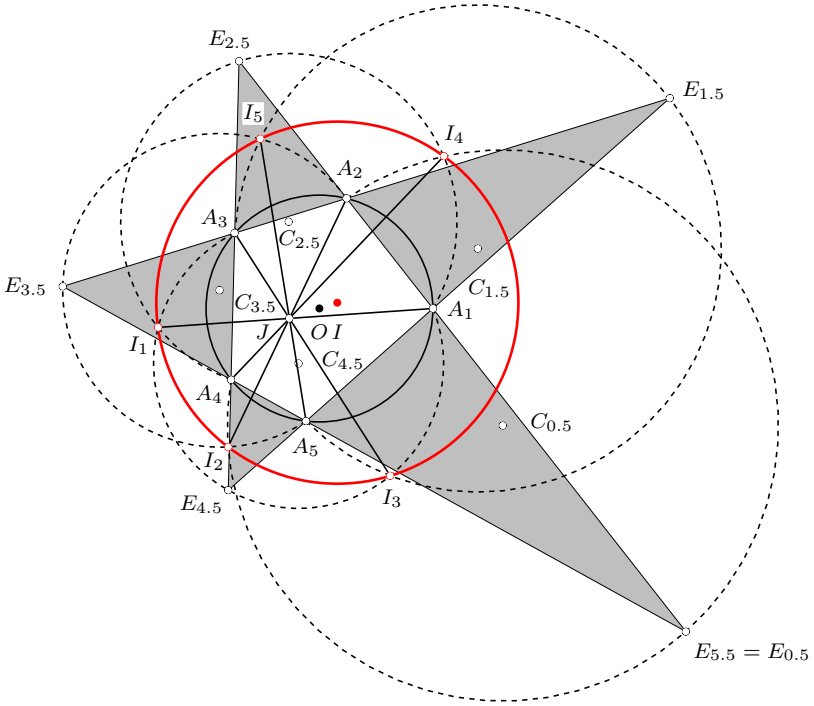

Figure 3

3. Related results

Along the same lines as in the proof of Theorem 2 one shows that the circumcenter of the ear $A_kE_{k+0.5}A_{k+1}$ is

$$\begin{aligned} C'_{k+0.5} &= \frac{a_{k-1}a_ka_{k+1} - a_ka_{k+1}a_{k+2}}{a_{k-1}a_k - a_{k+1}a_{k+2}} \\ &= e^{i(\alpha_k+\alpha_{k+1})/2} \sin\frac{\alpha_{k-1}-\alpha_{k+2}}{2} \csc\frac{\alpha_{k-1}+\alpha_k-\alpha_{k+1}-\alpha_{k+2}}{2} \end{aligned} \tag{8}$$

and its circumradius

$$r'_{k+0.5} = \left|\sin\frac{\alpha_k-\alpha_{k+1}}{2} \csc\frac{\alpha_{k-1}+\alpha_k-\alpha_{k+1}-\alpha_{k+2}}{2}\right|. \tag{9}$$

Formulæ (2), (4), (8), and (9) show (Figure 4) that the circumcircles of the ear and the rooted ear with apex $E_{k+0.5}$ are both tangent to the circles about O of radius

$$\left|\frac{\sin\frac{\alpha_{k-1}-\alpha_{k+2}}{2} \pm \sin\frac{\alpha_k-\alpha_{k+1}}{2}}{\sin\frac{\alpha_{k-1}+\alpha_k-\alpha_{k+1}-\alpha_{k+2}}{2}}\right|.$$

This proves the following theorem.

Theorem 3. *The circumcircle of an ear producing opposite sides of a cyclic quadrilateral and the circumcircle of the corresponding rooted ear are both tangent to the same two circles centered at the circumcenter of the quadrilateral* (Figure 4).

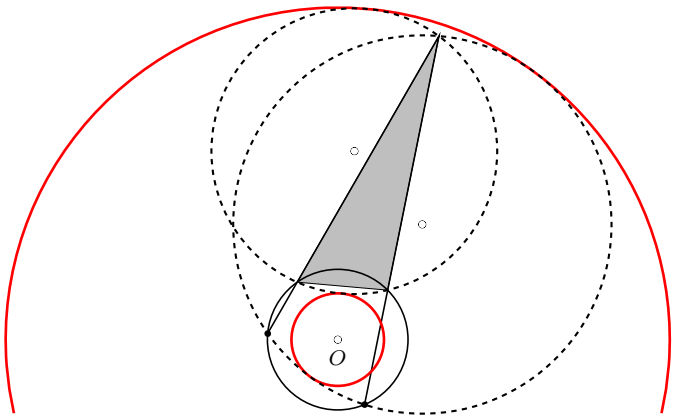

Figure 4

The circumcircles centered at $C'_{k+0.5}$ and $C'_{k-0.5}$ intersect at A_k and

$$I'_k = \frac{a_k(a_{k+1}+a_{k+2})a_{k+3}a_{k+4}-a_k a_{k+1}a_{k+2}(a_{k+3}+a_{k+4})+a_{k+1}^2 a_{k+2}a_{k+4}-a_{k+1}a_{k+3}a_{k+4}^2}{(a_k+a_{k+2}-a_{k+4})a_{k+3}a_{k+4}-(a_k-a_{k+1}+a_{k+3})a_{k+1}a_{k+2}}.$$

Miquel's circle of a pentagon inscribed in the unit circle is centered at

$$I' = \frac{\sum_{k=1}^{5} e^{i\alpha_k}\sin(\alpha_{k-1}-\alpha_{k+1})}{\sum_{k=1}^{5}\left[\sin(\alpha_k-\alpha_{k+2})+\sin(\alpha_k+\alpha_{k+1}-\alpha_{k+2}-\alpha_{k+3})\right]}$$

and the radical axes of all pairs of ear circumcircles concur at

$$J' = \frac{\sum_{k=1}^{5} e^{i\alpha_k}\sin(\alpha_{k-1}-\alpha_{k+1})}{\sum_{k=1}^{5}\sin(\alpha_k+\alpha_{k+1}-\alpha_{k+2}-\alpha_{k+3})}.$$

The points O, I', and J' are thus collinear. The following theorem is proven.

Theorem 4. *If a pentagram is obtained by producing the sides of a cyclic pentagon, the circumcircles of the ears have a common radical center.*

If a hexagon $A_1A_2A_3A_4A_5A_6$ is inscribed in the unit circle, the ears of the resulting hexagram have circumcenters $C'_{k+0.5}$ given by (8) (k is taken modulo 6) and the three lines $C'_{k+0.5}C'_{k+3.5}$ through opposite circumcenters concur at the point

$$\frac{\sum_{k=1}^{6} e^{i\alpha_k}\sin(\alpha_{k+1}+\alpha_{k+2}-\alpha_{k+4}-\alpha_{k+5})}{\sum_{k=1}^{6}\left[\sin(\alpha_k-\alpha_{k+2})-\sin(\alpha_k+\alpha_{k+1}-\alpha_{k+2}-\alpha_{k+3})\right]}.$$

(Note that $e^{i\alpha_k}$ and $e^{i\alpha_{k+3}}$ have opposite coefficients.) This is a direct proof of another experimental discovery of Dao [2, 4, 1].

As partially noted elsewhere [7], the following conjecture seems experimentally correct, but a formal proof is still missing (the implication (3) $\Rightarrow$ (2) follows as in Theorem 1).

Conjecture. The following properties of a cyclic hexagon $A_1A_2A_3A_4A_5A_6$ and its hexagram (obtained by producing the sides of the hexagon) are equivalent.

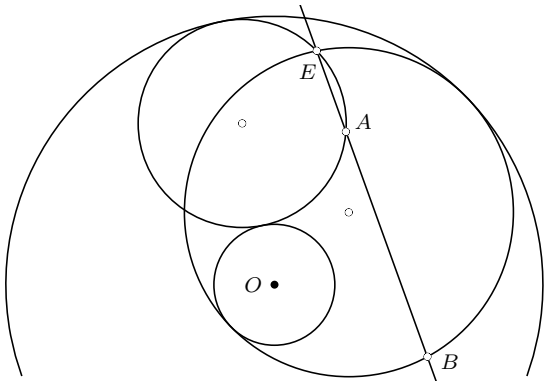

Figure 5

(1) The main diagonals A_kA_{k+3} concur.
(2) The alternate intersections of the circumcircles of consecutive ears are concyclic.
(3) The radical axes of all pairs of ear circumcircles concur.

Theorem 3 (Figure 4) has a kind of converse.

Theorem 5. *In* Figure 5*, the center O of the inner and outer circles is equidistant from A and B for all lines through E.*

Notice the particular collinearities when A and B are both on the inner or on the outer circle.

Proof. Without loss of generality, the inner circle is the unit circle, the circle $\mathcal{C}_A$ of radius r is centered at $(1+r)e^{i\varphi}$ and the circle $\mathcal{C}_B$ of radius $1+r$ at $re^{i\psi}$. The desired intersection of $\mathcal{C}_A$ and $\mathcal{C}_B$ is

$$E = (1+r)e^{i\varphi} + re^{i\psi},$$

clearly on both circles. Point A of $\mathcal{C}_A$ can be written as

$$A = (1+r)e^{i\varphi} + re^{i\alpha}.$$

Point B of $\mathcal{C}_B$ is then

$$B = re^{i\psi} + (1+r)e^{i(\alpha+\psi-\varphi)}$$

as $\overrightarrow{EA}$, parallel to $e^{i\alpha} - e^{i\psi}$, and $\overrightarrow{EB}$, parallel to $e^{i(\alpha+\psi-\varphi)} - e^{i\varphi}$, are both perpendicular to $e^{i(\alpha+\psi)/2}$ by (3). The segments OA and OB are congruent as they are diagonals of parallelograms with sides r and $1+r$ enclosing the angle $|\varphi - \alpha|$ modulo π (or simply as $e^{i\alpha}\overline{A} = e^{-i\psi}B$). □

References

[1] T. Cohl, A purely synthetic proof of Dao's theorem on six circumcenters associated with a cyclic hexagon, *Forum Geom.*, 14 (2014) 261–264.
[2] T. O. Dao, Message #1531, *Advanced Plane Geometry*, August 28, 2014. `https://groups.yahoo.com/neo/groups/AdvancedPlaneGeometry`

[3] T. O. Dao, Message #3274, *Advanced Plane Geometry*, May 30, 2016.
[4] N. Dergiades, Dao's theorem on six circumcenters associated with a cyclic hexagon, *Forum Geom.*, 14 (2014) 243–246.
[5] J. C. Fisher, L. Hoehn, and E. M. Schröder, A 5-circle incidence theorem, *Math. Mag.*, 87 (2014) 44–49.
[6] J. C. Fisher, E. M. Schröder, and J. Stevens, Circle incidence theorems, *Forum Geom.*, 15 (2015) 211–228.
[7] Q. D. Ngo, Some problems around Dao's theorem on six circumcenters associated with a cyclic hexagon configuration, *Int. J. Comp. Discov. Math.*, 1(2) (2016) 40–47.

Grégoire Nicollier: University of Applied Sciences of Western Switzerland, Route du Rawyl 47, CH–1950 Sion, Switzerland

E-mail address: gregoire.nicollier@hevs.ch

Forum Geometricorum
Volume 16 (2016) 355–366.

FORUM GEOM
ISSN 1534-1178

Some Monotonicity Results Related to the Fermat Point of a Triangle

Toufik Mansour and Mark Shattuck

Abstract. In this paper, we establish a Fermat point analogue of the Steiner-Lehmus theorem by proving a more general monotonicity property. We also consider four pairs of segment lengths determined by intersecting Fermat point cevians to unequal sides of a triangle and determine comparable properties for these segments. Our proofs make use of trigonometric inequalities.

1. Introduction

Starting with an isosceles triangle, if one were to draw the same type of segment to the congruent sides from the opposite angles, then the segments so obtained are always congruent, by symmetry. Conversely, one might wonder when congruence of some particular pair of internal segments within a triangle implies congruence of the two corresponding sides. For example, it is easy to show that congruence of medians or altitudes to two sides implies congruence of the sides. On the other hand, congruence of two angle bisectors implying congruence of the sides to which they are drawn is more difficult to show and is the content of the well-known Steiner-Lehmus theorem. The reader is referred to [2, 3, 4, 8] for various proofs of this theorem and to [5] for stronger versions of it. Results such as these are frequently particular cases of more general monotonic behavior. For example, a median, altitude or angle bisector to a longer side is always shorter, and conversely. On the other hand, congruence of some particular pair of segments that are congruent within an isosceles triangle due to symmetry need not imply that the triangle within which they lie is isosceles. See, e.g., [7] for such an example.

Here, we consider a variant of the Steiner-Lehmus result involving the Fermat point. The (external) Fermat point of a triangle ABC is obtained as follows. On sides AB, AC and BC, construct externally equilateral triangles ABH, ACG and BCI. Then the segments CH, BG and AI are concurrent at a point F, known as the *Fermat point*, see [3, p. 83]. See Figures 1-3 below. It is well-known [9] that the Fermat point provides a minimum when computing the sum of the distances from an arbitrary point to the vertices of triangle ABC. We will refer to the portion of either segment CH, BG or AI lying between the respective vertex of

Publication Date: November 8, 2016. Communicating Editor: Paul Yiu.

triangle ABC and the point where the segment intersects the opposite side (possibly extended) of triangle ABC as a *Fermat* (*point*) *cevian*. For instance, segments BD and CE in Figures 1-3 are Fermat cevians. Note that in the second figure, the side AC is extended, while both sides AB and AC are extended in the third.

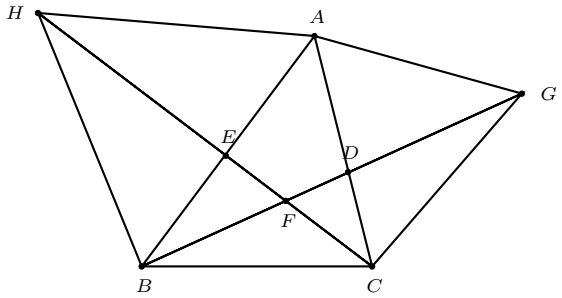

Figure 1. Position of F when all angles of triangle ABC are less than 120°.

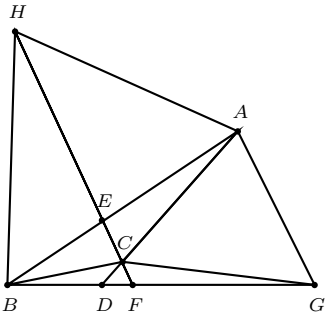

Figure 2. Position of F relative to BC when $\angle C > 120^\circ$.

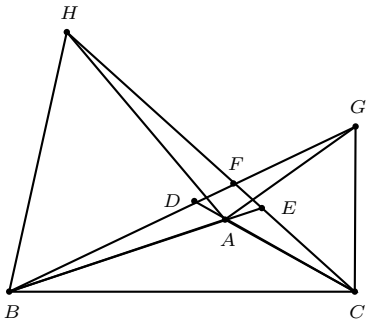

Figure 3. Position of F relative to BC when $\angle A > 120^\circ$.

In the next section, we show that a longer side always has a shorter Fermat cevian terminating on it, and conversely. In particular, if two Fermat cevians are congruent, then the sides to which they are drawn are congruent. In terms of the figures above, we have if $AB \geq AC$, then $BD \geq CE$, with equality holding if and only $AB = AC$. Note that this stands in contrast to the lengths of the segments BG and CH which are always equal. Our result here extends earlier work concerning a Gergonne point analogue of Steiner-Lehmus done in [10], where the question of looking at analogues involving other kinds of centers is mentioned. See also [1, 6] for related results involving extensions of the angle bisector and other types of cevians.

In the third section, we consider the same question for the two internal segments of a Fermat cevian determined by F as well as for the segments obtained by the intersection of a cevian with the opposite side. That is, we consider the segments BF and FD on line $\overleftrightarrow{BD}$ in Fig's 1-3, and segments AD and CD on side AC (possibly extended) in these figures, and compare each of these four segment lengths with the analogous segments involving CE and AB. In two of the cases, one gets the same type of monotonicity as that demonstrated by the Fermat cevians themselves (see Theorems 4 and 9 below). In the other cases, the monotonicity demonstrated depends upon the measure of the vertex angle.

In our proofs, we consider cases based off of the figures above. That is, we consider separately the cases when (i) all angles in triangle ABC are less than 120°, (ii) one of the base angles, $\angle B$ or $\angle C$ (from which cevians are drawn), is greater than 120°, or (iii) the vertex angle, $\angle A$, exceeds 120°. Note that the case when one of the angles of triangle ABC is exactly 120° can be degenerate and thus is sometimes excluded from consideration. Our proofs are trigonometric in nature and involve establishing certain inequalities (see, for example, Lemmas 5 and 8).

At times, we will make use of the following result (see, e.g., [3, p. 65]) concerning the Fermat point.

Lemma 1. *The segments BG and CH in Figures 1-3 are always congruent and meet at a 60° angle.*

In the proofs that follow, we will always take $BC = 1$ for convenience, which can be done without loss of generality.

2. A Fermat analogue of the Steiner-Lehmus result

In this section, we prove a version of the Steiner-Lehmus result for the Fermat point. In the theorem that follows (and subsequent theorems), the segment lengths refer to those defined in Figures 1-3 above.

Theorem 2. *If $AB > AC$ in triangle ABC, then $BD > CE$.*

Proof. Let $x = \angle CBF$ and $y = \angle BCF$. First assume all angles of triangle ABC are less than $\frac{2\pi}{3}$. By the law of sines applied to triangle BCD in Figure 1 above, we have

$$\frac{1}{BD} = \frac{\sin(x + C)}{\sin C} = \frac{\sin x \cos C + \cos x \sin C}{\sin C} = \sin x \cot C + \cos x. \quad (1)$$

By the law of sines in triangle BCG, we have

$$\frac{1}{b} = \frac{1}{CG} = \frac{\sin\left(\frac{2\pi}{3} - C - x\right)}{\sin x} = \sin\left(\frac{2\pi}{3} - C\right)\cot x - \cos\left(\frac{2\pi}{3} - C\right) \quad (2)$$

and $\sin x = \frac{b}{BG}\sin\left(C + \frac{\pi}{3}\right)$. Therefore, by (1) and (2), we get

$$\begin{aligned}\frac{1}{BD} &= \sin x(\cot C + \cot x) = \sin x\left(\cot C + \frac{\frac{1}{b} + \cos\left(\frac{2\pi}{3} - C\right)}{\sin\left(\frac{2\pi}{3} - C\right)}\right) \\ &= \frac{b\sin\left(C + \frac{\pi}{3}\right)}{BG}\left(\cot C + \frac{\frac{1}{b} + \cos\left(\frac{2\pi}{3} - C\right)}{\sin\left(\frac{2\pi}{3} - C\right)}\right) \\ &= \frac{b}{BG}\left(\frac{\sin\left(\frac{2\pi}{3} - C\right)\cos C + \cos\left(\frac{2\pi}{3} - C\right)\sin C + \frac{\sin C}{b}}{\sin C}\right) \\ &= \frac{b}{BG}\left(\frac{\sin\left(\frac{2\pi}{3}\right) + \frac{\sin C}{b}}{\sin C}\right) = \frac{1}{BG}\left(\frac{\sqrt{3}b + 2\sin C}{2\sin C}\right),\end{aligned}$$

where we have made use of the sine-of-sum formula and the fact $\sin z = \sin(\pi - z)$. Noting that a comparable formula holds for $\frac{1}{CE}$, it follows that $BD > CE$ if and only if

$$\frac{1}{BG}\left(\frac{\sqrt{3}b + 2\sin C}{2\sin C}\right) < \frac{1}{CH}\left(\frac{\sqrt{3}c + 2\sin B}{2\sin B}\right).$$

Since $BG = CH$ by Lemma 1, this inequality reduces to $\frac{b}{\sin C} < \frac{c}{\sin B}$, i.e., $b^2 < c^2$, by the law of sines. Since the last inequality is true by assumption, this completes the proof of the theorem in the case when all angles of triangle ABC are less than $\frac{2\pi}{3}$.

If $\angle C > \frac{2\pi}{3}$ or if $\angle A > \frac{2\pi}{3}$, then one may verify that the same formulas hold for $\frac{1}{BD}$ and $\frac{1}{CE}$ and the result follows as before. If $\angle C = \frac{2\pi}{3}$, then the result follows from the fact that $\angle BEC > \angle BCE$ in the cyclic quadrilateral $ACBH$. On the other hand, if $\angle A = \frac{2\pi}{3}$, then the result is tautological as D and E both coincide with A in this case. □

Corollary 3. *If $BD = CE$, then $AB = AC$.*

3. Related monotonicity results

In this section, we prove further monotonicity results for four additional segments determined by a given pair of intersecting Fermat point cevians. The first two results below concern how a pair of cevians to sides of unequal length divide one another.

Theorem 4. *If $AB > AC$ in triangle ABC, then $BF > CF$.*

Proof. Let $x = \angle CBF$ and $y = \angle BCF$. Let $\ell = \frac{\pi}{3}$. First assume $\angle C < \frac{2\pi}{3}$. By the law of sines in triangles BCG and BCH (considering separately the cases when $\angle A < \frac{2\pi}{3}$ or $\angle A \geq \frac{2\pi}{3}$), we have $\sin x = \frac{CG\sin(\angle BCG)}{BG} = \frac{b\sin(C+\ell)}{BG}$ and

$\sin y = \frac{BH\sin(\angle CBH)}{CH} = \frac{c\sin(B+\ell)}{CH}$. By the law of sines in triangles BCF and ABC and since $BG = CH$, we then have

$$\frac{BF}{CF} = \frac{\sin y}{\sin x} = \frac{c\sin(B+\ell)}{b\sin(C+\ell)} = \frac{\sin C\sin(B+\ell)}{\sin B\sin(C+\ell)}.$$

To complete the proof in this case, note that $\angle C > \angle B$ implies $\sin(C-B) > 0$ so that

$$\frac{1}{2}\cos(C-B) + \frac{\sqrt{3}}{2}\sin(C-B) > \frac{1}{2}\cos(B-C) + \frac{\sqrt{3}}{2}\sin(B-C),$$

i.e., $\cos(C-B-\ell) > \cos(B-C-\ell)$. But then

$$\frac{1}{2}\left(\cos(C-B-\ell) - \cos(C+B+\ell)\right) > \frac{1}{2}\left(\cos(B-C-\ell) - \cos(B+C+\ell)\right),$$

whence $\sin C\sin(B+\ell) > \sin B\sin(C+\ell)$, which implies $BF > CF$ in this case.

Now suppose $\angle C \geq \frac{2\pi}{3}$. Since the case when $\angle C = \frac{2\pi}{3}$ is seen to be trivial, assume $\angle C > \frac{2\pi}{3}$. Then to show $BF > CF$ in this case is to show $\sin C\sin(B+\ell) > \sin B\sin(C-2\ell)$, i.e.,

$$\frac{1}{2}(\cos(C-B-\ell) - \cos(C+B+\ell)) > \frac{1}{2}(\cos(B-C+2\ell) - \cos(B+C-2\ell)).$$

This may be rewritten as

$$\cos(C-B-\ell) - \cos(C-B-2\ell) > 2\cos(B+C+\ell),$$

i.e., $2\sin\left(C-B-\frac{\pi}{2}\right)\sin\left(-\frac{\pi}{6}\right) > 2\cos(B+C+\ell)$. To show $\sin\left(C-B-\frac{\pi}{2}\right) < -2\cos(B+C+\ell)$ where $\angle C > 2\ell$, simply observe that $\sin\left(C-B-\frac{\pi}{2}\right) < 1 < -2\cos(B+C+\ell)$ since $\pi < B+C+\ell < \frac{4\pi}{3}$ implies $-1 < \cos(B+C+\ell) < -\frac{1}{2}$, which completes the proof. □

For the next result, we will need the following inequality.

Lemma 5. *Suppose $\angle B < \angle C < \frac{2\pi}{3}$ in triangle ABC. Then*

$$\frac{\sqrt{3}\sin B + 2\sin(B+C)\sin C}{\sin\left(\frac{2\pi}{3} - C\right)} > \frac{\sqrt{3}\sin C + 2\sin(B+C)\sin B}{\sin\left(\frac{2\pi}{3} - B\right)} \qquad (3)$$

if $\angle B + \angle C > \frac{\pi}{3}$, with the inequality reversed if $\angle B + \angle C < \frac{\pi}{3}$.

Proof. Let $\ell = \frac{2\pi}{3}$. Consider the function

$$h(u,v) = (\sqrt{3}\sin u + 2\sin(u+v)\sin v)\sin(\ell - u)$$

for $0 < u < v < \min\{\ell, \pi - u\}$. By the product-to-sum trigonometric identities, we get

$$\begin{aligned} h(u,v) &= \sqrt{3}\sin u \sin(\ell-u) + 2\sin(u+v)\sin(\ell-u)\sin v \\ &= \frac{\sqrt{3}}{2}(\cos(2u-\ell)-\cos\ell) + (\cos(2u+v-\ell)-\cos(v+\ell))\sin v \\ &= \frac{\sqrt{3}}{2}(\cos(2u-\ell)-\cos\ell) + \frac{1}{2}(\sin(\ell-2u)+\sin(2u+2v-\ell) \\ &\quad -\frac{1}{2}(\sin(-\ell)+\sin(2v+\ell)) \\ &= \frac{\sqrt{3}}{2}(\cos(2u-\ell)-\cos\ell) + \frac{1}{2}(\sin(2u+2v-\ell)+\sin(\ell)) \\ &\quad +\sin(-u-v)\cos(u-v-\ell), \end{aligned}$$

where we have applied the sine sum-to-product identity in the last equality. To show the inequality in question, we compare the quantities $h(u,v)$ and $h(v,u)$. Note that $h(u,v) > h(v,u)$ if and only if

$$\frac{\sqrt{3}}{2}\cos(2u-\ell)-\sin(u+v)\cos(u-v-\ell) > \frac{\sqrt{3}}{2}\cos(2v-\ell)-\sin(u+v)\cos(v-u-\ell),$$

which may be rewritten as

$$\frac{\sqrt{3}}{2}(\cos(2u-\ell)-\cos(2v-\ell)) > \sin(u+v)(\cos(u-v-\ell)-\cos(u-v+\ell)),$$

i.e.,

$$\sqrt{3}\sin(v+u-\ell)\sin(v-u) > 2\sin(u+v)\sin(u-v)\sin\ell, \tag{4}$$

by the cosine difference-to-product formula.

Since $v > u$, inequality (4) is immediate if $u+v \geq \ell$ for then the left side is non-negative, while the right is negative. If $u+v < \ell$, then (4) reduces to $\sin(\ell-u-v) < \sin(u+v)$, which holds if $\frac{\ell}{2} < u+v < \ell$ for then $\sin(\ell-u-v) < \sin\left(\frac{\ell}{2}\right) < \sin(u+v)$ in that case. The reverse inequality is seen to hold if $u+v < \frac{\ell}{2}$, which completes the proof. □

We now prove a monotonicity result concerning the segments EF and DF in Figures 1-3 above. Note that when $\angle A = \frac{2\pi}{3}$, the points D, E and F coincide and so we exclude this case from consideration.

Theorem 6. *Suppose $\angle B < \angle C < \frac{2\pi}{3}$ in triangle ABC. Then $EF > DF$ if $\angle A < \frac{2\pi}{3}$ and $EF < DF$ if $\angle A > \frac{2\pi}{3}$.*

Proof. Let $x = \angle CBD$ and $y = \angle BCE$. First assume $\angle A < \frac{2\pi}{3}$. Then $DF = \frac{CF\sin(C-y)}{\sin(C+x)}$ and $EF = \frac{BF\sin(B-x)}{\sin(B+y)}$, by the law of sines in triangles CDF and BEF. Thus, we have

$$\frac{EF}{DF} = \left(\frac{\sin(C+x)\sin(B-x)}{\sin x}\right)\left(\frac{\sin y}{\sin(B+y)\sin(C-y)}\right), \tag{5}$$

by the law of sines in triangle BCF. Let $\ell = \frac{2\pi}{3}$. By the expressions for $\cot x$ and for $\cot x + \cot C$ found in the proof of Theorem 2 above, and the law of sines applied to triangles BCG and ABC, we get

$$\begin{aligned}\frac{\sin(C+x)\sin(B-x)}{\sin x} &= (\sin C\cot x + \cos C)(\sin B\cos x - \cos B\sin x)\\ &= \sin C(\cot x + \cot C)\sin x(\sin B\cot x - \cos B)\\ &= \sin C\left(\frac{\sin\ell + \frac{\sin C}{b}}{\sin C\sin(\ell - C)}\right)\left(\frac{CG\sin(C+\frac{\ell}{2})}{BG}\right)\\ &\quad\times\left(\frac{\sin B\left(\frac{1}{b} + \cos(\ell - C)\right) - \cos B\sin(\ell - C)}{\sin(\ell - C)}\right)\\ &= \left(\frac{\sqrt{3}\sin B + 2\sin(B+C)\sin C}{2\sin B\sin(\ell - C)}\right)\left(\frac{b}{BG}\right)\\ &\quad\times(\sin(B+C) + \sin(B+C-\ell)),\end{aligned}$$

where we have used the difference-of-sine formula in the last equality. Observe that the quotient $\frac{\sin(B+y)\sin(C-y)}{\sin y}$ is given by a comparable formula involving CH in place of BG. By Lemma 1, and the law of sines in triangle ABC, it follows from (5) that

$$\frac{EF}{DF} = \left(\frac{\sqrt{3}\sin B + 2\sin(B+C)\sin C}{\sin(\ell - C)}\right)\left(\frac{\sin(\ell - B)}{\sqrt{3}\sin C + 2\sin(B+C)\sin B}\right). \tag{6}$$

Since $\angle A < \frac{2\pi}{3}$, it follow from Lemma 5 that $\frac{EF}{DF} > 1$ in this case. If $\angle A > \frac{2\pi}{3}$, then one is led again to (6), and Lemma 5 implies $\frac{EF}{DF} < 1$, which completes the proof. □

We then obtain the following restricted Steiner-Lehmus type result.

Corollary 7. *If $EF = DF$ in triangle ABC where $\angle B, \angle C < \frac{2\pi}{3}$ (in particular, if triangle ABC is acute), then $AB = AC$.*

Remark. The results of the preceding theorem and corollary may not hold if $\angle C > \frac{2\pi}{3}$. For example, when $\angle B + \angle C = \frac{11\pi}{12}$, then $EF > DF$ if $\angle C = \frac{25\pi}{36}$, while $EF < DF$ if $\angle C = \frac{8\pi}{9}$. Note that $EF > DF$ if and only if $h(u,v) + h(v,u) > 0$ where $v = \angle C > \frac{2\pi}{3}$ and h is as above. Thus, by continuity, it is seen that when $\angle A = \frac{\pi}{12}$, there exists a triangle ABC where $C > \frac{2\pi}{3}$ (and thus $AB \neq AC$) such that $EF = DF$.

Before proving our next result, we will need the following trigonometric inequality.

Lemma 8. *If $0 < x < y$ with $x + y < \frac{\pi}{3}$, then*

$$\frac{\sin^2 x\sin(x+y) + \frac{\sqrt{3}}{2}\sin x\sin y}{\sin\left(\frac{2\pi}{3} - x\right)} < \frac{\sin^2 y\sin(x+y) + \frac{\sqrt{3}}{2}\sin x\sin y}{\sin\left(\frac{2\pi}{3} - y\right)}. \tag{7}$$

Proof. Let $\ell = \frac{2\pi}{3}$. Equivalently, we show

$$\sin^2 x \sin(x+y)\sin(\ell-y) + \frac{\sqrt{3}}{2}\sin x \sin y \sin(\ell-y) \\ < \sin^2 y \sin(x+y)\sin(\ell-x) + \frac{\sqrt{3}}{2}\sin x \sin y \sin(\ell-x),$$

which can be rewritten as

$$\sin^2 x \sin(x+y)(\sin(\ell-y)-\sin(\ell-x)) + \frac{\sqrt{3}}{2}\sin x \sin y(\sin(\ell-y)-\sin(\ell-x)) \\ < (\sin^2 y - \sin^2 x)\sin(x+y)\sin(\ell-x). \tag{8}$$

If $\ell - y \geq \frac{\pi}{2}$, then $\sin(\ell-y) > \sin(\ell-x)$ since $\ell - x > \ell - y \geq \frac{\pi}{2}$. If $\ell - y < \frac{\pi}{2}$, then $\ell - y > \pi - (\ell - x)$ since $x + y < 2\ell - \pi = \frac{\pi}{3}$, by assumption, and thus $\sin(\ell-y) > \sin(\pi-(\ell-x)) = \sin(\ell-x)$. Dividing both sides of (8) by $\sin(\ell-y) - \sin(\ell-x) > 0$, we then must show

$$\sin^2 x \sin(x+y) + \frac{\sqrt{3}}{2}\sin x \sin y < \frac{(\sin^2 y - \sin^2 x)\sin(x+y)\sin(\ell-x)}{\sin(\ell-y)-\sin(\ell-x)}. \tag{9}$$

Using $\sin(\ell-y)-\sin(\ell-x) = 2\sin\left(\frac{x-y}{2}\right)\cos\left(\frac{x+y}{2}-\ell\right)$ and the identity $\sin^2 y - \sin^2 x = \sin(y-x)\sin(y+x)$, we have

$$\begin{aligned}\frac{(\sin^2 y - \sin^2 x)\sin(x+y)\sin(\ell-x)}{\sin(\ell-y)-\sin(\ell-x)} &= \frac{(\sin^2 y - \sin^2 x)\sin(x+y)\sin(\ell-x)}{2\sin\left(\frac{x-y}{2}\right)\cos\left(\frac{x+y}{2}-\ell\right)} \\ &= \frac{\sin(y-x)\sin^2(x+y)\sin(\ell-x)}{2\sin\left(\frac{y-x}{2}\right)\cos\left(\frac{x+y+\ell}{2}\right)} \\ &= \frac{\cos\left(\frac{y-x}{2}\right)\sin^2(x+y)\sin(\ell-x)}{\cos\left(\frac{x+y+\ell}{2}\right)}.\end{aligned}$$

Thus, we need to show

$$\sin^2 x \sin(x+y) + \frac{\sqrt{3}}{2}\sin x \sin y < \frac{\cos\left(\frac{y-x}{2}\right)\sin^2(x+y)\sin(\ell-x)}{\cos\left(\frac{x+y+\ell}{2}\right)}. \tag{10}$$

Since the cosine function is decreasing in the first quadrant, to prove (10), it suffices to show

$$\sin^2 x \sin(x+y) + \frac{\sqrt{3}}{2}\sin x \sin y < \frac{\cos\left(\frac{x+y}{2}\right)\sin^2(x+y)\sin(\ell-x)}{\cos\left(\frac{x+y+\ell}{2}\right)}.$$

Dividing both the numerator and denominator of the fraction in the last inequality by $\cos\left(\frac{x+y}{2}\right)$ gives

$$\sin^2 x \sin(x+y) + \frac{\sqrt{3}}{2}\sin x \sin y < \frac{\sin^2(x+y)\sin(\ell-x)}{\frac{1}{2} - \frac{\sqrt{3}}{2}\tan\left(\frac{x+y}{2}\right)},$$

which can be rewritten as

$$\frac{\sin^2 x \sin(x+y) + \frac{\sqrt{3}}{4}(\cos(x-y) - \cos(x+y))}{\sin(\ell - x)} < \frac{\sin^2(x+y)}{\frac{1}{2} - \frac{\sqrt{3}}{2}\tan\left(\frac{x+y}{2}\right)}. \quad (11)$$

Since the right-hand side of (11) depends on x and y only through the sum, our strategy is to fix $u = x + y$ and consider the left-hand side as a function of x which we seek to maximize.

Given $0 < u < \frac{\pi}{3}$, define the function $h(x)$ for $0 < x < \frac{u}{2}$ by

$$h(x) = \frac{\sin u \sin^2 x + \frac{\sqrt{3}}{4}(\cos(u-2x) - \cos u)}{\sin(\ell - x)}.$$

Then $h'(x) > 0$ if and only if

$$\sin(\ell - x)\left(2\sin u \sin x \cos x + \frac{\sqrt{3}}{2}\sin(u-2x)\right)$$
$$> -\cos(\ell - x)(\sin u \sin^2 x + \frac{\sqrt{3}}{4}(\cos(u-2x) - \cos u)). \quad (12)$$

Since $\sin(\ell - x) > -\cos(\ell - x) > 0$ for $0 < x < \frac{\pi}{6}$ and since $0 < x < \frac{u}{2}$, to show (12), it suffices to show

$$2\sin u \sin x \cos x > \sin u \sin^2 x + \frac{\sqrt{3}}{4}(\cos(u-2x) - \cos u).$$

Note that $0 < x < \frac{\pi}{6}$ implies $\sin u \sin x \cos x > \sin u \sin^2 x$ and

$$\sin u \sin x \cos x > \frac{\sqrt{3}}{4}(\cos(u-2x) - \cos u) = \frac{\sqrt{3}}{2}\sin x \sin y,$$

as $\sin u = \sin(x+y) > \sin y$ and $\cos x > \frac{\sqrt{3}}{2}$. Adding these inequalities then implies the desired inequality and shows that $h(x)$ is increasing on the interval $(0, \frac{u}{2})$.

Thus, to prove (11), it is enough to show that it holds when $x = \frac{u}{2}$ (where $u = x + y$). That is, we must show

$$(2\sin^2 v \sin(2v) + \sqrt{3}\sin^2 v)(1 - \sqrt{3}\tan v) < 4\sin^2(2v)\sin(\ell - v), \qquad 0 < v < \frac{\pi}{6},$$

i.e.,

$$(2\sin(2v) + \sqrt{3})(1 - \sqrt{3}\tan v) < 16\cos^2 v \sin(\ell - v).$$

The last inequality holds since

$$(2\sin(2v) + \sqrt{3})(1 - \sqrt{3}\tan v) < 2\sqrt{3} < 16\cos^2 v \sin(\ell - v)$$

for $0 < v < \frac{\pi}{6}$. This implies (11), which completes the proof. □

Our final two results concern the monotonicity of the segments determined when a Fermat cevian intersects the opposite side.

Theorem 9. *If $AB > AC$ in triangle ABC, then $BE > CD$.*

Proof. First suppose all angles of triangle ABC are less than $\frac{2\pi}{3}$. In this case, by the law of sines in triangles BCE and BCD in Figure 1, we have $BE = \frac{\sin y}{\sin(B+y)}$ and $CD = \frac{\sin x}{\sin(C+x)}$, where $x = \angle CBD$ and $y = \angle BCE$. Then $BE > CD$ if and only if

$$\sin B(\cot y + \cot B) < \sin C(\cot x + \cot C).$$

By the formulas found previously for $\cot x + \cot C$ and $\cot y + \cot B$ and the law of sines in triangle ABC, this last inequality is equivalent to

$$\frac{\sin B \sin(B+C) + \frac{\sqrt{3}}{2}\sin C}{\sin(\ell - B)\sin C} < \frac{\sin C \sin(B+C) + \frac{\sqrt{3}}{2}\sin B}{\sin(\ell - C)\sin B}, \qquad (13)$$

where $\ell = \frac{2\pi}{3}$. By Lemma 5 and since $\sin C > \sin B > 0$, the preceding inequality holds, as desired.

We now consider the remaining cases. If $\angle A = \frac{2\pi}{3}$ or $\angle C = \frac{2\pi}{3}$, then the result is clear. If $\angle A > \frac{2\pi}{3}$, then one may verify that $BE > CD$ if and only if (13) holds as before; in which case, the result now follows from Lemma 8. If $\angle C > \frac{2\pi}{3}$, then one may verify that $BE > CD$ if and only if

$$\frac{\sin B \sin(B+C) + \frac{\sqrt{3}}{2}\sin C}{\sin(\ell - B)\sin C} < \frac{\sin C \sin(B+C) + \frac{\sqrt{3}}{2}\sin B}{\sin(C - \ell)\sin B}. \qquad (14)$$

To show (14), first note that $\sin(C-\ell) < \sin(\ell - B)$ since $C - \ell < \frac{\ell}{2} < \ell - B < \ell$. Hence, $\frac{\sin B \sin(B+C)}{\sin(\ell-B)\sin C} < \frac{\sin C \sin(B+C)}{\sin(C-\ell)\sin B}$ (since $\sin B < \sin C$) and $\frac{\sqrt{3}}{2\sin(\ell-B)} < \frac{\sqrt{3}}{2\sin(C-\ell)}$. Thus (14) follows from adding these two inequalities, which completes the proof. □

Theorem 10. *Let $AB > AC$ in triangle ABC where $\angle A \neq \frac{2\pi}{3}$. Then $AE < AD$ if $\angle A < \frac{\pi}{3}$ or $\angle A > \frac{2\pi}{3}$ and $AE > AD$ if $\frac{\pi}{3} < \angle A < \frac{2\pi}{3}$, with $AE = AD$ if $\angle A = \frac{\pi}{3}$.*

Proof. First assume that all angles in triangle ABC are less than $\frac{2\pi}{3}$. Using the formula for EB found in the proof of Theorem 9 and the fact that $\sin C = c\sin(B +$

C), we have

$$\begin{aligned}
AE = AB - EB &= c\left(1 - \frac{\sin\left(\frac{2\pi}{3} - B\right)\sin(B+C)}{\sin B\sin(B+C) + \frac{\sqrt{3}}{2}\sin C}\right) \\
&= c\left(\frac{\sin(B+C)\left(\sin B + \sin\left(B - \frac{2\pi}{3}\right)\right) + \frac{\sqrt{3}}{2}\sin C}{\sin B\sin(B+C) + \frac{\sqrt{3}}{2}\sin C}\right) \\
&= 2c\left(\frac{2\sin(B+C)\sin\left(B - \frac{\pi}{3}\right)\cos\left(\frac{\pi}{3}\right) + \frac{\sqrt{3}}{2}\sin C}{\cos C - \cos(C+2B) + \sqrt{3}\sin C}\right) \\
&= \frac{c}{2}\left(\frac{\cos\left(C + \frac{\pi}{3}\right) - \cos\left(C + 2B - \frac{\pi}{3}\right) + \sqrt{3}\sin C}{\sin\left(C + \frac{\pi}{6}\right) - \frac{1}{2}\cos(C+2B)}\right) \\
&= \frac{c}{2}\left(\frac{\cos\left(C - \frac{\pi}{3}\right) - \cos\left(C + 2B - \frac{\pi}{3}\right)}{\sin\left(C + \frac{\pi}{6}\right) - \frac{1}{2}\cos(C+2B)}\right) = \frac{c\sin\left(B + C - \frac{\pi}{3}\right)\sin B}{\sin\left(C + \frac{\pi}{6}\right) - \frac{1}{2}\cos(C+2B)},
\end{aligned}$$

where we have made use of several trigonometric identities. Noting the comparable expression for AD, it follows that $AE < AD$ if and only if

$$\frac{c\sin\left(B + C - \frac{\pi}{3}\right)\sin B}{\sin\left(C + \frac{\pi}{6}\right) - \frac{1}{2}\cos(C+2B)} < \frac{b\sin\left(C + B - \frac{\pi}{3}\right)\sin C}{\sin\left(B + \frac{\pi}{6}\right) - \frac{1}{2}\cos(B+2C)}.$$

Since $\sin\left(B + C - \frac{\pi}{3}\right)$ is positive (as $\angle A < \frac{2\pi}{3}$) and since $c\sin B = b\sin C$, this last inequality is equivalent to

$$\frac{1}{2}(\cos(C+2B) - \cos(B+2C)) < \sin\left(C + \frac{\pi}{6}\right) - \sin\left(B + \frac{\pi}{6}\right),$$

i.e.,

$$\sin\left(\frac{C-B}{2}\right)\sin\left(\frac{3(B+C)}{2}\right) < 2\sin\left(\frac{C-B}{2}\right)\cos\left(\frac{B+C}{2} + \frac{\pi}{6}\right).$$

Thus, we have $AE < AD$ if

$$\sin\left(\frac{3(B+C)}{2}\right) < 2\sin\left(\frac{\pi}{3} - \frac{B+C}{2}\right), \tag{15}$$

since $AB > AC$ implies that the $\sin\left(\frac{C-B}{2}\right)$ factor is positive. Note that $AE > AD$ if (15) is reversed.

We now consider cases on the sum $\angle B + \angle C$. First suppose $\angle B + \angle C > \frac{2\pi}{3}$ and let $u = \frac{B+C}{2} - \frac{\pi}{3}$ where $0 < u < \frac{\pi}{6}$. Then (15) holds if and only if

$$2\sin u < -\sin(3u + \pi) = \sin 3u = 3\sin u - 4\sin^3 u,$$

i.e., $4\sin^2 u < 1$, which is true since $0 < u < \frac{\pi}{6}$. Thus $AE < AD$ if $AB > AC$ in this case. If $\frac{\pi}{3} < \angle B + \angle C < \frac{2\pi}{3}$, then let $u = \frac{\pi}{3} - \frac{B+C}{2}$ where $0 < u < \frac{\pi}{6}$. In this case, the reverse of inequality (15) holds since $\sin 3u > 2\sin u$, whence $AE > AD$ if $AB > AC$. If $\angle B + \angle C = \frac{2\pi}{3}$, then there is equality in (15). Combining the preceding cases thus implies the theorem whenever all angles in $\angle ABC$ are less than $\frac{2\pi}{3}$.

If $\angle A > \frac{2\pi}{3}$, then $AE = EB - AB$ and one gets

$$AE = \frac{c \sin\left(\frac{\pi}{3} - B - C\right) \sin B}{\sin\left(C + \frac{\pi}{6}\right) - \frac{1}{2}\cos(C + 2B)}$$

in this case and a comparable expression for AD. Since $\angle B + \angle C < \frac{\pi}{3}$, the factor of $\sin\left(\frac{\pi}{3} - B - C\right)$ is positive and thus cancels out when comparing AE and AD, which leads to inequality (15) as before. Let $u = \frac{\pi}{3} - \frac{B+C}{2}$, so $\frac{\pi}{6} < u < \frac{\pi}{3}$. Then (15) is seen to hold in this case since $\sin 3u < 2 \sin u$, whence $AE < AD$ if $AB > AC$. Finally, if $\angle C \geq \frac{2\pi}{3}$, then one gets

$$AD = AC + CD = b\left(1 + \frac{\sin\left(C - \frac{2\pi}{3}\right)\sin(B + C)}{\sin C \sin(B + C) + \frac{\sqrt{3}}{2}\sin B}\right),$$

which is seen to yield the same formula as before. Note that the expression for AE also does not change in this case and we are again led to inequality (15). Since (15) holds if $\angle B + \angle C > \frac{2\pi}{3}$, we have $AE < AD$ if $AB > AC$ when $\angle C \geq \frac{2\pi}{3}$, which completes the proof. □

Corollary 11. *If $AE = AD$ in triangle ABC where $\angle A \neq \frac{\pi}{3}, \frac{2\pi}{3}$, then $AB = AC$.*

References

[1] S. Abu-Saymeh, M. Hajja, and H. A. ShahAli, Another variation on the Steiner-Lehmus theme, *Forum Geom.*, 8 (2008) 131–140.

[2] H. S. M. Coxeter, *Introduction to Geometry*, John Wiley & Sons, Inc., 1961.

[3] H. S. M. Coxeter and S. L. Greitzer, *Geometry Revisited*, Random House, Inc., 1967.

[4] M. Hajja, A short trigonometric proof of the Steiner-Lehmus theorem, *Forum Geom.*, 8 (2008) 39–42.

[5] M. Hajja, Stronger forms of the Steiner-Lehmus theorem, *Forum Geom.*, 8 (2008) 157–161.

[6] M. Hajja, Cyril F. Parry's variations on the Steiner-Lehmus theme, pre-print.

[7] T. Mansour and M. Shattuck, Monotonicity results concerning certain lengths within a triangle, *J. Adv. Math. Appl.*, 2 (2013) 59–64.

[8] R. Oláh-Gál and J. Sándor, On trigonometric proofs of the Steiner-Lehmus theorem, *Forum Geom.*, 9 (2009) 155–160.

[9] L. Sanger and J. Wales, Wikipedia, under `https://en.wikipedia.org/wiki/Fermat_point`.

[10] K. R. S. Sastry, A Gergonne analogue of the Steiner-Lehmus theorem, *Forum Geom.*, 5 (2005) 191–195.

Toufik Mansour: Department of Mathematics, University of Haifa, 3498838 Haifa, Israel
E-mail address: `tmansour@univ.haifa.ac.il`

Mark Shattuck: Department of Mathematics, University of Tennessee, Knoxville, Tennessee 37996, USA
E-mail address: `shattuck@math.utk.edu`

Forum Geometricorum
Volume 16 (2016) 367–369.

FORUM GEOM
ISSN 1534-1178

On a new generalization of the Droz-Farny line

Cyril Letrouit

Abstract. We prove a new generalization of the Droz-Farny line theorem, which is based on some reflections about similar triangles.

We will prove the following generalization of the Droz-Farny line theorem.

Theorem 1. *Let ABC be a triangle with orthocenter H. Let ℓ_1 and ℓ_2 be two lines intersecting perpendicularly at H. For $i = 1, 2$, let ℓ_i intersect the lines BC, CA, AB respectively at A_i, B_i, C_i. Let A_3, B_3, C_3 be points in the plane such that the triangles $A_1A_2A_3$, $B_1B_2B_3$, $C_1C_2C_3$ are directly similar. Then A_3, B_3, C_3 are collinear.*

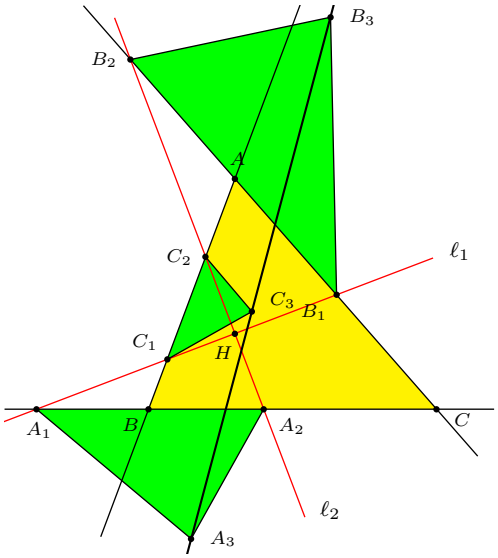

Figure 1

We call this line the generalized Droz-Farny line.

The case where A_3, B_3, C_3 are midpoints of the segments A_1A_2, B_1B_2, C_1C_2 is the one first studied by Droz-Farny in [2]. The more general case with A_3, B_3, C_3 dividing A_1A_2, B_1B_2, C_1C_2 in the same ratio was found by van Lamoen in [3].

Publication Date: November 8, 2016. Communicating Editor: Paul Yiu.

This proof uses similarities. Let us first mention a classical proposition, with the same notations as in the statement of the main theorem.

Proposition 2. *The circles with diameters A_1A_2, B_1B_2 and C_1C_2 are concurrent in a point M (different from H) which lies on the circumcircle of ABC.*

See Ayme [1, §3] for a proof.

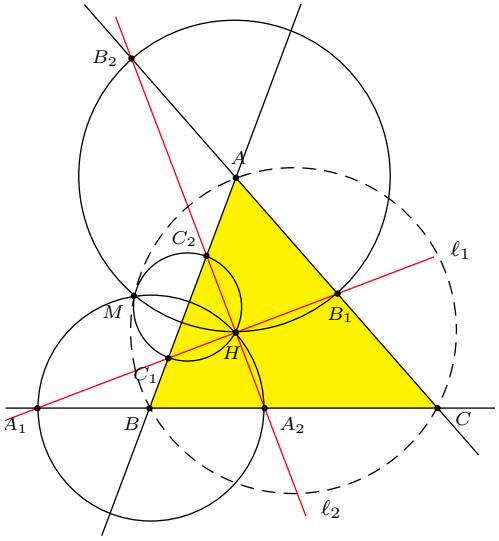

Figure 2

Proposition 3. *The points A, B_1, C_1, M are concyclic.*

Proof. M is on the circumcircles of HC_1C_2 and HB_1B_2. Hence, M is the point of intersection of the four circumcircles associated to the complete quadrilateral defined by HB_1, B_1B_2, B_2C_2, C_2A. It follows that M is on the circumcircle of AB_1C_1. □

This implies in particular that $\angle MB_1B_2 = \angle MC_1C_2$. By a cyclic argument, one can prove that we also have $\angle MA_1A_2 = \angle MB_1B_2$. Hence, since $\angle A_1MA_2 = \angle B_1MB_2 = C_1MC_2 = \frac{\pi}{2}$, we get that $MA_1A_2 \sim MB_1B_2 \sim MC_1C_2$.

Moreover, the similarity of center M that maps MA_1A_2 onto MB_1B_2 also maps A_3 onto B_3. From this, we get that there is a similarity S_1 of center M that maps A_2 onto A_3 and B_2 onto B_3. The same argument gives that there is a similarity S_2 of center M that maps B_2 onto B_3 and C_2 onto C_3. But there is only one similarity of center M that maps B_2 onto B_3. Hence $S_1 = S_2$, and so this similarity maps A_2, B_2 and C_2 onto A_3, B_3 and C_3. Since A_2, B_2 and C_2 are collinear, A_3, B_3 and C_3 are also collinear. This proves Theorem 1.

Corollary 4. *All the corresponding points of the three similar triangles lie on a line too (that means points which verify all the same relations, which is possible because the triangles are similar).*

For example, their three orthocenters lie on a line. To prove this, denote by A_3, B_3 and C_3 three corresponding points. Then $A_1A_2A_3$, $B_1B_2B_3$ and $C_1C_2C_3$ are directly similar. Hence A_3, B_3 and C_3 lie on a line by Theorem 1.

References

[1] J.-L. Ayme, A synthetic proof of the Droz-Farny line theorem, *Forum Geom.*, 4 (2004) 219–224.
[2] A. Droz-Farny, Question 14111, *Educational Times*, 71 (1899) 89–90.
[3] F. M. van Lamoen, Hyacinthos messages 6140, 6144, December 11, 2002.
[4] C. Pohoata and Son Hong Ta, A short proof of Lamoen's generalization of the Droz-Farny line theorem, *Mathematical Reflections*, 3 (2011).

Cyril Letrouit: Department of Mathematics and Applications, École Normale Supérieure (Paris), PSL Research University, 45 rue d'Ulm, 75005 Paris, France
E-mail address: cyril.letrouit@ens.fr

Forum Geometricorum
Volume 16 (2016) 371–372.

FORUM GEOM
ISSN 1534-1178

Euler Line in the Golden Rectangle

Tran Quang Hung

Abstract. We establish a relationship between a golden rectangle and the Euler line of a triangle contained in the rectangle.

The golden rectangle and the Euler line are two beautiful concepts of geometry. Let $\varphi := \frac{\sqrt{5}+1}{2}$ be the golden ratio. A golden rectangle is one whose dimensions are in the ratio φ. Since $\varphi^2 - \varphi - 1 = 0$, or equivalently $\varphi = 1 + \frac{1}{\varphi}$, it is clear that if a square is constructed inside a golden rectangle sharing one side, then the complement is also a golden rectangle.

In this note we construct a triangle in a given golden rectangle and show how its Euler line is related to the rectangle.

Proposition 1. *Let $ABCD$ be a golden rectangle with $\frac{AD}{AB} = \varphi$. Construct the squares $CDMN$, $BNQP$ inside the rectangles $ABCD$ and $ABNM$ respectively. Let E be the reflection of M in A. Then the line EC is the Euler line of triangle MNP.*

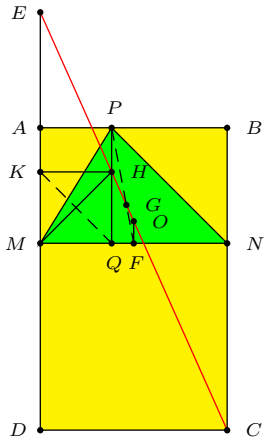

Figure 1

Proof. Clearly, $BNMA$ and $MQPA$ are golden rectangles, and $\frac{AD}{AM} = \frac{AD}{AB} \cdot \frac{AB}{AM} = \varphi \cdot \varphi = \varphi^2$. Construct the square $MQHK$ inside $MQPA$. Then $AKHP$ is also a golden rectangle, and $\frac{AK}{AM} = \frac{1}{\varphi^2}$.

Publication Date: November 10, 2016. Communicating Editor: Paul Yiu.

Consider triangle MNP. Since $MH \perp KQ$, and $KQ \parallel PN$, it follows that MH is the altitude on PN. It intersects the altitude PQ at the orthocenter H of the triangle.

Now,

$$\frac{KH}{DC} = \frac{MQ}{MN} = \frac{MQ}{AM} \cdot \frac{AM}{MN} = \frac{1}{\varphi} \cdot \frac{1}{\varphi} = \frac{1}{\varphi^2}.$$

Also,

$$\frac{EK}{ED} = \frac{EA + AK}{EA + AD} = \frac{AM + AK}{AM + AD} = \frac{1 + \frac{AK}{AM}}{1 + \frac{AD}{AM}} = \frac{1 + \frac{1}{\varphi^2}}{1 + \varphi^2} = \frac{1}{\varphi^2}.$$

Hence, $\frac{KH}{DC} = \frac{EK}{ED}$. By Thales' theorem, EC passes through H.

Let O and F be the midpoints of the segments EC and MN respectively. Since EM and CN are both perpendicular to MN, applying the midline theorem to the trapezoid $EMNC$, we have $OF \perp MN$, and

$$\begin{aligned} 2 \cdot OF &= EM - NC = 2AM - MN = AM + PQ - (MQ + QN) \\ &= AM - MQ = AM - KM = AK = PH. \end{aligned}$$

This means that the line EC intersects the perpendicular bisector of MN at O such that $PH = 2 \cdot OF$. This shows that O is the circumcenter of triangle MNP, and EC is the Euler line of the triangle. □

The intersection of EC with the median PF is the centroid G of the triangle MNP.

References

[1] A. Bogomolny, Golden ratio in geometry, *Interactive Mathematics Miscellany and Puzzles*, http://www.cut-the-knot.org/do_you_know/GoldenRatio.shtml.

[2] E. A. J. García and P. Yiu, Golden sections of triangle centers in the golden triangles, *Forum Geom.*, 16 (2016) 119–124.

Tran Quang Hung: High school for Gifted students, Hanoi University of Science, Vietnam National University, Hanoi, Vietnam

E-mail address: analgeomatica@gmail.com

Forum Geometricorum
Volume 16 (2016) 373–379.

FORUM GEOM
ISSN 1534-1178

Distances Among the Feuerbach Points

Sándor Nagydobai Kiss

Abstract. We find simple formulas for the distances from the Feuerbach points of a triangle to the vertices, and among themselves.

Consider a triangle ABC with the midpoints X, Y, Z of its sides BC, CA, AB respectively, circumcenter O, the incenter I, and the excenters I_a, I_b, I_c. The radii of the circumcircle, incircle, and excircles are denoted by R, r, r_a, r_b, r_c respectively. The nine-point circle is the circle through X, Y, Z; it has center N and radius $\frac{R}{2}$. By the famous Feuerbach theorem, the nine-point circle is tangent to the incircle and each of the excircles. The points of tangency are the Feuerbach points, F_{e} with the incircle, and F_a, F_b, F_c with the excircles (I_a), (I_b), (I_c) respectively.

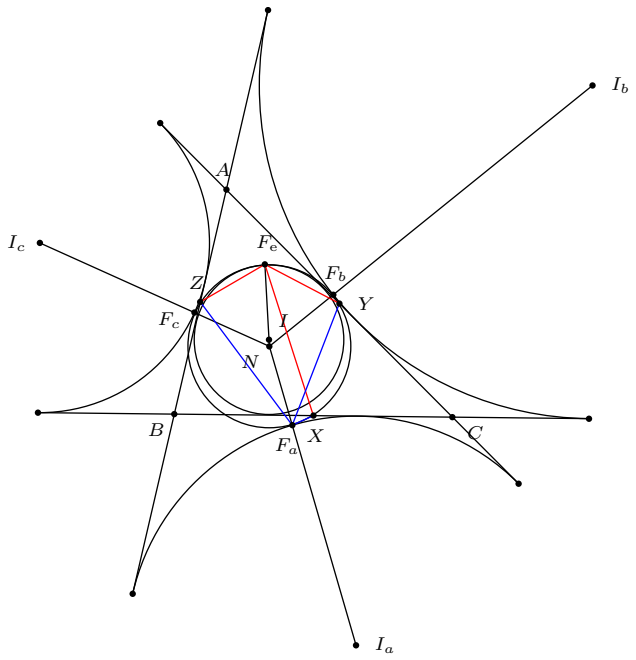

Figure 1

In [2], we have computed the distances from the Feuerbach points to X, Y, Z (see Figure 1). Specifically, if the lengths of the sides BC, CA, AB are a, b, c,

Publication Date: November 10, 2016. Communicating Editor: Paul Yiu.

then

$$F_{\mathrm{e}}X = \frac{|b-c|R}{2\cdot OI}, \quad F_{\mathrm{e}}Y = \frac{|c-a|R}{2\cdot OI}, \quad F_{\mathrm{e}}Z = \frac{|a-b|R}{2\cdot OI}; \tag{1}$$

$$F_aX = \frac{|b-c|R}{2\cdot OI_a}, \quad F_aY = \frac{(c+a)R}{2\cdot OI_a}, \quad F_aZ = \frac{(a+b)R}{2\cdot OI_a}. \tag{2}$$

By Euler's formula, $OI^2 = R(R-2r)$ and $OI_a^2 = R(R+2r_a)$, (see [1, Theorems 152, 153]), these are equivalent to the following formulas.

$$F_{\mathrm{e}}X^2 = \frac{(b-c)^2R}{4(R-2r)}, \quad F_{\mathrm{e}}Y^2 = \frac{(c-a)^2R}{4(R-2r)}, \quad F_{\mathrm{e}}Z^2 = \frac{(a-b)^2R}{4(R-2r)}; \tag{3}$$

$$F_aX^2 = \frac{(b-c)^2R}{4(R+2r_a)}, \quad F_aY^2 = \frac{(c+a)^2R}{4(R+2r_a)}, \quad F_aZ^2 = \frac{(a+b)^2R}{4(R+2r_a)}. \tag{4}$$

In this note, we find simple formulas analogous to (1), (2) for the distances among the Feuerbach points. We begin with the distances to the vertices (see Figure 2).

Proposition 1. *The distances from the Feuerbach point F_{e} to the vertices of triangle ABC are given by*

$$AF_{\mathrm{e}}^2 = \frac{(s-a)^2R - rS_A}{R-2r}, \quad BF_{\mathrm{e}}^2 = \frac{(s-b)^2R - rS_B}{R-2r}, \quad CF_{\mathrm{e}}^2 = \frac{(s-c)^2R - rS_C}{R-2r},$$

where s is the semiperimeter of the triangle, and $S_A := \frac{b^2+c^2-a^2}{2}$, $S_B = \frac{c^2+a^2-b^2}{2}$, and $S_C = \frac{a^2+b^2-c^2}{2}$.

Proof. We apply the median theorem for the triangles $F_{\mathrm{e}}BC$, $F_{\mathrm{e}}CA$, $F_{\mathrm{e}}AB$. From (3) above, we have

$$F_{\mathrm{e}}X^2 = \frac{BF_{\mathrm{e}}^2 + CF_{\mathrm{e}}^2}{2} - \frac{a^2}{4}, \tag{5}$$

$$F_{\mathrm{e}}Y^2 = \frac{CF_{\mathrm{e}}^2 + AF_{\mathrm{e}}^2}{2} - \frac{b^2}{4}, \tag{6}$$

$$F_{\mathrm{e}}Z^2 = \frac{AF_{\mathrm{e}}^2 + BF_{\mathrm{e}}^2}{2} - \frac{c^2}{4}. \tag{7}$$

The combination $-(5)+(6)+(7)$ gives

$$-F_{\mathrm{e}}X^2 + F_{\mathrm{e}}Y^2 + F_{\mathrm{e}}Z^2 = AF_{\mathrm{e}}^2 - \frac{b^2+c^2-a^2}{4}.$$

Hence,

$$\begin{aligned} AF_{\mathrm{e}}^2 &= -F_{\mathrm{e}}X^2 + F_{\mathrm{e}}Y^2 + F_{\mathrm{e}}Z^2 + \frac{b^2+c^2-a^2}{4} \\ &= \frac{(-(b-c)^2+(c-a)^2+(a-b)^2)R}{4(R-2r)} + \frac{S_A}{2} \\ &= \frac{2(a-b)(a-c)R}{4(R-2r)} + \frac{2(R-2r)S_A}{4(R-2r)} \\ &= \frac{(2(a-b)(a-c)+2S_A)R - 4rS_A}{4(R-2r)}. \end{aligned}$$

Since

$$2(a-b)(a-c)+2S_A = 2(a-b)(a-c)+(b^2+c^2-a^2) = (b+c-a)^2 = 4(s-a)^2,$$

we have $AF_{\mathrm{e}}^2 = \frac{(s-a)^2R-rS_A}{R-2r}$. The other two expressions follow similarly. □

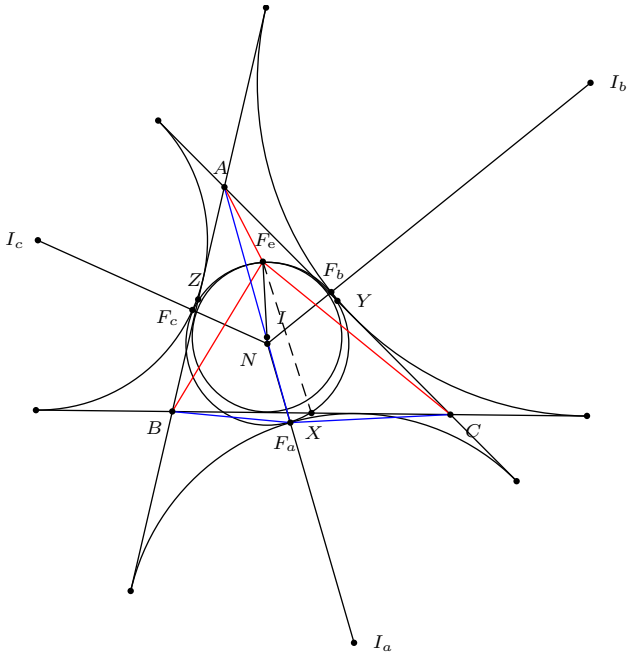

Figure 2

Proposition 2. *The distances from the Feuerbach point F_a to the vertices of triangle ABC are given by*

$$AF_a^2 = \frac{s^2R + r_aS_A}{R+2r_a}, \quad BF_a^2 = \frac{(s-c)^2R + r_aS_B}{R+2r_a}, \quad CF_a^2 = \frac{(s-b)^2R + r_aS_C}{R+2r_a}.$$

Proof. We applying the median theorem to triangles F_aBC, F_aCA, F_aAB. From (4) above, we have

$$F_aX^2 = \frac{BF_a^2 + CF_a^2}{2} - \frac{a^2}{4}, \tag{8}$$

$$F_aY^2 = \frac{CF_a^2 + AF_a^2}{2} - \frac{b^2}{4}, \tag{9}$$

$$F_aZ^2 = \frac{AF_a^2 + BF_a^2}{2} - \frac{c^2}{4}. \tag{10}$$

The combination $-$(8)+(9)+(10) gives

$$-F_aX^2 + F_aY^2 + F_aZ^2 = AF_a^2 - \frac{b^2 + c^2 - a^2}{4}.$$

Hence,

$$\begin{aligned} AF_a^2 &= -F_aX^2 + F_aY^2 + F_aZ^2 + \frac{S_A}{2} \\ &= \frac{(-(b-c)^2 + (c+a)^2 + (a+b)^2)R}{4(R+2r_a)} + \frac{S_A}{2} \\ &= \frac{2(a+b)(a+c)R}{4(R+2r_a)} + \frac{2(R+2r_a)S_A}{4(R+2r_a)} \\ &= \frac{(2(a+b)(a+c) + 2S_A)R + 4r_aS_A}{4(R+2r_a)}. \end{aligned}$$

Since

$$2(a+b)(a+c) + 2S_A = 2(a+b)(a+c) + (b^2 + c^2 - a^2) = (a+b+c)^2 = 4s^2,$$

we have $AF_a^2 = \frac{s^2R + r_aS_A}{R+2r_a}$.

On the other hand, the combination (8)$-$(9)+(10) gives

$$F_aX^2 - F_aY^2 + F_aZ^2 = BF_a^2 - \frac{c^2 + a^2 - b^2}{4}.$$

Therefore,

$$\begin{aligned} BF_a^2 &= F_aX^2 - F_aY^2 + F_aZ^2 + \frac{S_B}{2} \\ &= \frac{((b-c)^2 - (c+a)^2 + (a+b)^2)R}{4(R+2r_a)} + \frac{S_B}{2} \\ &= \frac{(2(a+b)(b-c) + 2S_B)R + 4r_aS_B}{4(R+2r_a)}. \end{aligned}$$

Since

$$2(a+b)(b-c) + 2S_B = 2(a+b)(b-c) + (c^2 + a^2 - b^2) = (a+b-c)^2 = 4(s-c)^2,$$

we have

$$BF_a^2 = \frac{(s-c)^2R + r_aS_B}{R+2r_a}.$$

The proof of the expression for CF_a^2 is similar. □

Now we compute the distances among the Feuerbach points.

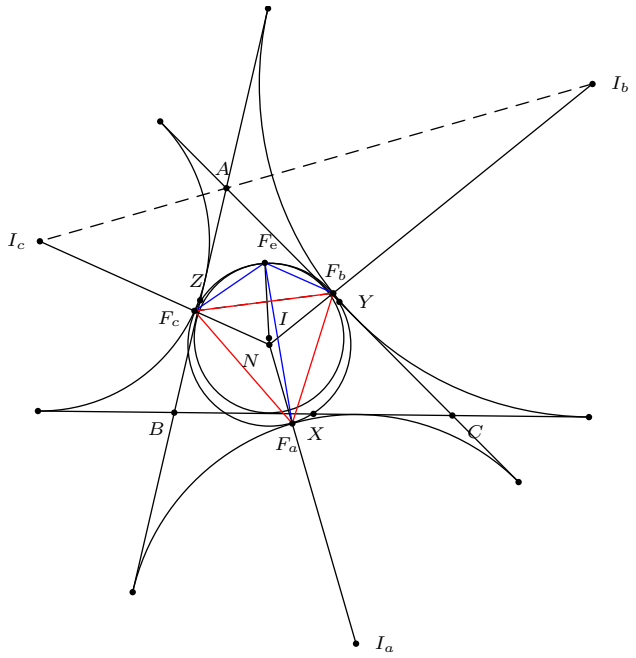

Figure 3

Theorem 3. $F_bF_c = \frac{(b+c)R^2}{OI_b \cdot OI_c}$, $F_cF_a = \frac{(c+a)R^2}{OI_c \cdot OI_a}$, $F_aF_b = \frac{(a+b)R^2}{OI_a \cdot OI_b}$.

Proof. It is enough to prove the first formula. Triangle NF_bF_c is isosceles with $NF_b = NF_c = \frac{R}{2}$; we have

$$F_bF_c^2 = \frac{R^2}{2}(1 - \cos F_bNF_c).$$

Applying the law of cosines to triangles NI_bI_c, noting that $I_bI_c = 4R\cos\frac{A}{2}$, we have

$$\begin{aligned}
&\left(4R\cos\frac{A}{2}\right)^2 \\
=\ & NI_b^2 + NI_c^2 - 2 \cdot NI_b \cdot NI_c \cos I_bNI_c \\
=\ & \left(\frac{R}{2} + r_b\right)^2 + \left(\frac{R}{2} + r_c\right)^2 - 2\left(\frac{R}{2} + r_b\right)\left(\frac{R}{2} + r_c\right)\cos I_bNI_c \\
=\ & \left[\left(\frac{R}{2} + r_b\right) - \left(\frac{R}{2} + r_c\right)\right]^2 + 2\left(\frac{R}{2} + r_b\right)\left(\frac{R}{2} + r_c\right)(1 - \cos F_bNF_c) \\
=\ & (r_b - r_c)^2 + \frac{1}{2}(R + 2r_b)(R + 2r_c)(1 - \cos F_bNF_c).
\end{aligned}$$

Therefore,

$$F_bF_c^2 = = \frac{R^4\left(\left(4R\cos\frac{A}{2}\right)^2-(r_b-r_c)^2\right)}{OI_b^2\cdot OI_c^2}.$$

Since $s = 4R\cos\frac{A}{2}\cos\frac{B}{2}\cos\frac{C}{2}$, $s\left(\tan\frac{B}{2}-\tan\frac{C}{2}\right) = 4R\cos\frac{A}{2}\sin\left(\frac{B}{2}-\frac{C}{2}\right)$. From this,

$$F_bF_c^2 = \frac{16R^6\cos^2\frac{A}{2}\left(1-\sin^2\left(\frac{B}{2}-\frac{C}{2}\right)\right)}{OI_b^2\cdot OI_c^2} = \frac{16R^6\cos^2\frac{A}{2}\cos^2\left(\frac{B}{2}-\frac{C}{2}\right)}{OI_b^2\cdot OI_c^2},$$

and

$$\begin{aligned}F_bF_c &= \frac{4R^3\cos\frac{A}{2}\cos\left(\frac{B}{2}-\frac{C}{2}\right)}{OI_b\cdot OI_c} = \frac{2R^3\left(\cos\left(\frac{A}{2}-\frac{B}{2}+\frac{C}{2}\right)+\cos\left(\frac{A}{2}+\frac{B}{2}-\frac{C}{2}\right)\right)}{OI_b\cdot OI_c}\\ &= \frac{2R^3\left(\cos\left(\frac{\pi}{2}-B\right)+\cos\left(\frac{\pi}{2}-C\right)\right)}{OI_b\cdot OI_c} = \frac{2R^3(\sin B+\sin C)}{OI_b\cdot OI_c} = \frac{(b+c)R^2}{OI_b\cdot OI_c}.\end{aligned}$$

□

Theorem 4. $F_eF_a = \frac{|b-c|R^2}{OI\cdot OI_a}$, $F_eF_b = \frac{|c-a|R^2}{OI\cdot OI_b}$, $F_eF_c = \frac{|a-b|R^2}{OI\cdot OI_c}$.

Proof. Again, it is enough to prove the first formula. Triangle NF_eF_a is isosceles with $NF_e = NF_a = \frac{R}{2}$ (see Figure 3); we have

$$F_eF_a^2 = \frac{R^2}{2}(1-\cos F_eNF_a).$$

Applying the law of cosines to triangle NII_a, we have, noting that $II_a = 4R\sin\frac{A}{2}$,

$$\begin{aligned}&\left(4R\sin\frac{A}{2}\right)^2\\ &= NI^2+NI_a^2-2NI\cdot NI_a\cos INI_a\\ &= \left(\frac{R}{2}-r\right)^2+\left(\frac{R}{2}+r_a\right)^2-2\left(\frac{R}{2}-r\right)\left(\frac{R}{2}+r_a\right)\cos INI_a\\ &= \left[\left(\frac{R}{2}-r\right)-\left(\frac{R}{2}+r_a\right)\right]^2+2\left(\frac{R}{2}-r\right)\left(\frac{R}{2}+r_a\right)(1-\cos F_eNF_a)\\ &= (r+r_a)^2+\frac{1}{2}(R-2r)(R+2r_a)(1-\cos F_eNF_a).\end{aligned}$$

Therefore,

$$F_eF_a^2 = \frac{R^2\left(\left(4R\sin\frac{A}{2}\right)^2-\left((b+c)\tan\frac{A}{2}\right)^2\right)}{(R-2r)(R+2r_a)} = \frac{R^4\left(\left(4R\sin\frac{A}{2}\right)^2-\left((b+c)\tan\frac{A}{2}\right)^2\right)}{OI^2\cdot OI_a^2}.$$

Since $(b+c)\tan\frac{A}{2} = 2R(\sin B+\sin C)\tan\frac{A}{2} = 4R\sin\frac{B+C}{2}\cos\frac{B-C}{2}\tan\frac{A}{2} = 4R\sin\frac{A}{2}\cos\frac{B-C}{2}$,

$$F_eF_a^2 = \frac{R^4\left(\left(4R\sin\frac{A}{2}\right)^2-\left(4R\sin\frac{A}{2}\cos\frac{B-C}{2}\right)^2\right)}{OI^2\cdot OI_a^2} = \frac{16R^6\sin^2\frac{A}{2}\sin^2\frac{B-C}{2}}{OI^2\cdot OI_a^2},$$

and

$$F_{\mathrm{e}}F_a = \left|\frac{4R^3 \sin\frac{A}{2}\sin\frac{B-C}{2}}{OI\cdot OI_a}\right| = \left|\frac{2R^3\left(\cos\left(\frac{A}{2}-\frac{B}{2}+\frac{C}{2}\right)-\cos\left(\frac{A}{2}+\frac{B}{2}-\frac{C}{2}\right)\right)}{OI\cdot OI_a}\right|$$
$$= \left|\frac{2R^3\left(\cos\left(\frac{\pi}{2}-B\right)-\cos\left(\frac{\pi}{2}-C\right)\right)}{OI\cdot OI_a}\right|$$
$$= \left|\frac{2R^3(\sin B-\sin C)}{OI\cdot OI_a}\right| = \frac{|b-c|R^2}{OI\cdot OI_a}.$$

□

References

[1] N. Altshiller-Court, *College Geometry*, Dover Reprint, 2007.

[2] S. N. Kiss, A distance property of the Feuerbach point and its extension, *Forum Geom.*, 16 (2016) 283–290.

[3] M. J. G. Scheer, A simple vector proof of Feuerbach's theorem, *Forum Geom.*, 11 (2011) 205–210.

S. Nagydobai Kiss: 'Constatin Brâncuşi' Technology Lyceum, Satu Mare, Romania
E-mail address: d.sandor.kiss@gmail.com

Forum Geometricorum
Volume 16 (2016) 381–395.

FORUM GEOM
ISSN 1534-1178

A Group Theoretic Interpretation of Poncelet's Theorem – The Real Case

Albrecht Hess, Daniel Perrin, and Mehdi Trense

Abstract. Poncelet's theorem about polygons that are inscribed in a conic and at the same time circumscribe another one has a greater companion, in which the second conic is substituted by possibly different conics for different sides of the polygon, while all conics belong to a fixed pencil. Here, a construction is presented that gives a visual group theoretic interpretation of both theorems and, eventually, leads to a generalization exposing the role of commutativity in Poncelet's theorem. There is no new thing about the ingredients but we hope that a dynamical view sheds new light on them. Finally, the occurrence of conics in a Poncelet grid [14] of lines constructed on a pencil of circles is explained with a simple proof.

1. Introduction

In [9, p. 285], Jacobi derives a formula relating the 'circuminscribed' polygons in Poncelet's theorem to the repeated addition of a parameter t in the argument of an elliptic function. Further ahead on p. 291 he shows that in the general case of tangents to circles of a pencil one has to add in the argument of the same elliptic function parameters t, t', t'', ... depending on the elements of this pencil. In [3] there is a summary of Jacobi's approach. Geometrizing this idea, we present here a group action on Poncelet configurations, that have been studied with other means elsewhere (see e.g. [1, 2, 3, 4, 7, 8, 11, 13, 14]). The construction applies to Poncelet configurations for pencils of circles without common points in the real plane. For other types of pencils this method yields the action of a local group.

2. The Group Action

Let $\mathcal{K} = \{k_t,\ 0 \le t \le \infty\}$ be the set of those elements of a pencil of non-intersecting circles in the real plane which are in the interior of the circle k_0. If k_0 and the limit circle k_∞ have the equations $k_0(X) = M_0X^2 - r_0^2 = 0$ and $k_\infty(X) = M_\infty X^2 = 0$, then the equation of the circle k_t is $k_t(X) = k_0(X) + tk_\infty(X) = 0$. Moreover, the radical axis r of $\mathcal{K}$ has the equation $r(X) = k_0(X) - k_\infty(X) = 0$.

Based on $\mathcal{K}$, we will define a group $\mathcal{G}$ and its action on k_0 as follows. As a set, the group $\mathcal{G}$ consists of the indices of the circles k_t, every index except 0 and ∞ counted twice, positively and negatively, thus $\mathcal{G} = \mathbb{R} \cup \{\infty\} \cong \mathbb{R}/\mathbb{Z}$.

Publication Date: November 15, 2016. Communicating Editor: Paul Yiu.

To construct the action of $t > 0$ on a point P of k_0, we draw the line from P tangent to k_t at S, leaving k_t on its left-hand side as seen from P. Its second intersection with k_0 is the image $Q = t + P$ of P under the action of t. In a similar manner, the other tangent from P to k_t gives the image $Q' = -t + P$ of P under the action of $-t$, leaving k_t on its right-hand side. The self-inverse action of ∞ maps P to $\infty + P$, which is the second intersection of the line through P and k_∞ with k_0. The neutral element 0 acts as identity (see Figure 1).

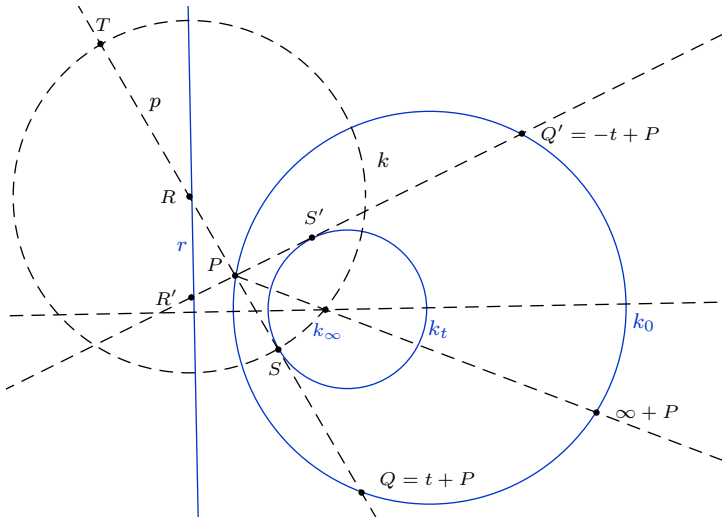

Figure 1

The line $p = (PQ)$ meets the axis r at a point R, except in the obvious case of parallel lines. Therefore, the circle k with center R through S is orthogonal to all circles k_t and

$$RP \cdot RQ = RS^2. \tag{1}$$

The second intersection T of k and p, together with P, Q and S, forms a harmonic range:

$$(P, Q, S, T) = -1, \tag{2}$$

which remains true, by sending T to infinity, even in the case of parallel lines p and r. The point T is the contact of p and a circle k_t from the complete pencil with the elements k_0 and k_∞. But this circle k_t, lying on the other side of r, has a negative parameter t.

Before showing that $(s + t)(P) = s + (t + P) = s + Q$ indeed defines a group law on $\mathcal{G}$ (i.e. independently of P, the lines through P and $s + (t + P)$ touches the same circle $k_{|s+t|}$ on the same side), we prove that the action of $\mathcal{G}$ is simply transitive and commutative.

Lemma 1 (Simple transitivity of the group action)**.** *For any chord $[PQ]$ of k_0 there exists a unique circle k_t of the pencil $\mathcal{K}$ that is tangent to $[PQ]$ at an interior point S, or the same in terms of the group action: For any elements P and Q of k_0 there exists a unique t from $\mathcal{G}$ with $Q = t + P$. We write $t = Q - P$.*

Proof. The line p through P and Q meets the radical axis r at R. The circle k around R through k_∞ intersects p at S and T. By (2), exactly one of both intersections is an interior point of $[PQ]$; this is the point S. Only one circle k_t from $\mathcal{K}$ goes through S. Hence, $[PQ]$ is tangent to k_t at S by (1) and $Q - P = t$ if k_t is on the left-hand side of $[PQ]$, as seen from P, and $Q - P = -t$ otherwise. If p does not intersect r, the circle k_t touches $[PQ]$ in its midpoint S. □

The definition of $t = Q - P$ allows us to give an orientation to the chords of k_0, at least to those that do not go through k_∞. The orientation of PQ is the sign of $t = Q - P$.

The commutativity of the group action

$$s + (t + P) = t + (s + P) \tag{3}$$

follows from the next lemmas; the first two are from [10, pp. 91–92](see Figure 2).

Lemma 2. *If a complete quadrangle is cyclic, a transversal line that forms an isosceles triangle with two opposite sides forms isosceles triangles with each pair of opposite sides.*

Proof. Let the line meet the sides (AD) and (BC) at the points G and H, so that it forms together with (AD) and (BC) an isosceles triangle. Then it will form with (AC) and (BD) another isosceles triangle. Look at the equal angles at G and H and C and D respectively.

A similar argument applies for the triangle formed by the transversal line (AB) and (CD). □

Lemma 3. *If a transversal line forms isosceles triangles with each pair of opposite sides of cyclic quadrangle, a circle can be drawn tangent to each pair where this line meets them; and these circles are coaxal with the circumcircle of the quadrangle.*

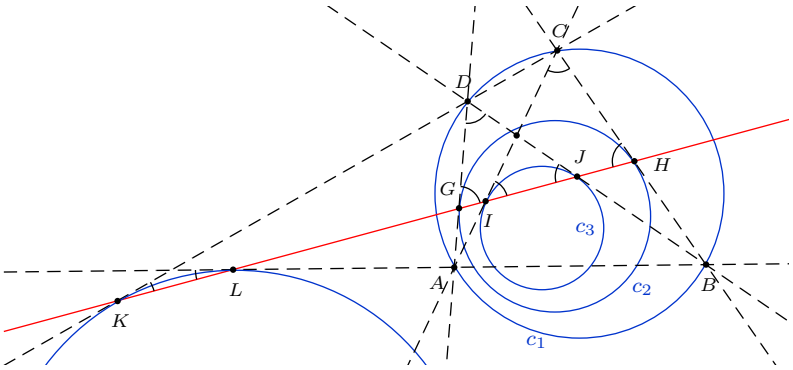

Figure 2

Proof. Let us look at the circle c_1 passing through A, B, C, D; the circle c_2, that is tangent to (AD) and (BC) at G and H, and the circle c_3, that is tangent to (AC)

and (BD) at I and J. With help of their equations $F_i(X) = M_iX^2 - r_i^2 = 0$, $i = 1, 2, 3$, one can determine as well the powers of A, B, C, D with respect to c_i by $AG^2 = F_2(A)$, $AI^2 = F_3(A)$, etc. The ratios $AG : AI = BH : BJ = CH : CI = DG : DJ$ are equal by the law of sines. Denoting their common value by u we get $-(1-u^2)F_1 + F_2 - u^2F_3 = 0$, since this linear equation has four intersections A, B, C, D with the circle c_1. Hence c_1, c_2, c_3 belong to the same pencil.

If we repeat this argument with c_3 replaced by the circle tangent to (AB) at L and to (CD) at K we obtain that all four circles of Figure 2 belong to the same pencil. □

Lemma 4 (Butterfly lemma)**.** *The circles k, k' and k'' are coaxal and the chords $[AB]$ and $[AC]$ of k touch k' at S' and k'' at S'', respectively. Let the line (SS'') meet k' again at T' and k'' at T''. Then (CT') is tangent to k' and (BT'') to k'' and these lines intersect at D on k.*

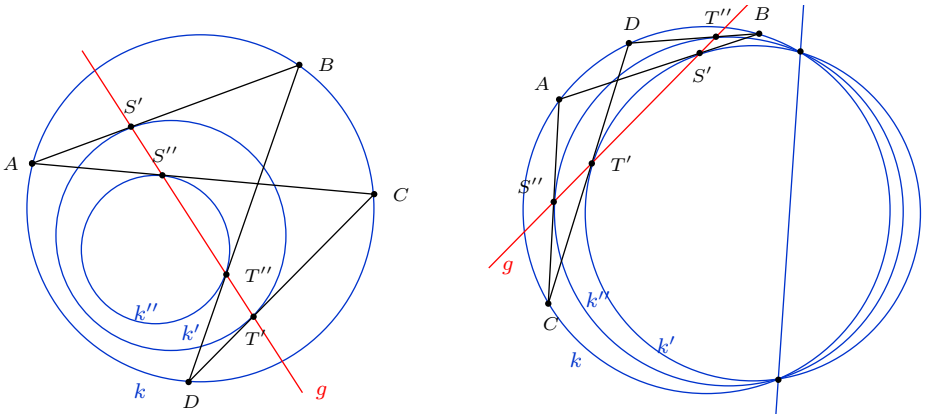

Figure 3

Proof. The circles k, k', k'' belong to a pencil $\mathcal{K}$ with radical axis r. If the intersections of r with (AB) and (AC) are U and V, respectively, then by (1),

$$UA \cdot UB = US'^2, \tag{4}$$

$$VA \cdot VC = VS''^2. \tag{5}$$

Let T' be on the line g through S' and S'', so that (CT'), (AB) and g delimit an isosceles triangle with equal angles at T' and S'. Let D be the second intersection of (CT') with k. Let g meet (BD) at T''. This gives a cyclic quadrangle $ABCD$ as in Lemma 2.

By Lemma 3, the circles c' and c'', a priori distinct from k' and k'', touching (AB) and (CD) at S' and T', (AC) and (BD) at S'' and T'', respectively, belong together with k to a pencil $\mathcal{C}$. But (4) and (5) reveal U and V on r as points on the radical axis of $\mathcal{C}$.

Having the same axis r and a common element k, $\mathcal{K}$ and $\mathcal{C}$ coincide, implying that $k' = c'$ and $k'' = c''$. Hence, g intersects at T' and T'' not only the lines (CD) and (BD) but also the circles k' and k''. Therefore, (CD) and (BD) touch k' and k'' at T' and T'', respectively. □

Proof of (3). (Commutativity of the action). Let P, $Q = s + P$, $R = t + P$ be on k_0 with $[PQ]$ tangent to $k_{|s|}$ at S and $[PR]$ to $k_{|t|}$ at T. The line g through S and T intersects $k_{|s|}$ again at S' and $k_{|t|}$ at T' (see Figure 4). By Lemma 4 the line through R and S' is tangent to $k_{|s|}$ and meets k_0 again at U. Being P, U and Q, R on distinct sides of g, the segment $[SS']$ as well as the circle $k_{|s|}$, are on the same side of $[PQ]$ and $[RU]$, as seen from P and R, respectively. Hence, these two chords have the same orientation. This proves that $U = s + R = s + (t + P)$. The same argument applies to the line through Q and T', passing through U by Lemma 4, and gives $U = t + Q = t + (s + P)$.

Corollary 5. *For P and Q on k_0 and t from $\mathcal{G}$ we have*

$$(t + Q) - (t + P) = Q - P. \tag{6}$$

This means that the group $\mathcal{G}$ acts transitively on chords from k_0; equally oriented and tangent to a fixed circle from $\mathcal{K}$.

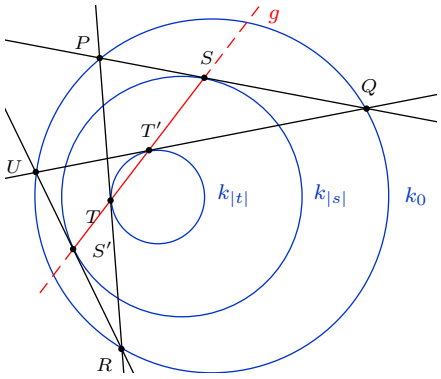

Figure 4

Proof. If $s = Q - P$, i.e. $Q = s + P$ by Lemma 1, then $t + Q = s + (t + P)$ by (3). □

The next Lemma, defining the group law, can be proved in the same manner.

Corollary 6 (Group law)**.** *For some P on k_0 and s, t from $\mathcal{G}$ we put*

$$s + t = (s + (t + P)) - P. \tag{7}$$

Since

$$(s + (t + P)) - P = (s + (t + Q)) - Q \tag{8}$$

for any Q from k_0, definition (7) *is correct, i.e. independent of P.*

Proof. If $Q = u+P$ by Lemma 1, then $s+(t+Q) = s+(t+(u+P)) = u+(s+(t+P))$ by (3). Hence, $(s+(t+Q))-Q = u+(s+(t+P))-(u+P) = (s+(t+P))-P$ by (6). □

Now the definition of the group $\mathcal{G}$ is completed by giving it a commutative group law. The identity is 0; t and $-t$ are mutually inverse; $t = \infty$ is self-inverse. Associativity of the group law and compatibility $(s + t) + P = s + (t + P)$ are obviously satisfied.

Poncelet's theorem in its general form results from an iterated application of (7) and (8).

Theorem 7 (Poncelet's Theorem)**.** *If for $t_1, \ldots, t_n$ from $\mathcal{G}$ the equation*

$$0 = (t_n + \cdots (t_2 + (t_1 + P))) - P \tag{9}$$

holds for some $P \in k_0$, then $t_n + \cdots + t_1 = 0$ and (9) *holds for every point from k_0.*

Here is the translation of this very condensed algebraic form of Poncelet's theorem into a more geometrical setting.

Theorem 8 (Geometrical form of Poncelet's Theorem)**.** *The vertices P_i of the polygonal chain $\{P_0, \ldots, P_n\}$ lie on the circle k_0, so that each chord $[P_{i-1}P_i]$ touches one of the circles k_t, situated in the interior of k_0, which belong together with k_0 to the same pencil. If that chain is closed, $P_0 = P_n$, for the starting point P_0, then a chain with another starting point Q_0 on k_0 will be closed too, provided that the Q-chords touch the same circles k_t in the same order and on the same sides as the P-chords.*

Remark. The Q-chain will be closed even if the order of the circles k_t is permuted thanks to the commutativity of the group law.

Proof. For $i = 1, 2, \ldots, n$, put $Q_i = (P_i - P_{i-1}) + Q_{i-1}$. Since $Q_i - Q_{i-1} = P_i - P_{i-1}$, the chords $[P_iP_{i-1}]$ and $[Q_iQ_{i-1}]$ touch the same circle on the same side. A repeated application of (8) gives $Q_i - Q_0 = P_i - P_0$, for $i = 1, \ldots, n$, and shows that the Q-chain is closed once the P-chain is. □

Poncelet's 'little' theorem is just the case of two circles k_0 and $k_{|t|}$ and equal parameters $t_1 = \cdots = t_n = t$.

In the case of a pencil $\mathcal{K}$ of circles passing all through one or two common points we get similar results for an action of a local group on an arc AB of the circle k_0, the two-point-case is shown above. The local action can be defined as in the case of disjoint circles, as far as the tangency points of the chords [PQ] with the circles of the pencil $\mathcal{K}$ stay in the interior of k_0 (see Figure 5).

3. Involutions

In [14] there is another method to prove Poncelet's theorem by using involutions. This is basically the same idea as in euclidean geometry the decomposition of rotations into reflections. After showing how these transformations fit into the

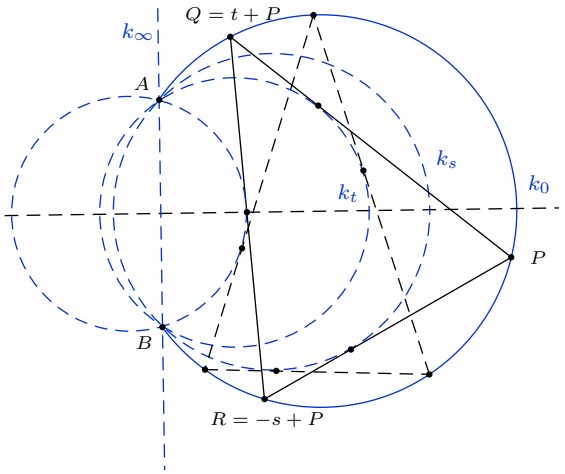

Figure 5

terminology introduced in the previous section, we will extend the group $\mathcal{G}$ to include both: translations $\tau_t(P) = t + P$ by elements t of $\mathcal{G}$ and involutions.

The formal definition of an involution with center P is $\sigma_P(Q) = (P - Q) + P$. To see the geometrical meaning of this formula, have a look at Figure 6.

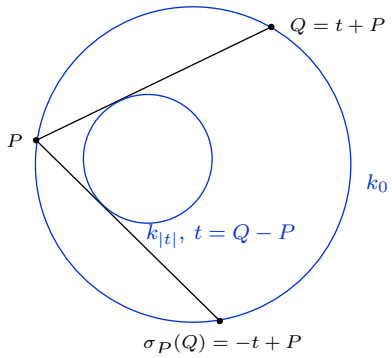

Figure 6

The transitive action of $\mathcal{G}$ guarantees the existence of a $t = Q - P \in \mathcal{G}$, such that $Q = t + P$. This was established in Lemma 1. There it was shown that the circle $k_{|t|}$ is the unique element of $\mathcal{K}$, that touches the segment $[PQ]$ in an interior point. The sign of t represents the orientation of $[PQ]$. Applying $-t = P - Q$ to P in the formula of $\sigma_P(Q)$ means, that $[P_{\sigma_P}(Q)]$ is just the other tangent from P to $k_{|t|}$.

The properties of these involutions will be derived in the following from the group laws of G. Things will become very transparent and reminiscent of the group of transformations of the unit circle generated by reflections, if we fix a point $O \in$

k_0 and write, thanks to the transitivity, all points of k_0 as translations of O by elements of $\mathcal{G}$. We have, e.g., that

$$\sigma_P(Q) = (2p - q) + O \quad \text{for } P = p + O; \quad Q = q + O,\ p, q \in \mathcal{G}. \tag{10}$$

Lemma 9. *For $P, Q \in k_0$ and $s \in \mathcal{G}$ we have $\sigma_P(s + Q) = -s + \sigma_P(Q)$, or $\sigma_P \circ \tau_s = \tau_{-s} \circ \sigma_P$.*

Proof. Substituting q in (10) by $s + q$ and using the commutativity of the group law, we get $\sigma_P(s + Q) = (2p - s - q) + O = -s + \sigma_P(Q)$. □

Lemma 10. *For $P, Q \in k_0$ we have $\sigma_P(\sigma_Q(R)) = 2(P - Q) + R$, or $\sigma_P \circ \sigma_Q = \tau_{2(P-Q)}$.*

Proof. In the same manner, putting $P = p + O$, $Q = q + O$, $R = r + O$ with $p, q, r \in \mathcal{G}$, we get from (10) that both sides of $\sigma_P(\sigma_Q(R)) = 2(P - Q) + R$ are equal to $(2p - 2q + r) + O$. □

Corollary 11. *The transformations σ_P are involutions, $\sigma_P \circ \sigma_P = \tau_0 = \mathrm{id}$.*

Corollary 12. *The transformations σ_P and σ_Q are equal if and only if $Q = P$ or $Q = \infty + P$.*

Proof. If $\sigma_P = \sigma_Q$ then by multiplication with σ_P we get $\sigma_P \circ \sigma_Q = \tau_{2(P-Q)} = \mathrm{id} = \tau_0$. Putting $t = Q - P$, the last equation can be written as $t = -t$. If $t \neq 0$ this means that both tangents drawn from any point of k_0 to the circle $k_{|t|}$ coincide. But this is only possible for the degenerated circle k_∞ and gives $t = \infty$. □

Just as any rotation of the unit circle can be decomposed into a product of two reflections, every translation τ_t can be written as a product of two involutions. How this is achieved is explained in the next proposition.

Proposition 13. *Let t be an element of $\mathcal{G}$.*

(1) *There exists an element $s \in \mathcal{G}$ with $t = 2s$.*

(2) *For every involution σ_Q there exists a unique involution σ_P with $\tau_t = \sigma_P \circ \sigma_Q$.*

Remarks. (a) The uniqueness does not hold in the first statement since $2(s + \infty) = 2s$. It is only claimed in the second statement.

(b) The second statement does not claim the uniqueness of P, which does not hold because of $\sigma_P = \sigma_{\infty+P}$. We get the uniqueness of σ_P from $\sigma_{P'} \circ \sigma_Q = \sigma_P \circ \sigma_Q$ multiplying it with σ_Q.

Proof. (1) On the circle k_0 there exist points R, $S = t + R$, such that the chord $[RS]$ is tangent to the circle $k_{|t|}$ and perpendicular to the line c that contains the centers of the circles from the pencil. If necessary, rename the points of the chord $[RS]$ in order to match with the sign of t. See Figure 7, where the case of $t > 0$ is shown, i.e. $k_{|t|}$ on the left hand side of $[RS]$ as seen from R. Let R' be one of the intersections of c with k_0. For $s = R' - R \in \mathcal{G}$ we have by symmetry $S = 2s + R$, i.e. $t = 2s$.

(2) With $s \in \mathcal{G}$, $t = 2s$, determined by part (1), for a given $Q \in k_0$ we put $P = s + Q$ and get $\sigma_P \circ \sigma_Q = \tau_t$ by Lemma 10. □

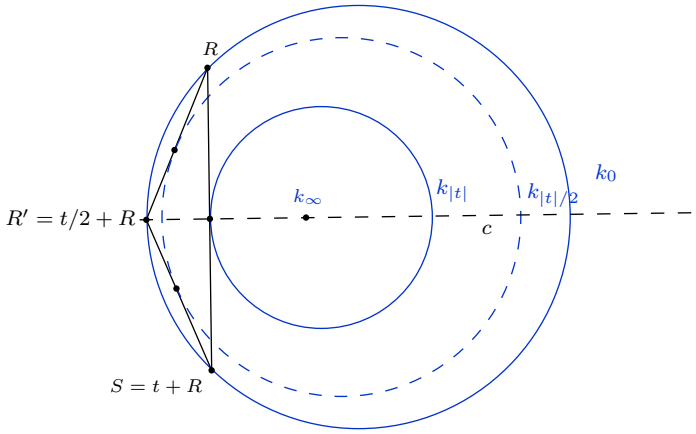

Figure 7

It is very instructive to see how a noncommutative extension $\mathcal{G}'$ of the group $\mathcal{G}$ and the same construction of its action on k_0 as explained in Section 2 - namely by drawing tangents to circles from a larger part $\mathcal{K}' \supset \mathcal{K}$ of the pencil and by taking their second intersection with k_0 as the image of the action - includes the involutions introduced above.

To $\mathcal{K}'$ belong besides the circles k_t from $\mathcal{K}$ with $k_t(X) = k_0(X) + tk_\infty(X) = 0$, $0 \leq t \leq \infty$, the circles beyond the radical axis with indices $\Omega \leq t \leq -1$, where k_Ω is the other limit circle and $r = k_{-1}$ is the radical axis.

As a set, the group $\mathcal{G}'$ consists of the indices $\Omega \leq t \leq -1$ and $0 \leq t \leq \infty$ of the circles from $\mathcal{K}'$, every index except Ω, -1, 0 and ∞ counted twice, positively and negatively. At this point, the problem arises that a negative sign can have two meanings: firstly, as a sign of a circle index of the new elements, and, secondly, as a sign describing the position of the circle relative to the tangent. But this possible confusion will disappear after the identification of the new elements from $\mathcal{G}' \setminus \mathcal{G}$ with involutions σ_P and their indexing with the center P.

To construct the action of t, $\Omega < t < -1$, on a point P in the positive direction, we draw a line through P tangent to k_t at S, leaving k_t on its left-hand side as seen from P. Its second intersection with k_0 is the image $Q = t + P$ of P under the action of t. In a similar manner, the other tangent from P to k_t produces the image $Q' = -t + P$ of P under the action of t in the negative direction, leaving k_t on its right hand side (see Figure 8).

For both indices $t = \Omega$, -1, there exists only one line tangent to k_t, in the first case it is the line Pk_Ω, and in the second case a parallel to the radical axis k_{-1} through P. Their second intersections with k_0 are the images of P under the corresponding mappings.

Proposition 14. *Let t be an element of $\mathcal{G}' \setminus \mathcal{G}$. Then there exist a point $R \in k_0$ for which the mapping $P \mapsto t + P$ is the involution σ_R.*

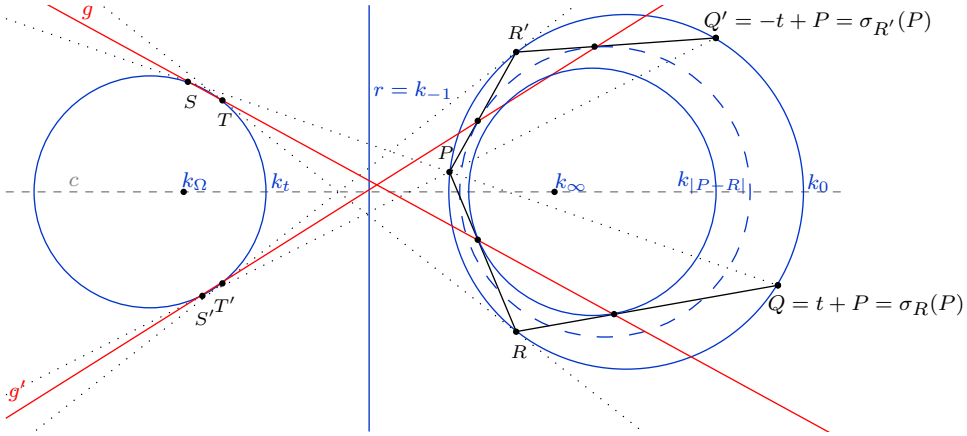

Figure 8

Proof. We adopt the notations used before, see Figure 8. For t different from Ω and -1, let (RT) (in the positive direction) and $(R'T')$ (in the negative direction) be the common inner tangents to k_0 and k_t. An application of corresponding modifications of Lemmas 2 and 3 to the case of the degenerated cyclic quadrilateral $PQRR$, in which two points coincide (or angle chasing using the theorem of inscribed and tangent angles) proves that the line g through S and T and the chords $[RP]$ and $[RQ]$ delimit an isosceles triangle. The intersections of g with $[RP]$ and $[RQ]$ are the points where the circle $k_{|P-R|}$ from the pencil touches these chords. This shows that $Q = t + P = \sigma_R(P)$ and that in this case the group action for a $t < 0$ is given by the involution σ_R. In a similar manner we obtain $-t + P = \sigma_{R'}(P)$ for the tangent from P' to the circle k_t, which leaves the circle on its right hand side.

As for the involutive actions of Ω and -1, we find that $P \mapsto \Omega + P$ is the involution σ_O, whose center O is one of the points of tangency from k_Ω to k_0. The mapping $P \mapsto (-1) + P$, i.e. the reflection in the line c, is the involution σ_E, whose center E is one of the intersections of c and k_0 (see Figure 9). □

Let us say some words about the difference between the involutions of the circle, that first come to mind when speaking about mappings with this name, and those introduced in this section. The former are self-inverse elements f in the group of homographies of a circle k (or more generally a conic), that can be defined with help of a so called Frégier point $F \notin k$ according to $(FP) \cap k = \{P, f(P)\}$ (see [2, Chap. 16.3]). From this definition follows, that they are birational automorphisms of the circle. The involutions considered here are not rational mappings, because already the determination of the points S and S', where tangents from P touch the circle k_t, requires the solution of a quadratic equation. Once S (or S') have been found, the second intersection $Q = t + P$ of the line (SP) with the circle k_0 depends rationally on S and P. The only elements of $\mathcal{G}'$ that act as Frégier involutions are τ_∞, σ_O, σ_E, the Frégier point of the latter is the infinite point on the radical axis.

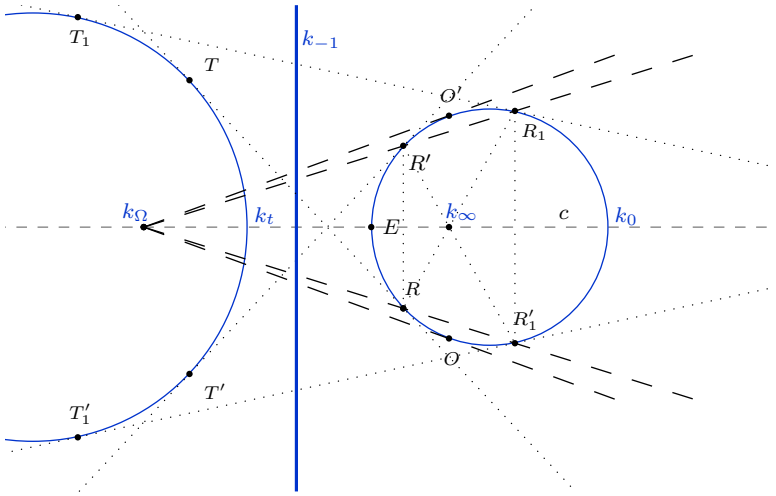

Figure 9

Before concluding this section about involutions with the theorems about the generalized Poncelet configurations, we show that these Frégier involutions together with the identity τ_0 form a group and determine its orbits.

Proposition 15. *Let* $\mathcal{V} = \{\tau_0,\ \tau_\infty, \sigma_O, \sigma_E\}$.

(1) *Then* $\mathcal{V}$ *is a subgroup of* $\mathcal{G}'$ *that is isomorphic to the Klein four-group.*

(2) *Let* RT, $R'T'$ *be the inner and* R_1T_1, $R_1'T_1'$ *the outer common tangents to a circle* k_t, $t < 0$, *and* k_0 (see Figure 9). *Then* $\{R, R', R_1, R_1'\}$ *is an orbit of* $\mathcal{V}$.

Proof. (1) Recall that O and O' are the tangency points from k_Ω to k_0. Since k_Ω and k_∞ are mutually inverse points with respect to k_0, the polar OO') of k_Ω with respect to k_0 goes through k_∞. Hence, $\tau_\infty(O) = O' = \sigma_E(O)$. This shows that the involution $\sigma_E \circ \tau_\infty$ has the fixed point O and therefore coincides with σ_O. We leave it to the reader to complete the multiplication table of $\mathcal{V}$ using e.g. that all elements of $\mathcal{V}$ are self-inverse.

(2) The symmetry with respect to the line c implies $\sigma_E(R) = R'$.
Let $R_0 = \tau_\infty(R)$. From Lemma 9 we get $\sigma_R(R_0) = \sigma_R(\tau_\infty(R)) = \tau_\infty(R) = R_0$. This means that the tangent line from R_0 to k_t has a double intersection with k_0 in R_0 and is a common tangent of both circles. Therefore, $R_0 = \tau_\infty(R) = R_1$. From (1) it follows that $\sigma_O(R) = \sigma_E(\tau_\infty)R)) = \sigma_E(R_1) = R_1'$. □

Summarizing the results obtained so far we can state the following theorems.

Theorem 16 (Generalized group action on Poncelet configurations)**.** *The group* $\mathcal{G}'$ *acts by translations* $\tau_{\pm t}$ *for* $0 \le t \le \infty$ *and involutions* σ_R *for* $R \in k_0$ *on a circle* k_0 *from a given pencil of non-intersecting circles in the real plane. The involutions generate the group* $\mathcal{G}'$, *that is the semidirect product of* $\mathbb{R}/\mathbb{Z}$ *and* $\mathbb{Z}/2\mathbb{Z}$ *with the*

multiplication table

$$\tau_s \circ \tau_t = \tau_{s+t}, \tag{11}$$

$$\tau_t \circ \sigma_R = \sigma_R \circ \tau_t = \sigma_{t/2+R}, \tag{12}$$

$$\sigma_R \circ \sigma_S = \tau_{2(R-S)}. \tag{13}$$

The image of a point $P \in k_0$ under the action of $\gamma \in \mathcal{G}'$ is the second intersection with k_0 of the tangent from P to another circle from the pencil. In the case of a translation $\gamma = \tau_{\pm t}$, this is a circle inside the circle k_0 and the contact point is an interior point of the chord $[P\gamma(P)]$. In the case of an involution $\gamma = \sigma_R$, this is a circle outside k_0, both having a common inner tangent touching k_0 in R, and the contact point on the line $(P\gamma(P))$ is an exterior point of the chord $[P\gamma(P)]$.

Theorem 17 (Generalized Poncelet Theorem)**.** *Let k_0 belong to a pencil $\mathcal{K}$ of circles without common points in the real plane and let the vertices P_i of a closed polygonal chain $\{P_0, \ldots, P_n\}$, $P_0 = P_n$, lie on k_0, so that each line $(P_{i-1}P_i)$ touches one of the circles of $\mathcal{K}$. The assumption that an even number (or none) of the contact points on $(P_{i-1}P_i)$ are outside the chord $[P_{i-1}P_i]$ is a necessary and sufficient condition for the possibility to construct, starting from any point Q_0 of k_0, a closed polygonal chain $\{Q_0, \ldots, Q_n\}$ with vertices on k_0 in such a way that the Q-chords (or their prolongations) touch the same circles in the same order and on the same side as the P-chords.*

Proof. If the circle $k_j \in \mathcal{K}$ touches in the interior of the chord $[P_{j-1}P_j]$, then $P_j = \tau_j(P_{j-1})$ for some translation $\tau_j \in \mathcal{G}$. If k_j touches the line $(P_{j-1}P_j)$ outside $[P_{j-1}P_j]$, then $P_j = \sigma_j(P_{j-1})$ for some involution $\sigma_j \in \mathcal{G}' \setminus \mathcal{G}$. Put, thanks to the transitivity, $t = Q_0 - P_0$, so that $\tau_t(P_0) = Q_0$. Then $\tau_t \circ \tau_j = \tau_j \circ \tau_t$ and $\tau_t \circ \sigma_j = \sigma_j \circ \tau_{-t}$ by Lemmas 9 and 10.

If in the product π of τ's and σ's that transform P_0 successively into $P_1, \ldots, P_n$ there is an even number of involutions σ_j, then τ_t commutes with π. The Q-chain defined by $Q_j = \tau_j(Q_{j-1})$, or $Q_j = \sigma_j(Q_{j-1})$ respectively, in the same order as the P-chain, touch the same circles in the same order and on the same side as the P-chain and terminates in $\pi(Q_0) = \pi \circ \tau_t(P_0) = \tau_t \circ \pi(P_0) = Q_0$.

If an odd number of involutions enters in π, reducing with (11), (12), (13) gives $\pi = \sigma_R$ for some $R \in k_0$. Because such a π has exactly two fixed points, R and $\infty + R$, one of them has to be P_0. For a chain of chords, beginning at Q_0 and touching the circles in the same way as the P-chords, there is, apart from $Q_0 = P_0$, the only possibility of a happy closed ending if $Q_0 = \infty + P_0$. Hence, there is only one more closed polygonal chain touching the circles in the same way as the P-chords in this case. □

4. The Poncelet grid

A nice construction based on the configuration of Poncelet's 'little' theorem was presented by R. E. Schwartz. He considered a 'regular' Poncelet n-gon inscribed in a circle, drew tangents to this circle at all vertices and obtained a grid of lines whose intersections are located on a family of ellipses and hyperbolas. The author called it Poncelet grid. A picture with a checkerboard effect is on [14, p.3].

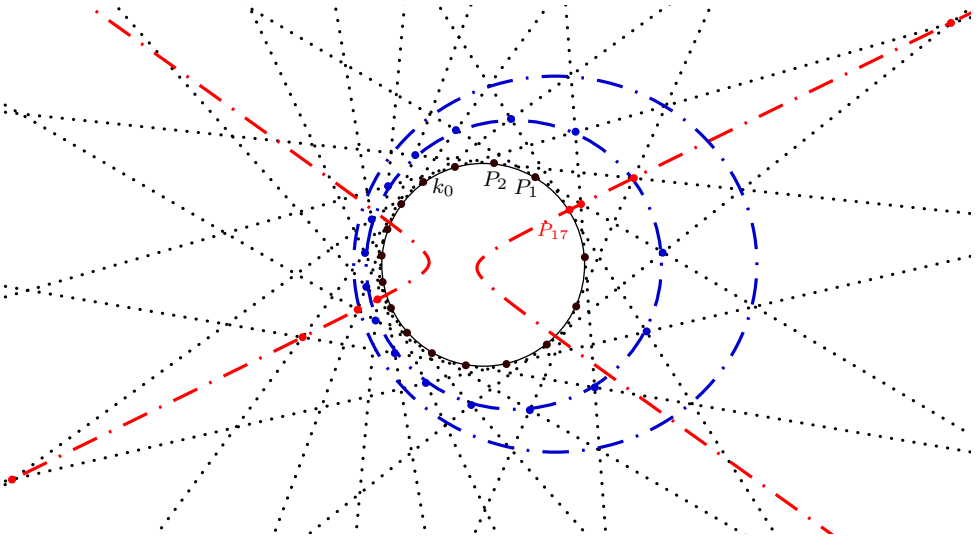

Figure 10

To explain the occurrence of ellipses and hyperbolas within the setting of a circle k_0, a pencil $\mathcal{K}'$ of non intersecting circles in the real plane, of which k_0 is a member, and the group $\mathcal{G}'$ introduced in Section 3, let τ_t for $t \in \mathcal{G}$. $t > 0$, be a translation of order $n \geq 3$. Starting with any point $P_0 \in k_0$ define $P_i = \tau_t(P_{i-1})$, $i = 1, \ldots, n$. Since τ_t is of order n the polygonal chain $\{P_0, \ldots, P_n\}$ is closed, $P_n = P_0$, and forms a 'regular' Poncelet n-gon, see Theorem 7. This allows us to make all further calculations of indices modulo n.

Proposition 18. *Let l_i be the tangents to k_0 at P_i, $i = 0, \ldots, n-1$, and P_{ij} the intersections of l_i and l_j, $P_{ii} = P_i$. Then there exist two families of conics C_d, $d = 0, \ldots, \left[\frac{n}{2}\right]$ and D_s, $s = 0, \ldots, n-1$, such that all P_{ij} are intersections of $C_{|i-j|}$ and D_{i+j}.*

Proof. For any pair of vertices P_i, P_j of the Poncelet n-gon $\{P_0, \ldots, P_n\}$ there exist two transformations from the group $\mathcal{G}'$ mapping P_i to P_j. They correspond to the two circles of the the pencil $\mathcal{K}'$ that are tangent to the line $g = (P_iP_j)$. The first circle k_u, $u = (j-i)t$, depends on the absolute value of the difference $j - i$ and produces a translation τ_u, the second circle k_v depends on the sum $i + j$ and produces an involution σ_R, $R = P_{(i+j)/2}$, both transforming P_i into P_j. The point P_{ij} is the pole of the line g with respect to the circle k_0. Since g touches the circles k_u and k_v, P_{ij} is located on the two conics that are the duals of the circles k_u and k_v with respect to k_0; see Figure 11. □

5. Final remarks

Most of the statements of this article, in particular, Theorems 8, 16, 17, are invariant under real projective transformations as long as only tangents, intersections, cross ratios and conics as projective images of circles are involved. They

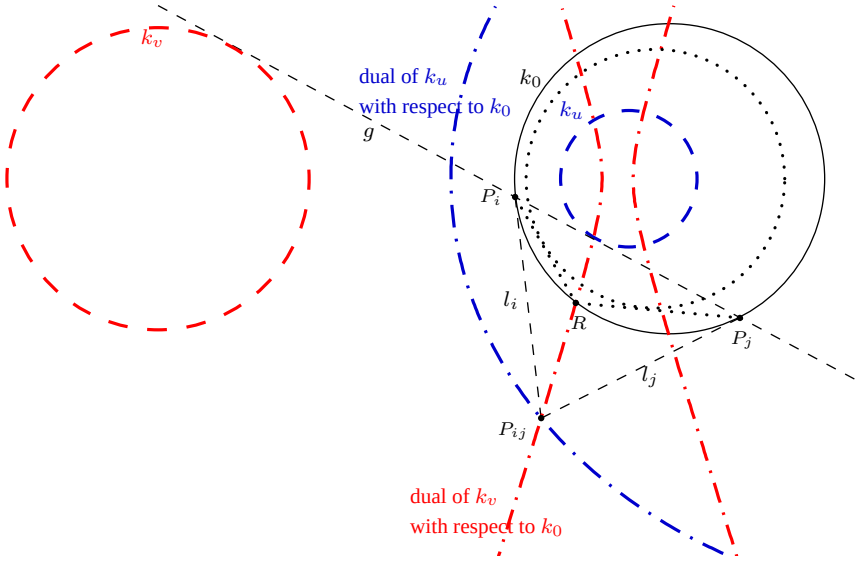

Figure 11

could have been formulated and proved in their general form for pencils of conics without common points, but little would have been gained. It was intended to keep the proofs as elementary as possible. In the general case, that includes also pencils of conics with common points in the real plane, Desargues involution theorem, stating that the pairs of intersections of a line with the conics of a pencil generate an involution on that line (see [2, 5, 6]), can be used to prove a "conical butterfly lemma" as a substitute for Lemma 4. The main results with reference to the transformation group of a real Poncelet configuration of non intersecting conics remains unchanged.

References

[1] W. Barth and T. Bauer, Poncelet theorems, *Expos. Math.*, 14 (1996) 125–144.
[2] M. Berger, *Geometry II*, Springer, 2009. ch. 16.6: The great Poncelet Theorem.
[3] H. J. M. Bos, C. Kers, et al., Poncelet's closure theorem, *Expos. Math.*, 5 (1987) 289–364.
[4] A. Cayley, On the porism of the in-and-circumscribed polygon, *Phil. Trans. R. Soc. Lond.*, 151 (1861) 225–239; available at `rstl.royalsocietypublishing.org/content/151/225`.
[5] H. S. M. Coxeter, *The Real Projective Plane*, Springer, third edition, 1993.
[6] H. Dörrie, *One Hundred Great Problems of Elementary Mathematics*, Dover reprint, 1965. 265–272: Desargues' Involution Theorem.
[7] P. Griffiths and J. Harris, A Poncelet theorem in space, *Comment. Math. Helv.*, 52 (1977) 145–160.
[8] P. Griffiths and J. Harris, On Cayley's explicit solution to Poncelet's porism, *Enseign. Math.*, 24 (1978) 31–40.
[9] C. G. J. Jacobi, Über die Anwendung der elliptischen Transcendenten auf ein bekanntes Problem der Elementargeometrie, in *Gesammelte Werke*, Band 1, 277–293; available at `gallica.bnf.fr/ark:/12148/bpt6k90209g/f292.item`.
[10] R. A. Johnson, *Advanced Euclidean Geometry*, Dover reprint, 2007.

[11] H. Lebesgue, *Les Coniques*, Gauthier-Villars, 1942. ch. 4: Polygones de Poncelet, available at gallica.bnf.fr/ark:/12148/bpt6k65374350/f131.image.
[12] J. V. Poncelet, *Traité des propriétés projectives des figures*, volumes 1, 2, Gauthier-Villars, second edition, 1865–66; available at gallica.bnf.fr/ark:/12148/bpt6k9608143v, gallica.bnf.fr/ark:/12148/bpt6k5484980j.
[13] R. E. Schwartz. The Poncelet grid, *Advances in Geometry*, 7 (2007) 157–175, available at www.math.brown.edu/~res/Papers/grid.pdf.
[14] M. Trense, Le grand théorème de Poncelet, to appear in *Quadrature*, 2016.

Albrecht Hess: Deutsche Schule Madrid, Calle Monastesio Guadelupe 7, 28049 Madrid, Spain
E-mail address: albrecht.hess@gmail.com

Daniel Perrin: 6 rue Einstein, 92160 Antony, France
E-mail address: daniel.perrin@math.u-psud.fr

Mehdi Trense: Lycée Louis-le-Grand, 123 rue Saint-Jacques, 75005 Paris, France
E-mail address: trense@clipper.ens.fr

Forum Geometricorum
Volume 16 (2016) 397–398.

FORUM GEOM
ISSN 1534-1178

Minimal Proof of a Generalized Droz-Farny Theorem

Grégoire Nicollier

Abstract. We give a simple proof of a recent generalization of the Droz-Farny line theorem by using complex numbers.

Theorem. ([2]) (1) *Let H be the orthocenter of a triangle ABC and ℓ, ℓ' two perpendicular lines through H that cut the sidelines BC, CA, and AB at D, E, F and D', E' F', respectively* (*see Figure 1*)*. If one erects directly similar triangular ears on the segments DD', EE', and FF', the ear apices are collinear.*

(2) *The ratio in which one ear apex cuts the segment of the other two is independent of the ear shape.* (*In particular, the ratios for D, E, F and D', E', F' are equal.*)

We present here a very simple proof. Droz-Farny took the midpoints of the segments as ear apices (see [1, 2] for further references).

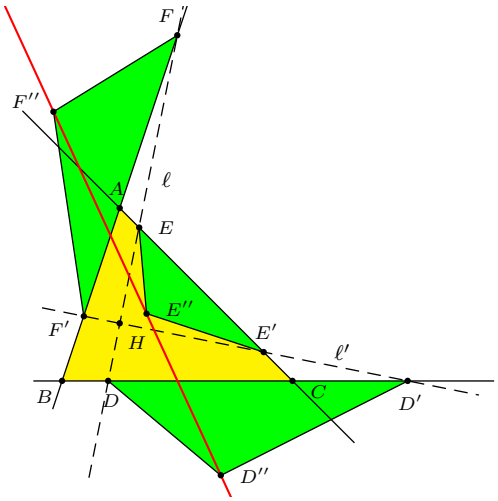

Figure 1

Proof. Without loss of generality, we choose in the complex plane

$$A = ia, \quad B = -b, \text{ and } C = c \text{ with } a, b, c > 0.$$

Publication Date: November 15, 2016. Communicating Editor: Paul Yiu.

The altitude through B being the line $y = \frac{c(x+b)}{a}$, the orthocenter is $H = ih$ for $h = \frac{bc}{a}$. The perpendiculars through H are

$$\ell:\ y = mx + h \quad \text{and} \quad \ell':\ y = -\frac{x}{m} + h,\ m \neq 0,\ m \notin \left\{0, -\frac{a}{c}, \frac{c}{a}, \frac{a}{b}, -\frac{b}{a}\right\}$$

as they have to intersect the sidelines of the triangle, which are

$$BC:\ y = 0, \qquad CA:\ y = -\frac{a}{c}(x-c), \qquad AB:\ y = \frac{a}{b}(x+b).$$

One finds at once

$$\begin{aligned}
D &= -\frac{h}{m}, & D' &= hm;\\
E &= \frac{c(a^2-bc)}{a(cm+a)} + i\frac{c(am+b)}{cm+a}, & E' &= \frac{cm(a^2-bc)}{a(am-c)} + i\frac{c(bm-a)}{am-c};\\
F &= \frac{b(a^2-bc)}{a(bm-a)} + i\frac{b(am-c)}{bm-a}, & F' &= \frac{-bm(a^2-bc)}{a(am+b)} + i\frac{b(cm+a)}{am+b}.
\end{aligned}$$

In order to erect triangular ears directly similar to the triangle with vertices 1, 0, and w on the segments DD', EE', and FF', one has to take the ear apices

$$D'' = wD + (1-w)D', \qquad E'' = wE + (1-w)E', \qquad F'' = wF + (1-w)F'.$$

The apices D'', E'', F'' are collinear as a straightforward computation gives the real quotient

$$\frac{F''-D''}{E''-D''} = \frac{\left(m+\frac{a}{c}\right)\left(m-\frac{c}{a}\right)}{\left(m-\frac{a}{b}\right)\left(m+\frac{b}{a}\right)}.$$

E'' divides segment $D''F''$ in a ratio depending on the slopes of ℓ and the sidelines of triangle ABC, but not on the ear shape! □

References

[1] J.-L. Ayme, A synthetic proof of the Droz-Farny line theorem, *Forum Geom.*, 4 (2004) 219–224.
[2] C. Letrouit, On a new generalization of the Droz-Farny line, *Forum Geom.*, 16 (2016) 367–369.

Grégoire Nicollier: University of Applied Sciences of Western Switzerland, Route du Rawyl 47, CH–1950 Sion, Switzerland

E-mail address: gregoire.nicollier@hevs.ch

Forum Geometricorum
Volume 16 (2016) 399–405.

FORUM GEOM
ISSN 1534-1178

On the Existence of a Triangle with Prescribed Bisector Lengths

Sergey F. Osinkin

Abstract. We suggest a geometric visualization of the process of constructing a triangle with prescribed bisectors that makes the existence of such a triangle geometrically evident.

1. Introduction

Since antiquity, in construction problems of elementary geometry main attention has been paid to possibility or impossibility of such constructions with only ruler and compass, and problems of constructing regular n-gons, trisection of angle or squaring of a circle has played an important role in the development of mathematics. Existence and number of solutions of these construction problems when one is not confined to using ruler and compass only is often evident and as a rule is not discussed in much detail. However, situation changes when one turns to other problems such as, for example, problems of constructing triangles with prescribed its three elements. In particular, a triangle with given lengths of its sides can be constructed if the 'triangle inequalities' are fulfilled and then the triangle is unique up to an isometry. In a similar way, the problems of constructing a triangle with given lengths of its medians or altitudes can be considered and these constructions with ruler and compass are possible under conditions that certain inequalities are fulfilled. Interestingly enough, the problem of constructing a triangle with prescribed lengths of its bisectors is very different: it was shown that such a construction with only ruler and compass is impossible (see, e.g., [1]). Then the question arises: Given three lengths l_a, l_b, l_c, does there exist a triangle with its angle bisectors equal to these lengths? Positive answer to this question was given by Mironescu and Panaitopol in [2] by analytical method with the use of the Brower fixed point theorem. More elementary analytical proof was suggested by Zhukov and Akulich in [3]. Being absolutely strict, these proofs lack, in our opinion, geometric clearness. In this note we suggest such a geometric visualization of the process of constructing a triangle with prescribed bisectors that makes the possibility of such a construction practically evident. Thus, our aim in this note is to present an elementary visual proof of the Mironescu and Panaitopol theorem that reads:

Publication Date: November 17, 2016. Communicating Editor: Paul Yiu.

Theorem 1. *For any given segments with lengths l_a, l_b, l_c there exists a triangle whose bisectors are equal to these prescribed lengths.*

Informal discussion. Before going to the strict proof of this theorem, we give an informal description of the idea of our proof in which the process of constructing a triangle with prescribed bisector lengths is reduced to two transformations. Let, for definiteness, the prescribed lengths of bisectors satisfy inequalities $l_c < l_a < l_b$. We start from an equilateral triangle with three equal bisector lengths equal to l_b. The first transformation is the decreasing of the angle B in such a way that the triangle becomes isosceles with decreasing equal sides $a = c$ and constant bisector l_b. It is evident that bisectors l_a and l_c decrease also remaining all the time equal to each other. As a result of this first transformation we can reach such an isosceles triangle that its two changing bisectors become equal to the prescribed value l_a. Further decrease of the angle B would lead to decrease of l_a, therefore we combine change of B with rotation of the side b around the intersection point of l_b and b in such a way that l_a remains fixed (as well as l_b) and l_c decreases reaching finally the prescribed value. Possibility of such transformation follows from geometrically evident observation that if angles A and B decrease under condition that l_a and l_b remain constant, then the third angle C increases whereas its bisector l_c decreases. In the limit $\angle A \to 0$, $\angle B \to 0$ we have $l_c \to 0$ and hence l_c can reach any prescribed value $l_c < l_a$, l_b. This visualization of the construction makes intuitively plausible that a triangle with prescribed bisector lengths $l_c < l_a < l_b$ does exist.

2. Preliminary lemmas

Now we turn to formal realization of the above idea. As a preliminary step, we shall prove several Lemmas about angles and sides of a triangle, and its bisectors.

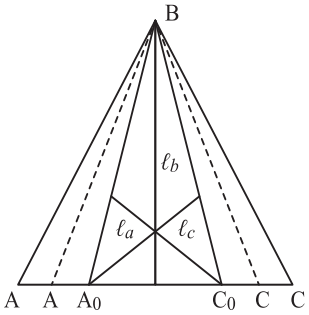

Figure 1. Transformation of equilateral triangle ABC with bisectors $l_a = l_b = l_c = l_1$ to isosceles triangle A_0BC_0 with bisectors $l_a = l_c = l_2$ and $l_b = l_1$ by decreasing the angle $\angle B$.

The above informal description of the idea of the proof actually introduces the elements of the triangle ABC as functions of the angle $\angle B$ under conditions that lengths of one or two bisectors are kept constant. Therefore it is convenient to distinguish the changing variables l_a, l_b, l_c equal to the bisectors lengths of our

varying triangle from their prescribed fixed values. To this end, from now on we denote the fixed prescribed values as $l_3 < l_2 < l_1$.

We shall start with formulation of an obvious Lemma 2 that describes the variation of elements of an isosceles triangle in the first type of our transformations.

Lemma 2. *In an isosceles triangle ABC with equal sides $AB = CB$ and fixed length of the bisector $l_b = l_1$ (see Figure 1) the angles $\angle A = \angle C = (180^\circ - \angle B)/2$ are decreasing functions of $\angle B$ and the sides $AB = CB$ as well as bisectors $l_a = l_c$ are increasing functions of $\angle B$. When $\angle B$ changes from 60° to zero, the bisectors l_a, l_c change from $l_b = l_1$ to zero.*

In the second type of our transformations the length of two bisectors l_b and l_a are kept constant and we are interested in dependence of the angles $\angle A$, $\angle C$ and the length of the bisector l_c on the angle $\angle B$.

Lemma 3. *Let in a triangle ABC the bisector l_a (of the angle $\angle A$) be equal to $l_a = l_2$, the bisector l_b (of angle $\angle B$) be equal to $l_b = l_1$, and the angles $\angle A$, $\angle B$, $\angle C$ satisfy the condition $\angle B < \angle A < \angle C$ (see Figure 2). Then the following inequalities hold*

$$\frac{1}{2}l_2 < b < a < c < l_1 + l_2. \tag{1}$$

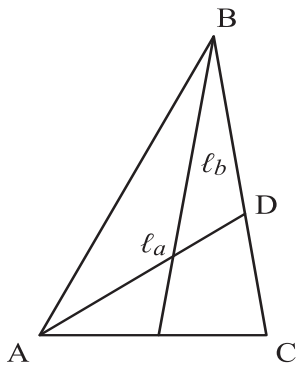

Figure 2. Sketch of triangle $\angle B < \angle A < \angle C$ and $l_a = l_2 < l_b = l_1$.

Proof. Since $\angle ADC = \angle BAD + \angle ABD$, we have $\angle ADC > \angle BAD = \angle CAD$ and, consequently, $CD < AC$. Therefore, we have $AD < AC + CD < 2AC$, hence $AC = b > \frac{1}{2}AD = \frac{1}{2}l_2$. At last, $AB = c$ is less than the sum of the two other sides of a triangle formed by AB and pieces of the bisectors $l_b = l_1$ and $l_a = l_2$. □

Now we consider a continuous set of triangles ABC parameterized by their smallest angle $\angle B$, so that $\angle B < \angle A < \angle C$, and we assume that in all these triangles the bisectors l_a and l_b have the same values. Thus, the angles $\angle A$ and $\angle C$ become some functions of the angle $\angle B$: if we change the angle $\angle B$, then

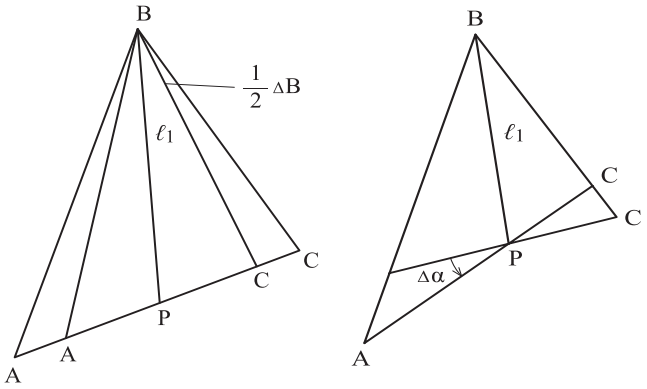

Figure 3. Transformation of the isosceles triangle with bisectors $l_a = l_c = l_2$ and $l_b = l_1$ to the final triangle with bisectors with $l_b = l_1$, $l_a = l_2$ and $l_c = l_3$.

the angles $\angle A$ and $\angle C$ will also change whereas the bisectors l_a and l_b remain constant. At first we shall prove the following simple property of these functions.

Lemma 4. *If there exists such a transformation of a triangle ABC that the conditions $\angle B < \angle A < \angle C$ are satisfied, the bisectors l_a and l_b are kept constant, and $\angle B \to 0$, then $\angle A \to 0$ and $\angle C \to 180^\circ$.*

Proof. From identities $\sin\angle A/a = \sin\angle B/b = \sin\angle C/c$ and inequalities (1) we find that in the limit $\angle B \to 0^\circ$ and, consequently, $\sin\angle B \to 0$, we have $\sin\angle A \to 0^\circ$, $\sin\angle C \to 0^\circ$. These limiting values of $\angle A$ and $\angle B$ can be realized in two cases

$$\angle A \to 0^\circ, \qquad \angle C \to 180^\circ;$$
$$\angle A \to 180^\circ, \qquad \angle C \to 0^\circ.$$

However in the second case we must have $l_a \to 0$ and that contradicts to the conditions of the Lemma, so this case must be excluded. We note also that inequalities (1) exclude such "exotic" situations as $\angle B \to 0^\circ$, $b \to 0$ or $\angle B \to 0^\circ$, $a \to \infty$, $c \to \infty$ that admit any limiting values of angles A and B provided $\angle A + \angle C \to 180^\circ$ and $\angle A < \angle C$. This completes the proof of Lemma 4. □

Now we concretize the transformation of the second type by combining the decrease of the angle $\angle B$ with rotation of the side AC around the point P at which the bisector l_b and the side AC meet. Let the angle $\angle B$ be decreased by the value ΔB (see Figure 3, left) and the side AC be rotated counterclockwise around point P by the angle $\Delta\alpha$ (Figure 3, right). Then after such a transformation we have $\angle B < \angle C$ since $l_a < l_b$ and also we have $\angle A < \angle C$ since $\Delta A = \frac{1}{2}\Delta B - \Delta\alpha$ and $\Delta C = \frac{1}{2}\Delta B + \Delta\alpha$. Thus, we have proved the following

Lemma 5. *In the defined above transformation we always have $\angle B < \angle A < \angle C$.*

This means that the conditions of Lemma 4 are always fulfilled for our concrete realization of the transformation.

Now we shall study the behavior of the bisector l_c under action of our transformation.

Lemma 6. *When angle $\angle B$ decreases from its value B_0, corresponding to the isosceles triangle with $l_a = l_c = l_2$, to zero, and the bisectors $l_b = l_1$, $l_a = l_2$ are kept constant, then the length of the bisector l_c is a continuous function of $\angle B$ taking all values from the interval $[0, l_2]$.*

Proof. From inspection of Figure 3 (left) it is clear that decrease of the angle $\angle B$ leads to the decrease of the sides AB and AC and to the increase of the angle $\angle A$. Consequently, from the known equation

$$l_a = \frac{2AB \cdot AC}{AB + AC} \cos\frac{\angle A}{2} = \frac{2}{\frac{1}{AB} + \frac{1}{AC}} \cos\frac{\angle A}{2} \tag{2}$$

we find that the length l_a also decreases with decrease of the angle $\angle B$, when the angles $\angle A$ and $\angle C$ are kept constant. To prevent such a decrease of l_a with decrease of $\angle B$ by the value ΔB, we combine it with rotation of the side AB around the point P by the angle $\Delta\alpha$, where $\alpha = \angle APB$. Considered separately, such a rotation increases the sides AB and AC monotonously to infinitely large values, decreasing at the same time the angle $\angle A$ to infinitesimally small values. Then, according to Eq. (2), the length l_a can be increased by such a rotation as we wish and, consequently, we can compensate the decrease of l_a after diminishing of $\angle B$ by the rotation of AC and make the bisector of the angle $\angle A$ equal to $l_a = l_2$. This construction shows that each value of the angle $\angle B$ corresponds to a definite value of the angle $\angle A$ at which $l_a = l_2$ and the function $\angle A = \angle A(\angle B)$ is continuous. The function $l_c(\angle B)$ is also continuous and in the described above transformation the conditions $\angle B < \angle A < \angle C$, $l_a = l_2 = \text{const}$, $l_b = l_1 = \text{const}$ of Lemma 4 are fulfilled and when $\angle B$ tends to zero we have $\angle A \to 0$ and $\angle C \to 180^\circ$, consequently $l_c \to 0$ as $\angle B$ tends to zero. Thus, we arrive at the conclusion that with decrease of $\angle B$ from B_0 to zero the bisector l_c as a continuous function of $\angle B$ takes all values from the interval $[0, l_2]$. □

Remark. As we shall see later, the function is not only continuous but also single-valued and, hence, monotonous.

3. Proof of Theorem 1

Now we can prove Theorem 1 about existence of a triangle with prescribed lengths of its bisectors.

Let three segments be given whose lengths l_1, l_2, l_3 satisfy the conditions $l_3 < l_2 < l_1$. Let us consider an equilateral triangle ABC with bisectors equal to $l_a = l_b = l_c = l_1$. We fix the position and the length of the bisector l_b and decrease the angle $\angle B$ in a way shown in Figure 1 down to the moment when we get an isosceles triangle A_0BC_0 with bisectors $l_a = l_c = l_2$ and $l_b = l_1$. Existence of such a triangle follows from Lemma 2: since the bisector lengths l_a and l_c ($l_a = l_c$) are continuous functions of the angle $\angle B$ and they decrease with $\angle B$ to zero value in the limit $\angle B \to 0$, then they take all values in the interval $[0, l_1]$ including the

value $l_a = l_c = l_2$ that belongs to this interval due to inequality $0 < l_2 < l_1$. The corresponding value of the angle $\angle B$ will be denoted as $\angle B_0$.

Then we continue transformation of the triangle ABC but now keeping the values of the bisectors l_a and l_b constant and decreasing the length l_c of the third bisector by further decrease of the angle $\angle B$ with simultaneously rotation of the side AC counterclockwise around the point P as is shown in Figure 3. As was shown in Lemma 6, during such an evolution the function $l_c(\angle B)$ behaves as a continuous function taking all values from the interval $[0, l_2]$ including the value $l_c = l_3$ thanks to inequality $0 < l_3 < l_2$. Hence by means of our transformation we arrive at such a triangle whose bisectors have the prescribed lengths. Thus the main Theorem 1 is proved.

We conclude with a few remarks.

Remarks. (1) In [3] an elementary proof is given that if a triangle with prescribed lengths does exist then it is unique up to isometry. Combining this theorem with our proof of existence of such a triangle, we conclude that in our transformation a single value of each parameter $\angle A$, $\angle C$ and l_c corresponds to a given value of $\angle B$; otherwise there would exist several such triangles. Consequently, these continuous functions of the angle $\angle B$ must be monotonous: with decrease of $\angle B$ the angle $\angle A$ and the bisector l_c monotonously decrease whereas the angle $\angle C$ monotonously increases.

(2) The above proof shows that the angles of the final triangle satisfy the inequalities $0^\circ < \angle A < \angle A_0$, $0^\circ < \angle B < \angle B_0$, $\angle C_0 < \angle C < 180^\circ$, where $\angle A_0 = \angle C_0 = (180^\circ - \angle B_0)/2$. These inequalities can be made stronger if one introduces an angle β such that $\angle C = 180^\circ - 2\beta$. Let $\beta = \arcsin(l_3/(l_1 + l_3))$, then we obtain the following estimate for l_c:

$$l_c = \frac{2ab}{a+b}\cos\frac{\angle C}{2} = \frac{2ab}{a+b}\cdot\frac{l_3}{l_1+l_3} < \frac{2a^2}{2a}\cdot\frac{l_3}{l_1+l_3} = l_3\cdot\frac{a}{l_1+l_3} < l_3. \quad (3)$$

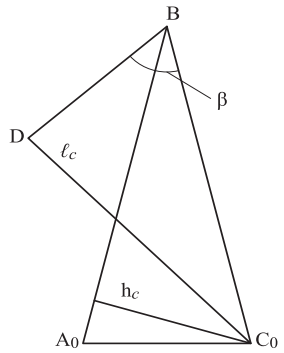

Figure 4. Estimates of the angles $\angle B$ and $\angle A$.

Since the angle $\angle C$ increases monotonously with decrease of $\angle B$ ($\Delta C = \frac{1}{2}\Delta B + \Delta\alpha$) and the length l_c monotonously decreases, then we find from Eq. (3) that $\angle C < 180^\circ - 2\beta$.

For estimation of the angle $\angle A$ we prolong the bisector line l_c up to the point D with $BD \perp CD$; see Figure 4. Then $\angle DBC = 90^\circ - \frac{1}{2}\angle C = \beta$ and we get $\angle B < \beta$. Indeed, if we assume that during our transformation at some moment we reach $\angle B > \beta$, then by continuity argument there exists a triangle $A'BC'$ such that $\angle B = \beta$. Consequently, $\angle B + \frac{1}{2}\angle C = \angle B + (90^\circ - \beta) = 90^\circ$, that is $AB \perp l_c$ and the triangle $A'BC'$ must be isosceles, $AC = BC$, what is impossible because of $l_a \neq l_b$. Hence, taking into account that $\angle A + \angle B + \angle C = 180^\circ$, we arrive at inequality $\angle A > \beta$. Thus, with account of monotonicity of our functions, we conclude that the angles of the triangle ABC satisfy the inequalities $\beta < \angle A < \angle A_0$, $0^\circ < \angle B < \angle B_0$, $\angle C_0 < \angle C < 180^\circ - 2\beta$.

(3) At last we notice that the suggested here method gives actually the algorithm for numerical calculation of the elements of the triangle with prescribed values of its bisectors.

References

[1] Yu. I. Manin, On solvability of constructing with compass and ruler problems, in *Encyclopedia of Elementary Mathematics*, vol. 4, pp. 205–227, Moscow, Nauka (1961) (in Russian).

[2] P. Mironescu and L. Panaitopol, The existence of a triangle with prescribed angle bisector lengths, *Amer. Math. Monthly*, 101 (1994) 58–60.

[3] A. Zhukov and N. Akulich, Kvant, N1 (2003) 29–31 (in Russian).

Sergey F. Osinkin: Moscow State University, Russia
E-mail address: osinkin1947@yandex.ru

Forum Geometricorum
Volume 16 (2016) 407–414.

FORUM GEOM
ISSN 1534-1178

How to Compute a Triangle with Prescribed Lengths of Its Internal Angle Bisectors

Gerhard Heindl

Dedicated to my friend Professor Dr. Ewald Reinhart
on the occasion of his 80th birthday

Abstract. In 1994 P. Mironescu and L. Panaitopol published a non-constructive proof that any three given positive real numbers are the lengths of the internal angle bisectors of a triangle which is unique up to isometries. In the present paper it will be shown that this result can be obtained also by a constructive proof which in addition leads to an efficient method for computing the lengths of the sides of the triangle in question.

1. Preliminaries

Let $\langle A, B, C\rangle$ be a triangle, $a = |\overrightarrow{BC}|$, $b = |\overrightarrow{CA}|$, $c = |\overrightarrow{AB}|$ the lengths of its sides, and $\alpha = \angle(CAB)$, $\beta = \angle(ABC)$, $\gamma = \angle(BCA)$ its angles. The lengths a, b, c are positive real numbers satisfying the triangle inequalities

$$a < b + c,\ b < c + a,\ c < a + b. \tag{1}$$

Conversely, if a, b, c are positive real numbers satisfying the inequalities (1), then there is a triangle $\langle A, B, C\rangle$, unique up to isometries, such that $|\overrightarrow{BC}| = a$, $|\overrightarrow{CA}| = b$, $|\overrightarrow{AB}| = c$. The line through A bisecting α is given by $\left\{A + \lambda(\frac{\overrightarrow{AC}}{b} + \frac{\overrightarrow{AB}}{c}) : \lambda \in \mathbb{R}\right\}$. It cuts the side $\langle B, C\rangle$ of the triangle at

$$X = A + \lambda'\left(\frac{\overrightarrow{AC}}{b} + \frac{\overrightarrow{AB}}{c}\right) = B + \tau'\overrightarrow{BC}, \tag{2}$$

where $\lambda' = \frac{bc}{b+c}$ and $\tau' = \frac{c}{b+c}$ (see Figure 1). The segment $\langle A, X\rangle$ is the so called internal angle bisector (of $\langle A, B, C\rangle$) at A. For the length $t_A = |\overrightarrow{AX}|$ of $\langle A, X\rangle$ the well-known formula

$$t_A^2 = bc\left(1 - \frac{a^2}{(b + c)^2}\right) \tag{3}$$

Publication Date: November 22, 2016. Communicating Editor: Paul Yiu.

can be easily derived from (2). The internal angle bisectors $\langle B, Y\rangle$ and $\langle C, Z\rangle$ at B and C, as well as t_B and t_C are defined similarly.

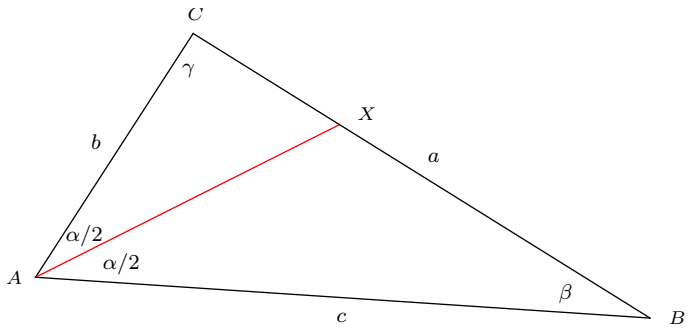

Figure 1. Triangle $\langle A, B, C\rangle$ with internal angle bisector $\langle A, X\rangle$

Whereas it is well-known, that a triangle can be reconstructed up to isometries by compass and ruler from the lengths of its altitudes or of its medians, it is not possible in general to reconstruct it by compass and ruler from the lengths of its internal angle bisectors, as was shown probably first by A. Korselt in 1897 [4] (see also [7]). It was even not clear for a long time, whether a triangle is uniquely defined up to isometries by the lengths of its internal angle bisectors, and if there is a relation between these lengths. These questions were answered by P. Mironescu and L. Panaitopol in 1994 [5]. Their surprising result was the following theorem.

Theorem (Mironescu and Panaitopol)**.** *Given any three positive real numbers m, n, p, then there is always a triangle $\langle A, B, C\rangle$ such that $t_A = m$, $t_B = n$, and $t_C = p$. This triangle is unique up to isometries.*

Their proof however was not constructive and therefore did not show up an efficient way how to compute a triangle with the desired property. Nevertheless, the first part of their proof is also the basis of the computational method to be developed in the present paper. This first part consists of the derivation of a relation of t_A, t_B, and t_C to the positive numbers

$$u = \frac{b+c-a}{2},\ v = \frac{c+a-b}{2},\ w = \frac{a+b-c}{2}, \tag{4}$$

appearing in several formulas for triangles.

We will deduce this relation here for the sake of completeness.
Solving (4) for a, b, c gives

$$a = v + w,\ b = w + u,\ c = u + v. \tag{5}$$

Using the identity $bc = \frac{1}{4}((b+c)^2 - (b-c)^2)$, it is easily verified that

$$t_A^2 + v^2 = \frac{1}{4}\left(b + c + \frac{a(c-b)}{b+c}\right)^2. \tag{6}$$

Since $a(c-b) = v^2 - w^2$, we have

$$b + c + \frac{a(c-b)}{b+c} = \frac{4u^2 + 2v^2 + 4wu + 2wv + 4uv}{b+c} > 0.$$

Hence (6) implies

$$\sqrt{t_A^2 + v^2} = \frac{1}{2}\left(b + c + \frac{a(c-b)}{b+c}\right). \tag{7}$$

Interchanging b and c in this formula, we get

$$\sqrt{t_A^2 + w^2} = \frac{1}{2}\left(b + c - \frac{a(c-b)}{b+c}\right). \tag{8}$$

Adding (7) and (8) results in

$$b + c = \sqrt{t_A^2 + v^2} + \sqrt{t_A^2 + w^2}. \tag{9}$$

Replacing $b + c$ by $w + 2u + v$, (9) can be written as

$$u = \frac{\sqrt{t_A^2 + v^2} - v}{2} + \frac{\sqrt{t_A^2 + w^2} - w}{2}. \tag{10}$$

By symmetry we have also

$$v = \frac{\sqrt{t_B^2 + w^2} - w}{2} + \frac{\sqrt{t_B^2 + u^2} - u}{2}, \tag{11}$$

and

$$w = \frac{\sqrt{t_C^2 + u^2} - u}{2} + \frac{\sqrt{t_C^2 + v^2} - v}{2}. \tag{12}$$

2. The approach of Mironescu and Panaitopol

After the derivation of the relations (10), (11), (12), Mironescu and Panaitopol introduced for every real $q > 0$ the function f_q defined for all $t \in \mathbb{R}$ by

$$f_q(t) = \frac{\sqrt{q^2 + t^2} - t}{2} \in \mathbb{R}, \tag{13}$$

and for every triple (m, n, p) of positive real numbers, the mapping $F_{(m,n,p)}$ defined for all $x = (x_1, x_2, x_3)^T \in \mathbb{R}^3$ by

$$F_{(m,n,p)}(x) = \begin{pmatrix} f_m(x_2) + f_m(x_3) \\ f_n(x_3) + f_n(x_1) \\ f_p(x_1) + f_p(x_2) \end{pmatrix} \in \mathbb{R}^3. \tag{14}$$

Then the relations (10), (11), (12) are restated as: $(u, v, w)^T$ is a fixed point of $F_{(t_A,t_B,t_C)}$. The main result however is, that for every triple (m, n, p) of positive real numbers, $F = F_{(m,n,p)}$ has a unique fixed point, and that this fixed point is located in the interior of $Q = [0, x_u]$, where $0 = (0, 0, 0)^T$, $x_u = (m, n, p)^T$,

and $[x, y]$ denotes the set of all $z \in \mathbb{R}^3$ satisfying $x \leq z \leq y$ with the usual order relation

$$x = (x_1, x_2, x_3)^T \leq y = (y_1, y_2, y_3)^T \text{ if and only if } x_i \leq y_i,\ i = 1, 2, 3.$$

We rewrite the proof, using also the strict order relation

$$x = (x_1, x_2, x_3)^T < y = (y_1, y_2, y_3)^T \text{ if and only if } x_i < y_i,\ i = 1, 2, 3.$$

Obviously $F(x) > 0$ for all $x \in \mathbb{R}^3$. This implies $x' > 0$ if x' is a fixed point of F. Now, $0 < f_q(t) < \frac{q}{2}$ for all $t > 0$ implies $F(x) < x_u$ if $x > 0$. Hence $0 < x' < x_u$ if x' is a fixed point of F. If $0 \leq x \leq x_u$, then $0 < F(x) \leq x_u$. Hence the continuous mapping F maps the convex compact set Q into Q, implying by Brouwer's fixed point theorem that F has a fixed point x' in Q, for which in fact $0 < x' < x_u$ must hold. From $-\frac{1}{2} < f_q'(t) < 0$ if $t > 0$, the authors concluded $||F(x) - F(y)||_2 < ||x - y||_2$ if $x, y \in Q$ and $x \neq y$, i.e. $F|Q$ is strictly nonexpansive with respect to the euclidean norm $|| \cdot ||_2$. But this shows the uniqueness of x'.

Actually a much easier proof of the existence of x' (attributed in [3] to a communication from M. Krein) can be given:

$F(Q)$ is a compact subset of Q. Hence there is an $x' \in F(Q)$ such that

$$||F(x') - x'||_2 \leq ||F(x) - x||_2 \text{ for all } x \in F(Q).$$

If we assume $F(x') \neq x'$, then

$$||F(F(x')) - F(x')||_2 < ||F(x') - x'||_2,$$

which is a contradiction since $x = F(x') \in F(Q)$.

In order to verify that there is a triangle $\langle A', B', C' \rangle$ such that $m = t_{A'}$ $n = t_{B'}$, $p = t_{C'}$, we set $a' = x_2' + x_3'$, $b' = x_3' + x_1'$, $c' = x_1' + x_2'$. Then $a' + b' > c'$, $b' + c' > a'$, $c' + a' > b'$. Hence there is a triangle $\langle A', B', C' \rangle$ such that $a' = |\overrightarrow{B'C'}|,\ b' = |\overrightarrow{C'A'}|,\ c' = |\overrightarrow{A'B'}|$.

Let us show $m = t_{A'}$. The first equation of the identity $x' = F_{(m,n,p)}(x')$ is

$$x_1' = \frac{\sqrt{m^2 + x_2'^2} - x_2'}{2} + \frac{\sqrt{m^2 + x_3'^2} - x_3'}{2}.$$

It is equivalent to

$$b' + c' = 2x_1' + x_2' + x_3' = \sqrt{m^2 + x_2'^2} + \sqrt{m^2 + x_3'^2}.$$

Squaring gives

$$(b' + c')^2 = 2m^2 + x_2'^2 + x_3'^2 + 2\sqrt{(m^2 + x_2'^2)(m^2 + x_3'^2)}.$$

Rearranging and squaring once more results in

$$((b' + c')^2 - 2m^2 - (x_2'^2 + x_3'^2))^2 = 4(m^2 + x_2'^2)(m^2 + x_3'^2).$$

Expanding, cancelling and rearranging gives

$$4(b' + c')^2 m^2 = (b' + c')^4 - 2(b' + c')^2(x_2'^2 + x_3'^2) + (x_2'^2 + x_3'^2)^2 - 4x_2'^2 x_3'^2.$$

Since $x_2' = \frac{c'+a'-b'}{2}$ and $x_3' = \frac{a'+b'-c'}{2}$, we get

$$\begin{aligned}(x_2'^2 + x_3'^2)^2 - 4x_2'^2x_3'^2 = \ & (x_3'^2 - x_2'^2)^2 = ((x_3' + x_2')(x_3' - x_2'))^2 = \ (a'(b'-c'))^2,\\ x_2'^2 + x_3'^2 = \ & \frac{a'^2 + (b'-c')^2}{2}, \text{ and}\\ 4(b'+c')^2m^2 = \ & (b'+c')^4 - (b'+c')^2(a'^2 + (b'-c')^2) + (a'(b'-c'))^2\\ = \ & (b'+c')^4 - 4a'^2b'c' - (b'+c')^2(b'-c')^2.\end{aligned}$$

Consequently,

$$m^2 = \frac{(b'+c')^2}{4} - \frac{a'^2b'c'}{(b'+c')^2} - \frac{(b'-c')^2}{4} = b'c'\left(1 - \frac{a'^2}{(b'+c')^2}\right),$$

which is equivalent to $m = t_{A'}$. Similarly, or by symmetry, we get $n = t_{B'}$ and $p = t_{C'}$.

The uniqueness of $\langle A', B', C'\rangle$ up to isometries is seen as follows: Assuming that $(m, n, p) = (t_A, t_B, t_C)$ holds also for the triangle $\langle A, B, C\rangle$, then, if u, v, w are defined by (4), $(u, v, w)^T$ is a fixed point of $F_{(m,n,p)}$ as shown in Section 1. Hence $(u, v, w)^T = x'$. But this implies

$$a = x_2' + x_3' = a', \quad b = x_3' + x_1' = b', \quad c = x_1' + x_2' = c'.$$

Hence $\langle A, B, C\rangle$ and $\langle A', B', C'\rangle$ are congruent.

3. Existence, uniqueness and computability of x' by Banach's fixed point theorem.

In the sequel we write x_l instead of

$$F(x_u) = (f_m(n) + f_m(p),\ f_n(p) + f_n(m),\ f_p(m) + f_p(n))^T.$$

A first suggestion for approximating x' was made by G. Dinca and J. Mawhin [1]. They considered the perturbed mappings $\lambda F|Q$, $0 < \lambda < 1$, which are contractions of Q into Q. By Banach's fixed point theorem there is a unique fixed point x_λ of $\lambda F|Q$ which can be approximated (theoretically) with arbitrary precision by the iteration $x_0 \in Q,\ x_k = \lambda F(x_{k-1}), k = 1, 2, \ldots$. For λ close to 1, x_λ is used as an approximation of x'.

Actually, a Theorem of M. Edelstein [2] (see also [6, 12.3.6]) shows that for any $x_0 \in Q$ the sequence $\{x_k\}$ defined by $x_{k+1} = F(x_k), k = 0, 1, \ldots$, converges to x'. In both cases, however, error estimates are not given.

In the following it will be demonstrated how Banach's fixed point theorem can be applied to a restriction of F to a suitable subset of Q.

We introduce the absolute value $|x| = (|x_1|, |x_2|, |x_3|)^T$ and the 1-norm $||x||_1 = |x_1|+|x_2|+|x_3|$ for all $x = (x_1, x_2, x_3)^T \in \mathbb{R}^3$. Since $f_q'(t) = \frac{1}{2}\left(\frac{t}{\sqrt{q^2+t^2}} - 1\right) < 0$ for all $t \in \mathbb{R}$, f_q is strictly decreasing. But this implies that F is order-reversing, i.e. $F(y) \leq F(x)$ if $x \leq y$. An important consequence of this property is the following

Proposition 1. *If F maps $[x, y]$ into itself, then it also maps $[F(y), F(x)]$ into itself.*

Proof. If $F(y) \le z \le F(x)$ then $F(F(x)) \le F(z) \le F(F(y))$. Since $x \le F(y)$ implies $F(F(y)) \le F(x)$, and $F(x) \le y$ implies $F(y) \le F(F(x))$, we have $F(y) \le F(F(x)) \le F(z) \le F(F(y)) \le F(x)$. □

A consequence of Proposition 1 is: Since F maps $[0, x_u]$ into itself, it maps also $[F(x_u), F(0)] = [x_l, x_u]$ into itself. If x' is a fixed point of F, we have seen already that $0 < x' < x_u$ must hold. $F(0) \ge F(x') = x' \ge F(x_u)$ shows that x' must be contained even in $[x_l, x_u]$.

Next we use the fact that we have for all $t_0 > 0$, $0 < -f_q'(t_0) < 1/2$, and $|f_q(t_2) - f_q(t_1)| \le -f_q'(t_0)|t_2 - t_1|$ if $t_1, t_2 \ge t_0$. This implies for all $x, y \ge x_l$ (> 0), $|F(y) - F(x)| \le P|y - x|$, where

$$P = \begin{pmatrix} 0 & -f_m'(x_{l2}) & -f_m'(x_{l3}) \\ -f_n'(x_{l1}) & 0 & -f_n'(x_{l3}) \\ -f_p'(x_{l1}) & -f_p'(x_{l2}) & 0 \end{pmatrix}. \tag{15}$$

Consequently we have $||F(y) - F(x)||_1 \le \lambda ||y - x||_1$ with

$$\lambda = \max\{-f_n'(x_{l1}) - f_p'(x_{l1}), -f_m'(x_{l2}) - f_p'(x_{l2}), -f_m'(x_{l3}) - f_n'(x_{l3})\}$$

for all $x, y \ge x_l$. $\lambda < 1$ since $-f_q'(t) < \frac{1}{2}$ if $t > 0$.

Now we can conclude from Banach's fixed point theorem: There is exactly one fixed point x' of F, $x' \in [x_l, x_u]$, and starting the iteration

$$x_{k+1} = F(x_k),\ k = 0, 1, \ldots,$$

with any $x_0 \in [x_l, x_u]$, then $||x' - x_{k+1}||_1$ is bounded above by $\frac{\lambda^{k+1}}{1-\lambda}||x_1 - x_0||_1$ (a priori error estimate), and by $\frac{\lambda}{1-\lambda}||x_{k+1} - x_k||_1$ (a posteriori error estimate).

Componentwise error estimates can be obtained from the inequalities

$$|x' - x_{k+1}| \le (I - P)^{-1} P^{k+1} |x_1 - x_0|$$

and

$$|x' - x_{k+1}| \le (I - P)^{-1} P |x_{k+1} - x_k|,$$

where I denotes the 3×3 unit matrix (see e.g. [6, 13.1.2]).

The evaluation of the considered error estimates can be avoided however if $x_0 = x_u$ is chosen. In this case the subsequence $\{x_{2k}\}$ of $\{x_k\}$ converges monotonically decreasing to x', and the subsequence $\{x_{2k+1}\}$ converges monotonically increasing to x'. This can be deduced by applying Proposition 1 iteratively: By Proposition 1 we get $[x_1, x_0] \supseteq [x_1, x_2] \supseteq [x_3, x_2]$, and by induction $[x_{2k-1}, x_{2(k-1)}] \supseteq [x_{2k-1}, x_{2k}] \supseteq [x_{2k+1}, x_{2k}], k = 2, 3, \ldots$. Since then $x_{2k-1} \le x' \le x_{2k}, k = 1, 2, \ldots$, it is possible to get lower and upper bounds of x' which are as close to x' as one wants.

Let us illustrate these results with the numerical example

$$(m, n, p)^T = (17, 12, 19.36)^T = x_u = x_0.$$

The following data were delivered by a simple MATLAB program using the standard output rounding:

$$x_1 = F(x_0) = x_l = (7.6066, 3.6130, 9.7709)^T,$$

($0 < x_l < x_0$ for the exact value of x_l),

$$x_{15} = (10.4995, 5.0363, 13.2461)^T,$$
$$x_{16} = (10.4996, 5.0364, 13.2462)^T,$$

($x_{15} \le x' \le x_{16}$ for the exact values of x_{15} and x_{16}),

$$P = \begin{pmatrix} 0 & 0.3961 & 0.2508 \\ 0.2323 & 0 & 0.1843 \\ 0.3172 & 0.4083 & 0 \end{pmatrix},$$

$\lambda = 0.8043$, and 9.7853×10^{-4} as the resulting upper bound for $||x' - x_{16}||_1$, $10^{-3} \times (0.1109, 0.0852, 0.1206)^T$ as the resulting upper bound of $|x' - x_{16}|$, and 3.1664×10^{-4} as the resulting upper bound of $|||x' - x_{16}|||_1$.

From the approximation x_{16} of x', $a = 18.8825$, $b = 23.7458$, $c = 15.5360$ were derived. The computation of t_A, t_B, t_C from a, b, c resulted in

$$t_A = 17.0000, \quad t_B = 12.0000, \quad t_C = 19.3600,$$

as it should be.

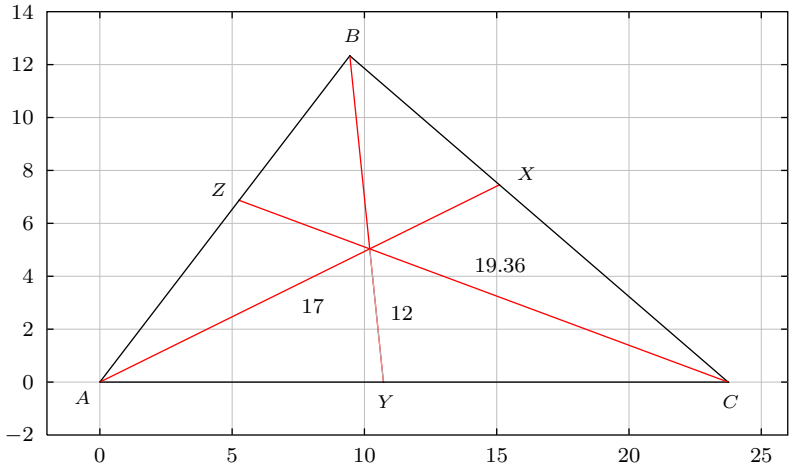

Figure 2. Triangle $\langle A, B, C\rangle$ with prescribed $(t_A, t_B, t_C) = (17, 12, 19.36)$

References

[1] G. Dinca and J. Mawhin, A constructive fixed point approach to the existence of a triangle with prescribed angle bisector lengths, *Bull. Belg. Math. Soc.*, 17 (2010), 333–341.

[2] M. Edelstein, On fixed and periodic points under contractive mappings, *J. London Math. Soc.*, 37 (1962), 74–79.

[3] L. W. Kantorovich and G. P. Akilov, *Functional Analysis in Normed Spaces*, Pergamon Press, Oxford, 1964.

[4] A. Korselt, Über die Unmöglichkeit der Konstruktion eines Dreiecks aus den drei Winkelhalbierenden, *Z. Math. Naturwiss. Unterricht*, 28 (1897) 81–83.
[5] P. Mironescu and L. Panaitopol, The existence of a triangle with prescribed angle bisector lengths, *Amer. Math. Monthly*, 101 (1994) 58–60.
[6] J. Ortega and W. Rheinboldt, *Iterative Solution of Nonlinear Equations in Several Variables*, Academic Press, New York, 1970.
[7] V. Zajic, Triangle From Angle Bisectors, 2003, `www.cut-the-knot.org/triangle/TriangleFromBisectors.shtml`.

Gerhard Heindl: Faculty of Mathematics and Natural Sciences, University of Wuppertal, Germany

E-mail address: `gerhard.heindl@math.uni-wuppertal.de`

Forum Geometricorum
Volume 16 (2016) 415–418.

FORUM GEOM
ISSN 1534-1178

A Generalization of the Droz-Farny Line Theorem with Orthologic Triangles

Ngo Quang Duong and Vu Thanh Tung

Abstract. We prove a generalization of the Droz-Farny line theorem with orthologic triangles.

In 1899, Arnold Droz-Farny [3] discovered and published without proof the following beautiful result.

Theorem 1 (Droz-Farny line theorem)**.** *Two perpendicular lines ℓ_1 and ℓ_2 pass through the orthocenter of triangle ABC. If ℓ_1 intersects BC, CA, AB at D_1, E_1, F_1, and ℓ_2 intersects BC, CA, AB at D_2, E_2, F_2, then the midpoints of D_1D_2, E_1E_2, F_1F_2 are collinear.*

The line containing these midpoints is called the Droz-Farny line associated with ℓ_1 and ℓ_2. There are a number of generalizations of the Droz-Farny line theorem, notably by van Lamoen [5] (see also [4, 8]), Thas, [10], and Bradley [2]. The most recent one is by Letrouit [6]. If directly similar triangles DD_1D_2, EE_1E_2, FF_1F_2 are constructed on D_1D_2, E_1E_2, F_1F_2 respectively, then D, E, F are collinear (see also Nicollier [7]).

In this note we prove a generalization associated with a pair of orthologic triangles. Consider a pair of orthologic triangles $A_1B_1C_1$ and $A_2B_2C_2$ with orthology centers P_1, P_2. In other words,

$$A_1P_1 \perp B_2C_2, \quad B_1P_1 \perp C_2A_2, \quad C_1P_1 \perp A_2B_2;$$
$$A_2P_2 \perp B_1C_1, \quad B_2P_2 \perp C_1A_1, \quad C_2P_2 \perp A_1B_1.$$

Theorem 2. *Let ℓ_1 and ℓ_2 be two perpendicular lines, passing through P_1 and P_2 respectively. For $i = 1, 2$, let ℓ_i intersect the lines B_iC_i at D_i, C_iA_i at E_i, and A_iB_i at F_i. If directly similar triangles DD_1D_2, EE_1E_2, FF_1F_2 are constructed on D_1D_2, E_1E_2, F_1F_2 respectively, then D, E, F are collinear* (*see Figure 1*).

When the triangles $A_1B_1C_1$ and $A_2B_2C_2$ are identical, and D, E, F are the midpoints of D_1D_2, E_1E_2, F_1F_2, Theorem 2 is the original Droz-Farny line theorem. In the proofs below, we shall make use of the notion of cross ratio of four collinear points $(A, B, C, D) := \frac{\frac{AC}{AD}}{\frac{BC}{BD}}$, and for four concurrent lines,

$$(PA, PB, PC, PD) = (A, B, C, D).$$

The infinite point of a line ℓ is denoted by Ω_ℓ.

Publication Date: November 29, 2016. Communicating Editor: Paul Yiu.

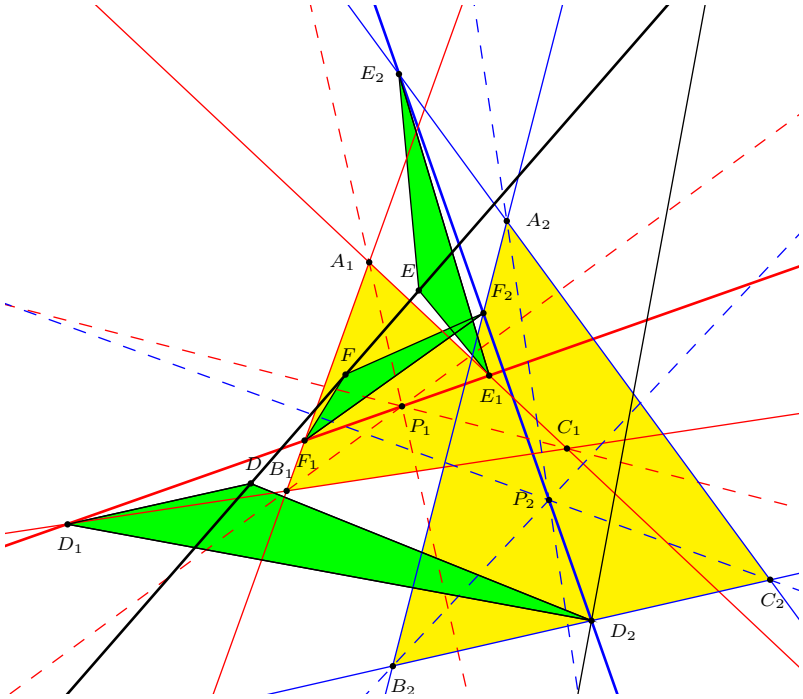

Figure 1

Lemma 3. $\frac{D_1B_1}{D_1C_1} = \frac{P_2F_2}{P_2E_2}$, $\frac{E_1C_1}{E_1A_1} = \frac{P_2D_2}{P_2F_2}$, $\frac{F_1A_1}{F_1B_1} = \frac{P_2E_2}{P_2D_2}$.

Proof. Denote the infinite point on the line AB by Ω_{AB}. Using cross ratios, we have

$$\frac{D_1B_1}{D_1C_1} = (D_1,\ \Omega_{B_1C_1},\ B_1,\ C_1) = (P_1D_1,\ P_1\Omega_{B_1C_1},\ P_1B_1,\ P_1C_1).$$

Since P_1D_1, $P_1\Omega_{B_1C_1}$, P_1B_1, P_1C_1 are perpendicular to ℓ_2, A_2P_2, A_2C_2, A_2B_2 respectively,

$$\begin{aligned}(P_1D_1,\ P_1\Omega_{B_1C_1},\ P_1B_1,\ P_1C_1) &= (A_2\Omega_{\ell_2},\ A_2P_2,\ A_2C_2,\ A_2B_2)\\ &= (A_2\Omega_{\ell_2},\ A_2P_2,\ A_2E_2,\ A_2F_2)\\ &= (\Omega_{\ell_2},\ P_2,\ E_2,\ F_2)\\ &= \frac{P_2F_2}{P_2E_2}.\end{aligned}$$

Therefore, $\frac{D_1B_1}{D_1C_1} = \frac{P_2F_2}{P_2E_2}$. The other two follow similarly. □

Lemma 4. $\frac{D_1E_1}{D_1F_1} = \frac{D_2E_2}{D_2F_2}$.

Proof. For $i = 1, 2$, applying Menelaus' theorem to triangle $A_iE_iF_i$ with transversal $D_iB_iC_i$, we have

$$\frac{E_iD_i}{D_iF_i} \cdot \frac{F_iB_i}{B_iA_i} \cdot \frac{A_iC_i}{C_iE_i} = -1 \implies \frac{D_iE_i}{D_iF_i} = \frac{B_iA_i}{B_iF_i} \cdot \frac{C_iE_i}{C_iA_i}.$$

By Lemma 3,

$$\frac{B_1A_1}{B_1F_1} = 1 - \frac{A_1F_1}{B_1F_1} = 1 - \frac{E_2P_2}{D_2P_2} = \frac{D_2E_2}{D_2P_2},$$
$$\frac{C_1A_1}{C_1E_1} = 1 - \frac{A_1E_1}{C_1E_1} = 1 - \frac{F_2P_2}{D_2P_2} = \frac{D_2F_2}{D_2P_2}.$$

Therefore,

$$\frac{D_1E_1}{D_1F_1} = \frac{B_1A_1}{B_1F_1} \cdot \frac{C_1E_1}{C_1A_1} = \frac{D_2E_2}{D_2P_2} \cdot \frac{D_2P_2}{D_2F_2} = \frac{D_2E_2}{D_2F_2}.$$

□

Proof of Theorem 2. Let ℓ_1 intersect ℓ_2 at P and the circles PE_1E_2 and PF_1F_2 intersect at M other than P. M is the Miquel point of the quadrilateral defined by the lines E_1F_1, E_2F_2, E_1E_2, F_1F_2. It is also the center of the spiral similarities $\Phi : E_1E_2 \to F_1F_2$ and $\Psi : E_1F_1 \to E_2F_2$. Since $\frac{D_1E_1}{D_1F_1} = \frac{D_2E_2}{D_2F_2}$, Ψ maps D_1 into D_2. Thus, the triangles MD_1D_2, ME_1E_2, MF_1F_2 are directly similar, and the triangles DD_1D_2, EE_1E_2, FF_1F_2 are also directly similar. Therefore triangles MD_1F_1 and MDF are directly similar, triangles MD_1E_1 and MDE are directly similar. Hence, we conclude that D, E, F are collinear.

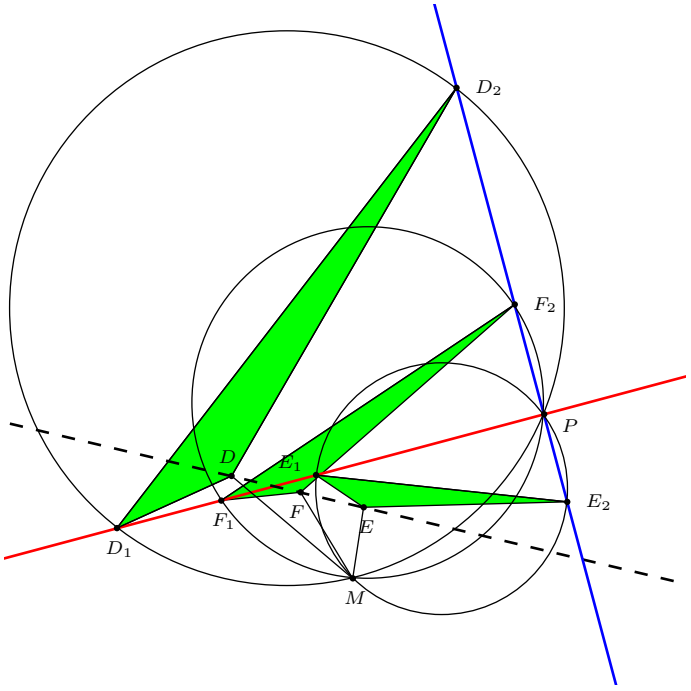

Figure 2

References

[1] J. L. Ayme, A purely synthetic proof of the Droz-Farny line theorem, *Forum Geom.*, 4 (2004) 219–224.
[2] C. J. Bradley, Generalisation of the Droz-Farny lines, *Math. Gazette*, 92 (2008) 332–335.
[3] A. Droz-Farny, Question 14111, *Educational Times*, 71 (1899) 89–90.
[4] J.-P. Ehrmann and F. M. van Lamoen, A projective generalization of the Droz-Farny line theorem, *Forum Geom.*, 4 (2004) 225–227.
[5] F. M. van Lamoen, Hyacinthos message 10716, October 17, 2004.
[6] C. Letrouit, On a new generalization of the Droz-Farny line, *Forum Geom.*, 16 (2016) 367–369.
[7] G. Nicollier, Minimal proof of a generalized Droz-Farny theorem, *Forum Geom.*, 16 (2016) 397–398.
[8] C. Pohoata and S. H. Ta, A short proof of Lamoen's generalization of the Droz-Farny line theorem, *Mathematical Reflections*, 3 (2011).
[9] I. F. Sharygin, *Problemas de geometria*, (spanish translation), Mir Edition, 1986.
[10] C. Thas, The Droz-Farny theorem and related topics, *Forum Geom.*, 6 (2006) 235–240.
[11] T. T. Vu, Advanced Plane Geometry, message 2495, May 1, 2015.

Ngo Quang Duong: High School for Gifted Students, Hanoi University of Science, Vietnam National University, Hanoi, Vietnam
E-mail address: tenminhladuong@gmail.com

Vu Thanh Tung: 250 Quang Trung, Nam Dinh, Vietnam
E-mail address: tungvtt@gmail.com

Forum Geometricorum
Volume 16 (2016) 419–427.

FORUM GEOM
ISSN 1534-1178

Circle Chains Inscribed in Symmetrical Lenses and Integer Sequences

Giovanni Lucca

Abstract. We derive the conditions for inscribing, inside a symmetrical lens, a chain of tangent circles having the property that the ratio between the largest circle radius and the radius of any other circle of the chain is an integer.

1. Introduction

A lens is the common area between two intersecting circles. If the radii of the circles are equal, the lens is symmetrical. The aim of this paper is to show some connections between the infinite chains of tangent circles that can be inscribed in a symmetrical lens and certain integer sequences. A generic example of circle chain is shown in Figure 1.

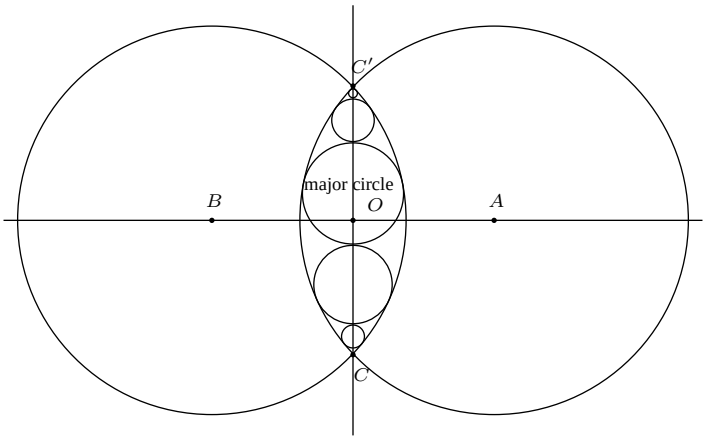

Figure 1. Example of a circle chain inscribed inside a symmetrical lens

To the best of our knowledge, only two papers ([1, 2]) can be found in literature dealing with the problem of an infinite chain of mutually tangent circles inscribed inside a lens. In the paper [2], by using the circular inversion technique, the present author derived, expressions for center coordinates and radius of the circles belonging to the chain. The results are general and they are valid also for a generic lens not necessarily symmetrical. In [1], J. Kocik, by using a different approach, showed that the radii relevant to chains of mutually tangent circles inscribed in a symmetrical lens can be obtained by a non-homogeneous linear recurrence formula.

Publication Date: December 1, 2016. Communicating Editor: Paul Yiu.

2. Some definitions and useful expressions

A circle chain in the symmetrical lens is doubly infinite. We label the circles $\mathcal{C}_k$, with radius r_k, for integers k. It is convenient to define the *major circle* $\mathcal{C}_0$ (see Figure 1) This induces a subdivision of the chain into two sub-chains:
(i) an *up-chain* $\mathcal{C}_{\mathrm{u}k} = \mathcal{C}_k$, $k = 0, 1, 2, \ldots$, starting from the major circle and converging to point C', and
(ii) a *down-chain* $\mathcal{C}_{\mathrm{d}k} = \mathcal{C}_{-k}$, $k = 0, 1, 2, \ldots$, starting from the major circle and converging to point C.

With a Cartesian coordinate system with axes along the line AB and its perpendicular bisector, the circle chain and its up- and down-subchains are completely determined by the ordinate of the center of the major circle (see Figure 2). We shall assume

- $R =$ the common radius of the circles forming the lens,
- $2a$ (with $a < R$) the distance between the centers of the two intersecting circles,
- the two circles intersect at $C(0, -h)$ and $C'(0, h)$, $h = \sqrt{R^2 - a^2}$,
- y_0 is the ordinate of the center K of the major circle in the chain; note that $y_0 \in \left[-\frac{R^2-a^2}{2R},\ \frac{R^2-a^2}{2R}\right]$,
- the radius of the major circle is

$$r_0(y_0) = R - \sqrt{a^2 + y_0^2}. \tag{1}$$

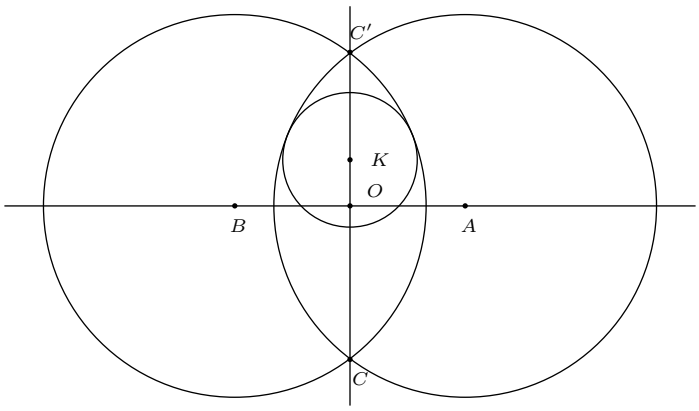

Figure 2. Symmetrical lens with major circle of the chain

For two particular values for y_0, the up- and down-chains are symmetrical.

- If $y_0 = 0$, we have $r_0 = R - a$, and the major circle is bisected by the x-axis (central symmetry; see Figure 3).
- If $y_0 = \pm\frac{R^2-a^2}{2R}$, we have $r_0 = \frac{R^2-a^2}{2R}$ and two equal major circles (see Figure 4). The up- and down-chains are symmetrical about the x-axis. In order to avoid complication of re-indexing, we exclude this case in the discussion below.

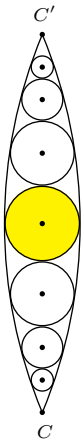

Figure 3

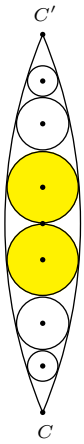

Figure 4

In this paper, we investigate the conditions for which the ratios $\tau_k := \frac{r_0}{r_k}$ ($k = \pm 1, \pm 2, \dots$) between the radii of the major circle and the generic k-th circle are integers for both the up- and down-sub-chains. In other words, we find conditions (provided they exist) for the radius of any generic circle of the chain is a submultiple of the major circle radius.

In [2], we applied inversion techniques (see [4]) and obtained expressions for the radii and the coordinates of the centers of the circles in the up- and down-chains. We choose the circle of inversion with center C and radius $\rho = 2h$, passing through C'. Here is a summary of the main formulas and results.

(a) The two intersecting circles forming the lens are transformed into the two straight lines

$$y = \pm \frac{a}{h} x + h, \tag{2}$$

through C'.

(b) The major circle is transformed into a circle with radius

$$R_0 = \left| \frac{\rho^2}{(y_0 + h)^2 - r_0^2} \right| r_0. \tag{3}$$

(c) The inversive images of the circles of the chain form another chain tangent to two lines given by (2) in (a). Their centers and radii are

$$(x'_k,\ y'_k) = \left(0,\ \frac{\omega^{-k} R R_0}{h} + h\right),$$
$$r'_k = \omega^{-k} R_0,$$

for $k = 0, \pm 1, \pm 2, \dots$. Here,

$$\omega = \frac{R - h}{R + h}.$$

(d) The centers and radii of the circles in the lens are

$$(x_k,\ y_k) = \left(0,\ s_k\left(\frac{\omega^k RR_0}{h} + 2h\right) - h\right),$$
$$r_k = |s_k|\omega^k R_0,$$

for $k = 0, \pm 1, \pm 2, \ldots$. Here

$$s_k = \left(-\frac{\omega^{2k}R_0^2}{4h^2} + \left(1 + \frac{\omega^k RR_0}{2h^2}\right)^2\right)^{-1}.$$

In Figure 5 an example of a circle chain inside a symmetrical lens is shown with the inversive images of the circles.

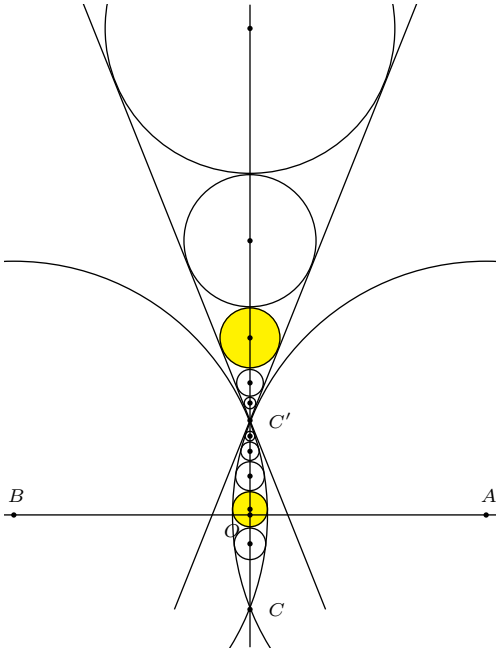

Figure 5

With the aids of the formulas, we have, for $k = 0, \pm 1, \pm 2, \ldots$,

$$r_k = r_0\left((G_k + G_k^{-1})\frac{a(R - \sqrt{a^2 + y_0^2})}{2h^2} + \frac{R(R - \sqrt{a^2 + y_0^2})}{h^2}\right)^{-1}, \qquad (4)$$

where

$$G_k = \frac{\omega^k a(R - \sqrt{a^2 + y_0^2})}{y_0 h - a^2 + R\sqrt{a^2 + y_0^2}}.$$

If k is positive, we have the up-chain while, if k is negative, we have the down-chain.

From (4), we define the sequence (τ_k) of the ratios between the major circle radius and the k-th circle radius:

$$\tau_k = \frac{r_0}{r_k} = (G_k + G_k^{-1})\frac{a(R-\sqrt{a^2+y_0^2})}{2h^2} + \frac{R(R-\sqrt{a^2+y_0^2})}{h^2}. \tag{5}$$

By means of algebra, we can show that for $k = 0, \pm1, \pm2, \ldots,$

$$\tau_k = \alpha\omega^k + \beta\omega^{-k} + \gamma, \tag{6}$$

for

$$\begin{aligned}
\alpha &= \frac{a^2(R-\sqrt{a^2+y_0^2})^2}{2h^2(hy_0 - a^2 + R\sqrt{a^2+y_0^2})},\\
\beta &= \frac{hy_0 - a^2 + R\sqrt{a^2+y_0^2}}{2h^2},\\
\gamma &= \frac{R(R-\sqrt{a^2+y_0^2})}{h^2}.
\end{aligned}$$

It is important, for the following, to point out that in [1], J. Kocik showed how Binet-like formulas can be expressed by means of a recursive relation of the type:

$$\tau_{k+2} = \left(\omega + \frac{1}{\omega}\right)\tau_{k+1} - \tau_k + \gamma\left(2 - \omega - \frac{1}{\omega}\right). \tag{7}$$

3. Conditions for integer sequences

In general, the doubly infinitely sequence (τ_k) is composed of real numbers. Here we want to find the conditions for which τ_k, $k = 0, \pm1, \pm2, \ldots,$ are integers. In other words, what are the values of $\frac{a}{R}$ and $\frac{y_0}{R}$ to guarantee (τ_k) to be an integer sequence?

First of all, by (5), it is possible to assign two specific values μ and λ (both > 1) to τ_1 and τ_{-1} respectively.

By making the substitutions

$$\begin{cases} X &= \frac{a}{R}, \quad 0 < X < 1,\\ Y &= \frac{y_0}{R}, \quad -\frac{1-X^2}{2} \le Y \le \frac{1-X^2}{2}, \end{cases} \tag{8}$$

we rewrite, for $k = 1$ and $k = -1$, (5) as

$$\begin{cases} \mu &= \left(\frac{\frac{1-\sqrt{1-X^2}}{1+\sqrt{1-X^2}}X(1-\sqrt{Y^2+X^2})}{Y\sqrt{1-X^2}-X^2+\sqrt{Y^2+X^2}} + \frac{Y\sqrt{1-X^2}-X^2+\sqrt{Y^2+X^2}}{\frac{1-\sqrt{1-X^2}}{1+\sqrt{1-X^2}}X(1-\sqrt{Y^2+X^2})}\right)\frac{X(1-\sqrt{Y^2+X^2})}{2(1-X^2)}\\ &\quad +\frac{1-\sqrt{Y^2+X^2}}{1-X^2},\\ \lambda &= \left(\frac{\frac{1+\sqrt{1-X^2}}{1-\sqrt{1-X^2}}X(1-\sqrt{Y^2+X^2})}{Y\sqrt{1-X^2}-X^2+\sqrt{Y^2+X^2}} + \frac{Y\sqrt{1-X^2}-X^2+\sqrt{Y^2+X^2}}{\frac{1+\sqrt{1-X^2}}{1-\sqrt{1-X^2}}X(1-\sqrt{Y^2+X^2})}\right)\frac{X(1-\sqrt{Y^2+X^2})}{2(1-X^2)}\\ &\quad +\frac{1-\sqrt{Y^2+X^2}}{1-X^2}. \end{cases} \tag{9a}$$

One can verify that the only solution of system (9a) satisfying the constraints in (8) is

$$\begin{cases} X = \frac{2}{\sqrt{(\lambda+1)(\mu+1)}}, \\ Y = \frac{1}{\lambda+1} - \frac{1}{\mu+1}. \end{cases} \tag{10a}$$

Similarly, one can impose from (5) $\tau_1 = \lambda$ and $\tau_{-1} = \mu$ and obtain

$$\begin{cases} \lambda &= \left(\frac{\frac{1-\sqrt{1-X^2}}{1+\sqrt{1-X^2}} X(1-\sqrt{Y^2+X^2})}{Y\sqrt{1-X^2}-X^2+\sqrt{Y^2+X^2}} + \frac{Y\sqrt{1-X^2}-X^2+\sqrt{Y^2+X^2}}{\frac{1-\sqrt{1-X^2}}{1+\sqrt{1-X^2}} X(1-\sqrt{Y^2+X^2})} \right) \frac{X(1-\sqrt{Y^2+X^2})}{2(1-X^2)} \\ &\quad + \frac{1-\sqrt{Y^2+X^2}}{1-X^2}, \\ \mu &= \left(\frac{\frac{1+\sqrt{1-X^2}}{1-\sqrt{1-X^2}} X(1-\sqrt{Y^2+X^2})}{Y\sqrt{1-X^2}-X^2+\sqrt{Y^2+X^2}} + \frac{Y\sqrt{1-X^2}-X^2+\sqrt{Y^2+X^2}}{\frac{1+\sqrt{1-X^2}}{1-\sqrt{1-X^2}} X(1-\sqrt{Y^2+X^2})} \right) \frac{X(1-\sqrt{Y^2+X^2})}{2(1-X^2)} \\ &\quad + \frac{1-\sqrt{Y^2+X^2}}{1-X^2}, \end{cases} \tag{9b}$$

having the unique solution

$$\begin{cases} X = \frac{2}{\sqrt{(\lambda+1)(\mu+1)}}, \\ Y = -\left(\frac{1}{\lambda+1} - \frac{1}{\mu+1} \right). \end{cases} \tag{10b}$$

Hence, the solutions (10a)-(10b) are the conditions relevant to the half width $R - a$ of the lens and to the ordinate y_0 of the center of the major circle in order to have the ratios $\tau_1 = \mu$ and $\tau_{-1} = \lambda$ or $\tau_1 = \lambda$ and $\tau_{-1} = \mu$ respectively. It is useful to notice that, by applying the Pythagorean theorem to the right triangle OAC in Figure 2, one has from (10a):

$$AC = \frac{1}{\lambda+1} + \frac{1}{\mu+1}.$$

In particular, we are interested to the case where $\mu = n - 1$ and $\lambda = m - 1$ for integers $m, n \geq 2$. With reference to Figure 2, we state the following property:

For a symmetrical lens with a given ratio $\frac{a}{R}$, the condition of a circle chain with integer ratios τ_k is

$$\begin{cases} AK &= \left(\frac{1}{m} + \frac{1}{n}\right) R, \\ OK &= \left|\frac{1}{m} - \frac{1}{n}\right| R, \end{cases}$$

where m, n are integers ≥ 2 and $(m, n) \neq (2, 2)$.

From (10a), we have

$$\frac{y_0}{R} = \frac{1}{m} - \frac{1}{n}, \tag{11}$$

$$\frac{a}{R} = \frac{2}{\sqrt{mn}}. \tag{12}$$

By splitting up (6) into two sequences for the up- and down-chains respectively one has, for $k = 0, 1, 2, \ldots$,

$$\tau_{\mathrm{u}k} = \alpha\omega^k + \beta\omega^{-k} + \gamma,$$

$$\tau_{\mathrm{d}k} = \beta\omega^k + \alpha\omega^{-k} + \gamma,$$

Moreover, by taking (11) and (12) into account, we have

$$\begin{aligned}
\omega &= \left(\frac{\sqrt{mn}-\sqrt{mn-4}}{2}\right)^2,\\
\alpha &= \frac{(m-n)\sqrt{mn-4}+(m+n-4)\sqrt{mn}}{2\sqrt{mn}(mn-4)},\\
\beta &= \frac{-(m-n)\sqrt{mn-4}+(m+n-4)\sqrt{mn}}{2\sqrt{mn}(mn-4)},\\
\gamma &= \frac{mn-m-n}{mn-4}.
\end{aligned}$$

With a little algebra, we can show that

$$\begin{aligned}
\omega+\frac{1}{\omega} &= mn-2,\\
\gamma\left(2-\omega-\frac{1}{\omega}\right) &= m+n-mn.
\end{aligned}$$

Furthermore,

$$\tau_{\mathrm{u}0}=\tau_{\mathrm{d}0}=\alpha+\beta+\gamma=1.$$

Note also that

$$\begin{cases}\tau_{\mathrm{u}1}=n-1,\\ \tau_{\mathrm{d}1}=m-1.\end{cases}$$

Now, let us focus on the up-chain. $\tau_{\mathrm{u}0}$, $\tau_{\mathrm{u}1}$, $\gamma\left(2-\omega-\frac{1}{\omega}\right)$, and $\omega+\frac{1}{\omega}$ being integers, $\tau_{\mathrm{u}2}$ is also an integer from (7). It follows that $\tau_{\mathrm{u}k}$ is an integer for all $k>0$.

The same reasoning applies to the down-chain. Therefore, the sequence $\{\tau_k\}$ consists entirely of integers.

To conclude, *given a symmetrical lens of ratio* $\frac{a}{R}$*, if a pair* (m,n) *of integers exists so that relation* (12) *is satisfied, then by choosing the ordinate* y_0 *to satisfy* (11)*, it is possible to inscribe inside the lens a circle chain generating two integer sequences* $(\tau_{\mathrm{u}k})$ *and* $(\tau_{\mathrm{d}k})$.

Conversely, relations (12) and (11) can be used to create an inscribed chain starting from an arbitrary pair of integers (m,n) provided that $(m,n)\neq(2,2)$.

4. Symmetrical chains

Some interesting particular cases are represented by the symmetrical chains . As mentioned in Section 2, depending on the ordinate y_0 of the major circle center, one can have two different kinds of symmetrical chains that, consequently, generate identical sequences $\{\tau_{\mathrm{u}k}\}$ and $\{\tau_{\mathrm{d}k}\}$:

- the case with $m=n\geq 3$, central symmetry;
- the case with (m,n) with $m=2$ and $n\geq 3$, or $m\geq 3$ and $n=2$, bicentral symmetry.

A certain number of these sequences can be found in OEIS (*The On Line Encyclopedia of Integer Sequences* [3]). In Table I, some of them are listed.

Table I: Some sequences listed in OEIS related to circle chains in a symmetric lens

(m,n)	Sequence in OEIS
$(3,3)$	$A064170$
$(4,4)$	$A011922$
$(6,6)$	$A076218$
$(2,3),\ (3,2)$	$A101265$
$(2,4),\ (4,2)$	$A011900$
$(2,5),\ (5,2)$	$A182432$
$(2,6),\ (6,2)$	$A054318$
$(2,7),\ (7,2)$	$A253621$
$(2,8),\ (8,2)$	$A156712$
$(2,10),\ (10,2)$	$A246641$
$(2,12),\ (12,2)$	$A254782$
$(2,14),\ (14,2)$	$A253458$
$(2,16),\ (16,2)$	$A253447$
$(2,22),\ (22,2)$	$A054318$
$(2,32),\ (32,2)$	$A131751$

We conclude with two examples of circle chains generated by sequences listed in OEIS.

Example 1. Circle chain with central symmetry derived from sequence

$A064170:$ $\quad 1,\ 2,\ 10,\ 65,\ 442,\ 3026,\ \ldots$

From the second term we have $\tau_{-1} = \tau_1 = 2$. This yields $m = n = 3$ and finally from (11) and (12), one has

$$\frac{y_0}{R} = 0, \qquad \frac{a}{R} = \frac{2}{3}.$$

Example 2. Circle chain with bicentral symmetry derived from sequence

$A101265:$ $\quad 1,\ 2,\ 6,\ 21,\ 77,\ 286,\ \ldots$

Due to the fact that we are considering a chain with bicentral symmetry, we have $r_0 = |y_0|$. From (1) one can write:

$$y_0 = R - \sqrt{a^2 + y_0^2}.$$

By considering the up-chain (with $y_0 > 0$) and by substituting (11) and (12) in the previous formula, we obtain $m = 2$. Moreover, from the second term of the sequence, we have that $\tau_1 = 2$. This yields $n = 3$ and finally from (11) and (12) one has:

$$\frac{y_0}{R} = \frac{1}{6}, \qquad \frac{a}{R} = \frac{2}{\sqrt{6}}.$$

References

[1] J. Kocik: Lens Sequences, arXiv: 0710.3226v1[math.NT], October 17, 2007, http://arxiv.org/pdf/0710.3226.pdf

[2] G. Lucca: Catene di cerchi all'interno di lunule e lenti, *Matematicamente Magazine*, n.17, Aprile 2012, http://www.matematicamente.it/rivista-il-magazine/numero-17-aprile-2012/168-catene-di-cerchi-allinterno-di-lunule-e-lenti/

[3] N. J. A. Sloane, editor, *The On-Line Encyclopedia of Integer Sequences*, published electronically at https://oeis.org

[4] E. W. Weisstein, Inversion, *MathWorld - A Wolfram Web Resource*, http://mathworld.wolfram.com/Inversion.html.

Giovanni Lucca: Via Corvi 20, 29122 Piacenza, Italy
E-mail address: vanni_lucca@inwind.it

Forum Geometricorum
Volume 16 (2016) 429–430.

FORUM GEOM
ISSN 1534-1178

Iterated Harmonic Divisions and the Golden Ratio

Frank Leitenberger

Abstract. On the projective real line we consider sequences of points in which every four consecutive points form two harmonic point pairs. Surprisingly, the asymptotic behavior of one type of these sequences is characterized by the golden ratio. Another type of these sequences is projectively equivalent to a dense set on the unit circle generated by an irrational rotation by nearly 137.5°.

We consider point pairs (A, B) and (C, D) on the projective real line $\mathbb{R} \cup \infty$, which are harmonic conjugate, i.e. their cross ratio $\frac{AC}{AD} \cdot \frac{DB}{CB}$ is -1. Because of the relevance of harmonic division it seems worth to consider also various types of iterated applications of this notion.

Starting with three different points P_0, P_1, P_2 on the projective real line there are three possibilities to define a fourth harmonic point in order to obtain two harmonic conjugate point pairs. Correspondingly, we consider three types of sequences (P_n) defined by a successive harmonic division:

Type 1: P_n is defined as the harmonic conjugate of P_{n-3} with respect to P_{n-1} and P_{n-2} for $n > 2$.

Type 2: P_n is defined as the harmonic conjugate of P_{n-2} with respect to P_{n-1} and P_{n-3} for $n > 2$.

Type 3: P_n is defined as the harmonic conjugate of P_{n-1} with respect to P_{n-2} and P_{n-3} for $n > 2$.

In the following we discuss a few properties of these sequences.

Sequences of type 1. At first we look for sequences of this type of a very simple form. A good candidate are geometric sequences q^n. q satisfies the condition

$$-1 = \frac{(q^n - q^{n-1})(q^{n-2} - q^{n-3})}{(q^n - q^{n-2})(q^{n-1} - q^{n-3})} = \frac{q}{(q+1)^2},$$

i.e. $q^2 + 3q + 1 = 0$ with the solutions $q_1 = \frac{-3+\sqrt{5}}{2} = -\Phi^{-2} = \Phi - 2$ and $q_2 = \frac{-3-\sqrt{5}}{2} = -\Phi^2 = -1 - \Phi$, where $\Phi = \frac{1+\sqrt{5}}{2}$ is the golden ratio. For an arbitrary sequence of type 1 we have a projective isomorphism $f : t \to \frac{at+b}{ct+d}$ with

Publication Date: December 1, 2016. Communicating Editor: Paul Yiu.

$(-\Phi^{-2})^n \to P_n$. It follows $\lim_{n\to\infty} P_n = f(0)$. For a finite limit we have $d \neq 0$ and

$$\lim_{n\to\infty} \frac{P_{n+2}P_{n+1}}{P_{n+1}P_n} = \lim_{n\to\infty} \frac{\frac{aq_1^{n+2}+b}{cq_1^{n+2}+d} - \frac{aq_1^{n+1}+b}{cq_1^{n+1}+d}}{\frac{aq_1^{n+1}+b}{cq_1^{n+1}+d} - \frac{aq_1^{n}+b}{cq_1^{n}+d}} = \frac{q_1(cq_1^n+d)}{(cq_1^{n+2}+d)} = -\Phi^{-2},$$

i.e. $P_{n+2}P_{n+1} \approx -\Phi^{-2}\, P_{n+1}P_n$ for large n. For an infinite limit we have $d = 0$ and

$$\lim_{n\to\infty} \frac{P_{n+2}P_{n+1}}{P_{n+1}P_n} = \lim_{n\to\infty} \frac{\frac{aq_1^{n+2}+b}{cq_1^{n+2}} - \frac{aq_1^{n+1}+b}{cq_1^{n+1}}}{\frac{aq_1^{n+1}+b}{cq_1^{n+1}} - \frac{aq_1^{n}+b}{cq_1^{n}}} = \frac{1}{q_1} = -\Phi^2.$$

Therefore, although projective transformations do not preserve ratios, not only cross ratios but also limits of certain ratios are preserved after projective transformations.

We can consider $q_2^n = (-\Phi^2)^n$ as a real subsequence of the complex geometric sequence $(i\Phi)^n$ or as a real subset of the golden spiral $(e^{t(\ln\Phi + i\frac{\pi}{2})})_{t\in\mathbb{R}}$ in the complex plane. The author has not found hints in the literature that four consecutive points of the intersection of the golden spiral with a line through the center form two harmonic point pairs.

Sequences of type 2. By Definition we have $P_{n+4} = P_n$. (P_n) is a 4-periodic sequence of two harmonic conjugate pairs (P_0, P_2) and (P_1, P_3).

Sequences of type 3. Looking for a geometric sequence of this type we require

$$-1 = \frac{(q^n - q^{n-2})(q^{n-3} - q^{n-1})}{(q^n - q^{n-3})(q^{n-2} - q^{n-1})} = \frac{(q+1)^2}{q^2+q+1}.$$

i.e. $q^2 + \frac{3}{2}q + 1 = 0$ with complex solutions $q_\pm = \frac{-3\pm i\sqrt{7}}{4}$. We remark that $|q_\pm^n| = 1$. For an arbitrary sequence of type 3 we have a projective isomorphism from the unit circle to the projective real line with $q_+^n \to P_n$ by a complex Möbius transformation. We obtain q_+^{n+1} by rotating q_+^n through an angle $\arg(q_+)$. q_+ is not a root of unity, because the minimal polynomial $2q^2 + 3q + 2$ is not a cyclotomic polynomial, cf. [1]. Consequently $\arg(q_+)$ is an irrational angle and the points q_+^n lie dense on the unit circle and correspondingly (P_n) is dense on the projective real line.

We remark that even though type 3 sequences seem not to be related to the golden ratio, the rotation angle $\arg(q_+) \approx 138.59^\circ$ is curiously very near to the golden angle $\frac{360^\circ}{\Phi^2} \approx 137.5^\circ$.

Reference

[1] I. Stewart, *Galois Theory*, Chapman and Hall, London, 1973.

Frank Leitenberger: Burgstr. 19, D-06618 Naumburg, Germany
E-mail address: leitenbe@web.de

Forum Geometricorum
Volume 16 (2016) 431–433.

FORUM GEOM
ISSN 1534-1178

Author Index